Methods in Molecular Biology 1447

Springer Protocols

Rafael Pulido *Editor*

Protein Tyrosine Phosphatases

Methods and Protocols

EXTRAS ONLINE

Humana Press

METHODS IN MOLECULAR BIOLOGY

Series Editor
John M. Walker
School of Life and Medical Sciences
University of Hertfordshire
Hatfield, Hertfordshire, AL10 9AB, UK

For further volumes:
http://www.springer.com/series/7651

Protein Tyrosine Phosphatases

Methods and Protocols

Edited by

Rafael Pulido

BioCruces Health Research Institute, Barakaldo, Bizkaia, Spain

Humana Press

Editor
Rafael Pulido
BioCruces Health Research Institute
Barakaldo, Bizkaia, Spain

ISSN 1064-3745 ISSN 1940-6029 (electronic)
Methods in Molecular Biology
ISBN 978-1-4939-3744-8 ISBN 978-1-4939-3746-2 (eBook)
DOI 10.1007/978-1-4939-3746-2

Library of Congress Control Number: 2016941685

Printed on acid-free paper

This Humana Press imprint is published by Springer Nature
The registered company is Springer Science+Business Media LLC New York

Preface

Protein tyrosine phosphatases (PTPs) are major direct regulators of the phosphotyrosine cellular content and essential drivers of the tyrosine-phosphorylation status of key cell signaling proteins. Tyrosine phosphatases include proteins from the Cys-based PTP superfamily (containing a PTP catalytic domain and a CxxxxxR signature catalytic motif) as well as enzymes from other gene families (Asp- and His-based phosphatases) that have converged to perform dephosphorylation of biological moieties by a two-step, nucleophile-based catalytic mechanism. Such convergence illustrates the adaptive relevance and the wide variety of the dephosphorylation functions mediated by these enzymes, whose manipulation could be important for specific therapeutic targeting in human disease, including cancer, neurodevelopmental, and metabolic diseases. Moreover, since mutations in many PTP genes are associated with hereditary diseases, several PTP family members are currently relevant in disease prevention and early molecular diagnosis. Tyrosine phosphatases are versatile enzymes in terms of substrate specificity and regulatory properties. Classical PTPs dephosphorylate specific phosphotyrosine residues from protein substrates, whereas dual-specificity PTPs dephosphorylate phosphotyrosine, phosphoserine, and phosphothreonine residues, as well as non-proteinaceous substrates, including phosphoinositides (the tumor suppressor PTEN being a hallmark) and carbohydrates, among others. In addition, several PTPs have impaired catalytic activity as a result of amino acid substitutions at their active sites but retain regulatory functions related to phosphotyrosine or phosphoinositide signaling. The substrate specificity and biological function of PTPs, as well as their regulation during cell homeostasis, is facilitated by a diverse array of protein-interaction and protein-targeting domains, and reversible oxidation of their active sites is a major physiological regulatory mechanism of the catalysis of many Tyr phosphatases.

This book is aimed to provide coverage, methodology, and laboratory protocols on the more essential aspects of PTP function and regulation, including the use of standardized in vitro functional assays, suitable cell systems, and animal and microorganism models. Chapters covering state-of-the-art technical approaches suitable to decipher the physiologic roles of PTPs, and their involvement in tissue-specific functions, are also included, which will be of utility for both newcomers and experienced researchers in the field of tyrosine- and phosphoinositide-phosphorylation/dephosphorylation. I wish to thank all authors for their valuable input and contribution to this issue of *Methods in Molecular Biology*. We think the book will be of interest to chemists, biochemists, molecular biologists, and cell biologists, as well as to clinicians focusing their attention on the role of protein kinases and phosphatases in human disease. It is our hope that the methods and protocols from the chapters of this book will help researchers to better define the common and individual features of the PTP family members, and how this knowledge can translate into PTP-based therapy for human disease.

Barakaldo, Bizkaia, Spain ***Rafael Pulido***

Contents

Contributors

James Adams • *Faculty of Life Sciences, University of Manchester, Manchester, UK*

Andrés Alonso • *Instituto de Biología y Genética Molecular (IBGM), CSIC-Universidad de Valladolid, Valladolid, Spain*

Mathieu Amand • *Immunology and Infectious Diseases Laboratory, GIGA-Signal Transduction Unit, University of Liège, Liège, Belgium*

Laura Amo • *Biocruces Health Research Institute, Barakaldo, Spain*

Olaia Aurtenetxe • *Biocruces Health Research Institute, Barakaldo, Spain*

Rodica A. Badea • *Department of Enzymology, Institute of Biochemistry of the Romanian Academy, Bucharest, Romania*

Yunpeng Bai • *Department of Biochemistry and Molecular Biology, Indiana University School of Medicine, Indianapolis, IN, USA*

Namrata Bali • *Division of Biology and Biological Engineering, California Institute of Technology, Pasadena, CA, USA*

Yolanda Bayón • *Instituto de Biología y Genética Molecular (IBGM), CSIC-Universidad de Valladolid, Valladolid, Spain*

Lorena Blanco • *Biocruces Health Research Institute, Barakaldo, Spain*

Frank-D. Böhmer • *Institute of Molecular Cell Biology, CMB, Jena University Hospital, Jena, Germany*

Sylvia-Annette Böhmer • *Institute of Molecular Cell Biology, CMB, Jena University Hospital, Jena, Germany*

Christopher J. Caunt • *Department of Biology and Biochemistry, University of Bath, Claverton Down, Bath, UK*

Lena Claesson-Welsh • *Department of Immunology, Genetics and Pathology, Rudbeck Laboratory, Uppsala University, Uppsala, Sweden*

Céline Delierneux • *Laboratory of Thrombosis and Haemostasis, GIGA-Cardiovascular Sciences Unit, University of Liège, Liège, Belgium*

Jeroen den Hertog • *Hubrecht Institute-KNAW & University Medical Center Utrecht, Utrecht, The Netherlands; Institute of Biology, Leiden University, Leiden, The Netherlands*

Ari Elson • *Department of Molecular Genetics, The Weizmann Institute of Science, Rehovot, Israel*

Charlotte Erpicum • *Laboratory of Tumor and Developmental Biology, GIGA-Cancer, University of Liège, Liège, Belgium*

Eynat Finkelshtein • *Department of Molecular Genetics, The Weizmann Institute of Science, Rehovot, Israel*

Mathew S. Gentry • *Department of Molecular and Cellular Biochemistry, Center for Structural Biology, University of Kentucky, Lexington, KY, USA*

Christine Gilles • *Laboratory of Tumor and Developmental Biology, GIGA-Cancer, University of Liège, Liège, Belgium*

Alexander James Hale • *Hubrecht Institute-KNAW & University Medical Center Utrecht, Utrecht, The Netherlands; Institute of Biology, Leiden University, Leiden, The Netherlands*

Makoto Hayashi • *Department of Immunology, Genetics and Pathology, Rudbeck Laboratory, Uppsala University, Uppsala, Sweden; Department of Physiology and Cell Biology, Graduate School of Medicine, Kobe University, Kobe, Japan*
Alexandre Hego • *Laboratory of Thrombosis and Haemostasis, GIGA-Cardiovascular Sciences Unit, University of Liège, Liège, Belgium*
Irene Helbing • *Department of Immunology, Genetics and Pathology, Rudbeck Laboratory, Uppsala University, Uppsala, Sweden; Alere Technologies GmbH, Jena, Germany*
Wiljan J. Hendriks • *Department of Cell Biology, Nijmegen Centre for Molecular Life Sciences, Radboud University Nijmegen Medical Centre, Nijmegen, The Netherlands*
Riet Hilhorst • *PamGene International BV, 's-Hertogenbosch, The Netherlands*
Shantá D. Hinton • *Department of Biology, Integrated Science Center, College of William and Mary, Williamsburg, VA, USA*
Liesbeth Hovestad-Bijl • *PamGene International BV, 's-Hertogenbosch, The Netherlands*
Aura E. Ionescu • *Department of Enzymology, Institute of Biochemistry of the Romanian Academy, Bucharest, Romania*
Stephen M. Keyse • *Cancer Research UK Stress Response Laboratory, Division of Cancer Research, Jacqui Wood Cancer Centre, Ninewells Hospital & Medical School, University of Dundee, Dundee, UK*
Andrew M. Kidger • *Cancer Research UK Stress Response Laboratory, Division of Cancer Research, Jacqui Wood Cancer Centre, Ninewells Hospital & Medical School, University of Dundee, Dundee, UK*
Sina Koch • *Department of Immunology, Genetics and Pathology, Rudbeck Laboratory, Uppsala University, Uppsala, Sweden; Max-Planck-Institute for Molecular Physiology, Dortmund, Germany*
Hyung-Kook (Peter) Lee • *Division of Biology and Biological Engineering, California Institute of Technology, Pasadena, CA, USA*
Nicholas R. Leslie • *Institute of Biological Chemistry, Biophysics and Bioengineering, Heriot Watt University, Edinburgh, UK*
Colin Levy • *Manchester Protein Structure Facility, Manchester Institute of Biotechnology, Manchester, UK*
Einat Levy-Apter • *Department of Molecular Genetics, The Weizmann Institute of Science, Rehovot, Israel*
Rob Liskamp • *School of Chemistry, University of Glasgow, Glasgow, UK; Medicinal Chemistry and Chemical Biology, Utrecht University, Utrecht, The Netherlands*
Sandra Luna • *Biocruces Health Research Institute, Barakaldo, Spain*
Sujay T. Mallikarjuna • *Department of Enzymology, Institute of Biochemistry of the Romanian Academy, Bucharest, Romania*
Humberto Martín • *Departamento de Microbiología II, Facultad de Farmacia, Instituto Ramón y Cajal de Investigaciones Sanitarias (IRYCIS), Universidad Complutense de Madrid, Madrid, Spain*
Mihaela Mentel • *Department of Enzymology, Institute of Biochemistry of the Romanian Academy, Bucharest, Romania*
Janire Mingo • *Biocruces Health Research Institute, Barakaldo, Spain*
María Molina • *Departamento de Microbiología II, Facultad de Farmacia, Instituto Ramón y Cajal de Investigaciones Sanitarias (IRYCIS), Universidad Complutense de Madrid, Madrid, Spain*

Lucia Musumeci • *Immunology and Infectious Diseases Laboratory, GIGA-Signal Transduction Unit, University of Liège, Liège, Belgium; Laboratory of Thrombosis and Haemostasis, GIGA-Cardiovascular Sciences Unit, University of Liège, Liège, Belgium*

Agnès Noël • *Laboratory of Tumor and Developmental Biology, GIGA-Cancer, University of Liège, Liège, Belgium*

Caroline E. Nunes-Xavier • *Centro de Investigación Príncipe Felipe, Valencia, Spain; Department of Tumor Biology, Institute for Cancer Research, Oslo University Hospital Radiumhospitalet, Oslo, Norway; Biocruces Health Research Institute, Barakaldo, Spain*

Cécile Oury • *Laboratory of Thrombosis and Haemostasis, GIGA-Cardiovascular Sciences Unit, University of Liège, Liège, Belgium*

Rebecca Page • *Department of Molecular Biology, Cell Biology and Biochemistry, Brown University, Providence, RI, USA*

Wolfgang Peti • *Department of Molecular Pharmacology, Physiology and Biotechnology, Brown University, Providence, RI, USA; Department of Chemistry, Brown University, Providence, RI, USA*

Georgiana Necula - Petrareanu • *Department of Enzymology, Institute of Biochemistry of the Romanian Academy, Bucharest, Romania*

Dirk Pijnenburg • *PamGene International BV, 's-Hertogenbosch, The Netherlands*

Rafael Pulido • *Biocruces Health Research Institute, Barakaldo, Bizkaia, Spain; IKERBASQUE, Basque Foundation for Science, Bilbao, Spain*

Vegesna Radha • *Centre for Cellular and Molecular Biology, Hyderabad, India*

Souad Rahmouni • *Immunology and Infectious Diseases Laboratory, GIGA-Signal Transduction Unit, University of Liège, Liège, Belgium*

Madushi Raththagala • *Department of Molecular and Cellular Biochemistry, Center for Structural Biology, University of Kentucky, Lexington, KY, USA*

Carlos Romá-Mateo • *Department of Physiology, School of Medicine and Dentistry, University of Valencia, Valencia, Spain; Centro de Investigación Biomédica en Red de Enfermedades Raras (CIBERER), Valencia, Spain*

Rob Ruijtenbeek • *PamGene International BV, 's-Hertogenbosch, The Netherlands*

Almudena Sacristán-Reviriego • *Departamento de Microbiología II, Facultad de Farmacia, Instituto Ramón y Cajal de Investigaciones Sanitarias (IRYCIS), Universidad Complutense de Madrid, Madrid, Spain*

Pascual Sanz • *Instituto de Biomedicina de Valencia, CSIC, Valencia, Spain; Centro de Investigación Biomédica en Red de Enfermedades Raras (CIBERER), Valencia, Spain*

Jan Schepens • *Department of Cell Biology, Nijmegen Centre for Molecular Life Sciences, Radboud University Nijmegen Medical Centre, Nijmegen, The Netherlands*

Ola Söderberg • *Department of Immunology, Genetics and Pathology, Rudbeck Laboratory, Uppsala University, Uppsala, Sweden; Department of Immunology, Genetics and Pathology, Science for Life Laboratory, Uppsala University, Uppsala, Sweden*

Laura Spinelli • *Institute of Biological Chemistry, Biophysics and Bioengineering, Heriot Watt University, Edinburgh, UK; Division of Cell Signalling and Immunology, School of Life Sciences, University of Dundee, Dundee, UK*

Andrew William Stoker • *UCL Institute of Child Health, University College London, London, UK*

Stefan E. Szedlacsek • *Department of Enzymology, Institute of Biochemistry of the Romanian Academy, Bucharest, Romania*

Lydia Tabernero • *Faculty of Life Sciences, University of Manchester, Manchester, UK*
Lutz Tautz • *NCI-Designated Cancer Center, Sanford Burnham Prebys Medical Discovery Institute, La Jolla, CA, USA*
Jeroen van Ameijde • *Janssen Prevention Center, Crucell Holland BV, Leiden, The Netherlands*
Odile Wéra • *Laboratory of Thrombosis and Haemostasis, GIGA-Cardiovascular Sciences Unit, University of Liège, Liège, Belgium*
Zhi-Hong Yu • *Department of Biochemistry and Molecular Biology, Indiana University School of Medicine, Indianapolis, IN, USA*
Zhong-Yin Zhang • *Department of Biochemistry and Molecular Biology, Indiana University School of Medicine, Indianapolis, IN, USA*
Kai Zinn • *Division of Biology and Biological Engineering, California Institute of Technology, Pasadena, CA, USA*

Chapter 1

The Extended Family of Protein Tyrosine Phosphatases

Andrés Alonso, Caroline E. Nunes-Xavier, Yolanda Bayón, and Rafael Pulido

Abstract

In higher eukaryotes, the Tyr phosphorylation status of cellular proteins results from the coordinated action of Protein Tyrosine Kinases (PTKs) and Protein Tyrosine Phosphatases (PTPs). PTPs have emerged as highly regulated enzymes with diverse substrate specificity, and proteins with Tyr-dephosphorylation or Tyr-dephosphorylation-like properties can be clustered as the PTPome. This includes proteins from the PTP superfamily, which display a Cys-based catalytic mechanism, as well as enzymes from other gene families (Asp-based phosphatases, His-based phosphatases) that have converged in protein Tyr-dephosphorylation-related functions by using non-Cys-based catalytic mechanisms. Within the Cys-based members of the PTPome, classical PTPs dephosphorylate specific phosphoTyr (pTyr) residues from protein substrates, whereas VH1-like dual-specificity PTPs dephosphorylate pTyr, pSer, and pThr residues, as well as nonproteinaceous substrates, including phosphoinositides and phosphorylated carbohydrates. In addition, several PTPs have impaired catalytic activity as a result of amino acid substitutions at their active sites, but retain regulatory functions related with pTyr signaling. As a result of their relevant biological activity, many PTPs are linked to human disease, including cancer, neurodevelopmental, and metabolic diseases, making these proteins important drug targets and molecular markers in the clinic. Here, a brief overview on the biochemistry and physiology of the different groups of proteins that belong to the mammalian PTPome is presented.

Key words Tyrosine phosphatase, Lipid phosphatase, Asp-phosphatase, His-based phosphatase, Phosphorylation, Dephosphorylation

1 Tyr Phosphatases: Positive and Negative Protein Regulators of Cell Signaling

Tyr phosphorylation/dephosphorylation is a profuse regulatory mechanism of the responses of the cells to physiologic and pathologic changes in their environment, and it is exerted in holozoan organisms by the coordinated action of Protein Tyrosine Kinases (PTKs) and Protein Tyrosine Phosphatases (PTPs) [1, 2]. Unlike protein kinases, PTPs have evolved independently of the Ser/Thr Phosphatases, displaying a characteristic PTP domain, a CxxxxxR conserved catalytic loop (where C is the catalytic Cys, x is any amino acid, and R is an Arg), and a Cys-based catalysis [1, 3–7].

Rafael Pulido (ed.), *Protein Tyrosine Phosphatases: Methods and Protocols,* Methods in Molecular Biology, vol. 1447,
DOI 10.1007/978-1-4939-3746-2_1,

Beyond that, the mammalian PTPome, considered as the cluster of proteins with Tyr-dephosphorylation or Tyr-dephosphorylation-like activity, includes proteins distributed in several families (Cys-based, His-based, Asp-based), among which the PTP family itself contributes with most of the members. In line with this, we have defined the concept of an open and extended PTPome whose members fulfill the following criteria: (a) harboring of a structurally defined PTP domain; *or* (b) presence of a CxxxxxR signature catalytic motif within a non-PTP phosphatase domain; *or* (c) displaying experimentally validated Tyr phosphatase activity; *or* (d) displaying high sequence similarity to members with demonstrated Tyr phosphatase activity. This updated human PTPome contains 125 genes, which encode both catalytically active and inactive (pseudophosphatases) proteins [8] (Fig. 1 and Table 1).

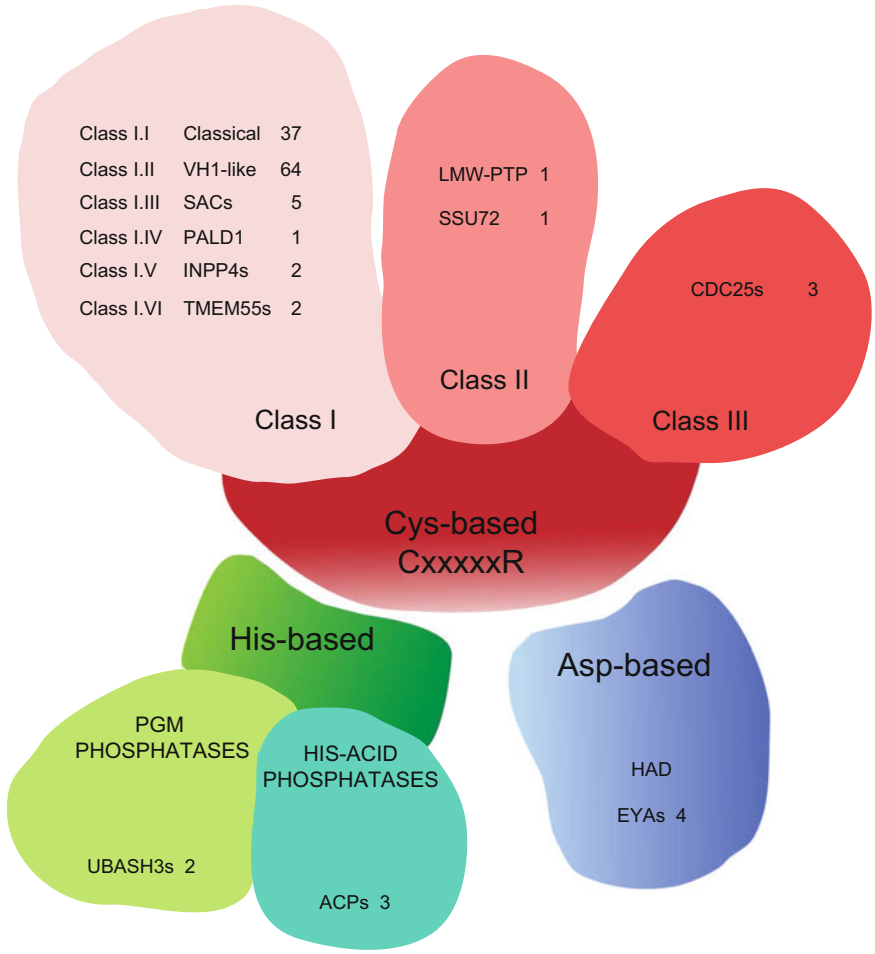

Fig. 1 Scheme of the extended family of Tyr phosphatases (extended PTPome). The classification is based on the nucleophilic catalytic residue (Cys, Asp, or His) and on protein topology. *Numbers* indicate the members included in each group. *See* Table 1 for a complete list of the members of the extended PTPome. *HAD* haloacid dehalogenase, *PGM* phosphoglyceromutase

Table 1
The extended human PTPome

Classical protein tyrosine phosphatases (PTPs) (Class I.I Cys-based)									
Classical receptor protein tyrosine phosphatases (RPTPs)									
1	PTPRA	5	PTPRE	9	PTPRJ	13	PTPRN2	17	PTPRS
2	PTPRB	6	PTPRF	10	PTPRK	14	PTPRO	18	PTPRT
3	PTPRC	7	PTPRG	11	PTPRM	15	PTPRQ	19	PTPRU
4	PTPRD	8	PTPRH	12	PTPRN[a]	16	PTPRR	20	PTPRZ1
Classical non-receptor protein tyrosine phosphatases (NRPTPs)									
21	PTPN1	25	PTPN5	29	PTPN11	33	PTPN18	37	PTPN23
22	PTPN2	26	PTPN6	30	PTPN12	34	PTPN20A/B		
23	PTPN3	27	PTPN7	31	PTPN13	35	PTPN21		
24	PTPN4	28	PTPN9	32	PTPN14	36	PTPN22		
Dual-specificity VH1-like PTPs (DUSPs) (Class I.II Cys-based)									
Dual-specificity MAPK phosphatases (MKPs)									
38	DUSP1	41	DUSP5	44	DUSP8	47	DUSP16		
39	DUSP2	42	DUSP6	45	DUSP9	48	STYXL1[a]		
40	DUSP4	43	DUSP7	46	DUSP10				
Dual-specificity atypical phosphatases (Atypical DUSPs)									
Small-size atypical DUSPs									
49	DUSP3	52	DUSP14	55	DUSP19	58	DUSP23	61	DUSP28
50	DUSP13	53	DUSP15	56	DUSP21	59	DUSP26	62	PTPMT1
51	DUSP13	54	DUSP18	57	DUSP22	60	DUPD1	63	STYX[a]
Other atypical DUSPs									
64	RNGTT	65	DUSP11	66	DUSP12	67	EPM2A	68	DUSP27[a]
Slingshots									
69	SSH1	70	SSH2	71	SSH3				
Phosphatases of regenerating liver (PRLs)									
72	PTP4A1	73	PTP4A2	74	PTP4A3				
CDC14s									
75	CDC14A	76	CDC14B	77	CDKN3	78	PTPDC1		
PTEN-like									
79	PTEN	81	TPTE2	83	TNS3[a]	85	DNAJC6[a]		
80	TPTE[a]	82	TNS1[a]	84	TENC1	86	GAK[a]		

(continued)

Table 1
(continued)

Myotubularins (MTMs)									
87	MTM1	90	MTMR3	93	MTMR6	96	MTMR9[a]	99	MTMR12[a]
88	MTMR1	91	MTMR4	94	MTMR7	97	MTMR10[a]	100	SBF2[a]
89	MTMR2	92	SBF1[a]	95	MTMR8	98	MTMR11[a]	101	MTMR14
SAC phosphoinositide phosphatases (Class I.III Cys-based)									
102	SACM1L	103	INPP5F	104	FIG4	105	SYNJ1	106	SYNJ2
Paladin (Class I.IV Cys-based)									
107	PALD1								
INPP4 inositol polyphosphate phosphatases 4′ (Class I.V Cys-based)									
108	INPP4A	109	INPP4B						
TMEM55 inositol polyphosphate phosphatases 4′ (Class I.VI Cys-based)									
110	TMEM55A	111	TMEM55B						
Low molecular weight PTP (LMW-PTP) (Class II Cys-based)									
112	ACP1								
SSU72 (Class II Cys-based)									
113	SSU72								
CDC25 (Class III Cys-based)									
114	CDC25A	115	CDC25B	116	CDC25C				
Eyes absent haloacid dehalogenase phosphatases (HAD-EYAs) (Asp-based)									
117	EYA1	118	EYA2	119	EYA3	120	EYA4		
UBASH3 HIS-PGM phosphatases (TULAs) (Branch 1 His-based)									
121	UBASH3A	122	UBASH3B						
ACP HIS-acid phosphatases (Branch 2 His-based)									
123	ACPP	124	ACP2	125	ACPT				

Official gene names are provided. PTPN20A and B are two duplicated identical genes located in the same locus. The two entries from DUSP13 correspond to DUSP13A and DUSP13B, two different genes located in the same locus
[a]Inactive phosphatases. PTPRN, TPTE, and TNS3, different to other inactive phosphatases which lack essential catalytic residues, contain all essential residues in their catalytic signature motif, making possible that these enzymes are active toward unknown substrates

Although Tyr phosphatases were initially considered cell signaling shutting-off enzymes, it is now widely known that Tyr phosphatases work both as positive and negative regulators of cell signaling, switching on and off with high specificity the biological activity of signal transduction molecules. Early after the first report of the amino acid sequence of a PTP in 1988 [9], findings of Tyr phosphatases working as positive signaling regulators followed and PTPRC/CD45 was shown to be essential for activation of the Src-family kinase (SFK)

Lck in T lymphocytes, by virtue of dephosphorylation of its inactivating C-terminal Tyr residue [10, 11]. Later on, PTPRA/RPTPα overexpression was reported to cause cell transformation of rat embryo fibroblasts, in association with dephosphorylation and activation of Src [12]. In fact, several PTPs are bona fide positive regulators of SFKs by specific Tyr dephosphorylation [13]. A classic example of targeted negative regulation of cell signaling by Tyr phosphatases is that of the kinase interaction motif (KIM)-containing MAPK-PTPs (PTPRR, PTPN5, and PTPN7), which specifically dephosphorylate the activating Tyr residue in the catalytic loop of MAPKs upon KIM-mediated binding [14, 15]. Thus, Tyr phosphatases may display exquisite substrate specificity and drive distinct signal outputs in coordination with specific TKs, as it has been recently illustrated in the case of PTPN1/PTP1B [16]. Some other examples of the positive and negative role of Tyr phosphatases in cell signaling, using EGFR-mediated signaling as a paradigm, are schematically depicted in Fig. 2.

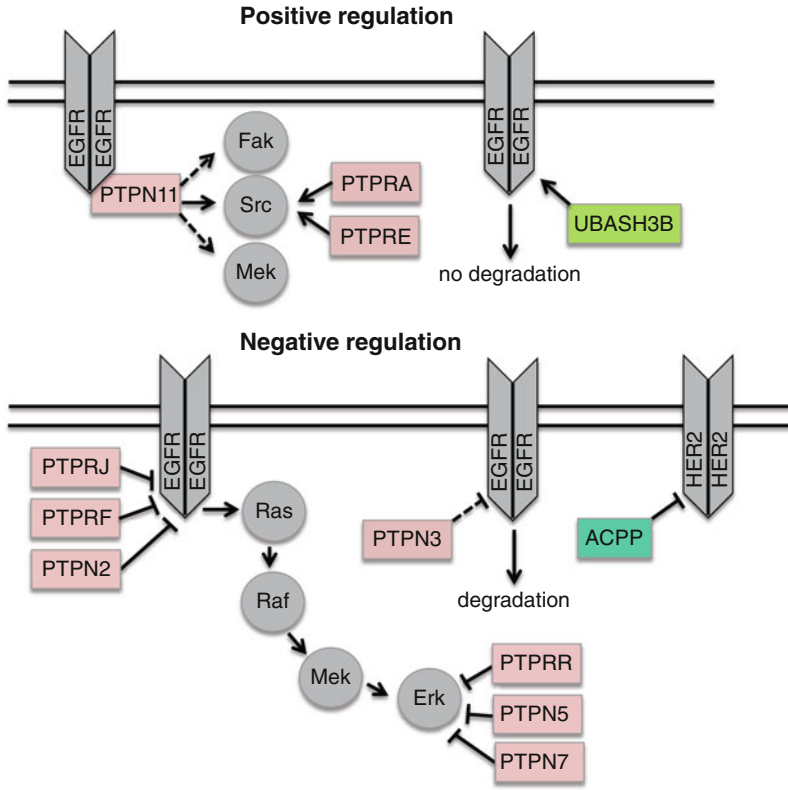

Fig. 2 Examples of positive and negative regulation of cell signaling exerted by different Tyr phosphatases. Examples were chosen using EGF receptor-mediated signaling as paradigm, and Tyr phosphatases acting on kinases upstream or downstream in the pathway. Direct dephosphorylation of regulatory pTyr on kinases is indicated by *solid lines*. Indirect effect on the Tyr phosphorylation status of kinases is indicated by *broken lines*. In most of the examples shown, Tyr dephosphorylation directly affects the catalytic activity of the kinase targeted. In the case of UBASH3B, both direct and indirect effects on EGFR have been documented to block the degradation of the receptor

Next, a brief account of the properties of Tyr phosphatases, as exemplified by the mammalian PTPome members, is presented.

2 Classification of Tyr Phosphatases

Here, we will follow the classification of PTPs by Alonso et al. [3], updated according to Alonso et al. [8] (Fig. 1 and Table 1). As shown, most of the PTPome members (116 genes) are Cys-based Tyr phosphatases, although many of those do not have pTyr as their physiologic substrate but rather phosphoinositides (PIPs). The rest includes the EYAs Asp-based (four genes) and the His-based (five genes) Tyr phosphatases.

3 Class I Cys-Based Phosphatases

Class I of Tyr phosphatases includes most of the Tyr phosphatases identified so far in the human genome. Over 100 phosphatases form part of this group of enzymes, characterized by a similar topology, the presence of common essential catalytic residues and a similar catalytic mechanism [7]. In our classification, six major groups can be differentiated in this class: classical PTPs (subclass I.I), VH1-like/DUSPs (subclass I.II), SACs (subclass I.III), Paladin (subclass I.IV), INPP4s (subclass I.V), and TMEM55s (subclass I.VI) phosphatases.

3.1 Classical PTPs

The most homogeneous group is that of classical PTPs. Alignments of their primary sequence and determination of the structures of the PTP domains (about 250 amino acids in length) from most of the classical Tyr phosphatases have allowed the identification of structural motifs conserved in this family and their implication in catalysis and physiological function [17, 18]. Classical PTPs are pTyr specific enzymes. This pTyr specificity is due to a loop present in classical PTPs structure and named pTyr loop that deepens the active site and impedes access of pSer/Thr to the catalytic Cys. In spite of this, the classical PTPs PTPRN2 and PTPRQ dephosphorylate phosphoinositides. This group is further divided into receptor and non-receptor phosphatases. Apart from the presence of a transmembrane domain that localizes the receptor enzymes in the plasma membrane, 13 out of 20 of these phosphatases contain two PTP domains. The domain close to the membrane, named D1, harbors the catalytic activity, while the second domain, D2, is mostly inactive and its function seems to be regulatory. D2 domains in RPTPs show a high degree of sequence conservation, indicating a conserved function through evolution [19]. Despite presenting receptor-like extracellular domains, ligands have only been

identified in some cases. For instance, PTPRK/RPTPκ, PTPRM/RPTPμ, PTPRU, and PTPRT interact by homotypic interactions, which seem to be involved in cell-cell adhesion processes that limit cell growth. On the other hand, the proteolysis of these PTPs generates extracellular and intracellular independent domains, which have been proposed as important mediators of oncogenicity [20, 21]. Other RPTPs, such as PTPRD/RPTPδ, PTPRF/LAR, and PTPRS/RPTPσ, bind membrane-bound ligands on adjacent cells and orchestrate cell signaling at specific cell compartments, like the synaptic junctions [22, 23]. In this regard, heparan sulfate proteoglycans (HSPGs) bind to PTPRF increasing its phosphatase activity, while another ligand, the protein Dallylike, inhibits its activity, regulating the function of this phosphatase in the formation of synapses [24]. Sugar components from PTPRC/CD45 bind to the endogenous lectin Galectin-1, which reduces PTPRC phosphatase activity and facilitates T cell death during thymic maturation [25, 26]. Remarkably, binding of Galectin-3 to PTPRC from B cells also diminishes PTPRC phosphatase activity, but conferring resistance to apoptosis-inducing agents [27], illustrating the cell type-dependent tuned specificity of the biological activity of PTPs. Another interesting example is that of PTPRZ1/RPTPζ, which binds to pleiotrophin and contactins. Binding to the cytokine pleiotrophin leads to a decrease in its phosphatase activity, and to an increase in Tyr phosphorylation of β-catenin and the ALK TK receptor [28, 29].

Non-receptor classical PTPs are 17 phosphatases which in addition to the PTP domain present additional regulatory and targeting domains and motifs. Some of these domains (FERM, BRO1, FYVE, or C2) are involved in binding to lipids in cellular membranes. Other domains, like the SH2 domain present in PTPN6/SHP1 and PTPN11/SHP2, regulate the activity of the phosphatase, whereas Pro-rich motifs permit the interaction with SH3 or F-BAR domains [30, 31]. As mentioned above, by virtue of these protein-interaction motifs and domains, as well as by intrinsic specificity for substrate recognition in the catalytic domains, PTPs show a physiologically well-tuned substrate specificity that exerts both positive and negative inputs in cell signaling pathways (Fig. 2).

3.2 VH1-Like/Dual-Specificity Phosphatases (DUSPs)

VH1-like/DUSP PTPs are more diverse than classical PTPs and present a phosphatase domain much smaller, usually 100 amino acids shorter. The first phosphatase of this group was identified in the vaccinia poxvirus and was named VH1 [32]. Then many others were identified up to the 64 genes that are included in this group in the human genome. The phosphatases in this group show a great diversity of substrates, from RNA to lipids, and include pTyr, pSer, and pThr phosphatases. Several groups can be distinguished among VH1-like phosphatases [3, 8]. Among them, the ten active MAP kinase (MAPK) phosphatases (MKPs), which target with

great specificity MAPKs thanks to the presence of specific binding domains, are major players in the regulation of cell growth, survival, and differentiation [33, 34]. Myotubularins (MTMs) dephosphorylate PI(3)P and PI(3,5)P2 to produce PtdIns(5)P, and constitute an important VH1-like/DUSP subfamily, with nine phosphatase-active and six phosphatase-inactive members (Table 1). They regulate endocytosis and membrane and vesicle trafficking, and have been genetically linked with human myopathies and neuropathies [35, 36]. A major human disease-related enzyme which belongs to the VH1-like/DUSP phosphatases is the PTEN tumor suppressor, which targets as the major substrate the PI(3,4,5)P3 product of the oncogenic PI3K. PTEN is a physiologic homeostatic regulator whose involvement in human disease goes beyond cancer [36]. Interestingly, some VH1-like/DUSP phosphatases are the lowest expression of a phosphatase, being almost exclusively a PTP domain of around 150 amino acids, like DUSP23/VHZ [37]. Some of these small phosphatases also dephosphorylate MAPKs, like DUSP3/VHR [38, 39].

3.3 SAC Phosphatases

The SAC phosphoinositide phosphatases have in common the presence of a SAC catalytic domain, whose core is topologically similar to that of the PTP catalytic domain of some VH1-like/DUSPs and contains a CxxxxxR catalytic motif [40]. The SAC enzymes included in the human PTPome display substrate specificity towards mono- and multi-phosphorylated PIPs, and form part of two subgroups: SACML1/SAC1, INPP5F/SAC2, and FIG4/SAC3, which possess the SAC domain as the only catalytic domain; and SYNJ1/Synaptojanin 1 and SYNJ2/Synaptojanin 2, which possess a non-Cys-based Mg^{2+}-dependent 5-phosphatase domain in addition to the SAC domain [41–44].

3.4 Paladin

Paladin/PALD1 is a protein that presents two putative PTP domains that contain the signature motif CxxxxxR. However, no phosphatase activity has been demonstrated yet for Paladin [45]. The phosphatase domains of Paladin belong to the PTP-like phytase (PTP-LP) type. Phytases are phosphatases that hydrolyze phosphate from myo-inositol hexakisphosphate, also called phytate [46], and they are found in different families of enzymes: histidine acid phosphatases, β-propeller phytases, purple acid phosphatases, and PTP-like phytases [46, 47]. PTP-LPs are found in anaerobic bacteria in ruminants [48], and in some human pathogens, such as *Clostridium botulinum*. The phytase domain from *Selenomonas ruminantium* (PhyAsr) has been crystallized, showing a similar topology to VH1-like phosphatases [49], with a PTP-loop that contains the catalytic Cys. Paladin expression is regulated during embryonic development [50–52] and it has been implicated in vascular biology [53]. A mouse knockout has been generated, but no phenotype has been reported for the loss of expression of this gene [53]. Paladin has also been involved in the regulation of insulin signaling [45].

3.5 INPP4 and TMEM55 Phosphatases

These two groups of Cys-based phosphatases have been recently added to the PTPome based on the presence on their four members of a conserved CxxxxxR motif (Tables 1 and 2) and phosphatase activity towards inositol polyphosphates and phosphoinositides [8].

INPP4A and INPP4B are two related enzymes that dephosphorylate the D4 position from PI(3,4)P2, Ins(3,4)P3, and Ins(1,3,4)P2. By virtue of their relative specificity towards PI(3,4)P2, INPP4A and INPP4B are involved in the negative regulation of PI3K-mediated signaling and AKT activation [54–56]. INPP4A has been related with Huntington's disease because of its involvement in the control of excitotoxic cerebellar- and striatum-neuronal cell death [57, 58], as well as with the regulation of platelet aggregation and asthma-related inflammation [59–61]. INPP4B exerts tumor suppressor activities in different human cancers by both PI3K/AKT-dependent and -independent mechanisms [56, 62–65]. In addition, INPP4B has been related with osteoporosis by its negative regulatory role on osteoclast differentiation [66].

TMEM55A and TMEM55B are two small phosphoinositide phosphatases that dephosphorylate the D4 position of PI(4,5)P2 [67]. TMEM55A and TMEM55B regulate EGFR lysosomal degradation [67], and a role for TMEM55B in p53 stabilization of nuclear p53 has also been reported [68].

4 Class II Cys-Based Phosphatases

The Class II of Cys-based PTPs now includes two phosphatases, the former member LMW-PTP/ACP1, and the new addition Ssu72 (suppressor of Sua72), which has been added to this family due to its structural homology with LMW-PTP [69]. LMW-PTP has been studied for many years and it has been linked with diseases related with the immune response, inflammation, and cancer [70, 71]. However, the physiological role of this phosphatase is still poorly defined. LMW-PTP and Ssu72 present the typical PTP CxxxxxR signature motif at the N-terminus of the PTP domain, and the Asp acid involved in catalysis is C-terminal, more than 100 amino acids away in the primary sequence, in contrast with Class I PTPs, where precedes the signature motif. LMW-PTP and Ssu72 are evolutionarily related to bacterial arsenate-reductases coupled to thioredoxin, which present the PTP CxxxxxR signature motif and display the same topology [72, 73]. Unlike LMW-PTP, which is specific for pTyr, Ssu72 dephosphorylates specifically pSer5 and pSer7 in the C-terminal domain (CTD) of RNA polymerase II [74–76], and thus Ssu72 is involved in mRNA processing. Ssu72 has also been recently involved in sister chromatid segregation during cell division [77] through the regulation of the cohesin protein complex [78].

Table 2
Catalytic motifs and substrate specificity from some PTPome members

Gene/protein	Catalytic motif	Specificity	Consensus catalytic motif
(Classical; Class I.I Cys-based) (37)			
PTPRA/RPTPα(D1)	**HCS**AG**V**G**R**	pTyr	**HCS**x**G**x**GR**
PTPRQ	**HCS**AG**V**G**R**	PIPs	
PTPN1/PTP1B	**HCS**AG**I**G**R**	pTyr	
(VH1-like/DUSPs; Class I.II Cys-based) (64)			
DUSP1/MKP1	**HC**QAG**I**S**R**	pSer/Thr/Tyr	**HC**xx**G**xx**R**
DUSP3/VHR	**HC**REG**Y**S**R**	pSer/Thr/Tyr	
PTPMT1/PLIP	**HC**KAG**R**S**R**	pGP,PIPs	
EPM2A/Laforin	**HC**NAG**V**G**R**	pGlycogen,pTyr	
SSH1	**HC**KMG**V**S**R**	pSer	
PTP4A3/PRL-3	**HC**VAG**L**G**R**	pSer/Thr/Tyr,PIPs	
CDC14A	**HC**KAG**L**G**R**	pSer/Thr	
PTEN	**HC**KAG**K**G**R**	PIPs/pSer/Thr/Tyr	
MTM1	**HC**SDG**W**D**R**	PIPs	
MTMR4	**HC**SDG**W**D**R**	PIPs,pSer	
(SACs; Class I.III Cys-based) (5)			**C**xxxxx**R**
SACML1/SAC1	N**C**MDCLD**R**	PIPs	
SYNJ1	S**C**ERAGT**R**	PIPs	
(Paladin; Class I.IV Cys-based) (1)			
PALD1(D1)	S**C**QMGVG**R**	?	
PALD1(D2)	S**C**LSGQG**R**	?	
(INPP4s; Class I.V Cys-based) (2)			
INPP4A	S**C**KSAKD**R**	PIPs	
(*TMEM55s; Class I.VI Cys-based) (2)*			
TMEM55A	I**C**KDTSR**R**	PIPs	
(LMW-PTP; Class II Cys-based) (1)			
ACP1/LMW-PTP	V**C**LGNIC**R**	pTyr	
(SSU72; Class II Cys-based) (1)			
SSU72	V**C**SSNQN**R**	pSer	
(CDC25s; Class III Cys-based) (3)			
CDC25A	H**C**EFSSE**R**	pThr/Tyr	
(EYAs; Asp-based) (4)			
EYA1	WDLDET	pSer/Tyr	
(UBASH3s; His-based) (2)			
UBASH3A/TULA/Sts-2	RHGE	pTyr	
(ACPs; His-based) (3)			
ACPP	RHGD	Nonproteinaceous,pSer/Thr/Tyr	

Only some members from the distinct PTPome subfamilies are shown. For a complete list of PTPome members, see Table 1. The consensus catalytic motifs are shown for the Cys -based Tyr phosphatases. For PTPRA, only the catalytic motif from the active PTP D1 domain is shown. For PALD1, the catalytic motifs from the two PTP domains are shown. Note that VH1-like/DUSP subfamily constitutes a heterogeneous group of enzymes. The numbers in brackets indicate the number of genes in each category. PIPs, phosphoinositides; pGP, phosphatidylglycerophosphate.

5 Class III Cys-Based Phosphatases

This class contains three members, cell division cycle (CDC) 25A, B, and C (CDC25A, CDC25B, and CDC25C), which activate CDKs by dephosphorylating Thr14 and Tyr15 in the ATP binding loop of CDKs [79]. Thus, CDC25 phosphatases are involved in cell-cycle progression and in the checkpoint pathways that control DNA damage response [80]. This family has expanded through evolution from a single gene in yeast to three genes in mammals. The catalytic domain of CDC25 is a Rhodanese domain [81, 82], which was first found in a sulfurtransferase called rhodanese [83]. This domain presents an ample distribution in living organisms, being present in Eukarya, Archaea, and Eubacteria. An inactive rhodanese domain, named CDC25 homology domain (CH2), in which the catalytic Cys is replaced by another amino acid, is present in MKPs [84]. This CH2 domain includes a kinase interaction motif (KIM) involved in binding to MKPs [14, 85]. CDC25s present an extended catalytic loop. Whereas other rhodanese enzymes present four amino acids between the catalytic Cys and Arg, CDC25s contain five amino acids by insertion of one extra residue, to generate the signature motif of Cys-based PTPs. The addition of this extra amino acid seems to change the enzyme activity from a sulfur transfer reaction to phosphate hydrolysis [86]. This family lacks a WPD loop containing the general acid/base that works in the second step of the catalysis in Classes I and II. In this sense, it has been proposed that, in CDC25 phosphatases, the initial proton donor is the monoprotonated phosphate that acts as its substrate in lieu of the bisanionic phosphate used by Class I PTPs. An invariant Glu, placed in the CDC25s PTP-loop contiguous to the catalytic Cys, has been proposed to be involved in the catalysis [87, 88].

6 Asp-Based Phosphatases

Among the members of the large family of Asp-based phosphatases, aka Haloacid Dehalogenase (HAD) phosphatases, there are a few that possess Tyr phosphatase activity [89]. We refer to the four members of the Eyes absent (**EYA**) family of transcription factors, which are involved in the formation of many tissues and organs [90]. They contain a poorly conserved N-terminal domain, responsible for its transactivation activity [91], and a highly conserved C-terminal domain, called EYA domain, that participates in protein interactions, mainly with the Six family proteins, and through these interactions, in DNA binding [92]. EYA domain shares the active core of the HAD phosphatases and presents Tyr phosphatase activity [93–95]. EYA proteins also have Thr phosphatase activity, but this activity is catalyzed by other active sites located in the

N-terminal domain and not related to HAD phosphatase activity [96, 97]. Hence, EYA proteins have a dual specificity that is based on two separated catalytic domains that probably act on different substrates. The only avowed substrate for the Tyr phosphatase activity of EYA proteins is the histone H2AX [98, 99], whereas no substrate for the Thr phosphatase activity has been discovered.

7 His-Based Phosphatases

The His phosphatase (HP) superfamily includes numerous enzymes that dephosphorylate a great variety of substrates, from proteins to small molecules involved in metabolism [100]. Two branches are distinguished in this family. Branch one is called PGM (phosphoglycerate mutase) group, because the enzyme Diphosphoglycerate mutase (dPGM) is here included. The second branch is termed AP (acid phosphatases). The PGM subfamily is better represented in prokaryotes, while the AP subfamily is more abundant in eukaryotic organisms. Tyr phosphatases have been identified in both subfamilies, UBASH3 phosphatases in the PGM branch and some acid phosphatases in the second branch [8].

The **UBASH3** (Ubiquitin-associated and SH3 domain-containing protein) group of phosphatases includes UBASH3A and UBASH3B [101–104]. UBASH3 proteins contain an N-terminal UBA (ubiquitin-associated) domain, an SH3 (Src homology 3) domain, and a phosphatase domain similar to the PGM branch of the His phosphatases. The UBA domain interacts with ubiquitin and ubiquitylated proteins, including UBASH3 phosphatases [101, 103, 105]. The PGM domain, in addition to phosphatase activity, allows dimerization of these phosphatases. Expression of UBASH3B is ubiquitous, while UBASH3A expression is restricted to lymphocytes [103, 106]. The phosphatase activity of UBASH3B is much higher than UBASH3A [107–109].

UBASH3A and UBASH3B Tyr phosphatases dephosphorylate ZAP70 and Syk Tyr kinases [106, 109–111] with exquisite specificity, as they just dephosphorylate a few Tyr in these kinases [107, 109, 111, 112]. UBASH3B has also been implicated in dephosphorylation of the EGFR, where it also targets specific Tyr [112].

UBASH3 phosphatases can work both as negative or positive regulators. In the immune system, they seem to function as negative regulators, mainly through the regulation of immunoreceptor tyrosine-based activation motif (ITAM) associated receptors, such as TCR and FcεR. Identification of several SNPs associated with autoimmune diseases in these phosphatases further supports their relevance in the immune system [113]. On the other hand, it has been found that UBASH3B works as positive regulator of EGFR. Upon EGFR stimulation, UBASH3B is recruited to the EGFR

through the interaction with the E3 ubiquitin ligase CBL [101, 103]. UBASH3 SH3 domain binds to the central Pro-rich region of CBL [101, 103], and this complex dephosphorylates EGFR and inhibits its subsequent degradation, which is dependent on EGFR ubiquitination by CBL. In this sense, it has been found that UBASH3 is overexpressed in triple negative breast cancer (TNBC), as well as in prostate cancer cells [114]. UBASH3B is involved in tumor growth and metastasis mainly by inhibiting EGFR degradation, and for this reason it seems that UBASH3B could behave as an oncogenic phosphatase in TNBC.

The group of His-based **acid phosphatases** related with Tyr dephosphorylation includes ACPP/PAP, ACP2/LAP, and ACPT (Table 1). They dephosphorylate small organic nonproteinaceous moieties, as well as pTyr from peptides and proteins [115]. In particular, ACPP and ACPT have been associated with Tyr dephosphorylation and inactivation of distinct members of the EGFR family [116–118]. ACPP, which is abundant in prostate tissue, has been proposed as a tumor suppressor for prostate cancer [119, 120].

8 Catalytic Mechanism of Tyr Phosphatases

Hydrolysis of phosphate from Tyr-phosphorylated proteins is initiated by a nucleophilic attack. The nucleophile that starts the reaction is different in each family of PTPs: Cys in Cys-based phosphatases, Asp in Eya HAD, and His in HPs [3, 115, 121]. The catalytic mechanism for Cys, Asp, and His phosphatases has been well established and involves two steps. The reaction is initiated by a nucleophilic attack carried out by the catalytic amino acids, Cys, Asp, or His. A phospho-enzyme intermediate is formed and the dephosphorylated substrate is released. In addition to the catalytic residue that starts the nucleophilic attack, in the first step of the reaction, an Asp participates donating a proton to the tyrosyl leaving group of the substrate. Next, in the second step of the reaction, the phosphate is released and the phosphatase is regenerated. In this step, a water molecule acting as nucleophile breaks the phospho-enzyme intermediate. This molecule of water is deprotonated by an Asp, which is the same that intervened as a general acid in the first step of the reaction, and now works as a general base (Fig. 3). Representative catalytic signature motifs from the distinct groups of Cys-based Tyr phosphatases are shown in Table 2. Note that these groups can be classified, at least in part, based on the sequence of this motif.

The correct orientation of the phosphate for catalysis as well as the stabilization of the transition state during the reaction is mediated by the Arg present in the catalytic pocket at the end of the P-loop, which is part of the signature motif (CxxxxxR) in the Cys-based PTPs. In HPs, the function of this Arg in Cys-based

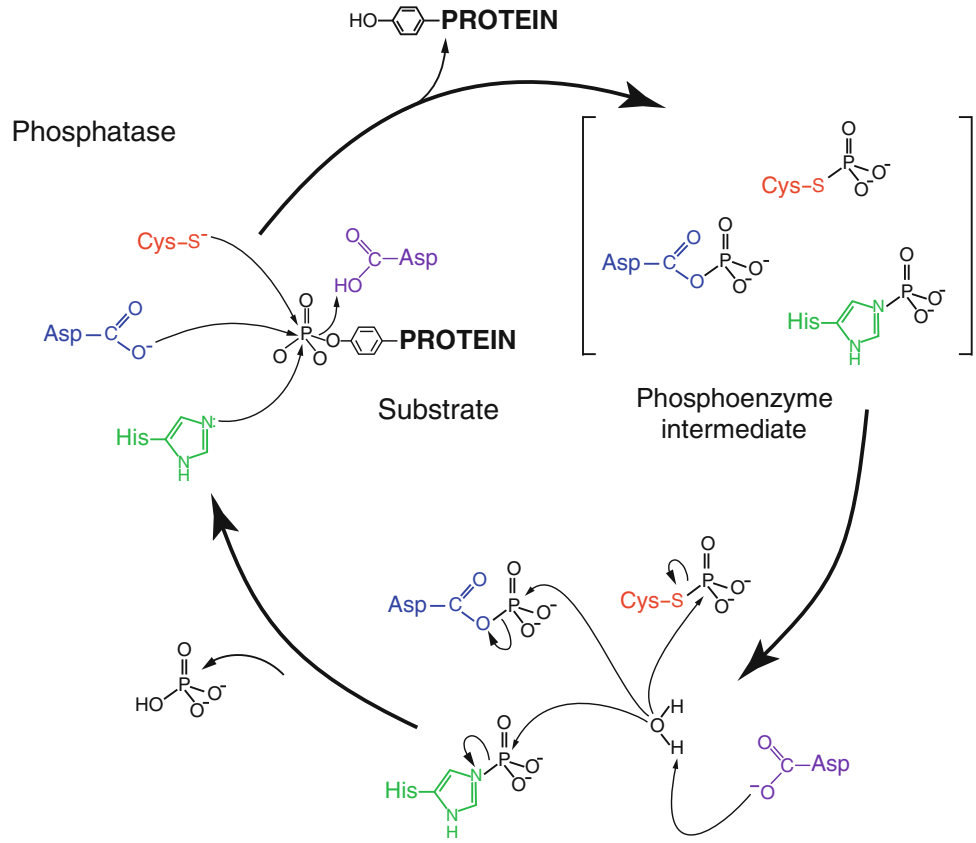

Fig. 3 Scheme of the two-step catalytic mechanism used by Tyr phosphatases. The scheme is shown with a pTyr-protein as the substrate. In the first step, the Cys-, His-, or Asp-catalytic residue from each family of phosphatases initiates a nucleophilic attack on the phosphate group of the substrate forming a transient phospho-enzyme intermediate and releasing the substrate dephosphorylated. In many cases, an Asp works as general acid in this step of the reaction, donating a proton to the tyrosyl group. In the second step of the reaction, the enzyme is restored after hydrolysis of the phospho-enzyme intermediate. In general, the catalytic Asp, working as a general base, deprotonates a water molecule, which now acts as nucleophile over the phospho-enzyme intermediate to release the phosphate group from the enzyme

phosphatases seems to be mediated by two Arg and a His within the catalytic pocket, which together with the catalytic His form the quartet of residues conserved in all HPs. On the other hand, HAD phosphatases use an Asp as the catalytic residue and Mg^{2+} as a cofactor to stabilize the transition state (Table 2) [122].

In contrast to the diversity found in the initial nucleophile in these families of phosphatases, they have adopted an Asp as the general acid/base. Nevertheless, in UBASH3 phosphatases, HPs of the PGM branch, it seems that a Glu develops this function [107, 123]. In most of the Cys-based PTPs, the general acid/base Asp is usually located in an additional loop in the active site. In Class I PTPs this Asp precedes by 30–40 amino acids the P-loop that contains the Cys. This loop contains a conserved stretch of amino

acids, WPD, in classical PTPs that is used to name this loop as WPD loop. However, these residues are not conserved outside this group of phosphatases. On the other hand, in Class II the Asp-loop is 100 amino acids C-terminal to the catalytic Cys. Interestingly, it has been suggested than in Class III phosphatases a Glu in the P-loop develops this function [87, 88], as well as in Myotubularins [36]. Similarly, in the EYAs HADs, the Asp is found in the same loop that the catalytic Asp at a +2 position (Table 2) [121].

9 The PTPome in Model Organisms

PTPome human and mouse genes are well conserved, with the exception of *PTPRV/Ptprv*, which is a transcribed pseudogene in human and a normal gene in mouse [124]. In addition, the two human *TPTE* and *TPTE2* genes are represented with one single gene in mouse [125]. *Dario rerio* (zebrafish) and *Drosophila melanogaster* (fruit fly), two widely used metazoan model organisms, contain members from all Tyr phosphatase families. Within the group of classical PTPs, *D. rerio* ortholog genes to all the mammalian PTPs have been found, with the exception of PTPN7, PTPN12, and PTPN14. In addition, at least 14 classical PTP genes are duplicated in *D. rerio* [126, 127]. In the case of *D. melanogaster*, the representation of Cys-based phosphatases covers about half of the human Cys-based phosphatase genes, with all the *D. melanogaster* Tyr phosphatases having orthologs in humans [127, 128]. The PTPome of the yeast *Saccharomyces cerevisiae* (budding yeast), the more used experimental model from Fungi kingdom, is mostly composed of Tyr-specific and dual-specificity Cys-based phosphatases dedicated to MAPKs dephosphorylation, as well as of dual-specificity phosphatases of unknown function [127, 129, 130]. Two SAC members are present in *S. cerevisiae* [131], as well as Ssu72 [75].

10 Conclusion and Future Perspectives

A variety of mammalian phosphatases from different gene families (PTPome) dephosphorylate pTyr residues or show topological similarity in their catalytic domains with the canonical PTP domain. This has been used to establish classifications and evolutionary relationships between these enzymes [3–6, 132, 133]. We have summarized here our concept of an open and extended PTPome which includes proteins that: (a) harbor a structurally defined PTP domain; *or* (b) contain a CxxxxxR signature catalytic motif within a non-PTP phosphatase domain; *or* (c) display experimentally validated Tyr phosphatase activity; *or* (d) display high sequence similarity to members with demonstrated Tyr phosphatase activity.

The relative conservation of Tyr phosphatase functions in distant Phyla, and the evolutionary convergence of several PTPome members towards Tyr- or PIP-dephosphorylation, outlines the physiologic importance of such functions. In this regard, bacteria and protozoan parasite Tyr phosphatases have a pathogenic role in several infectious diseases, which make them direct drug targets for therapeutic intervention [134–136]. Moreover, Tyr phosphatases have direct roles in the etiology of many hereditary and nonhereditary human diseases, including cancer, neurodegenerative, metabolic, immune, and heart diseases [33, 136–152]. The dual role of many of the Tyr phosphatases in relation with human disease constitutes both a challenge and an open scenario for the implementation of therapies based on these enzymes. For instance, many classical PTPs display pro-oncogenic or anti-oncogenic roles depending on the tissue and the physiologic context [134, 135, 140, 144]. A clinically relevant example is the lipid phosphatase PTEN, whose reconstitution, activation, or delivery could be beneficial in cancer therapy, whereas its inhibition could be beneficial in the treatment of neuroregeneration-related diseases [153–156]. The feasibility of Tyr phosphatases as both potential targets for inhibition and active drugs in human disease therapy will be under dedicated scrutiny in the upcoming future.

Acknowledgements

The work in RP laboratory is supported in part by grants SAF2013-48812-R from Ministerio de Economía y Competitividad (Spain), 2013111011 from Gobierno Vasco, Departamento de Salud (Basque Country, Spain), and BIO13/CI/001/BC from BIOEF/EITB maratoia (Basque Country, Spain).

References

1. Tonks NK (2013) Protein tyrosine phosphatases—from housekeeping enzymes to master regulators of signal transduction. FEBS J 280: 346–378
2. Hunter T (2014) The genesis of tyrosine phosphorylation. Cold Spring Harb Perspect Biol 6:a020644
3. Alonso A, Sasin J, Bottini N, Friedberg I, Friedberg I, Osterman A, Godzik A, Hunter T, Dixon J, Mustelin T (2004) Protein tyrosine phosphatases in the human genome. Cell 117:699–711
4. Andersen JN, Jansen PG, Echwald SM, Mortensen OH, Fukada T, Del Vecchio R, Tonks NK, Moller NP (2004) A genomic perspective on protein tyrosine phosphatases: gene structure, pseudogenes, and genetic disease linkage. FASEB J 18:8–30
5. Li X, Wilmanns M, Thornton J, Kohn M (2013) Elucidating human phosphatase-substrate networks. Sci Signal 6:rs10
6. Hatzihristidis T, Liu S, Pryszcz L, Hutchins AP, Gabaldon T, Tremblay ML, Miranda-Saavedra D (2014) PTP-central: a comprehensive resource of protein tyrosine phosphatases in eukaryotic genomes. Methods (San Diego, Calif) 65:156–164
7. Tautz L, Critton DA, Grotegut S (2013) Protein tyrosine phosphatases: structure, function, and implication in human disease. Methods Mol Biol (Clifton, NJ) 1053: 179–221

8. Alonso A, Pulido R (2016) The extended human PTPome: a growing tyrosine phosphatase family. FEBS J 283:1404–1429
9. Charbonneau H, Tonks NK, Walsh KA, Fischer EH (1988) The leukocyte common antigen (CD45): a putative receptor-linked protein tyrosine phosphatase. Proc Natl Acad Sci U S A 85:7182–7186
10. Mustelin T, Coggeshall KM, Altman A (1989) Rapid activation of the T-cell tyrosine protein kinase pp56lck by the CD45 phosphotyrosine phosphatase. Proc Natl Acad Sci U S A 86:| 6302–6306
11. Ostergaard HL, Shackelford DA, Hurley TR, Johnson P, Hyman R, Sefton BM, Trowbridge IS (1989) Expression of CD45 alters phosphorylation of the lck-encoded tyrosine protein kinase in murine lymphoma T-cell lines. Proc Natl Acad Sci U S A 86:8959–8963
12. Zheng XM, Wang Y, Pallen CJ (1992) Cell transformation and activation of pp60c-src by overexpression of a protein tyrosine phosphatase. Nature 359:336–339
13. Roskoski R Jr (2005) Src kinase regulation by phosphorylation and dephosphorylation. Biochem Biophys Res Commun 331:1–14
14. Pulido R, Zuniga A, Ullrich A (1998) PTP-SL and STEP protein tyrosine phosphatases regulate the activation of the extracellular signal-regulated kinases ERK1 and ERK2 by association through a kinase interaction motif. EMBO J 17:7337–7350
15. Saxena M, Williams S, Brockdorff J, Gilman J, Mustelin T (1999) Inhibition of T cell signaling by mitogen-activated protein kinase-targeted hematopoietic tyrosine phosphatase (HePTP). J Biol Chem 274:11693–11700
16. Fan G, Aleem S, Yang M, Miller WT, Tonks NK (2015) Protein tyrosine phosphatase and kinase specificity in regulation of SRC and BRK. J Biol Chem 290(26):15934–15947
17. Andersen JN, Mortensen OH, Peters GH, Drake PG, Iversen LF, Olsen OH, Jansen PG, Andersen HS, Tonks NK, Moller NP (2001) Structural and evolutionary relationships among protein tyrosine phosphatase domains. Mol Cell Biol 21:7117–7136
18. Barr AJ, Ugochukwu E, Lee WH, King ON, Filippakopoulos P, Alfano I, Savitsky P, Burgess-Brown NA, Muller S, Knapp S (2009) Large-scale structural analysis of the classical human protein tyrosine phosphatome. Cell 136:352–363
19. Ahuja LG, Gopal B (2014) Bi-domain protein tyrosine phosphatases reveal an evolutionary adaptation to optimize signal transduction. Antioxid Redox Signal 20:2141–2159
20. Mohebiany AN, Nikolaienko RM, Bouyain S, Harroch S (2013) Receptor-type tyrosine phosphatase ligands: looking for the needle in the haystack. FEBS J 280:388–400
21. Craig SE, Brady-Kalnay SM (2015) Regulation of development and cancer by the R2B subfamily of RPTPs and the implications of proteolysis. Semin Cell Dev Biol 37:108–118
22. Takahashi H, Craig AM (2013) Protein tyrosine phosphatases PTPdelta, PTPsigma, and LAR: presynaptic hubs for synapse organization. Trends Neurosci 36:522–534
23. Um JW, Ko J (2013) LAR-RPTPs: synaptic adhesion molecules that shape synapse development. Trends Cell Biol 23: 465–475
24. Johnson KG, Tenney AP, Ghose A, Duckworth AM, Higashi ME, Parfitt K, Marcu O, Heslip TR, Marsh JL, Schwarz TL, Flanagan JG, Van Vactor D (2006) The HSPGs Syndecan and Dallylike bind the receptor phosphatase LAR and exert distinct effects on synaptic development. Neuron 49:517–531
25. Walzel H, Schulz U, Neels P, Brock J (1999) Galectin-1, a natural ligand for the receptor-type protein tyrosine phosphatase CD45. Immunol Lett 67:193–202
26. Earl LA, Bi S, Baum LG (2010) N- and O-glycans modulate galectin-1 binding, CD45 signaling, and T cell death. J Biol Chem 285:2232–2244
27. Clark MC, Pang M, Hsu DK, Liu FT, de Vos S, Gascoyne RD, Said J, Baum LG (2012) Galectin-3 binds to CD45 on diffuse large B-cell lymphoma cells to regulate susceptibility to cell death. Blood 120:4635–4644
28. Meng K, Rodriguez-Pena A, Dimitrov T, Chen W, Yamin M, Noda M, Deuel TF (2000) Pleiotrophin signals increased tyrosine phosphorylation of beta beta-catenin through inactivation of the intrinsic catalytic activity of the receptor-type protein tyrosine phosphatase beta/zeta. Proc Natl Acad Sci U S A 97:2603–2608
29. Perez-Pinera P, Zhang W, Chang Y, Vega JA, Deuel TF (2007) Anaplastic lymphoma kinase is activated through the pleiotrophin/receptor protein-tyrosine phosphatase beta/zeta signaling pathway: an alternative mechanism of receptor tyrosine kinase activation. J Biol Chem 282:28683–28690
30. Marcos T, Ruiz-Martin V, de la Puerta ML, Trinidad AG, Rodriguez Mdel C, de la Fuente MA, Sanchez Crespo M, Alonso A, Bayon Y (2014) Proline-serine-threonine phosphatase interacting protein 1 inhibition of T-cell

receptor signaling depends on its SH3 domain. FEBS J 281:3844–3854

31. Veillette A, Rhee I, Souza CM, Davidson D (2009) PEST family phosphatases in immunity, autoimmunity, and autoinflammatory disorders. Immunol Rev 228:312–324
32. Guan KL, Broyles SS, Dixon JE (1991) A Tyr/Ser protein phosphatase encoded by vaccinia virus. Nature 350:359–362
33. Nunes-Xavier C, Roma-Mateo C, Rios P, Tarrega C, Cejudo-Marin R, Tabernero L, Pulido R (2011) Dual-specificity MAP kinase phosphatases as targets of cancer treatment. Anticancer Agents Med Chem 11:109–132
34. Caunt CJ, Keyse SM (2013) Dual-specificity MAP kinase phosphatases (MKPs): shaping the outcome of MAP kinase signalling. FEBS J 280:489–504
35. Hnia K, Vaccari I, Bolino A, Laporte J (2012) Myotubularin phosphoinositide phosphatases: cellular functions and disease pathophysiology. Trends Mol Med 18:317–327
36. Pulido R, Stoker AW, Hendriks WJ (2013) PTPs emerge as PIPs: protein tyrosine phosphatases with lipid-phosphatase activities in human disease. Hum Mol Genet 22:R66–R76
37. Alonso A, Burkhalter S, Sasin J, Tautz L, Bogetz J, Huynh H, Bremer MC, Holsinger LJ, Godzik A, Mustelin T (2004) The minimal essential core of a cysteine-based protein-tyrosine phosphatase revealed by a novel 16-kDa VH1-like phosphatase, VHZ. J Biol Chem 279:35768–35774
38. Todd JL, Tanner KG, Denu JM (1999) Extracellular regulated kinases (ERK) 1 and ERK2 are authentic substrates for the dual-specificity protein-tyrosine phosphatase VHR. A novel role in down-regulating the ERK pathway. J Biol Chem 274:13271–13280
39. Alonso A, Saxena M, Williams S, Mustelin T (2001) Inhibitory role for dual specificity phosphatase VHR in T cell antigen receptor and CD28-induced Erk and Jnk activation. J Biol Chem 276:4766–4771
40. Manford A, Xia T, Saxena AK, Stefan C, Hu F, Emr SD, Mao Y (2010) Crystal structure of the yeast Sac1: implications for its phosphoinositide phosphatase function. EMBO J 29:1489–1498
41. Sasaki T, Takasuga S, Sasaki J, Kofuji S, Eguchi S, Yamazaki M, Suzuki A (2009) Mammalian phosphoinositide kinases and phosphatases. Prog Lipid Res 48:307–343
42. Hughes WE, Cooke FT, Parker PJ (2000) Sac phosphatase domain proteins. Biochem J 350(Pt 2):337–352
43. Dyson JM, Fedele CG, Davies EM, Becanovic J, Mitchell CA (2012) Phosphoinositide phosphatases: just as important as the kinases. Subcell Biochem 58:215–279
44. Hsu F, Mao Y (2015) The structure of phosphoinositide phosphatases: insights into substrate specificity and catalysis. Biochim Biophys Acta 1851:698–710
45. Huang SM, Hancock MK, Pitman JL, Orth AP, Gekakis N (2009) Negative regulators of insulin signaling revealed in a genome-wide functional screen. PLoS One 4:e6871
46. Mullaney EJ, Ullah AH (2003) The term phytase comprises several different classes of enzymes. Biochem Biophys Res Commun 312:179–184
47. Puhl AA, Gruninger RJ, Greiner R, Janzen TW, Mosimann SC, Selinger LB (2007) Kinetic and structural analysis of a bacterial protein tyrosine phosphatase-like myo-inositol polyphosphatase. Protein Sci 16: 1368–1378
48. Huang H, Zhang R, Fu D, Luo J, Li Z, Luo H, Shi P, Yang P, Diao Q, Yao B (2011) Diversity, abundance and characterization of ruminal cysteine phytases suggest their important role in phytate degradation. Environ Microbiol 13:747–757
49. Chu HM, Guo RT, Lin TW, Chou CC, Shr HL, Lai HL, Tang TY, Cheng KJ, Selinger BL, Wang AH (2004) Structures of Selenomonas ruminantium phytase in complex with persulfated phytate: DSP phytase fold and mechanism for sequential substrate hydrolysis. Structure 12:2015–2024
50. Adams MS, Gammill LS, Bronner-Fraser M (2008) Discovery of transcription factors and other candidate regulators of neural crest development. Dev Dyn 237:1021–1033
51. Gammill LS, Bronner-Fraser M (2002) Genomic analysis of neural crest induction. Development 129:5731–5741
52. Roffers-Agarwal J, Hutt KJ, Gammill LS (2012) Paladin is an antiphosphatase that regulates neural crest cell formation and migration. Dev Biol 371:180–190
53. Wallgard E, Nitzsche A, Larsson J, Guo X, Dieterich LC, Dimberg A, Olofsson T, Ponten FC, Makinen T, Kalen M, Hellstrom M (2012) Paladin (X99384) is expressed in the vasculature and shifts from endothelial to vascular smooth muscle cells during mouse development. Dev Dyn 241:770–786
54. Ivetac I, Munday AD, Kisseleva MV, Zhang XM, Luff S, Tiganis T, Whisstock JC, Rowe T, Majerus PW, Mitchell CA (2005) The type Ialpha inositol polyphosphate 4-phosphatase generates and terminates phosphoinositide 3-kinase signals on endosomes and the plasma membrane. Mol Biol Cell 16:2218–2233

55. Barnache S, Le Scolan E, Kosmider O, Denis N, Moreau-Gachelin F (2006) Phosphatidylinositol 4-phosphatase type II is an erythropoietin-responsive gene. Oncogene 25:| 1420–1423
56. Gewinner C, Wang ZC, Richardson A, Teruya-Feldstein J, Etemadmoghadam D, Bowtell D, Barretina J, Lin WM, Rameh L, Salmena L, Pandolfi PP, Cantley LC (2009) Evidence that inositol polyphosphate 4-phosphatase type II is a tumor suppressor that inhibits PI3K signaling. Cancer Cell 16:115–125
57. Nystuen A, Legare ME, Shultz LD, Frankel WN (2001) A null mutation in inositol polyphosphate 4-phosphatase type I causes selective neuronal loss in weeble mutant mice. Neuron 32:203–212
58. Sasaki J, Kofuji S, Itoh R, Momiyama T, Takayama K, Murakami H, Chida S, Tsuya Y, Takasuga S, Eguchi S, Asanuma K, Horie Y, Miura K, Davies EM, Mitchell C, Yamazaki M, Hirai H, Takenawa T, Suzuki A, Sasaki T (2010) The PtdIns(3,4)P(2) phosphatase INPP4A is a suppressor of excitotoxic neuronal death. Nature 465:497–501
59. Sharma M, Batra J, Mabalirajan U, Sharma S, Nagarkatti R, Aich J, Sharma SK, Niphadkar PV, Ghosh B (2008) A genetic variation in inositol polyphosphate 4 phosphatase a enhances susceptibility to asthma. Am J Respir Crit Care Med 177:712–719
60. Marjanovic J, Wilson MP, Zhang C, Zou J, Nicholas P, Majerus PW (2011) The role of inositol polyphosphate 4-phosphatase 1 in platelet function using a weeble mouse model. Adv Enzyme Regul 51:101–105
61. Aich J, Mabalirajan U, Ahmad T, Agrawal A, Ghosh B (2012) Loss-of-function of inositol polyphosphate-4-phosphatase reversibly increases the severity of allergic airway inflammation. Nat Commun 3:877
62. Agoulnik IU, Hodgson MC, Bowden WA, Ittmann MM (2011) INPP4B: the new kid on the PI3K block. Oncotarget 2:321–328
63. Hodgson MC, Deryugina EI, Suarez E, Lopez SM, Lin D, Xue H, Gorlov IP, Wang Y, Agoulnik IU (2014) INPP4B suppresses prostate cancer cell invasion. Cell Commun Signal 12:61
64. Chew CL, Lunardi A, Gulluni F, Ruan DT, Chen M, Salmena LPD, Nishino M, Papa A, Ng C, Fung J, Clohessy JG, Sasaki J, Sasaki T, Bronson RT, Hirsch E, Pandolfi PP (2015) In vivo role of INPP4B in tumor and metastasis suppression through regulation of PI3K/AKT signaling at endosomes. Cancer Discov 5(7):740–751
65. Kofuji S, Kimura H, Nakanishi H, Nanjo H, Takasuga S, Liu H, Eguchi S, Nakamura R, Itoh R, Ueno N, Asanuma K, Huang M, Koizumi A, Habuchi T, Yamazaki M, Suzuki A, Sasaki J, Sasaki T (2015) INPP4B is a PtdIns(3,4,5)P3 phosphatase that can act as a tumor suppressor. Cancer Discov 5(7): 730–739
66. Ferron M, Boudiffa M, Arsenault M, Rached M, Pata M, Giroux S, Elfassihi L, Kisseleva M, Majerus PW, Rousseau F, Vacher J (2011) Inositol polyphosphate 4-phosphatase B as a regulator of bone mass in mice and humans. Cell Metab 14:466–477
67. Ungewickell A, Hugge C, Kisseleva M, Chang SC, Zou J, Feng Y, Galyov EE, Wilson M, Majerus PW (2005) The identification and characterization of two phosphatidylinositol-4,5-bisphosphate 4-phosphatases. Proc Natl Acad Sci U S A 102:18854–18859
68. Zou J, Marjanovic J, Kisseleva MV, Wilson M, Majerus PW (2007) Type I phosphatidylinositol-4,5-bisphosphate 4-phosphatase regulates stress-induced apoptosis. Proc Natl Acad Sci U S A 104:16834–16839
69. Xiang K, Nagaike T, Xiang S, Kilic T, Beh MM, Manley JL, Tong L (2010) Crystal structure of the human symplekin-Ssu72-CTD phosphopeptide complex. Nature 467:729–733
70. Souza AC, Azoubel S, Queiroz KC, Peppelenbosch MP, Ferreira CV (2009) From immune response to cancer: a spot on the low molecular weight protein tyrosine phosphatase. Cell Mol Life Sci 66:1140–1153
71. Alho I, Costa L, Bicho M, Coelho C (2013) The role of low-molecular-weight protein tyrosine phosphatase (LMW-PTP ACP1) in oncogenesis. Tumour Biol 34:1979–1989
72. Zegers I, Martins JC, Willem R, Wyns L, Messens J (2001) Arsenate reductase from S. aureus plasmid pI258 is a phosphatase drafted for redox duty. Nat Struct Biol 8:843–847
73. Bennett MS, Guan Z, Laurberg M, Su XD (2001) Bacillus subtilis arsenate reductase is structurally and functionally similar to low molecular weight protein tyrosine phosphatases. Proc Natl Acad Sci U S A 98:13577–13582
74. Xiang K, Manley JL, Tong L (2012) An unexpected binding mode for a Pol II CTD peptide phosphorylated at Ser7 in the active site of the CTD phosphatase Ssu72. Genes Dev 26:2265–2270
75. Krishnamurthy S, He X, Reyes-Reyes M, Moore C, Hampsey M (2004) Ssu72 Is an RNA polymerase II CTD phosphatase. Mol Cell 14:387–394

76. Zhang DW, Mosley AL, Ramisetty SR, Rodriguez-Molina JB, Washburn MP, Ansari AZ (2012) Ssu72 phosphatase-dependent erasure of phospho-Ser7 marks on the RNA polymerase II C-terminal domain is essential for viability and transcription termination. J Biol Chem 287:8541–8551
77. Kim HS, Baek KH, Ha GH, Lee JC, Kim YN, Lee J, Park HY, Lee NR, Lee H, Cho Y, Lee CW (2010) The hsSsu72 phosphatase is a cohesin-binding protein that regulates the resolution of sister chromatid arm cohesion. EMBO J 29:3544–3557
78. Kim HS, Kim SH, Park HY, Lee J, Yoon JH, Choi S, Ryu SH, Lee H, Cho HS, Lee CW (2013) Functional interplay between Aurora B kinase and Ssu72 phosphatase regulates sister chromatid cohesion. Nat Commun 4:2631
79. Boutros R, Lobjois V, Ducommun B (2007) CDC25 phosphatases in cancer cells: key players? Good targets? Nat Rev Cancer 7:495–507
80. Boutros R, Dozier C, Ducommun B (2006) The when and wheres of CDC25 phosphatases. Curr Opin Cell Biol 18:185–191
81. Reynolds RA, Yem AW, Wolfe CL, Deibel MR Jr, Chidester CG, Watenpaugh KD (1999) Crystal structure of the catalytic subunit of Cdc25B required for G2/M phase transition of the cell cycle. J Mol Biol 293:559–568
82. Fauman EB, Cogswell JP, Lovejoy B, Rocque WJ, Holmes W, Montana VG, Piwnica-Worms H, Rink MJ, Saper MA (1998) Crystal structure of the catalytic domain of the human cell cycle control phosphatase, Cdc25A. Cell 93:617–625
83. Ploegman JH, Drent G, Kalk KH, Hol WG, Heinrikson RL, Keim P, Weng L, Russell J (1978) The covalent and tertiary structure of bovine liver rhodanese. Nature 273:124–129
84. Bordo D, Bork P (2002) The rhodanese/Cdc25 phosphatase superfamily. Sequence-structure-function relations. EMBO Rep 3:741–746
85. Tanoue T, Nishida E (2003) Molecular recognitions in the MAP kinase cascades. Cell Signal 15:455–462
86. Cipollone R, Ascenzi P, Visca P (2007) Common themes and variations in the rhodanese superfamily. IUBMB Life 59:51–59
87. Rudolph J (2002) Catalytic mechanism of Cdc25. Biochemistry 41:14613–14623
88. Arantes GM (2008) The catalytic acid in the dephosphorylation of the Cdk2-pTpY/CycA protein complex by Cdc25B phosphatase. J Phys Chem 112:15244–15247
89. Patterson KI, Brummer T, O'Brien PM, Daly RJ (2009) Dual-specificity phosphatases: critical regulators with diverse cellular targets. Biochem J 418:475–489
90. Tadjuidje E, Hegde RS (2013) The Eyes Absent proteins in development and disease. Cell Mol Life Sci 70:1897–1913
91. Xu PX, Woo I, Her H, Beier DR, Maas RL (1997) Mouse Eya homologues of the Drosophila eyes absent gene require Pax6 for expression in lens and nasal placode. Development 124:219–231
92. Ohto H, Kamada S, Tago K, Tominaga SI, Ozaki H, Sato S, Kawakami K (1999) Cooperation of six and eya in activation of their target genes through nuclear translocation of Eya. Mol Cell Biol 19:6815–6824
93. Li X, Oghi KA, Zhang J, Krones A, Bush KT, Glass CK, Nigam SK, Aggarwal AK, Maas R, Rose DW, Rosenfeld MG (2003) Eya protein phosphatase activity regulates Six1-Dach-Eya transcriptional effects in mammalian organogenesis. Nature 426:247–254
94. Rayapureddi JP, Kattamuri C, Steinmetz BD, Frankfort BJ, Ostrin EJ, Mardon G, Hegde RS (2003) Eyes absent represents a class of protein tyrosine phosphatases. Nature 426:295–298
95. Tootle TL, Silver SJ, Davies EL, Newman V, Latek RR, Mills IA, Selengut JD, Parlikar BE, Rebay I (2003) The transcription factor Eyes absent is a protein tyrosine phosphatase. Nature 426:299–302
96. Okabe Y, Sano T, Nagata S (2009) Regulation of the innate immune response by threonine-phosphatase of Eyes absent. Nature 460:520–524
97. Sano T, Nagata S (2011) Characterization of the threonine-phosphatase of mouse eyes absent 3. FEBS Lett 585:2714–2719
98. Cook PJ, Ju BG, Telese F, Wang X, Glass CK, Rosenfeld MG (2009) Tyrosine dephosphorylation of H2AX modulates apoptosis and survival decisions. Nature 458:591–596
99. Krishnan N, Jeong DG, Jung SK, Ryu SE, Xiao A, Allis CD, Kim SJ, Tonks NK (2009) Dephosphorylation of the C-terminal tyrosyl residue of the DNA damage-related histone H2A.X is mediated by the protein phosphatase eyes absent. J Biol Chem 284(24):16066–16070
100. Rigden DJ (2008) The histidine phosphatase superfamily: structure and function. Biochem J 409:333–348
101. Kowanetz K, Crosetto N, Haglund K, Schmidt MH, Heldin CH, Dikic I (2004)

Suppressors of T-cell receptor signaling Sts-1 and Sts-2 bind to Cbl and inhibit endocytosis of receptor tyrosine kinases. J Biol Chem 279:32786–32795

102. Carpino N, Kobayashi R, Zang H, Takahashi Y, Jou ST, Feng J, Nakajima H, Ihle JN (2002) Identification, cDNA cloning, and targeted deletion of p70, a novel, ubiquitously expressed SH3 domain-containing protein. Mol Cell Biol 22:7491–7500
103. Feshchenko EA, Smirnova EV, Swaminathan G, Teckchandani AM, Agrawal R, Band H, Zhang X, Annan RS, Carr SA, Tsygankov AY (2004) TULA: an SH3- and UBA-containing protein that binds to c-Cbl and ubiquitin. Oncogene 23:4690–4706
104. Wattenhofer M, Shibuya K, Kudoh J, Lyle R, Michaud J, Rossier C, Kawasaki K, Asakawa S, Minoshima S, Berry A, Bonne-Tamir B, Shimizu N, Antonarakis SE, Scott HS (2001) Isolation and characterization of the UBASH3A gene on 21q22.3 encoding a potential nuclear protein with a novel combination of domains. Hum Genet 108:140–147
105. Hoeller D, Crosetto N, Blagoev B, Raiborg C, Tikkanen R, Wagner S, Kowanetz K, Breitling R, Mann M, Stenmark H, Dikic I (2006) Regulation of ubiquitin-binding proteins by monoubiquitination. Nat Cell Biol 8:163–169
106. Carpino N, Turner S, Mekala D, Takahashi Y, Zang H, Geiger TL, Doherty P, Ihle JN (2004) Regulation of ZAP-70 activation and TCR signaling by two related proteins, Sts-1 and Sts-2. Immunity 20:37–46
107. Mikhailik A, Ford B, Keller J, Chen Y, Nassar N, Carpino N (2007) A phosphatase activity of Sts-1 contributes to the suppression of TCR signaling. Mol Cell 27:486–497
108. Agrawal R, Carpino N, Tsygankov A (2008) TULA proteins regulate activity of the protein tyrosine kinase Syk. J Cell Biochem 104:953–964
109. San Luis B, Sondgeroth B, Nassar N, Carpino N (2011) Sts-2 is a phosphatase that negatively regulates zeta-associated protein (ZAP)-70 and T cell receptor signaling pathways. J Biol Chem 286:15943–15954
110. Thomas DH, Getz TM, Newman TN, Dangelmaier CA, Carpino N, Kunapuli SP, Tsygankov AY, Daniel JL (2010) A novel histidine tyrosine phosphatase, TULA-2, associates with Syk and negatively regulates GPVI signaling in platelets. Blood 116:2570–2578
111. Chen X, Ren L, Kim S, Carpino N, Daniel JL, Kunapuli SP, Tsygankov AY, Pei D (2010) Determination of the substrate specificity of protein-tyrosine phosphatase TULA-2 and identification of Syk as a TULA-2 substrate. J Biol Chem 285:31268–31276
112. Raguz J, Wagner S, Dikic I, Hoeller D (2007) Suppressor of T-cell receptor signalling 1 and 2 differentially regulate endocytosis and signalling of receptor tyrosine kinases. FEBS Lett 581:4767–4772
113. Tsygankov AY (2013) TULA-family proteins: a new class of cellular regulators. J Cell Physiol 228:43–49
114. Lee ST, Feng M, Wei Y, Li Z, Qiao Y, Guan P, Jiang X, Wong CH, Huynh K, Wang J, Li J, Karuturi KM, Tan EY, Hoon DS, Kang Y, Yu Q (2013) Protein tyrosine phosphatase UBASH3B is overexpressed in triple-negative breast cancer and promotes invasion and metastasis. Proc Natl Acad Sci U S A 110: 11121–11126
115. Veeramani S, Lee MS, Lin MF (2009) Revisiting histidine-dependent acid phosphatases: a distinct group of tyrosine phosphatases. Trends Biochem Sci 34:273–278
116. Veeramani S, Yuan TC, Chen SJ, Lin FF, Petersen JE, Shaheduzzaman S, Srivastava S, MacDonald RG, Lin MF (2005) Cellular prostatic acid phosphatase: a protein tyrosine phosphatase involved in androgen-independent proliferation of prostate cancer. Endocr Relat Cancer 12:805–822
117. Chuang TD, Chen SJ, Lin FF, Veeramani S, Kumar S, Batra SK, Tu Y, Lin MF (2010) Human prostatic acid phosphatase, an authentic tyrosine phosphatase, dephosphorylates ErbB-2 and regulates prostate cancer cell growth. J Biol Chem 285: 23598–23606
118. Fleisig H, El-Din El-Husseini A, Vincent SR (2004) Regulation of ErbB4 phosphorylation and cleavage by a novel histidine acid phosphatase. Neuroscience 127:91–100
119. Muniyan S, Ingersoll MA, Batra SK, Lin MF (2014) Cellular prostatic acid phosphatase, a PTEN-functional homologue in prostate epithelia, functions as a prostate-specific tumor suppressor. Biochim Biophys Acta 1846:88–98
120. Quintero IB, Herrala AM, Araujo CL, Pulkka AE, Hautaniemi S, Ovaska K, Pryazhnikov E, Kulesskiy E, Ruuth MK, Soini Y, Sormunen RT, Khirug L, Vihko PT (2013) Transmembrane prostatic acid phosphatase (TMPAP) interacts with snapin and deficient mice develop prostate adenocarcinoma. PLoS One 8:e73072
121. Seifried A, Schultz J, Gohla A (2013) Human HAD phosphatases: structure, mechanism,

and roles in health and disease. FEBS J 280: 549–571

122. Allen KN, Dunaway-Mariano D (2009) Markers of fitness in a successful enzyme superfamily. Curr Opin Struct Biol 19:658–665
123. Chen Y, Jakoncic J, Carpino N, Nassar N (2009) Structural and functional characterization of the 2H-phosphatase domain of Sts-2 reveals an acid-dependent phosphatase activity. Biochemistry 48:1681–1690
124. Cousin W, Courseaux A, Ladoux A, Dani C, Peraldi P (2004) Cloning of hOST-PTP: the only example of a protein-tyrosine-phosphatase the function of which has been lost between rodent and human. Biochem Biophys Res Commun 321:259–265
125. Tapparel C, Reymond A, Girardet C, Guillou L, Lyle R, Lamon C, Hutter P, Antonarakis SE (2003) The TPTE gene family: cellular expression, subcellular localization and alternative splicing. Gene 323:189–199
126. van Eekelen M, Overvoorde J, van Rooijen C, den Hertog J (2010) Identification and expression of the family of classical protein-tyrosine phosphatases in zebrafish. PLoS One 5:e12573
127. Hatzihristidis T, Desai N, Hutchins AP, Meng TC, Tremblay ML, Miranda-Saavedra D (2015) A Drosophila-centric view of protein tyrosine phosphatases. FEBS Lett 589: 951–966
128. Morrison DK, Murakami MS, Cleghon V (2000) Protein kinases and phosphatases in the Drosophila genome. J Cell Biol 150:F57–F62
129. Martin H, Flandez M, Nombela C, Molina M (2005) Protein phosphatases in MAPK signalling: we keep learning from yeast. Mol Microbiol 58:6–16
130. Roma-Mateo C, Sacristan-Reviriego A, Beresford NJ, Caparros-Martin JA, Culianez-Macia FA, Martin H, Molina M, Tabernero L, Pulido R (2011) Phylogenetic and genetic linkage between novel atypical dual-specificity phosphatases from non-metazoan organisms. Mol Genet Genomics 285:341–354
131. Hsu F, Mao Y (2013) The Sac domain-containing phosphoinositide phosphatases: structure, function, and disease. Front Biol (Beijing) 8:395–407
132. Duan G, Li X, Kohn M (2015) The human DEPhOsphorylation database DEPOD: a 2015 update. Nucleic Acids Res 43: D531–D535
133. Pons T, Paramonov I, Boullosa C, Ibanez K, Rojas AM, Valencia A (2014) A common structural scaffold in CTD phosphatases that supports distinct catalytic mechanisms. Proteins 82:103–118
134. Heneberg P (2009) Use of protein tyrosine phosphatase inhibitors as promising targeted therapeutic drugs. Curr Med Chem 16: 706–733
135. Heneberg P (2012) Finding the smoking gun: protein tyrosine phosphatases as tools and targets of unicellular microorganisms and viruses. Curr Med Chem 19:1530–1566
136. Bohmer F, Szedlacsek S, Tabernero L, Ostman A, den Hertog J (2013) Protein tyrosine phosphatase structure-function relationships in regulation and pathogenesis. FEBS J 280:413–431
137. Ostman A, Hellberg C, Bohmer FD (2006) Protein-tyrosine phosphatases and cancer. Nat Rev Cancer 6:307–320
138. Tonks NK (2006) Protein tyrosine phosphatases: from genes, to function, to disease. Nat Rev 7:833–846
139. Keyse SM (2008) Dual-specificity MAP kinase phosphatases (MKPs) and cancer. Cancer Metastasis Rev 27:253–261
140. Pulido R, Hooft van Huijsduijnen R (2008) Protein tyrosine phosphatases: dual-specificity phosphatases in health and disease. FEBS J 275:848–866
141. Vang T, Miletic AV, Arimura Y, Tautz L, Rickert RC, Mustelin T (2008) Protein tyrosine phosphatases in autoimmunity. Annu Rev Immunol 26:29–55
142. Hardy S, Julien SG, Tremblay ML (2012) Impact of oncogenic protein tyrosine phosphatases in cancer. Anticancer Agents Med Chem 12:4–18
143. Julien SG, Dube N, Hardy S, Tremblay ML (2011) Inside the human cancer tyrosine phosphatome. Nat Rev Cancer 11:35–49
144. Rhee I, Veillette A (2012) Protein tyrosine phosphatases in lymphocyte activation and autoimmunity. Nat Immunol 13:439–447
145. Hendriks WJ, Elson A, Harroch S, Pulido R, Stoker A, den Hertog J (2013) Protein tyrosine phosphatases in health and disease. FEBS J 280:708–730
146. Nunes-Xavier CE, Martin-Perez J, Elson A, Pulido R (2013) Protein tyrosine phosphatases as novel targets in breast cancer therapy. Biochim Biophys Acta 1836:211–226
147. Tsou RC, Bence KK (2012) Central regulation of metabolism by protein tyrosine phosphatases. Front Neurosci 6:192
148. Knobler H, Elson A (2014) Metabolic regulation by protein tyrosine phosphatases. J Biomed Res 28:157–168

149. Rios P, Nunes-Xavier CE, Tabernero L, Kohn M, Pulido R (2014) Dual-specificity phosphatases as molecular targets for inhibition in human disease. Antioxid Redox Signal 20:2251–2273
150. Stebbing J, Lit LC, Zhang H, Darrington RS, Melaiu O, Rudraraju B, Giamas G (2014) The regulatory roles of phosphatases in cancer. Oncogene 33:939–953
151. Zhao S, Sedwick D, Wang Z (2015) Genetic alterations of protein tyrosine phosphatases in human cancers. Oncogene 34(30):3885–3894
152. Lee H, Yi JS, Lawan A, Min K, Bennett AM (2015) Mining the function of protein tyrosine phosphatases in health and disease. Semin Cell Dev Biol 37:66–72
153. Leslie NR (2012) PTEN: an intercellular peacekeeper? Sci Signal 5:pe50
154. Boosani CS, Agrawal DK (2013) PTEN modulators: a patent review. Expert Opin Ther Pat 23:569–580
155. Papa A, Chen M, Pandolfi PP (2013) Pills of PTEN? In and out for tumor suppression. Cell Res 23:1155–1156
156. Pulido R (2015) PTEN: a yin-yang master regulator protein in health and disease. Methods (San Diego, Calif) 77–78:3–10

Chapter 2

Global RT-PCR and RT-qPCR Analysis of the mRNA Expression of the Human PTPome

Caroline E. Nunes-Xavier and Rafael Pulido

Abstract

Comprehensive comparative gene expression analysis of the tyrosine phosphatase superfamily members (PTPome) under cell- or tissue-specific growth conditions may help to define their individual and specific role in physiology and disease. Semi-quantitative and quantitative PCR are commonly used methods to analyze and measure gene expression. Here, we describe technical aspects of PTPome mRNA expression analysis by semi-quantitative RT-PCR and quantitative RT-PCR (RT-qPCR). We provide a protocol for each method consisting in reverse transcription followed by PCR using a global platform of specific PTP primers. The chapter includes aspects from primer validation to the setup of the PTPome RT-qPCR platform. Examples are given of PTP-profiling gene expression analysis using a human breast cancer cell line upon long-term or short-term treatment with cell signaling-activation agents.

Key words Protein tyrosine phosphatase, Reverse transcription PCR, Real-time quantitative PCR, PTPome

1 Introduction

The global analysis of changes in the expression of well-defined gene or protein families during physiological or pathological conditions provides valuable information to understand the regulation of cell physiology in health and disease. Genome-wide DNA microarray analyses generate reliable comparative global information on gene expression patterns and on major changes in the expression of individual genes. However, the wide scope of genome-wide analysis may hamper the optimization and comparison of the gene expression changes on specific groups of genes. In addition, small changes in gene expression, especially for genes expressed at low levels, may be overlooked due to the limited sensitivity of the DNA microarray assays [1–3]. Reverse transcription quantitative real-time PCR (RT-qPCR) may overcome these problems because of its very high sensitivity and dynamic range and the possibility of individualized choosing and optimization of primers specific for

Rafael Pulido (ed.), *Protein Tyrosine Phosphatases: Methods and Protocols*, Methods in Molecular Biology, vol. 1447,
DOI 10.1007/978-1-4939-3746-2_2,

the genes of interest, including mRNA isoform-specific primers [4, 5]. Semi-quantitative reverse transcription PCR (RT-PCR) provides limited quantitative information, but can be useful to compare the expression of related mRNA variants which can be differentiated by size, or the relative expression of a mRNA of interest versus a reference mRNA, if coupled to agarose gel electrophoresis [6, 7].

The protein tyrosine phosphatase (PTP) superfamily is composed of members that belong to several gene families, which differ in the number and type of catalytic domains, as well as in their catalytic mechanism and overall substrate specificity. As such, an array of enzymes or enzyme-like proteins directly related with Tyr dephosphorylation can be considered as the PTPome. A former version of the human PTPome was defined as formed by about 107 members, and in an extended updated form expands to about 125 members [8, 9]. Many PTPome members harbor different noncatalytic regulatory domains, whereas others are small proteins only composed of the catalytic domain [8, 10–18]. The classical PTP enzymes (class I Cys-based classical PTPs) and the dual-specificity (DSPs) VH1-like PTPs (class I Cys-based DSPs) form the core of the PTPome and account for most of its members. They harbor one or two (classical PTPs), or only one (DUSPs), conserved catalytic PTP domains, and contain the conserved HCxxGxxR catalytic signature motif. The classical PTPs form a homogeneous group of enzymes with substrate specificity mostly restricted towards pTyr residues, whereas the DSPs include several subfamilies with different substrate specificities, including specificity towards pTyr/pSer/pThr, phosphoinositides, phosphorylated carbohydrates, and mRNA. Other PTPome enzymes contain a less-conserved CxxxxxR catalytic motif and employ a Cys-based catalysis to dephosphorylate pTyr/pSer/pThr residues or phosphoinositides, but harbor different classes of catalytic domains [arsenate reductase domain (class II-Cys based); rhodanese domain (class III Cys based)]. Finally, some phosphatases dephosphorylate pTyr using catalytic mechanisms non-Cys based, which belong to independent phosphatase gene families (Asp-based phosphatases, His-based phosphatases) [9]. This is of importance since the catalytic active sites of each of these enzyme families, as well as the physiologic regulation of their activities, display differences, making possible phosphatase family specific drug targeting with experimental or therapeutic purposes.

The PTPome is well suited to perform RT-PCR and RT-qPCR approaches to analyze comparatively the gene expression of their members [19–23]. We describe here methods to perform comparative semi-quantitative (RT-PCR) and quantitative (RT-qPCR) analysis of the gene expression of the human PTPome. Examples are shown using the MCF-7 human breast cancer cell line grown under different experimental conditions.

2 Materials

All solutions are prepared in double-distilled, RNase-free water. Cell culture and transfection procedures require sterile conditions.

2.1 Analysis of Human PTPome mRNA Expression by Semi-quantitative RT-PCR

1. Tissue-cultured cells, or biological samples, as a source of RNA.
2. Specific primer sets for amplification of the PTPs of interest and the reference control genes (*see* **Notes 1** and **2**).
3. RNA isolation kit (*see* **Note 3**).
4. cDNAs of the PTPs of interest, for primer specificity validation.
5. RT and PCR reagents (*see* **Note 4**).
6. Thermocycler.
7. Agarose gel electrophoresis and DNA visualization reagents (*see* **Note 5**).
8. Ultraviolet light detection system.

2.2 Global Analysis of Human PTPome mRNA Expression by Quantitative RT-PCR

1. Tissue-cultured cells, or biological samples, as a source of RNA.
2. Validated primer sets for quantitative RT-PCR (RT-qPCR) (*see* **Note 6**).
3. RT-qPCR reagents (*see* **Notes 4** and **7**).
4. RNA isolation kit (*see* **Note 3**).
5. cDNAs of the PTPs of interest, for primer amplification efficiency validation.
6. Plate setup suitable for loading the qPCR PTPome set.
7. Real-time thermocycler.

3 Methods

The first method (Subheading 3.1) is aimed to monitor semi-quantitatively (band intensity) and qualitatively (band size) the expression of mRNAs from different related PTPs under different experimental conditions. This approach is useful when the relative size of the amplified bands provides information on the expression of highly related PTP isoforms or variants, which may display different functional properties [7, 24]. In addition, this methodology can provide a good and sensitive overall view of the relative expression of the members of PTP subfamilies (*see* Fig. 1). The second method (Subheading 3.2) is designed to perform a global and quantitative monitoring of the mRNA expression of the PTPome under different experimental conditions. Our setting uses real-time RT-qPCR methodology scaled to accommodate, in 96-well (96-w) or in 384-well (384-w) plates, primers that amplify individually the members of the PTPome in a single experiment (*see* Fig. 3)

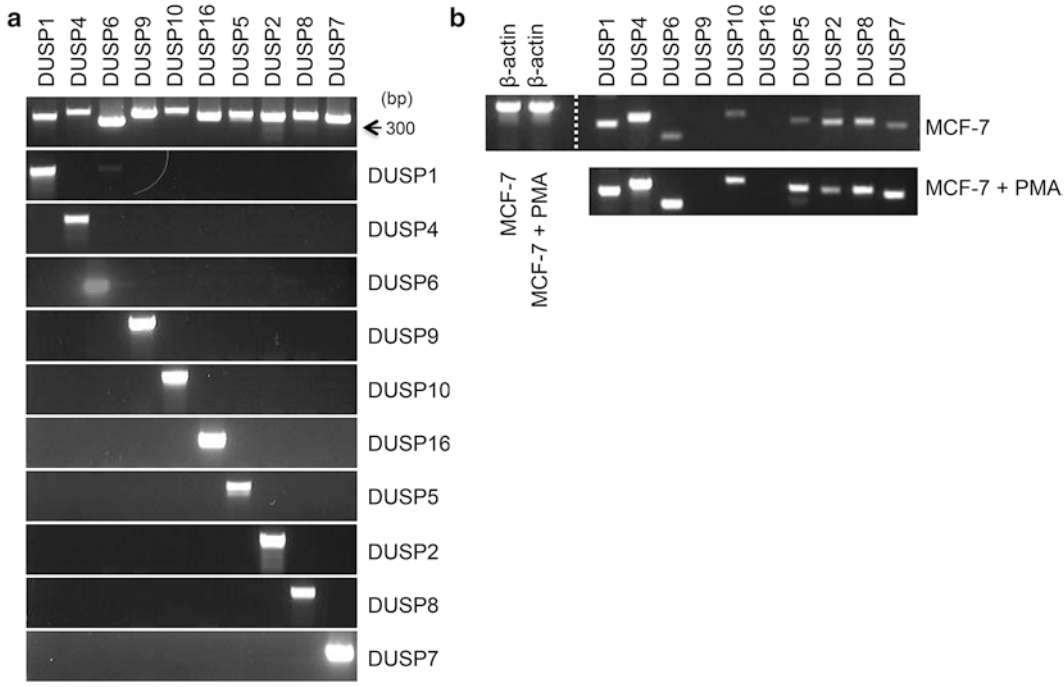

Fig. 1 (**a**) PCR analysis of oligonucleotide primer sets for the members of the human MKP family of active PTPs. Plasmids that contained cDNAs encoding each MKP were used as the template for each PCR reaction with the respective primer set (*upper row*), or with the primer sets of the ten different MKPs (*lower rows*). As shown, all primer sets amplified the expected DNA fragment from their corresponding cDNA template, and did not amplify DNA fragments from the other members of the MKP family. Thus, the ten primer sets designed are specific for the ten different MKP genes. Samples were resolved on 1 % agarose gels, and the amplified DNA was stained with ethidium bromide. In the *right* of the *upper row*, size in base pairs (bp) is indicated. Note that, when samples are run together, the slight differences in the size of the amplified bands (see Table 1) serve as internal controls. (**b**) Semi-quantitative RT-PCR analysis of the mRNA expression of the human MKP family of active PTPs. Poly(A) RNA obtained from human breast carcinoma MCF-7 cells untreated or treated with PMA (50 ng/ml) for 96 h was subjected to retrotranscription, and the resulting cDNA (50–200 ng/reaction) was processed for PCR using oligonucleotide primers specific for ACTB/β-actin (as a reference gene) and the ten active members of the MKP family, as in (**a**). mRNAs from DUSP1, DUSP4, DUSP6, DUSP10, DUSP5, DUSP2, DUSP8, and DUSP7 were detected in non-treated MCF-7 cells, while mRNAs for DUSP9 and DUSP16 were not detected in MCF-7 cells. PMA-treated MCF-7 cells displayed upregulation of DUSP6 and DUSP5 mRNAs, and, to a lower extent, of DUSP10 and DUSP7. These results have been previously published in [21]

3.1 Analysis of Human PTPome mRNA Expression by Semi-quantitative RT-PCR

1. Design specific oligonucleotide primer sets for the group of PTPs of interest, and perform PCR tests for primer specificity and cross-reactivity using as templates plasmids containing the distinct PTP cDNAs (*see* **Note 8**). An example of primer specificity test, using primers that amplify the members of the human MKP family of active PTPs (Table 1), is shown in Fig. 1a. Each PCR reaction contained 10 ng template, 0.5 mM dNTP mix (2.5 μl from 10 mM stock [2.5 mM each dNTP]), 0.3 μM of each primer (1.5 μl from 10 μM stock),

Table 1
Oligonucleotide primers specific for the members of the human MKP family of PTPs and human β-actin[a]

Gene/protein	Sense primer (5′–3′) Antisense primer (5′–3′)	Amplified fragment size (bp)	Localization[b]
DUSP1/MKP1	GTG GGC ACC CTG GAC GCT GCT GAG CCC CAT GGG GGT	426	C-term
DUSP4/MKP2	GAC TGC AGT GTG CTC AAA AGG AAC CGG GGG TGG GAT GGC	483	C-term
DUSP6/MKP3	ATA GAT ACG CTC AGA CCC GTG CTC GCC GCC CGT ATT CTC G	333	C-term
DUSP9/MKP4	GAG GGT CTG GGC CGC TCG CGC CAT GCT GGA GCC GGC	450	C-term
DUSP10/MKP5	GCA CTA TCT AGG CCC GTC C GTT GTA CTC CAT GAA GGG CC	516	C-term
DUSP16/MKP7	CAT GAG ATG ATT GGA ACT CAA A AGG GAC TAG AGT GGA TTT TCC T	426	C-term
DUSP5	TCG CTC GAC GGG CGC CAG CTC ACT CTC AAT CTT CTC TTG T	450	C-term
DUSP2	CTG GAG TGC GCG GCG CTG CAG CGC AGG GGC GGG GG	429	C-term
DUSP8	GGG GAC CGG CTC CCG AG GCT CAT GGG TAG CAG GGC A	438	C-term
DUSP7/MKPX	AAC GCC TTC GAG CAC GGC G GGA CTC CAG CGT ATT GAG TG	408	N-term
ACTB/β-actin	CCA AGG CCA ACC GCG AGA AGA TGA C AGG GTA CAT GGT GGT GCC GCC AGA C	562	Core

[a]Primers were used for experiments shown in Fig. 1
[b]The protein region targeted by each pair of primers is indicated

and 1 U GC-rich DNA Polymerase (0.5 μl from 2 U/μl stock) (*see* **Note 4**) in a final volume of 50 μl. PCR conditions were a denaturation step, 95 °C, 5 min, followed by 35 cycles: denaturation, 95 °C, 1 min; annealing, 55 °C, 2 min; extension, 72 °C, 1 min.

2. Isolate total RNA, or poly(A) RNA, from the cells or tissues of interest (*see* **Note 3**) and measure RNA concentration and purity in a nanodrop spectrophotometer (*see* **Note 9**).
3. Incubate (12.5 μl final volume) 1 μg total RNA, or 10 ng poly(A) RNA (*see* **Note 3**), and oligo(dT)18 primers (1 μl from 100 μM stock) at 70 °C, 10 min to denature RNA secondary structure, and transfer to ice to let the primers to anneal to the RNA.

4. To perform the reverse transcription reaction, add 4 mM dNTP mix (2 μl from 40 mM stock [10 mM each dNTP]), RNase inhibitor (0.5 μl, 20 U), reverse transcriptase (RT; 1 μl from 200 U/μl stock), and RT buffer (4 μl 5×), to give a final volume of 20 μl (*see* **Note 4**). Incubate at 42 °C, 1 h.
5. Optional: Incubate at 70 °C, 10 min, to inactivate the RT enzyme.
6. Measure concentration and purity of cDNA in a nanodrop spectrophotometer (*see* **Note 10**).
7. Perform the PCR reaction using the validated primer sets and 50–200 ng cDNA/reaction, as described in **step 1** (*see* **Note 11**).

An example of the relative expression of the mRNAs from the MKP family of PTPs, in human breast carcinoma MCF-7 cells untreated or treated with phorbol 12-myristate 13-acetate (PMA), is shown in Fig. 1b.

3.2 Global Analysis of Human PTPome mRNA Expression by Quantitative RT-PCR (RT-qPCR)

The high sensitivity of RT-qPCR makes necessary maximal accuracy in the manipulation and processing of the samples, as well as in the design and control of the experiment itself [25].

1. Choose or design the appropriate set of oligonucleotide primers sets for the members of the PTPome and for the reference genes (*see* **Note 6**). It is recommended to test individually the specificity of the primers by checking that a single sharp peak is obtained in the melt curve at the end of the PCR reaction (*see* **Note 12**).
2. Efficiency of the primers: it is recommended (especially when the primers are not prevalidated commercially) to test that the efficiency (E) of the amplification reaction is close to 2.0 (two-fold amplification per cycle = 100 % efficiency). This can be calculated from the slope of the quantification cycle (Cq) standard curve, which is made by running PCR reactions using decimal dilutions (e.g. 1:1, 1:10, 1:100) of the cDNA to be analyzed or of a template plasmid (starting with 10 ng) containing the cDNA amplified by the primers, and representing Cq (y) vs. LOG template concentration (x) [$y = \text{slope} \times x + \text{Cq}_{(x=0)}$; $E = 10^{(-1/\text{slope})}$] (*see* **Note 13**). The Pearson's correlation coefficient (r) of the standard curve should be >0.990. Examples of Cq standard curves for a set of commercial primers (QIAGEN) for the human MKP family of active PTPs, and the calculation of the efficiency for one of them (DUSP10), are given in Fig. 2.
3. Obtain cDNA by retrotranscription of the RNA of interest, as in Subheading 3.1, to be used as template.
4. Setup of plates: primers for all PTPs and controls are aliquoted at 10 μM in stock plates (Fig. 3). From the stock plate, a multipipette is used to make 384-w PCR working plates

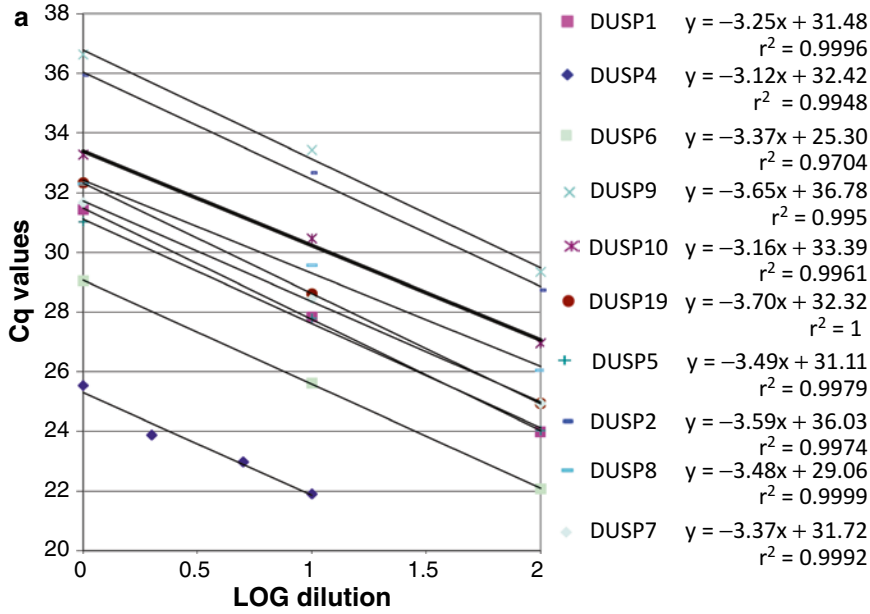

b

Primer	Dilutions	times	LOG	Cq	Slope	Efficiency
DUSP10	1:1	100	2	26,95	−3,16	2,069930511
	1:10	10	1	30,46		
	1:100	1	0	33,28		

$E = 10^{(-1/\text{slope})}$

Fig. 2 Validation of qPCR primers for efficiency. (**a**) Primer efficiency (*E*) [$E = 10^{(-1/\text{slope})}$] of human MKP primers is calculated from the slope of the plot, generated by running reactions using decimal dilutions (1:1, 1:10, and 1:100) of a template cDNA (starting at 100 ng) from control cells. (**b**) An example for DUSP10 primers is shown in the *bottom*

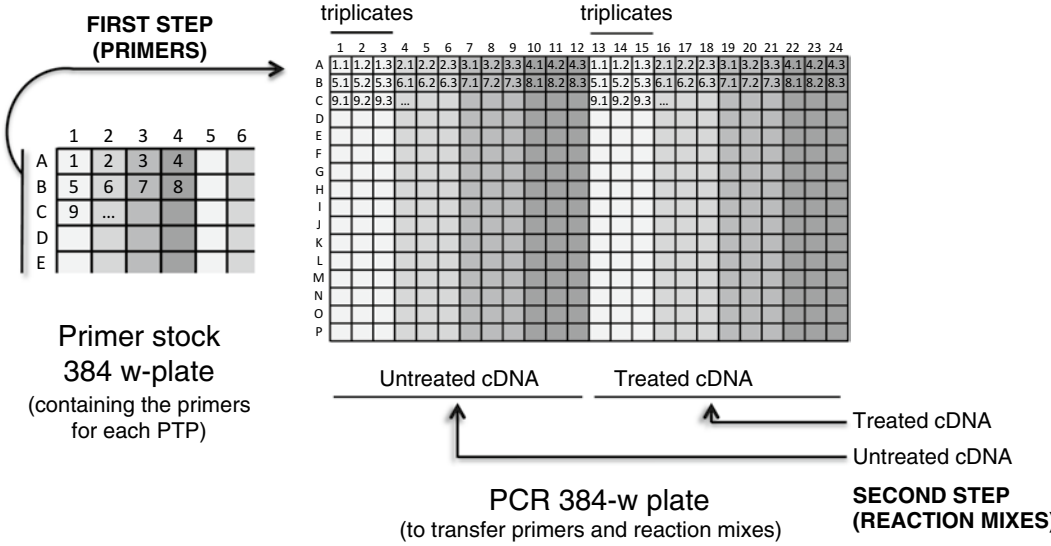

Fig. 3 Setup for the RT-qPCR analysis of the PTPome. A stock plate with primer aliquots for each PTP (numbered as *1*, *2*, etc., as an example) is used to transfer the primers to the PCR working plate, in triplicate (1.1, 1.2, 1.3, 2.1, 2.2, 2.3, etc., as an example) or in duplicate (not shown), for both untreated and treated conditions. Reaction mix is then added to the working plate and PCR is run

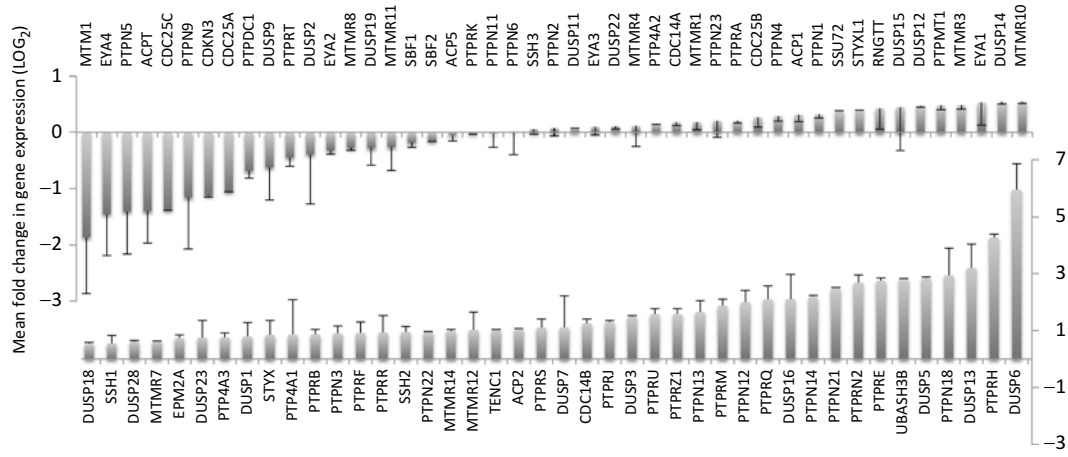

Fig. 4 Example of RT-qPCR expression analysis of the PTPome in MCF-7 cells treated with PMA. MCF-7 cells were left untreated or treated with PMA (50 ng/ml) for 72 h, and total RNA was purified and used for retrotranscription. cDNA was processed for PCR using a set of commercial primers (QuantiTect, QIAGEN). For this example, PCR was performed using technical duplicates. Relative expression values in LOG_2 scale are shown. Only a fraction of the PTPome, ordered from lower to higher fold change, is shown

containing 2 μl of each primer set per well, in duplicate or in triplicate, including in the same plate the experimental conditions to be compared (e.g., "untreated" vs. "treated") (Fig. 3) (*see* **Note 14**). All plates are always kept on ice.

5. Reaction mix (20 μl/reaction): 2 μl primers, 5 μl cDNA (50–200 ng) in PCR-grade H_2O, 3 μl PCR-grade H_2O, 10 μl Master Mix (2×) (containing DNA polymerase, dNTPs, Dye, and reaction buffer) (*see* **Note 7**).
6. Add reaction mix with a multipipette. When pipetting of working plate is finished, cover the plate with sealing foil and keep covered with aluminum foil, on ice, until placed in the thermocycler.
7. Run the reaction (*see* **Note 15**). An example of the mRNA expression of most of PTPome members from MCF-7 cells untreated or treated with PMA for 72 h, using a set of commercial primers (QuantiTect, QIAGEN), is shown in Fig. 4. PCR conditions were a denaturation step, 95 °C, 10 min, followed by 40 cycles: denaturation, 95 °C, 15 s; annealing, 55 °C, 20 s; extension, 72 °C, 15 s.
8. Analyze the data using the appropriate software. A common way to present the data is in logarithmic scale (LOG_2), where significant changes are usually considered > or equal to 2, or < or equal to −2. For relative changes, fold change can be calculated using the ΔΔCq equation: $\Delta\Delta Cq = 2^{-\left[\left(Cq_{ptp.treat} - Cq_{ref.treat}\right) - \left(Cq_{ptp.untreat} - Cq_{ref.untreat}\right)\right]}$; where the Cq from the reference (ref) genes is subtracted to the Cq of each PTP in both the "untreated" (untreat.) and "treated" (treat.) conditions. For the choosing of reference genes, *see* **Note 16**.

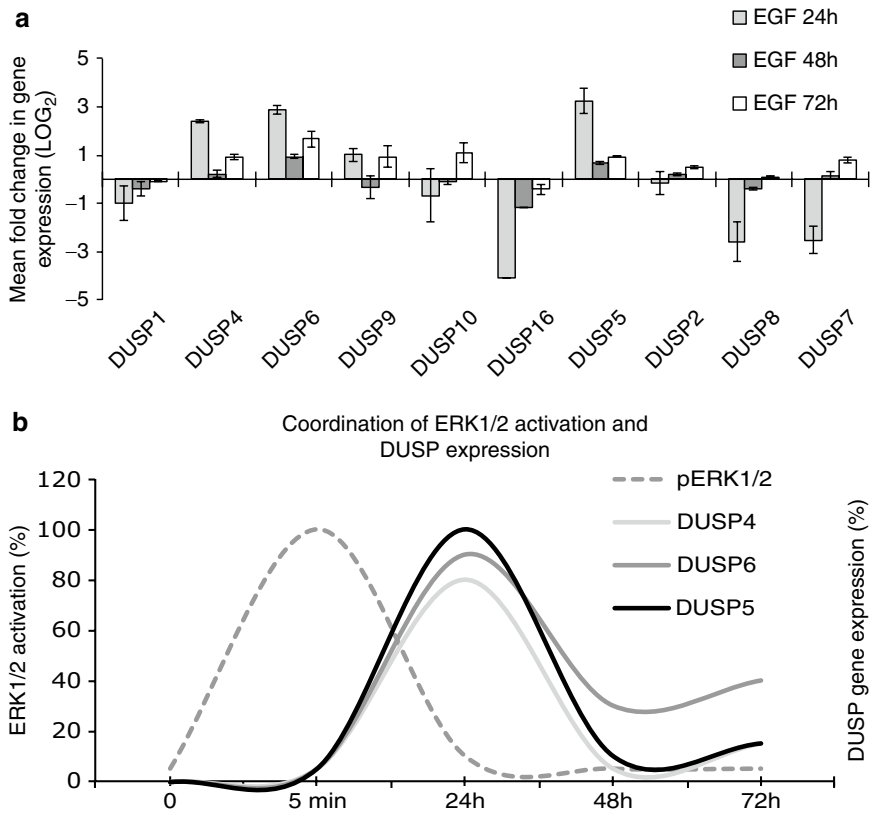

Fig. 5 (**a**) RT-qPCR analysis of the mRNA expression of the human MKP family of active PTPs from MCF-7 cells treated with EGF. MCF-7 cells were left untreated or treated with EGF (50 ng/ml) 24, 48, and 72 h, and processed for RT-qPCR as in Fig. 4. Mean fold change in gene expression is represented as LOG_2. DUSP4, DUSP6, and DUSP5 were significantly upregulated. (**b**) Example of coordination of ERK1/2 activation and DUSP4, DUSP6, and DUSP5 expression during transient activation of ERK1/2 by EGF stimulation. Data are normalized from (**a**) and from [21]

As an example, we show the mRNA expression of MKPs from MCF-7 cells stimulated with Epidermal Growth Factor (EGF), an ERK1/2-activating stimulus (Fig. 5). Six MKPs showed significant changes in gene expression after 24 h of EGF treatment, which declined after 48 and 72 h. The highest upregulated MKPs were DUSP4, DUSP6, and DUSP5 (Fig. 5a). In Fig. 5b, a comparative schematic kinetics of ERK1/2 activation, and DUSP4, DUSP6, and DUSP5 mRNA upregulation by EGF, is shown.

4 Notes

1. When comparison between groups of PTPome members is going to be done, the primers should target nonconserved regions, and amplify fragments of similar size (*see* also **Notes 8** and **12**).

2. The reference gene chosen for the experiment shown in Fig. 1b is ACTB/β-actin. Note that the expression of ACTB/β-actin mRNA, as that of many other commonly used reference genes, may change under your study conditions [26, 27]. An evaluation of the more appropriate reference genes for each study conditions should be made [28, 29].
3. There are many kits suitable for isolation of total or poly(A) RNA. As a rough estimation, poly(A) RNA constitutes 1 % of total RNA cellular content, which has to be taken in consideration for the amount of RNA used in the RT reaction. In general, total RNA works well for a reliable relative quantification of large sets of different target mRNAs [30]. For the experiments shown here, we have used Illustra QuickPrep *Micro* mRNA Purification Kit and IllustraRNAspin Mini Kit (GE Healthcare Life Sciences).
4. Many retrotranscriptase and DNA-polymerase options are available. For analytical purposes (nonpreparative), any high-amplification efficiency and high GC content tolerant Taq-polymerase is well suited. We commonly use RevertAid™ reverse transcriptase, oligo(dT)18 primers (stock 100 μM), and RiboLock RNase inhibitor from Fermentas. In the experiments shown in Fig. 1, GC-rich DNA polymerase from Roche was used. dNTPs mixes often come in the Master mix of some commercial kits or can be purchased separately. For RT, we use a commercial dNTP mix (4 × 10 mM; 40 mM total) from Fermentas. For PCR, we prepare a stock dNTP mix 4 × 2.5 mM (10 mM total) from the individual dNTPs.
5. When small differences in size (for amplicons between 250 and 750 bp), or when small amplicons have to be compared, 1%–2 % agarose gels are convenient. The gels shown in Fig. 1 were visualized by staining with 0.6 μg/ml ethidium bromide, but alternative less-toxic DNA stainers, such as GelRed™ or GelGreen™, are already available.
6. There are a wide variety of programs and online tools for qPCR primer design (see, for instance, http://molbiol-tools.ca/PCR.htm). When a relatively large number of different genes are going to be analyzed, as in the case of the PTPome analysis, the use of sets of prevalidated commercial primers from the same source gives the advantage of more homogeneous optimal amplification conditions. In the experiments shown in Figs. 2, 4 and 5, we have used QuantiTect Primer Assays (QIAGEN) primers.
7. In the experiments shown here, we have used SYBR® Green-based reagents (Roche Applied Science), but other dyes are also suitable for use.
8. For proper comparison, the DNA amplified fragments should be of similar size, and the pairs of primers should have a similar

Tm. For the experiments shown in Fig. 1, the length of the MKP primers was between 18 and 22 mer, and the Tm (calculated as $(G+C)\times 4+(A+T)\times 2$) was 62–64.

9. The ratio of absorbance at 260/280 nm for RNA should be around 2.0.
10. The ratio of absorbance at 260/280 nm for cDNA should be around 1.8. Sometimes removal of the template RNA is necessary by treating the RT reaction with RNase H before performing the PCR reaction.
11. In this method, the amplified band is the end product of the PCR reaction. This makes important to work with amounts of RNA and cDNA that allow visualization of differences. The number of PCR cycles for semi-quantitative PCR should be optimized to avoid oversaturation of the PCR reaction product. 30–35 cycles is a good range depending on the relative intensity of the bands of interest. To avoid false negatives and false positives, sometimes it is convenient to separate the reactions in two groups and amplify each group with different number of cycles. Note that in such case, comparisons have to be made within each group of PTPs.
12. A typical run for the melting curve is 95 °C, 15 s; 55 °C, 40 s. An additional control of specificity is to run the PCR product on an agarose gel to check the appropriate size of the amplicon. Note that sometimes amplicons from qPCR are of small size (*see* **Note 5**).
13. In practical terms, for a standard curve made with decimal dilutions of template, $E=2$ means that 3.32 cycles more are needed to reach the Cq when using ten times less template (slope = –3.32 means 100% efficiency).
14. It is convenient to have the PTPome primers in a 384-w primer stock plate, and make the transferring to the PCR working plate using a 12-channel 384-w multipipette. Alternatively, transferring can be made using an 8-channel 96-w multipipette, but taking six alternate wells each transfer, two transfers per row (an 8-channel 96-w multipipette will dispense samples to alternate wells in a 384-w plate). For two conditions ("untreated" vs. "treated") and technical triplicates, 48 genes can be analyzed in one 384-w plate. For two conditions ("treated" vs. "untreated") and technical duplicates, 72 genes can be analyzed in one 384-w plate. It is recommended to use technical triplicates.
15. There are different qPCR devices and detection systems, which have to be compatible. In the experiments shown here, we have used a LightCycler™ 480 thermocycler and the corresponding SYBR™ Green I Master Mix (Roche Applied Science).

16. The reference genes chosen for the experiments shown in Figs. 4 and 5 were HPRT1/hypoxanthine phosphoribosyltransferase 1, ACTB/β-actin, and GAPDH/glyceraldehyde-3-phosphate dehydrogenase (*see* also **Note 2**).

Acknowledgements

This work was supported in part by grants SAF2009-10226 from Ministerio Ciencia e Innovación (Spain and Fondo Europeo de Desarrollo Regional), SAF2013-48812-R from Ministerio de Economía y Competitividad (Spain), and EU Research Training Network (MRTN-CT-2006-035830).

References

1. Draghici S, Khatri P, Eklund AC, Szallasi Z (2006) Reliability and reproducibility issues in DNA microarray measurements. Trends Genet 22(2):101–109. doi:10.1016/j.tig.2005.12.005
2. Katagiri F, Glazebrook J (2009) Overview of mRNA expression profiling using DNA microarrays. Curr Protoc Mol Biol Chapter 22:Unit 22 24. doi:10.1002/0471142727.mb2204s85
3. Mehta JP (2011) Microarray analysis of mRNAs: experimental design and data analysis fundamentals. Methods Mol Biol 784:27–40. doi:10.1007/978-1-61779-289-2_3
4. Kubista M, Andrade JM, Bengtsson M, Forootan A, Jonak J, Lind K, Sindelka R, Sjoback R, Sjogreen B, Strombom L, Stahlberg A, Zoric N (2006) The real-time polymerase chain reaction. Mol Aspects Med 27(2–3):95–125. doi:10.1016/j.mam.2005.12.007
5. VanGuilder HD, Vrana KE, Freeman WM (2008) Twenty-five years of quantitative PCR for gene expression analysis. Biotechniques 44(5):619–626. doi:10.2144/000112776
6. Marone M, Mozzetti S, De Ritis D, Pierelli L, Scambia G (2001) Semiquantitative RT-PCR analysis to assess the expression levels of multiple transcripts from the same sample. Biol Proced online 3:19–25. doi:10.1251/bpo20
7. Pulido R, Krueger NX, Serra-Pages C, Saito H, Streuli M (1995) Molecular characterization of the human transmembrane protein-tyrosine phosphatase delta. Evidence for tissue-specific expression of alternative human transmembrane protein-tyrosine phosphatase delta isoforms. J Biol Chem 270(12):6722–6728
8. Alonso A, Sasin J, Bottini N, Friedberg I, Friedberg I, Osterman A, Godzik A, Hunter T, Dixon J, Mustelin T (2004) Protein tyrosine phosphatases in the human genome. Cell 117(6):699–711. doi:10.1016/j.cell.2004.05.018
9. Alonso A, Pulido R (2015) The extended human PTPome: a growing tyrosine phosphatase family. FEBS J. doi:10.1111/febs.13600
10. Andersen JN, Jansen PG, Echwald SM, Mortensen OH, Fukada T, Del Vecchio R, Tonks NK, Moller NP (2004) A genomic perspective on protein tyrosine phosphatases: gene structure, pseudogenes, and genetic disease linkage. FASEB J 18(1):8–30. doi:10.1096/fj.02-1212rev
11. Bhaduri A, Sowdhamini R (2003) A genome-wide survey of human tyrosine phosphatases. Protein Eng 16(12):881–888. doi:10.1093/protein/gzg144
12. Hatzihristidis T, Liu S, Pryszcz L, Hutchins AP, Gabaldon T, Tremblay ML, Miranda-Saavedra D (2014) PTP-central: a comprehensive resource of protein tyrosine phosphatases in eukaryotic genomes. Methods 65(2):156–164. doi:10.1016/j.ymeth.2013.07.031
13. Li X, Wilmanns M, Thornton J, Kohn M (2013) Elucidating human phosphatase-substrate networks. Sci Signal 6(275):rs10. doi:10.1126/scisignal.2003203
14. Patterson KI, Brummer T, O'Brien PM, Daly RJ (2009) Dual-specificity phosphatases: critical regulators with diverse cellular targets. Biochem J 418(3):475–489
15. Sadatomi D, Tanimura S, Ozaki K, Takeda K (2013) Atypical protein phosphatases: emerging players in cellular signaling. Int J Mol Sci 14(3):4596–4612. doi:10.3390/ijms14034596
16. Tautz L, Critton DA, Grotegut S (2013) Protein tyrosine phosphatases: structure, function, and implication in human disease.

Methods Mol Biol 1053:179–221. doi:10.1007/978-1-62703-562-0_13

17. Nunes-Xavier C, Roma-Mateo C, Rios P, Tarrega C, Cejudo-Marin R, Tabernero L, Pulido R (2011) Dual-specificity MAP kinase phosphatases as targets of cancer treatment. Anticancer Agents Med Chem 11(1):109–132
18. Rios P, Nunes-Xavier CE, Tabernero L, Kohn M, Pulido R (2014) Dual-specificity phosphatases as molecular targets for inhibition in human disease. Antioxid Redox Signal 20(14):2251–2273. doi:10.1089/ars.2013.5709
19. Arora D, Kothe S, van den Eijnden M, Hooft van Huijsduijnen R, Heidel F, Fischer T, Scholl S, Tolle B, Bohmer SA, Lennartsson J, Isken F, Muller-Tidow C, Bohmer FD (2012) Expression of protein-tyrosine phosphatases in Acute Myeloid Leukemia cells: FLT3 ITD sustains high levels of DUSP6 expression. Cell Commun Signal 10(1):19. doi:10.1186/1478-811X-10-19
20. Nunes-Xavier CE, Elson A, Pulido R (2012) Epidermal growth factor receptor (EGFR)-mediated positive feedback of protein-tyrosine phosphatase epsilon (PTPepsilon) on ERK1/2 and AKT protein pathways is required for survival of human breast cancer cells. J Biol Chem 287(5):3433–3444. doi:10.1074/jbc.M111.293928
21. Nunes-Xavier CE, Tarrega C, Cejudo-Marin R, Frijhoff J, Sandin A, Ostman A, Pulido R (2010) Differential up-regulation of MAP kinase phosphatases MKP3/DUSP6 and DUSP5 by Ets2 and c-Jun converge in the control of the growth arrest versus proliferation response of MCF-7 breast cancer cells to phorbol ester. J Biol Chem 285(34):26417–26430. doi:10.1074/jbc.M110.121830, M110.121830 [pii]
22. Pulido R, Serra-Pages C, Tang M, Streuli M (1995) The LAR/PTP delta/PTP sigma subfamily of transmembrane protein-tyrosine-phosphatases: multiple human LAR, PTP delta, and PTP sigma isoforms are expressed in a tissue-specific manner and associate with the LAR-interacting protein LIP.1. Proc Natl Acad Sci U S A 92(25):11686–11690
23. Schmidt F, van den Eijnden M, Pescini Gobert R, Saborio GP, Carboni S, Alliod C, Pouly S, Staugaitis SM, Dutta R, Trapp B, Hooft van Huijsduijnen R (2012) Identification of VHY/Dusp15 as a regulator of oligodendrocyte differentiation through a systematic genomics approach. PLoS One 7(7):e40457. doi:10.1371/journal.pone.0040457
24. Erdmann KS, Kuhlmann J, Lessmann V, Herrmann L, Eulenburg V, Muller O, Heumann R (2000) The Adenomatous Polyposis Coli-protein (APC) interacts with the protein tyrosine phosphatase PTP-BL via an alternatively spliced PDZ domain. Oncogene 19(34):3894–3901. doi:10.1038/sj.onc.1203725
25. Taylor S, Wakem M, Dijkman G, Alsarraj M, Nguyen M (2010) A practical approach to RT-qPCR-Publishing data that conform to the MIQE guidelines. Methods 50(4):S1–S5. doi:10.1016/j.ymeth.2010.01.005
26. Ruan W, Lai M (2007) Actin, a reliable marker of internal control? Clin Chim Acta 385(1–2):1–5. doi:10.1016/j.cca.2007.07.003
27. Schmittgen TD, Zakrajsek BA (2000) Effect of experimental treatment on housekeeping gene expression: validation by real-time, quantitative RT-PCR. J Biochem Biophys Methods 46(1–2):69–81
28. Sturzenbaum SR, Kille P (2001) Control genes in quantitative molecular biological techniques: the variability of invariance. Comp Biochem Physiol B Biochem Mol Biol 130(3):281–289
29. Hellemans J, Vandesompele J (2014) Selection of reliable reference genes for RT-qPCR analysis. Methods Mol Biol 1160:19–26. doi:10.1007/978-1-4939-0733-5_3
30. Petersen K, Oyan AM, Rostad K, Olsen S, Bo TH, Salvesen HB, Gjertsen BT, Bruserud O, Halvorsen OJ, Akslen LA, Steen VM, Jonassen I, Kalland KH (2007) Comparison of nucleic acid targets prepared from total RNA or poly(A) RNA for DNA oligonucleotide microarray hybridization. Anal Biochem 366(1):46–58. doi:10.1016/j.ab.2007.03.013

Chapter 3

Expression, Purification, and Kinetic Analysis of PTP Domains

Mihaela Mentel, Rodica A. Badea, Georgiana Necula - Petrareanu, Sujay T. Mallikarjuna, Aura E. Ionescu, and Stefan E. Szedlacsek

Abstract

Protein tyrosine phosphatases (PTP) are a large group of enzymes which work together with protein tyrosine kinases to control the tyrosine phosphorylation of proteins, thus playing a major role in cellular signaling. Here, we provide detailed protocols for expression and purification of the catalytic domain of RPTPμ and full length Eya3 as well as the extracellular region of PTPBR7. Methods are described for evaluation of the purity of the recombinant proteins thus obtained. For the purified Eya3 phosphatase we provide protocols for enzyme activity assay using either chromogenic, fluorescent, or peptide substrates. Determination of kinetic parameters by different graphical and computer-based procedures is also described.

Key words PTP domains, 6×His and GST tagged recombinant proteins, Prokaryotic expression, Eukaryotic expression, PTP purification, PTP kinetics, pNPP, DiFMUP, Phosphopeptide

1 Introduction

Since the discovery of tyrosine phosphorylation in proteins [1, 2] major progress has been made in elucidating its role in cellular signaling. The balance of tyrosine phosphorylation in cell, which is crucial for normal cellular homeostasis and disease, is a result of opposing actions of protein tyrosine kinases (PTKs) and protein tyrosine phosphatases (PTPs). Although early investigations regarding tyrosine phosphorylation were almost exclusively centered on PTKs, later studies clearly revealed that PTPs play a key role in signal transduction [3].

The superfamily of PTPs has a large number of representatives. Thus, there are 107 PTP genes in human genome [4]. They can be classified into four subfamilies based on their amino acid sequences and functional characteristics. Class I, the major group of PTPs, shares the conserved $(H/V)C(X)_5R(S/T)$ sequence called "PTP signature motif." This sequence contains the active-site cysteine which plays the essential role of nucleophile in the catalytic

Rafael Pulido (ed.), *Protein Tyrosine Phosphatases: Methods and Protocols*, Methods in Molecular Biology, vol. 1447,
DOI 10.1007/978-1-4939-3746-2_3,

mechanism of dephosphorylation. There are two subclasses in Class I PTPs: the subclass of classical, phospho-tyrosine-specific PTPs and the subclass of dual-specific phosphatases which recognize and dephosphorylate not only phospho-tyrosine but also phospho-serine/phospho-threonine. Class II contains the low molecular weight or acid phosphatases which act on tyrosine phosphorylated proteins as well as on some natural and synthetic aryl- and acyl-phosphates. Members of Class III contain also an essential, active-site cysteine and include several cell-cycle regulatory phosphatases. Class IV diverges from the other classes as its members do not share the PTP signature motif and do not use cysteine as a nucleophile in catalytic mechanism. Instead, they use a nucleophilic aspartic acid residue in a metal ion-dependent catalytic mechanism.

The structural architecture of PTPs is frequently multimodular due to the presence of various functional domains. Thus, the receptor-like PTP (RPTPs) group of classical PTPs contains in the extracellular region domains like: CAH (carbonic anhydrase-like), MAM (meprin/A5/μ), Ig (Immunoglobulin-like), or Fn (fibronectin type III-like). The intracellular region of RPTPs contains a membrane-proximal catalytic domain and, in case of some representatives, also a membrane-distal domain which is either inactive or has residual catalytic activity. The non-transmembrane group of classical PTPs contains, besides the catalytic domain, various noncatalytic domains like: HD (histidine domain), Pro (Proline-rich), SH2 (Src-homology 2), Sec14 (Sec14/cellular retinaldehyde-binding protein-like), KIM (kinase-interaction motif), FERM (4.1 protein/ezrin/radixin/moesin), or PDZ (PSD95/Dlg1/zo-1) [5].

Although PTPs have been studied since decades, there are still numerous unknowns concerning their molecular characteristics which need in-depth investigations. For example, novel crystal structures of PTPs are expected to be obtained. Despite the relatively high number of crystal structures of PTP catalytic domains so far reported, there are very few structures of extracellular regions of RPTPs, full-length non-receptor-like PTPs, or complexes between PTPs and their protein ligands (including phosphotyrosine-containing protein substrates). On the other hand protein crystallization as other experimental approach requires reasonable amounts of pure, active protein preparations. Another example of research area which needs purified protein and which can lead to finding novel molecular characteristics of PTPs is substrate specificity studies. Indeed, identification of factors that determine substrate specificity, identification of novel substrates, and characterization of PTPs interaction with their physiological substrates are major research targets for many representatives of PTPs superfamily.

Here, we provide robust expression, purification, and kinetic analysis protocols for catalytic domains of an RPTP from Class I,

subclass R2A (human RPTPμ or PTPRM), a full-length PTP from Class IV (human Eya3), and the extracellular region of an RPTP from Class I, subclass R7 (mouse PTPBR7 or PTPRR). The protocols described here contain specific experimental details for the mentioned PTPs. However, the protocols can be easily extended to other similar PTP representatives.

2 Materials

All mentioned chemicals should be of reagent grade. All solutions should be prepared in ultrapure water (deionized water purified to attain a resistivity of 18 MΩ at 25 °C) and filtered through a 45 μm filter. Solutions are stored at room temperature unless indicated.

2.1 PTP Domains Expression

2.1.1 Prokaryotic Expression of PTP Domains (Exemplified by Expressions of hEya3 and hRPTPμD1)

1. Prokaryotic expression vectors (*see* **Note 1**).
2. Chemically competent *E. coli* strains (*see* **Note 2**).
3. Liquid Luria-Bertani (LB) medium: add 10 g Bacto-Tryptone, 5 g Bacto-Yeast extract, and 10 g NaCl to 900 mL of ultrapure water. Adjust pH to 7.0 with NaOH and bring to a final volume of 1 L. Autoclave 20 min at 121 °C.
4. Ampicillin (Amp) stock solution: make 100 mg/mL solution in ultrapure water, filter sterilize using a 0.22 μm filter, and aliquot to an appropriate volume. Make aliquots and store at −20 °C. Use it at a final concentration of 100 μg/mL in LB medium.
5. LB agar plates with Amp (*see* **Note 3**).
6. Isopropyl-thio-β-D-galactopyranoside (IPTG), stock solution: prepare a 500 mM solution and filter sterilize. Make 1 mL aliquots and store at −20 °C, in the dark.
7. Block heater.
8. Shaker incubator.
9. Spectrophotometer.

2.1.2 Eukaryotic Expression of PTP Domains (Exemplified by Expression of the Extracellular Region of PTPBR7–Ecto-PTPBR7)

1. Eukaryotic expression vector pHLsec-Ecto-PTPBR7, containing the gene encoding for the extracellular region of PTPBR7 fused with a 6×His-tag (*see* **Note 4**).
2. Mammalian HEK293T (ATCC CRL-3216) and 293S (ATCC® CRL-3022) cell lines.
3. The complete growth media used Dulbecco's Modified Eagle's Medium (DMEM) high glucose with Glutamax supplemented with 1× non-essential amino acids (NEAA) and 10% fetal bovine serum (FBS).
4. Plasmid DNA purification kit.

5. Transfection reagent: polyethylenimine (PEI). Make an aqueous stock solution of 1 mg/mL PEI, adjust to pH 7 with HCl, filter sterilize and make aliquots and store at –20°C (*see* **Note 5**).
6. Expanded surface polystyrene roller bottles of 2125 cm^2.
7. Phosphate-buffered saline 1× (PBS-1×): 1.8 mM KH_2PO_4, 10 mM Na_2HPO_4, 137 mM NaCl, and 2.7 mM KCl, pH 7.4.
8. 0.05% Trypsin-EDTA.
9. Sterile serological pipettes (2, 5, 10, 25 mL).
10. Sterile cell culture plastics.
11. Rotating incubator (37 °C, 5% CO_2).

2.2 Recombinant Protein Purification

For hRPTPμ D1 catalytic domain (hRPTPμD1):

2.2.1 Affinity Chromatography on Glutathione-Sepharose

1. Glutathione-Sepharose 4B.
2. GST-LyB buffer (lysis buffer): 137 mM NaCl, 4.3 mM Na_2HPO_4, 1.47 mM KH_2PO_4, 2.7 mM KCl, pH 7.4, 1% Triton X-100, 4 mM DTT, 1 mM PMSF, and protease inhibitor cocktail EDTA-free.
3. GST-WB buffer (washing buffer): 137 mM NaCl, 4.3 mM Na_2HPO_4, 1.47 mM KH_2PO_4, 2.7 mM KCl, pH 7.4, 1% Triton X-100, 4 mM DTT, and 1 mM PMSF.
4. GST-EB buffer (elution buffer): 50 mM Tris–HCl pH 8.0, and 10 mM reduced glutathione.
5. Conical centrifuge tubes.
6. Amicon Ultra-4 centrifugal filter unit with 50 kDa Nominal Molecular Weight Limit (NMWL).
7. 0.2 μm membrane filters.
8. Eppendorf tubes.
9. Cooling centrifuge.
10. French press.

2.2.2 Affinity Chromatography on Ni-Sepharose

For hEya3:

1. HisTrap HP—5 mL immobilized metal ion affinity chromatography (IMAC) columns (GE Healthcare).
2. Lysis buffer (LyB): 50 mM Tris–HCl pH 7.4, 350 mM NaCl, 20 mM imidazole, 2 mM DTT, 2 mM $MgCl_2$, 0.1% Triton X-10, and 1× protease inhibitor cocktails or 1 mM PMSF (*see* **Note 6**).
3. Binding buffer for affinity purification (BBAP): 50 mM Tris–HCl pH 7.4, 350 mM NaCl, 20 mM imidazole, 2 mM DTT, 2 mM $MgCl_2$, and 0.1% Triton X-10 (*see* **Note 6**).

4. Elution buffer for affinity purification (EBAP): 50 mM Tris–HCl pH 7.4, 350 mM NaCl, 500 mM imidazole, 2 mM DTT, 2 mM $MgCl_2$, and 0.1 % Triton X-100 (*see* **Note 6**).
5. Amicon Ultra-4 and -15 Centrifugal filter Units with 50 kDa NMWL.
6. 0.2 μm membrane filters.
7. Probe Sonicator.

For Ecto-PTPBR7:

1. Ni-Sepharose High Performance.
2. Sepharose washing buffer 1: 10 mM Tris–HCl, 150 mM NaCl, and 2 mM imidazole pH 8.0.
3. Sepharose washing buffer 2: 10 mM Tris–HCl, 150 mM NaCl, and 5 mM imidazole pH 8.0.
4. Elution buffer: 10 mM Tris–HCl, 150 mM NaCl, and 250 mM imidazole pH 8.0.
5. 0.2 μm membrane filters.
6. Centricon Plus-70 Centrifugal filter unit with 10 kDa NMWL.
7. Empty columns for collecting the Ni-Sepharose beads.
8. Endo-H enzyme.
9. PNGase F enzyme (NEB).

2.2.3 Anion Exchange Chromatography

For hEya3:

1. MonoQ 5/50GL strong anion exchange column.
2. Binding buffer for anion exchange (BBAE): 50 mM Tris–HCl pH 7.4, 50 mM NaCl, 2 mM DTT, and 2 mM $MgCl_2$ (*see* **Note 6**).
3. Elution buffer for anion exchange (EBAE): 50 mM Tris–HCl pH 7.4, 1 M NaCl, 2 mM DTT, and 2 mM $MgCl_2$ (*see* **Note 6**).

2.2.4 Size Exclusion Chromatography

For hEya3, hRPTPμD1 and Ecto-PTPBR7:

1. Superdex 75 10/300 GL prepacked, high-resolution, size exclusion chromatography column.
2. 20 % ethanol (*see* **Note 6**).
3. Fraction collecting tubes.
4. Gel filtration buffers (GFB) (*see* **Note 6**).
   - GFB for hEya3: 50 mM Tris–HCl pH 7.4, 100 mM NaCl, 2 mM DTT, 2 mM $MgCl_2$.
   - GFB for hRPTPμD1: 50 mM Tris–HCl pH 7.5, 150 mM NaCl, 10 % glycerol, 4 mM DTT, and 0.5 mM PMSF.
   - GFB for Ecto-PTPBR7: 10 mM HEPES pH 7.5, and 150 mM NaCl.

2.3 Analysis of Purified Proteins by SDS-PAGE and Western Blotting

1. Solutions for SDS-PAGE gels (*see* **Note 7**):
   - 4× running gel buffer: 1.5 M Tris–HCl pH 8.8.
   - 4× stacking gel buffer: 0.5 M Tris–HCl pH 6.8.
   - 30% acrylamide/bis-acrylamide solution (37.5:1).
   - 10% sodium dodecyl sulfate solution (SDS).
   - 10% ammonium persulfate (APS) solution.
   - *N*,*N*,*N*′,*N*′-tetramethyl-ethylenediamine (TEMED).
2. 5× SDS-PAGE running buffer pH 8.3: 125 mM Tris Base, 960 mM glycine, and 0.5% SDS. The pH should be around 8.3 without adjusting. Dilute 1:5 with ultrapure water, before usage.
3. 5× SDS-PAGE reducing loading buffer (5× RLB): 60 mM Tris–HCl pH 6.8, 2% SDS, 0.01% bromophenol blue, 10% glycerol, and 100 mM β-mercaptoethanol. Store at −20 °C in small aliquots.
4. Coomassie blue staining solution: 2.4 g/L Coomassie blue, 0.5 L ethanol, 0.48 L acetic acid, 0.12 L distilled water.
5. Destaining solution: 20% acetic acid in ultrapure water.
6. 10× Transfer buffer: 250 mM Tris Base, and 1.9 M glycine. The pH should be around 8.3 without adjusting. Store at 4 °C. Before use, dilute 1:10 with ultrapure water plus 10% methanol or ethanol (*see* **Note 8**).
7. TBS-T buffer: 20 mM Tris–HCl pH 7.5, 150 mM NaCl, and 0.1% Tween-20.
8. Blocking buffer: 5% non-fat skim milk in TBS-T.
9. Methanol (100%) or ethanol (96–100%) for activation of PVDF membrane (*see* **Note 8**).
10. Polyvinylidene fluoride (PVDF) membrane, 45 μm pore size.
11. Primary antibody polyclonal rabbit anti-GST.
12. PentaHis monoclonal primary antibody.
13. Secondary antibodies: anti-rabbit and anti-mouse conjugated with HRP.
14. Chemiluminescence (ECL) detection kit.
15. X-ray films.
16. Plastic box.
17. Molecular weight markers for SDS-PAGE and Western blotting.
18. Mini-Protean protein electrophoresis system.
19. Semidry transfer system.

2.4 Mass Spectrometric Analysis

1. Purified recombinant 6×His-hEya3 protein.
2. Bradford assay kit.
3. Water LC-MS CHROMASOLV®.

4. Eppendorf tubes.
5. Nitrile gloves.
6. Protein denaturation buffer: 8 M urea solution in 50 mM Tris–HCl pH 8, freshly prepared.
7. Protein reduction buffer: 200 mM DTT solution in 50 mM $(NH_4)_2CO_3$ (LC-MS grade) freshly prepared with LC-MS CHROMASOLV® water.
8. Protein alkylation buffer: 200 mM iodoacetamide solution in 50 mM $(NH_4)_2CO_3$, freshly prepared with LC-MS CHROMASOLV® water.
9. rLysC, Mass Spec Grade.
10. Chymotrypsin, Sequencing Grade.
11. Pierce™ C18 Tips 100 µL.
12. Sample treatment solution: 2.5% trifluoroacetic acid (TFA) in water.
13. Elution solution: 0.1% formic acid (FA, LC-MS Grade) in 70% acetonitrile (ACN, LC-MS Grade), up to 100 µL per sample.
14. SpeedVac®, for removing the solvent from peptide solution obtained after desalting procedure.
15. Nano-liquid chromatography (nLC) vials.
16. Resuspension buffer and mobile phase A for nLC: 0.1% FA in 2% ACN:water.
17. Mobile phase B for nLC: 0.1% FA in ACN. nLC coupled with a hybrid LTQ-Orbitrap mass spectrometer. The chromatographic system should be composed of a desalting C18 trap column connected with an analytical C18 column for peptide separation.
18. Proteome Discoverer v1.4 program, containing SEQUEST or Sequest HT algorithms, or v1.3, containing SEQUEST.

2.5 Tyrosine Phosphatase Assays

1. Bradford assay kit.
2. pNPP (*para*-nitrophenyl phosphate) as a chromogenic PTP substrate.
   - 100 mM pNPP stock solution (*see* **Note 9**).
   - 10 mM pNP in ethanol (for standard curve).
   - 10× Assay buffer: 200 mM HEPES pH 7, 1500 mM NaCl, and 100 mM $MgCl_2$.
   - Disposable cuvettes.
3. DiFMUP (6,8-difluoro-4-methylumbelliferyl phosphate) as a fluorescent PTP substrate.
   - 10 mM DiFMUP in DMSO, store at −20 °C in single-use aliquots.

- Assay buffer: 20 mM MES pH 6.5, 100 mM NaCl, 10 mM $MgCl_2$ and 5 mM DTT.
- Black 96-well plates, flat bottom, nontreated.

4. Phospho-H_2AX as a peptide substrate for hEya3 PTP.
   - H2AX-pY142 peptide sequence: Acetyl-CPSGGKKATQ ASQE(pY)-NH_2.
   - 10× Assay buffer: 200 mM MES pH 6.5, 1 M NaCl, 100 mM $MgCl_2$, and 50 mM DTT (*see* **Note 10**).
   - 2 mM H_2AX-pY142 phosphopeptide: dissolve 2.5 mg of peptide in 100 µL of 50% DMSO and 650 µL of 50 mM Tris-Cl pH 7.6, 150 mM NaCl (*see* **Note 11**).
   - Clear 96-well plates, flat bottom, nontreated.
   - BIOMOL Green reagent for phosphate detection (Enzo Life Sciences).

3 Methods

3.1 D1 Domain of Human Receptor Protein Tyrosine Phosphatase µ (hRPTPµD1)

3.1.1 Prokaryotic Expression of hRPTPµD1

1. Transform DH5α competent cells with pGEX-KT-hRPTPµD1 prokaryotic expression vector (*see* **Note 1**). Thaw a 50 µL aliquot of DH5α competent cells on ice. Add 1 µL (~100–200 ng DNA) of the vector and incubate ~10 min on ice. Heat shock the cells for 1 min at 42 °C and put them quickly on ice for 2 min. Spread the cell suspension on a LB agar plate supplemented with Amp using a sterile spreader. Incubate overnight at 37 °C (*see* **Note 12**).
2. Prepare a starter culture, pick a single colony of the transformed DH5α to inoculate 40 mL of LB medium with 100 µg/mL Amp (LB-Amp). Incubate the bacterial inoculum at 37 °C overnight with shaking (*see* **Note 13**).
3. Next morning, centrifuge the starter culture 5 min at 5000 × *g* at room temperature, resuspend the pellet into 10 mL fresh LB medium, and add into 990 mL LB-Amp. In our lab, we typically use cultures of 2 L for prokaryotic expression of hRPTPµD1 (*see* **Note 14**).
4. Incubate the culture with shaking at 37 °C until the optical density of the culture at 600 nm ($OD_{600\ nm}$) (measured with a spectrophotometer/colorimeter covering the visible region of the spectrum) reaches 0.3 (*see* **Note 15**). This typically takes about 3 h.
5. Shift the culture temperature to 25 °C and continue the culture growth, until $OD_{600\ nm}$ is between 0.6 and 0.7 (*see* **Note 16**).
6. Induce protein expression by adding IPTG stock solution to 0.1 mM final concentration. Keep shaking overnight at

25 °C. Before induction, take a "before induction sample" (BI) by collecting the cells from 1 mL culture. Store the sample at −20 °C.

7. After about 16–18 h of expression, harvest the cells by centrifugation at 7000 × *g* for 10 min, at 4 °C, and use the cells directly for protein purification or store the cells at −80 °C until processing.

3.1.2 Purification of hRPTPμD1

1. Thaw the bacterial pellet on ice.
2. Resuspend the pellet in GST-Ly buffer (~35 mL for a cell pellet collected from 1 L bacterial culture) and homogenize thoroughly using a glass douncer (*see* **Note 17**).
3. Pass the homogenized suspension through a French press four times (pressure: 1000 psi) to disrupt the membrane of the bacterial cells (*see* **Note 18**). Take now the "whole lysate" sample (WL), collecting a small volume (~20–30 μL) of cell suspension for SDS-PAGE.

   Centrifuge the lysate at 20,000 × *g*, for 20 min at 4 °C. Take the "soluble protein" sample (S) by collecting a small volume (~20–30 μL) of supernatant for SDS-PAGE. Next, discard the pellet and submit the supernatant to the first purification step.
4. Affinity chromatography on Glutathione-Sepharose:
   - Prepare the Glutathione-Sepharose resin: gently shake the bottle of Glutathione-Sepharose to resuspend the resin and pick up 700 μL slurry. Cut off with a scissors about 1 mm of the pipet tip and use this tip to pipette the slurry. Equilibrate the beads by washing with at least 3 volumes of GST-WB buffer for three times. Between washes, spin down the beads 3 min, 1000 × *g*, at 4 °C.
   - Put the supernatant resulted after cell lysis in a 50 mL falcon tube. Add ~700 μL Glutathione-Sepharose resin (50% slurry equilibrated with GST-WB buffer) and incubate 1 h at 4 °C, on a tube rotator.
   - Spin down the resin by centrifugation 3 min at 1000 × *g* and transfer it into a 2 mL Eppendorf tube. Take the "flow through" (FT) sample by collecting a small volume (20–30 μL) from the supernatant, after protein adsorption on the resin.
   - Wash the resin three to five times, 10 min each, at 4 °C, with 1.5 mL GST-WB. Centrifuge the resin 3 min at 1000 × *g*. Take a small volume of beads (10 μL) for SDS-PAGE, using a cut-off pipet tip. This sample is "protein adsorbed on the beads" (denoted "B").
   - Elute the resin with GST-EB buffer four times (~1 mL GST-EB to 350 μL beads). For each elution incubate

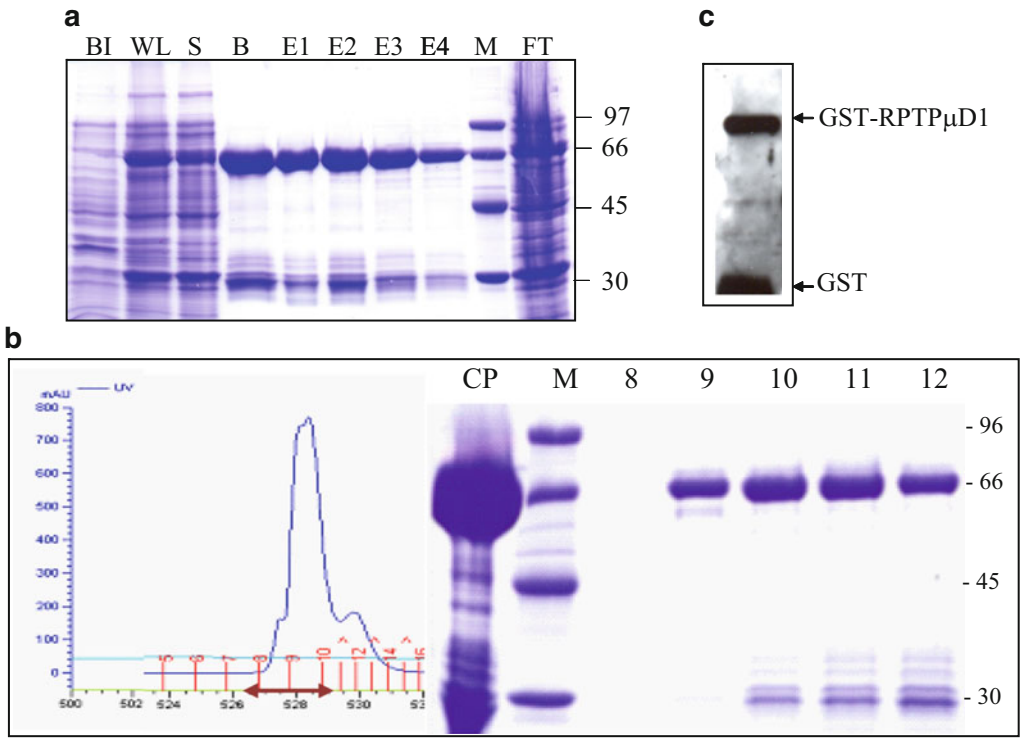

Fig. 1 Analysis of expression and purification of hRPTPμD1. (**a**) SDS-PAGE analysis of the expression and purification by affinity chromatography of RPTPμD1, N-terminally fused with GST. Gel was stained with Coomassie: *BI* bacterial cells before induction of the protein expression with IPTG, *WL* whole lysate, *S* soluble proteins, *B* protein adsorbed on Glutathione-Sepharose beads, *E1–E4* eluted protein, *FT* flow through, *M* low molecular weight marker. (**b**)RPTPμD1 elution profile after size exclusion chromatography (*left*) and SDS-PAGE analysis of the peak fractions (*right*): *CP* protein purified by affinity chromatography and concentrated on Amicon Ultra 50-K, *8–12* fractions of purified protein. Gel was stained with Coomassie. (**c**) Immunoblotting detection of the purified Glutathione *S*-transferase (GST) GST-RPTPμD1, detected with anti-GST antibody. All electrophoretic separations of proteins were performed in 10 % SDS-PAGE gels

5 min at 4 °C rotating the tube on a tube rotator. Take a small volume (20–30 μL) of each eluted fraction for SDS-PAGE.

- Analyze the collected elution fractions (E1–E4) together with the previous samples: BI, WL, S, B and FT by 10% SDS-PAGE (Fig. 1a).
- Put together the eluted fractions containing the purified protein, add 10% glycerol, and resuspend gently (without making foam) (*see* **Note 19**). Store the protein at −80 °C until the next purification step.

5. Size exclusion chromatography:
   - Start the FPLC-ÄKTA system (*see* **Note 20**).
   - Connect the Superdex 75 10/300 GL column to the system (*see* **Note 21**).

- Wash the column with at least one column volume (25 mL) of ultrapure degassed water, to remove the column storage solution (20% ethanol) and then equilibrate it with at least one column volume (25 mL) of GFB buffer (flow rate of 0.8 mL/min).
- Thaw the protein purified by affinity chromatography from −80 °C, and centrifuge at 20,000 × *g* for at least 15 min, at 4 °C (to remove the precipitated protein). Collect the supernatant carefully.
- Concentrate the supernatant to ~250 μL volume by centrifugation on Amicon Ultra-4 centrifugal filter unit with 50 kDa NMWL at 5000 × *g*, 4 °C.
- Inject the prepared sample into the column using a suitable loop.
- Wash the column with at least 1 volume GFB (flow rate of 0.8 mL/min) and collect fractions of 1 mL volume.
- After protein separation wash the column with 50 mL water (flow rate of 0.8 mL/min) and then with 30 mL of 20% ethanol (*see* **Note 26**). Detach the column from the ÄKTA system and keep it at 4 °C (*see* **Note 21**).
- Analyze the collected fractions by 10% SDS-PAGE (Fig. 1b).
- Put together the fractions containing the pure protein, add 10% glycerol, and mix gently (to avoid foaming).
- Determine the total protein concentration by Bradford method (or any other method used in your lab).
- Make aliquots of volumes adequate for your next assays and store aliquots at −80 °C (*see* **Note 22**).

3.1.3 Analysis of the Expression and Purification of hRPTP μD1 by SDS-PAGE

1. Prepare 10% SDS-PAGE gels using your lab protocol.
2. Prepare SDS samples: mix the samples taken after each step of protein expression and purification with 5× RLB, boil the samples for 5 min at 100 °C, then centrifuge at 13,000 × g for 1 min at room temperature. Prepare the molecular marker as specified by the manufacturer.
3. Prepare the electrophoresis system according to the manufacturer's instructions.
4. Load 10 μL of each prepared sample on gel. Do not forget to load the molecular weight marker on the gel.
5. Run gels about 40 min at 35 mA/gel. When the blue line is out of the gel, stop the device and place the gels into a clean plastic box with lid, suitable for microwave device.
6. Coomassie blue staining of gels: add solution to fully cover the gels (the volume depends on the box size), place the box in a

microwave device for 30–60 s then incubate for 3 min on a rocker (*see* **Note 23**).

7. Destaining of the gels: wash gels with plenty of distilled water and cover gels with destaining solution, place the box again in a microwave for 30–60 s and let on a rocker for 5 min. Repeat the destaining steps until the protein bands become visible (usually is enough three to four times).
8. Analyze the gels. Collect the fractions containing the protein of interest (the molecular weight of RPTPμD1 is 68.6 kDa).

3.1.4 Detection of hRPTPμ by Western Blotting

1. Run the SDS samples on a 10% SDS-PAGE gel (use the same procedure like in Subheading 3.1.3, **steps 1–5**).
2. Prepare the PVDF membrane (*see* **Note 24**).
3. Transfer the proteins from the gel on a PVDF membrane for 1 h at 80 mA/gel, using a semidry transfer system.
4. Take the membrane from the transfer system, remove the excess membrane by cutting its margins with a scissors and lay the membrane into a plastic box.
5. Add blocking buffer to cover the PVDF membrane and incubate for 1 h at room temperature or overnight at 4 °C, on a rocker.
6. Cover the membrane with the primary antibody, anti-GST in blocking buffer and incubate for 1 h at room temperature.
7. Rinse the membrane with 10–20 mL TBS-T, three times for 10 min at room temperature, to remove the unbound primary antibody.
8. Cover the membrane with the appropriate secondary antibody and incubate for 1 h at room temperature.
9. Rinse the membrane with 10–20 mL TBS-T, three times for 10 min at room temperature, to remove the excess of secondary antibody.
10. Incubate the membrane with mixed ECL kit solutions according to the manufacturer's instructions.
11. Expose the membrane to a X-ray film. The time of exposure depends on the protein concentration, antibodies affinity, and ECL kit sensitivity (Fig. 1c).

3.2 Human Eya3 (hEya3) Tyrosine Phosphatase

3.2.1 Prokaryotic Expression of hEya3 Tyrosine Phosphatase

1. Introduce the $pHAT_2$-hEya3 plasmid carrying the hEya3 gene into *BL21(DE3)RIL* cells by heat-shock transformation (*see* **Note 12**). Proceed like in Subheading 3.1.1, **step 1**.
2. Pick one colony from the plate and inoculate 20 mL of LB-Amp and incubate it at 37 °C overnight (*see* **Note 13**).
3. Centrifuge the 20 mL overnight culture in a sterile falcon tube at 5000 × *g* for 10 min, remove the supernatant and resuspend

the pellet in fresh 30 mL of LB-Amp, and finally add to 1 L LB-Amp (*see* **Note 14**). Incubate the culture at 30 °C under shaking at 120 rpm until $OD_{600\ nm}$ is about 0.7–0.9 (*see* **Note 15**). Add IPTG to a final concentration of 0.3 mM, and return the flask to the incubator (keep the same parameters) for 16–18 h. Take the "before induction" sample as in Subheading 3.1.1, **step 6** (Fig. 2a).

4. Next day, centrifuge the culture at 7000 × *g* for 10 min. Then, either proceed to protein purification or store the pellet at −80 °C.

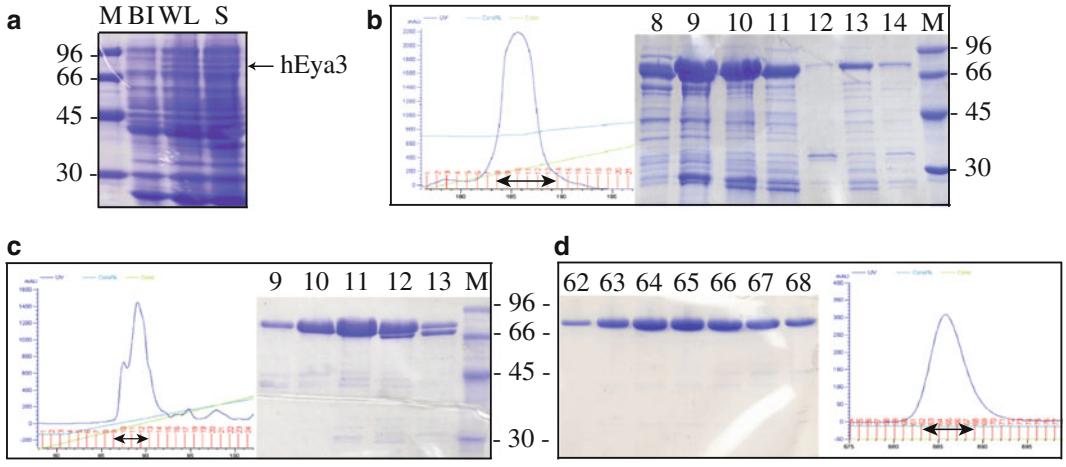

e

MEEEQDLPEQ PVKKAKMQES GEQTISQVSN PDVSDQKPET SSLASNLPMS EEIMTCTDYI
PRSSNDYTSQ MYSAKPYAHI LSVPVSETAY PGQTQYQTLQ QTQPYAVYPQ ATQTYGLPPF
GALWPGMKPE SGLIQTPSPS QHSVLTCTTG LTTSQPSPAH YSYPIQASST NASLISTSST
IANIPAAAVA SISNQDYPTY TILGQNQYQA CYPSSSFGVT GQTNSDAEST TLAATTYQSE
KPSVMAPAPA AQRLSSGDPS TSPSLSQTTP SKDTDDQSRK NMTSKNRGKR KADATSSQDS
ELERVFLWDL DETIIIFHSL LTGSYAQKYG KDPTVVIGSG LTMEEMIFEV ADTHLFFNDL
EECDQVHVED VASDDNGQDL SNYSFSTDGF SGSGGSGSHG SSVGVQGGVD WMRKLAFRYR
KVREIYDKHK SNVGGLLSPQ RKEALQRLRA EIEVLTDSWL GTALKSLLLI QSRKNCVNVL
ITTTQLVPAL AKVLLYGLGE IFPIENIYSA TKIGKESCFE RIVSRFGKKV TYVVIGDGRD
EEIAAKQHNM PFWRITNHGD LVSLHQALEL DFL

Fig. 2 Analysis of expression and purification of hEya3 phosphatase. (**a**) SDS-PAGE analysis of the expression of recombinant hEya3 phosphatase: *M* low molecular weight protein marker, *BI* before induction, *WL* whole lysate, *S* soluble proteins. (**b**) Affinity chromatography elution profile of hEya3 phosphatase (*left*) and SDS-PAGE analysis of peak fractions visualized on a 10 % SDS-PAGE (*right*). *M* low molecular weight protein marker, *8–14* eluted fractions containing Eya3 phosphatase. (**c**) Anion exchange chromatography elution profile of hEya3 phosphatase (*left*) and SDS-PAGE analysis of peak fractions visualized on a 10 % SDS-PAGE (*right*). *M* low molecular weight protein marker, *9–13* eluted fractions containing Eya3 phosphatase. (**d**) Gel filtration elution profile of hEya3 phosphatase (*right*) and SDS-PAGE analysis of peak fractions visualized on a 10 % SDS-PAGE (*left*). *M* low molecular weight protein marker, *62–68* eluted fractions containing Eya3 phosphatase. All gels were stained with Coomassie. (**e**) Example of sequence coverage of hEya3 (Q99504) obtained after sequential digestion with rLysC and Chymotrypsin and analysis by Collision-induced dissociation (CID). *Underlined* are the identified hEya3 peptides

3.2.2 Purification of hEya3

1. Cell lysis: thaw on ice the cellular pellet and resuspend it in 25 mL LyB buffer (*see* **Note 17**). Disrupt the cells by sonication for 10–15 times, 10 s each at 70% power with a Bandelin Sonicator (for efficient cell lysis split the resuspended pellet in three tubes, with about 10 mL of culture, and perform sonication for each of them). Take the "whole lysate" sample like in Subheading 3.1.2, **step 3** (Fig. 2a). After sonication, centrifuge the cell lysate for 25 min at 20,000 × *g* and 4 °C. Keep the supernatant which contains the 6×His-tagged hEya3 phosphatase and discard, as appropriate, the cellular pellet. Take "soluble protein" sample, like in Subheading 3.1.2, **step 3** (Fig. 2a). hEya3 phosphatase is further purified by a three-step purification protocol using a FPLC-ÄKTA system (**steps 2–4**).
2. Affinity chromatography:
   - Prepare the HisTrap HP column for purification: connect the column to the system (*see* **Notes 20** and **21**).
   - Wash the column with 25 mL water to remove the 20% ethanol storage solution; wash the column with 25 mL EBAP and finally equilibrate it on BBAP buffer (flow rate of 5 mL/min).
   - Inject the supernatant on the column, using a 50 mL SuperLoop (flow rate of 5 mL/min) (*see* **Note 25**).
   - Wash column with BBAP until the absorbance 280 nm ($A_{280\ nm}$) reaches the baseline (flow rate of 5 mL/min).
   - Elute the 6×His-tagged hEya3 protein with EBAP buffer in gradient. Set the gradient to reach 50% of EBAP buffer in 40 min (flow rate 1 mL/min). Collect 1 mL fractions.
   - Prepare the column for storage: set the gradient to reach 100% of EBAP buffer and run five column volumes (25 mL) to clean the column. Next, wash with 25 mL water and then with 25 mL of 20% ethanol.
   - All peak fractions are analyzed by SDS-PAGE, and those corresponding to the protein of interest are saved for further purification steps and stored with 10% glycerol at −80 °C (Fig. 2b).
3. Anion exchange chromatography:
   - Prepare the MonoQ 5/50 GL column: connect the column to the system (*see* **Notes 20** and **21**); use 5 mL water to remove the 20% ethanol storage solution; wash the column with 5 mL EBAE and finally equilibrate it on BBAE buffer (flow rate of 1 mL/min).
   - Thaw on ice the protein saved from the previous purification step (**step 2**), centrifuge at 4 °C and 20,000 × *g* for 30 min. Carefully, take the supernatant and exchange protein buffer to BBAE buffer using Amicon Ultra-15

Centrifugal filter Units. Collect the sample from the Amicon filter unit into an Eppendorf tube and centrifuge it at 4 °C and 20,000 × *g* for 10 min. Inject the supernatant into the column using an appropriate size loop (flow rate of 1 mL/min) (*see* **Note 25**).

- Wash unbound proteins until $A_{280\,nm}$ reached baseline with BBAE.
- Elute hEya3 phosphatase in gradient of EBAE. Set the gradient to reach 50% of EBAP buffer in 40 min (flow rate 1 mL/min). Collect 1 mL fractions.
- Prepare the column for storage: set the gradient to reach 100% of EBAE buffer and run for 5 mL. Next, wash with 5 mL water and then with 5 mL of 20% ethanol and store it at 4 °C (*see* **Note 26**).
- All peak fractions are analyzed by SDS-PAGE. Fractions corresponding to the protein of interest are saved for further purification steps and stored with 10% glycerol at −80 °C (Fig. 2c).

4. Size exclusion chromatography:
   - Prepare Superdex 75 10/300 GL column: connect the column to the system (*see* **Notes 20** and **21**).
   - Thaw on ice the protein fraction stored at −80 °C (from **step 3**), then centrifuge at 4 °C and 20,000 × *g* for 30 min. Carefully, take the supernatant and concentrate it to at least 250–300 μL using Amicon Ultra-4 Centrifugal filter Units with 50 kDa cutoff.
   - Collect the supernatant into an Eppendorf tube and centrifuge it at 4 °C and 20,000 × *g* for 10 min. Inject the supernatant onto the column using a 500 μL loop (flow rate of 0.8 mL/min) (*see* **Note 25**).
   - Run at least one column volume on GFB and collect 1 mL fractions.
   - Proceed like in Subheading 3.1.2, **step 5**.
   - Analyze all peak fractions by SDS-PAGE. All fractions containing the pure hEya3 protein are mixed together and aliquoted in 100 μL fractions (single-use aliquots). Proteins are stored with 10% glycerol at −80 °C until are used in further experiments (Fig. 2d).

3.2.3 Analysis of the Expression and Purification of hEya3 by SDS-PAGE

1. Prepare the 10% SDS-PAGE gels using your lab protocol.
2. SDS sample preparation: mix 10 μL from each fraction with 10 μL of 5× RLB, boil for 5 min at 100 °C. Centrifuge samples for 1 min to 13,000 × *g*.
3. Prepare the electrophoresis system, load the samples in the gel and run the gel.

4. Stain and then destain the gels to visualize the protein bands (*see* Subheading 3.1.3, **steps 6** and 7).
5. Analyze the gels and collect the fractions which contain the highest quantity of pure hEya3 protein.

3.2.4 Mass Spectrometric Identification of hEya3 Using Bottom-Up Approach

1. Preparation of the protein for in-solution digestion: thaw an aliquot of hEya3 on ice. Centrifuge it for 20–25 min, at 4 °C and 20,000 × *g*. Carefully transfer the protein solution in a new Eppendorf tube. Measure the protein concentration using the Bradford assay kit. Take a volume corresponding to 2 μg of hEya3 and transfer it into a new Eppendorf tube.
2. In-solution digestion:
   - Denaturation: add 8 M urea in 50 mM Tris–HCl pH 8 so the final concentration of urea in sample volume is 4 M.
   - Reduction: add protein reduction buffer until you reach a final concentration of 10 mM DTT in the sample volume. Incubate for 45–60 min at room temperature with moderate shaking. Do not heat the sample.
   - Alkylation: add protein alkylation buffer until the final concentration of 55 mM iodoacetamide has been reached in the sample volume. Incubate in the dark for 45–60 min at room temperature with moderate shaking.
   - Inactivation of the alkylating agent: add the same volume as the volume of iodoacetamide solution, from the protein reduction buffer. Incubate for 45–60 min at room temperature with moderate shaking.
   - Protein digestion with rLysC: add rLys-C Mass Spec Grade (10 ng/μL), to a final protease: protein ratio of 1:30 (w/w) and incubate sample for 16–18 h at 37 °C (*see* **Notes 27** and **28**).
   - Digestion with Chymotrypsin: add Chymotrypsin Sequencing Grade (10 ng/μL) to a final protease: protein ratio of 1:20 and incubate the sample for 16–18 h at 25 °C (*see* **Note 29**).
   - Stop the reaction by adding 2.5% TFA solution in sample, so that the final concentration in sample volume is 0.5% TFA; keep the sample on ice until desalting; avoid repeated freezing (−20 °C) and thawing of the peptide sample.
3. Desalting procedure:
   - Adjust sample to 0.5%TFA (with Sample treatment solution).
   - Desalting was performed according to the manufacturer's instructions (Thermo Scientific™ Pierce™ C18 Tips 100 μL bed) (also *see* **Note 30**).

- Eluting the sample: slowly aspirate 50 µL of 0.1% FA in 70% ACN and dispense in a new Eppendorf tube. Repeat once and reunite the eluates.
- Dry the eluate in a SpeedVac® to dryness.
- Keep the resulted sample at −20 °C until LC-MS/MS analysis.

4. LC-MS/MS analysis:
   - Resuspend the dried peptides in 20 µL of 0.1% FA in 2% ACN.
   - Transfer the solution obtained into a nLC vial or well plate (depending on the nLC type).
   - Set the parameters for the LC-MS/MS analysis (*see* **Note 31**).
5. Protein identification
   - Search the spectrum files acquired over the entire run with Proteome Discoverer v1.4, using SEQUEST or Sequest HT as algorithms, or v1.4, using SEQUEST (*see* **Note 32**).
   - Set the following parameters in SEQUEST or Sequest HT: database UniProtKB/Swiss-Prot; enzymes used: rLysC (full), chymotrypsin (full), each with maximum two missed cleavages; precursor mass tolerance of 10 ppm; fragment mass tolerance of 0.6 Da; methionine oxidation as dynamic modification and carbamidomethylation on cysteine set as static modification.
   - Perform a decoy database (with reversed sequences) search using a target false discovery rate (FDR) of 0.1% to eliminate the false positive results from the search (*see* **Note 33**).
   - The protein sequence obtained is displayed in Fig. 2e.

3.2.5 hEya3 Tyrosine Phosphatase Assays

1. Enzyme preparation: thaw an aliquot of hEya3 phosphatase on ice and then centrifuge at 4 °C and 20,000 × *g* for 20–25 min and carefully transfer the protein solution to a new Eppendorf tube. Determine the protein concentration using Bradford assay kit.
2. Phosphatase assay using pNPP as substrate:
   - Open the spectrophotometer and set the temperature controller at 37 °C.
   - Prepare 100 mM pNPP stock (*see* **Note 34**) and 5× pNPP assays buffer (*see* **Note 35**), keep both on ice. In a disposable cuvette pipette 40 µL of 5× pNPP assay buffer, *X*µL of 100 mM pNPP (*see* **Note 36**) and MilliQ water to the 195 µL final volume. Prepare also a cuvette for blank (use instead of enzyme solution the same amount of enzyme storage buffer). Incubate the reaction mixtures for 5 min in spectrophotometer (allow to reach 37 °C). Set up the

"Kinetics" program on the spectrophotometer. Measure the blank. Add 5 μL of hEya3 enzyme solution (0.122 mg/mL), mix well, and begin measuring the reaction immediately, for 5 min. Make sure the ΔA_{405} vs. time stays linear. The spectrophotometer will display a slope, but it may be incorrect if the rate is not constant! Note the slope in your lab book. Follow the same procedure for all concentrations of pNPP. The initial rate values ΔA_{405}/min (calculated from the linear portion of the progress curves) are converted into concentration of product per min (mM^{-1} min^{-1}) using the molar extinction coefficient of the reaction product pNP. Next, the values are plotted against the corresponding substrate concentrations and the steady-state constants K_m and k_{cat} can be obtained using different methods (*see* Subheading 3.2.6).

- Determine the molar extinction coefficient for pNP (the product formed), which depends on both assay buffer and equipment used. Prepare different concentrations of pNP, ranging from 0 to 0.1 mM in the same assay buffer and read the absorbance at A_{405}. Plot the values obtained vs. the concentrations of pNP used.

3. Phosphatase assay using DiFMUP as substrate:
   - Open the microplate reader and set the temperature controller to 25 °C. Create a kinetic measurement protocol, setting the parameters: filters Ex/Em 360/460, Gain 1955 (depends on the instrument used), 70 reading cycles (10s per cycle, ten flashes per well per cycle), and set to shake plate 5 s before reading.
   - Prepare 1 mM DiFMUP in assay buffer (*see* **Note 37**), keep it on ice.
   - The reactions are done in a 96-well black microplate. For each substrate concentration use three wells, one for the blank and two for enzyme reactions. Pipette *X*μL DiFMUP (depending on the substrate concentration made), then add assay buffer to 97.5 μL. Incubate the plate in microplate reader for 5 min to reach 25 °C, take out the plate and add 2.5 μL of hEya3 phosphatase (0.122 mg/mL) (*see* **Note 38**). Insert the plate and run the kinetic protocol immediately (*see* **Note 39**). Initial velocity values measured in fluorescence per minute (RFU/min) are converted into concentration of product per minute (μM/min) using the extinction coefficient calculated for DiFMU.
   - The extinction coefficient for DiFMU is calculated using known amounts of DiFMUP and DiFMU (Fig. 3a) (*see* **Note 40**). Plot the fluorescence intensity versus μM of DiFMU and the steady-state constants K_m and k_{cat} can be obtained using different methods (*see* Subheading 3.2.6).

a

μM DiFMU	100μM DiFMU	100μM DIFMUP
0	0 μl	100 μl
0.25	0.25 μl	99.75 μl
0.50	0.50 μl	99.50 μl
0.75	0.75 μl	99.25 μl
1	1 μl	99 μl
1.25	1.25 μl	98.75 μl
2	2 μl	98 μl
3	3 μl	97 μl

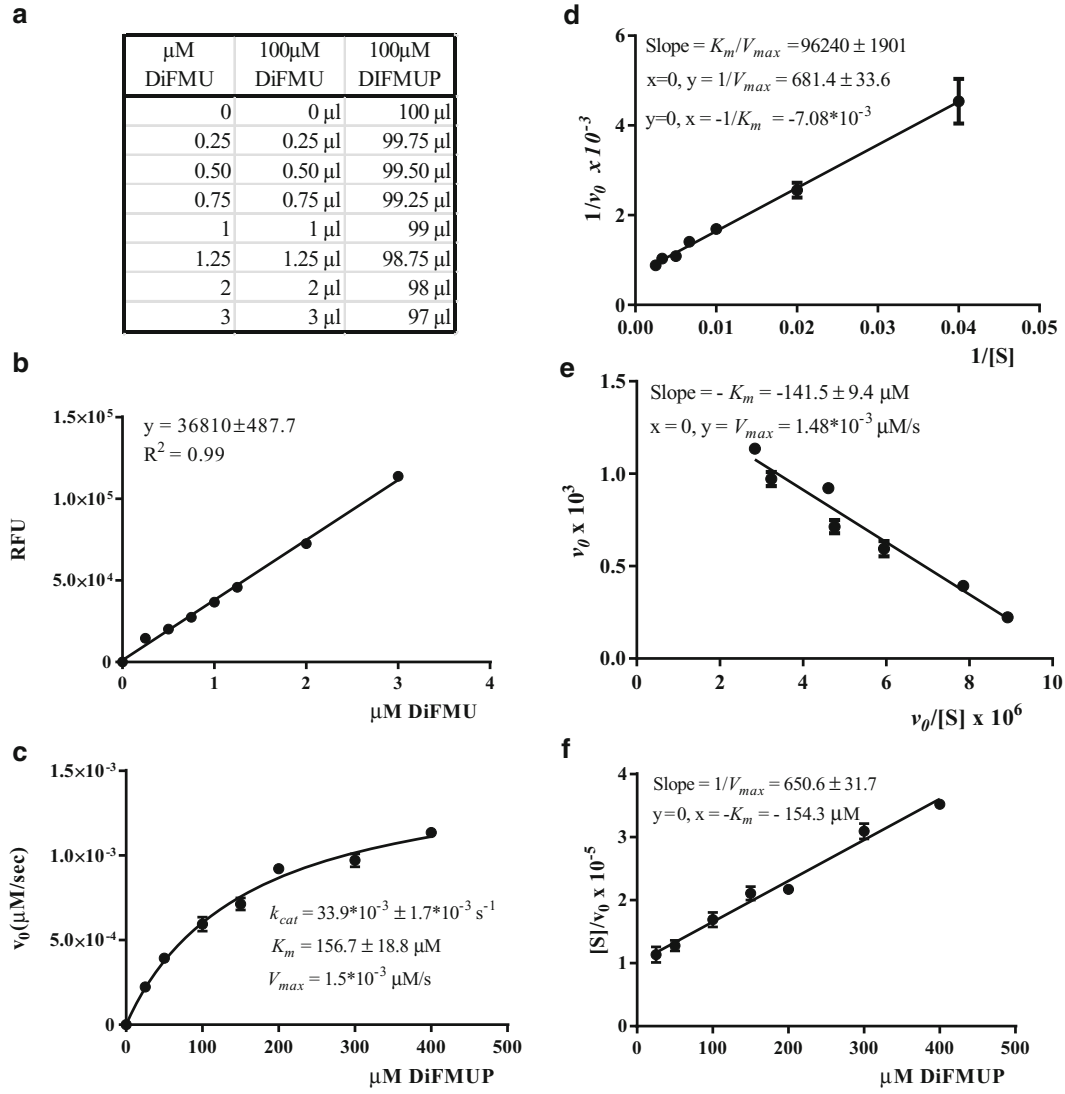

Fig. 3 Determination of the kinetic parameters of hEya3 phosphatase assay using DIFMUP as substrate. (**a**) Standard series of DiFMU/DiFMUP solutions used for DiFMU Standard Calibration Curve. (**b**) DiFMU Standard Calibration Curve. (**c**) Michaelis-Menten plot for DiFMUP as substrate for hEya3 phosphatase. Various concentrations of DiFMUP (0–400 μM) were incubated with purified hEya3 phosphatase and substrate conversion monitored in kinetic mode using 360 nm excitation and 460 nm emission. Initial velocities (v_0) for each substrate concentration were determined and were plotted against the concentration of substrate and V_{max} and K_m were calculated using Michaelis-Menten equation in GraphPad Prism. (**d**) Kinetic analysis of recombinant hEya3 phosphatase on DiFMUP as substrate using Lineweaver Burk plot. (**e**) Kinetic analysis of recombinant hEya3 phosphatase on DiFMUP as substrate using Eadie-Hofstee plot. (**f**) Kinetic analysis of recombinant hEya3 phosphatase on DiFMUP as substrate using Hanes-Woolf plot

4. Phosphatase assay using H_2AX-pY142 phosphopeptide: the phosphate released in the reaction was measured using BIOMOL Green (*see* **Note 41**).
   - Open the absorbance reading mode of the microplate reader and set wavelength at 620 nm. Choose to read absorbance with 1 cm path length correction.
   - Prepare 1 mM peptide stock in assay buffer. Pipette different volumes of peptide, from 0 to 400 μM, in a 96-well black plate, add 5 μL of 10× assay buffer and MilliQ water to the final volume of 30 μL. Incubate plate for 5 min at 37 °C, then add 20 μL of hEya3 enzyme (the enzyme was diluted in the reaction buffer to 0.034 mg/mL) and further incubate plate at the same temperature. After 40 min add 100 μL BIOMOL Green and reactions are further incubated 30 min at room temperature. Finally, read the absorbance at 620 nm.
   - Prepare a standard curve using the phosphate standard supplied with the BIOMOL Green kit according to the manufacturer instructions.
   - The steady-state constants K_m and k_{cat} can be obtained using different methods (*see* Subheading 3.2.5).

3.2.6 Determination of Kinetic Parameters of hEya3 Phosphatase

Exemplification of kinetic parameters determination on a set of data collected from DiFMUP phosphatase assay.

1. Plot the standard curve: the fluorescence intensity (RFU at Ex360/Em460) of standard series of DiFMU/DiFMUP solutions is measured and the calibration curve is generated by plotting concentration (μM) of the standard series vs. RFU (Fig. 3b). Standard curve fits the linear equation: $y = mx$ in which y = fluorescence intensity (RFU), x = concentration, and the slope is the extinction coefficient for DiFMU.
2. For each substrate concentration record the product formed over time, subtract the blank (reaction containing only DiFMUP, no enzyme), and determine the initial slope of RFU time-dependence curve (RFU/min). Divide the RFU/min to the extinction coefficient of DiFMU (in our case 36,810 RFU/μM) thus obtaining the initial reaction rates v_0 (μM of product/min). Divide to 60 to convert μM/min to μM/s (Table 1). For each substrate concentration perform reactions in duplicate. Duplicate values are mentioned in Table 1.
3. Graphical procedures for estimation of kinetic parameters (K_m, and k_{cat}). All graphs were created using GraphPad Prism software:
   - Nonlinear regression procedures based on initial rate dependence (v_0) on substrate concentration [S] (Fig. 3c) (*see* **Note 42**).

Table 1
Data collected when DiFMUP is used as substrate for hEya3 phosphatase. Values of the slope of RFU time-dependence curve and of the corresponding initial rates for two replicates are mentioned

DiFMUP (μM)	RFU/min		Initial rate v_0 (×10² μM DiFMU/s)	
25	546.66	438.41	0.025	0.020
50	923.25	810.51	0.042	0.037
100	1402.86	1223.00	0.064	0.055
150	1654.60	1496.65	0.075	0.068
200	1983.20	2088.62	0.090	0.095
300	2230.25	2060.11	0.101	0.093
400	2549.78	2468.16	0.115	0.112

- Lineweaver Burk representation (Fig. 3d): $1/v_0$ versus $1/[S]$
- Eadie-Hofstee representation (Fig. 3e): v_0 versus $v_0/[S]$
- Hanes-Woolf representation (Fig. 3f): $[S]/v_0$ versus $[S]$

All four types of representation give roughly similar results, but nonlinear regression procedure is preferred because no data transformation is required.

3.3 Extracellular Domain of PTPBR7 (Ecto-PTPBR7)

3.3.1 Cell Culture

1. We usually use HEK293T and HEK293S-GnTI⁻ cells that are easy to transfect, produce a high amount of recombinant protein, and are economically efficient. The HEK293S-GnTI⁻cells [6] are deficient in *N*-Acetylglucosaminyltransferase I and consequently do not produce complex N-linked glycans.
2. Cells grown in 175 cm² flasks were used to seed the roller bottles.
3. Remove the medium from one flask of 175 cm² with a 25 mL serological sterile pipette, in a way that no medium remains in the flask and the cells are not disturbed.
4. Wash two times with 10 mL of PBS, remove the PBS and discard it (*see* **Note 43**).
5. Add 5 mL Trypsin/EDTA to the cells and incubate for maximum 5 min at room temperature.
6. Dislodge the cells by tapping the flask gently.
7. Add 21 mL of complete medium (DMEM with Glutamax, NEAA, 10% FCS).
8. Pour 200 mL of complete medium into a fresh roller bottle, using the measure on the side of the roller bottle to estimate the amount.

9. Tap the 175-cm² flask several times so that no cell clumps are present in the solution and transfer all the cells to the roller bottle. Place the roller bottle into the rolling incubator at 0.8 rpm at 37 °C for 3–4 days for the cells to reach about 90% confluence.

3.3.2 Large-Scale Transfection

1. For a successful transfection a high-quality plasmid DNA, without endotoxins, is necessary. Plasmid DNA is purified from a bacterial culture grown overnight, initially transformed with pHLsec-Ecto-PTPBR7 vector.
2. Large-scale cultures for protein production are performed in expanded surface polystyrene roller bottles.
3. Transfection cocktail: 0.5 mg of Endotoxin-free plasmid DNA is required/2125 cm² roller bottle.
4. Add 80 μL of chloroform to 1 mL of plasmid DNA and vortex (to remove the contaminants).
5. Centrifuge for 10 min at 13,000 × *g* and take off the DNA leaving behind the chloroform.
6. For each roller bottle add 0.5 mg of chloroform treated plasmid DNA into 50 mL serum-free media in a separate tube and mix well.
7. Add 0.75 mL of PEI (1 mg/mL) to the serum-free media with plasmid DNA, mix well and incubate at room temperature for about 15 min for the complex to be formed. The resulting mixture is termed "transfection cocktail."
8. After 3 days of culture, remove by pouring the medium from the roller bottles.
9. Add 200 mL of serum-reduced medium (DMEM with Glutamax, NEAA, 2% FBS) into each roller bottle.
10. Add into each roller bottle, in this order, 0.25 mL of kifunensine (inhibitor of the mannosidase I enzyme), 5 mL of HEPES 1 M, and 50 mL of transfection cocktail.
11. Place the roller bottle back in the incubator at 37 °C at 0.8 rpm for 3–4 days (this is dependent on the state of the cells, if they start to detach, it is time to collect the media).
12. 4 days post-transfection collect the conditioned medium in which secreted protein of interest is present and purify it in order to obtain pure protein.
13. The collected medium is centrifuged at 3500 × *g* for 10 min at 4 °C to separate the detached cells from the media, and then filtered using 0.2 μm membrane filters to remove the leftover debris.
14. This medium is diluted threefold with ice-cold PBS and adjusted to pH 8 by adding 1 M Tris buffer pH 8.0.

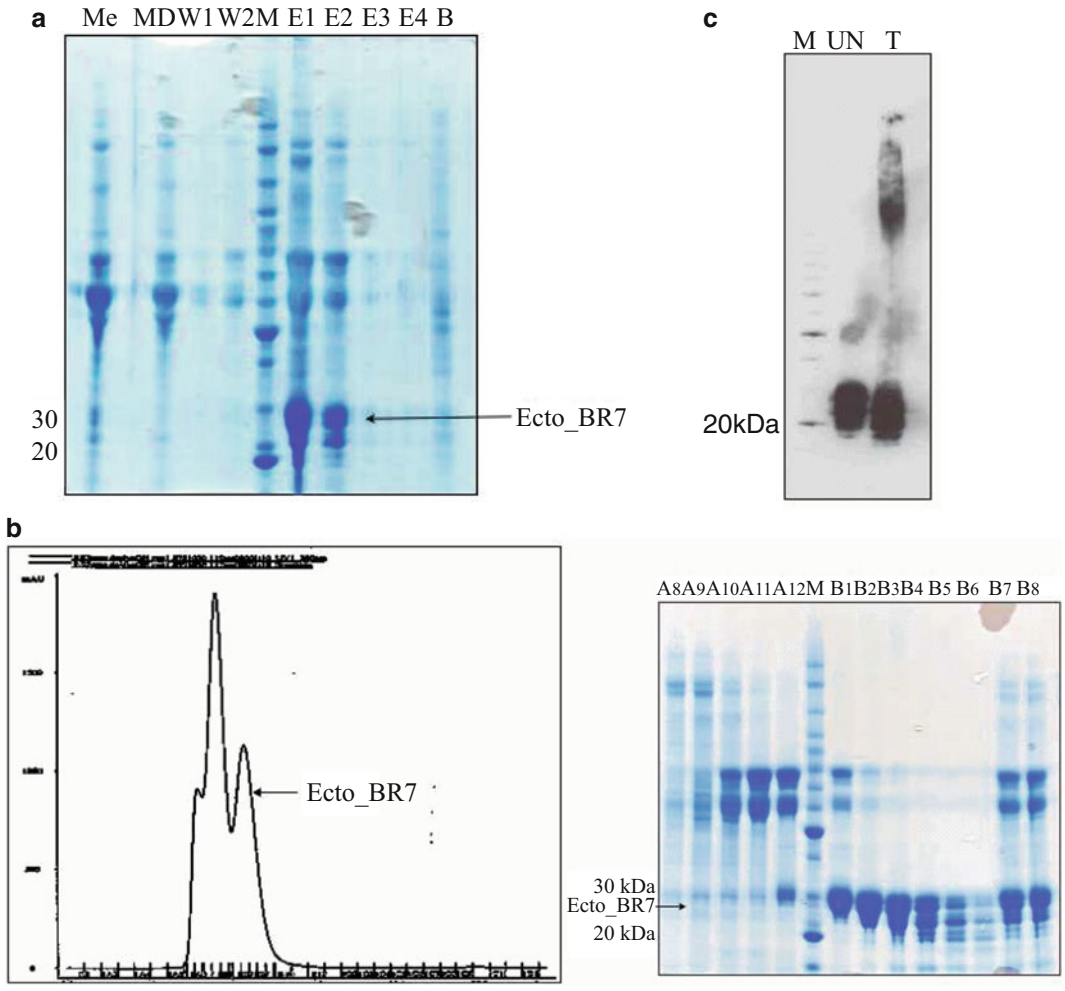

Fig. 4 Analysis of expression and purification of PTPBR7. (**a**) SDS-PAGE analysis of the samples of IMAC purification of PTPBR7. *Me* conditioned medium, *MD* medium after dilution, *W1* wash1, *W2* wash2, *M* marker, *E1* elution1, *E2* elution2, *E3* elution3, *E4* elution4, *B* beads after elution. (**b**) Gel filtration elution profile of ecto PTPBR7 (*left*) and peak fractions of gel filtration profile of ecto PTPBR7 visualized on a 12% SDS-PAGE (*right*). (**c**) Western Blot analysis of deglycosylation of purified PTPBR7 by PNGase. *M* marker, *UN* PNGase untreated, *T* PNGase treated

3.3.3 Protein Purification

1. Immobilized metal ion affinity chromatography (IMAC):
   - Nickel-coated chelating Sepharose beads, previously washed and equilibrated with PBS, are added to the filtered conditioned medium (from Subheading 3.3.2, **steps 13** and **14**).
   - The protein is allowed to bind to the beads by incubating in an orbital shaker at 120 rpm at 16 °C for about 90 min.
   - The suspension of beads and conditioned medium is loaded into an empty column.

- The beads are washed with 50 mL Sepharose washing buffer 1, followed by a second wash with 50 mL of Sepharose washing buffer 2 in order to remove nonspecific proteins that are bound to the beads.
- The protein is eluted in 15 mL of Elution buffer, and the eluted samples are analyzed by 12% SDS-PAGE and fractions containing the protein of interest (Fig. 4a) are collected for further purification (**step 2**).
- Proteins samples pooled after IMAC are partially deglycosylated with endo-H enzyme, before the next round of purification. The protein samples are diluted twofold with PBS and 50 µL (1.2 mg/mL) of endo-H enzyme is added to it and incubated overnight at room temperature.

2. Size exclusion chromatography:
   - Prepare Superdex 75 10/300 GL column: connect the column to the system (*see* **Notes 20** and **21**).
   - The samples containing the protein of interest are pooled and concentrated to 250 µL using membrane filter Centricon Plus-70 Centrifugal filter unit 10-kDa, according to manufacturer's instructions.
   - Inject the concentrated protein and collect the fractions (0.8 mL/min) (proceed as in Subheading 3.1.2, **step 5**).
   - Analyze the fractions by 12% SDS-PAGE.

The PTPBR7 purified protein showed multiple lower bands to the expected molecular weight of 24 kDa (theoretical MW of non-glycosylated protein) (Fig. 4b, right). The N-glycosylation prediction site NetNGlyc server predicted only one glycosylation site. Deglycosylation with PNGase F was done to see if all the bands collapsed to lesser number of bands post-deglycosylation.

3.3.4 Deglycosylation of Protein

1. Purified protein sample was denatured with glycoprotein denaturing buffer at 100 °C for 10 min. This was then mixed with reaction G7 buffer (50 mM sodium phosphate pH 7.5), 1% NP40 and PNGase F and incubated at 37 °C for 1 h. Both G7 buffer and NP40 are provided with the commercial PNGase F preparation. Samples were analyzed by western blot (semidry transfer on PVDF membrane, PentaHis monoclonal primary antibody, followed by the appropriate secondary antibody).

The Western blot showed a small shift in all bands, but the bands did not collapse into a single band. Therefore, it can be speculated that PTPBR7 is somehow susceptible to proteolytic cleavage during the large-scale production of the protein (Fig. 4c).

4 Notes

1. We used the following vectors: (a) pHAT$_2$-hEya3—containing 6×His-tagged human Eyes absent 3 (hEya3) gene; and (b) pGEX-KT-hRPTPμD1—containing the gene fragment encoding for the D1 catalytic domain (residues 818–1190) of human receptor-like protein tyrosine phosphatase μ (RPTPμ) tagged with glutathione *S*-transferase (GST).
2. We used calcium competent cells: (a) BL21(DE3)RIL strain for 6×His-hEya3; and (b) DH5α for GST-hRPTPμD1 protein expression. Competent bacteria cells can be either prepared in the lab or purchased from a biotech company.
3. To prepare LB plates weigh 15 g agar (Bacto) and add to 1 L with LB. Autoclave 20 min at 120 °C. Then, allow medium to cool or cool it with cold water until bottle can be held in hands without burning, then add 1 mL Amp stock solution (100 mg/mL), mix by gentle swirling, and put ~20 mL into each sterile Petri dish (100 mm diameter). Hold plates at room temperature until agar solidifies, then invert them to avoid condensation on lid of plates and store at 4 °C until usage (no more than 1 month).
4. pHLSec, kindly provided by R. Aricescu, is a mammalian expression vector designed to obtain a high yield of secreted protein [7].
5. PEI is extremely viscous liquid which cannot be pipetted. To prepare the PEI solution first tare an empty flask, put some PEI with a spatula into the empty flask and weigh the flask again. Add the calculated volume of water to reach the indicated concentration of PEI solution. Stir it until completely dissolved.
6. All buffers for FPLC-purification must be degassed 10 min using an ultrasonic bath and cooled at 4 °C before usage.
7. Running gel and stacking gel buffers can be kept at 4 °C not longer than about 3 month. Ammonium persulfate solution can be either freshly prepared or can be frozen in single-use aliquots at −20 °C.
8. You can change methanol with ethanol (96–100%), to avoid methanol toxicity. Using ethanol for activation of PVDF membrane and for preparation of transfer buffer we obtained similar results as in the case of methanol.
9. It is very important to make this stock solution in cold distilled water; otherwise it is very quickly hydrolyzed to pNP. We currently use 40 mg tablets of Phosphatase substrate from Sigma-Aldrich.
10. It is very important to keep this buffer phosphate-free; therefore, we usually prepare it in sterile plastic tubes.

11. Add 50% DMSO in water over the phosphopeptide, allow 5 min to dissolve, then add TBS buffer.
12. Manipulate the competent cells in sterile area, either in a bacterial hood or close to a flame. Using this short heat-shock transformation protocol we obtain enough colonies on plate to be further used in protein expression.
13. Do not keep the culture more than 16 h at 37 °C.
14. A dilution of 1:50–1:100 of the overnight starter culture into fresh LB-Amp medium is optimal for bacterial growth. The volume of the culture flask should be at least three times higher than the volume of the media. For example, in a 5 L flask add no more than 1.5–1.6 L medium.
15. To measure the $OD_{600\ nm}$ we use disposable plastic cuvettes and a standard spectrophotometer/colorimeter. We read $OD_{600\ nm}$ of 1 mL of culture with LB medium as a background blank.
16. The culture must be cooled at 25 °C prior to IPTG addition in order to obtain a good yield of soluble protein.
17. It is important to homogenize well the bacterial pellet in lysis buffer; otherwise the disruption of the bacterial cells will not be efficient.
18. Lysis is complete when the cloudy cell suspension becomes translucent.
19. It is important to add glycerol to the protein samples before freezing to preserve protein stability.
20. Before connecting any column to the ÄKTA system it is very important to check whether all parameters are within column specifications; otherwise the column may be damaged.
21. Connecting and detaching of the column has to be performed at a low flow rate (0.5 mL/min).
22. Make aliquots sufficiently small so that they should not be freeze-thaw cycled more than three times. Repeated freezing and thawing can cause protein inactivation. We typically make aliquots of 250–300 μL.
23. Coomassie staining solution can be reused several times.
24. Activate the PVDF membrane by soaking into methanol or ethanol for 2 min at room temperature. Then equilibrate the membrane in 1× Transfer buffer.
25. For the first 2 ml of supernatant passing through the column use a reduced flow rate (0.25 mL/min) and then increase it gradually to 5 mL/min.
26. Running on ethanol usually increases the back pressure of the column, so for this final step decrease flow rate to 0.5 mL/min.

27. Check the pH of the solution before performing the digestion. The pH should be between 7 and 9 for the protease to have maximum enzyme activity.
28. After incubation with rLysC keep the sample at 4 °C, until incubation with chymotrypsin.
29. Before digestion with chymotrypsin, dilute the sample with 50 mM Tris–HCl pH 8 so that the final concentration of urea is less than 1 M and the DTT concentration is less than 10 mM in sample volume.
30. Set pipettor to 100 μL then secure the pipette tip tightly to the end of the pipettor for optimum sample aspiration. Do not introduce air through the membrane at any time during the procedure.
31. For our instrument we set the following parameters: LC method—40 min linear gradient of 2–30 % mobile phase B; LTQ-Orbitrap method, Scan Event details: initial survey MS scan between 300 and 1800 m/z at a resolution of 60,000 at m/z 400 (in the Orbitrap), followed by a data-dependent analysis of the five most intense peaks from the survey scan with +2, +3, and +4 charge using CID (Collision-Induced Dissociation) fragmentation method. Make at least two technical replicates from one sample (two consecutive runs).
32. Separately search each run (technical replicate) to reveal protein identification.
33. Assign a positive identification of a protein when there are at least two unique peptides with high confidence (99 %) present in the sample.
34. 100 mM pNPP stock can be stored at −20 °C in single-use aliquots.
35. All assay buffers are stored at −20 °C in 10 mL aliquots. 5× pNPP assay buffer is prepared fresh from 10× assay buffer and is supplemented with 25 mM DTT.
36. pNPP final concentration in the assay varies from 0.5 to 30 mM.
37. DiFMUP solution is very sensitive to light, so either use a black Eppendorf tube or cover one with tinfoil. Make up fresh daily.
38. First add enzyme storage buffer in blank well and then add enzyme in reaction wells.
39. Do not forget to subtract the values corresponding to the blank wells from those corresponding to the reaction wells.
40. For the standard curve of DiFMU, prepare 100 μM solution of both DiFMUP and DiFMU in assay buffer. We usually prepare

400 μL of each standard point in a tube, then split in three wells.

41. For this phosphatase assay method it is very important to check all reaction components, including enzyme solution, for phosphate contaminants. Pipette the maximum amount of each component of reaction; add MilliQ water to 50 and 100 μL of BIOMOL Green. Read the absorbance at 620 nm and compare with blank, which contains 50 μL water. Free phosphate present on labware and in reagent solutions will greatly increase the background absorbance of the assay.
42. To determine the k_{cat} parameter the value obtained for V_{max} has to be divided to the enzyme concentration used in assay.
43. To keep the cells in the flask, washing should be performed by adding PBS on the opposite side of the flask without disturbing the cells.

Acknowledgments

This work was financially supported by the Romanian National Council for Higher Education Research (PN-II-ID-PCE-2011-3-0743, PN-II-PT-PCCA-2011-79/2012 (THERION) and PN-II-ID-PCCE-2011-2-0024), Programme Human Resources Development (POSDRU/89/1.5/S/60746) (SES, MM and GP), "CERO—Career profile: Romanian Researcher" project (POSDRU/159/1.5/S/135760) cofinanced by the European Social Fund for Sectoral Operational Programme Human Resources Development 2007–2013 (AEI), The European Commission (project P-CUBE-227764) (MM, GP) and in part by European Research Community Funds to PTPNET (MRTN-CT-2006-035830) (S.E.S. and S.T.M.).

References

1. Eckhart W, Hutchinson MA, Hunter T (1979) An activity phosphorylating tyrosine in polyoma T antigen immunoprecipitates. Cell 18:925–933
2. Ushiro H, Cohen S (1980) Identification of phosphotyrosine as a product of epidermal growth factor-activated protein kinase in A-431 cell membranes. J Biol Chem 255:8363–8365
3. Tonks NK (2013) Protein tyrosine phosphatases—from housekeeping enzymes to master regulators of signal transduction. FEBS J 280:346–378
4. Alonso A, Sasin J, Bottini N et al (2004) Protein tyrosine phosphatases in the human genome. Cell 117:699–711
5. Lee H (2015) Mining the function of protein tyrosine phosphatases in health and disease. Semin Cell Dev Biol 37:66–72
6. Reeves PJ, Callewaert N, Contreras R, Khorana HG (2002) Structure and function in rhodopsin: high-level expression of rhodopsin with restricted and homogeneous N-glycosylation by a tetracycline-inducible N-acetylglucosaminyltransferase I-negative HEK293S stable mammalian cell line. Proc Natl Acad Sci U S A 99:13419–13424
7. Aricescu AR, Lu W, Jones EY (2006) A time- and cost-efficient system for high-level protein production in mammalian cells. Acta Crystallogr D Biol Crystallogr 62:1243–1250

Chapter 4

Peptide Microarrays for Real-Time Kinetic Profiling of Tyrosine Phosphatase Activity of Recombinant Phosphatases and Phosphatases in Lysates of Cells or Tissue Samples

Liesbeth Hovestad-Bijl, Jeroen van Ameijde, Dirk Pijnenburg, Riet Hilhorst, Rob Liskamp, and Rob Ruijtenbeek

Abstract

A high-throughput method for the determination of the kinetics of protein tyrosine phosphatase (PTP) activity in a microarray format is presented, allowing real-time monitoring of the dephosphorylation of a 3-nitro-phosphotyrosine residue. The 3-nitro-phosphotyrosine residue is incorporated in potential PTP substrates. The peptide substrates are immobilized onto a porous surface in discrete spots. After dephosphorylation by a PTP, a 3-nitrotyrosine residue is formed that can be detected by a specific, sequence-independent antibody. The rate of dephosphorylation can be measured simultaneously on 12 microarrays, each comprising three concentrations of 48 clinically relevant peptides, using 1.0–5.0 μg of protein from a cell or tissue lysate or 0.1–2.0 μg of purified phosphatase. The data obtained compare well with solution phase assays involving the corresponding unmodified phosphotyrosine substrates. This technology, characterized by high-throughput (12 assays in less than 2 h), multiplexing and low sample requirements, facilitates convenient and unbiased investigation of the enzymatic activity of the PTP enzyme family, for instance by profiling of PTP substrate specificities, evaluation of PTP inhibitors and pinpointing changes in PTP activity in biological samples related to diseases.

Key words Tyrosine phosphatase, Phosphatase activity, Peptide microarray, Multiplex assay, Phosphatase substrate identification, Phosphatase activity profiling, Phosphatase kinetics, Phosphatase inhibition, Phospho-nitrotyrosine, Nitrotyrosine

1 Introduction

Reversible tyrosine phosphorylation is a fundamental signaling mechanism controlling a diversity of cellular processes. Whereas protein tyrosine kinases have long been implicated in many diseases, aberrant protein tyrosine phosphatase (PTP) activity is increasingly being associated with a wide spectrum of disorders. PTPs are now regarded as key regulators of biochemical processes, e.g., cell differentiation, proliferation, and oncogenic

Rafael Pulido (ed.), *Protein Tyrosine Phosphatases: Methods and Protocols*, Methods in Molecular Biology, vol. 1447,
DOI 10.1007/978-1-4939-3746-2_4,

transformation, instead of simple "off" switches operating in tyrosine kinase signaling pathways [1].

The interplay between tyrosine phosphatase and tyrosine kinase assays can be illustrated by the phosphatase SHP-2. The levels of tyrosine phosphorylated SHP-2 in CD4+ T-cells of human melanoma specimens decrease with tumor progression, leading to a modulated downstream activity of SHP-2. CTLA4 or PD1 is able to recruit and activate SHP-2 which contributes to the negative regulation of T cell activation. This suggests an important role for SHP-2 in preventing melanoma progression and metastasis [2].

Measuring both phosphorylation as well as dephosphorylation of different kinase and tyrosine phosphatase substrates in a multiplex mode might provide a better understanding of cascades.

Modification of the flow-through microarray technology used for measuring (rates of) kinase substrate phosphorylation [3–6] resulted in the development of a kinetic PTP assay [7, 8].

The principle of the assay is shown in Fig. 1. Three concentrations of 48 tyrosine phosphatase peptide substrates containing a 3-nitro-phosphotyrosine residue are covalently coupled onto Anopore aluminum oxide membranes that are activated with a functionalized spacer. The peptide substrates have been selected for their therapeutic relevance, e.g., SIGLEC2 for its role in autoimmune diseases [9] and ZAP70 for its importance in leukemia [10]. As a positive control for detection, a nitrotyrosine peptide substrate (nSTAT3) is present among the substrates spotted on the array.

The dephosphorylated 3-nitro-tyrosine is detected by a monoclonal mouse anti-nitrotyrosine antibody and a FITC-labeled goat

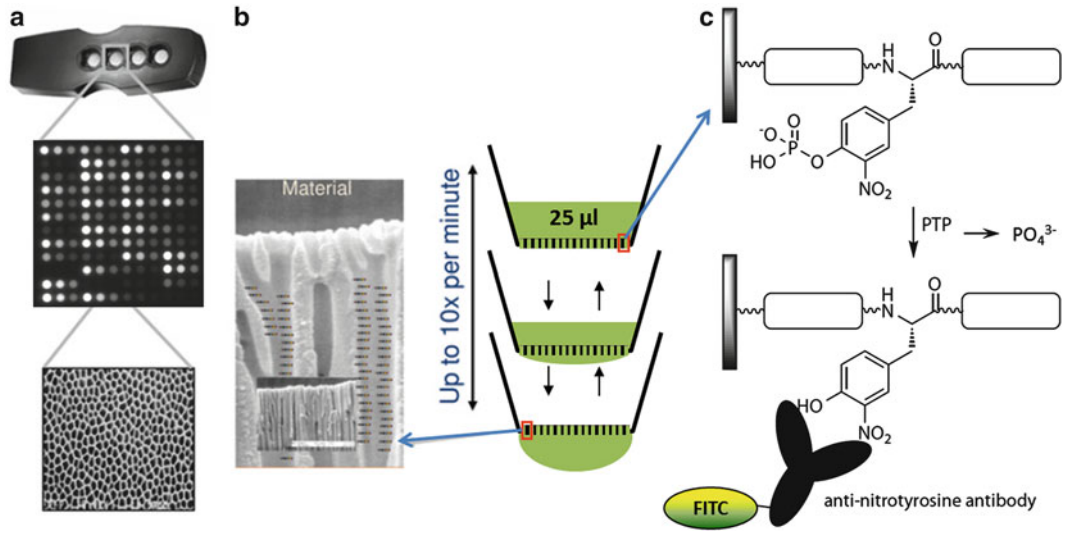

Fig. 1 Schematic view of the PTP assay. (**a**) PamChip® disposable with four arrays on which peptide substrates are spotted, 12 × 12 per array. (**b**) PTP containing sample is pumped through the array. (**c**) 3-nitro-phosphotyrosine detection strategy. Fluorescent images are recorded when the solution is underneath the membrane

anti-mouse secondary antibody that is simultaneously present in this assay. The reaction kinetics of dephosphorylation of the substrate is monitored in time by imaging the membranes every 5 min for 1 h. The fluorescence intensity of every peptide spot on every image is quantitated to yield reaction rates. The method is rapid, because apart from preparation of the lysates, no preprocessing is required. The activity of the enzymes in the lysate can be determined and modulated by addition of phosphatase inhibitors, allowing the investigation of their effect ex vivo on phosphatases with relevant post-translational modifications in naturally occurring protein complexes.

Note that this dynamic, sensitive, high-throughput PTP substrate microarray assay is inventive because it allows detection of product formation rather than disappearance of the substrate. Dephosphorylation by a PTP leaves a 3-nitrotyrosine residue that can be detected by a selective, sequence-independent antibody, which uniquely allows a real-time product formation assay (Fig. 1c) [8]. Several phosphatase assays have been described [11–16] but they suffer from several drawbacks, like the necessity for the PTP to compete with phosphotyrosine antibody prior to reaction and/or problems associated with detector-signal saturation, as discussed extensively in [8].

In summary, in combination with the existing protein tyrosine kinase (PTK) peptide microarray-based assay, the novel PTP assay creates a tool to measure phosphorylation as well as dephosphorylation in a multiplex way that will contribute to a better understanding of (the regulation of) biological processes.

2 Materials

Prepare all dilutions with ultrapure water. Use analytical grade chemicals to prepare solutions that are not provided in the reagent kit.

2.1 Preparation of Lysates for Analysis of Tyrosine Phosphatase Activity

1. Mammalian extraction buffer (M-PER) (Thermo Scientific).
2. Halt Protease Inhibitor Cocktail, EDTA free (Thermo Scientific).
3. Phosphate buffered saline (PBS, 10× stock).
4. Bradford protein concentration assay reagents.

2.2 Analysis of the Tyrosine Phosphatase Activity of a Recombinant or Purified Phosphatase or of a Cell Lysate

1. PamChip® PTP peptide microarrays (PamGene International BV, 's-Hertogenbosch, The Netherlands).
2. PamStation®12 (PamGene International BV, 's-Hertogenbosch, The Netherlands).
3. PTP reagent kit (PamGene International BV, 's-Hertogenbosch, The Netherlands). The kit contains:

- Blocking buffer: 20 mg/ml Bovine Serum Albumin (BSA).
- 10× PTP buffer (*see* **Note 1**).
- DTT (1 M).
- 100× BSA (10 mg/ml).
- Mouse anti-nitrotyrosine antibody (StressMarq).
- Goat anti-mouse FITC antibody (Southern Biotech).

All materials should be stored as indicated in the information provided with the kit.

3 Methods

Phosphatase activity can be measured with phosphatases expressed as recombinant and purified proteins or with crude lysates prepared from cell lines or tissues. When phosphatase inhibitors are added before thawing, the same lysates can be used for kinase activity determination. The preparation of these lysates is described in Subheading 3.1. The phosphatase activity assay itself is described in Subheading 3.2.

3.1 Preparation of Lysates for Analysis of Tyrosine Phosphatase Activity

1. Lyse at most four to six samples simultaneously. Aliquot final lysates in multiple tubes. Biological replicates are samples prepared separately.
2. Cool on ice Mammalian Extraction Buffer (M-PER) supplemented with protease inhibitor cocktail as indicated by the supplier (1:100) (*see* **Note 2**).
3. Label tubes for lysate aliquots of every sample and precool tubes on dry ice. This will cause the lysate to freeze immediately. Alternatively, lysates can be snap-frozen in liquid nitrogen.
4. *Cells*. Remove culture medium from cells and wash twice with ice cold PBS. Add 100 µl of cold lysis buffer per 1×10^6 cells (*see* **Note 3**). Proceed with **step 9**.
5. *Tissue*: Fine needle biopsies and endoscope biopsies can be lysed without cutting of sections. For core biopsies, cut a number of sections that gives about 1 mm^3 of tissue. For cutting sections from larger tissue blocks several options are possible (*see* **Notes 4** and **5**). Either cut one section of 60 µm, or several thinner sections (total of 60 µm of material) of a 5 × 5 mm tissue block of a fresh frozen specimen (*see* **Note 6**). Make sure that the sections remain frozen during the cutting process. The integrity of the sections is less important than in histology, since protein will be extracted from the sections. Use first and last or middle sections for histological investigations if possible.
6. Place sections at the bottom of a precooled vial.

7. The material can be lysed immediately or stored at −80 °C for later use.
8. For lysis of tissues, add 100 µl cold lysis buffer to the first vial with frozen tissue to start the lysis procedure. Keep on ice.
9. Promote the lysis by slowly pipetting the mixture up and down (approximately ten times) in the vial until the solution is clear (no lumps should be visible). Expel the fluid gently from the pipette tip in order to prevent foaming and denaturation of the proteins.
10. Keep the lysate on ice for 15 min. Check the lysis process visually. Promote lysis by pipetting the liquid up and down a few times at intervals of about 5 min. Prolong the incubation time to 30 min when solution is not clear.
11. Centrifuge the lysate for 15 min at 16,000 × *g* at 4 °C in a precooled centrifuge.
12. Transfer the supernatant of each lysed sample to new precooled vials, mix and aliquot (for instance four times 5 µl/vial and four times 20 µl/vial). Lysates can be placed at the bottom of vials precooled on dry ice. Alternatively, vials can be snap-frozen in liquid nitrogen before storage. Store vials immediately at −80 °C. Keep a 5 µl aliquot for protein quantification purposes.
13. Repeat the procedure described above for the remainder of the samples.
14. Determine protein concentration with a standard Bradford protein quantitation assay.

3.2 Analysis of the Tyrosine Phosphatase Activity of a Recombinant or Purified Phosphatase or of a Cell Lysate

In a PamStation®12 instrument three PamChips® with four arrays each are placed, which allows analysis of 12 samples simultaneously (Fig. 2).

PamChip® 90121 comprises 48 peptide substrates spotted at three concentrations (125, 250, and 500 µM) on the same microarray. The rate of dephosphorylation depends on peptide concentration (Fig. 2) and on sample input as shown in Fig. 3.

Before the start of the experiment, an experimental set up and a pipetting scheme must be prepared. The experimental setup describes the distribution of the samples over the chips and arrays, based on the research question to be answered by the experiment and the desired statistical analysis. The pipetting scheme aims at reducing experimental variation between the arrays by making master mixes with as many common ingredients for the assays as possible. The scheme is based on the volumes per array and is shown in Table 1. Multiply the volumes by the number of arrays and add at least 10% additional volume to account for pipetting loss during transfer of solutions (e.g., for four arrays, multiply volumes with at least 4.4).

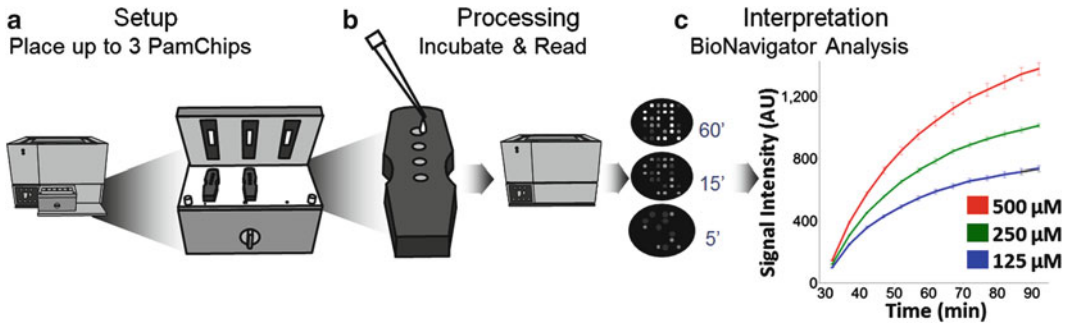

Fig. 2 Workflow for testing three PamChips® (12 microarrays) involving the setup (**a**) and processing (**b**). Dephosphorylation activity (**c**) depends on peptide substrate concentration and increases in time. Data are shown for a selected peptide substrate at three spot concentrations

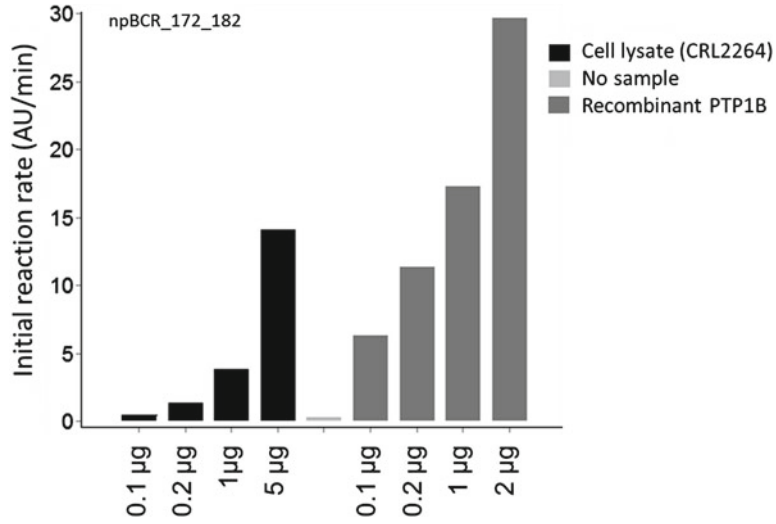

Fig. 3 The dephosphorylation rate depends on sample input for both recombinant phosphatase and lysate. Kinetic curves are fitted to signal intensities as a function of time and initial reaction rates are calculated [17]. In the concentration range tested, a sample input of 0.1–5 µg/array for the CRL2264 lysate and 0.1–2 µg/array for recombinant PTP1B enzyme results in good signals

Keep all solutions on ice, unless indicated otherwise.

1. Allow the PamChip® disposable(s) to come to room temperature.
2. Cool some ultrapure water on ice.
3. To prepare 5 ml 1× PTP wash buffer, dilute 10× PTP buffer tenfold in ultrapure water and add DTT from a freshly prepared 100 mM stock to a final concentration of 1 mM.
4. When performing experiments with inhibitors in the assay mix, pre-dilute the inhibitors to 50× the final concentration in DMSO. From these dilutions, add inhibitors just before the assay (*see* **Notes 7–9**).

Table 1
Composition of assay master mix per array

Solution	Volume (µl)
Water	To a final volume of 25 µl
10× PTP buffer	2.5
100 mM DTT	0.25
100× BSA stock solution	0.25
Mouse anti-nitrotyrosine	0.25
Goat anti-mouse FITC	0.05
(Inhibitor in 100% DMSO)	(0.5)
Sample (recombinant PTP or lysate)	max 10

5. Turn on the PamStation®12 following the instructions of the manufacturer and load the desired assay protocol into the Evolve software program. A more detailed protocol is given in the manual provided with the PamStation®12.
6. Place 1, 2, or 3 PamChip® PTP disposables in the incubator.
7. Place a syringe with 1× PTP wash buffer in the instrument at the position indicated in the assay protocol.
8. Apply 30 µl of blocking buffer to each array (*see* **Note 10**).
9. Start the blocking step in the assay protocol (*see* **Note 11**).
10. Prepare the assay master mix while the arrays are being blocked and washed. The assay master mix is prepared just before application onto the array and should not be stored. Mix gently, *do not vortex* and keep the assay mix on ice. Add components in the order indicated in Table 1. To reduce variation between arrays, prepare an assay master mix containing all components common to all arrays.
11. Divide the desired amount of the assay master mix over pre-cooled tubes representing the different conditions to be tested. Complement with other ingredients, according to experimental design.
12. Add the sample to the assay mix just before application to the arrays. The amount of input material required depends on the sample type used.
13. For recombinant phosphatases, the amount can vary from 1 to 100 nmol, depending on the activity of the recombinant phosphatase (*see* **Notes 12–14**).
14. For cell or tissue lysates, in general 0.2–5.0 µg protein per array will result in a robust phosphatase activity signal (*see* **Notes 15–18** and Figs. 3 and 4).

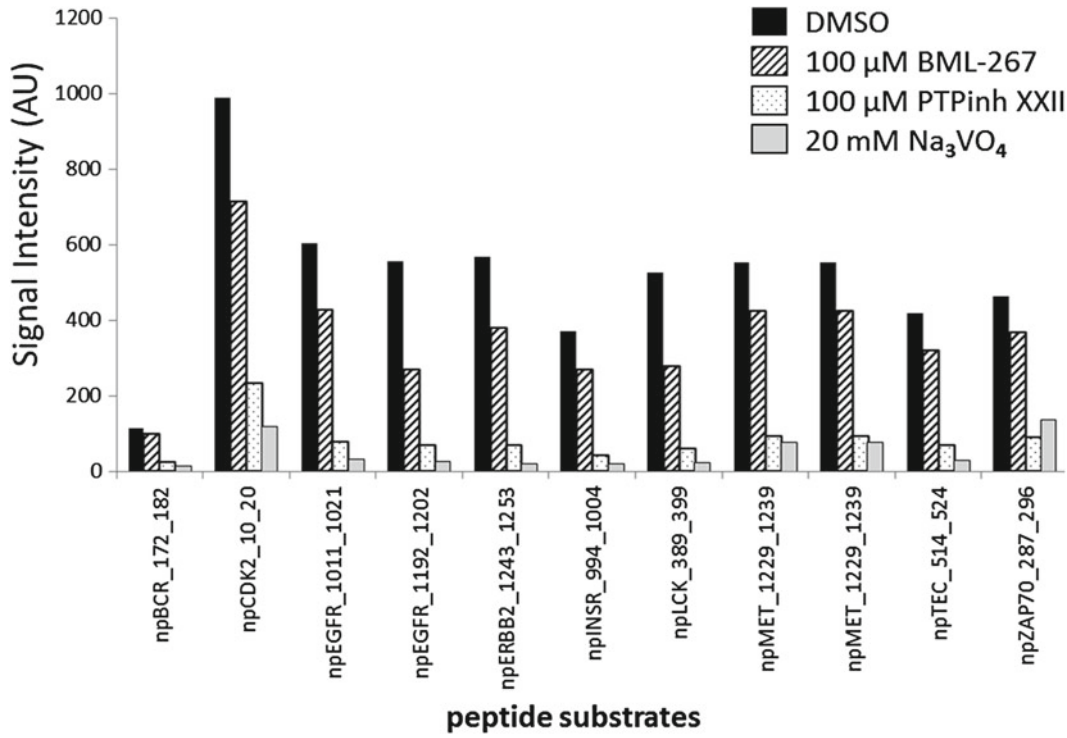

Fig. 4 Inhibition of dephosphorylation activity of recombinant full length PTP1B by three phosphatase inhibitors

15. Apply 25 µl assay mix per array (*see* **Note 19**).
16. Run the assay protocol.
17. During the run, (a run takes 60 min in the standard assay protocol), images are taken (Fig. 2), showing the signal increase on all peptide spots. At the end of the run, an automated washing step is performed, and images are taken at different exposure times.
18. When the running of the assay protocol is completed, remove the PamChip® disposable(s) and shut down the instrument according to the information in the PamStation®12 manual.
19. Use BioNavigator software (PamGene International BV, 's-Hertogenbosch, the Netherlands) to quantitate the signal intensities of all peptide spots on all images (*see* **Notes 20** and **21**). The software has an algorithm that recognizes the spots and their identity and places a grid on the array of spots on each image.
20. In BioNavigator, inspect the correct placement of each grid and identification of spots by the software as well as the occurrence of irregularities, fluorescent particles and other phenomena affecting data quality (*see* **Note 22**). The software calculates the intensity in each spot, the local background around each

spot and detects saturation in the pixels in the images. Subtraction of local background yields the value SigmBg (signal minus background) for each spot. These values are used for further analysis.

21. The data points can be inspected as a time series of signal intensity per peptide (Fig. 2). The initial rate of reaction can be calculated and used as basis for data analysis. Alternatively, the SigmBg end levels either before or after the washing step can be used for further analysis. In general, these values are very similar. In case a high phosphatase activity leads to saturation of many spots, the values at an earlier time point can be used as input for data analysis.
22. The dynamic range of the assay can be increased by making use of a combination of different exposure times. Therefore the slope of the signal as function of exposure time is used. Saturated signals can be excluded from this analysis.
23. The BioNavigator software provides several predefined statistical analysis and visualization methods for quick data analysis and interpretation. Furthermore the software provides building blocks for construction of alternative analysis methods and can easily be linked to R-modules.
24. A database function allows easy combination of the results of multiple experimental runs and analysis of such combined data sets.

4 Notes

1. Composition of the 10× PTP buffer: 250 mM potassium phosphate adjusted to pH 7.4, 500 mM NaCl, 50 mM EDTA, 0.5% Brij-35.
2. Some tissues are known to have a high protease content. Use 1:50 diluted inhibitors for such tissues.
3. Preferably scrape adhering cells because trypsin is known to induce kinase activity. The influence of trypsin treatment on phosphatase activity has not been investigated.
4. Grinding frozen tissue with a mixer-mill or pestle is a good alternative (Detailed instructions are available from PamGene International BV).
5. Cutting of sections makes it possible to use sections before and after for HE staining to determine for example the percentage of tumor cells.
6. Avoid the use Tissue-Tek® or OCT™, a wax-like substance used for embedding tissues before cryo-section. If it is used, remove as much as possible. Embedded material is compatible

with PamChip® array analysis when tissue sections contain less than 10% of such material.

7. When working with inhibitors, usually a stock solution of 10 mM inhibitor in DMSO is made that is then diluted in DSMO till 50× the desired final concentration. Just before the assay, this solution is diluted in the final assay mixture. Per 25 μl assay mix, 0.5 μl of this solution is added, resulting in 2% DSMO in the final assay mix. When no replicates are tested, prepare higher volumes to prevent variation due to small volumes.
8. When dissolving and diluting inhibitors, the experimenter should check that all material dissolves. Depending on the inhibitor concentration, dilution in water may result in precipitation. When this happens, a less concentrated solution can be made. Up to 2% DMSO in the assay mixture is tolerated by phosphatases, but may result in lower activity.
9. Some inhibitors might bind slowly to the phosphatase. To assure proper binding, pre-incubation of the inhibitor to the phosphatase can be considered.
10. The material the arrays are made of is very brittle. Do not touch the arrays with the pipette tip to prevent breaking. Place the pipette tip in the dedicated area in the plastic housing adjacent to the array or let the fluid wet the array by touching the surface with the drop hanging from the pipette tip.
11. Complete drying of arrays after blocking affects assay performance negatively. When a long time passes between washing and application of the assay mixture, the arrays may dry completely (white appearance). When it is expected that the time between the end of the washing step and application of assay mix will be more than 15 min, the PamChip® disposable(s) may be removed from the instrument and stored in the original pouch to prevent further drying.
12. For a recombinant phosphatase the optimal input must be determined by testing a concentration series of the phosphatase. The input suggested by the supplier is a good starting point. When such information is not available, a range between 1 and 100 nmol or 1 and 1000 ng per array can be tested to determine the optimal concentration.
13. When preparing a concentration series of a phosphatase, one assay master mix containing the highest concentration phosphatase is made and one without. The latter is used to dilute the phosphatase containing assay master mixture. This method avoids errors due to variation in pipetting small volumes.
14. Since recombinant phosphatases may be sensitive to freeze–thaw cycles, they must be treated according to the instruction of the manufacturer. In many cases, preparing aliquots of the recombinant phosphatase is suggested to avoid freeze–thaw cycles.

15. Lysates should be centrifuged shortly in a precooled centrifuge before addition to the assay mix to remove precipitates that could be present.
16. The optimal amount of lysate per array must be determined. In general, 0.2–5 μg of protein per array results in a robust signal (Fig. 3). For an optimization experiment, it is suggested to test three input concentrations, with the middle concentration repeated with a generic phosphatase inhibitor like 1.0 mM sodium vanadate spiked-in to confirm that the activity determined can also be inhibited. Signals increase with input concentration till an optimum is reached.
17. It is advised to dilute the samples in M-PER lysis buffer with freshly added protease inhibitors since the inhibitors are not resistant to freeze–thaw cycles.
18. Although the phosphatase activity in some samples can withstand several freeze–thaw cycles, other lysates are more susceptible to freezing–thawing. Therefore, it is advised to aliquot samples after lysis so as to avoid freeze–thaw cycles.
19. To establish that *bona fide* phosphatase activity is measured controls should be performed to assure that activity depends on the phosphatase input concentration and that it can be inhibited by a generic phosphatase inhibitor like sodium vanadate.
20. Other programs can be used for signal quantitation, but are not designed to deal with a large number of arrays nor with the kinetic readouts.
21. The grid is placed on the last image of a series. When the camera position has slightly shifted during the run, grid placement may be inaccurate. In such cases separate analysis of images (see manual for more instructions) is helpful.
22. When fluorescent speckles are visible on many arrays, precipitates in the antibody solution may be the cause. Remove those by centrifugation of the antibody solutions and transfer to clean tubes.

References

1. Hatzihristidis T, Liu S, Pryszcz L et al (2014) PTP-central: a comprehensive resource of protein tyrosine phosphatases in eukaryotic genomes. Methods 65:156–164
2. Zhang T (2013) Loss of SHP-2 activity in CD4+ T cells promotes melanoma progression and metastasis. Sci Rep 3:2845. doi:10.1038/srep02845
3. Lemeer S, Ruijtenbeek R, Pinkse MW, Jopling C, Heck AJ, den Hertog J, Slijper M (2007) Endogenous phosphotyrosine signaling in zebrafish embryos. Mol Cell Proteomics 6(12):2088–2099
4. Lemeer S, Jopling C, Naji F, Ruijtenbeek R, Slijper M, Heck AJ, den Hertog J (2007) Protein-tyrosine kinase activity profiling in knock down zebrafish embryos. PLoS One 2(7):e581
5. Versele M, Talloen W, Rockx C, Geerts T, Janssen B, Lavrijssen T, King P, Gohlmann HW, Page M, Perera T (2009) Response prediction to a multitargeted kinase inhibitor in

cancer cell lines and xenograft tumors using high-content tyrosine peptide arrays with a kinetic readout. Mol Cancer Ther 8(7): 1846–1855

6. Hilhorst R, Houkes L, Mommersteeg M et al (2013) Kinase activity profiling on peptide microarray. In: Bina M (ed) Gene regulation: methods and protocols, vol 977, Methods in molecular biology. Springer, Heidelberg, pp 259–271. doi:10.1007/978-1-62703-284-1_21
7. van Ameijde J, Overvoorde J, Knapp S et al (2014) A versatile spectrophotometric protein tyrosine phosphatase assay based on 3-nitrophosphotyrosine containing substrates. Anal Biochem 448:9–13
8. van Ameijde J, Overvoorde J, Knapp S et al (2013) Real-time monitoring of the dephosphorylating activity of protein tyrosine phosphatases using microarrays with 3-nitrophosphotyrosine substrates. ChemPlusChem 78(11):1349–1357. doi:10.1002/cplu.201300299
9. Hatta Y, Tsuchiya N, Matsushita M et al (1999) Identification of the gene variations in human CD22. Immunogenetics 49:280–286
10. Hamblin AD, Hamblin TJ (2005) Functional and prognostic role of ZAP-70 in chronic lymphocytic leukaemia. Expert Opin Ther Targets 9:1165–1178
11. Kalesh KA, Tan LP, Lu K, Gao L, Wang J, Yao SQ (2010) Peptide-based activity-based probes (ABPs) for target-specific profiling of protein tyrosine phosphatases (PTPs). Chem Commun 46:589–591. doi:10.1039/B919744C
12. Wisastra R, Poelstra K, Bischoff R, Maarsingh H, Haisma HJ, Dekker FJ (2011) Antibody-free detection of protein tyrosine nitration in tissue sections. ChemBioChem 12:2016–2020. doi:10.1002/cbic.201100148
13. Yang J, Cheng Z, Niu T, Liang X, Zhao ZJ, Zhou GW (2000) Structural basis for substrate specificity of protein-tyrosine phosphatase SHP-1. J Biol Chem 275:4066–4071. doi:10.1074/jbc.275.6.4066
14. Ames BN (1966) Assay of inorganic phosphate, total phosphate and phosphatases. Methods Enzymol 8:115–118. doi:10.1016/0076-6879(66)08014-5
15. Hess HH, Derr JE (1975) Assay of inorganic and organic phosphorus in the 0.1–5 nanomole range. Anal Biochem 63(2):p607–p613
16. Webb MR (1992) A continuous spectrophotometric assay for inorganic phosphate and for measuring phosphate release kinetics in biological systems. Proc Natl Acad Sci U S A 89(11):4884–4887
17. Hilhorst R, Houkes L, van den Berg A, Ruijtenbeek R (2009) Peptide microarrays for detailed, high-throughput substrate identification, kinetic characterization, and inhibition studies on protein kinase A. Anal Biochem 387:150–161. doi:10.1016/j.ab.2009.01.022

Chapter 5

Tailor-Made Protein Tyrosine Phosphatases: In Vitro Site-Directed Mutagenesis of PTEN and PTPRZ-B

Sandra Luna, Janire Mingo, Olaia Aurtenetxe, Lorena Blanco, Laura Amo, Jan Schepens, Wiljan J. Hendriks, and Rafael Pulido

Abstract

In vitro site-directed mutagenesis (SDM) of protein tyrosine phosphatases (PTPs) is a commonly used approach to experimentally analyze PTP functions at the molecular and cellular level and to establish functional correlations with PTP alterations found in human disease. Here, using the tumor-suppressor PTEN and the receptor-type PTPRZ-B (short isoform from *PTPRZ1* gene) phosphatases as examples, we provide a brief insight into the utility of specific mutations in the experimental analysis of PTP functions. We describe a standardized, rapid, and simple method of mutagenesis to perform single and multiple amino acid substitutions, as well as deletions of short nucleotide sequences, based on one-step inverse PCR and DpnI restriction enzyme treatment. This method of SDM is generally applicable to any other protein of interest.

Key words Site-directed mutagenesis, PCR, Protein tyrosine phosphatase, PTEN, PTPRZ-B, PTPRZ1

1 Introduction

The directed alteration of cDNA sequences to modulate protein function in in vitro or in vivo experimental settings constitutes one of the basic approaches to establish, at the molecular and cellular level, protein structure-activity relationships governing biological processes. Together with structural and functional studies, SDM applied to relevant proteins has emerged as an indispensable technique to test and validate experimental hypothesis and to characterize intrinsic protein biological activities, as well as to define the mechanism of action of specific drugs. Site-directed mutagenesis is especially well suited for studying the biological activities of enzymes, since protocols for the readout of activity are usually available. In the case of PTPs, different experimental approaches exist to study in vitro PTP biological properties, including catalytic activity towards different substrates, sensitivity to inhibitors or redox regulatory agents, and binding to ligands, substrates, and

Rafael Pulido (ed.), *Protein Tyrosine Phosphatases: Methods and Protocols*, Methods in Molecular Biology, vol. 1447,
DOI 10.1007/978-1-4939-3746-2_5,

regulatory proteins, among others [1–9]. In this regard, mutations at the PTP active site have been used to engineer binding sites for specific inhibitors [10], as well as to obtain antibodies that specifically recognize the oxidized conformation of the PTP and keep the enzyme in its inactive state [11].

All Cys-based PTPs follow a two-step enzymatic mechanism that starts with a nucleophilic attack on the phospho-substrate by the catalytic Cys (located on the CxxxxxR signature motif-containing catalytic P-loop), which is aided by a general acid donating-proton residue, generally an Asp (located in the WPD-loop), to release the dephosphorylated substrate. This generates a characteristic phospho-enzyme intermediate. In a second step, a water molecule is deprotonated by the catalytic Asp (which now acts as a general base) and the remaining hydroxyl group attacks the P-O thiol-phosphate bond from the phospho-enzyme intermediate, releasing the phosphate moiety [12–16]. The conservative substitution of the catalytic Cys by a Ser (C/S mutation) is the standard enzyme-inactivating mutation used in PTP studies [17]. Importantly, C/S PTP mutations may act as dominant negative PTP variants, likely by binding to substrates (without dephosphorylating them) or by competing with effectors [18–22]. The substitution of the catalytic Asp by an Ala (D/A mutation) renders an enzyme with very low activity, which usually binds to substrates with higher affinity than the C/S mutation, being referred as a substrate-trapping mutation [23]. Substrate-trapping D/A mutations have been used successfully to identify *bona fide* substrates of different PTPs, alone [24–28] or in combination with the C/S mutation [29]. A list of residues important for catalysis of PTPs, using PTPN1/PTP1B as a model, is provided in reference [30].

Protein-protein interactions constitute a major regulatory mechanism in the control of PTP biological activity, not only by conferring substrate specificity but also by regulating the compartmentalization and subcellular location of PTPs. This is aided by the existence of a domain modular organization on many PTPs that specifically orchestrate their differential binding to effectors and regulators [31–33]. In addition, linear C-terminal amino acid motifs that represent canonical binding sites for PDZ protein domains are present in some PTPs, including PTEN (-Thr-Lys-Val; -TKV motif) and PTPRZ-B (-Ser-Leu-Val; -SLV motif), as well as in some myotubularins. PDZ domains exist in many scaffolding and regulatory proteins, and are considered as major elements in the compartmentalization of the cell at the molecular level, with important implications in human disease [34, 35]. PDZ-domain binding to protein partners can be experimentally manipulated by PDZ-domain rearrangements, as well as by mutation of the residues from the PDZ-binding motif on the protein partners [36, 37].

PTEN is a lipid- and protein-phosphatase that controls cell homeostasis. PTEN behaves as a major tumor-suppressor protein

in humans by dephosphorylating PIP3, the product of the oncogenic PI3K, and PTEN functional alterations are strongly associated with human disease, especially cancer. *PTEN* gene is a frequent target of mutations in human tumors, and patients with PTEN hamartoma tumor syndrome (PHTS) or with autism spectrum disorders (ASD) carry *PTEN* germ-line mutations [38–42]. Thus, the potential to introduce PTEN mutations for experimental purposes is required to study PTEN functionality or effects of PTEN disease-associated mutations [43, 44]. PTPRZ-B is a receptor-type PTP that is encoded by gene *PTPRZ1* and that is mainly (but not exclusively) expressed in the nervous system. *PTPRZ1*-encoded protein isoforms are involved in the regulation of cell-cell and cell-extracellular matrix interactions, and display both tumor suppressive and oncogenic properties [45–50]. In addition, *PTPRZ1* isoforms are involved in myelination processes [51–53], and they have been proposed as a target for Parkinson's disease and schizophrenia [54, 55]. Both PTEN and PTPRZ-B bind PDZ domains through their C-terminal PDZ-binding motifs, which impacts on their stability, subcellular location, and function [36, 56–59].

Mutations useful to study the functions of PTEN and PTPRZ-B in any cell system or experimental setting are illustrated in Table 1. These include specific mutations affecting the catalysis or the binding to PDZ domains of PTEN and PTPRZ-B, and may be extended to other PTPs. Using PTEN and PTPRZ-B cDNAs in different plasmid backgrounds, we describe a standardized, rapid, and simple mutagenesis method to obtain single and multiple amino acid substitutions, as well as short-length nucleotide deletions. The method is based on one-step inverse PCR followed by DpnI restriction enzyme treatment and direct *E. coli* transformation, and can potentially be applied to any other cDNA of interest.

Table 1
Amino acid substitution mutations of utility to study PTEN and PTPRZ-B function

Mutation	Location	Functional consequence	References
PTEN[a]			
C124S	PTP domain (P-loop)	Catalytically inactive (full)	[61–63]
G129E	PTP domain (P-loop)	Loss of lipid phosphatase activity	[64]
Y138L	PTP domain	Loss of protein phosphatase activity	[65]
D90A	PTP domain (WPD-loop)	Catalytically inactive; substrate trapping	[66]
V403A	C-terminal tail	Loss of PDZ-domain binding	[59]
PTPRZ-B[b]			
C1073S	PTP D1 domain (P-loop)	Catalytically inactive (full)	[57, 67]
D1041A	PTP D1 domain (WPD-loop)	Catalytically inactive; substrate trapping	[68]
S1453A	C-terminal tail	Loss of PDZ-domain binding	[58]
V1455A	C-terminal tail	Loss of PDZ-domain binding	Predicted

[a]Amino acid numbering corresponds to the major human PTEN isoform (NP_000305)
[b]Amino acid numbering corresponds to the short human PTPRZ-B isoform (NP_001193767)

2 Materials

All solutions are prepared in double-distilled, RNase-free water. Plasticware is autoclaved or sterilized by ethylene oxide.

2.1 Site-Directed Mutagenesis of PTPs

1. Plasmid containing the PTP cDNA to be mutagenized (*see* **Note 1**).
2. Mutagenic oligonucleotide primers (*see* **Note 2**).
3. High-fidelity DNA polymerase and dNTPs (*see* **Note 3**).
4. DpnI restriction enzyme (target sequence 5′-Gm^{6}ATC-3′) (*see* **Note 4**).
5. *E. coli* competent cells (*see* **Note 5**).
6. TNE buffer: 50 mM Tris–HCl pH 7.5, 100 mM NaCl, 5 mM EDTA.
7. 10× TCM buffer: 100 mM Tris–HCl pH 7.5, 100 mM $CaCl_2$, 100 mM $MgCl_2$.
8. LB medium: 1% Tryptone, 0.5% yeast extract, and 1% NaCl.
9. LB-Ampicillin (LB-Amp) plates: 1% Tryptone, 0.5% yeast extract, 1% NaCl, 0.01% NaOH, 1.5% agar, and 100 μg/ml ampicillin.
10. Plasmid DNA purification kit.
11. Agarose gel electrophoresis and DNA visualization reagents.
12. Thermocycler.
13. Shaking incubator.
14. Ultraviolet light detection system.

3 Methods

This mutagenesis method is based on the QuikChange™ Site-Directed Mutagenesis procedure, which consists of one-step inverse PCR from a methylated double-stranded DNA (dsDNA) plasmid followed by DpnI restriction enzyme treatment, eliminating the need for subcloning and single-stranded DNA (ssDNA) rescue. Our procedure utilizes a supercoiled dsDNA vector with the insert of interest, and synthetic oligonucleotide mutagenic primers with a standardized predesigned length (see below). The oligonucleotide primers are extended during temperature cycling by a high-fidelity DNA polymerase, which generates a non-methylated mutated nicked plasmid. The PCR product is directly treated with DpnI endonuclease to digest the parental methylated DNA template, followed by transformation into competent bacteria. Examples are provided for single-amino acid substitutions and

deletions on human PTEN (1.2 kb cDNA; NM_000314, NP_000305) (Figs. 1 and 2, Table 2) and for single and multiple-amino acid substitutions on human PTPRZ-B (4.3 kb cDNA; NM_001206838, NP_001193767) (Fig. 3). Note that for both single and multiple mutations we run a single PCR.

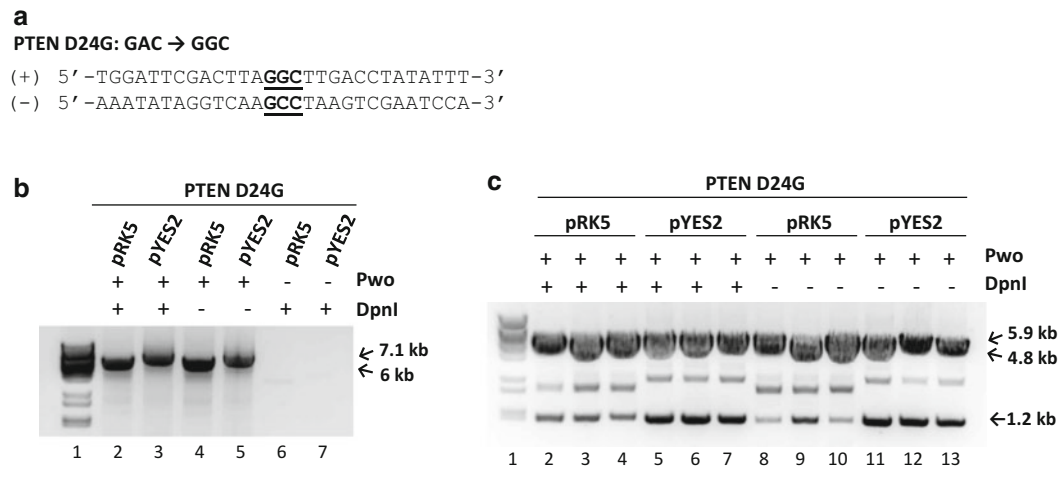

d

Mutagenesis conditions	Template plasmid	Number of colonies	Mutagenesis efficiency
+ Pwo + DpnI	pRK5-PTEN	198	3/3
	pYES2-PTEN	115	3/3
+ Pwo - DpnI	pRK5-PTEN	231	0/3
	pYES2-PTEN	172	0/3
-Pwo + DpnI	pRK5-PTEN	0	--
	pYES2-PTEN	0	--

Fig. 1 Monitoring of standardized site-directed mutagenesis using a PTEN amino acid substitution as an example. (**a**) Mutagenic primers of 29-mer predefined length (13 + 3 + 13, codon substituted *underlined*). The amino acid substitution (D24G) is indicated using the amino acid one-letter code. +, forward primer; –, reverse primer. (**b**) Linear DNA obtained on the mutagenic PCR, as resolved by 1 % agarose gel electrophoresis. pRK5 PTEN is 6 kb size, whereas pYES2 PTEN is 7.1 kb size. The parental circular DNA is in low amount and not visualized. Note the lack of PCR product in the absence of DNA polymerase (*lanes 6* and *7*). (**c**) Control restriction enzyme digestions (XbaI + SalI, cutting out the 1.2 kb PTEN insert) of plasmid DNA obtained from bacteria transformed with the mutagenic PCR product. Three colonies were analyzed from each condition. In *lanes 1* from (**b**) and (**c**), molecular markers (BstEII digestion of λ phage) are shown. (**d**) Efficiency of bacteria transformation with the mutagenic PCR product (number of bacteria colonies after transformation with the DpnI-treated PCR product) and mutagenesis efficiency (number of mutated samples with respect to the number of samples sequenced) achieved from each condition are indicated. Note that in the absence of DpnI, the parental template plasmid gives a background of non-mutated samples. In the absence of DNA polymerase (but presence of DpnI) no colonies should be obtained, as an indication of the efficiency of DpnI digestion

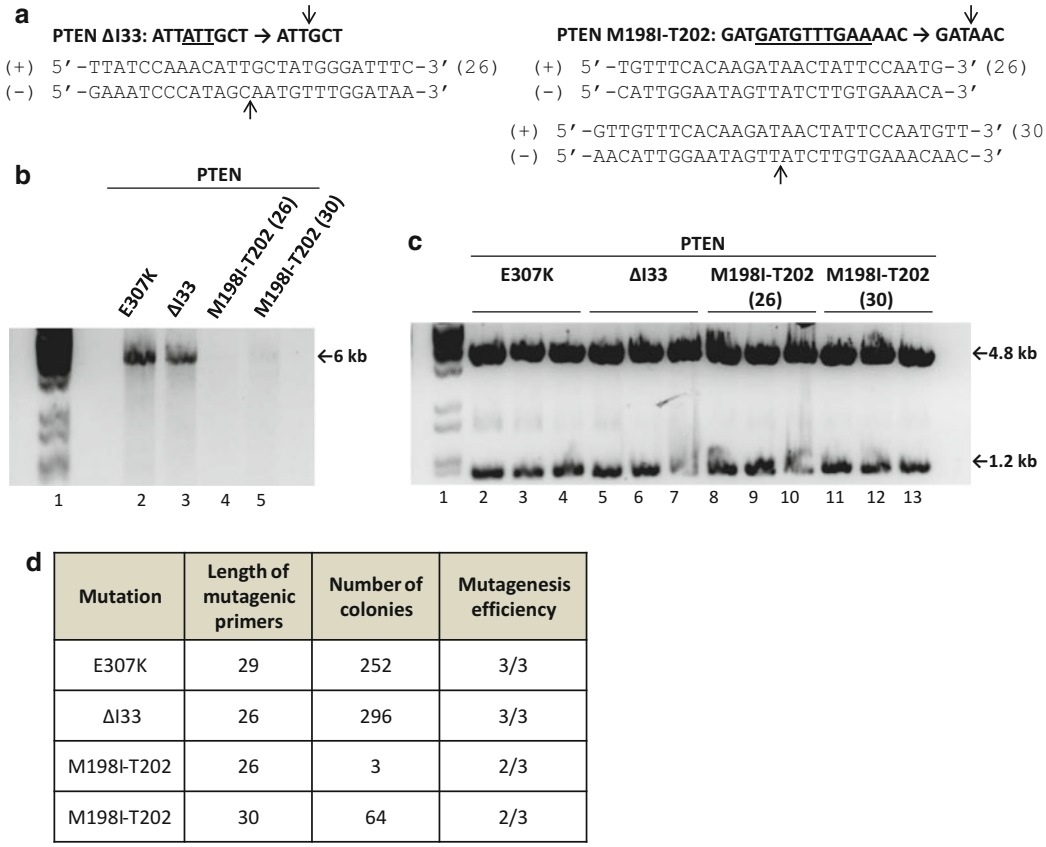

d

Mutation	Length of mutagenic primers	Number of colonies	Mutagenesis efficiency
E307K	29	252	3/3
ΔI33	26	296	3/3
M198I-T202	26	3	2/3
M198I-T202	30	64	2/3

Fig. 2 Monitoring of standardized site-directed mutagenesis using PTEN amino acid substitution and nucleotide deletions as examples. (**a**) Mutagenic primers of 26-mer or 30-mer predefined length (13 + 0 + 13 or 15 + 0 + 15, respectively, where 0 indicates the *underlined* deleted nucleotides). The *arrows* indicate the nucleotide junction after the deletion. The amino acid changes after the nucleotide deletion are indicated as follows: ΔI33, deletion of I33; M198I-T202, M198I substitution plus deletion of residues 199–201. +, forward primer; –, reverse primer. (**b**) Linear DNA obtained on the mutagenic PCR (pRK5 PTEN as template plasmid), as resolved by 1 % agarose gel electrophoresis. The E307K amino acid substitution (29-mer mutagenic primers) was included for comparison. (**c**) Control restriction enzyme digestions (XbaI + SalI, cutting out the 1.2 kb PTEN insert) of plasmid DNA obtained from bacteria transformed with the mutagenic PCR product. Three colonies were analyzed from each condition. In *lanes 1* from (**b**) and (**c**), molecular markers (BstEII digestion of λ phage) are shown. (**d**) Efficiency of bacteria transformation with the DpnI-treated PCR product, and mutagenesis efficiency are indicated. Note that two different set of primers (26-mer or 30-mer) were used for the M198I-T202 mutagenesis. Note that sometimes the amplified PCR product is barely detected [see *lanes 4* and *5* from panel (**b**)], but it is enough to obtain colonies with the desired mutation

3.1 Site-Directed Mutagenesis of PTPs

1. Design the mutagenic oligonucleotide primers. In our protocol for amino acid substitutions, the mutagenic primers are two fully complementary primers of standardized predefined length (usually 29-mer), with the mutated codon in the center (Fig. 1a) (*see* **Note 2**) (Mingo et al., submitted). For deletions of short sequences of nucleotides, the design of mutagenic primers follows similar rules, with the junction of the deleted sequence in the center (Fig. 2a).

Table 2
Efficiency of amino acid substitution-standardized mutagenesis of PTEN[a]

Mutation[b]	GC content (%)	Tm[c]	Number of colonies	Mutagenesis efficiency
M1I (ATG → ATA)	48	75	22	1/1
K6E[d] (AAA → GAA)	48	75	12	1/1
K6I[d] (AAA → ATA)	45	74	8	1/1
N12T[e] (AAC → ACC)	41	72	12	1/1
R14G[d] (AGG → GGG)	41	72	20	1/2
D24G (GAC → GGC)	38	71	58	1/1
E43G (GAA → GGA)	48	75	11	1/1
I50T (ATT → ACT)	31	68	19	1/1
Y65C[e] (TAC → TGC)	34	69.5	8	1/1
Y68N[e] (TAC → AAC)	34	69.5	9	2/3
Y68H[e] (TAC → CAC)	38	71	15	1/1
Y68C[e] (TAC → TGC)	38	71	32	1/1
L70P[e] (CTT → CCT)	38	71	14	1/1
K80E[d] (AAA → GAA)	41	72	5	1/1
I101T[d] (ATC → ACC)	41	72	20	1/1
D107G[d] (GAT → GGT)	48	75	10	1/1
L112P (CTA → CCA)	45	74	10	1/1
H123R (CAC → CGC)	45	74	25	1/1
R130L (CGA → CTA)	45	74	38	1/1
G132D[d] (GGT → GAT)	38	71	32	1/2
R142P (CGG → CCG)	24	65	44	1/1
R159G[d] (AGG → GGG)	48	75	39	1/1
Q171E (CAG → GAG)	48	75	15	1/2
M205V (ATG → GTG)	45	74	19	1/1
D252V (GAT → GTT)	41	72	55	1/1
K254T[e] (AAA → ACA)	45	74	26	1/1
V255A (GTA → GCA)	41	72	100	1/1

[a]Mutagenesis was performed using the plasmid pYES2 PTEN as the template, and 29-mer-length mutagenic primers, as shown in Fig. 1a
[b]The nucleotide substitutions and the resulting amino acid changes (one-letter amino acid code) are indicated
[c]Tm was calculated according to the QuikChange™ manual (Agilent Technologies)
[d]One of the primers from the mutagenic primer pair has G or C in 3′ position
[e]Both primers from the mutagenic primer pair have G or C in 3′ position
Data are shown as in Fig. 1d

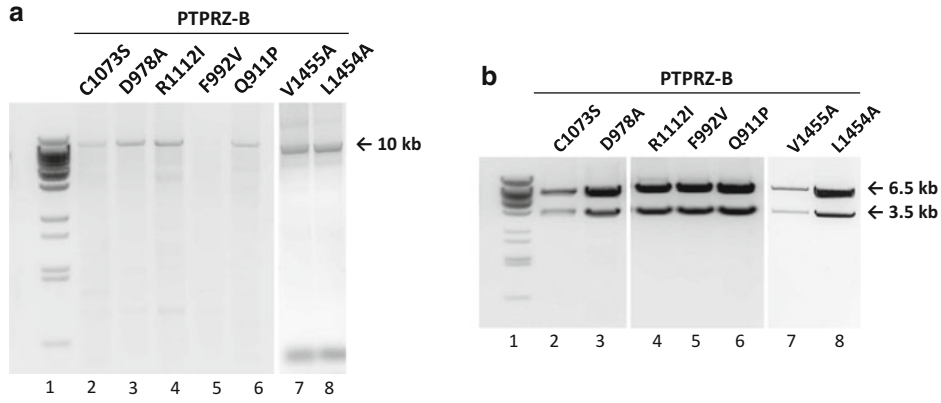

c

Mutation	Number of colonies	Mutagenesis efficiency
C1073S	13	2/2
D978A	50	1/2
R1112I	37	2/2
F992V	8	2/2
Q911P	15	2/2
V1455A	16	1/2
L1454A	37	2/2

Mutation	Number of colonies	Mutagenesis efficiency		
		D978A	C1073S	D978A/ C1073S
D978A/ C1073S	10	4/6	0/6	2/6

Fig. 3 Monitoring of standardized site-directed mutagenesis using PTPRZ-B amino acid substitutions as examples. (**a**) Linear DNA obtained on the mutagenic PCR (pCDNA3 PTPRZ-B as template plasmid, 10 kb size), as resolved by 1 % agarose gel electrophoresis. The amino acid substitutions are indicated using the amino acid one-letter code. (**b**) Control restriction enzyme digestions (XbaI, cutting out a 3.5 kb fragment of PTPRZ-B insert) of plasmid DNA obtained from bacteria transformed with the mutagenic PCR product. Two colonies were analyzed from each condition (see *left panel* c; digestion is only shown for one colony each). In *lanes 1* from (**a**) and (**b**), molecular markers (BstEII digestion of λ phage) are shown. (**c**) In the *left panel*, the efficiency of bacteria transformation with the DpnI-treated PCR product and mutagenesis efficiency are indicated, corresponding to the mutagenesis shown in (**a**). Note that sometimes the amplified PCR product is barely detected [see *lane 5* from panel (**a**)], but it is enough to obtain colonies with the desired mutation. In the *right panel*, data are shown for the simultaneous obtaining of two mutations at two distinct target sites, running a single PCR reaction with a mix of two pairs of mutagenic primers

2. Prepare the mutagenic PCR mix (25 μl): 14.25 μl H_2O, 5 μl template plasmid (at 5 ng/μl) (*see* **Note 1**), 1.25 μl dNTP mix (at 4×2.5 mM), 2.5 μl buffer Pwo 10× (Roche), 0.1 μl DNA polymerase Pwo (at 5 U/μl; Roche), and, in the case of a single mutation (one primer pair), 1 μl of each mutagenic primer (at 10 μM). In the case of multiple mutations (one primer pair/mutation), we keep constant the final concentration of primers preparing a mix of primer pairs from the 10 μM primer stocks (same volume each primer) and adding 2 μl of the mix to the mutagenic PCR mix.

3. Run the mutagenic PCR, using the following cycling conditions (*see* **Note 6**):
   - For PTEN mutagenesis: 1 min at 95 °C, followed by 18 cycles of 50 s at 95 °C (denaturation), 50 s at 60 °C (annealing), and 5 min at 68 °C (extension), and followed by a final 7-min extension at 68 °C and cooling at 4 °C.
   - For PTPRZ-B mutagenesis: 1 min at 95 °C, followed by 18 cycles of 50 s at 95 °C (denaturation), 50 s at 60 °C (annealing), and 7 min at 68 °C (extension), and followed by a final 7-min extension at 68 °C and cooling at 4 °C.
4. Transfer 10 μl of the PCR product to a new Eppendorf tube and add 0.15 μl of the DpnI restriction enzyme (20 U/μl) (*see* **Note 4**). Mix carefully the solution and incubate at 37 °C for 2–3 h (*see* **Note 7**). For long-term storage, keep the undigested PCR product at 4 °C, and the DpnI-digested PCR product at −20 °C (*see* **Note 8**).
5. *Optional*: Run 5–10 μl of the undigested PCR product on 1% agarose gel to monitor the efficiency of the PCR amplification. A linear DNA migrating as the size of the template should be detected (*see* **Note 9**).
6. Transform bacteria: Mix, in a 14 ml polypropylene round-bottom tube, 10 μl of TCM 10×, 10 μl of TNE, and 2 μl of the DpnI-treated PCR product (*see* **Note 10**). Keep on ice for 5 min; then, add 20 μl *E. coli* competent cells (*see* **Note 5**) and incubate on ice for 15–30 min. Heat-shock the mix by incubating the tube in a 42 °C water bath for 90 s, followed by incubation at 20 °C for 10 min. Add 300 μl of LB medium, and incubate under shaking at 37 °C for 80 min.
7. Plate the transformation mix on LB-ampicillin agar plates, air-dry, and incubate inverted at 37 °C for 16 h (*see* **Note 11**).
8. Pick individual colonies to inoculate 3 ml of LB-ampicillin and grow for 16 h at 37 °C under constant shaking.
9. Purify the plasmid DNA according to standard procedures and check the resulting plasmid for the presence of the desired mutation by restriction enzyme and DNA sequencing analysis (*see* **Notes 12** and **13**).

An example of an amino acid substitution mutagenesis on PTEN, using different template plasmids and a pair of 29-mer predefined length mutagenic primers, is provided in Fig. 1. These experiments illustrate the monitoring of the mutagenesis by analyzing the efficiency of the PCR (amount of amplicon and number of bacteria colonies after transformation) and of the mutagenesis (number of sequencing-confirmed mutated samples per number of samples sequenced). Examples of mutagenesis results obtained using different template plasmids (different vectors with PTEN

and PTPRZ-B cDNA inserts) and mutagenic primers are shown in Figs. 2 and 3. In all cases, the PCR product resolved by agarose gel electrophoresis is shown. Note that the amount of this amplified linear DNA correlates with the number of bacteria colonies obtained after transformation with the DpnI-digested PCR product. Data on the mutagenesis efficiency are also provided. In addition, an example of the simultaneous incorporation of two separate mutations in the PTPRZ-B cDNA (resulting in two different amino acid substitutions) is provided in Fig. 3c. Finally, examples from an extensive mutagenesis of PTEN are also given in Table 2.

4 Notes

1. Mutagenesis protocols coupled to digestion with DpnI restriction enzyme (target sequence 5′-Gm^{6}ATC-3′) require a Dam-methylated DNA plasmid template, which is produced by most of laboratory cloning *E. coli* strains (*dam*+).
2. In our standardized protocol, we use mutagenic primers of predefined length, irrespective of their Tm, GC content, and GC localization (Table 2) (Mingo et al., submitted). As a general rule, for single-amino acid substitutions, we use 29-mer mutagenic primers (13 + 3 + 13; 13 nucleotides flanking each side of the codon to be changed [underlined]). For deletion of one amino acid, we use 26-mer primers (13 + 0 + 13; where 0 indicates the deleted nucleotides). For larger nucleotide deletions we increase the length of the mutagenic primers (15 + 0 + 15) (see an example in Fig. 2). It is possible that for templates difficult to amplify, the design of the mutagenic primers needs further optimization. For simultaneous mutagenesis of several target sequences (multiple mutagenesis), we prepare a mix of all the mutagenic primer pairs and use the same final amount of total primers than for a single mutagenesis. In our experience, double and triple mutations are easily obtained by this procedure in a single PCR reaction.
3. High-fidelity thermostable DNA polymerases are required to avoid incorporation of undesired mutations. In addition, some thermostable DNA polymerases, such as Taq polymerase, add undesired "A-tails" in the PCR product. The examples shown here have been performed using Pwo DNA polymerase (Roche), but many other high-fidelity thermostable DNA polymerases are suitable.
4. The efficiency of the digestion of the PCR product with the DpnI restriction enzyme determines the amount of undesired parental plasmid that is transformed into bacteria, which produces wild-type (parental plasmid) colonies. This constitutes one of the key parameters of the mutagenesis efficiency.

Examples of control experiments to test DpnI efficiency are shown in Fig. 1. Note that in the absence of DNA polymerase no colonies should be obtained if the DpnI enzyme is fully efficient. The examples shown have been performed using DpnI from New England Biolabs, but many other DpnI enzymes are suitable.

5. We routinely use $CaCl_2$-competent DH5α *E. coli* cells [60] for direct transformation of the DpnI-digested PCR product. To make a stock of competent bacteria from 50 ml culture, we resuspend the final bacteria pellet in a volume of 2 ml $CaCl_2$ 0.1 M, and keep frozen at −80 °C in aliquots of 50 μl. Commercial ultra-competent bacteria, available from different vendors, are also suitable.
6. Optimization of PCR cycling conditions may be necessary if the template plasmid is of large size or difficult to amplify. As a general rule, 1 min of extension is recommended per kb of template size. Number of cycles can be increased, although this may raise the frequency of undesired mutations. In addition, the amount of parental template plasmid can be increased, although this may result (depending on the DpnI efficiency) in higher background from the parental plasmid (the transformation efficiency of the circular parental plasmid exceeds that of the linear PCR product) (*see* also **Note** 7).
7. It is advisable to test the efficiency of the DpnI digestion with different incubation times, taking into consideration the amount of template plasmid used (*see* Fig. 1). For convenience with time distribution, overnight digestion with DpnI can be performed, although nonspecific digestion will decrease the mutagenesis efficiency.
8. If required, the PCR product can be stored at 4 or −20 °C for some time before being treated with DpnI. Similarly, the DpnI-digested PCR product may be stored for longer periods at −20 °C before the transformation of bacteria is taken up.
9. In general, the number of colonies obtained from the mutagenesis is proportional to the amount of amplified DNA from the mutagenic PCR (monitored by agarose gel electrophoresis in **step 5**; the parental template plasmid is not detectable at these amounts). It is recommended to transform bacteria with the DpnI-digested PCR product even when the amplicon is not detectable on gel, since a small number of colonies is enough to obtain the desired mutation (*see* Figs. 2 and 3).
10. The amount of DpnI-digested PCR product to transform bacteria can be increased, although this may increase background due to the parental plasmid (depending on the DpnI efficiency; *see* also **Note** 7).

11. Our routine mutagenesis experiments yield 20–200 colonies after transformation with 2 μl of DpnI-digested PCR product. If no colonies are obtained, *see* **Notes 2**, **6**, and **10**.
12. Before sequencing, we routinely check by restriction analysis that the amplified DNA corresponds to the template plasmid.
13. The mutation efficiency under our standardized mutagenesis conditions is about 85 %. Sequencing of one to three colonies should be enough to obtain the desired mutation from a single mutagenesis experiment. In the case of multiple mutagenesis, take into consideration that a mix of individual and multiple mutations is likely to be obtained, necessitating the analysis of a larger number of colonies (*see* Fig. 3c, right panel).

Acknowledgements

This work was supported in part by grants SAF2013-48812-R from Ministerio de Economía y Competitividad (Spain), 2013111011 from Gobierno Vasco, Departamento de Salud (Basque Country, Spain), and BIO13/CI/001/BC from BIOEF/EITB maratoia (Basque Country, Spain) (to RP).

References

1. Blanchetot C, Chagnon M, Dube N, Halle M, Tremblay ML (2005) Substrate-trapping techniques in the identification of cellular PTP targets. Methods 35(1):44–53. doi:10.1016/j.ymeth.2004.07.007
2. Boivin B, Yang M, Tonks NK (2010) Targeting the reversibly oxidized protein tyrosine phosphatase superfamily. Sci Signal 3(137):pl2. doi:10.1126/scisignal.3137pl2
3. Gao L, Sun H, Yao SQ (2010) Activity-based high-throughput determination of PTPs substrate specificity using a phosphopeptide microarray. Biopolymers 94(6):810–819. doi:10.1002/bip.21533
4. Karisch R, Neel BG (2013) Methods to monitor classical protein-tyrosine phosphatase oxidation. FEBS J 280(2):459–475. doi:10.1111/j.1742-4658.2012.08626.x
5. Montalibet J, Skorey KI, Kennedy BP (2005) Protein tyrosine phosphatase: enzymatic assays. Methods 35(1):2–8. doi:10.1016/j.ymeth.2004.07.002
6. Persson C, Kappert K, Engstrom U, Ostman A, Sjoblom T (2005) An antibody-based method for monitoring in vivo oxidation of protein tyrosine phosphatases. Methods 35(1):37–43. doi:10.1016/j.ymeth.2004.07.006
7. Gil A, Rodríguez-Escudero I, Stumpf M, Molina M, Cid VJ (2015) A functional dissection of PTEN N-terminus: implications in PTEN subcellular targeting and tumor suppressor activity. PLoS One 10(4):e0119287
8. Stoker A (2005) Methods for identifying extracellular ligands of RPTPs. Methods 35(1):80–89. doi:10.1016/j.ymeth.2004.07.011
9. Tautz L, Mustelin T (2007) Strategies for developing protein tyrosine phosphatase inhibitors. Methods 42(3):250–260. doi:10.1016/j.ymeth.2007.02.014
10. Bishop AC, Zhang XY, Lone AM (2007) Generation of inhibitor-sensitive protein tyrosine phosphatases via active-site mutations. Methods 42(3):278–288. doi:10.1016/j.ymeth.2007.02.005
11. Haque A, Andersen JN, Salmeen A, Barford D, Tonks NK (2011) Conformation-sensing antibodies stabilize the oxidized form of PTP1B and inhibit its phosphatase activity. Cell 147(1):185–198. doi:10.1016/j.cell.2011.08.036
12. Barford D, Flint AJ, Tonks NK (1994) Crystal structure of human protein tyrosine phosphatase 1B. Science 263(5152):1397–1404

13. Barford D, Jia Z, Tonks NK (1995) Protein tyrosine phosphatases take off. Nat Struct Biol 2(12):1043–1053
14. Denu JM, Dixon JE (1998) Protein tyrosine phosphatases: mechanisms of catalysis and regulation. Curr Opin Chem Biol 2(5):633–641
15. Stuckey JA, Schubert HL, Fauman EB, Zhang ZY, Dixon JE, Saper MA (1994) Crystal structure of Yersinia protein tyrosine phosphatase at 2.5 A and the complex with tungstate. Nature 370(6490):571–575. doi:10.1038/370571a0
16. Zhang ZY (1998) Protein-tyrosine phosphatases: biological function, structural characteristics, and mechanism of catalysis. Crit Rev Biochem Mol Biol 33(1):1–52. doi:10.1080/10409239891204161
17. Guan KL, Dixon JE (1990) Protein tyrosine phosphatase activity of an essential virulence determinant in Yersinia. Science 249(4968):553–556
18. Dustin LB, Plas DR, Wong J, Hu YT, Soto C, Chan AC, Thomas ML (1999) Expression of dominant-negative src-homology domain 2-containing protein tyrosine phosphatase-1 results in increased Syk tyrosine kinase activity and B cell activation. J Immunol 162(5):2717–2724
19. Furukawa T, Itoh M, Krueger NX, Streuli M, Saito H (1994) Specific interaction of the CD45 protein-tyrosine phosphatase with tyrosine-phosphorylated CD3 zeta chain. Proc Natl Acad Sci U S A 91(23):10928–10932
20. Liu F, Chernoff J (1997) Protein tyrosine phosphatase 1B interacts with and is tyrosine phosphorylated by the epidermal growth factor receptor. Biochem J 327(Pt 1):139–145
21. Milarski KL, Zhu G, Pearl CG, McNamara DJ, Dobrusin EM, MacLean D, Thieme-Sefler A, Zhang ZY, Sawyer T, Decker SJ et al (1993) Sequence specificity in recognition of the epidermal growth factor receptor by protein tyrosine phosphatase 1B. J Biol Chem 268(31):23634–23639
22. Sun H, Charles CH, Lau LF, Tonks NK (1993) MKP-1 (3CH134), an immediate early gene product, is a dual specificity phosphatase that dephosphorylates MAP kinase in vivo. Cell 75(3):487–493
23. Flint AJ, Tiganis T, Barford D, Tonks NK (1997) Development of "substrate-trapping" mutants to identify physiological substrates of protein tyrosine phosphatases. Proc Natl Acad Sci U S A 94(5):1680–1685
24. Cote JF, Charest A, Wagner J, Tremblay ML (1998) Combination of gene targeting and substrate trapping to identify substrates of protein tyrosine phosphatases using PTP-PEST as a model. Biochemistry 37(38):13128–13137. doi:10.1021/bi9812591
25. Fukada M, Kawachi H, Fujikawa A, Noda M (2005) Yeast substrate-trapping system for isolating substrates of protein tyrosine phosphatases: isolation of substrates for protein tyrosine phosphatase receptor type z. Methods 35(1):54–63. doi:10.1016/j.ymeth.2004.07.008
26. Garton AJ, Flint AJ, Tonks NK (1996) Identification of p130(cas) as a substrate for the cytosolic protein tyrosine phosphatase PTP-PEST. Mol Cell Biol 16(11):6408–6418
27. Timms JF, Carlberg K, Gu H, Chen H, Kamatkar S, Nadler MJ, Rohrschneider LR, Neel BG (1998) Identification of major binding proteins and substrates for the SH2-containing protein tyrosine phosphatase SHP-1 in macrophages. Mol Cell Biol 18(7):3838–3850
28. Zhang SH, Liu J, Kobayashi R, Tonks NK (1999) Identification of the cell cycle regulator VCP (p97/CDC48) as a substrate of the band 4.1-related protein-tyrosine phosphatase PTPH1. J Biol Chem 274(25):17806–17812
29. Wu J, Katrekar A, Honigberg LA, Smith AM, Conn MT, Tang J, Jeffery D, Mortara K, Sampang J, Williams SR, Buggy J, Clark JM (2006) Identification of substrates of human protein-tyrosine phosphatase PTPN22. J Biol Chem 281(16):11002–11010. doi:10.1074/jbc.M600498200
30. Zhang ZY (2002) Protein tyrosine phosphatases: structure and function, substrate specificity, and inhibitor development. Annu Rev Pharmacol Toxicol 42:209–234. doi:10.1146/annurev.pharmtox.42.083001.144616
31. Sacco F, Perfetto L, Castagnoli L, Cesareni G (2012) The human phosphatase interactome: an intricate family portrait. FEBS Lett 586(17):2732–2739. doi:10.1016/j.febslet.2012.05.008
32. Tautz L, Critton DA, Grotegut S (2013) Protein tyrosine phosphatases: structure, function, and implication in human disease. Methods Mol Biol 1053:179–221. doi:10.1007/978-1-62703-562-0_13
33. Tonks NK (2006) Protein tyrosine phosphatases: from genes, to function, to disease. Nat Rev Mol Cell Biol 7(11):833–846. doi:10.1038/nrm2039
34. Facciuto F, Cavatorta AL, Valdano MB, Marziali F, Gardiol D (2012) Differential expression of PDZ domain-containing proteins in human diseases—challenging topics and novel issues. FEBS J 279(19):3538–3548. doi:10.1111/j.1742-4658.2012.08699.x
35. Subbaiah VK, Kranjec C, Thomas M, Banks L (2011) PDZ domains: the building blocks reg-

ulating tumorigenesis. Biochem J 439(2):195–205. doi:10.1042/BJ20110903

36. Sotelo NS, Schepens JT, Valiente M, Hendriks WJ, Pulido R (2015) PTEN-PDZ domain interactions: binding of PTEN to PDZ domains of PTPN13. Methods 77–78:147–156. doi:10.1016/j.ymeth.2014.10.017
37. Sotelo NS, Valiente M, Gil A, Pulido R (2012) A functional network of the tumor suppressors APC, hDlg, and PTEN, that relies on recognition of specific PDZ-domains. J Cell Biochem 113(8):2661–2670. doi:10.1002/jcb.24141
38. Ngeow J, Eng C (2015) PTEN hamartoma tumor syndrome: clinical risk assessment and management protocol. Methods 77–78:11–19. doi:10.1016/j.ymeth.2014.10.011
39. Pulido R (2015) PTEN: a yin-yang master regulator protein in health and disease. Methods 77–78:3–10. doi:10.1016/j.ymeth.2015.02.009
40. Song MS, Salmena L, Pandolfi PP (2012) The functions and regulation of the PTEN tumour suppressor. Nat Rev Mol Cell Biol 13(5):283–296. doi:10.1038/nrm3330
41. Worby CA, Dixon JE (2014) Pten. Annu Rev Biochem 83:641–669. doi:10.1146/annurev-biochem-082411-113907
42. Zhou J, Parada LF (2012) PTEN signaling in autism spectrum disorders. Curr Opin Neurobiol 22(5):873–879. doi:10.1016/j.conb.2012.05.004
43. Rodriguez-Escudero I, Fernandez-Acero T, Bravo I, Leslie NR, Pulido R, Molina M, Cid VJ (2015) Yeast-based methods to assess PTEN phosphoinositide phosphatase activity in vivo. Methods 77–78:172–179. doi:10.1016/j.ymeth.2014.10.020
44. Rodríguez-Escudero I, Oliver MD, Andrés-Pons A, Molina M, Cid VJ, Pulido R (2011) A comprehensive functional analysis of PTEN mutations: implications in tumor- and autism-related syndromes. Hum Mol Genet 20(21):4132–4142. doi:10.1093/hmg/ddr337
45. Deuel TF (2013) Anaplastic lymphoma kinase: "Ligand Independent Activation" mediated by the PTN/RPTPbeta/zeta signaling pathway. Biochim Biophys Acta 1834(10):2219–2223. doi:10.1016/j.bbapap.2013.06.004
46. Diamantopoulou Z, Kitsou P, Menashi S, Courty J, Katsoris P (2012) Loss of receptor protein tyrosine phosphatase beta/zeta (RPTPbeta/zeta) promotes prostate cancer metastasis. J Biol Chem 287(48):40339–40349. doi:10.1074/jbc.M112.405852
47. Makinoshima H, Ishii G, Kojima M, Fujii S, Higuchi Y, Kuwata T, Ochiai A (2012) PTPRZ1 regulates calmodulin phosphorylation and tumor progression in small-cell lung carcinoma. BMC Cancer 12:537. doi:10.1186/1471-2407-12-537
48. Mohebiany AN, Nikolaienko RM, Bouyain S, Harroch S (2013) Receptor-type tyrosine phosphatase ligands: looking for the needle in the haystack. FEBS J 280(2):388–400. doi:10.1111/j.1742-4658.2012.08653.x
49. Muller S, Kunkel P, Lamszus K, Ulbricht U, Lorente GA, Nelson AM, von Schack D, Chin DJ, Lohr SC, Westphal M, Melcher T (2003) A role for receptor tyrosine phosphatase zeta in glioma cell migration. Oncogene 22(43):6661–6668. doi:10.1038/sj.onc.1206763
50. Ulbricht U, Eckerich C, Fillbrandt R, Westphal M, Lamszus K (2006) RNA interference targeting protein tyrosine phosphatase zeta/receptor-type protein tyrosine phosphatase beta suppresses glioblastoma growth in vitro and in vivo. J Neurochem 98(5):1497–1506. doi:10.1111/j.1471-4159.2006.04022.x
51. Harroch S, Furtado GC, Brueck W, Rosenbluth J, Lafaille J, Chao M, Buxbaum JD, Schlessinger J (2002) A critical role for the protein tyrosine phosphatase receptor type Z in functional recovery from demyelinating lesions. Nat Genet 32(3):411–414. doi:10.1038/ng1004
52. Huang JK, Ferrari CC, Monteiro de Castro G, Lafont D, Zhao C, Zaratin P, Pouly S, Greco B, Franklin RJ (2012) Accelerated axonal loss following acute CNS demyelination in mice lacking protein tyrosine phosphatase receptor type Z. Am J Pathol 181(5):1518–1523. doi:10.1016/j.ajpath.2012.07.011
53. Kuboyama K, Fujikawa A, Masumura M, Suzuki R, Matsumoto M, Noda M (2012) Protein tyrosine phosphatase receptor type z negatively regulates oligodendrocyte differentiation and myelination. PLoS One 7(11):e48797. doi:10.1371/journal.pone.0048797
54. Herradon G, Ezquerra L (2009) Blocking receptor protein tyrosine phosphatase beta/zeta: a potential therapeutic strategy for Parkinson's disease. Curr Med Chem 16(25):3322–3329
55. Takahashi N, Sakurai T, Bozdagi-Gunal O, Dorr NP, Moy J, Krug L, Gama-Sosa M, Elder GA, Koch RJ, Walker RH, Hof PR, Davis KL, Buxbaum JD (2011) Increased expression of receptor phosphotyrosine phosphatase-beta/zeta is associated with molecular, cellular, behavioral and cognitive schizophrenia phenotypes. Transl Psychiatry 1:e8. doi:10.1038/tp.2011.8
56. Adamsky K, Arnold K, Sabanay H, Peles E (2003) Junctional protein MAGI-3 interacts with receptor tyrosine phosphatase beta (RPTP

beta) and tyrosine-phosphorylated proteins. J Cell Sci 116(Pt 7):1279–1289

57. Bourgonje AM, Navis AC, Schepens JT, Verrijp K, Hovestad L, Hilhorst R, Harroch S, Wesseling P, Leenders WP, Hendriks WJ (2014) Intracellular and extracellular domains of protein tyrosine phosphatase PTPRZ-B differentially regulate glioma cell growth and motility. Oncotarget 5(18):8690–8702
58. Kawachi H, Tamura H, Watakabe I, Shintani T, Maeda N, Noda M (1999) Protein tyrosine phosphatase zeta/RPTPbeta interacts with PSD-95/SAP90 family. Brain Res Mol Brain Res 72(1):47–54
59. Valiente M, Andrés-Pons A, Gomar B, Torres J, Gil A, Tapparel C, Antonarakis SE, Pulido R (2005) Binding of PTEN to specific PDZ domains contributes to PTEN protein stability and phosphorylation by microtubule-associated serine/threonine kinases. J Biol Chem 280(32):28936–28943. doi:10.1074/jbc.M504761200
60. Sambrook J (1989) Molecular cloning: a laboratory manual. Cold Spring Harbor Laboratory Press, Cold Spring Harbor, NY
61. Li DM, Sun H (1997) TEP1, encoded by a candidate tumor suppressor locus, is a novel protein tyrosine phosphatase regulated by transforming growth factor beta. Cancer Res 57(11):2124–2129
62. Maehama T, Dixon JE (1998) The tumor suppressor, PTEN/MMAC1, dephosphorylates the lipid second messenger, phosphatidylinositol 3,4,5-trisphosphate. J Biol Chem 273(22):13375–13378
63. Myers MP, Stolarov JP, Eng C, Li J, Wang SI, Wigler MH, Parsons R, Tonks NK (1997) P-TEN, the tumor suppressor from human chromosome 10q23, is a dual-specificity phosphatase. Proc Natl Acad Sci U S A 94(17):9052–9057
64. Myers MP, Pass I, Batty IH, Van der Kaay J, Stolarov JP, Hemmings BA, Wigler MH, Downes CP, Tonks NK (1998) The lipid phosphatase activity of PTEN is critical for its tumor suppressor function. Proc Natl Acad Sci U S A 95(23):13513–13518
65. Davidson L, Maccario H, Perera NM, Yang X, Spinelli L, Tibarewal P, Glancy B, Gray A, Weijer CJ, Downes CP, Leslie NR (2010) Suppression of cellular proliferation and invasion by the concerted lipid and protein phosphatase activities of PTEN. Oncogene 29(5):687–697. doi:10.1038/onc.2009.384
66. Gu J, Tamura M, Pankov R, Danen EH, Takino T, Matsumoto K, Yamada KM (1999) Shc and FAK differentially regulate cell motility and directionality modulated by PTEN. J Cell Biol 146(2):389–403
67. Meng K, Rodriguez-Pena A, Dimitrov T, Chen W, Yamin M, Noda M, Deuel TF (2000) Pleiotrophin signals increased tyrosine phosphorylation of beta beta-catenin through inactivation of the intrinsic catalytic activity of the receptor-type protein tyrosine phosphatase beta/zeta. Proc Natl Acad Sci U S A 97(6):2603–2608. doi:10.1073/pnas.020487997
68. Kawachi H, Fujikawa A, Maeda N, Noda M (2001) Identification of GIT1/Cat-1 as a substrate molecule of protein tyrosine phosphatase zeta/beta by the yeast substrate-trapping system. Proc Natl Acad Sci U S A 98(12):6593–6598. doi:10.1073/pnas.041608698

Chapter 6

Assays to Measure PTEN Lipid Phosphatase Activity In Vitro from Purified Enzyme or Immunoprecipitates

Laura Spinelli and Nicholas R. Leslie

Abstract

PTEN is a one of the most frequently mutated tumor suppressors in human cancers. It is essential for regulating diverse biological processes and through its lipid phosphatase activity regulates the PI 3-Kinase signaling pathway. Sensitive phosphatase assays are employed to study the catalytic activity of PTEN against phospholipid substrates. Here we describe protocols to assay PTEN lipid phosphatase activity using either purified enzyme (purified PTEN lipid phosphatase assay) or PTEN immunopurified from tissues or cultured cells (cellular IP PTEN lipid phosphatase assay) against vesicles containing radiolabeled PIP_3 substrate.

Key words PTEN, Phosphoinositide, Phosphatase, Phosphate, Tumor suppressor, PI3-Kinase, Cancer

1 Introduction

Phosphatase and tensin homolog deleted on chromosome 10 (PTEN) is a phosphatase that mainly localizes in the cytoplasm and antagonizes the phosphoinositide 3-kinase (PI3K) signaling pathway by dephosphorylating plasma membrane localized phosphatidylinositol-3,4,5-trisphosphate (PIP_3) and negatively regulating its downstream targets [1]. PTEN has been heavily studied due to its status as a tumor suppressor gene in which loss of function mutations are identified in many sporadic tumors and in the germ line of patients with Cowden disease and related phenotypes [2–6]. The predominant product of the *PTEN* gene is a 403-amino acid protein structured with an N-terminal phosphatase domain (residues 7–185) and a C-terminal C2 domain (residues 186–351). These two domains constitute the minimal catalytic unit [7, 8]. The phosphatase domain contains the highly conserved HCXXGXXR(S/T) (CX5R) active site motif, hallmark of protein tyrosine phosphatases [9], with Cysteine 124 required for catalysis as the active site nucleophile, and with many different mutations to

Rafael Pulido (ed.), *Protein Tyrosine Phosphatases: Methods and Protocols*, Methods in Molecular Biology, vol. 1447,
DOI 10.1007/978-1-4939-3746-2_6,

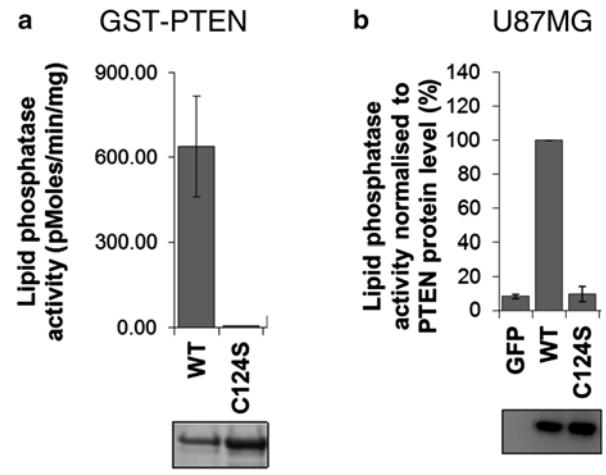

Fig. 1 PTEN assay data. Example experiments following the described protocol are shown using either (**a**) GST-PTEN (1 h and 500 ng enzyme at 30 °C assaying either wild-type enzyme or the phosphatase inactive mutant PTEN C124S) or (**b**) Untagged recombinant human PTEN protein was immunoprecipitated from 1 mg soluble protein extract derived from PTEN null U87MG cells. In the latter case, cells were transduced with viruses encoding either GFP, wild-type PTEN or PTEN C124S. Western blots using anti-PTEN antibodies display the amount of PTEN protein in each assay. This figure is adapted from data previously published [6]

the phosphatase domain resulting in loss of the phosphatase activity. As a lipid phosphatase, it is known that PTEN antagonizes PI3-Kinase, dephosphorylating at the D3 position, the PI3K lipid product PtdIns(3,4,5)P_3, which is generated by PI3K phosphorylation of PtdIns(4,5)P_2 [10, 11]. Through this mechanism PTEN affects AKT/PKB and other PIP_3-regulated proteins and thus a number of cell biological processes regulated by PI3K via PIP_3. Assaying PTEN lipid phosphatase activity in vitro is therefore a starting point to study PTEN function [12, 13]. Here, we describe in vitro protocols and present example data (Fig. 1), studying the catalytic activity of PTEN against phospholipid vesicle substrates containing radiolabeled PIP_3 that in our experience can give substantially greater sensitivity than assays detecting phosphate release using malachite green reagent and can detect low ng quantities of input enzyme.

2 Materials

2.1 Production of 3-(^{33}P)-PtdIns (3,4,5)P_3

1. PtdIns(4,5)P_2. Prepare 1 mM stock in methanol–chloroform 1:1. Store at −20 °C (*see* **Note 1**).
2. Phosphatidylserine (PS). Prepare a 5 mM stock in: chloroform–methanol 1:1. Store at −20 °C.

3. Resuspension buffer: 25 mM Hepes pH 7.4, 100 mM NaCl, and 1 mM EGTA.
4. γ-^{33}P ATP. Stored at −20 °C following radioisotope guidelines.
5. PI3K α (p110α and p85α heterodimer co-expressed and purified from insect cells or commercially available) and stored in small aliquots at −80 °C.
6. Reaction buffer: 25 mM Hepes pH 7.4, 100 mM NaCl, 1 mM EGTA, 0.2 mM EDTA, 2.5 mM $MgCl_2$, 1 mM DTT, 1 mM sodium orthovanadate, 0.2 mM PMSF, 1 mM benzamidine (*see* **Note 2**).
7. Assay termination buffer: chloroform–methanol–HCl (40:80:1) (*see* **Note 3**).
8. Chloroform ($CHCl_3$).
9. 0.1 M HCl.
10. Synthetic upper phase (*see* **Note 4**).
11. Phosphorylated substrate resuspension solvent: chloroform–methanol (2:1 v/v) (*see* **Note 5**).
12. Cup horn bath sonicator.
13. Centrifuge vacuum dryer.
14. Scintillation cocktail.
15. Liquid scintillation counter.

2.2 In Vitro PTEN Lipid Phosphatase Assay Components

1. Phosphatidylcholine (PC). Prepare a 33 mM stock in: chloroform–methanol 1:1. Store at −20 °C.
2. diC16 PtdIns(3,4,5)P_3. Prepare 1 mM stock in methanol–chloroform 1:1. Store at −20 °C (*see* **Note 6**).
3. ^{33}P-PtdIns(3,4,5)P_3 prepared and stored as described.
4. Lipid Vesicle resuspension buffer: 10 mM Hepes pH 7.4, 1 mM EGTA.
5. Purified recombinant PTEN protein (usually 100 ng per assay) in buffer containing: 50 mM Tris–HCl pH 7.4, 150 mM NaCl, 1 mM EGTA, 1 mM DTT, 10% glycerol. Store in small aliquots at −80 °C (*see* **Note 7**).
6. Reaction buffer: 50 mM Hepes pH 7.4, 150 mM NaCl, 1 mM EGTA, 10 mM DTT.
7. Bovine serum albumin (BSA) (10 mg/ml) (*see* **Note 8**).
8. 1 M perchloric acid (PCA) (*see* **Note 9**).
9. 10% (v/v) ammonium molybdate (*see* **Note 10**).
10. Toluene–isobutyl alcohol (1:1 v/v) (*see* **Note 11**).
11. Scintillation cocktail.

12. Centrifuge vacuum dryer.
13. Cup horn bath sonicator.
14. Scintillation counter.

2.3 Immunoprecipitated Cellular PTEN Lipid Phosphatase Assay Components

1. Tissue or cultured mammalian cells expressing PTEN.
2. Cell lysis buffer: 50 mM Tris–HCl pH 7.4, 150 mM NaCl, 1 mM EDTA, 1 mM EGTA, 5 mM sodium pyrophosphate, 10 mM β-glycerophosphate, 50 mM NaF, 1 % NP-40 and containing freshly added 0.2 mM phenylmethylsulfonyl fluoride (PMSF), 1 mM benzamidine, and 0.1 % β-mercaptoethanol.
3. 1× phosphate-buffered saline (PBS).
4. Protein G sepharose FastFlow beads (Sigma-Aldrich, St. Louis, MO, USA) (*see* **Note 12**).
5. Washing buffer: 50 mM Tris–HCl pH 7.4, 300 mM NaCl, 1 mM EDTA, 1 mM EGTA, 5 mM sodium pyrophosphate, 10 mM β-glycerophosphate, 50 mM NaF, 1 % NP-40 and containing freshly added 0.2 mM PMSF, 1 mM benzamidine, and 0.1 % β-mercaptoethanol.
6. Anti-PTEN antibody, e.g., Mouse monoclonal A2B1 unconjugated (Santa Cruz Biotechnology, Dallas, Texas, USA).
7. Phosphatidylcholine (PC) (Avanti Polar Lipids, Inc.). Prepare a 33 mM stock in: chloroform–methanol 1:1. Store at –20 °C.
8. diC16 PtdIns(3,4,5)P_3 (Cellsignals, Columbus, OH). Prepare 1 mM stock in methanol–chloroform 1:1. Store at –20 °C (*see* **Note 6**).
9. ^{33}P-PtdIns(3,4,5)P_3 prepared as described (*see* Subheading 3.1).
10. Lipid Vesicle resuspension buffer: 10 mM Hepes pH 7.4, 1 mM EGTA.
11. Reaction buffer: 50 mM Hepes pH 7.4, 150 mM NaCl, 1 mM EGTA, 10 mM DTT.
12. BSA (10 mg/ml) (*see* **Note 8**).
13. 1 M PCA (*see* **Note 9**).
14. 10 % (v/v) ammonium molybdate (*see* **Note 10**).
15. Toluene–isobutyl alcohol (1:1 v/v) (*see* **Note 11**).
16. Scintillation cocktail.
17. Centrifuge vacuum dryer.
18. Cup horn bath sonicator.
19. Liquid scintillation counter.
20. 4× lithium dodecyl sulfate (LDS) sample loading buffer.
21. β-mercaptoethanol.
22. 4–12 % precast SDS-polyacrylamide gel (SDS-PAGE) (*see* **Note 13**).

23. Polyvinylidene difluoride (PVDF) membrane.
24. PTEN antibody for immunoblotting. Several good antibodies are commercially available and the use of an antibody raised in a different species may allow immunoblotting for PTEN without interference from secondary antibody recognition of the primary anti-PTEN antibody originally used in immunoprecipitation.

3 Methods

Carry out all procedures on ice unless otherwise specified. Work with extreme care: remember you are using radioisotopes (*see* **Note 14**).

3.1 Production of 3-(^{33}P)-PtdIns(3,4,5)P_3 Substrate by Labeling at the D3 Position

1. Plan the scale of the substrate preparation required. Here we describe a 100 µl PI3K reaction but this could be scaled up or down. To a 2 ml screw cap Eppendorf tube add sufficient volume of lipid stocks (PS and PtdIns(4,5)P_2) that will give a final concentration of 100 µM phosphatidylserine (PS—2 µl from 5 mM stock) and 100 µM PtdIns(4,5)P_2 (10 µl from 1 mM stock) in the final total volume of aqueous reaction mix.
2. Dry the lipid mixture under vacuum to remove all organic solvents (*see* **Note 15**).
3. Submerge the lipid film in 50 µl of Lipid Reaction Buffer (LRB): 25 mM Hepes pH 7.4, 100 mM sodium chloride and 1 mM EGTA.
4. Sonicate the lipid mixture using a cup horn sonicator by three cycles of 15 s to resuspend the lipids, forming heterogeneous vesicles.
5. To the lipid vesicles add 25 µl of Kinase Buffer (25 mM Hepes pH 7.4, 100 mM sodium chloride, 1 mM EGTA, 0.2 mM EDTA, 2.5 mM $MgCl_2$, 1 mM dithiothreitol (DTT), 1 mM sodium orthovanadate, 0.2 mM phenylmethanesulfonyl fluoride (PMSF), 1 mM benzamidine) 500 µCi of (γ-^{33}P) ATP (18.5 MBq), and 10 µg of the PI3K to a total of 100 µl.
6. Incubate the mixture for 45 min in a water bath at 37 °C.
7. Add a second aliquot of PI3K and incubate for further 45 min at 37 °C.
8. Terminate the reaction by adding 750 µl of $CHCl_3$–CH_3OH–HCl (40:80:1).
9. Add 250 µl of chloroform and 400 µl 0.1 M HCl to make the ratio $CHCl_3$ (1)–CH_3OH (1)–aqueous (0.9).

10. Two layers will form. The sequential addition of solvent components is to allow acidification in a single phase before the phase split.
11. Remove and discard the all aqueous upper phase and any interphase precipitate (*see* **Note 16**).
12. Wash the lower organic phase three times with synthetic upper phase (*see* **Note 17**).
13. Dry the lower phase in a vacuum dryer (*see* **Note 18**).
14. Resuspend the dried substrate in 500 µl of $CHCl_3$–CH_3OH (2:1 v/v).
15. Add 2 µl of each of the three washes and 2 µl of substrate to individual tubes containing the scintillation cocktail and mix.
16. Determine the radioisotope incorporation into the ^{33}P labeled substrate by using a scintillation counter. Using the initial specific activity of the ATP, the concentration of ^{33}P-PIP_3 can be estimated.
17. Store the radiolabeled substrate at −20 °C following appropriate radioisotope guidelines.

3.2 In Vitro PTEN Lipid Phosphatase Assay

1. Determine the total volume of assay mix required for the day's experiments, using a volume of for example 100 µl per assay and with some residual.
2. Lipid vesicles are prepared by mixing sufficient lipid stocks to give a final concentration of 100 µM of phosphatidylcholine (PC—from 33 mM stock), 1 µM of diC16 PtdIns(3,4,5)P_3 in the final assay mixture along with a volume of ^{33}P-PtdIns(3,4,5)P_3 to give 100,000 dpm counts per assay (*see* **Note 19**).
3. Dry the lipids using a centrifuge vacuum dryer.
4. Submerge the dried substrate in a buffer containing 10 mM Hepes pH 7.4 and 1 mM EGTA.
5. Sonicate the mixture in a cup horn sonicator for three 15 s bursts, followed by 5 min of ice incubation to prepare lipid vesicles.
6. Dilute the enzyme (usually 100 ng (2 pmol) of recombinant PTEN per assay) in 50 µl of H_2O (*see* **Note 20**).
7. Add 25 µl of assay buffer containing 50 mM Hepes pH 7.4, 1 mM EGTA, 10 mM dithiothreitol (DTT) and 150 mM NaCl.
8. Add 25 µl of the radiolabeled substrate vesicles.
9. Incubate for 1 h or, in case of a time course, for the respective time points, at 37 °C on a shaker (*see* **Note 21**).
10. Terminate the reaction through the addition of 10 µl of BSA (10 mg/ml) and 500 µl of 1 M ice-cold PCA.

11. Mix the samples by vortex and incubate for 30 min on ice.
12. Centrifuge the samples at 14,000×*g* for 10 min at 4 °C to remove precipitated lipid and protein and transfer the supernatants to new tubes.
13. Add 10% (w/v) ammonium molybdate to the supernatant to form a complex with free phosphate released during the assay, which will become soluble in the later organic phase. Vortex and incubate for 10 min at room temperature.
14. Add 1 ml toluene–isobutyl alcohol (1:1 v/v). A two-phase mix will form.
15. Remove 500 μl of the upper organic phase containing the phosphate complex and mix it into 8 ml of liquid scintillation cocktail.
16. Determine the radioactivity using a liquid scintillation counter.

3.3 In Cell PTEN Lipid Phosphatase Assay

1. Seed cells, e.g., U87MG (PTEN null) or HEK293T cells (highly transfectable), in 10 cm dishes in 10 ml of recommended medium. Grow cells in a 37 °C incubator with 5% CO_2.
2. If necessary, express wild-type PTEN protein or mutants using plasmids transfection or lentiviral particles.
3. Immediately prior to lysis, wash the cells twice with 5 ml ice-cold 1× PBS.
4. Lyse cells on ice using 1 ml cell lysis buffer per 10 cm dish (50 mM Tris–HCl pH 7.4, 150 mM NaCl, 1 mM EDTA, 1 mM EGTA, 5 mM sodium pyrophosphate, 10 mM β-glycerophosphate, 50 mM NaF, 1% NP-40 and containing freshly added 0.2 mM PMSF), 1 mM benzamidine. Rotate the dish carefully to let the lysis buffer cover the entire area of grown cells.
5. Scrape the cells on ice with a cell scraper. Collect and transfer the cell lysates into a 1.5 ml microfuge tube on ice. Incubate the lysate on ice for 30 min.
6. Centrifuge the samples at 14,000×*g* for 15 min at 4 °C to remove any aggregated insoluble proteins and cellular debris.
7. Transfer the supernatant to a new ice-cold microfuge tube and keep on ice. Be careful not to transfer any pellet.
8. While the cell lysates are incubating on ice for 30 min, cut the narrow end of a P-200 pipette tip and transfer an appropriate amount of 50% protein G sepharose bead slurry (10 μl per sample) to a 1.5 ml microfuge tube (*see* **Notes 12** and **22**). Wash the beads thrice with 200 μl ice-cold PBS by centrifuging at 1000×*g* for 1 min.
9. Resuspend the beads in 500 μl of lysis buffer. Pre-couple the protein G sepharose beads with the antibody by incubating it

with PTEN A2B1 antibody at 4 °C for 1 h while gently mixing on a rotating shaker. Centrifuge the antibody-coupled beads at 2000 × *g* for 1 min at 4 °C and discard the supernatant. Pipette 10 μl of PTEN-antibody coupled beads to new Eppendorf tubes, one for each sample.

10. Add 1 ml of cell lysate to the PTEN-antibody coupled beads and incubate at 4 °C for 1 h with constant rotation.
11. Centrifuge the beads at 2000 × *g* for 1 min.
12. Wash the beads twice in lysis buffer with high salt (300 mM NaCl) and then with reaction buffer (50 mM Hepes pH 7.4, 1 mM EGTA, 10 mM dithiothreitol (DTT), and 150 mM NaCl) (*see* **Note 23**).
13. Aspirate the buffer and proceed for the assay as described above.
14. Together with cell lysate used for PTEN immunoprecipitation and assay, samples should be analyzed by western blotting in order to be able to monitor the level of PTEN expression.
15. For the samples to use for western blotting analysis, wash the beads thrice using centrifuge tube filters (*see* **Note 24**).
16. Add 30 μl of 1× LDS sample loading buffer and leave for 10 min at room temperature.
17. Spin down the samples. Discard the filters and add 10% β-mercaptoethanol to the samples.
18. Heat the samples at 70 °C for 10 min.
19. Resolve the samples on 4–12% SDS-PAGE gel.
20. After electrophoresis, transfer the proteins from a gel to a PVDF membrane, for 1 h at 30 V, in the presence of running buffer, using a tank wet transfer system and following standard protocols and manufacturer's guidelines.
21. Dry the PVDF membrane for 30 min and then block it with a solution of 5% (w/v) low fat milk protein or 5% (w/v) BSA made up in TBS-T (25 mM Tris–HCl pH 7.4, 150 mM NaCl, 2.5 mM KCl, 0.1% (v/v) Tween 20).
22. Wash the PVDF membrane for 30 min with three buffer changes of TBS-T, before its overnight incubation at 4 °C with a PTEN primary antibody made up in 5% (w/v) low fat milk protein or 5% (w/v) BSA in TBS-T.
23. Remove the primary antibody solution and wash the membrane for 30 min including three buffer changes of TBS-T.
24. Incubate the membrane with the appropriate HRP-linked secondary antibodies made up in 5% (w/v) low fat milk in TBS-T, for 1 h at room temperature.

25. Unbound secondary antibody is removed by washing the membrane over 30 min with three buffer changes of TBS-T.
26. Detect protein-antibody complexes using HRP chemiluminescence detection reagents following manufacturer' protocols (*see* **Note 25**).

4 Notes

1. The lipids used are available either in the acid form (Cellsignals, PtdIns(4,5)P_2-diC16 catalog number 902) or sodium salt form (PtdIns(4,5)P_2-diC16-Na catalog number 202). We recommend the latter.
2. Prepare the reaction buffer fresh each time. Use frozen aliquots of 1 M DTT. Add vanadate, PMSF, benzamidine, and DTT just before starting.
3. $CHCl_3$–CH_3OH–HCl (40:80:1) buffer can be made and stored at room temperature for short periods (weeks–months) in well-sealed glass containers. Evaporation of Chloroform during prolonged storage can change the ratio. Use glass pipettes or measuring cylinders to measure the solvents.
4. Synthetic upper phase refers to the upper phase solvent mixture after the phase split procedure and is prepared without dissolved solutes as a washing reagent. For precise replication of the synthetic upper phase solvent preparation,: use a 2 l separating funnel to mix methanol–chloroform–12 M HCl in a ratio 200:100:1 (750 ml final volume). Add 250 ml chloroform and 450 ml 0.1 M HCl. Mix thoroughly and leave to clarify overnight (shorter times tend to give a slightly cloudy phase split). Drain off the upper and lower phase separately and store separately at room temperature.
5. $CHCl_3$–CH_3OH (2:1 v/v) buffer can be made and stored at room temperature. Do not keep it for too long because evaporation of the components can change the ratio.
6. Cellsignals, sodium salt form (PtdIns(3,4,5)P_3-diC16-Na catalog number 208).
7. Recombinant PTEN protein can be expressed in E. coli cells as a fusion protein with glutathione *S*-transferase (GST). GST-PTEN is immobilized on GSH-Sepharose 4B bead slurry. Cleavage of the GST-tag from the fusion PTEN protein is then obtained by using PreScission protease enzyme. Add 10% glycerol to the untagged purified PTEN protein aliquots, snap-freeze in liquid nitrogen and store the aliquots at –80 °C.
8. We use essentially fatty acid free BSA prepared in water and stored at 4 °C.

9. Prepare 1 M PCA and store at 4 °C.
10. Prepare ammonium molybdate 10% w/v fresh every time. Vortex.
11. Prepare toluene–isobutyl alcohol (1:1 v/v) stock and store it at room temperature in a well-sealed glass bottle.
12. Resuspend the protein G sepharose beads thoroughly before dispensing.
13. Before loading the samples onto the Precast SDS-PAGE gels rinse the gels with tap water and gel wells at least three times with 1× running buffer.
14. Work in a designed area following the rules agreed by your institution. Always monitor the area of work, pipettes, equipment used, and yourself. If spillage occurs, clean and monitor the area of interest. Collect all the waste, liquid and/or solid, in a specific container.
15. The time required for the mixture to dry will vary based on the volume.
16. Be careful in removing the upper phase and make sure you avoid contamination of the lower phase. Alternatively, the lower phase can be removed from below the upper- and interphases to a fresh tube.
17. Add 2× lower phase volume of synthetic upper phase and leave for 5 min. Two layers will form. Keep 2 μl from each wash for radioactivity determination.
18. The time required for the mixture to dry will vary based on the volume.
19. Calculate the finale volume based on 100 μl for each sample (e.g., 100 μl × *N*—number of samples). Always prepare a sample where the enzyme is substituted with water. This will represent the assay background. If analyzing the activity of expressed PTEN mutant proteins always have in your assay a PTEN wild-type (positive control) and an inactive mutant, e.g., PTEN C124S (catalytically dead—negative control).

    The addition of a known excess concentration of non-radiolabeled PIP_3 provides a more confident substrate concentration and allows the more accurate analysis of reaction kinetics.
20. Keep proteins always on ice in order to preserve their catalytic activity.
21. If you are performing a phosphatase assay in a time point format, start from the longest time point and in a countdown manner add the substrate just before the beginning of the time point.
22. Remember to prepare a sample where the beads are incubated only with lysis buffer instead of cell lysate. This will represent

the assay background. Samples immunoprecipitated from cells lacking PTEN allow the assessment of any apparent activity derived from other contaminating phosphatases.

23. We use high salt (0.3 M NaCl) washing buffer so that nonspecific binding to the beads is reduced and thus likely to be specific to PTEN. Wash the beads at least three times to reduce background signals.
24. Use a bench centrifuge or, if available, a vacuum manifold.
25. Use X-ray film processed using an automatic developer or acquire the image directly using an imaging system.

Acknowledgements

We would like to thank the members of the NRL laboratory for their constructive discussions. Work developing and applying these assays was funded by the Medical Research Council (grant code G0801865).

References

1. Song MS, Salmena L, Pandolfi PP (2012) The functions and regulation of the PTEN tumour suppressor. Nat Rev Mol Cell Biol 13(5): 283–296
2. Cairns P et al (1997) Frequent inactivation of PTEN/MMAC1 in primary prostate cancer. Cancer Res 57(22):4997–5000
3. Dahia PL et al (1997) Somatic deletions and mutations in the Cowden disease gene, PTEN, in sporadic thyroid tumors. Cancer Res 57(21):4710–4713
4. Liaw D et al (1997) Germline mutations of the PTEN gene in Cowden disease, an inherited breast and thyroid cancer syndrome. Nat Genet 16(1):64–67
5. Marsh DJ et al (1997) Germline mutations in PTEN are present in Bannayan-Zonana syndrome. Nat Genet 16(4):333–334
6. Spinelli L et al (2015) Functionally distinct groups of inherited PTEN mutations in autism and tumour syndromes. J Med Genet 52(2): 128–134
7. Lee JO et al (1999) Crystal structure of the PTEN tumor suppressor: implications for its phosphoinositide phosphatase activity and membrane association. Cell 99(3):323–334
8. Vazquez F, Sellers WR (2000) The PTEN tumor suppressor protein: an antagonist of phosphoinositide 3-kinase signaling. Biochim Biophys Acta 1470(1):M21–M35
9. Denu JM, Dixon JE (1998) Protein tyrosine phosphatases: mechanisms of catalysis and regulation. Curr Opin Chem Biol 2(5): 633–641
10. Myers MP et al (1998) The lipid phosphatase activity of PTEN is critical for its tumor suppressor function. Proc Natl Acad Sci U S A 95(23):13513–13518
11. Engelman JA, Luo J, Cantley LC (2006) The evolution of phosphatidylinositol 3-kinases as regulators of growth and metabolism. Nat Rev Genet 7(8):606–619
12. McConnachie G et al (2003) Interfacial kinetic analysis of the tumour suppressor phosphatase, PTEN: evidence for activation by anionic phospholipids. Biochem J 371(Pt 3):947–955
13. Spinelli L, Leslie NR (2015) Assaying PTEN catalysis in vitro. Methods 77–78:51–57

Chapter 7

Assessing the Biological Activity of the Glucan Phosphatase Laforin

Carlos Romá-Mateo, Madushi Raththagala, Mathew S. Gentry, and Pascual Sanz

Abstract

Glucan phosphatases are a recently discovered family of enzymes that dephosphorylate either starch or glycogen and are essential for proper starch metabolism in plants and glycogen metabolism in humans. Mutations in the gene encoding the only human glucan phosphatase, laforin, result in the fatal, neurodegenerative, epilepsy known as Lafora disease. Here, we describe phosphatase assays to assess both generic laforin phosphatase activity and laforin's unique glycogen phosphatase activity.

Key words Glycogen, Lafora disease, Dual-specificity phosphatase

1 Introduction

Lafora progressive myoclonus epilepsy (LD, OMIM 254780) is a rare, fatal, neurological disorder characterized by neurodegeneration, epilepsy, and the accumulation of glycogen-like (polyglucosan) inclusions (named Lafora bodies, LBs) in neurons and other cell types in peripheral tissues. Two main causative genes have been identified, *EPM2A* that encodes the glucan phosphatase laforin and *EPM2B* that encodes the E3-ubiquitin ligase malin. It has been recently described that laforin and malin regulate glycogen biosynthesis [1–4], explaining why defects in any of these two proteins lead to the accumulation of LBs.

Laforin is the only human phosphatase with a carbohydrate-binding domain (CBM; belonging to the CBM20 family) in the same polypeptide [5, 6]. Laforin also contains a C-terminal dual-specificity phosphatase (DSP) domain, and utilizes a strictly conserved cysteine residue (Cys266) at the base of the active site to perform nucleophilic attack on the phosphorus atom of the substrate. The DSPs are a diverse clade of phosphatases within the larger protein tyrosine phosphatase superfamily that includes

Rafael Pulido (ed.), *Protein Tyrosine Phosphatases: Methods and Protocols*, Methods in Molecular Biology, vol. 1447,
DOI 10.1007/978-1-4939-3746-2_7,

members able to dephosphorylate pSer, pThr, and pTyr as well as members that dephosphorylate non-proteinaceous substrates such as phosphoinositols, nucleic acids, and glycogen or starch [7]. Accordingly, recombinant laforin is able to dephosphorylate in vitro artificial phosphatase substrates such as 4-*para*-nitrophenylphosphate (pNPP) and 3-*O*-methyl fluorescein phosphate (OMFP; a more sensitive substrate of DSPs) [8–10]. Laforin is the founding member of the glucan phosphatase family, phosphatases that dephosphorylate either glycogen or starch [1]. Biochemical data, glycogen analysis from mouse models, and the laforin crystal structure all demonstrate that laforin dephosphorylates glycogen in vivo [11–13].

More than 33 Lafora disease point mutations in laforin have been described to date [14]. These mutations are scattered between laforin's CBM and DSP domains and they affect the phosphatase activity of laforin to different extents [13]. In order to correlate the phosphatase activity found in the mutated forms of laforin with their pathological output, we describe methods to quantify both the generic phosphatase activity of laforin and its specific glycogen phosphatase activity.

2 Materials

Prepare all solutions using double-distilled, deionized MilliQ filtered water. Sterile conditions are not required for in vitro phosphatase assays. All manipulations can be performed at room temperature unless otherwise specified.

2.1 pNPP/OMFP Phosphatase Assay

1. Phosphatase buffer 1: 100 mM Tris–HCl pH: 8, 150 mM NaCl, 10 mM DTT, 0.5 mM OMFP.
2. Phosphatase buffer 2: 0.1 M sodium acetate, 0.05 M Tris, 0.05 M Bis-Tris, pH: 8, 10 mM DTT, 10 mM pNPP.
3. Recombinant protein: At least 0.5 μg of purified phosphatase enzyme.
4. Sodium vanadate (Na_3VO_4) and carbohydrate reagents (i.e., glycogen).
5. 96-Well ELISA plates and multi-plate spectrophotometer reader.

2.2 Glycogen Phosphatase Assay

1. Phosphatase buffer 3 (5× stock): 0.5 M Sodium acetate, 0.25 M Bis, 0.25 M Tris. Adjust to pH 6.5 with HCl.
2. Glycogen purified from rabbit skeletal muscle.
3. Recombinant laforin: 100–500 ng per reaction.

4. Malachite green reagent: Ammonium molybdate tetrahydrate and malachite green carbinol hydrochloride.
5. Tween 20, *N*-ethylmaleimide (NEM), dithiothreitol (DTT).
6. Spectrophotometer.

3 Methods

pNPP is a classical colorimetric substrate used in enzymatic activity assays. Dephosphorylation of pNPP produces an increase in absorbance at the wavelength of 405–410 nm, proportional to pNP formation by hydrolysis. pNPP is highly specific for the active-site pocket of tyrosine protein phosphatases (PTPs); however, it is less efficient in the subfamily of dual-specificity phosphatases (DSPs). DSPs exhibit a shallower active-site pocket in which the long and narrow structure of pNPP, resembling tyrosine-phosphorylated residues, is not as easily accommodated in the DSP phosphatase active site. The OMFP structure comprises a series of aromatic rings that confer a planar structure more appropriate for the active-site cleft in DSPs, which are able to dephosphorylate both pTyr and pSer/Thr residues, as well as other phosphorylated substrates ([15]; Fig. 1). The hydrolysis of OMFP to OMF produces a similar increment in absorbance as that observed in pNP, but in this case at a higher wavelength (around 490 nm).

Either substrate can be added to a phosphatase buffer reaction that includes a specific amount of the purified phosphatase, producing an increment in absorbance proportional to both phosphatase and substrate concentrations. The reaction can be analyzed by a unique measurement after a defined incubation time. However, in the present protocol we describe a method for obtaining enzymatic activity curves of phosphatase activity, by measuring long-term kinetics of increases in absorbance via multiple and consecutive measurements. Thus, the protocol avoids having to stop the reaction (classically with a NaOH solution which abolishes further

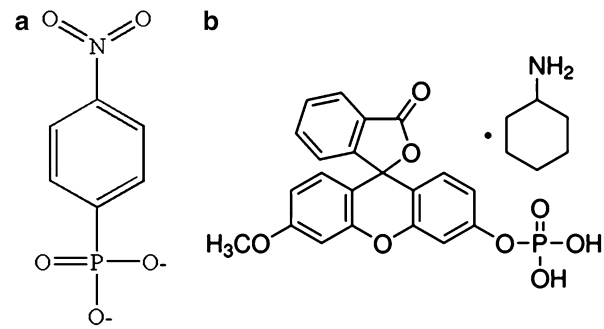

Fig. 1 pNPP (**a**) and OMFP (**b**) structures

dephosphorylation) and provides a first-glance overview of the kinetic features of the analyzed phosphatase. This method allows the evaluation of the effect of different compounds on the phosphatase activity of laforin, as in the case of the inhibitory action of glycogen, described below.

pNPP and OMFP assays (Subheading 3.1) are optimized to define the generic phosphatase activity of a specific phosphatase, i.e., laforin. These assays provide a fast, reproducible, colorimetric measurement of laforin's generic phosphatase activity. However, they do not utilize the biologically relevant substrate glycogen. The third assay in this chapter (Subheading 3.2) is specifically developed and optimized to detect glucan phosphatase activity of laforin using glycogen.

Malachite green-molybdate-based assays have been commonly used in the past for quantifying picomolar amounts of inorganic free phosphate [16–18]. Unlike OMFP and pNPP, malachite green reagent is not an artificial substrate. Instead, it forms a green color complex with free ortho phosphate in aqueous solutions under acidic conditions (*see* Fig. 4a). The malachite green phosphomolybdate complex is stable and provides a fast, nonradioactive way of detecting picomolar amounts of inorganic free phosphate at 620 nm. A recently developed malachite green-based assay is able to determine specific glucan phosphatase activity of laforin [19]. Also, a similar assay has been employed to detect phosphate release from laforin's physiological substrate, glycogen [11, 13]. Subheading 3.2 describes the methodology for quantifying phosphate release of rabbit skeletal muscle glycogen by laforin.

3.1 pNPP/OMFP Phosphatase Assay

1. *Preparation of phosphatase buffer*. First, determine the optimum pH for each phosphatase to be assayed (*see* **Note 1**). In the case of laforin the optimal pH is 8 [20]. DTT should be added just before use (in the case of laforin at 10 mM). A stock buffer solution (phosphatase buffers 1 and 2; *see* Subheading 2.1) should be prepared to use it as reaction buffer and to dilute the substrate of the reaction (pNPP/OMFP; *see* **Note 2** for details on solubility) and to prepare enzyme dilutions if needed. Once prepared, the buffer should be kept at 4 °C or in ice prior to use. The buffer should be freshly prepared, and DTT added immediately before the reaction starts.
2. *Preparation of protein dilutions*. Protein preparations should be in the range of 0.5–5 μg/μl (*see* **Notes 3** and **4**). In a standard phosphatase reaction, a minimum amount of 1 μg of protein will be required to obtain a relevant phosphatase activity. In the case of laforin we follow the reaction for 1 h for a good measurement of phosphatase activity under standard conditions.
3. *Preparation of the plates*. The final volume for the reaction is 200 μl. Each well will contain 100 μl of phosphatase buffer with purified protein (plus any other substance to be assayed,

e.g., vanadate or carbohydrates). One well should be left for a blank reaction containing only phosphatase buffer (*see* **Note 5**). The plate can be maintained on ice or at 4 °C.

4. *Preparation of the plate reader*. An automated program should be prepared to produce a series of consecutive measurements. The measuring parameters (interval between measurements; total duration of the assay) are dependent on the intrinsic phosphatase activity of the phosphatase used, the concentration of substrate, and the assayed conditions (i.e., presence of inhibiting compounds). These variables should be empirically evaluated in order to define the time needed to reach saturation, thus establishing the linear range of the reaction (*see* Fig. 2a for an example). The temperature should be set to the optimal for each phosphatase (37 °C for laforin and most human PTPs). Make sure that the reader has reached the desired temperature before starting the assay. For pNPP assays, absorbance should be measured at 405 nm; for OMFP assays, the absorbance measured is 490 nm.

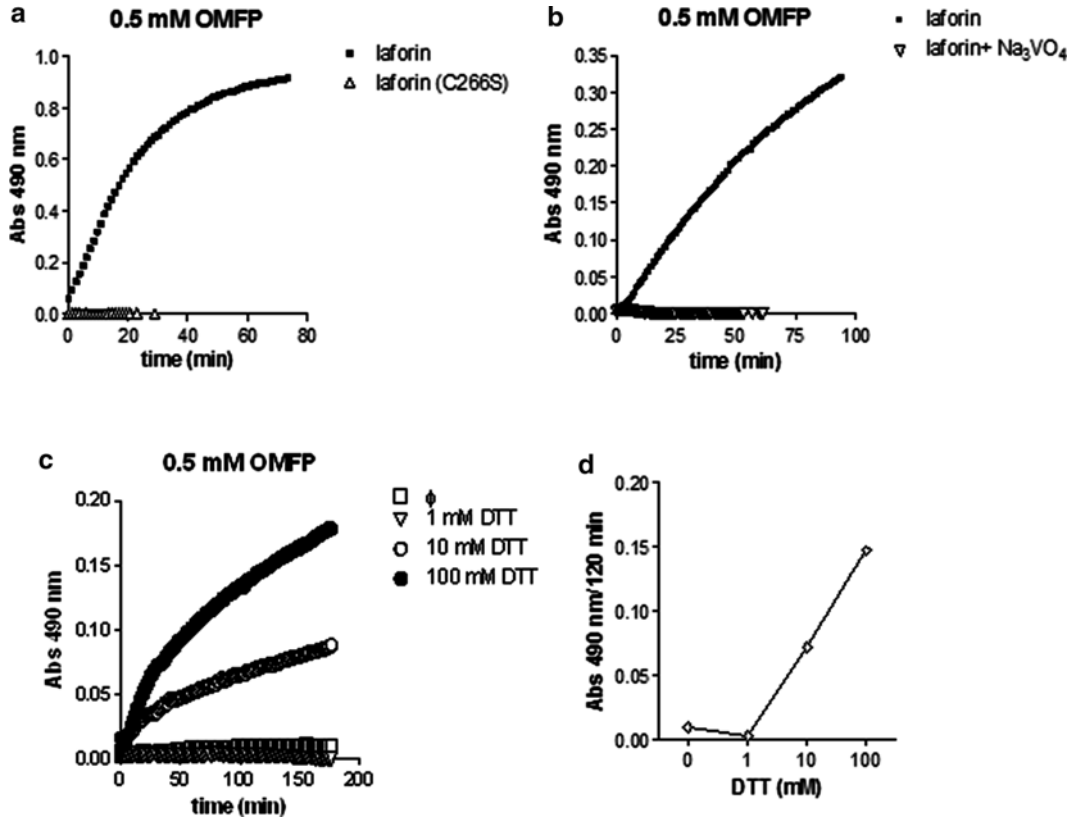

Fig. 2 Laforin phosphatase shows a typical enzymatic kinetics for OMFP dephosphorylation and a cysteine-dependent catalytic mechanism (**a**). Plots are shown for wild-type laforin and for the C226S laforin mutation, targeting the catalytic cysteine of the enzyme. (**b**) Vanadate inhibition. (**c**) Reducing environment dependence. (**d**) Plot of the maximal absorbance reached at different DTT concentrations

5. *Starting the reaction*. Since both pNPP and OMFP suffer slow but significant spontaneous dephosphorylation, all reactions including the blank should be started at the same time (*see* **Note 3**). Use a multichannel pipet to add 100 μl of reaction buffer containing the corresponding chromogenic substrate (*see* **Note 2**) quickly and equally to all the wells. Immediately after adding the substrate, initiate measuring via the plate reader.
6. *Displaying the results*. Absorbance values should be displayed in columns next to the corresponding time interval. If the reader software does not automatically normalize values, the absorbance value obtained for the blank well in any given time should be subtracted from the corresponding time interval in the rest of wells. Representing absorbance values in the Y-axis and time interval values in the X-axis will produce the curve for phosphatase activity (Fig. 2). Obtaining completely saturated curves is convenient for the determination of kinetic parameters (*see* **Note 6**). To compare the global dephosphorylation capacity of the enzyme, regardless of kinetics, maximum absorbance values can be displayed (*see* Fig. 2d). In order to compare different proteins or substrates, the absorbance values obtained with this method should be normalized and transformed adequately, converting absorbance values into amount of substrate hydrolyzed (the use of a pNP or OMF standard curve would be necessary) per protein amount and time unit; this final value is usually expressed as specific activity of the enzyme. The glucan phosphatase laforin displays a measurable phosphatase activity using pNPP or OMFP as a substrate, although OMFP is a more efficient substrate.

   Sodium vanadate is a specific inhibitor of cysteine-based PTPs that mimics the phosphate binding to the catalytic pocket of the enzyme, completely abolishing phosphatase activity [21]. Hence, addition of a final concentration of 1 mM sodium vanadate to the buffer solution provides a valuable tool as a negative control to distinguish artificial substrate dephosphorylation or contamination of the purified protein with non-PTP phosphatases (Fig. 2b).

   It has been described that glycogen decreases laforin activity against pNPP [9]. This effect could be explained by the binding of laforin to glycogen, which could interfere with the entry of the substrate to the catalytic pocket. The protocol described above can be used to assess the effect of any substance on the phosphatase reaction, just by including the compound in the phosphatase reaction buffer. As an example, we describe the use of the method to test the decrease in laforin OMFP activity by glycogen (Fig. 3). In these experiments, increasing concentrations of glycogen were used in the phosphatase reaction together with OMFP.

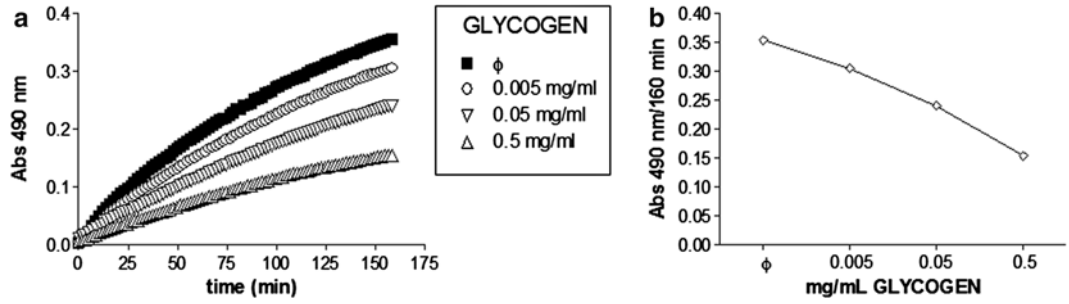

Fig. 3 Glycogen inhibition of the glucan phosphatase laforin

3.2 Glycogen Phosphatase Assay

1. *Preparation of assay buffer*. Similar to Subheading 3.1, it is important to determine the optimum pH for glycogen phosphatase activity. Laforin is active within a pH range of 6.5–8.0. The optimum pH for laforin's glycogen phosphatase activity is pH 6.5. Make a 5× assay buffer stock (phosphatase buffer 3; *see* Subheading 2.2) at the desired pH and store at 4 °C. Prior to the experiment, make a fresh 1× assay buffer solution with 10 mM DTT to prepare the necessary protein dilutions or substrate solutions (*see* **Note 7**).
2. *Standard curve for quantifying glycogen phosphatase activity*. Make a 100 mM stock solution of KH_2PO_4 using ultrapure H_2O (*see* **Notes 7** and **8**). Make serial dilutions to obtain solutions containing 100 pmol to 1 nmol of KH_2PO_4. Mix 40 µl of these solutions with 80 µl of malachite green reagent (with 0.01% Tween 20). Tween 20 stabilizes the malachite green phosphomolybdate complex for up to 48 h [22]. Incubate reactions for 30 min and measure absorbance at 620 nm using a spectrophotometer.
3. *Preparation of protein dilutions*. Protein dilutions should be in the range of 0.1–1.0 µg/µl. For example, laforin has a higher specific phosphatase activity compared to the plant glucan phosphatases (SEX4 and LSF2); therefore, the amount of protein must be appropriately calibrated to be within the linear range [2, 23, 24]. In a standard glucan phosphatase assay with amylopectin, a minimum amount of 100 ng of protein incubated for 10 min is sufficient to obtain absorbance values within the linear range [25]. However, rabbit skeletal muscle glycogen contains lower amounts of phosphate than potato amylopectin and the assay's color development depends on the amount of free phosphate present in the reaction (*see* **Note 9**). Therefore, begin the assay initially with 100 ng of protein and incubate for 30 min with 40–100 µg of glycogen to see whether there is detectable phosphatase activity under standard conditions. However, longer incubation times and higher substrate concentrations may be necessary depending on the amount of phosphate groups present in the rabbit skeletal muscle glycogen (*see* **Note 10**).

4. *Preparation of malachite green reagent.* Prepare malachite green reagent by making 1 volume of 4.2 % (w/v) ammonium molybdate tetrahydrate in 4 M HCl. Add 3 volumes of 0.045 % (w/v) malachite green carbinol hydrochloride (*see* **Note 7**). Stir the contents for 30 min at room temperature and filter with Whatman filter paper. Malachite green reagent can be stored at 4 °C away from light for a few weeks (*see* **Note 8**). Just before the experiment is initiated, add 10 % (v/v) Tween 20 to an aliquot of malachite green reagent to make the final concentration of Tween 20 to 0.01 % (v/v).
5. *Preparation of reaction tubes.* Each reaction is performed in a final volume of 20 µl, with six replicates for each enzyme to be tested. First, calculate the number of reactions to be performed and make a master mixture with all the assay components except the enzyme, as it will be added to start the reaction. For one reaction, mix 4 µl of 5× assay buffer of the desired pH, 9 µl of 5 mg/ml rabbit skeletal muscle glycogen, and 2 µl of 100 mM DTT in a 0.5 ml Eppendorf tube. These components will give a final concentration of 100 mM sodium acetate, 50 mM Bis-Tris, 50 mM Tris–HCl, 5 mM DTT, and 45 µg of rabbit skeletal muscle glycogen per reaction.
6. *Starting the assay.* The reaction starts when 5 µl of diluted enzyme (100–500 ng) are mixed with 15 µl of the assay components in the 0.5 ml Eppendorf tube. Timing is critical for the assay and a timer should be initiated once enzyme is added to the first reaction tube. Add enzyme to a tube in 30-s time intervals for subsequent reactions. Incubate all reactions for 30 min at 37 °C. Maintaining a constant and consistent incubation time for each tube is important in obtaining accurate and reproducible data (*see* **Note 11**).
7. *Terminating the assay.* The enzymatic activity of laforin can be stopped by adding 20 µl of 0.1 M NEM to the reaction mixture and vortexing the tube for 10 s. NEM modifies thiol groups and thereby irreversibly inhibits the phosphatase activity of all protein tyrosine phosphatases, including laforin [26]. Add 80 µl of malachite green reagent to each of the reaction tubes and vortex for 10 s. Incubate all reactions for 30 min at room temperature before measuring the absorbance at 620 nm using a spectrophotometer (*see* **Note 12**). The glucan phosphatase laforin has robust glycogen phosphatase activity while the human proteinaceous phosphatase VHR lacks this activity (Fig. 4b). Mutation of the laforin catalytic cysteine to serine (C266S) ablates the laforin glycogen phosphatase activity (Fig. 4b). Lafora disease patient mutations in the CBM (W32G) or DSP (T142A) domains dramatically decrease the laforin glycogen phosphatase activity (Fig. 4b) (*see* **Notes 13** and **14**).

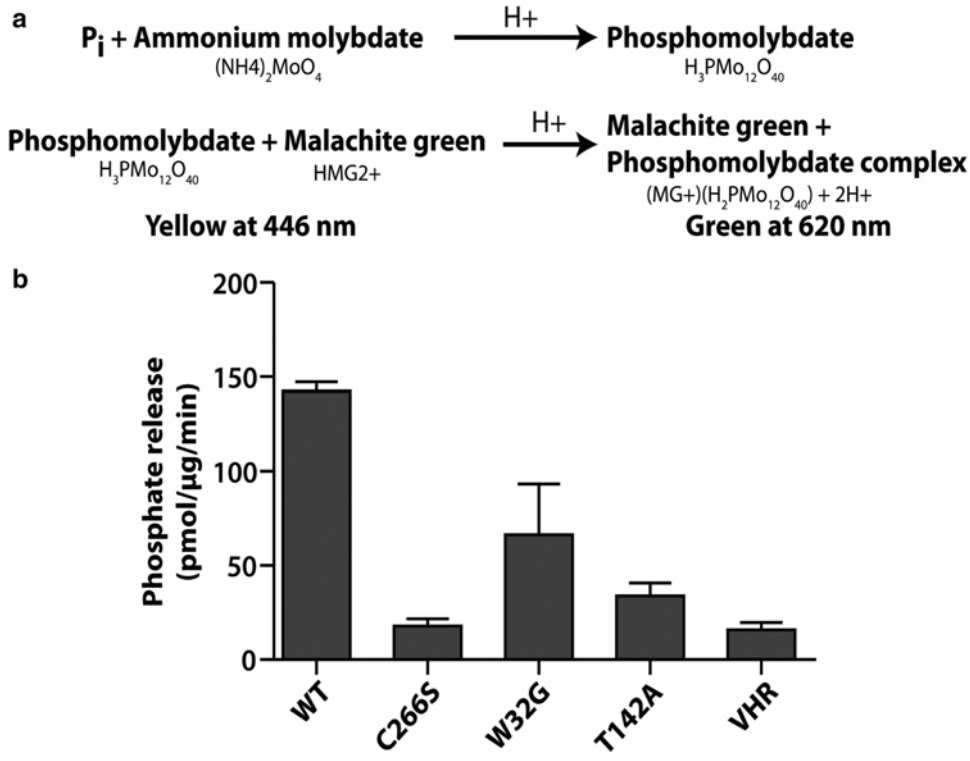

Fig. 4 Malachite green-based glycogen phosphatase assay. (**a**) When phosphate monoesters in glycogen are hydrolyzed, the free phosphate reacts with ammonium molybdate. At a low pH, the basic malachite green dye forms a complex with phosphomolybdate and shifts to its absorption maximum. This complex is stabilized by the addition of Tween 20, allowing for colorimetric detection at 620 nm that is linear with as little as 50–1000 pmol of P_i. (**b**) Specific activity of laforin wild type, laforin mutants, and human VHR against glycogen. A total of 100 ng of protein was incubated with 45 μg glycogen for 20 min. Each bar is the mean ± SEM of five replicates; $p < 0.05$

4 Notes

1. It is critical to assess the optimal pH for each phosphatase; the method presented in this chapter provides a straightforward way to assay different pH values in the phosphatase buffer, by comparing the enzyme kinetics in the same plate and experimental conditions.
2. The substrate for the phosphatase reaction should be prepared in a 2× concentration. Each substrate presents some particularities that should be considered. To prepare the *pNPP solution*, pNPP can be easily diluted in water, in concentrations ranging from 5 to 100 mM. For the reaction described here, a solution of 20 mM DTT in phosphatase reaction buffer should be prepared. When a volume of this solution is mixed with the same volume of phosphatase reaction buffer containing the

protein, a final concentration of 10 mM in the assay will be obtained. To prepare the *OMFP solution*, 1.05 mg OMFP should be first diluted in 1 ml methanol (other organic solvents can be assayed) and vortexed vigorously in order to obtain a homogeneous, milky-faint yellow 2 mM solution. Then, a 1:1 solution in phosphatase reaction buffer will produce a colorful, yellow 1 mM preparation that can be used as the 2× substrate solution. When a volume of this solution is mixed with the same volume of phosphatase reaction buffer containing the protein, a final concentration of 0.5 mM OMFP will be obtained.

3. The progress of the reaction must be observed to determine the proper measuring intervals. For very active phosphatases, a 10 mM pNPP solution can produce saturation within minutes; hence intervals in the range of 10–30 s should be sufficient to obtain a nice curve. In the case of laforin, the best curves are obtained using 0.5 mM OMFP as a substrate, and intervals in the minute range can lead to a nice curve in a period of ½ to 1 h.
4. Recombinant proteins often present either carboxy- or amino-terminal tags; it should be taken into account that these tags could affect phosphatase activity of the enzyme.
5. Given the catalytic requirements of the active site in cysteine-based PTPs, reducing conditions are required. Thus, reducing agents such as DTT, TCEP, or β-mercaptoethanol should be added to reaction mixtures. The dependence of each phosphatase to specific redox conditions should be assessed, since reducing agents can affect also the oligomerization state of proteins. In the example of the glucan phosphatase laforin, redox conditions affect oligomerization, and also affect phosphatase activity [20, 27] (Fig. 2c, d).
6. Performing phosphatase assays as those represented by Fig. 2 and using different substrate concentrations are useful to determine Michaelis-Menten constants. When using different substrate concentrations, a blank for each condition should be left without protein, since both pNPP and OMFP spontaneously dephosphorylate and dephosphorylation rate can be affected by concentration, as well as by any other substance added to the reaction buffer when comparing conditions and/or enzyme modifiers.
7. Malachite green reagent detects free phosphate in aqueous solutions. Prepare all solutions using ultrapure water that has the sensitivity of 18 MΩ cm at 25 °C. Diligently follow cleaning procedures as many soaps and dish detergents contain phosphate. All glassware should be rinsed extensively with ultrapure water before use to avoid any contaminations and to decrease the background absorbance of the assay.

8. Malachite green reagent is light sensitive and changes color from yellow to green/brown over time if it is exposed to light. Prepare new reagent in a timely manner before there is a color change, typically within weeks. Also, small divalent cations such as magnesium, calcium, and manganese have lower solubility in the presence of phosphate. Check water purity if precipitation occurs. A yellow color malachite green reagent with no precipitate gives reproducible and accurate measurements.
9. Mammalian glycogen contains small amounts of covalently attached phosphate groups. Use of commercially available glycogen as a substrate has not been successful. It may be due to the low availability/accessibility of phosphate groups in certain types of glycogen [1]. The Roach group reported that rabbit skeletal muscle glycogen is a substrate for malachite green-based glycogen dephosphorylating assays and they have published elegant methodology to purify glycogen from rabbit skeletal muscle [11, 28].
10. Glycogen consists of a series of concentric rings of glucose chains. This unique structure may hinder laforin's activity to remove phosphate groups in the inner regions of glycogen. Increased sensitivity may be achieved by adding alpha amylase and amyloglucosidase enzymes to the substrate to disrupt glycogen structure [11].
11. Low levels of color development may be due to inadequate amounts of substrate, enzyme, or incubation times. Optimize the assay with each preparation of rabbit skeletal muscle glycogen.
12. If a heavy precipitation is observed in the reaction with glycogen but not in the standard curve reactions, then there are two possibilities to consider. (a) The precipitation could be due to higher phosphate content on the rabbit skeletal muscle glycogen. If this is the case, then dilute the glycogen stock, using less glycogen per reaction. (b) The precipitation could be due to phosphate contamination in the enzyme or glycogen samples.
13. Kinetic studies are possible with the assay; however, interpreting kinetics of glycogen dephosphorylation by laforin is complex [11]. In addition to glycogen being polydispersed, laforin is a dimer containing two catalytic sites and two carbohydrate-binding modules. Unlike OMFP/pNPP assay described above, the progress of the color development cannot be assayed over time. Separate reactions are needed for each time point.
14. This method can be easily amenable to a 96-well plate or 396-well plate format if high-throughput detection is needed.

Acknowledgments

This study was supported by grants from the Spanish Ministry of Education and Science SAF2014-54604-C3-1-R (P.S.), Generalitat Valenciana (PrometeoII/2014/029) (P.S.), NIH Grants R01NS070899 (M.S.G.), P20GM103486 (M.S.G.), Mizutani Foundation for Glycoscience Award (M.S.G.), and NSF Grant IIA-1355438 (M.S.G.). C.R.-M. was supported by the *Saving Lives at Birth Consortium*.

References

1. Worby CA, Gentry MS, Dixon JE (2006) Laforin, a dual specificity phosphatase that dephosphorylates complex carbohydrates. J Biol Chem 281(41):30412–30418
2. Gentry MS, Dowen RH III, Worby CA, Mattoo S, Ecker JR, Dixon JE (2007) The phosphatase laforin crosses evolutionary boundaries and links carbohydrate metabolism to neuronal disease. J Cell Biol 178(3):477–488
3. Vilchez D, Ros S, Cifuentes D, Pujadas L, Valles J, Garcia-Fojeda B, Criado-Garcia O, Fernandez-Sanchez E, Medrano-Fernandez I, Dominguez J, Garcia-Rocha M, Soriano E, Rodriguez de Cordoba S, Guinovart JJ (2007) Mechanism suppressing glycogen synthesis in neurons and its demise in progressive myoclonus epilepsy. Nat Neurosci 10(11):1407–1413
4. Solaz-Fuster MC, Gimeno-Alcaniz JV, Ros S, Fernandez-Sanchez ME, Garcia-Fojeda B, Criado Garcia O, Vilchez D, Dominguez J, Garcia-Rocha M, Sanchez-Piris M, Aguado C, Knecht E, Serratosa J, Guinovart JJ, Sanz P, Rodriguez de Cordoba S (2008) Regulation of glycogen synthesis by the laforin-malin complex is modulated by the AMP-activated protein kinase pathway. Hum Mol Genet 17(5):667–678
5. Minassian BA, Ianzano L, Meloche M, Andermann E, Rouleau GA, Delgado-Escueta AV, Scherer SW (2000) Mutation spectrum and predicted function of laforin in Lafora's progressive myoclonus epilepsy. Neurology 55(3):341–346
6. Wang J, Stuckey JA, Wishart MJ, Dixon JE (2002) A unique carbohydrate binding domain targets the lafora disease phosphatase to glycogen. J Biol Chem 277(4):2377–2380
7. Tonks NK (2006) Protein tyrosine phosphatases: from genes, to function, to disease. Nat Rev 7(11):833–846
8. Ganesh S, Tsurutani N, Suzuki T, Ueda K, Agarwala KL, Osada H, Delgado-Escueta AV, Yamakawa K (2003) The Lafora disease gene product laforin interacts with HIRIP5, a phylogenetically conserved protein containing a NifU-like domain. Hum Mol Genet 12(18): 2359–2368
9. Wang W, Roach PJ (2004) Glycogen and related polysaccharides inhibit the laforin dual-specificity protein phosphatase. Biochem Biophys Res Commun 325(3):726–730
10. Girard JM, Le KH, Lederer F (2006) Molecular characterization of laforin, a dual-specificity protein phosphatase implicated in Lafora disease. Biochimie 88(12):1961–1971
11. Tagliabracci VS, Turnbull J, Wang W, Girard JM, Zhao X, Skurat AV, Delgado-Escueta AV, Minassian BA, Depaoli-Roach AA, Roach PJ (2007) Laforin is a glycogen phosphatase, deficiency of which leads to elevated phosphorylation of glycogen in vivo. Proc Natl Acad Sci U S A 104(49):19262–19266
12. Tagliabracci VS, Girard JM, Segvich D, Meyer C, Turnbull J, Zhao X, Minassian BA, Depaoli-Roach AA, Roach PJ (2008) Abnormal metabolism of glycogen phosphate as a cause for Lafora disease. J Biol Chem 283(49):33816–33825
13. Raththagala M, Brewer MK, Parker MW, Sherwood AR, Wong BK, Hsu S, Bridges TM, Paasch BC, Hellman LM, Husodo S, Meekins DA, Taylor AO, Turner BD, Auger KD, Dukhande VV, Chakravarthy S, Sanz P, Woods VL Jr, Li S, Vander Kooi CW, Gentry MS (2015) Structural mechanism of laforin function in glycogen dephosphorylation and lafora disease. Mol Cell 57(2):261–272
14. Singh S, Ganesh S (2009) Lafora progressive myoclonus epilepsy: a meta-analysis of reported mutations in the first decade following the discovery of the EPM2A and NHLRC1 genes. Hum Mutat 30(5):715–723
15. Gottlin EB, Xu X, Epstein DM, Burke SP, Eckstein JW, Ballou DP, Dixon JE (1996) Kinetic analysis of the catalytic domain of

human cdc25B. J Biol Chem 271(44): 27445–27449

16. Lanzetta PA, Alvarez LJ, Reinach PS, Candia OA (1979) An improved assay for nanomole amounts of inorganic phosphate. Anal Biochem 100(1):95–97
17. Harder KW, Owen P, Wong LK, Aebersold R, Clark-Lewis I, Jirik FR (1994) Characterization and kinetic analysis of the intracellular domain of human protein tyrosine phosphatase beta (HPTP beta) using synthetic phosphopeptides. Biochem J 298(Pt 2):395–401
18. McCain DF, Zhang ZY (2002) Assays for protein-tyrosine phosphatases. Methods Enzymol 345:507–518
19. Sherwood AR, Johnson MB, Delgado-Escueta AV, Gentry MS (2013) A bioassay for Lafora disease and laforin glucan phosphatase activity. Clin Biochem 46(18):1869–1876
20. Sanchez-Martin P, Raththagala M, Bridges TM, Husodo S, Gentry MS, Sanz P, Roma-Mateo C (2013) Dimerization of the glucan phosphatase laforin requires the participation of cysteine 329. PLoS One 8(7):e69523
21. Huyer G, Liu S, Kelly J, Moffat J, Payette P, Kennedy B, Tsaprailis G, Gresser MJ, Ramachandran C (1997) Mechanism of inhibition of protein-tyrosine phosphatases by vanadate and pervanadate. J Biol Chem 272(2):843–851
22. Itaya K, Ui M (1966) A new micromethod for the colorimetric determination of inorganic phosphate. Clin Chim Acta 14(3): 361–366
23. Meekins DA, Guo HF, Husodo S, Paasch BC, Bridges TM, Santelia D, Kotting O, Vander Kooi CW, Gentry MS (2013) Structure of the Arabidopsis glucan phosphatase like sex four2 reveals a unique mechanism for starch dephosphorylation. Plant Cell 25(6):2302–2314
24. Meekins DA, Raththagala M, Husodo S, White CJ, Guo HF, Kotting O, Vander Kooi CW, Gentry MS (2014) Phosphoglucan-bound structure of starch phosphatase Starch Excess4 reveals the mechanism for C6 specificity. Proc Natl Acad Sci U S A 111(20):7272–7277
25. Sherwood AR, Paasch BC, Worby CA, Gentry MS (2013) A malachite green-based assay to assess glucan phosphatase activity. Anal Biochem 435(1):54–56
26. Walton KM, Dixon JE (1993) Protein tyrosine phosphatases. Annu Rev Biochem 62:101–120
27. Dukhande VV, Rogers DM, Roma-Mateo C, Donderis J, Marina A, Taylor AO, Sanz P, Gentry MS (2011) Laforin, a dual specificity phosphatase involved in lafora disease, is present mainly as monomeric form with full phosphatase activity. PLoS One 6(8):e24040
28. DePaoli-Roach AA, Contreras CJ, Segvich DM, Heiss C, Ishihara M, Azadi P, Roach PJ (2015) Glycogen phosphomonoester distribution in mouse models of the progressive myoclonic epilepsy, Lafora disease. J Biol Chem 290(2):841–850

Chapter 8

Discovery and Evaluation of PRL Trimer Disruptors for Novel Anticancer Agents

Yunpeng Bai, Zhi-Hong Yu, and Zhong-Yin Zhang

Abstract

Overexpression of PRL phosphatases (PRL1, PRL2, and PRL3) has been found in a variety of late-stage tumors and their distant metastatic sites. Therefore, the oncogenic PRL phosphatases represent intriguing targets for cancer therapy. There is considerable interest in identifying small molecule inhibitors targeting PRLs as novel anticancer agents. However, it has been difficult to acquire phosphatase activity-based PRL inhibitors due to the unusual wide and shallow catalytic pockets of PRLs revealed by crystal structure studies. Here, we present a novel method to identify PRL1 inhibitors by targeting the PRL1 trimer interface and the procedure to characterize their biochemical and cellular activity.

Key words PRL phosphatases, Virtual screening, Trimerization, MTT assay, Wound healing assay, Transwell migration assay

1 Introduction

The PRL phosphatases, consisting of three members (PRL1, PRL2, and PRL3; gene names PTP4A1, PTP4A2, and PTP4A3), represent a novel subfamily of protein tyrosine phosphatases (PTPs) sharing a high degree (>75 %) of amino acid sequence identity [1–3]. As the first identified member, the expression of PRL1 was found to be elevated in many tumor cell lines, and cells expressing high levels of PRL1 exhibited enhanced proliferation and anchorage-independent growth [1, 2, 4, 5]. Overexpression of PRL2 was also observed in different cancers, such as prostate cancer [6]. PRL3 level was found to be highly increased in colon cancer liver metastasis but not in nonmetastatic tumors or in normal colorectal epithelium [7]. Both PRL1 and PRL3 expressing cells displayed enhanced cell motility and invasiveness and induced metastatic tumor formation in mice [3, 8]. Mechanistically, PRLs promote cell proliferation and migration through a number of signaling pathways, such as PI3K/Akt, Src, Rho family of small GTPases as well as p53 signaling pathways [9, 10]. All these

Rafael Pulido (ed.), *Protein Tyrosine Phosphatases: Methods and Protocols*, Methods in Molecular Biology, vol. 1447,
DOI 10.1007/978-1-4939-3746-2_8,

observations suggest that PRLs play a critical role in cancer progression, and that PRLs are potential targets for novel anticancer therapeutic strategies. Thus, considerable interest has been focused on identifying small molecule inhibitors targeting PRLs for novel anticancer agents. However, there has been no effective PRL inhibitors reported to date [11–13].

Structural studies showed that the catalytic pockets of the PRLs are unusually wide and shallow, which makes it difficult to design PRL inhibitors by targeting the active site [14]. However, all of the PRL1 crystal structures solved so far reveal an identical trimeric arrangement [14–17]. Trimerization provides a membrane-binding surface with the C-terminal polybasic residues and the adjacent prenylation group positioned to anchor the PRL1 on the acidic inner membrane. In addition, given the high homology among all three PRLs, trimerization revealed in PRL1 may be a general property for all PRL enzymes [16]. Moreover, PRL1 trimer formation appeared to be essential for the PRL1-mediated cell growth and migration [16]. Most importantly, PRLs are highly expressed in many human cancer types, but no evidence for point mutations in PRLs has been identified, suggesting that overexpression may increase the propensity for PRL trimerization and contribute to malignancies. Thus, targeting the trimer interface of PRLs is a novel approach to develop small molecule therapeutics for PRL driven cancer treatment.

Here, we present methods to identify and evaluate PRL1 trimer disruptors for anticancer therapy. The methods include the identification of small molecule compounds targeting PRL1 trimer interface by virtual screening; the validation of the compounds as PRL1 de-trimerizers by in vitro and in vivo cross-linking assays; and the evaluation of cellular activity of the compounds by cell-based assays. The methods are designed to establish a novel strategy to develop PRL inhibitors by targeting PRLs trimer interface and to demonstrate the potential therapeutic value of PRL trimer disruptors as novel anticancer agents.

2 Materials

Solutions and reagents are prepared using analytical grade reagents in deionized MilliQ filtered water at room temperature. Reagents for cell-based assay are prepared in sterile conditions.

2.1 Identification of Small Molecules Targeting PRL1 Trimer Interface by Virtual Screening

1. Dell OPTIPLEX 380 Workstation running Red Hat Enterprise Linux 5.
2. BigRed supercomputer in Indiana University.
3. PDBePISA [18] Online Server (http://www.ebi.ac.uk/pdbe/pisa/).
4. RCSB Protein Data Bank database (http://www.rcsb.org).

5. ZINC small molecule 3D-structure database [19] (http://zinc.docking.org/).
6. UCSF Chimera software package [20] (http://www.cgl.ucsf.edu/chimera/).
7. DOCK6.2 software package [21, 22] (http://dock.compbio.ucsf.edu/).
8. AutoDock4.01 software package [23, 24] (http://autodock.scripps.edu/).
9. AutoDockTools software package [25, 26] (http://mgltools.scripps.edu/).

2.2 Validation of PRL1 De-trimerization Compounds by In Vitro Cross-linking Assay

1. Bacterial expression vector pET21a-$(His)_6$-tagged-PRL1.
2. Luria broth (LB) medium, 100 mg/mL ampicillin, 1 M DTT, and 1 M IPTG.
3. Binding buffer: 500 mM NaCl, 20 mM Tris–HCl (pH 7.9), and 5 mM Imidazole.
4. Wash buffer: 500 mM NaCl, 20 mM Tris–HCl (pH 7.9), and 20 mM Imidazole.
5. Elution buffer: 500 mM NaCl, 20 mM Tris–HCl (pH 7.9), and 300 mM Imidazole.
6. Protease inhibitors: 1 M PMSF (Phenylmethylsulfonyl fluoride).
7. Ni-NTA agarose.
8. Phosphate-buffered saline (PBS): 1.85 mM NaH_2PO_4, 8.4 mM $NaHPO_4$, and 150 mM NaCl.
9. Cross-linker: Glutaraldehyde (25% glutaraldehyde solution, grade I).
10. Reaction termination buffer: 0.5 M Tris–HCl (pH 7.5).
11. 6× SDS sample buffer: 0.375 M Tris–HCl (pH 6.8), 12% SDS, 60% glycerol, 0.6 M DTT, 0.06% bromophenol blue.
12. SDS-PAGE gel reagents: Resolving gel buffer: 1.5 M Tris–HCl (pH 8.8); Stacking gel buffer: 0.5 M Tris–HCl (pH 6.8); 30% acrylamide/Bis solution, 10% SDS, 10% APS and TEMED.
13. 10× SDS-PAGE running buffer: 0.25 M Tris–HCl (pH 8.3), 1.92 M glycine, and 1% SDS.
14. Coomassie Blue Stain Reagent.

2.3 Validation of PRL1 De-trimerization Compounds by In Vivo Cross-linking Assay

1. Mammalian expression vector pcDNA3.1 (+)-HA-tagged PRL1.
2. Cell culture medium: DMEM supplemented with 10% fetal bovine serum (FBS), penicillin (50 U/mL), and streptomycin (50 μg/mL).
3. Cross-linker: Formaldehyde (16% formaldehyde solution).

4. Phosphate-buffered saline (PBS): 1.85 mM NaH_2PO_4, 8.4 mM $NaHPO_4$, and 150 mM NaCl.
5. Lysis buffer: 50 mM Tris–HCl (pH 7.4), 150 mM NaCl, 1% Triton-100, 10% glycerol supplemented with a complete protease inhibitor tablet.
6. Anti-HA primary antibody, HRP-linked secondary anti-rabbit IgG, protein A/G-agarose beads, and prestained molecular weight standard marker.
7. Nitrocellulose Membranes.
8. Filter Paper.
9. 1× Transfer buffer: 25 mM Tris base, 192 mM glycine, and 20% (v/v) methanol.
10. 10× TBST buffer: 200 mM Tris–HCl (pH 7.5), 1.5 M NaCl, and 0.5% Tween-20.
11. Blocking solution: 5% milk in TBST.
12. Chemiluminescent substrate.

2.4 Evaluation of the Cellular Activity of PRL1 De-trimerization Compounds

1. 5 mg/mL MTT (3-(4,5-Dimethylthiazol-2-yl)-2,5-Diphenyltetrazolium Bromide).
2. DMSO (Dimethyl sulfoxide).
3. Cell starvation medium: DMEM supplemented with penicillin (50 U/mL), and streptomycin (50 μg/mL).
   Also *see* materials in Subheading 2.3.

3 Methods

3.1 Identification of Small Molecules Binding at PRL1 Trimer Interface by Virtual Screening

PRL1 exists as a trimer in the crystal structure (Fig. 1a), which results in two intermolecular interfaces for each PRL1 molecule, i.e., the BA-interface and BC-interface for monomer B. A small molecule binding at either interface may disrupt the trimer formation, thus driving us to perform virtual screening simultaneously on each interface. A two-stage screening process is depicted in Fig. 1b: the Asinex and ChemBride subsets in the ZINC database were used as small molecule library for screening. Both libraries were firstly screened by rigid docking in DOCK6.2 program, and the top 10% molecules were chosen based on the docking score for the subsequent flexible docking in AutoDock4.01, then the final hit molecules were picked out based on binding energy ranking, binding mode inspection, and structure similarity analyses. The experimental details are described below step by step.

1. Prepare the receptor structure for rigid docking in DOCK6.2.
   Retrieve the PRL1 trimer structure (PDBID: 1ZCK) [14] from the RCSB Protein Data Bank database and save it as

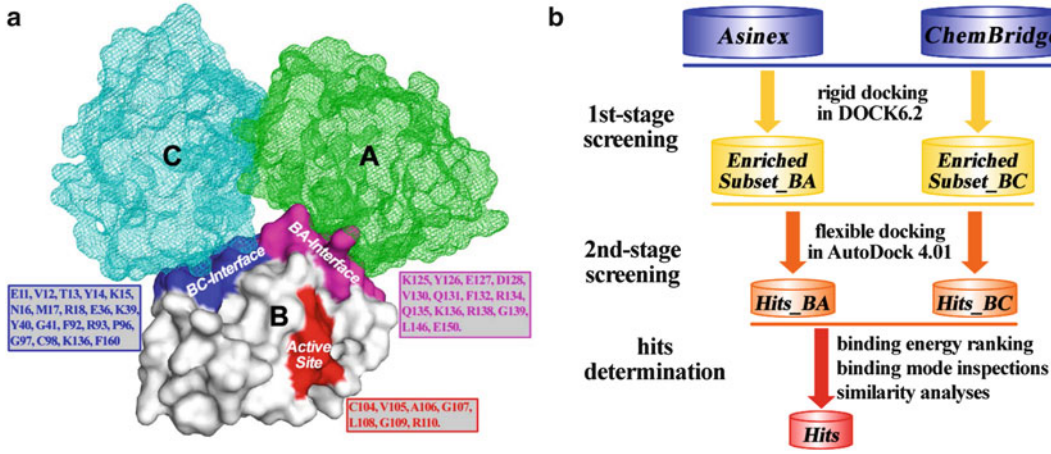

Fig. 1 (**a**) The PRL1 trimer arrangement in the crystal structure. By taking monomer B as a representative PRL1 monomer, two trimer interfaces, namely BA-interface and BC-interface, are highlighted in **purple** and **blue**, and residues constituting the interface surface are listed correspondingly. The CX_5R catalytic motif is colored in **red** to highlight the active site. (**b**) The pipeline of the two-stage virtual screening process

1zck.pdb. Load *1zck.pdb* into the UCSF Chimera software, remove waters and bound ligands, save it as *prl1.pdb*. Remove chain A and C, and process chain B using the "Dock Prep". Save the processed file as *prl1b.mol2*, as well as *prl1b.pdb*. Delete the newly added hydrogens and save as *prl1b_noH.pdb*.

2. Define the docking region for rigid docking.
   - At the PDBePISA Online Server (http://www.ebi.ac.uk/pdbe/pisa/), submit the *prl1.pdb* file for interface analyses to determine intermolecular interface residues within chain B. Two interfaces (BA-interface and BC-interface) were found, and residues constituted either interface are listed in Fig. 1a.
   - Generate the molecular surface of the receptor using dms program using a command "**dms prl1b_noH.pdb -n -w 1.4 -v -o prl1b.ms**".
   - Generate the spheres surrounding the receptor by running sphgen program, with *prl1b.ms* as input molecular surface file and *prl1b.sph* as output spheres file.
   - Select spheres to represent the binding site on either interface by running *sphere_selector* program with *prl1b.sph* as input sphere file. To represent binding site on the BA-interface, select all spheres within 8 Å distance of residues V130 and Q131, save the selected spheres in the file *selected_spheres_ba.sph*. To represent binding site on the BC-interface, select all spheres within 8 Å of residues N16 and M17, save the selected spheres in the file *selected_spheres_bc.sph*.

3. Prepare the energy grid files for rigid docking.
   - Create a rectangle box around the binding site using showbox program. To create the box surrounding BA-interface, use *selected_spheres_ba.sph* as input sphere file and set the extra margin to 5 Å, the output file is named as *ba_interface_box.pdb*. Similarly, to create the box surrounding BC-interface, use *selected_spheres_bc.sph* as input sphere file and set the extra margin to 5 Å, the output file is named as *bc_interface_box.pdb*.
   - Create an input file *grid_ba.in* to set essential parameters for running grid program to generate the energy grid around the BA-interface. In this file, set compute_grids, energy_score, bump_filter to "yes"; atom_model to "a"; energy_cutoff_distance to "999"; receptor_file to "prl1b.mol2"; box_file to "ba_interface_box.pdb"; score_grid_prefix to "grid_ba". Use default value for other parameters.
   - Execute the command "**grid -i grid_ba.in -o grid_ba.out**". Two energy grid files *grid_ba.nrg* and *grid_ba.bmp* will be generated once the computation is done.
   - Generate an input file *grid_bc.in* to set essential parameters for running grid program to generate the energy grid around the BC-interface. Set box_file to "*bc_interface_box.pdb*"; score_grid_prefix to "grid_bc". The other parameters are same with that in *grid_ba.in* above.
   - Execute the command "**grid -i grid_bc.in -o grid_bc.out**". Two energy grid files *grid_bc.nrg* and *grid_bc.bmp* will be generated once the computation is done.
4. Prepare the ligand structure for rigid docking.

   The Asinex and ChemBridge subsets in ZINC database (version 7) were used as small molecule library for virtual screening. The coordinates were downloaded from ZINC website (http://zinc.docking.org) in 28 mol2 files, which were sequentially named as *asin0.mol2*, …, *asin14.mol2* for Asinex subset, or *chbr0.mol2*, …, *chbr12.mol2* for ChemBridge subset. Each file contains 20,000 molecules; thus there are totally 560,000 molecules in the two libraries. The 3D structure of each small molecule is already in ready-to-dock mol2 format.
5. Create input files for docking calculation.
   - Create an input file *ba_asin0.in* to set essential parameters for screening 20,000 molecules in the file *asin0.mol2* on BA-interface. Set ligand_atom_file to "asin0.mol2"; receptor_site_file to "selected_spheres_ba.sph"; max_orientations to "1000"; grid_score_grid_prefix to "grid_ba";

ligand_outfile_prefix to "ba_asin0"; rank_ligands to "yes"; max_ranked_ligands to "2000". Use default value for other parameters. According to these parameters, the 20,000 molecules in *asin0.mol2* file will be docked at BA-interface; for each small molecule, it's automatically positioned for 1000 orientations, the lowest interaction energy and related conformation are recorded. All 20,000 molecules are ranked based on their lowest interaction energy, and the top 2000 molecules are saved to *ba_asin0.mol2* file.

- Copy *ba_asin0.in* as a new input file *ba_asin1.in*, in which only change ligand_atom_file to "asin1.mol2". Repeat this step to generate additional 26 input files for docking the other 26 mol2 files. Thus, there are 28 input files for docking calculation on BA-interface, namely *ba_asin0.in*, …, *ba_asin14.in* and *ba_chbr0.in*, …, *ba_chbr12.in*.
- Repeat the previous steps to generate 28 input files for docking calculation on BC-interface, namely *bc_asin0.in*, …, *bc_asin14.in* and *bc_chbr0.in*, …, *bc_chbr12.in*. In these input files, set receptor_site_file to "selected_spheres_bc.sph"; set grid_score_grid_prefix to "grid_bc".

6. Perform rigid docking in DOCK6.2.
   - Generate a job script file dock6_ba_asin0 for running docking calculation for molecules in the file asin0.mol2 on BA-interface. In this script file, the key command for performing docking calculation is: "mpirun -machinefile/tmp/machinelist.$LOADL_STEP_ID -np 16 dock6.mpi -i ba_asin0.in -o ba_asin0.out", which means that: DOCK6.2 parallel version is used for docking calculation; 16 CPUs are used for docking calculation; all docking parameters are read from the file ba_asin0.in; and the output will be saved in ba_asin0.out.
   - Use the command line "llsubmit dock6_ba_asin0" to submit the job to the job scheduler for queuing. The job will start once the requested CPUs are available.
   - Repeat the previous steps to submit additional 55 jobs. For the key command in each job script file, the input file ba_asin0.in needs to be changed to one of the other 55 docking input files, and the output file ba_asin0.out needs to be renamed correspondingly.
   - Once all jobs are finished, for each interface, 56,000 molecules (28 mol2 files, 2000 molecules in each file) are picked out and combined as an enriched binder subset at the trimer interface. These molecules were used for the subsequent flexible docking in AutoDock4.01.

7. Prepare the receptor structure for flexible docking in AutoDock4.01.

   Use *prl1b.pdb* as an input file and execute the command "**prepare_receptor4.py -r prl1b.pdb -o prl1b.pdbqt**". During this process, the nonpolar hydrogens are merged; the Gasteiger charge and autodock4 atom type are added for each atom. The resulted *prl1b.pdbqt* file will be used as receptor structure for docking in AutoDock4.01.

8. Define the docking region and generate energy grid for flexible.

   - Load *prl1b.pdbqt* file into AutoDockTools software. Click the menu "Grid → Macromolecule → Choose…" to choose prl1b as receptor. Click the menu "Grid → Set Map Types → Directly…" to set ligand atom type as "H HD HS C A N NA NS OA OS F P SA S Cl Br I" (see Note 1). Click the menu "Grid → Grid Box…" to open the "Grid Options" dialog and bring out a rectangle box. By adjusting the number of points in x, y, z dimension and the grid box center, move the box to cover the BA-interface. The number of points in x, y, z is set to 50, 50, 72, and the grid box center locates at (−0.2, −0.1, 25.9). Save these values and close the "Grid Options" dialog. Click the menu "Grid → Output → Save GPF…" to save as *ba_grid.gpf*.
   - Click the menu "Grid → Grid Box…" to open the "Grid Options" dialog again. Move the box to cover the BC-interface. The number of points in *x*, *y*, *z* is set to 50, 50, 72, and the grid box center locates at (−19.0, −5.0, 37.6). Save these values and close the "Grid Options" dialog. Click the menu "Grid → Output → Save GPF…" to save as *bc_grid.gpf*.
   - Make a directory *ba_maps*, copy *prl1b.pdbqt* and *ba_grid.gpf* into the directory. Execute the command "**autogrid4 -p ba_grid.gpf -l ba_grid.glg**" to generate 19 energy grid files (17 atom types plus electrostatic and desolvation potential) around BA-interface (*see* **Note 1**).
   - Make a directory *bc_maps*, copy *prl1b.pdbqt* and *bc_grid.gpf* into the directory. Execute the command "**autogrid4 -p bc_grid.gpf -l bc_grid.glg**" to generate 19 energy grid files (17 atom types plus electrostatic and desolvation potential) around BC-interface.

9. Prepare the ligand structure and docking parameter file for flexible.

   For the BA-interface, the 56,000 molecules from the rigid docking are saved in 28 mol2 files (namely *ba_asinN.mol2* (N = 0–14) and *ba_chbrN.mol2* (N = 0–12)), and each file contains 2000 molecule.

- Make a directory *ad4_ba_asin0*, copy *ba_asin0.mol2* to the directory, execute the command "**split_molecules.py ba_asin0.mol2**" to extract the coordinates of each molecule and save as single mol2 file, thus resulting in 2000 mol2 files. Delete the *ba_asin0.mol2* in current directory.
- Use *prepare_ligand4.py* and *prepare_dpf4.py* scripts to prepare structure information file (pdbqt file) and docking parameter file (dpf file). Execute the following bash script to process all 2000 mol2 files in current directory.

```
for f in `ls *.mol2`
do
   name=`basename ${f} .mol2`
   prepare_ligand4.py -l ${f} -o ${name}.pdbqt
   prepare_dpf4.py -r prl1b.pdbqt -l ${name}.pdbqt -o
     ${name}.dpf
done
```

- In current directory, create symbolic link to all files in the directory *ba_maps* using the command "**ln -s ../ba_maps/* .**"
- Repeat the previous steps to prepare pdbqt file and dpf file for the remaining 54,000 molecules in the other 27 mol2 files. Use different directory name correspondingly for different mol2 file, such as *ad4_ba_asin1* for *ba_asin1.mol2*, …, *ad4_ba_chbr12* for *ba_chbr12.mol2*.

  Similarly, for the BC-interface, the 56,000 molecules from the rigid docking are saved in another 28 mol2 files (namely *bc_asinN.mol2* (N=0–14) and *bc_chbrN.mol2* (N=0–12)), and each file contains 2000 molecule. Repeat the previous steps to prepare pdbqt file and dpf file for all 56,000 molecules potentially binding at BC-interface. Replace "ba_" whenever it appears to "bc_" in every repeat.

10. Perform flexible docking in AutoDock4.01.

    In **step 9**, 56 directories were created. Each directory contains 2000 molecules and their corresponding pdbqt and dpf file for running docking calculation in AutoDock4.01. Create a file *docking_job* containing the following bash script, and use it to perform docking calculations for all molecules in one directory. Execute the command "**./docking_job**" in each of 56 directories to run flexible docking simultaneously.

```
for f in `ls *.dpf`
do
   name=`basename ${f} .dpf`
   autodock4 -p ${f} -l ${name}.dlg
done
```

11. Determine the hits from the flexible docking.
    - In each directory starting with "ba_", execute the command "**grep -e '^ 1 | ' *.dlg >>../ba_bfe**" to extract the lowest BFE (binding free energy) for each molecule to the file *ba_bfe*. Execute the command "**cat ba_bfe | sort -k4n >ba_bfe.sort**" to sort all 56,000 BFE values and save the sorted values in the file *ba_bfe.sort*.
    - In each directory starting with "bc_", execute the command "**grep -e '^ 1 | ' *.dlg >>../bc_bfe**" to extract the lowest BFE (binding free energy) for each molecule to the file *bc_bfc*. Execute the command "**cat bc_bfe | sort -k4n >bc_bfe.sort**" to sort all 56,000 BFE values and save the sorted values in the file *ba_bfe.sort*.
    - Collect the docking result file (dlg file) for top 100 molecules in *ba_bfe.sort* file as well as *bc_bfe.sort* file. Determine the hit molecules by checking the structure similarity and visually examining the binding mode.
12. Purchase the hit molecules.

    After considering multiple factors like calculated binding free energy, structure similarity, structure diversity, binding mode rationality, and the commercial availability, 56 molecules were picked out as final hits, 34 of which were purchased from ChemBridge Corp. and the other 22 compounds were purchased from Asinex Corp.

3.2 Validation of PRL1 De-trimerization Compounds by In Vitro Cross-linking Assay

Since the 56 hits were identified by computer-based virtual screening, further evaluations were required to validate the activity of these compounds to disrupt PRL1 trimerization. Therefore, in vitro cross-linking assays were performed to test the de-trimerization activity of the 56 hits in vitro. The experimental procedure is described below.

1. PRL1 was cloned into pET21a bacterial expression vector with $(His)_6$-tag at the C-terminal. For protein expression, pET21A-PRL1 was transformed into *Escherichia coli* BL21-(DE3). Transformed cells were grown at 37 °C in LB culture medium containing 100 mg/mL ampicillin for 4 h until the OD_{600} reached 0.6, and then induced overnight at room temperature with 0.5 mM IPTG (*see* **Note 2**). Cells were harvested by centrifugation (6340 × *g* for 15 min at 4 °C).
2. The cell pellets from 1.5 L of LB medium were suspended in 30 mL of ice-cold lysis buffer (binding buffer with 0.1 mM PMSF). The suspensions were passed twice through a French press at 1000 psi, and the cell lysates were centrifuged at 4 °C for 45 min at 26,640 × *g*. The supernatants were mixed with 2 mL of nickel-nitrilotriacetic acid-agarose at 4 °C for 2 h, and then the mixture was transferred to an empty column.

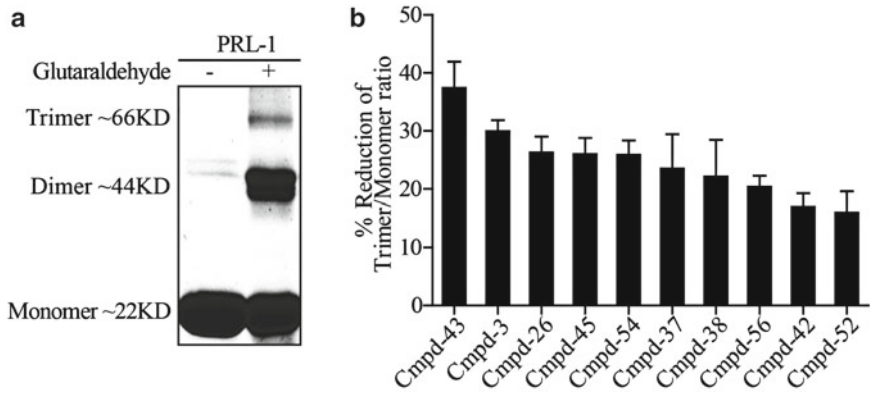

Fig. 2 (**a**) The representative PRL1 monomer, dimer, and trimer by in vitro trimerization assay. (**b**) Top ten hits of the PRL1 de-trimerization compounds that showed reduced Trimer/Monomer ratio compared to DMSO control

3. The column was washed with 100 mL of binding buffer, followed by 50 mL of wash buffer, and then eluted with 15 mL of elution buffer. The elution was centrifuged using ultracentrifugal filter at 2820×*g* to exchange the Tris buffer to PBS buffer (*see* **Note 3**), and to concentrate the PRL1 protein. The concentrated PRL1 protein was supplemented with 10 mM DTT (*see* **Note 4**) and then stored at −80 °C.
4. The in vitro cross-linking reactions were performed in 20 μL solution containing 5 μg of purified PRL1 protein in PBS buffer. Recombinant PRL1 was treated with 10 μM of each compound for 30 min, and then cross-linked by incubation with 0.005% glutaraldehyde (*see* **Note 5**) at room temperature for 10 min. The reaction was terminated by addition of pH 7.5 Tris–HCl (final concentration 50 mM) and 5 min incubation on ice.
5. The samples were separated on 10% SDS-PAGE gel and analyzed by Coomassie Blue staining for monomer (~22 kDa), dimer (~44 kDa), and trimer (~66 kDa) (Fig. 2a).
6. The trimer/monomer relative ratio was calculated by ImageJ software, and the top ten hits of the PRL1 trimer disruptors were determined (Fig. 2b).

3.3 Validation of PRL1 De-trimerization Compounds by In Vivo Cross-linking Assay

After validation of the de-trimerization activity of the 56 hits in vitro, the top ten hits were selected to further test the activity by cell-based in vivo cross-linking assay. This assay allows us to measure the permeability and in vivo de-trimerization activity of these compounds. The experimental procedure is described below.

1. Parental HEK293 cells were maintained in DMEM culture medium in a 37 °C incubator containing 5% CO_2, and then were seeded at 40% confluence in antibiotic-free medium and

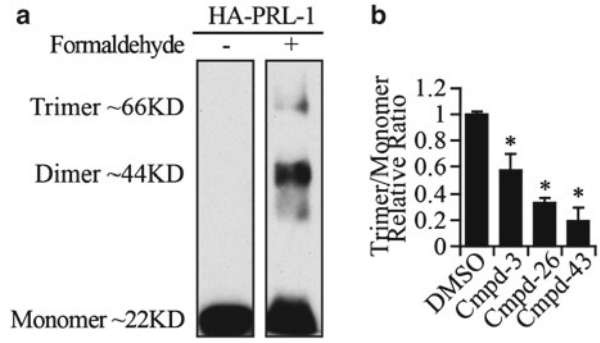

Fig. 3 (**a**) The representative PRL1 monomer, dimer, and trimer by in vivo trimerization assay. (**b**) Top three hits of PRL1 de-trimerization compounds that showed reduced Trimer/Monomer ratio compared to DMSO control by in vivo cross-linking assay

grown overnight in 6-well plates. Transfection was performed according to the suppliers' standard protocols (*see* **Note 6**), containing the pcDNA3.1 (+)-HA-tagged PRL1 and pIRES-EGFP-puro for selection.

2. 24 h after transfection, cells were trypsinized and reseeded in 10 cm plate. After the cells were attached, 2 μg/mL of puromycin was added for selection. After cell colonies were visible, single cell clones were trypsinized and transferred to a new 24-well plate. Stable cell lines overexpressing PRL1 was validated by Western blot with HA antibody (*see* **Note 7**).
3. HEK293 cells stably overexpressing HA-tagged PRL1 were maintained in DMEM culture medium in a 37 °C incubator containing 5% CO_2, and then seeded at 70% confluence and grown overnight in 6-well plates.
4. For in vivo cross-linking, HEK293 cells with 90% confluence were treated with 20 μM of each compound for 24 h, and then fixed with 1% formaldehyde (*see* **Note 5**) for 10 min at room temperature.
5. Cells were washed twice in ice-cold PBS and lysed on ice for 30 min following by immunoprecipitation with HA antibody.
6. The HA immunoprecipitants were analyzed by SDS-PAGE and detected by immunoblotting with anti-HA antibody for PRL1 monomer (~22 kDa), dimer (~44 kDa), and trimer (~66 kDa). A representative in vivo trimerization result was shown (Fig. 3a).
7. The trimer/monomer relative ratio was calculated by ImageJ software, and the top three hits of PRL1 trimer disruptors were determined (Fig. 3b).

3.4 Evaluation the Cellular Activity of PRL1 De-trimerization Compounds

It has been shown that overexpression of PRL1 enhances cell proliferation and migration, which requires the trimerization of PRL1 [16]. To evaluate whether PRL1 trimer disruptors inhibit PRL1-induced cell proliferation and migration, MTT assay, wound healing assay, and Transwell migration assay were performed by treating PRL1 overexpressing HEK293 cells with one of the top three hits, Cmpd-3. The experimental procedure is described below.

1. HEK293 cells stably overexpressing HA-tagged PRL1 were maintained in DMEM culture medium in a 37 °C incubator containing 5% CO_2.
2. MTT assay was used to measure the anti-proliferation activity of PRL1 de-trimer compound (*see* **Note 8**). Vector control cells and PRL1 overexpressing cells were seeded in a 96-well plate (3000 cells/well) overnight, and then PRL1 overexpressing cells were treated with various concentrations of Cmpd-3 for 48 h. 10 μL of 5 mg/mL MTT reagent was added to each well for 3.5 h until purple precipitate is visible. Medium was removed and 100 μL of DMSO was added to dissolve the precipitate. Mix to ensure complete solubilization and then record absorbance at 570 nm using a multiwall spectrophotometer. Relative proliferation rate compared with vector control cells was measured to determine the anti-proliferation activity of the compound (Fig. 4a).
3. Wound healing assay was used to measure the anti-migration activity of PRL1 de-trimerization compound in a convenient and inexpensive manner (*see* **Note 9**). Vector control cells and PRL1 overexpressing cells were grown to 90% confluence in a 12-well plate. Then a wound was created by scratching cells with a sterile 200 μL pipette tip. Cells were washed with PBS to remove the floating cells, and then PRL1 overexpressing cells were treated with fresh medium containing 20 μM of the compound for 24 h. The wounds were photographed at 0 and 24 h under ×10 magnitude microscope, and then the relative wound closure compared with vector control cells was measured to determine the anti-migration activity of each PRL1 de-trimerization compound (Fig. 4b).
4. Transwell migration assay, as a more sensitive and informative method, was also used to measure the anti-migration activity of PRL1 de-trimer compound (*see* **Note 10**). The assay was performed with Transwells (6.5 mM diameter; 8 μM pore size polycarbonate membrane). 3.75×10^5 in 1.5 mL of serum-free medium was placed in the upper chamber, whereas the lower chamber was loaded with 2.5 mL of medium containing 20% FBS. PRL1 overexpressing cells were then treated with 10 μM of each compound for 24 h incubation (37 °C, 5% CO_2). The total number of cells that had migrated into the lower chamber

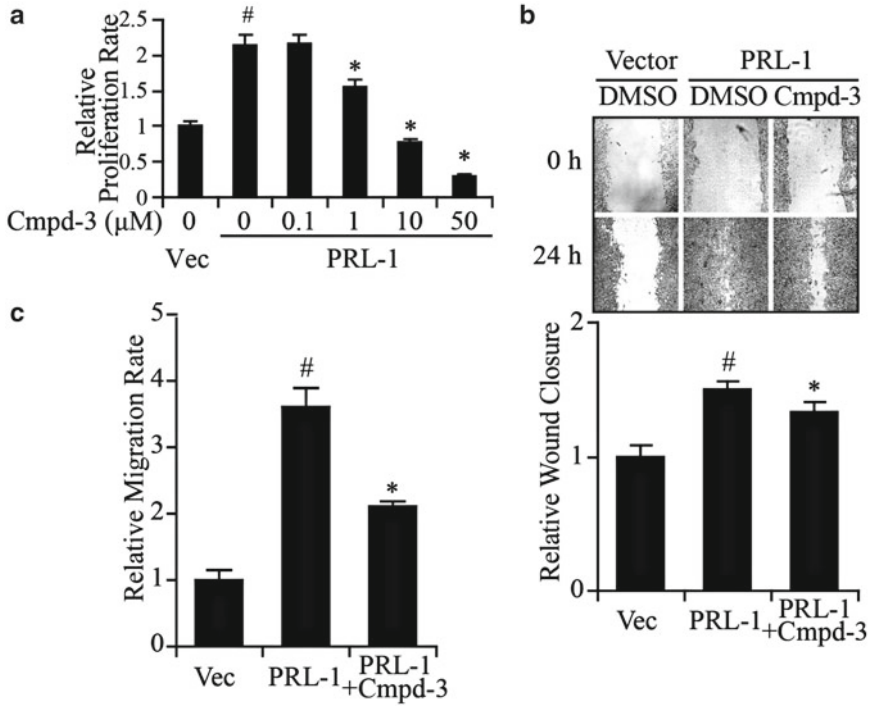

Fig. 4 (**a**) Cmpd-3 dose dependently reduced PRL1-induced cell proliferation in PRL1 overexpressing HEK293 cells by MTT assay. (**b**) Cmpd-3 inhibited PRL1-mediated wound closure in PRL1 overexpressing HEK293 cells by wound healing assay. (**c**) Cmpd-3 suppressed PRL1-induced cell migration in PRL1 overexpressing HEK293 cells by Transwell migration assay

was counted with a hemocytometer. The relative migration rate compared with vector control cells was measured to determine the anti-migration activity of the compound (Fig. 4c).

4 Notes

1. Since hundreds of thousands of molecules are used for the virtual screening, they may contain various types of atoms. To provide energy grid maps as much as possible for atom type in the library, all inherently supported atom types (except for metal element since the library only contains organic molecules) are manually set for the parameter ligand_type in the grid parameter file. While, autogrid4 program can only calculate energy grid map for maximal 14 atom types during each run. Thus, the gpf file generated in **step 8** in Subheading 3.1 needs to be split into two files for two runs of autogrid4 program. For example, for *ba_grid.gpf* file, copy this file to *ba_grid1.gpf* and *ba_grid2.gpf*. Edit *ba_grid1.gpf*, only keep the first 14 atom types and delete the atom type "Cl Br I" at line

5, delete line 23–25 and save the changes. Edit *ba_grid2.gpf*, delete the first 14 atom types "H HD HS C A N NA NS OA OS P S SA F" at line 5 and only keep the remaining three atom types "Cl Br I", delete line 9–22 and save the changes. Execute the command "**autogrid4 -p ba_grid2.gpf -l ba_grid2.glg**" and "**autogrid4 -p ba_grid1.gpf -l ba_grid1.glg**". Edit the generated *prl1b.maps.fld*, change "veclen=16" at line 18 to "veclen=19". Delete line 38 and 39, and insert the following five lines at line 38.

```
label=Cl-affinity       # component label for variable 15
label=Br-affinity       # component label for variable 16
label=I-affinity        # component label for variable 17
label=Electrostatics    # component label for variable 17
label=Desolvation       # component label for variable 18
```

Delete the last two lines and append the following five lines. Save all changes.

```
variable 15 file=prl1b.Cl.map filetype=ascii skip=6
variable 16 file=prl1b.Br.map filetype=ascii skip=6
variable 17 file=prl1b.I.map filetype=ascii skip=6
variable 18 file=prl1b.e.map filetype=ascii skip=6
variable 19 file=prl1b.d.map filetype=ascii skip=6
```

2. Purification of $(His)_6$-tagged PRL1 is done according to the manufacturer's handbook for high-level expression and purification of 6×His-tagged proteins. To get pure PRL1 protein, many conditions, including expressing vector, *Escherichia coli* strain, IPTG concentration as well as induction time and temperature, need to be optimized.
3. Since Tris buffer contains amine group, which will react with glutaraldehyde in vitro, the protein stock buffer needs to change to PBS buffer or other buffer without amine ends.
4. The phosphatase activity of PRL1 requires reducing conditions. Therefore, 10 mM DTT was added to the purified PRL1 to keep PRL1 activity.
5. Cross-linking is the process to chemically link two or more protein molecules through a covalent bond. Cross-linking reagents contain at least two reactive end groups that react toward certain functional groups on target protein, including amines and sulfhydryls. Based on the similarity of the reactive groups on both ends, cross-linking reagents can be divided into homobifunctional cross-linkers (same reactive ends) or heterobifunctional cross-linkers (different reactive ends). Different cross-linking reagents may perform differently for different target proteins. Many features should be taken into consideration

when choosing a cross-linker, such as the nature of reactive groups, the length of spacer arm, and the reaction condition required for conjugation. We screened different cross-linkers, including glutaraldehyde, formaldehyde, DSG (disuccinimidyl glutarate), and DSS (disuccinimidyl suberate). Glutaraldehyde is the best for in vitro cross-linking, while formaldehyde is the best for in vivo cross-linking. All the conditions, including cross-linker, reaction time as well as temperature, should be optimized for each protein and cell line assayed.

6. The transfection is done according to the suppliers' standard protocols. In fact, many transfection reagents and protocols are available for different cell lines. HEK293 cell was used because this cell line can be transfected with very high efficiency with a variety of commercial lipid reagents.
7. HEK293 cell lines stably overexpressing HA-tagged PRL1 were selected by adding 2 μg/mL of puromycin for about 2 weeks. The puromycin concentration and treating time was optimized based on the cell line we selected. In addition, control HEK293 cells without transfection of puromycin resistant gene are recommended to be used as selection control.
8. MTT assay is widely accepted as a reliable method to assess cell viability [27]. Dehydrogenase enzymes in metabolically active cells are capable of reducing the yellow tetrazolium MTT (3-(4,5-dimethylthiazolyl-2)-2,5-diphenyltetrazolium bromide) to its insoluble formazan. The resulting intracellular purple formazan can be solubilized and quantified to reflect cell proliferation. The optimal cell number and incubation time for the HEK293 stable cell lines should be optimized before the experiment.
9. The wound healing assay is widely adapted to study cell migration and proliferation [28]. In a typical wound healing assay, scratching is used to create a wound gap in a cell monolayer, and the closure of this gap is monitored and quantified to reflect cell migration and cell proliferation ability. The wound healing assay is simple and inexpensive. The optimization is required for the cell confluence and monitoring time after scratching.
10. Transwell assay is a commonly used method to study cell migration in response to different stimulation and inhibition. It was done according to the suppliers' standard protocols. During this assay, cells in the medium containing the testing reagent are placed on the upper chamber with a cell permeable membrane on the bottom. Following an incubation period, the cells that have migrated through the membrane are stained and counted to indicate the cell migration ability in the presence of certain reagent. The optimal cell number and incubation time for the HEK293 stable cell lines should be optimized before the experiment.

References

1. Cates CA, Michael RL, Stayrook KR, Harvey KA, Burke YD, Randall SK, Crowell PL, Crowell DN (1996) Prenylation of oncogenic human PTP(CAAX) protein tyrosine phosphatases. Cancer Lett 110(1–2):49–55
2. Diamond RH, Cressman DE, Laz TM, Abrams CS, Taub R (1994) PRL-1, a unique nuclear protein tyrosine phosphatase, affects cell growth. Mol Cell Biol 14(6):3752–3762
3. Zeng Q, Dong JM, Guo K, Li J, Tan HX, Koh V, Pallen CJ, Manser E, Hong W (2003) PRL-3 and PRL-1 promote cell migration, invasion, and metastasis. Cancer Res 63(11):2716–2722
4. Wang J, Kirby CE, Herbst R (2002) The tyrosine phosphatase PRL-1 localizes to the endoplasmic reticulum and the mitotic spindle and is required for normal mitosis. J Biol Chem 277(48):46659–46668. doi:10.1074/jbc.M206407200
5. Werner SR, Lee PA, DeCamp MW, Crowell DN, Randall SK, Crowell PL (2003) Enhanced cell cycle progression and down regulation of p21(Cip1/Waf1) by PRL tyrosine phosphatases. Cancer Lett 202(2):201–211
6. Wang Q, Holmes DI, Powell SM, Lu QL, Waxman J (2002) Analysis of stromal-epithelial interactions in prostate cancer identifies PTPCAAX2 as a potential oncogene. Cancer Lett 175(1):63–69
7. Saha S, Bardelli A, Buckhaults P, Velculescu VE, Rago C, St Croix B, Romans KE, Choti MA, Lengauer C, Kinzler KW, Vogelstein B (2001) A phosphatase associated with metastasis of colorectal cancer. Science 294(5545):1343–1346. doi:10.1126/science.1065817
8. Liang F, Liang J, Wang WQ, Sun JP, Udho E, Zhang ZY (2007) PRL3 promotes cell invasion and proliferation by down-regulation of Csk leading to Src activation. J Biol Chem 282(8):5413–5419. doi:10.1074/jbc.M608940200
9. Bessette DC, Qiu D, Pallen CJ (2008) PRL PTPs: mediators and markers of cancer progression. Cancer Metastasis Rev 27(2):231–252. doi:10.1007/s10555-008-9121-3
10. Rios P, Li X, Kohn M (2013) Molecular mechanisms of the PRL phosphatases. FEBS J 280(2):505–524. doi:10.1111/j.1742-4658.2012.08565.x
11. Pathak MK, Dhawan D, Lindner DJ, Borden EC, Farver C, Yi T (2002) Pentamidine is an inhibitor of PRL phosphatases with anticancer activity. Mol Cancer Ther 1(14):1255–1264
12. Ahn JH, Kim SJ, Park WS, Cho SY, Ha JD, Kim SS, Kang SK, Jeong DG, Jung SK, Lee SH, Kim HM, Park SK, Lee KH, Lee CW, Ryu SE, Choi JK (2006) Synthesis and biological evaluation of rhodanine derivatives as PRL-3 inhibitors. Bioorg Med Chem Lett 16(11):2996–2999. doi:10.1016/j.bmcl.2006.02.060
13. Campbell AM, Zhang ZY (2014) Phosphatase of regenerating liver: a novel target for cancer therapy. Expert Opin Ther Targets 18(5):555–569. doi:10.1517/14728222.2014.892926
14. Sun JP, Wang WQ, Yang H, Liu S, Liang F, Fedorov AA, Almo SC, Zhang ZY (2005) Structure and biochemical properties of PRL-1, a phosphatase implicated in cell growth, differentiation, and tumor invasion. Biochemistry 44(36):12009–12021. doi:10.1021/bi0509191
15. Jeong DG, Kim SJ, Kim JH, Son JH, Park MR, Lim SM, Yoon TS, Ryu SE (2005) Trimeric structure of PRL-1 phosphatase reveals an active enzyme conformation and regulation mechanisms. J Mol Biol 345(2):401–413. doi:10.1016/j.jmb.2004.10.061
16. Sun JP, Luo Y, Yu X, Wang WQ, Zhou B, Liang F, Zhang ZY (2007) Phosphatase activity, trimerization, and the C-terminal polybasic region are all required for PRL1-mediated cell growth and migration. J Biol Chem 282(39):29043–29051. doi:10.1074/jbc.M703537200
17. Bai Y, Luo Y, Liu S, Zhang L, Shen K, Dong Y, Walls CD, Quilliam LA, Wells CD, Cao Y, Zhang ZY (2011) PRL-1 protein promotes ERK1/2 and RhoA protein activation through a non-canonical interaction with the Src homology 3 domain of p115 Rho GTPase-activating protein. J Biol Chem 286(49):42316–42324. doi:10.1074/jbc.M111.286302
18. Krissinel E, Henrick K (2007) Inference of macromolecular assemblies from crystalline state. J Mol Biol 372(3):774–797. doi:10.1016/j.jmb.2007.05.022
19. Irwin JJ, Shoichet BK (2005) ZINC—a free database of commercially available compounds for virtual screening. J Chem Inf Model 45(1):177–182. doi:10.1021/ci049714+
20. Pettersen EF, Goddard TD, Huang CC, Couch GS, Greenblatt DM, Meng EC, Ferrin TE (2004) UCSF Chimera—a visualization system for exploratory research and analysis. J Comput Chem 25(13):1605–1612. doi:10.1002/jcc.20084
21. Moustakas DT, Lang PT, Pegg S, Pettersen E, Kuntz ID, Brooijmans N, Rizzo RC (2006) Development and validation of a modular, extensible docking program: DOCK 5.

J Comput Aided Mol Des 20(10–11): 601–619. doi:10.1007/s10822-006-9060-4

22. Lang PT, Brozell SR, Mukherjee S, Pettersen EF, Meng EC, Thomas V, Rizzo RC, Case DA, James TL, Kuntz ID (2009) DOCK 6: combining techniques to model RNA-small molecule complexes. RNA 15(6):1219–1230. doi:10.1261/rna.1563609
23. Morris GM, Goodsell DS, Halliday RS, Huey R, Hart WE, Belew RK, Olson AJ (1998) Automated docking using a Lamarckian genetic algorithm and an empirical binding free energy function. J Comput Chem 19(14):1639–1662. doi:10.1002/(Sici)1096-987x(19981115)19:14<1639::Aid-Jcc10>3.0.Co;2-B
24. Huey R, Morris GM, Olson AJ, Goodsell DS (2007) A semiempirical free energy force field with charge-based desolvation. J Comput Chem 28(6):1145–1152. doi:10.1002/jcc.20634
25. Sanner MF (1999) Python: a programming language for software integration and development. J Mol Graph Model 17(1):57–61
26. Morris GM, Huey R, Lindstrom W, Sanner MF, Belew RK, Goodsell DS, Olson AJ (2009) AutoDock4 and AutoDockTools4: automated docking with selective receptor flexibility. J Comput Chem 30(16):2785–2791. doi:10.1002/jcc.21256
27. Mosmann T (1983) Rapid colorimetric assay for cellular growth and survival: application to proliferation and cytotoxicity assays. J Immunol Methods 65(1–2):55–63
28. Lampugnani MG (1999) Cell migration into a wounded area in vitro. Methods Mol Biol 96:177–182. doi:10.1385/1-59259-258-9:177

Chapter 9

Analyzing Pseudophosphatase Function

Shantá D. Hinton

Abstract

Pseudophosphatases regulate signal transduction cascades, but their mechanisms of action remain enigmatic. Reflecting this mystery, the prototypical pseudophosphatase STYX (phospho-serine-threonine/tyrosine-binding protein) was named with allusion to the river of the dead in Greek mythology to emphasize that these molecules are "dead" phosphatases. Although proteins with STYX domains do not catalyze dephosphorylation, this in no way precludes their having other functions as integral elements of signaling networks. Thus, understanding their roles in signaling pathways may mark them as potential novel drug targets. This chapter outlines common strategies used to characterize the functions of pseudophosphatases, using as an example MK-STYX [mitogen-activated protein kinase (MAPK) phospho-serine-threonine/tyrosine binding], which has been linked to tumorigenesis, apoptosis, and neuronal differentiation. We start with the importance of "restoring" (when possible) phosphatase activity in a pseudophosphatase so that the active mutant may be used as a comparison control throughout immunoprecipitation and mass spectrometry analyses. To this end, we provide protocols for site-directed mutagenesis, mammalian cell transfection, co-immunoprecipitation, phosphatase activity assays, and immunoblotting that we have used to investigate MK-STYX and the active mutant MK-STYX$_{active}$. We also highlight the importance of utilizing RNA interference (RNAi) "knockdown" technology to determine a cellular phenotype in various cell lines. Therefore, we outline our protocols for introducing short hairpin RNA (shRNA) expression plasmids into mammalians cells and quantifying knockdown of gene expression with real-time quantitative PCR (qPCR). A combination of cellular, molecular, biochemical, and proteomic techniques has served as powerful tools in identifying novel functions of the pseudophosphatase MK-STYX. Likewise, the information provided here should be a helpful guide to elucidating the function of other pseudophosphatases.

Key words Pseudophosphatases, STYX domains, MAPK phosphatases, MK-STYX, Immunoprecipitation, shRNA knockdown

1 Introduction

Pseudophosphatases are catalytically inactive because they lack residues essential for catalytic activity within their protein tyrosine phosphatase (PTP) active site signature motif (HCX_5R) [1]. Many pseudophosphatases have been identified [2, 3]; yet their modes of action remain elusive. Importantly, however, they possess the characteristic PTP fold. Consequently, though catalytically inactive,

Rafael Pulido (ed.), *Protein Tyrosine Phosphatases: Methods and Protocols*, Methods in Molecular Biology, vol. 1447,
DOI 10.1007/978-1-4939-3746-2_9,

they maintain their ability to bind phosphorylated proteins, which makes them ideal for investigating the dynamics of protein-protein interactions and their effect on pathways such as Ras and apoptotic signaling. Exactly what are the functions of pseudophosphatases, and how can these proteins be investigated?

Identifying PTP substrates was essential for understanding the roles of these active phosphatases in signal transduction [4]. A key to identifying PTP substrates was the development of "substrate-trapping," a powerful technique in which mutations of invariant residues of the active site render an active enzyme a "substrate trap," in which the mutated PTP binds a phosphorylated residue but does not hydrolyze it [3, 11, 12]. The discovery of naturally occurring proteins structurally related to PTPs that resemble "substrate-trapping" mutants led to many questions. Why do they exist? Are they simply dominant-negative proteins? Do they function like substrate traps, similar to artificial mutants? Just as identifying substrates of PTPs led to many discoveries of their central role in signaling pathways, identifying interacting partners of the myotubularins, *C. elegans* EGGs, prototypical STYX, and MK-STYX has led to defining the molecular details of their functions.

The myotubularins (MTM) include several pseudophosphatases [5]. Seven of the 16 human MTM genes encode pseudophosphatases [6, 7] that function as scaffolds to form complexes with their active homologs, to regulate catalytic function and subcellular localization of the active phosphatase. For example, the pseudophosphatase MTM13 (MTM-related protein 13) binds the active enzyme MTMR2 [6]. A mutation in the MTMR13 pseudophosphatase or the active MTMR2 is associated with Charcot-Marie-Tooth disease, a neuropathy characterized by abnormal nerve myelination [5]. The *C. elegans* pseudophosphatases EGG-4 and EGG-5 trap MBK-2 (mini brain kinase 2) to regulate the oocyte-to-zygote transition though DYRK (dual-specificity tyrosine phosphorylated and regulated kinase) [8, 9]. The prototypical STYX, which competes for ERK binding, modulates cell-fate decisions and cell migration as a spatiotemporal regulator of ERK1/2 signaling [10].

MK-STYX is structurally related to dual-specificity phosphatases (DSPs). In particular, bioinformatic analysis revealed homology to MAP kinase phosphatases (MKPs), which dephosphorylate both threonine and tyrosine residues in the activation loop of members of the MAPK family [4]. It does not possess the active-site signature motif **HC**(X_5)**R** that is essential for phosphatase activity; instead it has the sequence I**FS**TQGIS**R**S, which renders it catalytically inactive [1, 4, 11]. For many years, little was known about MK-STYX, except that it is highly expressed in Ewing's sarcoma family tumors [11, 12]. More recently, significant advances have been made in understanding its functional role. It interacts with G3BP-1 (Ras-GTPase activating protein SH3 domain binding

protein-1) and decreases stress granule assembly [11, 13], thereby affecting the stress response pathway. In addition, it regulates mitochondrial dependent apoptosis [14]. It interacts with PTPM1 (PTP localized to the mitochondrion 1), and inhibits its catalytic activity, regulating cell viability [15]. MK-STYX also has implications in neuronal development [16], in which it induces neurite outgrowth and decreases RhoA activation. Furthermore, it affects the downstream player of RhoA, actin-binding protein cofilin. The presence of MK-STYX decreases the phosphorylation of cofilin in non-NGF-stimulated cells, but increased its phosphorylation in NGF-stimulated cells, whereas knocking it down caused an opposite effect [16].

These reports illustrate that the pseudophosphatases are key molecules in signaling pathways, highlighting the increasing importance of investigating the function of such pseudoenzymes. In this chapter, we present methodologies for designing catalytically active mutants, characterizing interacting partners, and assessing function of pseudophosphatases. While the molecular mechanisms of pseudophosphatases remain relatively uncharacterized, we expect that strategies to tackle these catalytically inactive members of the PTP family will lead to many novel discoveries.

2 Materials

All solutions are prepared in deionized MilliQ-filtered H_2O. Cell culture and transfection procedures require sterile conditions.

2.1 Conversion of a Pseudophos-phatase STYX Domain to an Active Signature Motif (HCX_5R)

1. Recombinant cDNA of the tagged pseudophosphatase of interest, cloned into a mammalian expression vector (*see* **Note 1**).
2. Site-directed mutagenesis kit (*see* **Note 2**).
3. PCR reagents (*see* **Note 3**).
4. PTP activity assay kit (*see* **Note 4**).

2.2 Immuno-precipitation and Immunoblotting

1. Mammalian cell lines suitable for transfection and transient overexpression of recombinant proteins (*see* **Note 5**).
2. Cell culture medium and any required supplements.
3. Lipofectamine 2000 and Opti-MEM Reduced Serum Medium or the lab's preferred transfection reagent.
4. 10× Phosphate-buffered saline (PBS): 0.2 M KH_2PO_4, 1.5 M NaCl, pH 7.2. Dilute as required to 1×.
5. Lysis buffer: 50 mM HEPES, pH 7.2, 150 mM NaCl, 10% glycerol, 10 mM NaF, 1% Nonidet P-40 alternate (e.g., IGEPAL), and Roche protease inhibitor cocktail tablets; or other appropriate protease and phosphatase inhibitors (*see* **Notes 6** and 7).

6. Cell lifters or scrapers.
7. Bradford protein concentration assay reagent (or the lab-preferred method to determine protein concentration).
8. Antibodies against the pseudophosphatase of interest (or an epitope tag in a mammalian expression vector) (*see* **Notes 1** and **8**).
9. Immunoglobulin (Ig) G beads (or protein A beads; dependent on primary antibody) (*see* **Note 9**).
10. 5× Laemmli sample loading buffer: 10% Sodium dodecyl sulfate, 30% glycerol, 250 mM Tris–HCl, pH 6.8, and 0.02% bromophenol blue.
11. Dithiothreitol (DTT) or β-mercaptoethanol.
12. 1.5 mL Centrifuge tubes (*see* **Note 10**).
13. Access to mass spectrometry facilities (*see* **Note 11**).
14. Sodium dodecyl sulfate-polyacrylamide gel electrophoresis (SDS-PAGE) reagents (*see* **Note 9**): 30% Acrylamide-bisacrylamide mix (29:1); 1.5 M Tris–HCl (pH 8.8); 1.0 M Tris–HCl (pH 6.8); 10% SDS; 10% ammonium persulfate; tetramethylethylenediamine (TEMED).
15. Protein standard molecular weight marker (pre-stained and unstained).
16. Protein stain (Coomassie blue and destain, or silver stain) (*see* **Note 12**).
17. Polyvinyl difluoride (PVDF) membrane or nitrocellulose membrane (*see* **Note 13**).
18. Blotting paper.
19. Transfer buffer: 48 mM Tris base, 39 mM glycine, 1.3 mM SDS, 20% methanol (*see* **Note 13**).
20. Blocking reagent (powdered milk, bovine serum albumin [BSA], or commercial blocking reagent) (*see* **Note 14**).
21. Anti-rabbit or anti-mouse antibodies conjugated to horseradish peroxidase (HRP), dependent on the source of primary antibody.
22. 10× Tween 20-Tris saline buffer (TTBS): 1.0 M Tris–HCl pH 7.5, 1.5 M NaCl, 0.1% Tween 20 (v/v). Dilute as required to 1×.
23. Enhanced chemiluminescence (ECL) Prime, or another chemiluminescence detection reagent.
24. Mild stripping buffer: 200 mM Glycine, 3.5 mM SDS, 1% Tween 20 (*see* **Note 15**).

2.3 Knockdown

1. Short hairpin (shRNA) expression plasmids specific for pseudophosphatase of interest (*see* **Notes 16–18**).

2. Lipofectamine 2000 transfection reagent and Opti-MEM (or other transfection reagent).
3. Aurum™ Total RNA Mini Kit or the lab's preferred RNA isolation kit (*see* **Note 19**).
4. SuperArray RT² First Strand Kit or the lab's preferred cDNA kit.
5. StepOne™ Real-Time PCR or a lab-preferred real-time quantitative polymerase chain reaction (qPCR) apparatus.
6. RT²SYBR Green/Fluorescein qPCR Master Mix or reagent designed for the lab's specific qPCR apparatus.
7. Primers for the pseudophosphatase of interest.

3 Methods

3.1 Creation of an Active PTP from a Pseudo-phosphatase

1. Design primers that will substitute the residues of the pseudophosphatase to residues that resemble a PTP signature active site (HCX_5R). For example, the PTP signature site of MK-STYX consists of FSTQGIRS; thus we designed primers that substituted HC for the FS to generate the sequence HCTQGIRS (*see* **Notes 1** and **18**).
2. Follow the protocol of the site-directed mutagenesis kit and PCR to construct a plasmid that contains the signature active site (*see* **Note 2**).
3. Sequence plasmid to confirm that the newly generated residues are equivalent to the PTP-active-site signature motive sequence [I/V**HC**XXGXX**R**[S/T]], in which the residues in bold play a critical role in catalysis.
4. Perform a PTP activity assay to determine whether the substituted residues of the pseudophosphatase confer PTP activity (*see* **Note 4**).

3.2 Identifying Interacting Partners of Pseudo-phosphatases

If the activity of a pseudophosphatase is "restored," this active mutant can serve as a powerful tool for functional studies of the wild-type pseudophosphatase. Therefore, when an active mutant is available, it should also be used for immunoprecipitation studies. The wild-type pseudophosphatase may bind different proteins than the active mutant (*see* **Notes 20** and **21**).

1. Transfect cells of interest with a mammalian expression plasmid containing the tagged pseudophosphatase (*see* **Note 1**). We transfect cells seeded on a 10 cm plate with 2 or 4 μg plasmid following the Lipofectamine 2000 protocol.
2. 24 or 48 h post-transfection remove medium (*see* **Note 19**), wash with 1× PBS, and remove PBS.

3. Add 1 mL (for 10 cm plates) lysis buffer with protease and phosphatase inhibitors (when warranted; *see* **Notes 6** and **7**), and make sure that all cells are covered by the buffer. Incubate cells (in plate) on ice for 3 min (*see* **Note 22**).
4. Use cell lifter to remove cells from plate, and pipet ~1 mL lysate into a pre-chilled 1.5 mL microcentrifuge tube. Incubate on ice for 5–10 min. Time is dependent on viscosity of samples; samples should not become too viscous.
5. Centrifuge for 15 min at 14,000 × *g* at 4 °C. Samples may be stored at −20 °C or protocol continued for immunoprecipitation.
6. Determine the protein concentration with Bradford reagent or another protein quantitative assay. The minimum amount of protein required for an immunoprecipitation is 500 μg/mL. We prefer to use 1 mg/mL or up to 2 mg/mL (*see* **Note 23**). Dilute samples with lysis buffer to a total volume of 1 mL.
7. Pre-clear lysate (*see* **Note 24**) by adding 20 μL protein A or G beads (dependent on antibody; *see* **Note 9**). Incubate on ice for 30 min, and centrifuge for 5 min at 14,000 × *g*, at 4 °C. Transfer lysate (not beads) to a new 1.5 mL centrifuge tube (*see* **Note 10**).
8. Save 40–50 μL lysate to analyze by immunoblotting to ensure that the immunoprecipitations were performed with equal amounts of protein.
9. Add 5 μL antibody probing for the pseudophosphatase of interest, and incubate on ice for 1 h. Make sure that the antibody is mixed well with the lysate by inverting the tube.
10. Add 25 μL of well-suspended protein A or G beads to lysate (sample) and antibody mixture. Gently pipette twice to release excess beads into solution, and invert tube and place on ice. Place tubes containing the lysates (samples), antibody, and beads on a rocker in a cold room (at 4 °C) for 1 h. Be careful to ensure that tubes are tightly sealed. We prefer an adjustable test tube rocker.
11. Centrifuge for 15 min at 14,000 × *g* at 4 °C; protein A or G agarose beads should be visible as a pellet.
12. Aspirate supernatant with a Pasteur pipette that has a gel loading (flat) tip connected to it. The extra tip minimizes the force of the aspiration and prevents aspiration of the beads (the immunoprecipitated sample). Be careful not to disturb beads; we suggest not to aspirate all of the supernatant until the final wash (*see* **Note 25**).
13. Wash three to four times with 1 mL ice-cold lysis buffer by centrifuging at 10,000 × *g* at 4 °C for 30–60 s. If complexes are stable, the washes may be done at room temperature.
14. After the final wash, aspirate as much as possible of the supernatant. Be consistent with the volume of beads (samples) left

in each tube because this is the sample that will be analyzed for complexes.

15. Elute the complexes from the beads with 50 μL sample loading buffer and 100 mM DTT. Heat to 85 °C (or boil) for 5 min, centrifuge briefly (~1 min), and load sample onto SDS-PAGE. Samples may also be stored at −20 °C for electrophoresis at a later time. Samples may be aliquoted into two separate tubes for staining and immunoblotting purposes.
16. Resolve samples on a 10% SDS-PAGE or appropriate percentage gel for size of pseudophosphatase of interest (*see* **Note 26**).
17. Stain gel with Coomassie Blue or silver stain to visualize proteins (*see* **Note 12**).
18. To identify the proteins of interest, cut out the bands (proteins), and send to a mass spectrometry facility for identification of the peptides (*see* **Note 11**). When a possible candidate is identified as an interacting partner of the pseudophosphatase, an immunoblot may be performed on the immunoprecipitated complex.
19. Resolve samples (20 μL from **step 15**) by 10% SDS-PAGE (or desired percentage gel), making sure that samples are heated and centrifuged before loading.
20. Transfer samples to a PVDF membrane, using desired transfer methods (*see* **Note 13**).
21. Detect the candidate determined to be the possible interacting partner by standard immunoblotting and chemiluminescence detection techniques, using the antibody against the candidate, and the appropriate secondary antibody.
22. Detect the pseudophosphatase by standard immunoblotting and chemiluminescent detection techniques, using the antibody against the pseudophosphatase or the tag, and appropriate secondary antibody. If the pseudophosphatase and possible interacting candidate are of sufficiently different molecular masses, cut the PVDF membrane so that each protein is separate and may be probed separately with appropriate antibodies. However, if the proteins are close in size, the membrane must be stripped (*see* **Note 15**).
23. Strip membrane by warming stripping buffer to 50 °C, and add enough buffer to cover the membrane placed in a small plastic container with lid. Or use the lab's established stripping protocol.
24. Add the membrane, and incubate at 50 °C while agitating for 45 min.
25. Dispose of the buffer as required by the institution.
26. Rinse the membrane under running tap water for 1–2 h.

27. Wash two times for 5 min with 1× TTBS before performing the immunoblotting procedure, blocking first.

3.3 Investigating the Biological Significance of Pseudophosphatases by Knockdown

1. Seed cells of interest that express the pseudophosphatase at 6×10^5 cells per 10 cm plate.
2. 24 h post-seeding, transfect cells with 10 μg of the pseudophosphatase shRNA expression plasmid (*see* **Notes 16–18**).
3. Incubate plates for 4–6 h, and replace medium with fresh medium. Success of transfection may be visualized with a fluorescence microscope, when using GFP-tagged shRNA plasmids.
4. To validate knockdown of the pseudophosphatase, mRNA levels may be examined by qPCR:
   - Analyze mRNA levels. 24 h post-transfection, purify RNA with the Aurum™ Total RNA Mini Kit (or lab's established RNA purification compatible with the qPCR apparatus; *see* **Note 19**).
   - Determine concentration of RNA; only use RNA with the following ratios: $A_{260/280} > 2.0$ and $A_{260/230} > 1.7$ for qPCR.
   - Synthesize cDNA from 0.735 μg RNA with the SuperArray Bioscience's RT² First Strand Kit or the lab's established cDNA protocol.
   - Use a 48-well plate to set up reactions; one reaction (total volume 25 μL) should contain 12.5 μL RT² SYBR Green/Fluorescein qPCR Master Mix specifically designed for the lab's preferred qPCR apparatus, 11.5 μL RNase-free water, 1.5 μL cDNA template, and 1 μL appropriate primer. A reaction should also be set up with a housekeeping gene (dependent on cell type) for each experimental sample to normalize the raw data. "No reverse transcriptase" controls should be included for each gene of interest and housekeeping gene to detect any genomic contamination.
   - Centrifuge the 48-well plate for 90 s at $400 \times g$.
   - Load the Applied Biosystems' StepOne™ Real-Time PCR apparatus or lab's preferred apparatus.
   - Run the qPCR at the following parameters: 10 min at 95 °C (for enzyme activation), and 40 cycles of 15 s at 95 °C, 35 s at 55 °C, and 30 s at 72 °C. The SYBR Green fluorescence should be detected and recorded during the annealing step of each cycle.
   - Perform a melting curve as a quality control measure, and analyze the qPCR data. When using the Applied Biosystems' StepOne™ Real-Time PCR apparatus, the $\Delta\Delta C_t$ (Livak) method is used with ABI StepOne software.

5. To further validate knockdown of the pseudophosphatase, protein expression levels may be examined by immunoblotting (*see* **Note 18**, and Subheading 3.2).
6. 24 h post-transfection observe cells with phase and fluorescence microscopy for any noticeable morphological changes (such changes may be noticed sooner than 24 h, so it is advisable to monitor cells over a time course). These morphological changes may suggest possible biological functions and proteins involved in these functions that the pseudophosphatase may regulate (*see* **Note 27**).
7. 24 post-transfection stimulate cells with the appropriate stimulus or inhibitors for the desired biological functional assay (*see* **Note 28**).
8. Perform immunoblot with the antibodies against the desired protein of interest (*see* Subheading 3.2). Analyze whether knocking down the pseudophosphatase changed the expression pattern of the chosen protein of interest (*see* **Note 29**).

4 Notes

1. MK-STYX was flanked by two FLAG epitopes, and then cloned into the vector of interest. We suggest using a tag such as a FLAG expression system. The FLAG expression system will allow numerous applications with the pseudophosphatase such as protein purification, immunoblotting, and immunoprecipitation. FLAG is a small hydrophilic peptide that is unlikely to interfere with protein folding or alter the function of the pseudophosphatase. In addition, the FLAG epitope may be detected with a commercially available anti-FLAG antibody.
2. Substituting amino acid residues is no longer labor intensive. Mutations to change nucleotide codons for amino acid residues may be accomplished by purchasing site-directed mutagenesis kits from companies such as Agilent Technologies (Quik Change II) or New England Bio Labs (site-directed mutagenesis kit). Furthermore, there are companies that will synthesize a DNA construct with the desired sequence (e.g., GeneArt, Life Technologies). Considering that there may be other important domains responsible for the function of PTPs such as the CH2 (cdc25 homology) in the MKPs family, we suggest that the sequence of such domains be closely examined for any possible substitution as well for possible future investigations.
3. PCR is a common technique widely used in cellular and molecular and biochemical laboratories. Therefore, the details of PCR are not discussed in this chapter.

4. A purified protein is required for PTP activity assay. When purified protein is unavailable, cells may be transfected with plasmids encoding the pseudophosphatase, and immunoprecipitation performed to obtain purified protein. Then, a PTP activity assay may be performed. PTP catalytic activity is very substrate specific; therefore, commercial PTP activity kits may not be specific enough to test for putative "restored" activity, and it may be necessary that specific substrates be radiolabeled with [γ-P^{32}]ATP.
5. MK-STYX has been successfully overexpressed in mammalian cell lines such as HEK-293, HeLa, COS-1, and PC12. The appropriate media such as Dulbecco's modified Eagle medium (DMEM), minimum essential medium (MEM), or Roswell Memorial Institute (RPMI) medium are required to culture each cell line successfully.
6. No one buffer is universal to sufficiently lyse all cells. Therefore, it is important to choose the appropriate buffer that allows the release of a recognizable antigen (pseudophosphatase) by the antibody. Various buffers such as NP-40 Lysis: 150 mM NaCl, 1% NP-40, and 50 mM Tris–HCl, pH 8.0 (nonionic detergent) or RIPA: 150 mM NaCl, 1% NP-40, 0.5% sodium deoxycholate, 0.1% SDS (combination of nonionic and ionic detergents, thus more denaturing), and 50 mM Tris–HCl, pH 8.0 should be tested to determine the most efficient way to release the pseudophosphatase and other proteins. Researchers may build their own lysis buffer by altering salt concentration, type of detergent, pH, and the presence of divalent cations, which are variables that may drastically alter the release of proteins in the cells.
7. The addition of phosphatase inhibitors or other inhibitors to the lysis buffer is dependent on the design of the experiment. When studying an active phosphatase, we suggest including phosphatase inhibitors in the lysis buffer. We add all inhibitors to the buffer immediately before lysing cells, providing enough time to dissolve in buffer on ice.
8. Although an antibody for MK-STYX (anti-STYXL1) is now available, we prefer to use anti-FLAG for immunoprecipitating over-expressed Flag-tagged MK-STYX for the following reasons: (1) reliability, (2) specificity to the over-expressed MK-STYX, and (3) cost. Therefore, we recommend when immunoprecipitation does not require pulling down the endogenous protein of interest, an antibody against the tag epitope is used. Furthermore, if an active mutant phosphatase is used as a comparison tool of the pseudophosphatase, then antibody against the tag epitope should be used. The success

of immunoprecipitation is dependent on the purification of the antigen, which is affected by the abundance of antigen in sample, and the affinity of the antibody for the antigen.

9. Purifying the immune complex (pseudophosphatase antibody, and possible unidentified binding partners) relies on the appropriate secondary reagent that binds the antibody. Therefore, the appropriate beads (recombinant protein A or G) should be chosen, based on the affinity to the immunoglobulin. Protein G or A differs in its binding strength to immunoglobulins from different species and subclasses. For example, anti-FLAG antibody produced in mouse has a greater affinity for isotope IgG1 (immunoglobulin); therefore, protein G beads were used to precipitate MK-STYX fused to FLAG.
10. It is helpful to pre-label tubes ahead of time with the correct lysate (sample), and antibody used. When we immunoprecipitate with two different antibodies, we prefer to use two different colors of 1.5 mL centrifuge tubes.
11. Collaboration should be established with a mass spectrometry facility during initial experiments so that the correct parameters for buffers and elution procedure may be established with the mass spectrometry facility performing the analysis. The decision may be not to elute samples from the beads with sample loading buffer, and/or not to use protein A or protein G beads to interact with the antibody. When mass spectrometry was performed on the immunoprecipitate for MK-STYX, the immunoprecipitation was performed with EZview™ RED ANTI-FLAG^{R} M2 Affinity Gel, and the mass spectrometry facility performed the elution.
12. Both Coomassie Blue and silver staining are used to visualize proteins. However, silver staining is 30-fold more sensitive and is compatible with mass spectrometric analysis. We use Coomassie Blue staining for initial analysis of complexes. When the decision is made to identify a specific protein, silver staining is used so that mass spectrometry may be performed. Coomassie Blue and silver stain may be purchased commercially. The manufacturer's protocol should be followed.
13. We have provided a protocol for the traditional way to transfer proteins to membranes. However, PVDF or nitrocellulose membranes may be purchased as stacks (membrane, blotting paper, cathode, anode, and the required buffers) for quick and reliable transfer. These stacks require the purchase of a specialized gel transfer device such as the iblot (GE, Health Care) or Trans-Blot Turbo System (BioRad). We use both traditional and newer techniques, and have found, with low protein

concentrations, that the iBlot provides the best results; we have not tested the Trans-Blot Turbo System for these purposes.

14. Various blocking reagents may be used, depending on the antibody required for the immunoblotting. 5% milk is a commonly used blocking reagent. To substitute for milk, many labs also use a commercial blocking reagent that accompanies the secondary antibodies. The antibody product sheet will provide specifications for antibody concentrations and/or ratios and blocking conditions to be used; some antibodies may require the use of BSA as a blocking agent.
15. When detecting (probing) proteins that migrate at or near each other, the membrane must be stripped and re-probed with the other primary antibody of interest. The reagents provided in this chapter are for a mild stripping buffer. However, a more stringent stripping buffer (when residual is seen from the first blot) may be used.
16. RNA interference (RNAi) is commonly used to examine intracellular protein functions; it allows sequence-specific repression of gene expression through mRNA degradation or translational repression [17]. RNAi may be accomplished by introducing small interfering RNAs (siRNAs) directly into cells, or by introducing plasmid expression vectors for short hairpin RNAs (shRNAs) [7, 18], or viral vectors for short hairpins (more stable conditions) [19]. Methods in this chapter describe transfection techniques using a commercially available plasmid that co-expresses green fluorescent protein (GFP) and shRNA against the pseudophosphatase MK-STYX. The advantage of coexpression of GFP is that transfection efficiency can be validated by viewing cells under a fluorescence microscope.
17. More than one shRNA should be included in the knockdown experiment to ensure that any results are not due to nonspecific, off-target effects. shRNAs with different efficacies of knockdown also provide an additional level of control and verify for dose dependency of functional effects [19].
18. RNAi experiments are only significant when knockdown of the specific gene is confirmed; therefore, knockdown must be validated. Knockdown of the transcript is confirmed by qPCR, and the knockdown of the protein product may be confirmed by immunnoblotting. Immunoblotting provides visualization of the protein knockdown (and may also provide semiquantitative validation), whereas qPCR allows highly accurate quantification of gene expression levels [3, 20]. We recommend using both methods in combination.
19. High-quality RNA is important for gene expression experiments and is essential for accurate, good-quality, and consistent real-time quantitative PCR analysis [3]; a BioAnalyzer

(Agilent) may also be used to quantitate the RNA as well as DNA or proteins.

20. Not all pseudophosphatases may be able to have their activity "restored." However, it is worthwhile to test whether, as in the case of the prototypical STYX [21] or MK-STYX [11], mutations could be introduced to generate a catalytically competent form. A comparison of the effects of the catalytically active and inactive form of a pseudophosphatase may exert different functions on signaling cascades, which may provide insight into a specific role of a pseudophosphatase.
21. In the enzymology arena the term "mutant" is normally associated with creating an inactive version of an enzyme. Therefore, we coined the term "active mutant" to avoid confusion.
22. Immunoprecipitation should be done on ice; therefore, buffers, centrifuges, and microcentrifuge tubes should be at 4 °C. It is not necessary for the experiment to be done in a cold room; however, the 1.5 mL microcentrifuge tubes should be prechilled, and buffers stored on ice during the procedure.
23. Another constraint of immunoprecipitation is determining the amount of antibody-antigen ratio (how much antibody should be used to efficiently interact with the antigen). The protocol provided has been optimized for 1 mg/mL protein lysate. Occasionally, we have used 2 mg/mL; however, when a larger amount of protein lysate is preferred, the amount of antibody as well as protein A or G agarose beads should be optimized.
24. Preclearing lowers the background and improves the signal-to-noise ratio by minimizing nonspecific binding (proteins in the lysates that bind nonspecifically are removed). Because of the commercial availability of protein A or G beads, and the thought that these products are immediately ready for immunoprecipitation, many investigators think that they can skip preclearing. However, we suggest preclearing the lysate (samples), at least with the beads. Preclearing may also be done by adding an irrelevant antibody to the lysate and following the immunoprecipitation procedure. We found that adding beads alone suffices, and provides an efficient control "mock" immunoprecipitation.
25. The most common concern about immunoprecipitation is background (nonspecific binding). However, it is important to note that background may be specific, when antigens are recognized by spurious antibodies used for the experiment, which gives rise to specific background bands. Methods to solve this problem are as follows: (1) remove the contaminated antibody by using an antigen affinity column to purify the antigen-specific antibody, and (2) block the contaminated antibody's activity by saturating it with the proteins that it

binds. Nonspecific background results from numerous sources. This problem is often solved by using more stringent washes, alternating wash buffers from high salt to low salt, and increasing the number of washes or length of wash.

26. SDS-PAGE gels may be made at various concentrations (6–12 %) dependent on molecular mass (size) of the protein of interest. Typically a 10 % gel is used for resolving proteins of a broad range of molecular weights. When the protein of interest resolves at large molecular weight, lower gel percentages are used and higher gel percentage for proteins that resolve at smaller molecular weights. A gradient gel with various acrylamide percentages may also be used. Instead of making SDS-PAGE gels, they may also be purchased commercially at the desired percentages or gradients.
27. Whether overexpressing MK-STYX or knocking down MK-STYX in PC12 cells, a morphological difference was immediately noticed. Over-expressing MK-STYX induced these cells to form neurite-like outgrowths, whereas knockdown prevented any outgrowth. Furthermore, RhoA activity decreased in the presence of MK-STYX, and increased when MK-STYX was knocked down [16].
28. To determine the role of MK-STYX in neuronal differentiation, we knocked down MK-STYX and stimulated cells with 100 ng/mL nerve growth factor (NGF) [16].
29. MK-STYX decreased RhoA activation; therefore, we evaluated MK-STYX′ effect on the RhoA downstream effector, cofilin. Knocking down MK-STYX increased cofilin phosphorylation in unstimulated cells, but decreased it 24 h post-NGF stimulation [16]. MK-STYX′ effects on RhoA and cofilin dynamics imply that this pseudophosphatase may have a role in biological functions where cytoskeletal reorganization is important.

Acknowledgements

We are grateful for researchers such as Jack E. Dixon who dared to investigate catalytically inactive members of the PTP family. Furthermore, we would like to thank Nicholas K. Tonks for introducing us to the pseudophosphatase MK-STYX; it is a fascinating protein to study. We would also like to thank Lizabeth A. Allison, for her interest and enthusiasm in our pursuit of the function of a "dead" phosphatase. Finally, I thank all my former undergraduates and Master's student who have tirelessly assisted with the projects related to MK-STYX. This work was supported in part by Jeffress

Memorial Trust Award J-931 (to S.D.H.), National Science Foundation grant MCB1113167 (to S.D.H.), and the Howard Hughes Medical Institute Undergraduate Science Education Grant awarded to the College of William and Mary.

References

1. Wishart MJ, Dixon JE (1998) Gathering STYX: phosphatase-like form predicts functions for unique protein-interaction domains. Trends Biochem Sci 23:301–306
2. Tonks NK (2009) Pseudophosphatases: grab and hold on. Cell 139:464–465
3. Kharitidi D, Manteghi S, Pause A (2014) Pseudophosphatases: methods of analysis and physiological functions. Methods 65:207–218
4. Tonks NK (2006) Protein tyrosine phosphatases: from genes, to function, to disease. Nat Rev Mol Cell Biol 7:833–846
5. Begley MJ, Dixon JE (2005) The structure and regulation of myotubularin phosphatases. Curr Opin Struct Biol 15:614–620
6. Robinson FL, Dixon JE (2005) The phosphoinositide-3-phosphatase MTMR2 associates with MTMR13, a membrane-associated pseudophosphatase also mutated in type 4B Charcot-Marie-Tooth disease. J Biol Chem 280:31699–31707
7. Prohits Interaction Repository (2012). http://prohits-web.lunenfeld.ca/GIPR/index.php?m_num=m1&DataSets_Sel=0
8. Cheng KC, Klancer R, Singson A, Seydoux G (2009) Regulation of MBK-2/DYRK by CDK-1 and the pseudophosphatases EGG-4 and EGG-5 during the oocyte-to-embryo transition. Cell 139:560–572
9. Parry JM, Velarde NV, Lefkovith AJ, Zegarek MH, Hang JS, Ohm J, Klancer R, Maruyama R, Druzhinina MK, Grant BD, Piano F, Singson A (2009) EGG-4 and EGG-5 link events of the oocyte-to-embryo transition with meiotic progression in C. elegans. Curr Biol 19:1752–1757
10. Reiterer V, Fey D, Kolch W, Kholodenko BN, Farhan H (2013) Pseudophosphatase STYX modulates cell-fate decisions and cell migration by spatiotemporal regulation of ERK1/2. Proc Natl Acad Sci U S A 110:E2934–E2943
11. Hinton SD, Myers MP, Roggero VR, Allison LA, Tonks NK (2010) The pseudophosphatase MK-STYX interacts with G3BP and decreases stress granule formation. Biochem J 427:349–357
12. Siligan C, Ban J, Bachmaier R, Spahn L, Kreppel M, Schaefer KL, Poremba C, Aryee DN, Kovar H (2005) EWS-FLI1 target genes recovered from Ewing's sarcoma chromatin. Oncogene 24:2512–2524
13. Barr JE, Munyikwa MR, Frazier EA, Hinton SD (2013) The pseudophosphatase MK-STYX inhibits stress granule assembly independently of Ser149 phosphorylation of G3BP-1. FEBS J 280:273–284
14. Niemi NM, Lanning NJ, Klomp JA, Tait SW, Xu Y, Dykema KJ, Murphy LO, Gaither LA, Xu HE, Furge KA, Green DR, MacKeigan JP (2011) MK-STYX, a catalytically inactive phosphatase regulating mitochondrially dependent apoptosis. Mol Cell Biol 31:1357–1368
15. Niemi NM, Sacoman JL, Westrate LM, Gaither LA, Lanning NJ, Martin KR, Mackeigan JP (2014) The pseudophosphatase MK-STYX physically and genetically interacts with the mitochondrial phosphatase PTPMT1. PLoS One 9:e93896
16. Flowers BM, Rusnak LE, Wong KE, Banks DA, Munyikwa MR, McFarland AG, Hinton SD (2014) The pseudophosphatase MK-STYX induces neurite-like outgrowths in PC12 cells. PLoS One 9:e114535
17. Obbard DJ, Gordon KH, Buck AH, Jiggins FM (2009) The evolution of RNAi as a defence against viruses and transposable elements. Philos Trans R Soc Lond B Biol Sci 364:99–115
18. Aagaard L, Rossi JJ (2007) RNAi therapeutics: principles, prospects and challenges. Adv Drug Deliv Rev 59:75–86
19. Moore CB, Guthrie EH, Huang MT, Taxman DJ (2010) Short hairpin RNA (shRNA): design, delivery, and assessment of gene knockdown. Methods Mol Biol 629:141–158
20. Derveaux S, Vandesompele J, Hellemans J (2010) How to do successful gene expression analysis using real-time PCR. Methods 50:227–230
21. Wishart MJ, Denu JM, Williams JA, Dixon JE (1995) A single mutation converts a novel phosphotyrosine binding domain into a dual-specificity phosphatase. J Biol Chem 270:26782–26785

Chapter 10

Crystallization of PTP Domains

Colin Levy, James Adams, and Lydia Tabernero

Abstract

Protein crystallography is the most powerful method to obtain atomic resolution information on the three-dimensional structure of proteins. An essential step towards determining the crystallographic structure of a protein is to produce good quality crystals from a concentrated sample of purified protein. These crystals are then used to obtain X-ray diffraction data necessary to determine the 3D structure by direct phasing or molecular replacement if the model of a homologous protein is available. Here, we describe the main approaches and techniques to obtain suitable crystals for X-ray diffraction. We include tools and guidance on how to evaluate and design the protein construct, how to prepare Se-methionine derivatized protein, how to assess the stability and quality of the sample, and how to crystallize and prepare crystals for diffraction experiments. While general strategies for protein crystallization are summarized, specific examples of the application of these strategies to the crystallization of PTP domains are discussed.

Key words Crystallogenesis, Se-methionine protein, Crystal seeding, Crystallization trials, Cryoprotectant

1 Introduction

Protein tyrosine phosphatases are important pharmacological targets [1–5] and therefore they have been extensively studied at the structural level [6–8]. A comprehensive list of available PTP structures, both of PTP domains and PTP extracellular regions, has been extracted from the Protein Data Bank (PDB) and can be found in the Appendix.

Protein crystallization has experienced a major evolution during the past 30 years with the introduction of faster cloning approaches, more sophisticated recombinant expression systems and the use of robotics to assist in setting up trials. Advances on all these fronts have transformed crystallogenesis from a "magic art"

The online version of this chapter (doi:10.1007/978-1-4939-3746-2_10) contains supplementary material, which is available to authorized users.

Rafael Pulido (ed.), *Protein Tyrosine Phosphatases: Methods and Protocols*, Methods in Molecular Biology, vol. 1447,
DOI 10.1007/978-1-4939-3746-2_10, © Springer Science+Business Media New York 2016

into a routine approach in structural biology laboratories around the world. These advances have evolved in parallel with major technical and engineering developments of X-ray generators, detectors and high-brilliance synchrotron beam lines, an increase in computing speed and the dissemination of new software packages that streamline data processing, structure determination and refinement. During this period, the number of protein structures deposited in the PDB [9] as grown from 186 in 1985 to more than 110,000 in 2015, 372 of which are PTPs.

However, the main challenge remains in the production of high quality crystals to yield good quality data from the X-ray diffraction experiments. A number of factors affect data quality, from the choice of the construct boundaries, to the freezing of the crystals in preparation for diffraction. A careful inspection and analysis of the protein sequence prior to cloning is essential to establish the correct sequence boundaries or to design mutations that may improve stability of the recombinant protein. The decisions taken at this stage will have a large impact on protein solubility, the purification process and its chances to crystallize. Even if crystals are readily obtained, the internal packing and therefore the diffraction quality and maximum resolution that can be achieved in determining the structure will depend in part, on the quality of the protein and its behavior in solution. If no crystals are obtained with the initial construct, we recommend a reinspection of the design to generate alternative boundaries, eliminate potentially disordered regions or to minimize surface entropy. PTP domains contain a compact and a well-conserved fold with an antiparallel β-sheet (five to eight strands) and surrounding helices (five to eight). Most variations in the constructs will affect the N-terminal region where more variability exists between PTPs. A sequence and structural alignment of several PTP structures related to your target PTP might help to define similar boundaries for your initial construct.

A main consideration for successful crystallization should be the solubility of the recombinant protein. Very soluble proteins can be concentrated to high levels (>10 mg/mL), which speeds up the initial nucleation process and facilitates crystallogenesis. Quality control of the protein sample is essential to ensure the purity (>95% pure) and homogeneity of the sample. For this, we recommend to characterize the behavior of your purified protein in solution by testing enzyme activity, if the wild-type PTP protein is expressed, as well as monodispersity of the sample to ensure that it contains only *one type* of particle, either monomer or dimer, or other oligomers. Polydispersity (i.e., a mix of monomer/oligomers) of the sample results inevitably in a lack of crystallogenesis or poorly diffracting crystals. Achieving monodispersity requires rigorous purification of the protein (*quality over quantity always!*) involving affinity purification, ion exchange and size exclusion chromatography. Often, an additional screening of different pH and buffer

conditions is necessary to prevent unspecific aggregation and precipitation of the protein. The use of additives such as EDTA/EGTA, reducing agents (DTT, TCEP, β-mercaptoethanol), metal ions and other ligands is sometimes needed to stabilize the protein or its oligomeric state, thus ensuring homogeneity.

PTPs are more stable in buffers that contain sulfonic groups such as HEPES or MES because these bind to the active site and maintain the P-loop in its extended open conformation. Often the active site in PTP crystals is occupied by either phosphate or sulfate that are captured from the culture media, contamination in the buffers (from glassware washing detergents), or the crystallization conditions (specially ammonium sulfate precipitant). These ligands will help crystallogenesis of the apo-enzyme, but may need to be removed if you are planning to do co-crystallization or soaking with other ligands (inhibitors, substrates or peptides).

Protein crystallogenesis consists of preliminary screens, using automation and robotics systems if available, testing a variety of preset precipitant conditions (mostly commercially available screens), followed by systematic optimization of the initial hits to produce larger or better quality crystals. Optimization approaches involve seeding with the initial crystals to grow larger crystals in larger drops and/or refining the crystallization conditions (precipitant concentration, pH, type of buffer, temperature, additives, or ligands). Once crystals are obtained, the next step is to identify a suitable cryoprotectant to allow efficient flash freezing of the crystals without compromising their integrity of the quality of X-ray diffraction.

The whole process, from protein purification, crystallogenesis to preparing crystals for X-ray diffraction, can take as little as a few days for high quality stable and well-behaved proteins, to several weeks if optimization is required. Most human PTPs will crystallize readily under standard and published conditions.

If no results are obtained, do not despair! There is always an alternative way for reluctant proteins. For example, co-crystallization with ligands or substrates, co-expression with chaperones or co-expression/purification with more biological protein partners to form stable complexes. Failing that, choosing an ortholog from another species may prove helpful, particularly if present in a thermophile.

2 Materials

All solutions should be prepared with ultra pure deionized water, filtered using a 0.22 μm filter and kept in glass containers. Chemical reagents should be of analytical grade with >98 % purity. We recommend storing all solutions at 4 °C except for high concentration salt buffers (>1 M), which should be stored at room temperature.

Polyethylene glycol solutions are susceptible to microbial contamination that can be prevented by adding 0.02% of sodium azide. Commercial solutions do not require further additives as they may already contain azide or other antimicrobials. Precautions should be taken when manipulating sodium azide or other toxic and hazardous chemicals; always follow manufacturer's instructions. Make sure that you adhere to good laboratory practice regulations and that you comply with health and safety guidelines for the disposal of chemicals and waste materials.

2.1 Se-Methionine Protein Production

1. LB media: Dissolve 10 g of tryptone, 5 g of yeast extract, and 10 g of NaCl in water and make up volume to 1 L. We recommend adding glucose up to 1% to stop any leaky expression. Sterilize by autoclaving and store at room temperature.
2. Minimal media: Prepare the M9 salts by dissolving 64.0 g $Na_2HPO_4{\cdot}7H_2O$, 15.0 g KH_2PO_4, 2.5 g NaCl, 5.0 g NH_4Cl in distilled deionized water and adjust to a final volume of 1 L. Sterilize by autoclaving. This is enough for 5 L of culture medium and can be split into aliquots and stored at 4 °C for future use. To prepare 1 L of minimal media, use 500 mL of sterile distilled deionized water, add 200 mL of the M9 salts stock (see above), 2 mL of 1 M $MgSO_4$ (sterile), 20 mL of 20% glucose or glycerol, 100 μL of 1 M $CaCl_2$ (sterile), 1 mL of the trace element mix and adjust pH to 7.4 with NaOH as needed. Adjust to a final volume of 1 L with sterile distilled deionized water (adapted from Sambrook [10]).
3. Trace element mix (1000×): use 800 mL of sterile distilled deionized water to dissolve 4.4 g of $ZnSO_4{\cdot}7H_2O$, 180 mg of $MnCl_2{\cdot}4H_2O$, 20 mg of $(NH_4)_6Mo_7O_{24}{\cdot}4H_2O$, 80 mg of $CuSO_4{\cdot}5H_2O$, 5.0 g of $FeSO_4{\cdot}7H_2O$, 250 mg of $CoCl_2$, and 1.0 g of H_3BO_3. Add 1 mL of concentrated H_2SO_4, adjust to a final volume of 1 L with distilled deionized water. Filter to sterilize (do not autoclave!).
4. Amino acid mix (powder): Phenylalanine (100 mg/L), threonine (100 mg/L), lysine (100 mg/L), isoleucine (50 mg/L), leucine (50 mg/L), valine (50 mg/L), and l-selenomethionine (80–120 mg/L).
5. Phosphate buffered saline (PBS): Dissolve 8.0 g of NaCl, 200 mg of KCl, 1.44 g of Na_2HPO_4, 240 mg of KH_2PO_4 in 800 mL distilled deionized water. Adjust pH to 7.4 with HCl and adjust to a final volume of 1 L. Sterilize by autoclaving.
6. Lysis buffer: use preferred lysis buffer. We recommend avoiding PBS if you plan to do co-crystallization with ligands. Phosphate binds to the active site and it may be difficult to displace by the ligand if used at low concentrations. Alternatively use a buffer containing 20 mM HEPES, 500 mM NaCl, 1 mM

TCEP, 0.1% Triton X-100, 10 mM imidazole, pH 7.4 for His-tagged proteins. For GST-tagged proteins use 20 mM HEPES, 150 mM NaCl, 3 mM TCEP, 0.1% Triton X-100, 2 mM EDTA, pH 7.4. Protease inhibitors can be also added if necessary (commercial cocktails are available). Follow with your established purification procedures.

2.2 Protein Crystallogenesis

1. Commercial screens for crystallogenesis. Several companies sell prefilled 96 deep well blocks screens ready for use with automated liquid-handling robotics systems or individual kits containing 24–96 reagents, each in 10 mL bulk that can be used to setup manual screens. A good starting screen is the JBScreen Phosphatase from MiTeGen, derived from data mining the PDB for successfully crystallized phosphatases [11]. Other popular general screens are the Morpheus (Molecular Dimensions [12]), Crystals Screen I and II (Hampton Research [13]), PEG/Ion [12, 13], PACT premier, JCSG$^+$, JCSG Core Suite (QIAGEN [14]).
2. Crystallization plates: MRC crystallization plates [12], 24-well "Linbro" plate [12], XTalQuest 24-well plates for sitting drops [11], Crystal Clear Sealing tape, siliconized glass cover slides for hanging drop crystallogenesis in "Linbro" style plates and Dow Corning high vacuum grease [12–14].
3. Seeding tools: Streak seeding tool [14], MicroSeed Beads for the preparation of seed stocks for use in microseeding and Matrix seeding protocols [12, 14].

2.3 Crystal Freezing and Mounting

1. Cryoproctectant oils: Parabar 10312 (formerly known as Paratone-N), Perfluoropolyether Cryo Oil, and Santovac Cryo Oil are all commonly used for cryoprotection of crystals [14]. Parabar 10312 is a viscous oil and it is recommended to mix with 50% mineral oil to lessen the mechanical stress on your crystals during the freezing procedure.
2. Two primary styles of cryo-loops are available, fiber-based loops [14] and Lithographic loops [11, 12]. A selection of loop sizes will be required, an ideal loop will match the crystal size, avoiding contact with the crystal whilst minimizing the surrounding liquor. Lithographic style loops are also available in a variety of shapes and meshes that can provide additional support when dealing with thin plate like crystals.
3. SPINE standard cryo-pins are compatible with the vast majority of synchrotron facilities worldwide. For a full list of compatibility *see* ref. 15.
4. Different Synchrotrons utilize different crystal positioning systems—it is important to check with your local synchrotron which system they are using as specialist equipment and tools

will be required. However basic cryo-cooling of crystal samples will require:

- Magnetic cryo-wand for spine caps [12, 13].
- Dewars, metal or foam [12, 13]. Modern foam-based Dewars are excellent for plunge freezing crystals. A shallow dewar holding no more than ~10 cm depth of liquid nitrogen is ideal for plunge freezing.
- Shipping Dewar. A popular option for shipping frozen crystals is the Taylor Wharton CX100 Dry Shipper and Shipping Case. This system can be matched with a variety of inserts to allow the safe transportation of cryogenically stored crystal samples internationally to your chosen synchrotron facility. The most appropriate dry shipper will vary depending upon the crystal positioning system utilized at your chosen synchrotron [12, 13].

3 Methods

3.1 Construct Design and Sequence Analysis

1. Use the XtalPred-RF website [16] to run a prediction on the crystallizability of your PTP construct. Paste the sequence of your protein construct in FASTA format and into the search box.
2. Tick boxes for the SERp analysis and the optional feature to find bacterial homologues.
3. Retrieve results. You will find information on the estimated isoelectric point (IP) of the protein (*see* **Note 1**), disorder prediction, crystallization classes and homologues in the PDB or other databases (Fig. 1).
4. Click on the "link to protein details", this will take you to a page containing the full analysis of your construct and its probability of crystallization in comparison to a pool of other proteins. It also contains links to homologues in either the PDB or a nonredundant database. It has a table with the protein features and predictions and a link to the construct design page (Fig. 2).
5. Click to the link "construct design" to access to the multiple sequence alignment and information on conservation, disorder, secondary structure, and others. When designing your construct it is important to consider a number of key factors and the bioinformatics analysis will help to guide you in choosing appropriate boundaries, avoiding regions of disorder whilst maintaining all highly conserved structural and catalytic elements (Fig. 2). It is wise to generate more than one construct with a series of termini varying by ~2 residues at a time, this will give you the greatest chance of hitting the ideal length for

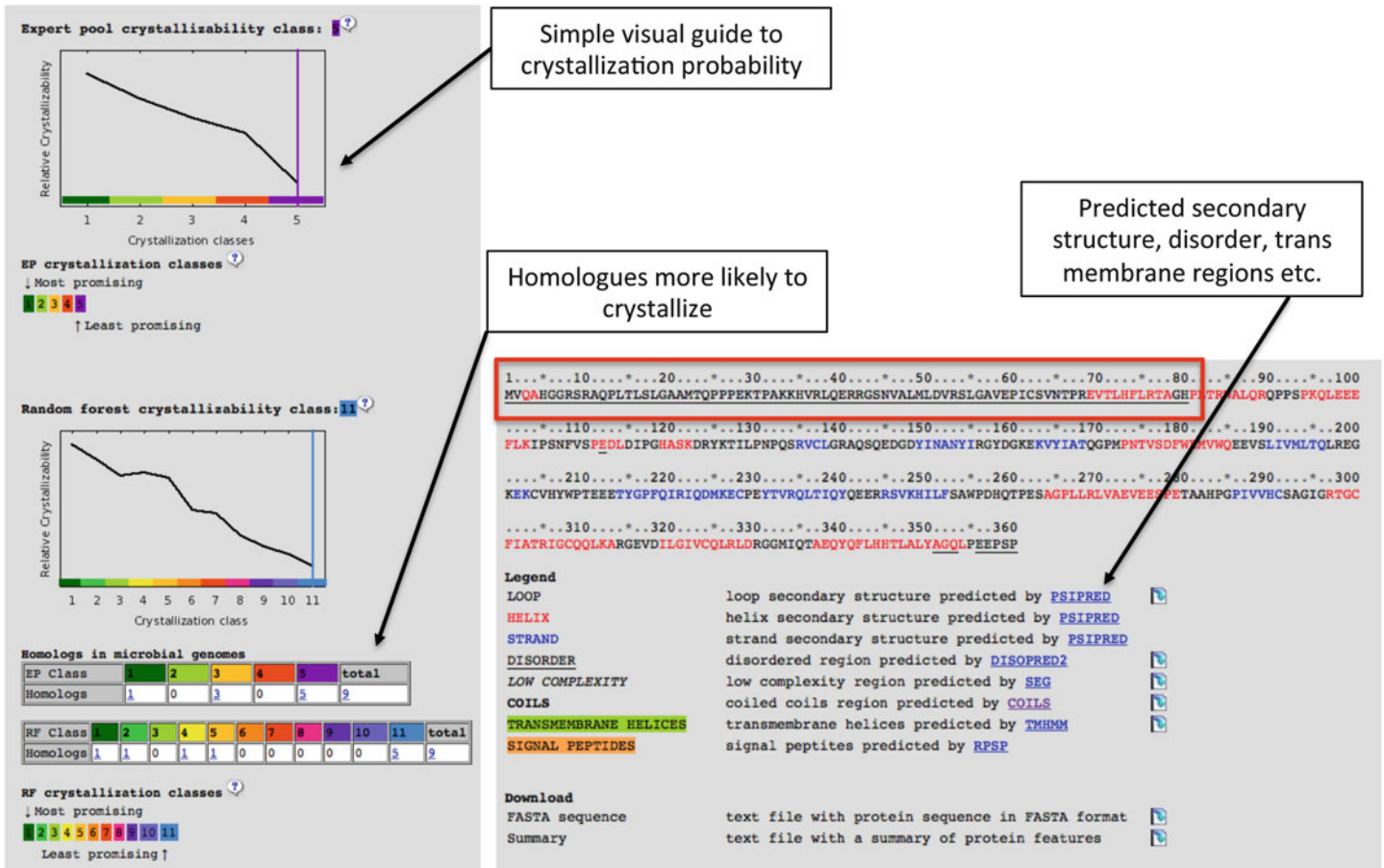

Fig. 1 Results obtained in a *XtalPred-SerP* query for PTPN7. Different parameters are provided: an estimated evaluation of the probability of successful crystallization of the construct, information of secondary structure predictions and homologues in microbial species that could be used as alternatives for crystallization. In this example, the full sequence has a very poor crystallizability score and the first 80 residues are predicted to be disordered, suggesting that a shorter version should be considered when designing the construct for protein expression

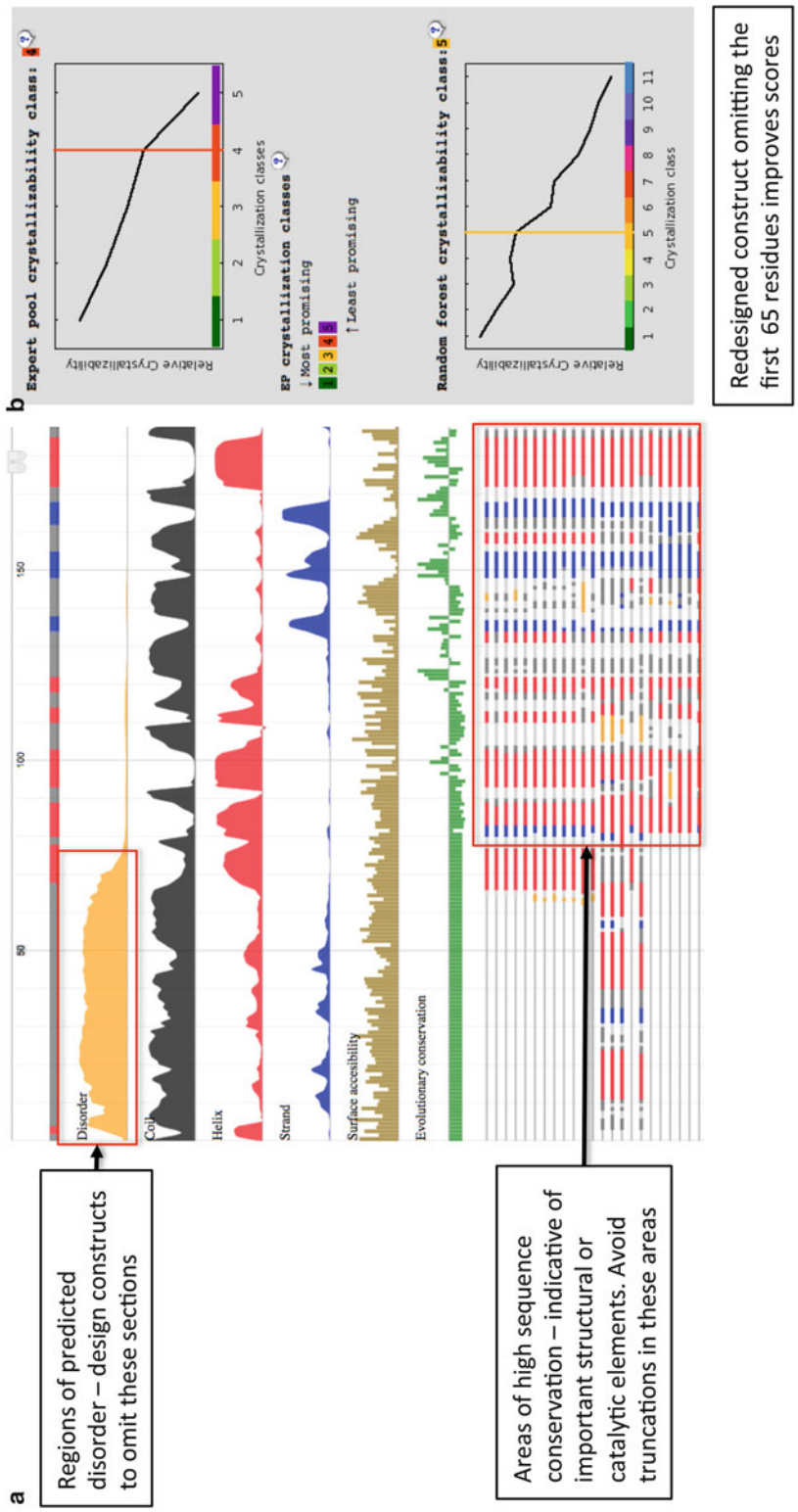

Fig. 2 (**a**) Example of results obtained for PTPN7 from the *XtalPred-SerP* "construct design" section. The prediction results highlight a disordered region at the N-terminus of the input construct sequence. Evolutionary conservation highlights areas to maintain in the construct, while others not conserved can be removed. A suggested strategy is to generate a series of constructs truncated in a stepwise manner, perhaps two residues at a time, to enhance the chances of obtaining a stable protein [17]. (**b**) Omision of the first 65 residues substantially improves the chances of crystallization as seen in the better scores. The prediction is confirmed in this case as the N-terminal truncation construct has yielded 15 structures (wt and mutants) deposited in the PDB

crystallogenesis [17] In addition it is useful when affinity tagging your protein for purification to design constructs with both N and C terminal cleavable tags. Many PTPs have been crystallized with their affinity His-tag in place, however as the tag can impede crystallogenesis or crystal packing in some instances (particularly with larger tags such as GST or MBP), designing the cleavage into your construct from the outset can save a lot of time later in the process.

3.2 Expression Systems Used to Produce PTP Proteins for Crystallographic Analyses

1. The preferred vectors for recombinant expression systems used for PTPs are those that provide His-tag fusions with the target PTP gene (pET, pNIC and their variations, *see* Appendix). Less common now is the use of GST-tag fusions using pGEX vectors, as these require protease cleavage of the GST tag prior to crystallization. GST-tags may also interfere with phosphatase activity and induce dimerization if left uncleaved. The use of proteases such as thrombin has additional liabilities because they may also cleave the target protein, therefore these should be avoided when possible. We recommend choosing a vector that contains a His-tag, a small linker and a very specific protease cleavage site (i.e., TEV protease) to minimize chances of proteolytic cleavage during preparation of the sample and generating undesirable heterogeneity.
2. The preferred host for expression of PTP catalytic domains is *E. coli* (Appendix). Bacterial hosts with T7 RNA polymerase systems are the most commonly used for large-scale expression because they are easy and relatively inexpensive to culture and produce high yield of recombinant protein. Common strains used are BL21 and all its derivatives (BL21 (DE3), BL21 pLysS, B834, C41 (DE3), CodonPlus, Rosetta, Shuffle, or Tuner). If you have difficulties optimizing expression on your chosen system, we recommend to try different hosts first (various bacterial strains) and then change your vector. Some strains such as C41, Rosetta, or Shuffle give better results with proteins that are toxic to bacterial growth.
3. Extracellular domains of PTPs are normally expressed in mammalian cells lines (CHO, HEK-293) (Appendix) or using cell-free systems (less common as yields are low). Mammalian cell expression allows for posttranslational modifications such a glycosylation, which may be essential for native protein folding. These expression systems are more expensive because of the medium used and the protein yield is sometimes lower than bacterial expression systems.

3.3 Preparing Se-Methionine Derivatized Protein

1. Prepare minimal media the day before the experiment as per materials instructions.
2. Grow a starter culture (20–50 mL), from your glycerol stocks or from plated colonies, in LB media supplemented with the

appropriate antibiotics and glucose (1%), at 37 °C overnight with agitation.

3. Next morning, transfer some (or all) of the overnight culture into 1 L of prewarmed unlabelled LB media, supplemented with antibiotic and glucose. Grow this culture at 37 °C with good aeration to promote rapid proliferation to reach an OD_{600} of 6–10 in about 2 h.
4. Harvest the grown culture at 3500 × *g* for 30 min in a refrigerated centrifuge, discard the supernatant medium and wash the pellet with autoclaved PBS buffer three to four times to remove completely the LB medium.
5. Prepare the Se-Met medium by dissolving the amino acid mix (without methionine!!) powder into the minimal media. Resuspend the pellet in warm Se-medium and incubate the culture for 2 h at 37 °C. The mix is designed to inhibit methionine biosynthesis and to allow the incorporation of Se-Met instead (*see* **Note 2**).
6. Induce your culture with IPTG according to the preestablished conditions (temperature, and length of time) for the unlabeled protein. In the new medium it may require a bit of extra time for the bacteria to adjust to the new growth conditions.
7. Harvest the cells in the usual manner 3500 × *g*, 4 °C, 15–30 min and flash-freeze the pellets in LN_2 and store at –80 °C.
8. When ready to proceed with the purification, thaw the tubes with the pellet in a bucket with ice, resuspend the pellet in enough lysis buffer to obtain a density of approximately 0.2 g/mL (e.g., 10 g topped to 50 mL), and then transfer to a beaker. You can vortex the tubes to help homogenizing the suspension. Make sure that the suspension is smooth with no clumps of pellet left.
9. Disrupt the cells by sonication or other means (French press, homogenizer) and separate the supernatant containing your overexpressed protein by centrifugation (12,000 × *g* 30 min, repeat twice to clarify the supernatant until it looks transparent). Proceed with your purification protocol the same as used for unlabeled protein.

3.4 Assessing the Quality of Your Sample

Critical to successful crystallization is the quality of the protein sample. This should be in a native conformation, preferably active, monodisperse, homogeneous, and soluble at high concentrations if possible. A number of biophysical techniques are now routine in many laboratories and biomolecular facilities that provide a quality profile of a given protein sample. These include circular dichroism, analytical ultracentrifugation (sedimentation velocity and equilibrium sedimentation), multi-angle laser light scattering, dynamic

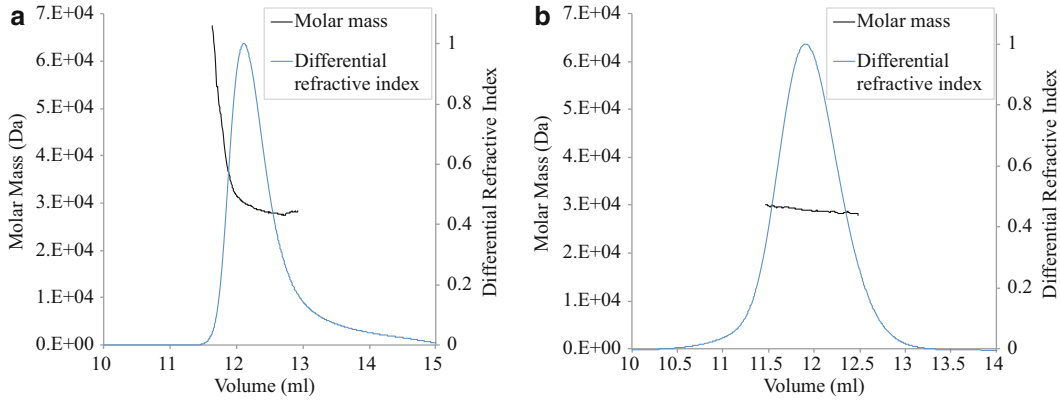

Fig. 3 Example of SEC-MALS (size-exclusion chromatography and multiangle light scattering) analysis of two different PTPs samples (**a**) protein sample, in 20 mM MES, 150 mM NaCl, 1 mM EDTA, pH 6.0, showing a polydisperse distribution of molecular mass values although it elutes in a single peak (11.5–13.3 mL). (**b**) Protein sample, in 20 mM HEPES, 150 mM NaCl, 1 mM EDTA, pH 7.4, showing a monodisperse distribution of molecular mass throughout the elution peak (11.3–12.7). Data courtesy of Dr. Andrew Currin

light scattering, 1-D NMR, and fluorescence spectroscopy (Thermofluor) [18]. These techniques allow the investigation of the size and shape of proteins particles, to calculate the hydrodynamic parameters, to estimate secondary structure content and the stability of your protein under different buffer and pH conditions [18]. This information is very valuable to design the best crystallization strategy and complements the structural analyses. Most of these techniques are conservative, do not destroy the protein and require small amounts of sample. An example of a monodisperse and polydisperse protein sample is shown in Fig. 3.

3.5 Assessing the Stability of Your Sample by Thermofluor

Thermofluor or Differential Scanning Fluorimetry (DSF) provides a fluorescence readout measurement of thermally induced melting in proteins. Knowledge about the temperature at which a given protein melts, T_m, is a good indicator of protein stability. It has been clearly shown that optimizing the stability of protein samples for crystallogenesis can aid the formation of crystals [19]. The three dimensional lattice is favored when all protein molecules present within the solution adopt a single structurally identical conformation. Thermofluor allows us to rapidly identify conditions that maximize the thermal stability of a protein and thus reduce the conformational heterogeneity of the protein dynamic states, leading to improved crystal formation [19]. Full protocols and extensive details available from refs. [19, 20].

3.6 Crystallogenesis

3.6.1 Pre-crystallization Test

1. Your sample will contain the purified protein at a concentration as high as it is reasonably achievable. We recommend that you aim to reach at least 10 mg/mL or higher. The sample buffer should contain some salt (100–150 mM minimum) to

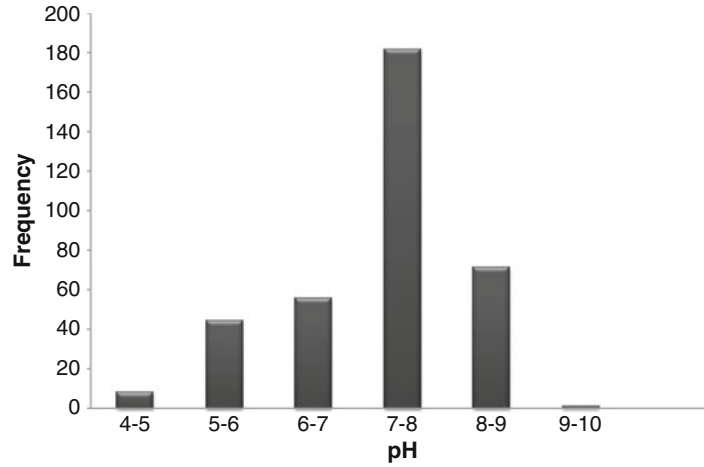

Fig. 4 Graph showing the frequency distribution of pH values in the crystallization conditions for PTPs. Most conditions are in the range of pH 7–8 although a large proportion of conditions are at pH 8–9, probably due to the increase in the p*K* of the fusion protein in the presence of the His-tag. Extracted from the PDB entries and published data as per list in Appendix

avoid premature precipitation and be at a pH that is compatible with activity and solubility of the protein (pH 6–8 is reasonable, although optimal pH for activity of most PTPs is pH 5–6). However, the pH of the crystallization conditions may be different than that of the sample buffer, as shown in a graph of the most common pH values from the crystallization conditions of PTPs (Fig. 4) extracted from the Appendix.

2. Mix 0.5 μL of sample with 30% PEG 5000 and check that the drop precipitates. If the drop remains clear then further concentrating of the sample will be required prior to crystallogenesis.

3.6.2 Crystallization Screening

Current automation favors sitting drop vapor diffusion as the means of crystallogenesis; however, alternative methods such as hanging drop, free interface diffusion and microfluidic techniques are all valid approaches and can be used according to sample availability and type of experiment. Crystals grow once the protein solution reaches super saturation. This can be achieved by either using highly concentrated protein samples or by increasing the precipitant concentration until the conditions in the drop have reached the metastable region of the saturation curve for the particular protein (Fig. 5). Factors such as buffer pH, salt concentration and temperature will all affect the saturation profile of your protein. A good screen should allow you to establish where the metastable region is for your sample and to identify conditions to drive nucleation and crystallogenesis [21, 22].

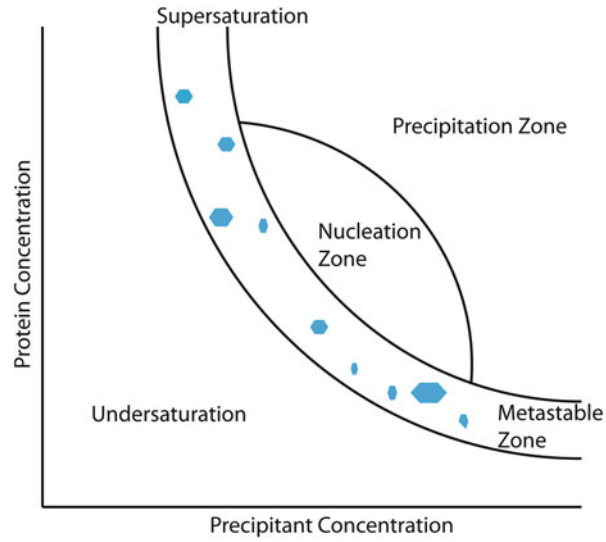

Fig. 5 Diagram showing a typical protein precipitation curve. Protein crystallization depends on reaching a metastable zone within the precipitation curve by either increasing the protein concentration or the precipitant concentration. The curve shape will vary for every protein according to its solubility and stability properties. Knowing the solubility of your protein under certain pH and salt concentration is critical to reach the metastable zone quicker, avoiding irreversible precipitation

1. Prior to setting drops it is good practice to spin down the sample (13,000 × *g* for 15 min). This will help to minimize the presence of detritus arising during the purification procedure including chromatography resin, plastic flakes, denatured and aggregated proteins (and fabric fibers if you are not wearing a lab coat!).
2. Protein samples should be stored on ice to minimize any degradation prior to screening.
3. Prepare the crystallization plates by adding the screen solutions (24-kit or 96-kit from commercial screens or homemade screens) to the reservoir wells (*see* **Note 3**). This can be done manually with a multichannel pipette or using a liquid handling automated system. The volume to add will vary depending on the plate (Appendix).
4. Protein sample and crystallization solution are mixed in a 1:1 ratio to form a drop, mixed and then sealed and incubated to allow vapor diffusion to equilibrate the precipitant concentration between the drop and the well.
5. Setting the drops manually: a total volume of 2 μL (1 μL of sample + 1 μL of reservoir solution) will be suitable for either hanging drops or sitting drops. Larger drops can be setup during optimization (up to 10 μL in hanging and 25 μL in sitting

drops) to grow bigger crystals, but during the initial screen you want to use minimal amounts of sample until you identify some hits.

6. Using a robotic platform to set the drops: use a total volume of 400 nL (200 nL of sample + 200 nL of reservoir). This is a good balance between minimizing sample consumption whilst still allowing for the growth of useable crystals.
7. Manual hanging drops: use 24-well Linbro Plates and fill reservoirs well with 0.8 mL of each screen condition. Cover the rim of the well with silicone grease (dispense from a 5 mL syringe previously filled with the grease), or vacuum oil. Take a round siliconized coverslip (22 mm), clean with wipe or spray with compressed air. Aliquot 1 μL or sample onto the coverslip. Aliquot 1 μL of reservoir solution and add to the sample drop, mixing by pipetting up and down three times. Invert the coverslip and seal over the siliconized rim of the well. Push gently to remove trapped air bubbles. Incubate (4 or 21 °C) for 24 h before checking for signs of crystal growth (*see* **Notes 4** and **5**) (Fig. 6).
8. Manual sitting drops using 24-well XTalQuest plates and fill well 0.8 mL. Aliquot 1–5 μL sample onto the central well. Aliquot 1–5 μL of reservoir solution and add to the sample drop, mixing by pipetting up and down three times. Seal the individual wells with a coverslip or with sealing tape over the entire plate. Incubate (4 or 21 °C) for 24 h before checking for

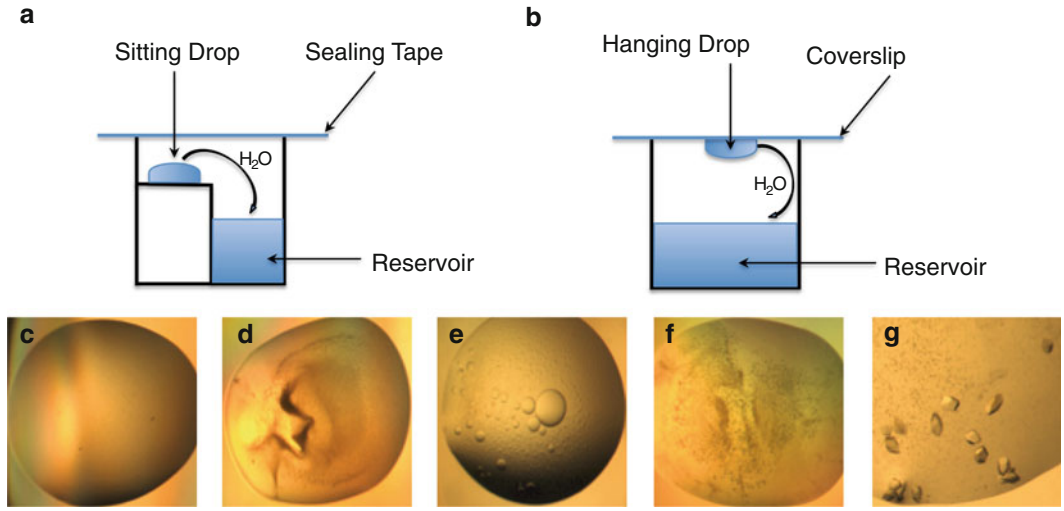

Fig. 6 Diagram showing vapor diffusion crystallization setup trials using either sitting drops (**a**) or hanging drops (**b**). Vapor diffusion allows equilibration of the concentration of precipitant between the reservoir and the drop to slowly reach the nucleation state. (**c**–**g**) Usual results from crystallization screens ranging: (**c**) clear drop, (**d**) precipitate, (**e**) phase separation, (**f**) microcrystals and (**g**) single crystals suitable for X-ray diffraction

signs of crystal growth (*see* **Notes 4** and **5**). Alternatively use MRC 48-well optimization plate [12]. This option maintains the Society for Biomolecular Sciences (SBS) standard footprint, allowing integration with high throughput screening automated systems.

9. Manual sitting drops using MRC 48-well plates (SBS footprint) or other 96-well format trays (MRC Maxi Optimization plates). Aliquot 200–400 μL of screen solution into the reservoir using a multichannel pipette. Aliquot 1–5 μL of protein into each of the drop well positions (some plates have two or three drop wells that allow testing different samples with the same precipitant condition) on the plate using a multichannel pipette or robotics systems if available. Aliquot 1–5 μL of the reservoir conditions into the respective protein drops already dispensed onto the plate. Seal the plate (sealing tape) and incubate (4 or 21 °C) for 24 h before checking for signs of crystal growth (*see* **Note 6**).
10. Requirements for drop size, well volume, protein sample amount and average crystal growth time, vary depending on the approach used (manual or automated). As guidance we have summarized the different parameters in Table 1.

3.6.3 Rapid Hit Optimization

Preliminary screening will routinely produce crystals that require some further optimization prior to data collection (Fig. 7). Grid based screening has been the method of choice to optimize these initial hits (Fig. 8). However, a powerful and rapid method of optimization is to utilize Matrix seeding as described by Darcy et al. [23]. Decoupling nucleation from crystal growth can very quickly optimize crystal growth and highlight areas of crystal space able to sustain growth but no nucleation of crystals.

1. Locate a preliminary hit containing some crystals or crystalline material.

Table 1
Typical values for crystallogenesis screens including both manual and automated systems

	Manual setup	Robotic setup
Drop volume	0.5–5 μL	100–500 nl
Reservoir volume	0.5–0.8 mL	30–50 μL
Growth time for crystals	3–5 days	24–48 h
Total protein volume required for initial screening (480 drops)	240–2400 μL	48–240 μL
Time for setup	~2–3 h	~30 min

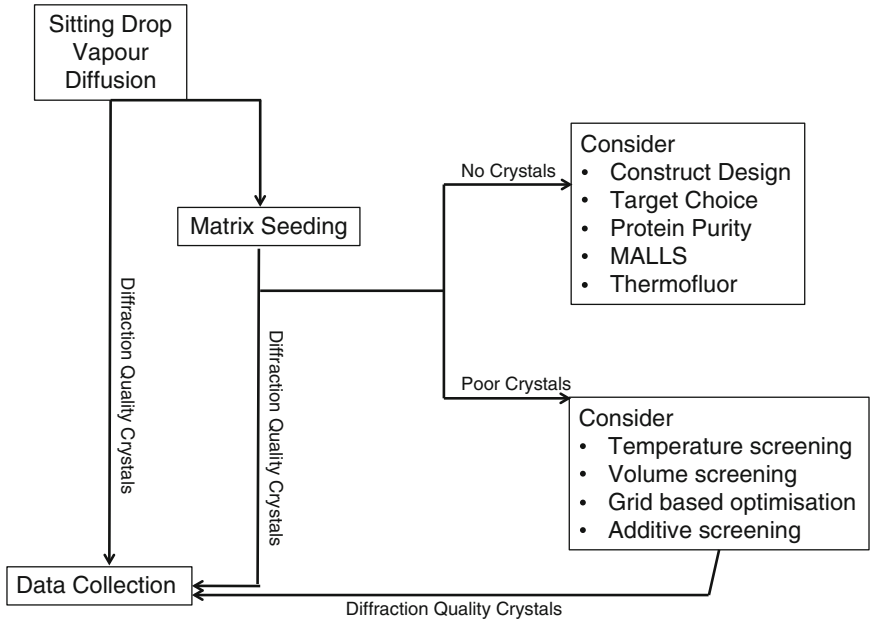

Fig. 7 Flowchart in a crystallization optimization protocol. Decision making points lead to either diffraction of suitable crystals or to reconsider new constructs or optimization of the initial crystals hit conditions to improve size/quality of the crystals. This is an iterative process that may require several runs of optimization depending on the difficulty of the project

2. Aspirate the entire drop containing the crystals along with ~50 μL of the mother liquor from the reservoir and dispense this into a Micro seed bead [12, 13].
3. Vortex this mixture for 90 s to generate the seed stock (*see* **Note 7**).
4. Transfer to ice.
5. Setup repeat screens as carried out for the primary screening but reduce the protein volume by 10% and substitute this volume with seed stock (*see* **Note 8**). Aliquot 180 nL of protein. Multi-aspirate (*see* **Note 9**) 20 nL of seed stock and 200 nL of crystallization cocktail and dispense these together into the protein drop (Fig. 9).
6. Seal and incubate as previous.
7. Alternative Optimization Strategies. Despite the power of Matrix seeding as a means of rapid hit optimization, it may still be necessary to utilize alternative approaches for some systems (Fig. 8). Optimization routes to consider include:
   - Temperature screening. If after a period of initial incubation trays do not show signs of crystal formation or precipitation it can be useful to move them to an alternative incubation temperature. Some systems will readily crystallize over

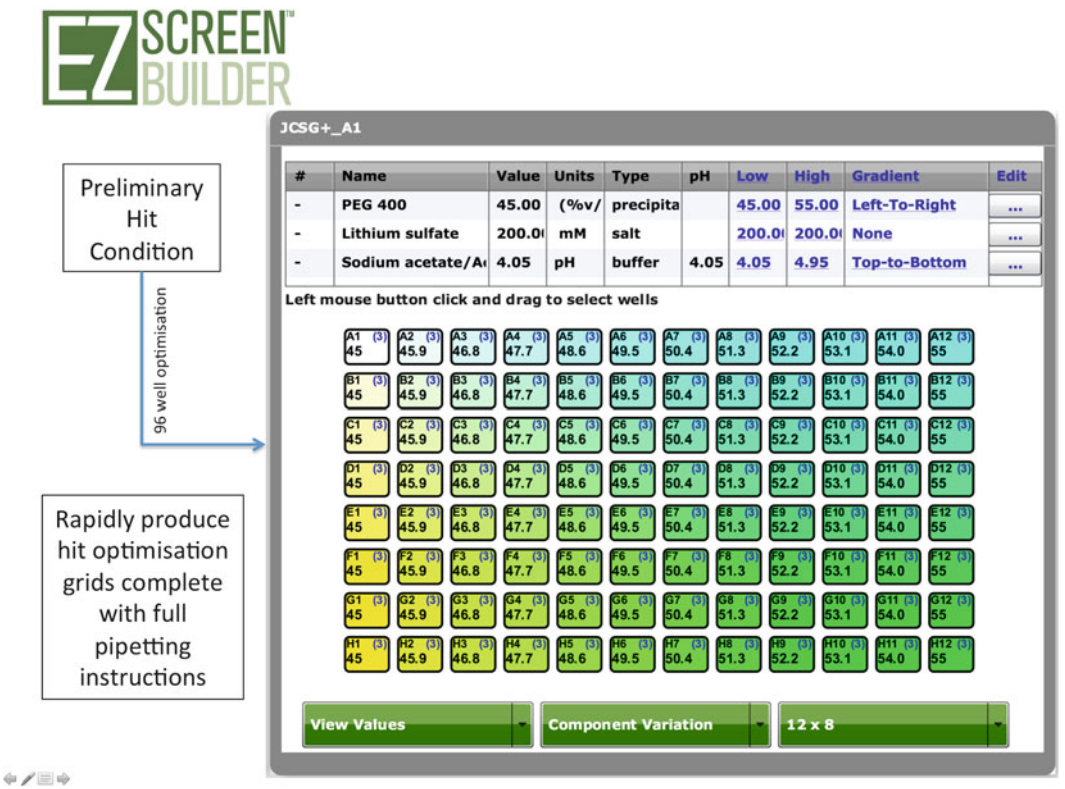

Fig. 8 EZ Screen builder allows designing a whole grid screen from the original hit conditions. It is a simple way to rapidly produce complete hit optimization grids with full pipetting instructions

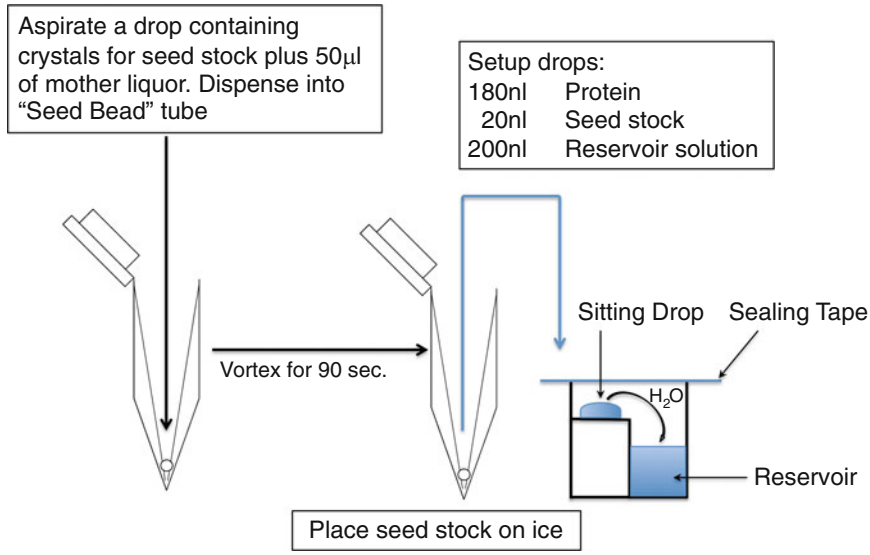

Fig. 9 Diagram showing how to prepare a seed stock from a drop containing initial crystals. Seed stocks can be used *as is* to rescreen using an optimization grid of conditions or to prepare serial dilutions to reseed into the original condition to grow larger crystals

a broad range of temperatures whilst others appear to only crystallize within a very narrow temperature window. Typical temperatures to test: 4, 15, 21, 25 °C.

- Varying drop volume. Drop volume is a much-underutilized screening variable and can have a marked impact on the equilibration rate, dynamics and on the crystal size. Larger drops will slow down the rate of equilibration whilst smaller volumes will lead to more rapid equilibration. Setting drops of total volume 400, 800 and 1200 nL on a single three well plate can be an excellent strategy to optimize initial hits obtained in 400 nL drops.
- Varying reservoir volume. This will similarly have an impact on the rate of equilibration of the drop. Reducing the reservoir volume will slow the rate of equilibration whilst increasing the reservoir volume will have the opposite effect.
- Once an initial hit condition has been located a grid screen expansion of this condition can help to optimize the crystals obtained (Fig. 8). Grid based optimization can be combined with seeding to further aid the process. An excellent free online tool for grid-based optimization is provided by Rigaku [24]. This tool will assist you in both designing and preparing your optimization grid screen. If funds are plenty you can simply have Rigaku make the optimized screen for you!

- Additive screening involves the introduction of additional components into an already located hit condition (ions, alcohols, organic solvents, etc.). Additive screens are available from a number of commercial suppliers [12, 13]. If your protein requires any ions or cofactors for activity these should be present in the sample buffer or added to the crystallization drop.
- Limited proteolysis screen. Some PTP constructs may have flexible or disordered regions that prevent crystallogenesis, as discussed in Subheading 3.1. One way to overcome this is to redesign your construct to eliminate those regions. Alternatively, you can use limited proteolysis during the optimization process by adding proteases into your crystallization drop. Protease kits are available commercially for example (Proti-Ace) [13], follow manufacturers recommendations to decide on the amount to add depending on your drop volume.

The ultimate goal is to obtain high quality diffracting crystals with size being dependent on the X-ray source to use (*see* **Note 10**).

3.7 Ligand Inhibitor Complexation

Preparation of PTP complexes with ligands (substrates, inhibitors, peptides) can be achieved in different ways: by incubating purified PTP with the ligand previous to crystallization, by co-crystallization mixing protein and ligand in the crystallization drop or by soaking apo-protein crystals in a solution containing the ligand. In all instances, ensuring that the active site is available for ligand binding is essential, as it will affect the efficiency of the binding as well as the final occupancy of the ligand in the crystal structure. We recommend minimizing the exposure of the PTP sample to phosphate and sulfate ions during purification by using Tris-based buffers. Another precaution is to rinse thoroughly your glassware with distilled water to wash off any phosphate traces in the detergents. In addition, you can include a desalting step at the end of your purification to exchange the purification buffer into a phosphate-free buffer. A simple and quick way to check the presence of phosphate in your buffer is to test it with malachite green reagent.

Small-molecule ligands may have very limited solubility in aqueous buffers and thus cosolvents (ethanol, DMSO, other alcohols or organic reagents) may be used to enhance their solubility. Unfortunately these solvents can have a negative impact upon crystallogenesis by preventing nucleation. One alternative method of overcoming this issue is to mix the ligand and protein at low concentration by directly dissolving the powder into the protein sample. Solvents can thus be minimized or avoided altogether, instead allowing the protein and ligand to complex over a protracted period.

1. Dissolve ligand compound (powder or stock solution) in the protein sample solution (before protein concentration). Gently mix on a roller shaker for 1–2 h if the ligand is very soluble or if used from a stock solution. Incubate for 16–24 h for ligands with limited solubility or if added as powder (*see* **Note 11**).
2. Following incubation, spin the mix to remove undissolved ligand or aggregates (13,000 × *g* for 15 min).
3. Concentrate the protein complex until the desired concentration for crystallogenesis is achieved (>10 mg/mL) (*see* **Note 12**).
4. Screening and Matrix optimization is carried out as described previously. Apo-protein crystals can often be used to assist in the nucleation of the complex.
5. Co-crystallization can also be achieved by adding a small volume of ligand stock directly into the crystallization drop already containing the protein sample, prior to the addition of the well solution. A good precaution is to test the solubility of the ligand solution in the presence of the precipitant as a control and to adjust the concentration of ligand in the drop. Set up a control drop containing sample buffer, add the ligand solution (<10% of total drop volume if it is in volatile solvents or DMSO) and then the well solution (volumes as per standard screening protocols). Incubate and check next day for precipitation or crystal growth from the ligand. Readjust the concentration of the ligand solution accordingly to avoid precipitation or change precipitant conditions if crystals of the ligand appear.
6. Crystal soaking: dissolve the ligand in the mother liquor (taken from the reservoir solution where the crystals had grown). Prepare a drop containing 5–10 μL of this solution in a sitting drop well. Transfer a few crystals from the crystallization drop into the ligand solution drop using a cryo-loop. Try to minimize the amount of liquid carried on from the original drop. Let the crystals soak for a couple of minutes and then fish them with the loop and freeze. Optimizing the soaking may take a few tests until the concentration of ligand is such that crystals do not crack, but that it is diffusing into the crystal in sufficient amounts to visualize it in the electron density maps.
7. Gradual soaking can be done using increasing amounts of ligand in the mother liquor. This is a more gentle approach and may prevent crystals from cracking or dissolving. If soaks are done with small concentrations of ligand we recommend extending the time of soaking to a few hours or even several days The soaks will be done in a sealed sitting drop plate for easy manipulation and the buffer changes can be done by simply aspirating 80% of the drop volume and then adding a drop with the new buffer. No need to mix, diffusion will take care of it. The gradual soaking can also include an initial step

of "soaking-out" phosphate or buffer components from the crystal by using a phosphate-free buffer.

3.8 Cryoprotection and Crystal Freezing

Prior to data collection crystals will require cryoprotection and freezing. Deciding on a suitable cryoprotectant can be difficult. However, as a general rule, crystals grown from polyethylene glycol (PEG) containing conditions will often tolerate the addition of low molecular weight PEGs (PEG 200, 400) at 10–20 % or glycerol (20–30 %), which will be sufficient to cryoprotect the crystal. For crystals of complexes with ligands, the cryoprotectant should contain a similar amount of ligand as used for crystallization to avoid soaking it out.

If crystals are grown in ammonium sulfate the best option would be to try an oil as the starting cryoprotectant; alternatively glycerol (20–30 %) or small PEGs may also work. Another option, longer and more risky for the integrity of the crystals, is to "desalt" the crystals by soaking them in a drop containing decreasing amounts of ammonium sulfate (decrease by 100 mM at a time) with increasing amounts of PEG (from 0 to 20 %). These soaks can be done changing the buffer every hour if the crystals are robust. If they start to crack, then leave them in the drop for a few hours and leave the last soak overnight (exchange the buffer as directed for the ligand soaking procedure).

3.8.1 Cryofreezing Using Glycerol or PEG

1. Use a large cryo-loop to check the status of your mother liquor (equilibrated reservoir) and determine if it is forming a vitreous glass. Using the largest (0.7 mm) loop available, pick up some of the liquor and plunge freeze it in LN_2 using a cryo-wand. Maintaining the wand and loop under the LN_2 bring the loop towards the surface of the LN_2 so you can observe the loop region itself. If the loop appears white then you will need to add additional components or find an alternative cryoprotectant, if, however, the loop is clear then you can be confident that the solution will not result in the formation of hexagonal ice.
2. If working in small volume drops, add 1 μL of mother liquor to the drop, this can make the mounting significantly easier. Add 1 μL of cryoprotectant solution (made with the reservoir solution), wash twice, use cryo-loops to lift the crystal from the drop and transfer to a second drop (1 μL) of cryoprotectant solution, then fish immediately and plunge freeze.

3.8.2 Cryofreezing in Oils

Oils can be excellent cryoprotectants; this is particularly the case when ligand complexes are being sought, as the oils will minimize any back soaking or competition effects from cryo-components that may decrease ligand occupancy.

1. Harvest the crystal as normal and then transfer the crystal to a drop containing 1 μL of the oil of choice. More viscous oils

such as Parabar 10312 will require more care to minimize mechanical damage during the crystal manipulation. Passing the crystal repeatedly through the air oil interface will cause the remaining mother liquor around the crystal to slowly be replaced, leaving the crystal surrounded by oil.

2. Prior to plunge freezing the crystal it is often useful to touch the tip of the loop on the surface of the plate. This will allow the excess oil to run off the surface and leave a loop containing only a very thin film of oil with the crystal suspended in it. Minimizing the oil in this way will not only enhance the subsequent rate of freezing but reduces the background noise during data collection and makes centering the sample significantly easier!

3.9 Online Tools and Resources

3.9.1 Online Links and Useful Websites

1. The Protein Data Bank (PDB) is a publicly available online database where all macromolecule structures are deposited (determined by X-ray crystallography and NMR) [9]: http://www.rcsb.org
2. XtalPred-RF is an online tool that provides a crystallizability classification and it is an useful aid in construct design [25]: http://ffas.burnham.org/XtalPred-cgi/xtal.pl
3. Series of online tutorials regarding crystallography techniques and many related links, news and others. Created by Bernhard Rupp: http://www.ruppweb.org/default.htm
4. Protein Crystal Structure Propensity Prediction Server [26] from the Northeast Structural Genomics Consortium: http://nmr.cabm.rutgers.edu:8080/PXS/
5. SERp, Surface Entropy Reduction prediction server that helps to identify sites that are most suitable for mutation, to aid in redesigning your construct and enhance crystallizability [17]: http://services.mbi.ucla.edu/SER/
6. Rigaku EZ-Screen Builder, grid based optimization tool to help building suitable crystallization grids to optimize initial hits: https://www.rigakureagents.com/escreentoolkit/escreen.html
7. Helpful tips and advice on standard procedures regarding crystallogenesis: https://hamptonresearch.com/growth_101_lit.aspx
8. Online tutorial covering the basic principles of X-ray crystallography: http://www.ruppweb.org/Xray/101index.html
9. Ray Salemme's website including links and references to protein structure and analysis, structure based drug discovery and many other useful links: www.beta-sheet.org
10. Videos on how to freeze crystals: https://www.youtube.com/watch?v=FENUWRYXMOM, https://www.youtube.com/watch?v=QcsaWowulDM

11. Demonstration on how to use the mosquito automated crystallization setup system https://www.youtube.com/watch?v=BZkyRu_UMw8
12. Structural Genomics Consortium, Oxford, UK: http://www.thesgc.org/

3.9.2 Databases Containing Information on Crystallization Conditions for Protein Phosphatases

1. Protein Data Bank (PDB) [9]: http://www.rcsb.org
2. Marseille Protein Crystallization Database (MPCD) [27]: www.cinam.univ-mrs.fr/mpcd/
3. Biological Macromolecule Crystallization Database (BMCD) [28]: http://xpdb.nist.gov:8060/BMCD4/index.faces
4. Large-Scale Structural Analysis of the Classical Human Protein Tyrosine Phosphatome [6] http://www.thesgc.org/resources/phosphatases

3.9.3 Crystallography Textbooks

1. Principles of Protein X-ray Crystallography [29].
2. Introduction to Macromolecular Crystallography [21].
3. Biomolecular Crystallography: Principles, Practice, and Application to Structural Biology [22].
4. Data mining crystallization databases: Knowledge-based approaches to optimize protein crystal screens [30].

4 Notes

1. The information of the estimated PI of your construct (including the tag) is useful to decide on the best buffer conditions during purification of your protein, particularly if you are using ionic exchange chromatography. At a pH above the PI the protein will have a net negative charge. Below the PI it will have a net positive charge. However, it is better to determine the actual PI values using isoelectric-focusing electrophoresis, this will also show if your sample has multiple isoform species with slightly different PI. This is another source of heterogeneity that it is worth minimizing if crystals are difficult to grow. A change in salt concentration or pH conditions may alleviate the issue followed by effective ion-exchange chromatography to separate the isoforms.
2. Some of the solids may not dissolve completely right away but they may eventually during culture growth.
3. Plastic plates should be cleaned prior to filling with screen solutions. Use compressed air to spray and remove dust and plastic debris. Alternatively you can wash with distilled water and leave to dry inverted on absorbent paper.

4. It is good practice to check the drops right after setting up the plate. If precipitate has already formed in all drops, this is a sign that protein concentration may be too high. If drops remain clear then check after 24 h. Monitoring the dynamics of the crystallization is important to understand the behavior of your sample and to aid decisions as to how to change concentration or buffer conditions during subsequent rounds of purification and sample preparation.
5. Single crystals with a clean and sharply faceted appearance are most suitable for crystallographic study. Clusters, needles and crystalline precipitates are all excellent sources of seeds for optimization.
6. As drop volumes increase the equilibration time of the drop will also increase. When using 5 + 5 μL or larger drops it is not uncommon for crystals not to form for several weeks following initial setup.
7. Seed stocks can be flash frozen and stored for future use.
8. Seed stocks can be serially diluted to control the levels of nucleation achieved (10^{-9}, 10^{-12} dilutions are typically used).
9. In order to maximize the stability of our seed stock we utilize a multi-aspirate step when dispensing this component. The robot will first aspirate 20 nL of seed stock before moving to the crystal screen and aspirating a further 200 nL of screen into the same tip as the seed. The high concentration of precipitants in the screen aid the stability of the seeds and the increased volume of liquor in the tip helps to ensure a more accurate dispense. It is important to always have seeds and screen mixed before adding them to the protein.
10. Modern synchrotron beam lines allow excellent data to be collected from even relatively small crystals (10–50 μm). The size of crystal necessary for successful data collection will vary on a protein-by-protein basis. Home source X-ray systems require larger crystals (100–200 μm).
11. The final concentration of the ligand will depend upon its maximal solubility and the effective concentration for binding. As a rule-of-thumb we recommend using a final concentration 10–20 times the K_m or K_i value. If the binding affinity is not known, use a molar ratio of at least 2:1 ligand–protein or higher if it is a small molecule. For peptide ligands 1–2 mM usually is sufficient for co-crystallization, for small molecules use 0.5–1 mM. If feasible, we recommend adding an excess of ligand to overcome potential competition with any ions or buffer bound to the active site, particularly if crystal soaking is used.
12. The concentration achievable for the complex may significantly differ to that of the Apo protein.

Acknowledgements

This work was supported by MRC funding (MR/K011049/1) to LT and BBSRC Doctoral Training Studentship, Sir Kenneth Murray Scholarship, Manchester Presidents Doctoral Scholar Award and a SCI Scholarship to JA. CL is a senior experimental officer at the Manchester Protein Structure Facility, University of Manchester. We thank Darel Macdonald, Andrew Currin, Efrain Ceh Pavia, and Deepankar Gahloth for sharing their data and protocols.

References

1. Tonks NK (2006) Protein tyrosine phosphatases: from genes, to function, to disease. Nat Rev Mol Cell Biol 7(11):833–846
2. Tautz L, Pellecchia M, Mustelin T (2006) Targeting the PTPome in human disease. Expert Opin Ther Targets 10(1):157–177
3. Eswaran J et al (2006) Crystal structures and inhibitor identification for PTPN5, PTPRR and PTPN7: a family of human MAPK-specific protein tyrosine phosphatases. Biochem J 395:483–491
4. Nunes-Xavier C et al (2011) Dual-specificity MAP kinase phosphatases as targets of cancer treatment. Anticancer Agents Med Chem 11(1):109–132
5. Rios P et al (2014) Dual-specificity phosphatases as molecular targets for inhibition in human disease. Antioxid Redox Signal 20(14):2251–2273
6. Barr AJ et al (2009) Large-scale structural analysis of the classical human protein tyrosine phosphatome. Cell 136(2):352–363
7. Tabernero L et al (2008) Protein tyrosine phosphatases: structure-function relationships. FEBS J 275(5):867–882
8. Bohmer F et al (2013) Protein tyrosine phosphatase structure-function relationships in regulation and pathogenesis. FEBS J 280(2): 413–431
9. Berman HM et al (2000) The protein data bank. Nucleic Acids Res 28(1):235–242
10. Sambrook J, Russell DW (2001) Molecular cloning: a laboratory manual, 3rd edn. Cold Spring Harbor Laboratory Press, New York, p A2.2
11. Mitigen. Available from http://www.mitegen.com/
12. Molecular Dimensions. Available from http://www.moleculardimensions.com/
13. Hampton Research. Available from http://hamptonresearch.com
14. Qiagen. Available from https://www.qiagen.com/gb/
15. Hampton Research, product detail. Available from http://hamptonresearch.com/product_detail.aspx?sid=152&pid=445
16. XtalPred. Available from http://ffas.burnham.org/XtalPred-cgi/xtal.pl
17. Goldschmidt L et al (2007) Toward rational protein crystallization: a web server for the design of crystallizable protein variants. Protein Sci 16(8):1569–1576
18. Cantor CR, Schimmel PR (1980) Schimmel biophysical chemistry, Part 2: Techniques for the study of biological structure and function (Pt. 2). W. H. Freeman, New York
19. Phillips K, de la Peña AH (2011) The combined use of the Thermofluor assay and ThermoQ analytical software for the determination of protein stability and buffer optimization as an aid in protein crystallization. Curr Protoc Mol Biol Chapter 10:Unit 10.28
20. Beta-sheet. Available from http://www.beta-sheet.org/resources/T11-Crystallization-ericsson.pdf
21. McPherson A (2009) Introduction to macromolecular crystallography, 2nd edn. Wiley, Hoboken, NJ
22. Rupp B (2009) Biomolecular crystallography: principles, practice, and application to structural biology. Garland Science, New York
23. D'Arcy A, Villard F, Marsh M (2007) An automated microseed matrix-screening method for protein crystallization. Acta Crystallogr D Biol Crystallogr 63(Pt 4):550–554
24. Rigaku EZ screen. Available from https://www.rigakureagents.com/escreentoolkit/escreen.html

25. Slabinski L et al (2007) XtalPred: a web server for prediction of protein crystallizability. Bioinformatics 23(24):3403–3405
26. Price WN et al (2009) Understanding the physical properties that control protein crystallization by analysis of large-scale experimental data. Nat Biotechnol 27(1):51–57
27. Charles M, Veesler S, Bonnete F (2006) MPCD: a new interactive on-line crystallization data bank for screening strategies. Acta Crystallogr D Biol Crystallogr 62(Pt 11):1311–1318
28. Tung M, Gallagher DT (2009) The Biomolecular Crystallization Database Version 4: expanded content and new features. Acta Crystallogr D Biol Crystallogr 65:18–23
29. Mesters J (2007). In: Drenth J (ed) Principles of protein X-ray crystallography. Practical Protein Cristallization. Springer, New York. pp 297–304
30. Kimber MS et al (2003) Data mining crystallization databases: knowledge-based approaches to optimize protein crystal screens. Proteins 51(4):562–568

Chapter 11

NMR Spectroscopy to Study MAP Kinase Binding to MAP Kinase Phosphatases

Wolfgang Peti and Rebecca Page

Abstract

NMR spectroscopy and other solution methods are increasingly being used to obtain novel insights into the mechanisms by which MAPK regulatory proteins bind and direct the activity of MAPKs. Here, we describe how interactions between the MAPK p38α and its regulatory proteins are studied using NMR spectroscopy, isothermal titration calorimetry, and small angle X-ray scattering (SAXS).

Key words Mitogen activated protein kinase (MAPK), p38α, Protein tyrosine phosphatases, Dual specificity phosphatase, Protein–protein interaction, Nuclear magnetic resonance (NMR) spectroscopy, Chemical shift perturbation (CSP), Isotopically labeled growth media, D_2O, Isothermal titration calorimetry (ITC), Small angle X-ray scattering (SAXS)

1 Introduction

Spatial and temporal regulation of mitogen activated protein kinases (MAPKs) is of essential importance for transducing environmental and developmental signals (growth factors, stress) into adaptive and programmed responses (differentiation, inflammation, apoptosis) [1, 2]. Although MAPKs are ubiquitously expressed, their activation is finely tuned in a cell-type specific and temporal manner [3]. The regulators that achieve this fine-tuning include: (1) upstream kinases, (2) downstream phosphatases, and (3) scaffolding proteins [4–6]. Over the years, many groups using a variety of techniques have advanced the field's understanding of how the activities of MAPKs are finely controlled by MAPK regulatory proteins. Clearly, understanding how these proteins interact at a molecular level is also essential [7–15]. X-ray crystallography has provided key insights into the regulation of MAPKs by their interacting proteins by mostly determining structures of MAPKs bound to different peptides derived from interacting proteins [7]; e.g., for the MAPK p38α a single structure of a full-length interacting protein (MK2—a substrate that binds with a K_d of 20 nM) has

Rafael Pulido (ed.), *Protein Tyrosine Phosphatases: Methods and Protocols*, Methods in Molecular Biology, vol. 1447,
DOI 10.1007/978-1-4939-3746-2_11,

Table 1
NMR and SAXS studies of p38α with its regulatory proteins

MAPK complex	Tech	BMRB[b]	Reference
p38α:MKK3b	NMR	6468	[8]
p38α[a]:HePTP$_{15–31}$	NMR	17471/6468	[17]
p38α:HePTP$_{15–56}$	NMR	17471/6468	[17]
p38α:HePTP$_{15–339}$	NMR	17471/6468/15680	[17]
p38α:STEP$_{214–229}$	NMR	17471/6468	[45]
p38α:STEP$_{214–256}$	NMR	17471/6468	[45]
p38α:STEP$_{214–539}$	NMR	17471/19046/6468	[45]
p38α:PTPSL$_{332–348}$	NMR	17471/6468	[45]
p38α:PTPSL$_{332–373}$	NMR	17471/6468	[45]
p38α:PTPSL$_{332–655}$	NMR	17471/6468	[45]
p38α:STEP/PTPSL$_{chimera}$	NMR	17471/6468	[45]
p38α:MKP5/DUSP10	NMR	17471/19330	[58]
*pTpY*p38α[c]:MBP$_{94–102}$	NMR	17940	[59]
p38α:HePTP$_{15–339}$	SAXS	–	[17]
p38α:STEP$_{214–539}$	SAXS	–	[45]
p38α:PTPSL$_{332–655}$	SAXS	–	[45]
p38α:STEP/PTPSL$_{chimera}$	SAXS	–	[45]
p38α:MKP5/DUSP10	SAXS	–	[58]

[a]82% of all expected resonances assigned
[b]BMRB references 6468 [21], 15680 [60], 17471 [17], 17940 [59]
[c]56% of all expected resonances assigned

been determined [16]. Over the last ~10 years, biomolecular NMR spectroscopy has complemented and, more critically, expanded these efforts [17–22]. By doing so, it has become apparent that regulatory proteins adopt distinct conformations when bound to MAPKs and have different degrees of flexibility upon complex formation, which contributes to the observed differences in their biological functions. Here we review the use of biomolecular NMR spectroscopy and other biophysical techniques to study complexes between the MAPK p38α and its regulatory proteins (Table 1).

2 Materials

Prepare all solutions using ultrapure Water (Milli-Q water purification system, Millipore). Chemicals should be at least ACS grade. Prepare and store reagents/solutions at temperatures and

conditions recommended by the manufacturer. Chemicals specific for NMR labeling, e.g., [^{13}C]D-glucose, [^{13}C]D-d^{7}-glucose (1,2,3,4,5,6,6-d^{7}), $^{15}NH_4Cl$, D_2O are typically purchased from Cambridge Isotope Laboratories (CIL) or Isotech (Sigma). Standard buffers are used for purification; when necessary, buffers are autoclaved when prepared in order to prevent unwanted proteolytic degradation. All buffers are stored at 4 °C and are filtered (0.22 μm PES filter, Millipore) prior to use. If possible uniform buffers should be used throughout all experiments. Furthermore, it is important to reduce the salt concentration and select the right buffer for NMR experiments as the sensitivity of cryoprobe significantly decreases with increasing amounts of salt (thus it is also better to use HEPES buffer than phosphate buffer) [23]. Buffers for ITC experiments must be degassed. NMR data analysis can be performed by a variety of software, including Cara (http://cara.nmr.ch), NMRVIEW [24], Sparky [25], and CCPN [26, 27].

1. M9 medium: Weigh 5.8 g Na_2HPO_4 anhydrous, 3.0 g KH_2PO_4, and 0.5 g NaCl. Add water to a volume of 900 mL. Mix and adjust pH to 7.1–7.3 with HCl. Volume up to 1 L with water. Sterilize by filtration and store at 4 °C.
2. Vitamin mix: BME mix (Sigma-Aldrich). Use directly for H_2O-based medium. Lyophilize and resuspend in D_2O for D_2O-based medium.
3. Solution Q: In a final volume of 1 L of water, add 8 mL 5 M HCl (*see* **Note 1**), 5 g $FeCl_2{\cdot}4H_2O$, 184 mg $CaCl_2{\cdot}2H_2O$, 64 mg H_3BO_3, 18 mg $CoCl_2{\cdot}6H_2O$, 4 mg $CuCl_2{\cdot}2H_2O$, 340 mg $ZnCl_2$, and 40 mg $Na_2MoO_4{\cdot}2H_2O$. Mix thoroughly. Aliquot into 2 mL Eppendorf tubes, freeze and store at –20 °C.
4. Glucose: Use [^{12}C]D-glucose for unlabeled protein expression; [^{13}C]D-glucose for ^{13}C labeled protein expression; [^{13}C]D-d^{7}-glucose (1,2,3,4,5,6,6-d^{7}) for fully deuterated protein expression.
5. Ammonium chloride: Use NH_4Cl for unlabeled protein expression and $^{15}NH_4Cl$ for NMR-active protein expression.
6. Preparation of medium: All plastic ware must be autoclaved before use; for large-scale expression we prefer Ultra-Yield 2 L expression flasks (six-times baffled for high aeration; Thomson Instrument Company); 250 mL of media for each Ultra-Yield 2 L expression flask [28].
7. NMR tubes: Different NMR tubes are available for measurements which differ both in diameter (1, 1.7, 3, and 5 mm [outdated: 8 and 10 mm]; 5 mm is the size most commonly used) and shape (distinct shapes can partially compensate the reduced sensitivity of high salt samples in cryo-probes). Shigemi has developed a set of tubes that use solvent-susceptibility matched glass and thus allows for lower sample volumes (~40% reduction), with similar tubes are also available from New Era Scientific.

3 Methods

3.1 Production of p38α and Regulatory Protein Tyrosine Phosphatases for NMR Studies

p38α and its regulatory proteins are large proteins (≥35 kDa) for biomolecular NMR spectroscopy [29, 30]. In order to analyze proteins using NMR spectroscopy, they must be uniformly labeled with NMR-active nuclei. NMR-active nuclei have a nuclear spin, preferably with a spin number of ½ (^{1}H, ^{13}C and ^{15}N nuclei have spin numbers of ½). Labeling is achieved by providing labeled precursors (e.g., [^{13}C]-D-glucose, $^{15}NH_4Cl$) during protein expression in a variety of expression systems, including *Escherichia coli* (*E. coli*) [28], yeast [31], insect cell [32], and human expression systems [33].

However, in order to overcome the broad line-widths that are characteristic of proteins ≥35 kDa, MAPKs must be expressed in D_2O-based medium and TROSY [34] versions of all 2D and 3D experiments must be recorded using a high-field NMR spectrometer (800–1000 MHz ^{1}H Larmor frequency) [35]. Deuteration reduces the dipole–dipole ^{1}H–^{1}H relaxation, as deuterium has a ~7-fold lower gyromagnetic ratio than protons [36]. However, as most NMR experiments rely on the excitation and detection of ^{1}H (largest gyromagnetic ratio; 99.9% natural abundance), deuteration limits the available experimental approaches for such proteins. Most $^{1}H^{N}$ will rapidly back-exchange during protein purification in H_2O-based buffers. However, H/D exchange can be slow in β-sheets and in hydrophobic pockets where access of water or strong hydrogen bonds can significantly limit the exchange rates. If possible, protein refolding either by chemicals or pressure in H_2O-based buffers can be helpful; however, refolding of larger signaling enzymes, such as p38α or tyrosine phosphatases, is not readily achievable. For many years expression of deuterated proteins was limited to the *E. coli* expression system, but recently it has become economically feasible to express ^{2}H-labeled proteins in insect cells [37]. To achieve the necessary high expression yields, *E. coli* cells must be adapted for growth in D_2O-based medium.

3.1.1 Fresh Transformation and Colony Expression Screening

1. Transform the expression plasmid into the appropriate *E. coli* expression cell line (*see* **Notes 2** and **3**).
2. Screen multiple (three to five) colonies for robust expression using a small scale growth and induction (i.e., β-D-1-thiogalactopyranoside [IPTG]) in Luria broth (LB) medium (3–5 mL). Allow expression to proceed for 2 h at 37 °C and evaluate the expression levels of the different colonies using sodium dodecyl sulfate polyacrylamide gel electrophoresis (SDS-PAGE) and Coomassie staining.

3.1.2 D_2O Adaption (see Table 2 and Fig. 1)

1. 20 µL of uninduced LB growth is transferred into 3 mL of freshly prepared 0% D_2O medium and grown for ~12–15 h (37 °C; 250 rpm shaking).

Table 2
D_2O adaption

	0% D_2O (10 mL)	30% D_2O (10 mL)	50% D_2O (10 mL)	70% D_2O (10 mL)	100% D_2O (10 mL)
D_2O	–	3 mL	5 mL	7 mL	8.84 mL
H_2O	8.84 mL	5.84 mL	3.84 mL	1.84 mL	–
10× M9	1 mL	1 mL	1 mL	1 mL	1 mL
1 M $MgSO_4$	20 µL	20 µL	20 µL	20 µL	20 µL
Vitamins	100 µL	100 µL	100 µL	100 µL	100 µL
Solution Q	20 µL	20 µL	20 µL	20 µL	20 µL
Glucose	40 mg	40 mg	40 mg	40 mg	40 mg
NH_4Cl	10 mg	10 mg	10 mg	10 mg	10 mg
Antibiotic	10 µL	10 µL	10 µL	10 µL	10 µL

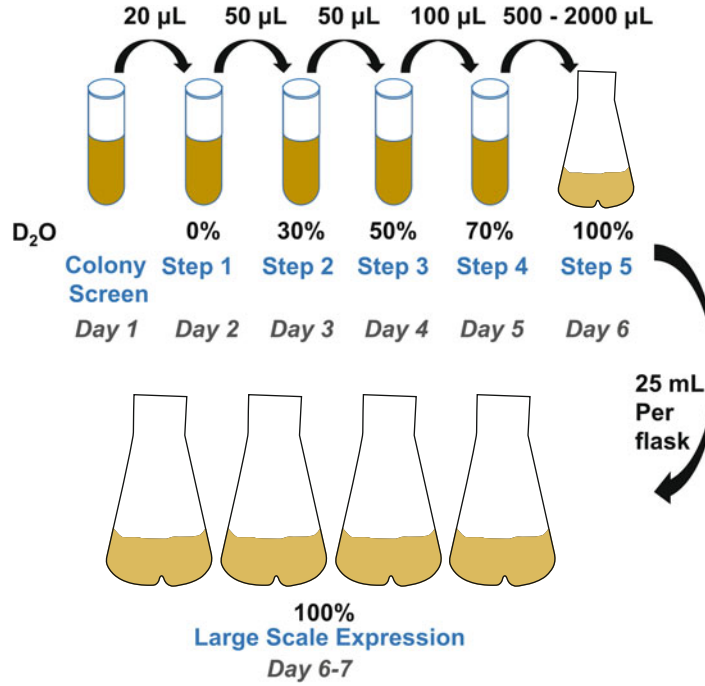

Fig. 1 Schematic of the D_2O adaption protocol. See text for details

2. 50 µL of the 0% D_2O culture is added to 3 mL of 30% D_2O and grown for ~12–15 h (37 °C; 250 rpm shaking).
3. 50 µL of the 30% D_2O culture is added to 3 mL of 50% D_2O and grown for ~12–15 h (37 °C; 250 rpm shaking).

4. 100 µL of the 50% D_2O culture is added to 3 mL of 70% D_2O and grown for ~12–15 h (37 °C; 250 rpm shaking).
5. 500–2000 µL (depending on protein) of the 70% D_2O culture is added to 100 mL of 100% D_2O medium in a 500 mL Ultra-Yield expression flask (*see* **Notes 4** and **5**) and grown for ~12–15 h (37 °C; 250 rpm shaking).

3.1.3 D_2O Large Scale Expression

25 mL of the 100% D_2O culture is added to 225 mL of 100% D_2O medium in a 2 L Ultra-Yield flask and the cells grown to OD_{600} of ~0.6–0.8 (37 °C; 250 rpm shaking with the appropriate antibiotics). Cells are induced using the appropriate induction agent (i.e., IPTG) and then expressed at appropriate temperature (e.g., 18 °C; 18–20 h, 250 rpm shaking for p38α [*see* **Note 6**]). Large scale expression of [^{2}H,^{15}N]-p38α is done in M9 medium supplemented with $^{15}NH_4Cl$ (1 g per 1 L medium) in 99.8% D_2O, and [^{2}H,^{13}C,^{15}N]-p38α is expressed in M9 medium supplemented with $^{15}NH_4Cl$ (1 g per 1 L medium) and [^{13}C]D-d7-glucose (4 g per 1 L medium) in 99.8% D_2O.

3.1.4 D_2O Recycling

D_2O can be readily recycled and reused with a slightly (~10–15%) lower degree of deuteration, which is done in many laboratories.

1. Following the pelleting of the cell mass after the large-scale D_2O expression, the supernatant is collected and stored (RT or –20 °C; *see* **Note 7**).
2. Used D_2O is distilled in a standard glass apparatus, with a controlled heating mantle and a 4 L distillation flask with two inlets (*see* **Note 8**). Aluminum foil is used to lower the boiling temperature. Regular boiling stones are used to ensure to ensure uniform boiling.
3. During distillation, the distillation flask will accumulate debris. Used D_2O is added to the flask until 20–40 L has been distilled. At this point the flask is either cleaned or replaced.
4. Distilled D_2O is perfectly clear; however, it has nasty ammonia-like smell. To make the distilled D_2O suitable for culturing bacteria (*E. coli* will not grow on the freshly distilled, but nasty smelling D_2O), the distilled D_2O must be treated with ~20 g of acid-washed activated charcoal (Sigma) per 1 L of distilled D_2O under vigorous stirring for 12–24 h. The activated carbon is removed by filtering through a Buchner filter.
5. If necessary, the recycled D_2O can be filtered through a 2 µm bottle-top filter to remove any remaining debris/charcoal. At this point, the D_2O is completely clear and does not have any detectable odor. The recycled D_2O can then be used identically to fresh D_2O. Mass spectrometry will confirm a lower rate of deuteration (~85%) (*see* **Note 9**).

3.2 Interaction with Kinase Interaction Motif Protein Tyrosine Phosphatases (KIM-PTPs) and MAPK Protein Tyrosine Phosphatases

Rapid assessment of a protein–protein interaction can be achieved using size exclusion chromatography (SEC) by simply comparing the retention volume (or time) of the free and complex samples. SEC media varies widely in quality and size, leading to different numbers of theoretical plates and thus resolution. For protein studies, Superdex or Sephacryl (GE Healthcare) are the most commonly used media due to their high inertness to nonspecific interactions and their excellent separation capabilities. An earlier eluting peak indicates a higher molecular weight complex and can be readily compared with the SEC of the individual components (proteins). The best readout is SDS-PAGE, where both proteins should be present throughout the peak with similar intensities. In order to measure a full thermodynamic profile of a protein–protein interaction, isothermal titration calorimetry is the best method. Its drawback is the need for rather high amounts of protein. Malvern (VP-ITC and ITC_{200}) and TA Instruments (nano-ITC) are the main manufacturers of these instruments.

1. All ITC experiments should be performed at the same temperature.
2. All proteins and/or peptides must be in the identical buffer (*see* **Note 10**).
3. All proteins should be purified using SEC (e.g., Superdex 75 26/60; GE Healthcare) immediately prior to the experiment.
4. To carry out the ITC experiment, titrant (10 μL per injection) is injected into the sample cell over a period of 20 s with a 250 s interval between titrations to allow for complete equilibration and baseline recovery. About 28 injections are delivered during each experiment (example given for a VP-ITC system), and the solution in the sample cell is stirred at 307 rpm to ensure rapid mixing.
5. Data analysis, Origin: A nonlinear least-squares algorithm and the titrant and sample cell concentrations are used to fit the integrated heat per injection to an equilibrium binding equation, providing values of the stoichiometry (n), change in enthalpy (ΔH) and the binding constant (K). Subsequently, ΔG and ΔS are readily calculated. Data are most commonly analyzed with a one-site binding model assuming a binding stoichiometry of 1:1. Typically, Origin 7.0 software with a specific ITC module is used for data evaluation.
6. Data analysis, NITPIC [38] and SEDPHAT [39]: NITPIC is a stand-alone program that is used to integrate ITC data from a variety of instruments and prepare the data for analysis using SEDPHAT, a program designed to analyze multiple datasets from different biophysical methods, including ITC.

3.3 NMR Spectroscopy

NMR spectroscopy is one of the best techniques to measure interactions (e.g., protein–protein, protein–peptide, protein–DNA, protein–RNA, protein–inhibitor [small molecule], and any variation thereof) at a variety of binding strengths; it is especially well suited to detect weak and even very weak interactions (μM–mM).

3.3.1 NMR Sample Preparation

1. Identification of the optimal sample buffer: Perform a high-throughput buffer screen to identify the buffer, pH, and salt concentration at which the protein is most stable (*see* **Notes 11** and **12**).
2. Identification of the optimal temperature for NMR measurements: The faster a protein tumbles in solution, the shorter its overall correlation time (τ_c) and the better the spectral quality due to longer transverse relation times (R_2). Thus, once the optimal buffer has been identified, determine the melting temperature of the protein and set the measurement temperature at ~30 °C below the melting temperature (*see* **Note 13**).
3. A small amount of D_2O must be added to the sample (1–10% depending on the spectrometer and probe used (*see* **Note 14**).

3.3.2 NMR Experiments, Sequence Specific Backbone Assignment

1. Sequence specific backbone assignment: 2D [^{1}H,^{15}N]-TROSY, 3D HNCA [40], 3D HNCACB, 3D HN(CO)CA, 3D HN(CO)CACB, 3D HNCO, 3D HN(CA)CO, and a 3D ^{15}N-edited [^{1}H,^{1}H] NOESY spectrum are the most common NMR spectra used to achieve the sequence-specific backbone assignment for a protein (*see* **Notes 15** and **16**).
2. Verification of assignment accuracy, single amino acid labeling: Due to the significantly reduced number of experiments (*see* **Note 15**) and the potential reduced completion percentage of the sequence-specific backbone assignment in large proteins due to, for example, the lack of H/D back-exchange, it is critical to verify the accuracy of the assignment. One of the primary methods by which this is achieved is by using single amino acid labeled samples (see examples in [41, 42]), which can be rapidly produced for ^{15}N-Phe, ^{15}N-Ile, ^{15}N-Leu, and ^{15}N-Tyr. Here it is best to use a specially prepared medium that has all amino acids in unlabeled form except for the ones that should be labeled, which are added as ^{15}N-labeled amino acids. As these samples are produced using H_2O and not D_2O, sequence-specific backbone assignment problems arising from D_2O/H_2O back-exchange can be assayed.
3. Verification of assignment accuracy, CSPs: The sequence-specific backbone assignment can be further verified using ligand and/or inhibitor binding. Here, only residues known to interact with the ligand/inhibitor should show significant chemical shift perturbations (CSP) [43]. For example, we used C3′-(2,2,5,5-tetramethyl-3-pyrroline-1-oxyl-3-carboxylic acid

ester) adenosine triphosphate (SL-ATP, a generous gift from Dr. Pia Vogel, Southern Methodist University) [44] to verify the assignment of p38α. AMP-PNP and/or specific p38α inhibitors can be used to test for CSP changes. This allows for the rapid detection of potentially mis-assigned residues.

4. Data deposition: All NMR chemical shift information must be deposited in the BioMagResBank (www.bmrb.wisc.edu; p38α accession number is 17471) so it can be downloaded and used by other research scientists for additional analysis and/or for the design of novel experiments.

3.3.3 NMR Experiments, Protein–Protein Interactions

1. Identification of residues that mediate a protein–protein interaction: The formation of a protein–protein complex influences the local environment of chemical shifts, which can be readily measured using a concentration dependent recording of a series of 2D [^{1}H,^{15}N] HSQC spectra [43]. Specifically, one protein is ^{15}N-labeled (NMR-active) and the second protein is un-labeled (NMR-inactive). The bound, unlabeled protein will change the local environment of the amino acids that mediate binding, which can be readily detected in the NMR spectrum.
2. Measuring the K_d of the interaction: A concentration-dependent measurement is used to determine an amino acid specific K_d. Protein–protein binding events typically lead to a concentration dependent linear change in the chemical shift value. If a deviation from this linear change is detected, this means an additional conformational change is occurring during the binding event (*see* **Note 17**).
3. Reverse titrations: A reverse titration can be performed in which the previous unlabeled protein is now NMR active, while the previous NMR-active protein is now unlabeled. In this way, the complementary binding site can be determined.
4. NMR spectroscopy has a size limit; however, these CSP studies can be performed even with very high molecular weight proteins (depending on the labeling scheme up to 1 MDa). A further advantage of this technique is the ability to use peptides and full length proteins, which allows, for example, a small part of an interaction to be tested via a peptide [17, 45].

3.4 Global Structures

NMR spectroscopy has a limited set of experiments for measuring long-distance interactions. Nuclear Overhauser Effect (nOe) measurements (^{1}H–^{1}H dipole–dipole) are limited to ~5–6 Å (depending on labeling and the size of the B_0 field used for the measurements; NOE scales with $B_0^{3/2}$) [46]. Paramagnetic spin relaxation measurements (^{1}H–e^{-} dipole–dipole) allow for the measurements of longer distances (up to ~20 Å), but require routine modification of the protein (e.g., covalently attached via a cysteine or a

N/C-terminal residue) using a paramagnetic spin label (most commonly used spin-label is (1-Oxyl-2,2,5,5-tetramethylpyrroline-3-methyl)methanethiosulfonate [MTSL]) [47]. As the relaxation effects depend on the internal dynamics of the spin label as well as the proteins themselves, all quantitative distance interpretation of spin-label data must be performed with great care. Other possibilities to define tertiary and quaternary structures are the use of residual dipolar couplings (RDCs) [48]. Rapid isotropic overall tumbling of the proteins in solution usually cancels out dipolar couplings. However, introducing a slight preferred alignment relative to the external field, e.g., through changes in the solution environment or high magnetic field strengths, restores a portion of these couplings. The measurement of these RDC data makes it possible to derive the orientation of a large number of local NH vectors in relationship to the overall alignment tensor, and thus can define the relative orientation of distant parts of for example a multi-domain protein.

Another method to obtain long-distance information is the incorporation of overall distance and shape constrains from independent small angle X-ray scattering measurements (SAXS; this method reports on the isotropic scattering of X-ray photons on proteins in solution, which enables the measurements of the radius of gyration (R_g) among other parameters; *see* ref. 49 for a review). For example, to determine the structure of p38α in complex with HePTP, multiple experiments were performed. X-ray crystallography and NMR spectroscopy were used to achieve a high resolution local structure while SAXS allowed for the description of the global structure [17]. In recent years, a variety of computational methods have been introduced that allow data from multiple techniques to be optimally combined in order to determine the structure and/or the ensemble of structures that best fit the experimental results (HADDOCK [50, 51], EROS [18, 52], EROS-NMR [17], among other software [53]).

SAXS measurements can be performed either at a home source or at a synchrotron. Here we summarize steps we routinely perform when measuring this data.

1. Obtaining non-aggregated samples: SAXS is exceptionally sensitive to aggregation, as soluble aggregates, even if they represent less than 1% of the sample, are significantly larger and thus will have a major impact on the overall measured scattering. Thus, it is optimal to prepare the protein sample immediately (or as shortly as possible before) the SAXS measurements; to facilitate optimal sample preparation, some synchrotron beamlines offer in-line SEC purification prior to SAXS measurements. For some samples, it is possible to filter aggregates prior to measurement. For this, 0.02 μm syringe filters (GE Healthcare Anotop 10) are suitable (*see* **Note 10**).

2. Sample concentration: The optimal concentration for SAXS measurements depends on the X-ray source, the size and assembly of the cell (flow-through or static), among other parameters. For example, on our home source (BioSAXS, FRE+ anode, Rigaku), we measure samples at concentrations as low as 1.5 mg/mL. Typically, we initiate our measurements using samples with the lowest concentration possible. We then concentrate the sample and re-collect the SAXS data from the sample at as high of concentration as can be achieved before aggregation is detected (sometimes this can be as high as 30 mg/mL).
3. Aggregation detection: Some samples are not amenable to SAXS measurements as they exhibit aggregation even at low concentrations. Aggregation is readily detected by observing a concentration dependent change in the R_g as well as a change in the I/c_0 plot. In general, all experimental SAXS curves should be parallel at multiple concentrations; discrepancies are a clear indication of aggregation.
4. Radiation damage: Exposure to high energy photons can induce radiation damage. This is less of an issue at home sources, but can occur when using synchrotron radiation. Here, the use of flow cells can alleviate the problem [54].
5. SAXS data analysis: Numerous software packages are available to analyze SAXS data, with the two most widely used being ATSAS [55] and SCATTER, both of which also allow for the calculation of 3D envelops from the data; this calculations are usually performed with the highest signal/noise dataset (commonly highest measured concentration). This can also be done using Fast-SAXS-pro [56].

4 Notes

1. Warning: HCl must be diluted into H_2O or D_2O; do not add directly to metals.
2. For p38α expression, we use BL21 (DE3) RIL cells (Agilent) to overcome rare codon usage bias in *E. coli*.
3. A fresh transformation is essential for high yield expression of deuterated proteins.
4. 500 mL is the minimum flask volume to ensure sufficient culture aeration.
5. Generally, after the overnight growth step with 70% D_2O-based medium, the 1 L of D_2O-based medium is prepared with 100 mL distributed in a 500 mL Ultra-yield flask and the remaining 900 mL distributed equally into four 2 L Ultra-yield flasks.

6. For proteins that are expressed at 18 °C, cultures must be cooled to 18 °C prior to induction.
7. One typically waits until ~10–20 L of used D_2O have accumulated before initiating D_2O recycling.
8. Flasks with two inlets are optimal because they can be readily refilled.
9. We routinely recycle D_2O twice. The doubly recycled D_2O is only used for test expression, initial protein characterization and protein–protein interaction studies and sequence specific backbone assignment experiments.
10. Typically, we prepare 4–8 L of the appropriate ITC buffer that is then used for all subsequent experiments in order eliminate any heat of dilution from a buffer mismatch. The same approach is used for SAXS measurements, where accurate buffer subtraction is equally important.
11. We use the high-throughput thermofluor assay to identify optimal buffers for NMR samples [57].
12. Modern NMR spectrometers are most commonly equipped with cryogenically cooled NMR probes. Here, cold (~20 K) helium gas is used to cool the coil and the built-in signal preamplifier of the probe, which reduces thermal noise and increases the signal-to-noise ratio by an factor of 3–4. Because cryoprobes are very sensitive to salt concentrations, samples with lower ionic strength ($\leq$50 mM) are preferred. In addition, HEPES should be preferably used over phosphatase buffers.
13. We determine the melting temperature by following the transition of the 222 nM circular dichroism [CD] signal during heating from 25 to 90 °C.
14. The deuterium NMR signal (nuclear spin = 1) is used as an internal reference and allows for rapid compensation for changes of the magnetic field due to environmental changes (cars on nearby roads, etc.) or the stability of the superconductive magnet.
15. Due to their large gyromagnetic ratio, protons (42.58 MHz/T; ratio of magnetic dipole moment/angular momentum of proton) are most commonly used for excitation and detection of NMR experiments. Thus, in fully deuterated samples, where the only H_2O exchangeable protons are available for excitation and detection (specifically $^1H^N$), the number of useable NMR experiments are significantly reduced.
16. The sequence-specific backbone assignment allows for the identification (assignment) of each peak in an NMR spectrum specifically to its amino acid and atom in the protein under investigation. It is based on probability matching of measured chemical shifts—thus, the more the data points, the higher the

likelihood of a correct assignment. As a consequence, the higher the completion percentage of the sequence-specific backbone assignment is, the smaller the chance of errors in the sequence-specific backbone assignment.

17. Depending on the K_d, the interaction will be in the fast, intermediate or slow exchange regime. A fast and slow exchange regime titration can be most readily analyzed. In the fast exchange regime, the switching between chemical states is so rapid that one average chemical shift is reported and thus the change can be fully traced (K_d μM range). Here the experimenter needs to use ratios of 1:1, 1:2, 1:3, and higher until full saturation is achieved, i.e., until the peaks do not shift further upon the addition of more protein. An interaction in the slow exchange regime will lead to two peaks, whose intensities reflect their populations. An interaction in the intermediate exchange regime often leads to a broadening of the peaks beyond detectability. Here titration ratios of 1:0.1, 1:0.25, 1:0.5, etc. can be useful to be able to trace changes.

Acknowledgement

The authors thank the large numbers of highly skilled and ambitious coworkers for their strong support in the effort to better understand protein phosphatases. They are also deeply indebted to many members of the phosphatase field—too many to name—for their support, for their collaborations and their input. We thank Dr. Michael Clarkson (Brown University) for input for the document and Dr. Andrew Hink (UTHSCSA) for input in regard to D_2O recycling. This work was supported by NIH grant R01GM098482 to RP, R01GM100910 to WP.

References

1. Cuadrado A, Nebreda AR (2010) Mechanisms and functions of p38 MAPK signalling. Biochem J 429(3):403–417. doi:10.1042/BJ20100323, BJ20100323 [pii]
2. Kim EK, Choi EJ (2010) Pathological roles of MAPK signaling pathways in human diseases. Biochim Biophys Acta 1802(4):396–405. doi:10.1016/j.bbadis.2009.12.009, S0925-4439(10)00015-3 [pii]
3. Coulthard LR, White DE, Jones DL, McDermott MF, Burchill SA (2009) p38(MAPK): stress responses from molecular mechanisms to therapeutics. Trends Mol Med 15(8):369–379. doi:10.1016/j.molmed.2009.06.005, S1471-4914(09)00114-2 [pii]
4. Brown MD, Sacks DB (2009) Protein scaffolds in MAP kinase signalling. Cell Signal 21(4):462–469. doi:10.1016/j.cellsig.2008.11.013, S0898-6568(08)00345-8 [pii]
5. Imajo M, Tsuchiya Y, Nishida E (2006) Regulatory mechanisms and functions of MAP kinase signaling pathways. IUBMB Life 58(5–6):312–317. doi:10.1080/15216540600746393, N77103R4L425G181 [pii]
6. Koveal D, Schuh-Nuhfer N, Ritt D, Page R, Morrison DK, Peti W (2012) A CC-SAM, for coiled coil-sterile alpha motif, domain targets the scaffold KSR-1 to specific sites in the plasma membrane. Sci Signal 5(255):ra94. doi:10.1126/scisignal.2003289

7. Peti W, Page R (2013) Molecular basis of MAP kinase regulation. Protein Sci 22(12):1698–1710. doi:10.1002/pro.2374
8. Akella R, Min X, Wu Q, Gardner KH, Goldsmith EJ (2010) The third conformation of p38alpha MAP kinase observed in phosphorylated p38alpha and in solution. Structure 18(12):1571–1578. doi:10.1016/j.str.2010.09.015, S0969-2126(10)00368-0 [pii]
9. Akella R, Moon TM, Goldsmith EJ (2008) Unique MAP kinase binding sites. Biochim Biophys Acta 1784(1):48–55. doi:10.1016/j.bbapap.2007.09.016,S1570-9639(07)00281-6 [pii]
10. Canagarajah BJ, Khokhlatchev A, Cobb MH, Goldsmith EJ (1997) Activation mechanism of the MAP kinase ERK2 by dual phosphorylation. Cell 90(5):859–869, S0092-8674(00)80351-7 [pii]
11. Chang CI, Xu BE, Akella R, Cobb MH, Goldsmith EJ (2002) Crystal structures of MAP kinase p38 complexed to the docking sites on its nuclear substrate MEF2A and activator MKK3b. Mol Cell 9(6):1241–1249, S1097276502005257 [pii]
12. Goldsmith EJ, Akella R, Min X, Zhou T, Humphreys JM (2007) Substrate and docking interactions in serine/threonine protein kinases. Chem Rev 107(11):5065–5081. doi:10.1021/cr068221w
13. Wang Z, Harkins PC, Ulevitch RJ, Han J, Cobb MH, Goldsmith EJ (1997) The structure of mitogen-activated protein kinase p38 at 2.1-A resolution. Proc Natl Acad Sci U S A 94(6):2327–2332
14. Wilson KP, Fitzgibbon MJ, Caron PR, Griffith JP, Chen W, McCaffrey PG, Chambers SP, Su MS (1996) Crystal structure of p38 mitogen-activated protein kinase. J Biol Chem 271(44):27696–27700
15. Zhou T, Sun L, Humphreys J, Goldsmith EJ (2006) Docking interactions induce exposure of activation loop in the MAP kinase ERK2. Structure 14(6):1011–1019. doi:10.1016/j.str.2006.04.006, S0969-2126(06)00222-X [pii]
16. ter Haar E, Prabhakar P, Prabakhar P, Liu X, Lepre C (2007) Crystal structure of the p38 alpha-MAPKAP kinase 2 heterodimer. J Biol Chem 282(13):9733–9739. doi:10.1074/jbc.M611165200, M611165200 [pii]
17. Francis DM, Rozycki B, Koveal D, Hummer G, Page R, Peti W (2011) Structural basis of p38alpha regulation by hematopoietic tyrosine phosphatase. Nat Chem Biol 7(12):916–924. doi:10.1038/nchembio.707
18. Francis DM, Rozycki B, Tortajada A, Hummer G, Peti W, Page R (2011) Resting and active states of the ERK2:HePTP complex. J Am Chem Soc 133(43):17138–17141. doi:10.1021/ja2075136
19. Piserchio A, Francis DM, Koveal D, Dalby KN, Page R, Peti W, Ghose R (2012) Docking interactions of hematopoietic tyrosine phosphatase with MAP kinases ERK2 and p38alpha. Biochemistry 51(41):8047–8049. doi:10.1021/bi3012725
20. Piserchio A, Warthaka M, Devkota AK, Kaoud TS, Lee S, Abramczyk O, Ren P, Dalby KN, Ghose R (2011) Solution NMR insights into docking interactions involving inactive ERK2. Biochemistry 50(18):3660–3672. doi:10.1021/bi2000559
21. Vogtherr M, Saxena K, Grimme S, Betz M, Schieborr U, Pescatore B, Langer T, Schwalbe H (2005) NMR backbone assignment of the mitogen-activated protein (MAP) kinase p38. J Biomol NMR 32(2):175. doi:10.1007/s10858-005-2449-x
22. Vogtherr M, Saxena K, Hoelder S, Grimme S, Betz M, Schieborr U, Pescatore B, Robin M, Delarbre L, Langer T, Wendt KU, Schwalbe H (2006) NMR characterization of kinase p38 dynamics in free and ligand-bound forms. Angew Chem Int Ed Engl 45(6):993–997. doi:10.1002/anie.200502770
23. Wong M, Khirich G, Loria JP (2013) What's in your buffer? Solute altered millisecond motions detected by solution NMR. Biochemistry 52(37):6548–6558. doi:10.1021/bi400973e
24. Johnson BA (2004) Using NMRView to visualize and analyze the NMR spectra of macromolecules. Methods Mol Biol 278:313–352. doi:10.1385/1-59259-809-9:313
25. Lee W, Tonelli M, Markley JL (2015) NMRFAM-SPARKY: enhanced software for biomolecular NMR spectroscopy. Bioinformatics 31(8):1325–1327. doi:10.1093/bioinformatics/btu830
26. Vranken WF, Boucher W, Stevens TJ, Fogh RH, Pajon A, Llinas M, Ulrich EL, Markley JL, Ionides J, Laue ED (2005) The CCPN data model for NMR spectroscopy: development of a software pipeline. Proteins 59(4):687–696. doi:10.1002/prot.20449
27. Skinner SP, Goult BT, Fogh RH, Boucher W, Stevens TJ, Laue ED, Vuister GW (2015) Structure calculation, refinement and validation using CcpNmr Analysis. Acta Crystallogr D Biol Crystallogr 71(Pt 1):154–161. doi:10.1107/S1399004714026662
28. Peti W, Page R (2007) Strategies to maximize heterologous protein expression in Escherichia coli with minimal cost. Protein Expr Purif 51(1):1–10. doi:10.1016/j.pep.2006.06.024, S1046-5928(06)00195-1 [pii]

29. Tugarinov V, Hwang PM, Kay LE (2004) Nuclear magnetic resonance spectroscopy of high-molecular-weight proteins. Annu Rev Biochem 73:107–146. doi:10.1146/annurev.biochem.73.011303.074004
30. Frueh DP (2014) Practical aspects of NMR signal assignment in larger and challenging proteins. Prog Nucl Magn Reson Spectrosc 78:47–75. doi:10.1016/j.pnmrs.2013.12.001
31. Sugiki T, Ichikawa O, Miyazawa-Onami M, Shimada I, Takahashi H (2012) Isotopic labeling of heterologous proteins in the yeast Pichia pastoris and Kluyveromyces lactis. Methods Mol Biol 831:19–36. doi:10.1007/978-1-61779-480-3_2
32. Gossert AD, Jahnke W (2012) Isotope labeling in insect cells. Adv Exp Med Biol 992:179–196. doi:10.1007/978-94-007-4954-2_10
33. Hansen AP, Petros AM, Mazar AP, Pederson TM, Rueter A, Fesik SW (1992) A practical method for uniform isotopic labeling of recombinant proteins in mammalian cells. Biochemistry 31(51):12713–12718
34. Pervushin K, Riek R, Wider G, Wüthrich K (1997) Attenuated T2 relaxation by mutual cancellation of dipole-dipole coupling and chemical shift anisotropy indicates an avenue to NMR structures of very large biological macromolecules in solution. Proc Natl Acad Sci U S A 94(23):12366–12371
35. Barrett PJ, Chen J, Cho MK, Kim JH, Lu Z, Mathew S, Peng D, Song Y, Van Horn WD, Zhuang T, Sonnichsen FD, Sanders CR (2013) The quiet renaissance of protein nuclear magnetic resonance. Biochemistry 52(8):1303–1320. doi:10.1021/bi4000436
36. Gardner KH, Kay LE (1998) The use of 2H, 13C, 15N multidimensional NMR to study the structure and dynamics of proteins. Annu Rev Biophys Biomol Struct 27:357–406. doi:10.1146/annurev.biophys.27.1.357
37. Sitarska A, Skora L, Klopp J, Roest S, Fernandez C, Shrestha B, Gossert AD (2015) Affordable uniform isotope labeling with H, C and N in insect cells. J Biomol NMR. doi:10.1007/s10858-015-9935-6
38. Keller S, Vargas C, Zhao H, Piszczek G, Brautigam CA, Schuck P (2012) High-precision isothermal titration calorimetry with automated peak-shape analysis. Anal Chem 84(11):5066–5073. doi:10.1021/ac3007522
39. Zhao H, Piszczek G, Schuck P (2015) SEDPHAT—a platform for global ITC analysis and global multi-method analysis of molecular interactions. Methods 76:137–148. doi:10.1016/j.ymeth.2014.11.012
40. Bax A, Ikura M (1991) An efficient 3D NMR technique for correlating the proton and 15N backbone amide resonances with the alpha-carbon of the preceding residue in uniformly 15N/13C enriched proteins. J Biomol NMR 1(1):99–104
41. Francis DM, Page R, Peti W (2014) Sequence-specific backbone (1)H, (1)(3)C and (1)(5)N assignments of the 34 kDa catalytic domain of PTPN5 (STEP). Biomol NMR Assign 8(1):185–188. doi:10.1007/s12104-013-9480-8
42. Krishnan N, Koveal D, Miller DH, Xue B, Akshinthala SD, Kragelj J, Jensen MR, Gauss CM, Page R, Blackledge M, Muthuswamy SK, Peti W, Tonks NK (2014) Targeting the disordered C terminus of PTP1B with an allosteric inhibitor. Nat Chem Biol 10(7):558–566. doi:10.1038/nchembio.1528
43. Williamson MP (2013) Using chemical shift perturbation to characterise ligand binding. Prog Nucl Magn Reson Spectrosc 73:1–16. doi:10.1016/j.pnmrs.2013.02.001
44. Hoffman AD, Urbatsch IL, Vogel PD (2010) Nucleotide binding to the human multidrug resistance protein 3, MRP3. Protein J 29(5):373–379. doi:10.1007/s10930-010-9262-4
45. Francis DM, Kumar GS, Koveal D, Tortajada A, Page R, Peti W (2013) The differential regulation of p38alpha by the neuronal kinase interaction motif protein tyrosine phosphatases, a detailed molecular study. Structure 21(9):1612–1623. doi:10.1016/j.str.2013.07.003
46. Wüthrich K (1986) NMR of proteins and nucleic acids. Wiley-Interscience, New York
47. Gaponenko V, Howarth JW, Columbus L, Gasmi-Seabrook G, Yuan J, Hubbell WL, Rosevear PR (2000) Protein global fold determination using site-directed spin and isotope labeling. Protein Sci 9(2):302–309. doi:10.1110/ps.9.2.302
48. Tolman JR, Flanagan JM, Kennedy MA, Prestegard JH (1995) Nuclear magnetic dipole interactions in field-oriented proteins: information for structure determination in solution. Proc Natl Acad Sci U S A 92(20):9279–9283
49. Rambo RP, Tainer JA (2013) Super-resolution in solution X-ray scattering and its applications to structural systems biology. Annu Rev Biophys 42:415–441. doi:10.1146/annurev-biophys-083012-130301
50. de Vries SJ, van Dijk AD, Krzeminski M, van Dijk M, Thureau A, Hsu V, Wassenaar T, Bonvin AM (2007) HADDOCK versus HADDOCK: new features and performance of HADDOCK2.0 on the CAPRI targets. Proteins 69(4):726–733. doi:10.1002/prot.21723
51. Dominguez C, Boelens R, Bonvin AM (2003) HADDOCK: a protein-protein docking

approach based on biochemical or biophysical information. J Am Chem Soc 125(7):1731–1737. doi:10.1021/ja026939x

52. Rozycki B, Kim YC, Hummer G (2011) SAXS ensemble refinement of ESCRT-III CHMP3 conformational transitions. Structure 19(1): 109–116.doi:10.1016/j.str.2010.10.006,S0969-2126(10)00395-3 [pii]
53. Yang S, Blachowicz L, Makowski L, Roux B (2010) Multidomain assembled states of Hck tyrosine kinase in solution. Proc Natl Acad Sci U S A 107(36):15757–15762. doi:10.1073/pnas.1004569107, 1004569107 [pii]
54. Allaire M, Yang L (2011) Biomolecular solution X-ray scattering at the National Synchrotron Light Source. J Synchrotron Radiat 18(1):41–44. doi:10.1107/S0909049510036022
55. Petoukhov MV, Franke D, Shkumatov AV, Tria G, Kikhney AG, Gajda M, Gorba C, Mertens HD, Konarev PV, Svergun DI (2012) New developments in the program package for small-angle scattering data analysis. J Appl Crystallogr 45(Pt 2):342–350. doi:10.1107/S0021889812007662
56. Ravikumar KM, Huang W, Yang S (2013) Fast-SAXS-pro: a unified approach to computing SAXS profiles of DNA, RNA, protein, and their complexes. J Chem Phys 138(2):024112. doi:10.1063/1.4774148
57. Romanuka J, van den Bulke H, Kaptein R, Boelens R, Folkers GE (2009) Novel strategies to overcome expression problems encountered with toxic proteins: application to the production of Lac repressor proteins for NMR studies. Protein Expr Purif 67(2):104–112. doi:10.1016/j.pep.2009.05.008
58. Kumar GS, Zettl H, Page R, Peti W (2013) Structural basis for the regulation of the mitogen-activated protein (MAP) kinase p38alpha by the dual specificity phosphatase 16 MAP kinase binding domain in solution. J Biol Chem 288(39):28347–28356. doi:10.1074/jbc.M113.499178
59. Nielsen G, Schwalbe H (2011) NMR spectroscopic investigations of the activated p38alpha mitogen-activated protein kinase. Chembiochem 12(17):2599–2607. doi:10.1002/cbic.201100527
60. Jeeves M, McClelland DM, Barr AJ, Overduin M (2008) Sequence-specific 1H, 13C and 15N backbone resonance assignments of the 34 kDa catalytic domain of human PTPN7. Biomol NMR Assign 2(2):101–103. doi:10.1007/s12104-008-9095-7

Chapter 12

Visualizing and Quantitating the Spatiotemporal Regulation of Ras/ERK Signaling by Dual-Specificity Mitogen-Activated Protein Phosphatases (MKPs)

Christopher J. Caunt, Andrew M. Kidger, and Stephen M. Keyse

Abstract

The spatiotemporal regulation of the Ras/ERK pathway is critical in determining the physiological and pathophysiological outcome of signaling. Dual-specificity mitogen-activated protein kinase (MAPK) phosphatases (DUSPs or MKPs) are key regulators of pathway activity and may also localize ERK to distinct subcellular locations. Here we present methods largely based on the use of high content microscopy to both visualize and quantitate the subcellular distribution of activated (*p*-ERK) and total ERK in populations of mouse embryonic fibroblasts derived from mice lacking DUSP5, a nuclear ERK-specific MKP. Such methods in combination with rescue experiments using adenoviral vectors encoding wild-type and mutant forms of DUSP5 have allowed us to visualize specific defects in ERK regulation in these cells thus confirming the role of this phosphatase as both a nuclear regulator of ERK activity and localization.

Key words DUSP5, Ras/ERK signaling, Spatiotemporal regulation, High-content microscopy, Adenoviral expression

1 Introduction

The core Ras/extracellular signal-regulated kinase (ERK) mitogen-activated protein kinase (MAPK) signaling pathway comprises a three-component module in which a member of the Raf family of MAPK kinase kinases (MKKKs or MEKKs) phosphorylates and activates a MAPK kinase (MKK or MEK). The latter is a dual-specificity (Thr/Tyr) protein kinase, which phosphorylates both residues within the conserved T-X-Y activation loop motif to activate ERK1 and ERK2 [1]. This pathway mediates a wide variety of physiological outcomes in response to extracellular stimuli. These include cell proliferation, differentiation, transformation, migration, and survival [2–4]. In addition, Ras/MAPK signaling is frequently deregulated in human cancers, often due to activating mutations in upstream pathway components such as receptor tyrosine kinases (RTKs), the Ras family of small GTPases, the Braf

Rafael Pulido (ed.), *Protein Tyrosine Phosphatases: Methods and Protocols,* Methods in Molecular Biology, vol. 1447,
DOI 10.1007/978-1-4939-3746-2_12,

MAPK kinase kinase, and MAPK kinases [5]. Thus, Ras/ERK signaling components are a major focus of anticancer drug development with a range of small molecule inhibitors of RTKs, Braf and MEK either in development or clinical use [6, 7].

The diversity of physiological outputs of Ras/ERK signaling is due to the coordinated phosphorylation of a wide range of cellular ERK substrates. These include transcription factors, protein kinases, metabolic enzymes, and cytoskeletal proteins [8, 9]. Clearly, because these substrates either reside in or are associated with distinct subcellular compartments, the spatial as well as the temporal control of Ras/ERK signaling is a critical determinant of biological outcome. This may explain, at least in part, why ERK activation can result in quite different endpoints within the same cell type. A good example of the latter is the ability of nerve growth factor (NGF) to cause sustained activation and nuclear localization of ERK in rat PC12 cells leading to differentiation and neurite outgrowth, while exposure to epidermal growth factor (EGF) instead results in transient ERK activation and drives cell proliferation [10].

Exactly how the spatial organization of the Ras/ERK pathway is regulated is still unclear and likely to be complex. Various mechanisms have been proposed to underpin the growth factor-induced nuclear translocation of ERK itself, including activation-dependent dimerization, active/passive transport and the phosphorylation of additional regulatory sites on ERK that promote its association with importin7 [11]. In addition, it is clear that a diverse array of proteins can act as ERK binding partners and retain ERKs in specific subcellular locations. The latter include MKK/MEK, scaffold proteins such as β-arrestin and kinase suppressor of Ras (KSR), phosphoprotein enriched in astrocytes-15 (PEA-15), and cytoskeletal elements such as microtubule and actin filaments [12]. One class of ERK regulatory proteins that clearly plays a role in controlling both the activity and localization of ERK1 and ERK2 are the dual-specificity MAPK phosphatases (DUSPs or MKPs) exemplified by DUSP5 and DUSP6/MKP-3 [13].

DUSP6/MKP-3 is a cytoplasmic ERK-specific MKP that binds tightly to the common docking (CD) domain of ERKs via a kinase interaction domain (KIM) located within the amino-terminal noncatalytic domain of the protein [14–16]. The latter domain also carries a functional leucine-rich nuclear export signal (NES), which mediates the cytoplasmic localization of the protein [17]. DUSP6/MKP-3 is a transcriptional target of ERK itself and acts as a negative feedback regulator of pathway activity [18]. Once induced in response to ERK activation, DUSP6/MKP-3 would be expected to bind to, dephosphorylate, and retain ERK in the cytoplasm. Indeed, overexpression experiments have confirmed the ability of DUSP6/MKP-3 to act in this way to anchor ERKs in the cytosol: this anchoring function requires both a functional KIM and NES within the DUSP6/MKP-3 protein [17, 19]. In contrast to DUSP6/MKP-3, DUSP5 is an inducible nuclear ERK-specific MKP, which is also

transcriptionally regulated by ERK signaling and has been proposed to act as a nuclear anchor for ERK [20, 21]. Again, overexpression experiments confirm the ability of DUSP5 to anchor inactive ERK within the cell nucleus and this is also dependent on the integrity of both the KIM and a nuclear localization signal (NLS) located within the amino terminal domain of DUSP5 [20].

In order to study the precise role of DUSP5 in regulating ERK activation and function, we recently generated mice in which the DUSP5 gene was deleted. These animals and cells derived from them were then used to ask two key questions about the role of DUSP5. Firstly, is ERK signaling deregulated in the absence of DUSP5, if so how does this affect the distribution of ERK/phospho-ERK and what biological endpoints are affected? Secondly, does DUSP5 play a role in modulating the oncogenic potential of mutant Ras oncogenes in vivo? To address the latter, we used the DMBA/TPA model of skin carcinogenesis and found that loss of one or both copies of DUSP5 greatly sensitized mice to the development of skin papillomas. At the cellular level, we were able to show that loss of DUSP5 caused increased levels of nuclear phospho-ERK and gene expression studies identified a small cohort of ERK-dependent transcripts that were upregulated in cell lacking DUSP5. Prominent amongst the latter was serpinB2, a protease inhibitor previously linked to susceptibility to DMBA/TPA-induced carcinogenesis. Surprisingly, deletion of serpinB2 completely reversed the sensitivity of mice lacking DUSP5 to DMBA/TPA indicating that DUSP5 acts as a tumor suppressor in this model by regulating nuclear ERK signaling and suppressing the ERK-dependent expression of serpinB2 [22].

In order to study the precise spatiotemporal regulation of ERK activation in murine cells lacking DUSP5, we made extensive use of quantitative high-content microscopy to detect the subcellular distribution of endogenous total ERK and phosphorylated, activated ERK over time, either after stimulation with phorbol ester or expression of mutant Hras. This technique uses automated fluorescence microscopy to analyze thousands of individual cells per condition, thus allowing an accurate quantitation of the spatiotemporal regulation of ERK activation in cell populations [23]. To link this regulation to the biochemical activities and ERK-binding properties of DUSP5 itself, we also employed adenoviral vectors expressing either wild-type or mutant forms of DUSP5 under the control of the early growth response-1 (EGR-1) promoter. This allowed us to perform rescue experiments in which ERK-dependent DUSP5 expression was recapitulated in DUSP5 knockout cells at physiologically relevant levels. This differs from previous approaches, principally utilizing DUSP5 overexpression under the control of constitutive promoters whose activity is divorced from ERK regulation, which do not reveal the same dynamic functions of DUSP5 as a feedback regulator. These techniques, together with more conventional biochemical fractionation methods to

study the distribution of activated ERK are described in detail below and should be broadly applicable to the study of other MKPs which act to regulate ERK signaling such as DUSP1/MKP-2, DUSP2, DUSP4/MKP-2, and DUSP6/MKP-3.

2 Materials

2.1 MEF Cell Culture

1. Primary mouse embryo fibroblasts (MEFs) (*see* **Note 1**).
2. Dulbecco's Modified Eagle's Medium (DMEM) with GlutaMAX supplement, pyruvate, and 4.5 g/l D+glucose (Invitrogen).
3. Clear bottomed, black-walled 96-well plates (Corning Costar plate 3904).
4. Fetal bovine serum (FBS).
5. Trypsin (0.25%) and ethylenediamine tetraacetic acid (EDTA) mix dissolved in phosphate buffered saline (PBS).
6. PBS: 137 mM NaCl, 2.7 mM KCl, 4.3 mM Na_2HPO_4, and 1.47 mM KH_2PO_4, pH 7.4.
7. Tetra-decanoyl phorbol acetate (TPA) is stored in dimethyl sulfoxide (DMSO) in single use aliquots at −20 °C. Working stock is prepared by dilution in PBS.

2.2 Adenoviral Generation and Purification

1. Human embryonic kidney (HEK)293 cells (*see* **Note 2**).
2. Dulbecco's Modified Eagle's Medium (DMEM) with GlutaMAX supplement, pyruvate, and 4.5 g/l D+ glucose (Invitrogen).
3. Fetal bovine serum (FBS).
4. PacI restriction enzyme and 'Cutsmart' enzyme buffer (New England Biolabs) for digestion of Adenoviral backbone and shuttle vectors.
5. 2× HBS solution for calcium phosphate transfection: rinse a clean bottle 5× with ddH_2O, to remove residual detergent, then make up 280 mM NaCl, 10 mM KCl, 1.5 mM $Na_2HPO_4 \cdot 12H_2O$, 12 mM D+ glucose, 50 mM HEPES buffer. pH to 7.05 and filter through 0.22 μm syringe-driven filter into sterile 50 ml Falcon tubes. Store in 20–50 ml aliquots at −20 °C.
6. 2 M $CaCl_2$ for calcium phosphate transfection: make up and filter through 0.22 μm syringe-driven filter. Store in 5 ml aliquots at −20 °C.
7. 100 mM Tris–HCl, pH 7.5.
8. CsCl-saturated 100 mM Tris–HCl, pH 7.5.
9. 1:0.6 ratio 100 mM Tris–HCl and CsCl-saturated 100 mM Tris–HCl, pH 7.5.
10. 13 × 51 mm 'Quick-Seal' polyallomer ultracentrifuge tubes (Beckman Coulter).

11. NVTi 90 ultracentrifuge rotor (Beckman Coulter).
12. L-80 preparative ultracentrifuge (Beckman Coulter).
13. 21 G and 25 G needles and 5 ml syringes.
14. PBS containing 3% sucrose.
15. 0.5–3.0 ml 5 kDa cutoff 'Slide-a-Lyser' dialysis cassettes (Pierce).

2.3 Immunofluorescence Staining of ERK1/2, p-ERK1/2, and Myc

1. Paraformaldehyde (PFA) made up as a 4% stock solution in PBS (*see* **Note 3**).
2. 100% methanol.
3. Normal goat serum stored in single use aliquots at −20 °C. Working stock is prepared by dilution into a 2.5% solution with PBS and 0.01% sodium azide.
4. Anti-ERK1/2 rabbit monoclonal antibody (clone 137F5) (Cell Signaling Technology).
5. Anti-*p*-ERK1/2 mouse monoclonal antibody (clone MAPK-YT) (Sigma).
6. Anti-Myc epitope rabbit monoclonal antibody (clone 71D10) (Cell Signaling Technology).
7. Alexa 488-conjugated, highly cross-adsorbed goat anti-mouse secondary antibody (Invitrogen).
8. Alexa 546-conjugated, highly cross-adsorbed goat anti-rabbit secondary antibody (Invitrogen).
9. 3 mM DAPI (4,6-diamidino-2-phenylindole) stock in water. Dilute 1:5000 in PBS for working solution (600 nM).

2.4 Subcellular Fractionation and Immunoblot Analysis

1. NE-PER nuclear and cytoplasmic extraction reagents (Thermo Scientific).
2. Halt Protease and Phosphatase Inhibitor Single-Use Cocktail (100×) (Thermo Scientific).
3. Bradford Assay Reagent (Thermo Scientific).
4. NuPAGE® LDS Sample Buffer (4×) (Thermo Scientific).
5. NuPAGE® Novex® 4–12% Bis-Tris Protein Gels, 1.0 mm (Thermo Scientific).
6. Immobilon-FL PVDF 0.45 μm Blotting Membrane (Millipore).
7. Anti-ERK1/2 rabbit monoclonal antibody (clone 137F5) (Cell Signaling Technology).
8. Anti-ppERK1/2 rabbit monoclonal antibody (clone D13.14.4E) (Cell Signaling Technology).
9. Anti-DUSP5 sheep polyclonal antibody (*see* **Note 4**).
10. Anti-UBF sheep polyclonal antibody (*see* **Note 5**).
11. Anti-MEK rabbit polyclonal antibody (Cell Signaling Technology).

12. Alexa Fluor® 680 conjugate, Donkey anti-Sheep IgG (H + L) Secondary Antibody (Thermo Scientific).
13. DyLight™ 680 Conjugate, Goat anti-rabbit IgG (H + L) secondary antibody (Cell Signaling).

3 Methods

We have previously described methodology for sensitive detection of ERK and phosphorylated ERK in HeLa cells using high content microscopy [23]. Here, we describe similar approaches for studying ERK regulation by DUSP5 in primary MEFs by DUSP5 knockout and reconstitution using adenoviral (Ad) expression of Myc-tagged DUSP5, or mutants of DUSP5. An additional layer of complexity is added by the heterogeneity in cell shape and size in the non-monoclonal population, which presents new challenges for automated analysis. High quality monoclonal antibodies are available, which specifically recognize dual phosphorylated ERK1/2 (but neither mono-phosphorylated form), ERK1/2 (irrespective of phosphorylation state), and the Myc epitope tag, which are validated for use in immunofluorescence imaging and flow cytometry. The use of high-content microscopy and analysis is well suited to studying spatiotemporal aspects of DUSP5-ERK regulation, which requires quantitative assessment of ERK phosphorylation and subcellular distribution in multiple knockout rescue and stimulus conditions in parallel. Antibody detection allows multiplexed single cell assessment of *p*-ERK1/2, ERK1/2, and Myc intensity and distribution in the same samples, as suitable antibodies for detection are available as mouse or rabbit monoclonals. Our microscopy results were cross-validated using immunoblotting of biochemically fractionated cell lysates, and thus we have also included the methodology for this complementary approach here.

3.1 Generation of Recombinant Adenovirus

This method is based on the Iowa Gene Transfer Vector Core 'RapAd™' system [24]. All plasmids may be obtained from them directly:

http://www.medicine.uiowa.edu/vectorcore/products/

The RapAd™ plasmids used to make serotype 5 recombinant adenoviral vectors have left-hand ITR, E1a, and partial E1b sequence deletions. This modification greatly reduces the chances of wild-type non-recombinant virus from contaminating the final preparation. The backbone vector, pacAd5 9.2-100, contains the entire adenoviral genome, but lacks the first 9.2 map units, and must recombine with the shuttle vector, pacAd5 K-N pA, via homology regions flanking the multiple cloning site in the presence of the E1a protein (expressed by the HEK293 helper cell line) in order to undergo viral replication and enter a lytic cycle.

Therefore, the virus will not replicate in cells that do not harbor the E1a gene, and may be used safely as a vector delivery system for transgenes of interest (*see* **Note 6**).

1. Clone fragment of interest into pacAd5 K-N pA promoterless shuttle vector (in our case the EGR-1 promoter and DUSP5-Myc cDNA). This vector contains a Pac1 digestion site, Amp resistance, and large sections of the adenoviral genome necessary for viral replication.
2. Plate low passage (<50) University of Iowa HEK293 cells in DMEM + 10% FBS, 24 h prior to transfection with backbone and shuttle vectors. Cells should be 50–60% confluent in a T25 for the transfection (on day of transfection).
3. Digest 1.5 μg of pacAd5 9.2-100 backbone vector with 5 U of PacI in Cutsmart buffer in a total volume of 25 μl. Digest 4.5 μg pacAd5 EGR-1pDUSP5-Myc shuttle vector with 5 U of PacI in Cutsmart buffer in a total volume of 25 μl. Incubate digests at 37 °C overnight.
4. Combine PacI-digested shuttle and pacAd5 9.2-100 backbone, and make up to 140 μl total volume with sterile ddH_2O.
5. Add 20 μl of 2 M $CaCl_2$. Mix well.
6. Add 160 μl of 2× HBS. Add dropwise over a period of ~20 s (the dropwise addition is important to ensure precipitate formation). Incubate at room temperature for 20 min. Do not shake or mix the solution or the precipitate will not form properly.
7. Mix well by pipetting up and down and transfer to HEK293 cells by adding to medium. Return to 37 °C, 5% CO_2 for 3–4 h (can leave the transfection medium on O/N).
8. Remove medium from cells and wash once with PBS.
9. Add 5 ml of DMEM + 10% FBS and return to 37 °C, 5% CO_2.
10. Check daily for presence of plaques—these will appear initially as foci of clearance in the cell monolayer, where cells appear healthy apart from rounded cells with the appearance of 'bunches of grapes' at the periphery of the plaque. Gaps in the monolayer are easy to distinguish as cells will appear healthy and well spread at the periphery of the area devoid of cells. If plate is ready for harvest (>60% of cells lifted, then tapping the flask gently removes virtually all cells). If not, return to incubator.
11. If medium is low or appears exhausted before plaques start to form, add 2 ml medium on day 7 and 10. Recombination and plaque formation is usually obvious by 14 days.
12. To harvest: gently tap the side of the culture flask to remove residual cells and transfer medium and cells into a 5 ml sterile tube. Snap-freeze the cells in liquid N_2 and store at −80 °C.
13. Re-inoculate a T75 flask of HEK293 cells (in 15 ml medium) with 0.3–0.5 ml of viral lysate from the initial prep to check for

functional virus alongside a non-infected control flask, and a control flask of cells that are not transformed with the E1a gene (e.g., HeLa cells). A genuine adenovirus will cause lysis of the HEK293 flask within 24–72 h, and no effect should be seen on cell viability in either control flask. Harvest this lysate in a 50 ml tube as above. Snap-freeze the lysate in liquid N_2 and store at –80 °C for future large-scale amplification.

3.2 Large-Scale Amplification and Purification of Recombinant Adenovirus

1. Grow 10×T175 flasks of low passage (<50) HEK293 cells to 60% confluency. To achieve 60% confluency, split 1×T175 flask into 10×T175 flasks. Cells will be 60% confluent 1–2 days post-split.
2. Infect each flask with 0.5 ml of viral lysate/supernatant (from previous steps above).
3. Inoculate for 24–72 h until the cells are about to detach from the flask. Maximal yields are achieved if cells are harvested just prior to cell lysis, so it is important the cells are not all detached already: this means they have already released virus to the supernatant.
4. Tap the side of the flask to dislodge the cells. Collect the cells in the medium into 50 ml tubes.
5. Spin down the cells at 1000×*g* for 10 min.
6. Discard the supernatant, save some 5–15 ml aliquots by snap-freezing in liquid N_2 and storing at –80 °C for future large scale preps if necessary.
7. Resuspend the cell pellets and pool them in a total volume of 3 ml 100 mM Tris–HCl, pH 7.5.
8. Snap-freeze in liquid N_2 and store at –80 °C until ready for purification.
9. Thaw the harvested virus and cells (3 ml) on ice. This process can be accelerated using a 37 °C water bath, but it is important the mix does not warm to more than 4 °C. Snap-freeze in liquid N_2 and thaw (repeat process again a further three times to lyse cells).
10. Centrifuge at 3000×*g* for 10 min at 4 °C to remove cell debris.
11. Transfer the supernatant to an ultracentrifuge tube using a 5 ml syringe and 21 G needle.
12. Add 0.6 volumes of CsCl-saturated 100 mM Tris–HCl (prepare by adding CsCl to 100 mM Tris–HCl, pH 7.5 until salt precipitates and no longer enters solution).
13. Fill the tube(s) with 1 volume 100 mM Tris–HCl and 0.6 volumes CsCl-saturated 100 mM Tris–HCl.
14. Balance tubes to within 0.01 g of each other.
15. Close the tubes using a heat sealer.

16. Add balance caps to the tubes and place tubes in rotor. Coat the rotor screw-tops with 'Spinkote' lubricant and screw on.
17. Close the caps to 120 psi using a torque wrench.
18. Centrifuge at 65,000 rpm (292,000 × *g*) for 6–8 h.
19. Remove tubes from rotor using tweezers.
20. Place in a stand in such a position to ensure that the viral band will be visible. Insert 2 × 25 G needles into the top of the tube to equalize the pressure.
21. Remove the white viral particle band with a 19–21 G needle and a 5 ml syringe. Insert the needle just below the viral band, taking care only to puncture one side of the tube, slowly insert the needle and then angle the needle upwards into the viral particle band. Slowly remove the viral particles using the syringe plunger.
22. Transfer the viral particles into a fresh ultracentrifuge tube and fill with 1 volume 100 mM Tris: 0.6 volumes CsCl-saturated 100 mM Tris.
23. Balance, heat seal, place in rotor as above and centrifuge for a second time overnight.
24. Remove the virus particle band as above, and inject into a 'Slide-a-Lyser' dialysis cassette. Remove air from the cassette to allow maximal use of membrane surface area and efficient dialysis. Mark the entry point used for injection of the viral particles into the cassette, as the same one should not be used twice.
25. Insert the cassette into a floating holder and dialyze for 3 h with gentle stirring in PBS containing 3% w/v sucrose. Use 1 l of PBS–sucrose and change every hour (3 l total needed).
26. Remove virus from cassette using a needle inserted into a different corner from that used to introduce the virus. Aliquot into sterile 500 µl tubes at 20 µl/tube.
27. Snap freeze the aliquots in liquid N_2 and store at –80 °C.

3.3 Culture, Adenoviral Infection, and Staining of MEFs for ERK1/2, p*-ERK1/2, and Myc*

1. Wash subconfluent flasks of wild-type (WT) and DUSP5 knockout (KO) MEFs 2× with sterile PBS. Add 2 ml/flask of trypsin–EDTA mix, and incubate at 37 °C for 5 min, or until cells have detached from the bottom of the flask. Tap the side of the flask to dislodge remaining cells. Add 10 ml of DMEM containing 10% FBS to stop the action of trypsin. Transfer to 15 ml centrifuge tubes and spin at 800 × *g* for 5 min at room temperature. Discard the supernatant and resuspend cells in DMEM containing 10% FBS.
2. Dilute cells to a suspension containing 4000 cells per 100 µl of 10% FBS/DMEM. Plate cells on to 96-well back-wall imaging plates at 100 µl. Return cells to the incubator overnight.
3. Infect cells with empty adenoviral vector containing no transgene, or adenovirus expressing DUSP5-Myc (or alternatively a mutant,

such as R53/54A DUSP5 [20], which cannot associate with or dephosphorylate the ERK kinase target, despite being catalytically active) under the control of the EGR-1 promoter. Defrost a virus aliquot and dilute to $0.1–3\times10^6$ plaque forming units (pfu) per ml for reexpression of DUSP5-Myc in DUSP5 KO MEFs. Titres of $1–3\times10^5$ pfu/ml are usually sufficient to restore endogenous levels of DUSP5 expression in MEFs. Remove medium from cells and replace with 10% FBS DMEM containing adenovirus at 100 µl/well. Return cells to the incubator for 4–6 h.

4. Remove medium from all cells, wash once with PBS and replace with 90 µl/well 10% FBS DMEM overnight for stimulation with TPA the next day. For serum stimulus, replace with 90 µl/well DMEM without FBS to serum-starve cells overnight. Add 10 µl of 10× TPA or FBS to cells for required periods.
5. Tip off medium from cells and fix by adding 50 µl/well 4% PFA in PBS (*see* **Note 3**). Incubate on a rocking platform for 10 min at room temperature.
6. Tip off PFA and permeabilize the cells by adding 50 µl/well of −20 °C methanol. Incubate for 5 min in the freezer.
7. Remove methanol and wash cells with 100 µl/well PBS at room temperature.
8. Add 25 µl/well of 2.5% v/v normal goat serum and 0.01% w/v sodium azide in PBS (blocking buffer) and incubate plates at room temperature on a rocking platform for 2 h.
9. Tip away blocking buffer and add 25 µl/well 1:200 dilution of primary mouse anti-*p*-ERK1/2 and either rabbit anti-ERK1/2 or rabbit anti-Myc antibody diluted in blocking buffer. Incubate overnight on a rocking platform at 4 °C.
10. Retrieve antibody for reuse if required. Wash cells three times with 100 µl/well PBS at room temperature.
11. Remove PBS and add 25 µl/well 1:300 dilution of either or both Alexa 546 or 488 labeled goat anti-mouse or anti-rabbit secondary antibody diluted in blocking buffer. Incubate for 90 min on a rocking platform at room temperature.
12. Retrieve antibody for reuse if required. Wash cells three times with 100 µl/well PBS at room temperature.
13. Add 100 µl/well of 300 nM DAPI diluted in PBS. Store at 4 °C until ready to image.

3.4 High Content Microscopy and Analysis

These procedures are optimized for use with the GE Healthcare IN Cell Analyzer 2000 fluorescence microscope and proprietary "IN Cell" Investigator software. However, the same outcomes are achievable using most platforms. A schematic overview of the workflow involved in performing the analysis is given in Fig. 1 and representative images and quantitative data are shown in Fig. 2b.

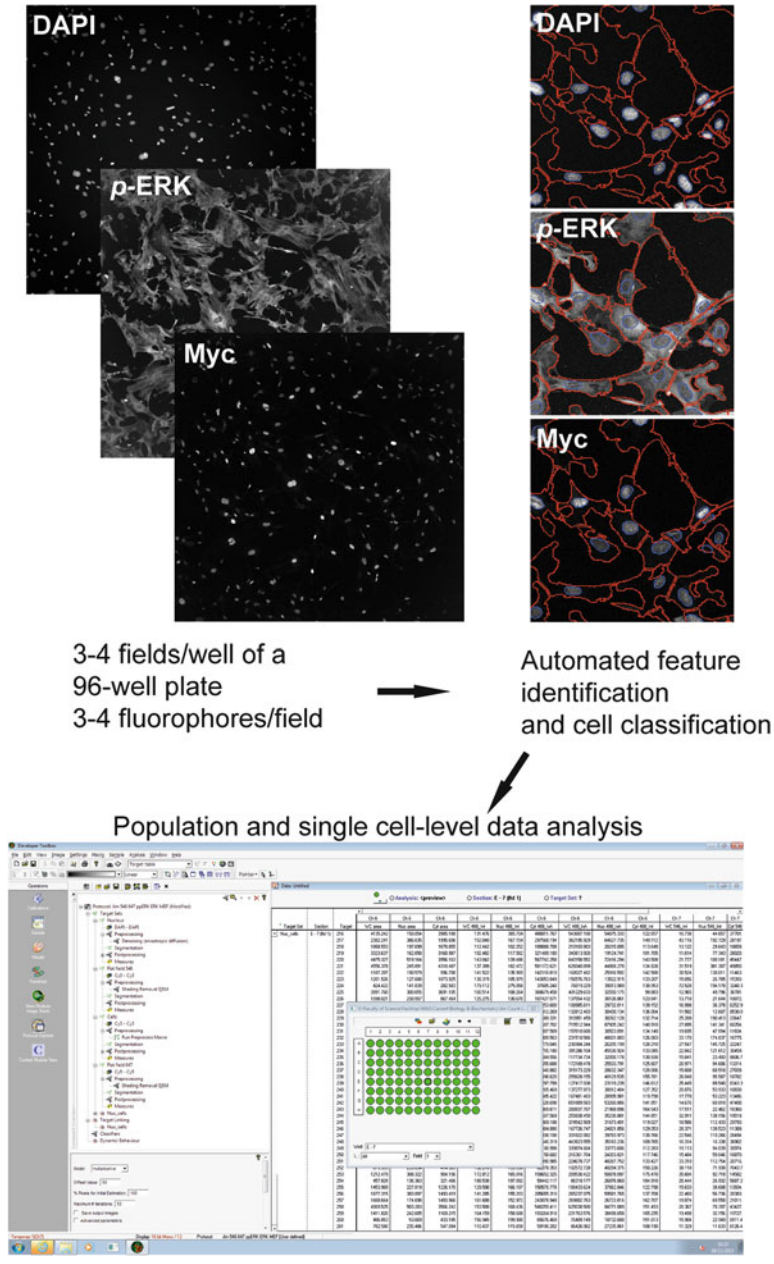

Fig. 1 Image acquisition and analysis workflow using high content microscopy. Mouse embryo fibroblasts were stained with up to three fluorophores (in this case, using DAPI, *p*-ERK, and Myc antibodies, as described in main text) and imaged using a 10 objective at 3–4 fields/well (capturing typically 100–500 cells/field) in 96-well plates using an IN Cell Analyzer 2000 microscope (GE Healthcare). Duplicate, triplicate, or quadruplicate wells per condition were used in individual experiments. Custom analysis algorithms were defined using IN Cell Developer software (GE Healthcare) to capture data related to cell and nuclear area, shape, and stain distribution and intensity. Typically, the DAPI stain was used to define a nuclear mask and *p*-ERK stain was used as a common readout between experiments to define the cell perimeter. Image processing functions were applied to enhance object definition as necessary. Mean, max and sum values per field, per well and per cell were captured and plotted in figures as appropriate

1. Plates must firstly be equilibrated to room temperature prior to imaging. This prevents condensation forming on the bottom of the plate and plate expansion during the run, which affect image consistency and quality.
2. In the microscope software 'acquisition mode' setup, be sure to select the Costar plate type 3904 from the list of options (or alternative if a different culture plate is being used). If the plate is not in the database, then the plate dimensions will need to be added using the 'plate manager' button in the drop-down menu (*see* **Note 7**).
3. Dock the plate into the microscope, using the 'insert/eject plate' button in the toolbar ensuring that well A1 is in the top left-hand corner of the plate-holder tray.
4. Set up an acquisition protocol to capture three fluorescent images per well, selecting excitation filters: 'DAPI' (350 ± 25 nm), 'FITC' (490 ± 10 nm), and 'Cy3' (543 ± 11 nm) and emission filters: 'DAPI' (455 ± 25 nm), 'FITC' (525 ± 10 nm), and 'Cy3'(604 ± 32 nm). Select the 'QUAD1' polychroic mirror and '2-D deconvolution' options. The latter applies an image processing function, which sharpens the images but does not influence the linear dynamic range of the image detection, and does not incur a time penalty. We often use the '2 × 2 binning' function, which pools fluorescence detection from four detectors per pixel (*see* **Note 8**). Set exposure times of 0.1, 0.3, and 0.2 s for DAPI, Alexa 488, and Alexa 546 images, respectively.
5. In the 'focus' window in the wizard, select the 'laser autofocus' (hardware autofocus) option and click the 'auto-offset' button above the list of filters and exposure times. The microscope should automatically find the optimal distance above the plastic–PBS interface of the sample plate at which to capture images with greatest in-focus clarity in the field of view. Problems at this stage normally arise from incorrect plate settings.
6. Move to several different wells by clicking on the plate map image in well areas. Click the 'AF' (autofocus) button next to each filter setting to ensure the autofocus/offset settings give

Fig. 2 (continued) (**b**) Representative images of WT and DUSP5 KO MEFs treated for 1 h with TPA prior to immunostaining for *p*-ERK, ERK, and DAPI. Scale bar = 75 μm. Note that cropped images are only 20 % of the area of a single field of view acquired per well. (**c**) Graphs represent population average normalized fluorescence values for nuclear (Nuc) and cytoplasmic (Cyt) *p*-ERK intensity, or nuclear (Nuc) ERK intensity derived from three separate experiments, each of which contained two to four replicate wells per condition. Data are shown as mean ± SEM, $n = 3$. The data clearly show the increase in nuclear *p*-ERK, which results from deletion of DUSP5, but also reveal the role of DUSP5 as a nuclear anchor for total ERK, with the knockout cells failing to accumulate total ERK in the cell nucleus at later times after stimulation. For further details of these and rescue experiments using adenoviral vectors encoding wild-type and mutant DUSP5 *see* ref. 22

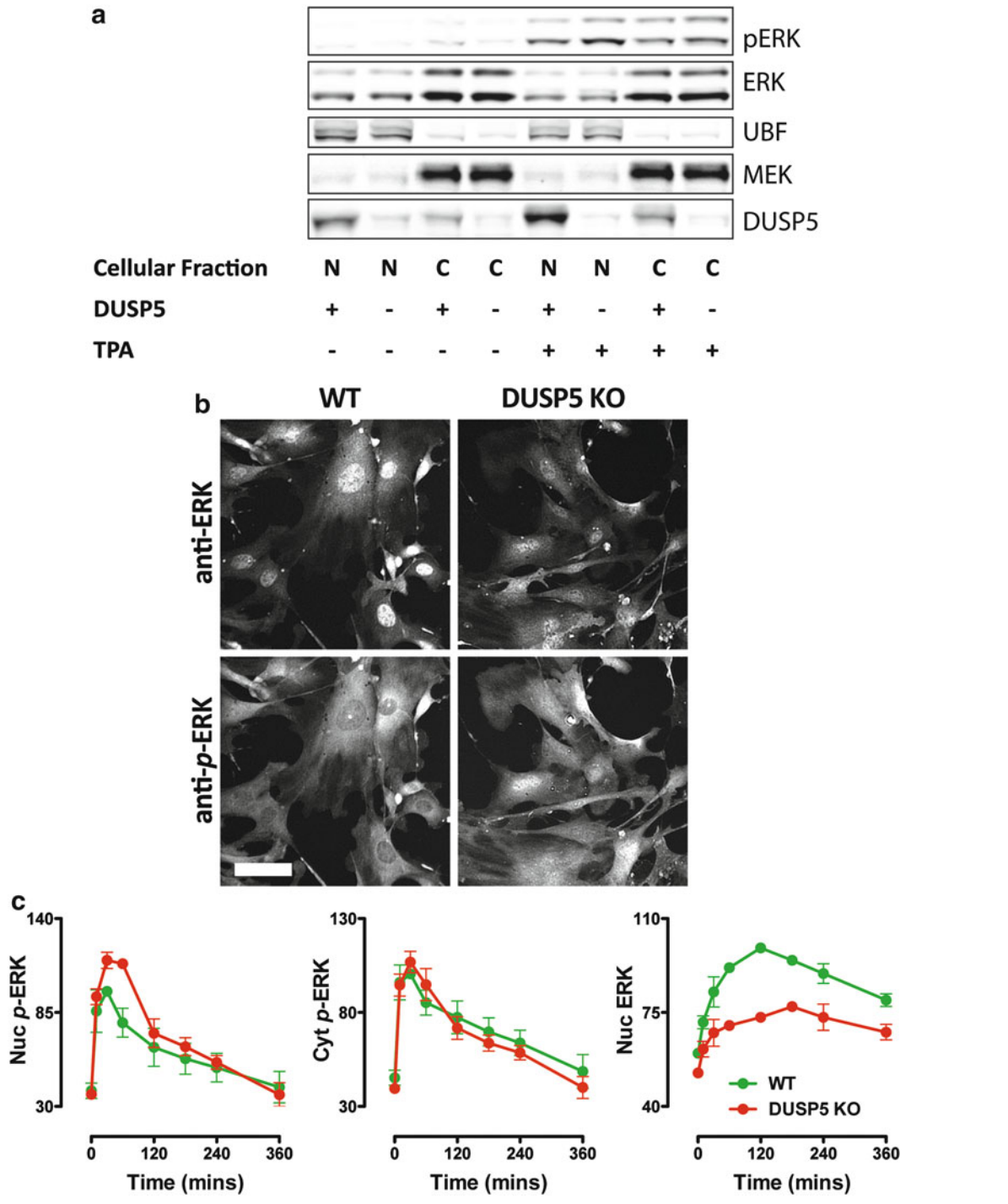

Fig. 2 Comparison of spatiotemporal ERK regulation using cell fractionation and high content microscopy. Primary MEFs derived from wild-type (WT) or DUSP5 knockout (KO) mice were maintained in 10 % FBS prior to stimulation with 100 ng/ml TPA phorbol ester as indicated. (**a**) Wild-type and DUSP5 KO MEFs were lysed and fractionated before analysis by SDS-PAGE and Western blotting using the antibodies indicated. Upstream binding factor (UBF) and MAP kinase kinase (MEK) were used as markers to verify efficient separation intoFig. 2 (continued) nuclear (N) and cytoplasmic (C) fractions respectively. Immunoblotting with antibodies against phosphorylated ERK (*p*-ERK) and total ERK clearly indicates that loss of DUSP5 leads to an increase in nuclear *p*-ERK.

in-focus images in a range of wells in different areas of the plate. Also check the pixel histograms by clicking on the button that looks like an artist's palette to ensure all detectors are acquiring fluorescence values within the dynamic range of the camera. If some pixels are saturated, the exposure time must be reduced. Other options for bright-field acquisition and the order in which wells are acquired are optional. Similarly, if a minimum cell number of required per well, an 'on the fly' cell count may be included based on the DAPI stain to ensure the microscope carries on acquiring images until the number has been achieved.

7. In the field selection button to the right of the plate image, select the number of fields per well to be acquired (usually 2–4 fields of view, giving roughly 500–1000 cells acquired/well).
8. Once the acquisition protocol is set up, it is not usually changed between assays, apart from to redefine the 'auto-offset' at the start of each session.
9. Acquire images by pressing the 'run protocol' button in the toolbar. Specify the file-path for the images (usually a server mapped to the computer) and type in an appropriate name for the experiment. Images will be directly saved to the server.
10. Once images are saved, proceed to image analysis. Note that this does not require the microscope—just a computer with access to the images. Open IN Cell Investigator software (or equivalent, such as 'Cell Profiler'). We use a bespoke analysis protocol for our staining procedure, so we include our settings merely as a guide.
11. Click on the 'View/Analyze Image Stack' button and navigate to image stack using the dialog box.
12. Open the 'Protocol Explorer' window and define the first 'Target set' in a new protocol as 'nuclei', choosing 'DAPI' as the input image (channel 1). Apply a 'Denoising-anisotropic diffusion' Preprocess function to the image to make segmentation of individual nuclei easier, using a 'kernel' size of 3 and a sensitivity of 6. Choose 'Object segmentation' parameters as a kernel size of 13 and a sensitivity of 24. Add a first Post-process function of 'Fill holes' and a second of 'Sieve' with settings of 'keep objects > 13 μm^2'.
13. Create a new 'Target set' called 'Cells'. Set up a 'Preprocess macro', which links the following image transformations and filters, using the *p*-ERK1/2 image (channel 2) as an input, and exporting the output image to channel 6: information equalisation > histogram equalisation > smooth > smooth. This has the effect of slightly blurring the image and enhancing boundary definition between stained cells and background. Choose

'Object segmentation' parameters as a kernel size of 27 and a sensitivity of 75. Add a first Post-process function of 'Sieve' with settings of 'Keep objects > 40 μm²' a second of 'Clump break' based on 'Nuclei' targets to ensure only single cells (one nucleus per cell) are counted, a third of 'Fill holes' and finally 'Border object removal-all borders'.

14. Create 'Target linking-one to one linking' between 'Nuclei' and 'Cells' target sets using 90% overlap of 'Nuclei' within 'Cells' as acceptable, defining the linked objects as 'Nuclei_Cells'.
15. If necessary, apply a flat field correction to acquired images in the Alexa 488 and 546 channels (*p*-ERK1/2 and either ERK1/2 or Myc images, respectively), using 'Shading removal-QSM' and an offset value of 30–50 in multiplicative mode.
16. Define measures (for example, average pixel intensity or cell area) by using the 'Add user defined measure' function by right-clicking in the 'Measures' panel (highlighted when the icon if the same name is selected underneath the 'Nuclei_Cells' icon). Double click the desired measure, then double click the linked 'Nuclei_Cells target path' to link the measure to the relevant objects. Apply statistical functions from the drop-down menu in the 'Measures' panel as necessary (e.g., 'Sum', 'Mean') to summarize population-level data. Ensure that the data is acquired from the relevant source image using the drop-down menu in the 'Measures' panel. For example, any measures relevant to *p*-ERK images must be linked to either the original acquired images in channel 2 or their flat field corrected derivatives.

3.5 Culture, Adenoviral Infection, and Subcellular Fractionation of MEFs for Immunoblot

These procedures are optimized for use with NE-PER nuclear and cytoplasmic extraction reagents (Thermo Scientific) and fluorescent immunoblots imaged on a Li-Cor Odyssey imaging system (LI-COR Biosciences) (*see* **Note 9**).

1. Perform **steps 1–4** of subheading 3.3 scaled up for use in 10 cm tissue culture treated plates. Seed 5×10^5 WT and KO MEFs per 10 cm plate in 10 ml DMEM containing 10% FBS. Infect with the required titre of adenovirus in 5 ml DMEM containing 10% FBS to minimize the amount of virus required.
2. Following the required stimulations remove medium from all cells and wash twice with PBS. Harvest cells by adding 5 ml/plate of trypsin–EDTA mix, and incubate at 37 °C for 5 min. Tap the flask to dislodge the remaining cells, add 10 ml of DMEM containing 10% FBS to quench the trypsin, then centrifuge at $500 \times g$ for 5 min at room temperature. Discard the supernatant and resuspend cells in 1 ml PBS.

3. Transfer the cell suspension to 1.5 ml microcentrifuge tubes and pellet by centrifugation at 500 × *g* for 3 min. Resuspend cells in 100 μl ice-cold CER I buffer (containing Halt protease and phosphatase inhibitors) from the NE-PER nuclear and cytoplasmic extraction reagent kit (Thermo Scientific).
4. Continue to use the NE-PER nuclear and cytoplasmic extraction reagents (Thermo Scientific) to isolate the cytoplasmic and nuclear fractions according to the manufacturer's instructions. Utilize the minimum reagent volumes recommended to obtain concentrated protein samples in the cellular fractions.
5. Perform a Bradford assay on the isolated cellular fractions to determine protein concentrations. The cytoplasmic fraction is usually three to four times more concentrated than the nuclear fraction. Normalize the protein concentrations within the samples and add NuPAGE LDS sample buffer (Thermo Scientific) and boil at 95 °C for 5 min.
6. Resolve equivalent quantities of protein by SDS-PAGE using NuPAGE® Novex® 4–12% gradient 4–12% Bis-Tris protein gels, transfer onto Immobilon-FL PVDF membranes, and block in 5% milk for 30 min at room temperature on a rocking platform.
7. Tip away blocking buffer and wash cells three times for 5 min with PBS–Tween at room temperature.
8. Incubate with the required primary antibodies, diluted in 5% BSA, overnight at 4 °C including:
   (a) Anti-DUSP5 (1:2000) (*see* **Note 4**).
   (b) Anti-pERK (1:1000).
   (c) Anti-ERK (1:1000).
   (d) Anti-MEK (1:1000).
   (e) Anti-UBF (1:1000) (*see* **Note 5**).
9. Retrieve antibody for reuse if required. Wash cells three times for 5 min with PBS–Tween at room temperature.
10. Place in corresponding fluorescent-tagged secondary antibodies, diluted in 5% milk, for 1 h at room temperature on a rocking platform, avoiding exposure to light.
11. Retrieve antibody for reuse if required. Wash cells three times for 5 min with PBS–Tween at room temperature.
12. Scan the membrane utilizing the 680 nm channel on a Li-Cor Odyssey imaging system (LI-COR Biosciences) to visualized reactive bands. Representative results of a fractionation experiment are shown in Fig. 2a.

4 Notes

1. A number of standard methods are available for the isolation and culture of primary MEFs from 12.5 to 13.5 postcoitum (p.c.) mouse embryos. In addition, Pierce now produce a commercial mouse embryonic fibroblast isolation kit (Cat No 88279) which claims to have improved performance over standard trypsin-based tissue digestion in the establishment of MEFs in culture.
2. Low passage HEK293 cells (<20) were obtained from Iowa Gene Transfer Vector Core, to ensure the strong E1A expression necessary for adenoviral propagation. There are quite large differences in HEK293 cell phenotype between different sources, which are likely due to subtle differences in selection pressure between the thousands of labs culturing this immortalized line. Therefore, some HEK293 lines more efficiently generate recombinant virus following co-transfection, while others form better monolayers for cell biological studies. Here, the strongest indicator of their utility as a 'helper' cell line is the expression of the E1A gene.
3. To make up 4% PFA, weigh PFA in a fume cupboard and add to PBS on a stirrer. Add concentrated NaOH dropwise until PFA dissolves, then restore to pH 7.2. Store in aliquots at –20 °C and defrost thoroughly before use.
4. We used an "in house" sheep polyclonal antibody raised against recombinant protein produced in *E. coli* to detect DUSP5 by Western blotting [20]. Commercial antibodies against DUSP5 are available, but are of variable quality. Specificity for DUSP5 should be verified by siRNA knockdown and Western blotting before use. The authors can provide samples of the antiserum used here on request.
5. We used a non-proprietary antibody against upstream binding factor (UBF) as our marker for the nuclear fraction. However, several commercial antibodies are available for this purpose. These include antibodies against lamin A, poly ADP ribose polymerase (PARP), histone deacetylase-2 (HDAC-2) and the transcription factor SP1.
6. All preparation of DNA and digestion, as well as the actual transfections, should be carried out under aseptic conditions in a class II sterile flow cabinet designed for cell culture. All materials and solutions that have been in contact with adenovirus or HEK293 helper cells must be sterilized by immersion in 1% hypochlorite or other peroxygen-based commercial disinfectant, such as 2% Virkon (Fisher Scientific).

7. Plate dimensions are usually available from the plate manufacturer, but an actual measure of plate thickness and skirt height can also be obtained using the 'laser autofocus trace' tool.
8. The '2 × 2 binning' function increases sensitivity and decreases image file size from 8 to 2 Mb but reduces image resolution. We have shown this does not influence the quality of data gathering from cells the size of MEFs acquired using a 10× lens and measuring fluorescence changes in nuclear and cytoplasmic compartments, and actually improves signal–noise ratios.
9. The same outcomes are achievable using a range of commercially available subcellular fractionation kits and reagents and standard (ECL) immunoblotting procedures.

Acknowledgements

Work in the Keyse laboratory is supported by a CR-UK programme grant (C8227/A12053). Work in the Caunt lab is funded by the BBSRC (South West Doctoral Training Partnership) and the Commonwealth Scholarship Commission.

References

1. Marshall CJ (1994) MAP kinase kinase kinase, MAP kinase kinase and MAP kinase. Curr Opin Genet Dev 4:82–89
2. Cobb MH, Hepler JE, Cheng M, Robbins D (1994) The mitogen-activated protein kinases, ERK1 and ERK2. Semin Cancer Biol 5:261–268
3. Shaul YD, Seger R (2007) The MEK/ERK cascade: from signaling specificity to diverse functions. Biochim Biophys Acta 1773: 1213–1226
4. Cowley S, Paterson H, Kemp P, Marshall CJ (1994) Activation of MAP kinase kinase is necessary and sufficient for PC12 differentiation and for transformation of NIH 3T3 cells. Cell 77:841–852
5. Dhillon AS, Hagan S, Rath O, Kolch W (2007) MAP kinase signalling pathways in cancer. Oncogene 26:3279–3290
6. Roberts PJ, Der CJ (2007) Targeting the Raf-MEK-ERK mitogen-activated protein kinase cascade for the treatment of cancer. Oncogene 26:3291–3310
7. Caunt CJ, Sale MJ, Smith PD, Cook SJ (2015) MEK1 and MEK2 inhibitors and cancer therapy: the long and winding road. Nat Rev Cancer 15:577–592
8. Davis RJ (1993) The mitogen-activated protein kinase signal transduction pathway. J Biol Chem 268:14553–14556
9. Carlson SM, Chouinard CR, Labadorf A, Lam CJ, Schmelzle K, Fraenkel E, White FM (2011) Large-scale discovery of ERK2 substrates identifies ERK-mediated transcriptional regulation by ETV3. Sci Signal 4:rs11
10. Marshall CJ (1995) Specificity of receptor tyrosine kinase signaling: transient versus sustained extracellular signal-regulated kinase activation. Cell 80:179–185
11. Plotnikov A, Zehorai E, Procaccia S, Seger R (2011) The MAPK cascades: signaling components, nuclear roles and mechanisms of nuclear translocation. Biochim Biophys Acta 1813:1619–1633
12. Wortzel I, Seger R (2011) The ERK cascade: distinct functions within various subcellular organelles. Genes Cancer 2:195–209
13. Caunt CJ, Keyse SM (2012) Dual-specificity MAP kinase phosphatases (MKPs): shaping the outcome of MAP kinase signalling. FEBS J 280:489–504
14. Groom LA, Sneddon AA, Alessi DR, Dowd S, Keyse SM (1996) Differential regulation of the MAP, SAP and RK/p38 kinases by Pyst1, a novel cytosolic dual-specificity phosphatase. EMBO J 15:3621–3632
15. Muda M, Boschert U, Dickinson R, Martinou JC, Martinou I, Camps M, Schlegel W, Arkinstall S (1996) MKP-3, a novel cytosolic

protein-tyrosine phosphatase that exemplifies a new class of mitogen-activated protein kinase phosphatase. J Biol Chem 271:4319–4326

16. Muda M, Theodosiou A, Gillieron C, Smith A, Chabert C, Camps M, Boschert U, Rodrigues N, Davies K, Ashworth A, Arkinstall S (1998) The mitogen-activated protein kinase phosphatase-3 N-terminal noncatalytic region is responsible for tight substrate binding and enzymatic specificity. J Biol Chem 273:9323–9329
17. Karlsson M, Mathers J, Dickinson RJ, Mandl M, Keyse SM (2004) Both nuclear-cytoplasmic shuttling of the dual specificity phosphatase MKP-3 and its ability to anchor MAP kinase in the cytoplasm are mediated by a conserved nuclear export signal. J Biol Chem 279:41882–41891
18. Ekerot M, Stavridis MP, Delavaine L, Mitchell MP, Staples C, Owens DM, Keenan ID, Dickinson RJ, Storey KG, Keyse SM (2008) Negative-feedback regulation of FGF signalling by DUSP6/MKP-3 is driven by ERK1/2 and mediated by Ets factor binding to a conserved site within the DUSP6/MKP-3 gene promoter. Biochem J 412:287–298
19. Brunet A, Roux D, Lenormand P, Dowd S, Keyse S, Pouysségur J (1999) Nuclear translocation of p42/p44 mitogen-activated protein kinase is required for growth factor-induced gene expression and cell cycle entry. EMBO J 18:664–674
20. Mandl M, Slack DN, Keyse SM (2005) Specific inactivation and nuclear anchoring of extracellular signal-regulated kinase 2 by the inducible dual-specificity protein phosphatase DUSP5. Mol Cell Biol 25:1830–1845
21. Kucharska A, Rushworth LK, Staples C, Morrice NA, Keyse SM (2009) Regulation of the inducible nuclear dual-specificity phosphatase DUSP5 by ERK MAPK. Cell Signal 21:1794–1805
22. Rushworth LK, Kidger AM, Delavaine L, Stewart G, van Schelven S, Davidson J, Bryant CJ, Caddye E, East P, Caunt CJ, Keyse SM (2015) Dual-specificity phosphatase 5 regulates nuclear ERK activity and suppresses skin cancer by inhibiting mutant Harvey-Ras (HRasQ61L)-driven SerpinB2 expression. Proc Natl Acad Sci U S A 111:18267–18272
23. Caunt CJ, Armstrong SP, McArdle CA (2010) Using high-content microscopy to study gonadotrophin-releasing hormone regulation of ERK. Methods Mol Biol 661:507–524
24. Anderson RD, Haskell RE, Xia H, Roessler BJ, Davidson BL (2000) A simple method for the rapid generation of recombinant adenovirus vectors. Gene Ther 2000(7):1034–1038

Chapter 13

In Situ Proximity Ligation Assay (In Situ PLA) to Assess PTP-Protein Interactions

Sina Koch, Irene Helbing, Sylvia-Annette Böhmer, Makoto Hayashi, Lena Claesson-Welsh, Ola Söderberg, and Frank-D. Böhmer

Abstract

Spatiotemporal aspects of protein-tyrosine phosphatase (PTP) activity and interaction partners for many PTPs are elusive. We describe here an elegant and relatively simple method, in situ proximity ligation assay (in situ PLA), which can be used to address these issues. The possibility to detect endogenous unmodified proteins in situ and to visualize individual interactions with spatial resolution is the major advantage of this technique. We provide protocols suitable to monitor association of the transmembrane PTPs PTPRJ/DEP-1/CD148 and PTPRB/VE-PTP with their substrates, the receptor tyrosine kinases FMS-like tyrosine kinase 3 (FLT3/CD135), and Tie2 and vascular endothelial growth factor receptor 2 (VEGFR2), respectively. Detailed description of method development and reagents as well as highlighting of critical factors will enable the reader to apply the method successfully to other PTP-protein interactions.

Key words In situ proximity ligation assay (in situ PLA), Protein-tyrosine phosphatase, Protein interaction, Receptor tyrosine kinase, Signal transduction, Imaging

1 Introduction

Protein-tyrosine phosphatases (PTPs) comprise an enzyme family encoded by approximately 100 genes in the human genome, which regulate cellular signaling by a variety of mechanisms [1]. Notably, many PTPs are specifically dephosphorylating phosphotyrosines on proteins, thereby reversing or modulating the action of protein-tyrosine kinases. Therefore, PTP activities are important in many contexts, such as regulation of growth factor and cytokine signaling [2, 3], and defects in PTP functions have been associated with severe diseases like cancer [4, 5]. Hence, identifying protein interaction partners of PTPs is of outmost importance for understanding PTP functions and potentially for developing treatment strategies. Interacting proteins can be regulatory molecules or substrates or both. In particular, identification of substrates poses technical challenges because their interaction with PTPs is usually

Rafael Pulido (ed.), *Protein Tyrosine Phosphatases: Methods and Protocols*, Methods in Molecular Biology, vol. 1447,
DOI 10.1007/978-1-4939-3746-2_13,

transient thereby precluding simple identification of PTP-substrate complexes by, e.g., immunoprecipitation. The use of PTP-substrate-trapping mutants [6] has been important in partially overcoming this problem and is now an inevitable component in the canon of methods for identifying physiologically relevant substrates [7]. Substrate trapping mutants have been used for assessing PTP complex formation in conjunction with a large number of techniques, such as yeast or mammalian two-hybrid assays [8–10] or visualization methods [11, 12]. Still, substrate trapping mutants are genetically modified, and exogenously expressed proteins, which may not properly reflect the spatiotemporal profile of endogenous PTP interactions.

Visual assessment of the interaction of PTPs with regulators and substrates in situ in cells and tissues provides important functional information. Several techniques for reporting complex formation have been employed for this purpose. These include Förster (fluorescence)-resonance energy transfer (FRET) [11, 13], bioluminescence resonance energy transfer (BRET) [12, 14], and bimolecular fluorescence protein complementation (BiFC) [15]. Also, monitoring alterations in the mobility of fluorescently labeled PTPs, e.g., by fluorescence recovery after photobleaching (FRAP) can be informative with respect to complex formation [16, 17]. While these methods are powerful and can provide valuable and unique information, they have in common that molecules and cells have to be extensively engineered, e.g., by generating fluorescent fusion proteins and transient or stable transfections. Moreover, they usually require laborious and costly microscopy techniques and very experienced users. The possible generation of artifacts is difficult to control and has to be kept in mind.

As an alternative to investigate endogenously interacting proteins, the in situ proximity ligation assay (in situ PLA) has emerged as a powerful technology allowing the detection of individual protein-protein interactions as bright fluorescent spots at the site, where the interaction occurred in situ. Hence, differences in the location and quantity of the interactions are easily accessible and cell-to-cell variations can be analyzed without expensive equipment. This method—which usually is performed within 1–2 days of work—is typically applied to individual fixed cells or tissue sections and does not require molecule or cell engineering. Instead, primary antibodies are used to probe two potentially interacting proteins, e.g., one PTP and its binding protein partner. Either, these two antibodies are directly conjugated to oligonucleotides and in that way converted to proximity probes or two primary antibodies from different species are probed with secondary, species-specific proximity probes—secondary antibodies carrying an oligonucleotide. Upon binding of two probes to the same protein complex, the oligonucleotides are brought into proximity and allow the hybridization of two additional oligonucleotides, these

forming a circular molecule. Subsequently, the circle-forming oligonucleotides are ligated, and a rolling circle amplification (RCA) can be performed, primed from one of the oligonucleotides coupled to the antibodies. Using a polymerase with a strong strand-displacement activity ~1000 concatemeric copies of the circular DNA molecules are created. This concatemer stays attached to the antibodies where it was primed from and collapses into a bundle of DNA. With the help of fluorophore-labeled oligonucleotides, which bind to the concatemer, the protein-protein complex is detected as one bright fluorescent spot at the site, where the antibodies were bound. These signals can be visualized using conventional epifluorescence or a confocal microscope (Fig. 1) and can be counted or spatially evaluated [18, 19].

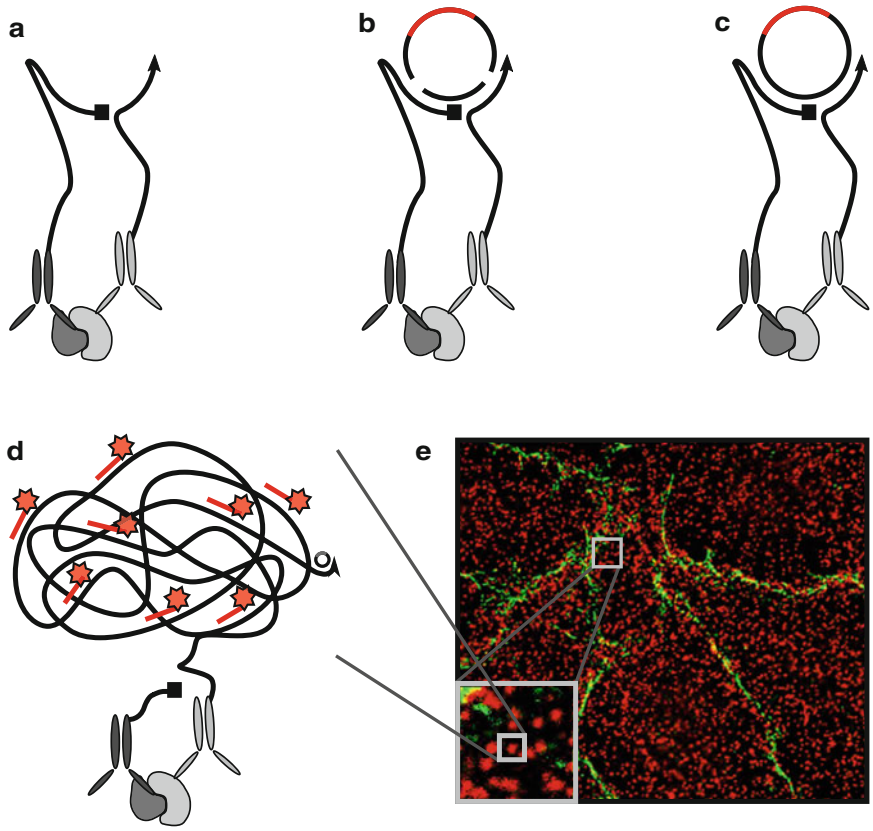

Fig. 1 Schematic presentation of the different steps of the in situ PLA assay. (**a**) Interacting proteins react with specific antibodies from two different species. Corresponding species-specific secondary antibodies coupled to DNA oligonucleotides ("PLA probes") are bound to the primary antibodies. Proximity of the interacting proteins results in proximity of the oligonucleotides. (**b**) By virtue of their proximity, the DNA oligonucleotides can hybridize with two further oligonucleotides, thereby bridging the probes. (**c**) Ligation of the hybridized oligonucleotides creates a closed circular DNA template enabling subsequent "rolling circle amplification (RCA)". (**d**) RCA of the circular DNA in the presence of a hybridizing, fluorescent detection probe causes bright fluorescent signals (RCA products) in places of the cell where complex formation of the two proteins occurred. (**e**) Example of RCA products indicating complex formation of Vascular Endothelial PTP (VE-PTP) in HUVEC cells (see paragraph 3.2 for details)

In situ PLA technology has been successfully applied to detect the interaction of PTPs at endogenous levels with other proteins, notably also with substrates. Examples include the binding of PTP1B/PTPN1 to an interacting protein designated PTPIP51 with yet incompletely understood regulatory relevance [20], association of PTPD1/PTPN21 with the epidermal growth factor receptor (EGFR) promoting EGFR signaling [17], and association of PTEN with the Thr308 phosphorylated form of the protein kinase AKT contributing to the depletion of nuclear pAKT subsequent to stimulation of purinergic receptors [21].

The transmembrane PTPs (RPTPs) DEP-1/PTPRJ and VE-PTP/PTPRB can negatively regulate different receptor tyrosine kinases (RTKs) and have important functions in tumor and vascular biology [5, 10, 22]. By in situ PLA, the association was demonstrated of DEP-1 with FLT3, a hematopoietic RTK frequently mutated in acute myeloid leukemia [23]. VE-PTP was shown to interact with the RTKs VEGFR2 and Tie2, both major regulators of angiogenesis. Notably, VEGFR2 is not directly interacting with VE-PTP, and Tie2 is required for dephosphorylation of VEGFR2 by VE-PTP complex formation [24, 25]. These in situ PLA experiments considerably strengthened the identification of both PTPs as *bona fide* regulators of the interacting RTKs and revealed spatiotemporal features of the PTPs' encounter with their substrates. We will describe and discuss the applied in situ PLA methodology in detail below.

It should be noted that the in situ PLA technology is rapidly developing, thereby potentially providing novel possibilities for the study of PTP-protein interactions despite certain limitations, e.g., the dependence on suitable binders for the proteins of interest. Some of these technical issues shall be briefly highlighted. As other methods like FRET or BRET, in situ PLA is a measure of the distance between two proteins. When a signal is obtained—which means that the distance between the interacting proteins is under a certain threshold—it is interpreted to represent an interaction. By changing the length or polarity of the oligonucleotides, the tolerated distance can be reduced or increased, if required [26]. However, given that the use of secondary antibody probes will permit a distance between the probed epitopes of ~40 nm, a positive reaction does not easily allow distinguishing direct physical interaction of two detected proteins from interactions mediated by further proteins. When studying larger complexes such as the VE-PTP, VEGFR2, and Tie2 complex, conditions allowing detection of more widely distributed epitopes can be an advantage. However, to more strictly assess direct associations, reducing the detected distances is desirable. Using primary conjugates the distance will be reduced to ~25 nm, but even this might be too large. One possibility involves replacement of antibodies with other, considerably smaller molecules, which specifically recognize and bind their

targets in situ, such as aptamers or darpins [27]. In these cases, the distance threshold between the anchoring points of the oligonucleotides of the proximity probes is below 10 nm, in the same range as FRET. Further recent advances in the in situ PLA technology, which may have bearing for PTP interaction studies, involve techniques for increasing the dynamic range [28], reducing the size of the in situ PLA product [29], and for parallel monitoring of multiple protein interactions [30]. Apart from assessing the association of PTPs to regulators and targets, PTP actions in intact cells may potentially be visualized by in situ PLA combining pan- and phosphosite-selective antibodies for monitoring substrate dephosphorylation [19].

2 Materials

2.1 In Situ PLA Detection of DEP-1/PTPRJ Interaction with Its Substrate Protein FLT3 in Hematopoietic Cells

1. Cell lines include: THP-1 cells, cultured in RPMI1640 medium (with 20 mM HEPES) supplemented with 10% heat-inactivated fetal bovine serum (FBS), and 1 mM sodium pyruvate; COS7 cells cultured in DMEM (4.5 g glucose/l) supplemented with 2 mM glutamine, 1 mM sodium pyruvate, 10% FBS; HEK293 cells, cultured in Ham's F12/DMEM 1:1 medium, 10% FBS. As required, media are supplemented with 100 U/ml Penicillin, and 100 μg/ml Streptomycin.
2. FLT3 ligand (FL), human recombinant, dissolved at 100 μg/ml in sterile Milli-Q H_2O, stored in aliquots at −80 °C. FLT3 inhibitor cpd. 102 (Merck-Calbiochem FLT3 inhibitor II, 343021).
3. DEP-1/PTPRJ siRNA DEP-1 duplex of [5′-UACUGUGUCUUGGAAUCUAdGdC-3′ (sense) and 5′-UAGAUUCCAAGACACAGUAdGdG-3′ (antisense)]. Control siRNA [(5′-AATTCTCCGAACGTGTCACGT-3′ (sense), 5′-ACGTGACACGTTCGGAGAATT-3′ (antisense)].
4. Amaxa® Cell Line Nucleofector® Kit V (Lonza, Cologne, Germany), including 4 mm electroporation cuvettes; Amaxa Nucleofector I (Amaxa Biosystems/Lonza, Cologne, Germany).
5. Phosphate-buffered saline (PBS): 8 g NaCl, 0.2 g KCl, 1.44 g Na_2HPO_4, 0.24 g KH_2PO_4 in 1 l H_2O, pH 7.4.
6. Secondary antibodies for immunostainings in pre-testing of antibodies: Goat anti-rabbit-IgG-Cy3, donkey anti-goat-IgG-Cy3, and goat anti-mouse-IgG-Cy3.
7. Coverslips 13 mm, #1 thickness, round, autoclaved before use. Tissue slides.
8. Poly-L-lysine, 250 μg/ml in PBS, filter sterilized.
9. Collagen, 100 μg/ml sterile in PBS.

10. Ethanol, Molecular Biology grade.
11. Wax pen—ImmEdge Pen.
12. Pipet tips connected via flexible plastic tubes to a vacuum driven aspiration apparatus with collection flask (can be self-made).
13. Wet chamber: Drain paper towels with sterile ultrapure water and place in a suitable plastic box with a lid.
14. Anti-FLT3 rabbit polyclonal antibodies (S18, sc-480, Santa Cruz Biotechnology, Heidelberg, Germany); anti-DEP-1 polyclonal goat antibodies (AF1934, R&D Systems, Wiesbaden, Germany).
15. DUOLINK® Kit: Duolink® In situ Orange Starter Kit Goat/Rabbit, DUO92106-1KT (Sigma-Aldrich, Taufkirchen, Germany), containing the following components: Duolink® In situ PLA® Probe Anti-Rabbit MINUS, DUO92005; Duolink® In situ PLA® Probe Anti-Goat PLUS, DUO92003 (The probe sets also include DUOLINK blocking solution and DUOLINK antibody solvent.); Duolink® In situ Detection Reagents Orange, DUO92007; Duolink® In situ Wash Buffers, A and B, DUO82049.
16. Secondary antibody for counterstaining FLT3: FITC-labeled anti-rabbit-IgG.
17. Mounting solutions: Vectashield mounting medium for fluorescence or Immu-Mount.
18. HOECHST 33347 staining dye for nuclei.
19. Nail polish, fast drying.
20. BlobFinder (Version 3.2) can be downloaded at http://www.cb.uu.se/~amin/BlobFinder/index_files/Page430.htm.
21. DNA constructs for expression of hDEP-1 C1239S and hFLT3 in HEK293 and COS7 cells were described previously [31, 32].

2.2 In Situ PLA Detection of VE-PTP/PTPRB Interaction with VEGFR2 or Tie2 in Endothelial Cells

Several of the required materials are listed under Subheading 2.1. The following materials were specifically used only in Subheading 3.2.

1. Human Umbilical Vein Endothelial Cells (HUVECs) were cultured in Endothelial Cell Basal Medium MV2 (EBM2, C-22221, PromoCell, Heidelberg, Germany) with supplemental pack C-39221, containing 5% fetal calf serum (FCS), epidermal growth factor (5 ng/ml), VEGF (0.5 ng/ml), fibroblast growth factor-2 (10 ng/ml), long R3 insulin growth factor-1 (20 ng/ml), hydrocortisone (0.2 µg/ml), and ascorbic acid (1 µg/ml) plus 15% heat-inactivated FCS. Only cells below passage 8 were used for experiments.

2. Murine VEGF164 (450-32, Peprotech Nordic, Stockholm) was dissolved in sterile ultrapure water to obtain a stock concentration of 100 μg/ml and stored in aliquots at −80 °C. COMP-Angiopoietin-1 (COMP-Ang1, kind gift from Gou Young Koh, Daejeon, Republic of Korea) was dissolved in sterile ultrapure water to obtain a stock concentration of 1 mg/ml and stored in aliquots at −80 °C. CompAng1 is a stable variant of Ang1 produced by the Koh lab [33]. The N-terminal portion of Ang1 is replaced with the short coiled-coil domain of cartilage oligomeric matrix protein (COMP), to generate a soluble, stable, and potent Ang1 variant.
3. Stealth RNA duplex oligoribonucleotides against human VE-PTP (HSS108847), human Tie2 (HSS110624), human Tie1 (HSS110625), or control siRNA (12935-300; all from Invitrogen/Life Technologies, Carlsbad, CA, USA).
4. Lipofectamine RNAiMax (Invitrogen/Life Technologies, Carlsbad, CA, USA).
5. Glass bottom 8-well chamber slides.
6. 4% paraformaldehyde (PFA) in PBS.
7. 0.2% Triton X-100 in PBS; 0.1% Tween 20 in PBS.
8. Polyclonal goat anti-human VEGFR2 (AF357, R&D Systems Europe, Ltd., Abingdon, UK) (Epitope: extracellular domain, Ala20-Glu764), polyclonal goat-anti-human Tie2 (AF313, R&D Systems Europe, Ltd., Abingdon, UK) (Epitope: extracellular domain, Ala23-Lys745), polyclonal rabbit anti-human VEPTP (kind gift from Dr. D. Vestweber [34]), and monoclonal rabbit anti-pY1175 VEGFR2 (cat.# 2478, Cell Signaling, Stockholm, Sweden) were used for PLA. The anti-VE-PTP antibody was produced by immunizing rabbits with a synthetic peptide raised against the VE-PTP juxtamembrane domain. The monoclonal mouse anti-human ZO-1 antibody (610966, BD Biosciences, Stockholm, Sweden) was used for immunofluorescence staining of cell-cell junctions.
9. Anti-mouse-IgG-conjugated to Alexa-488.
10. Tris-buffered saline (TBS): 6.05 g Tris-base and 8.76 g NaCl in 1 l H_2O, pH adjusted with HCl to 7.5.

3 Methods

3.1 In Situ PLA Detection of DEP-1/PTPRJ Interaction with Its Substrate Protein FLT3 in Hematopoietic Cells

This protocol describes first a method used for detecting FLT3-DEP-1 interaction in THP-1 cells, a hematopoietic cell line expressing wild-type FLT3 and DEP-1 at easily detectable levels. DEP-1 knockdown enhances FLT3 ligand (FL)-stimulated FLT3 signaling in these cells [35]. FL stimulation increases FLT3-DEP-1 complex formation in a time-dependent manner [23] (Fig. 2).

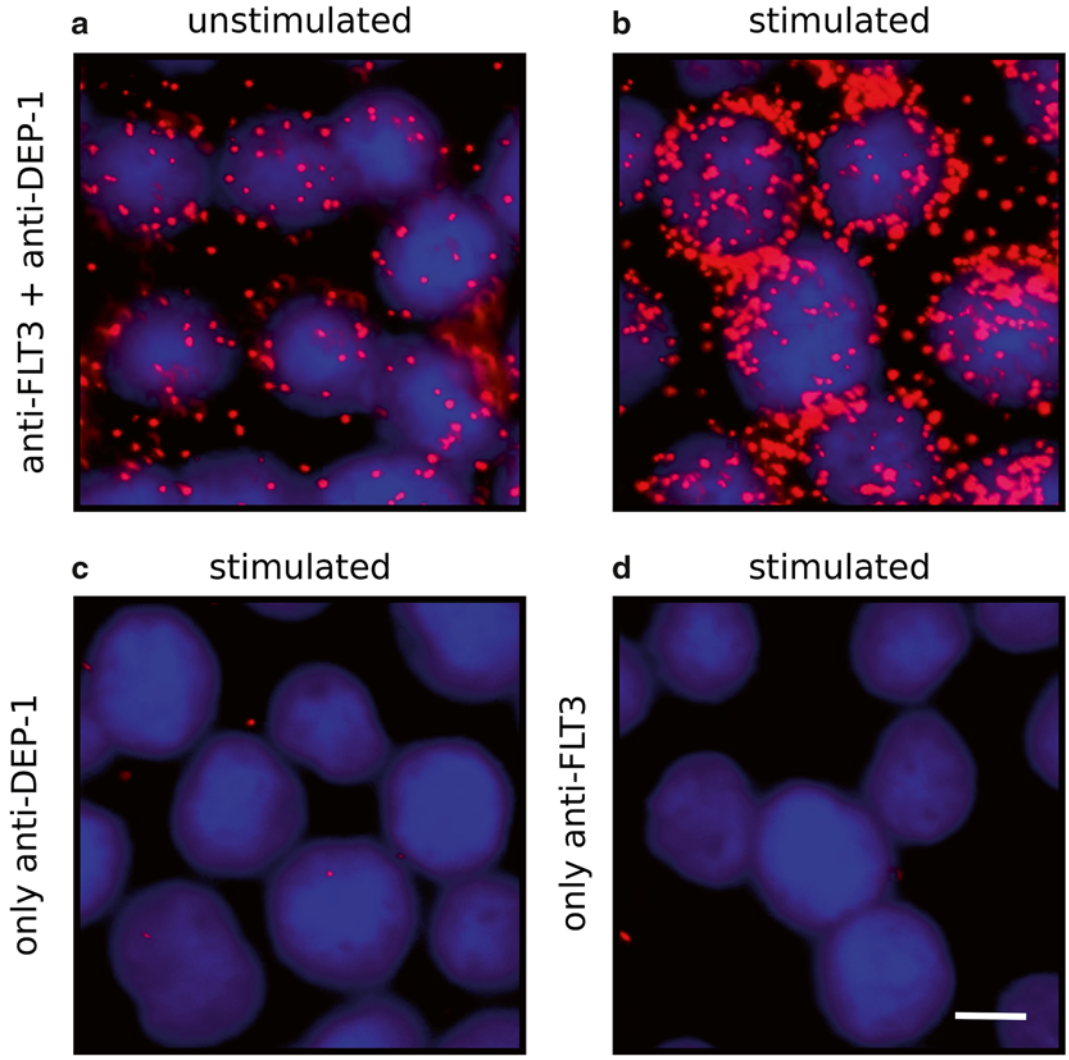

Fig. 2 Formation of DEP-FLT3 complexes in FLT3 ligand-stimulated THP-1 cells visualized by in situ PLA. THP-1 cells, which endogenously express both FLT3 and DEP-1, were starved and left unstimulated (**a**) or were stimulated with 100 ng/ml FLT3 ligand for 20 min (**b**–**d**). Fixed cells were subjected to in situ PLA. (**a** and **b**) Both anti-FLT3 antibody (rabbit) and anti-DEP-1 antibody (goat) were bound to fixed and permeabilized cells before performing the in situ PLA detection. (**c**) Stimulated cells were exposed to anti-DEP-1 antibody only before in situ PLA. (**d**) Stimulated cells were exposed to anti-FLT3 antibody only before in situ PLA. Lack of staining in (**c**) and (**d**) indicates specificity of the in situ PLA detection. (*Red channel*—RCA signals; *blue channel*—HOECHST 33347 staining of nuclei; scale bar 5 μm)

For establishment of the in situ PLA protocol, different variables were tested (*see* **Note 1**). Control experiments using siRNA for DEP-1 and transient transfections in COS7 cells and HEK293 cells were also performed. Finally, inhibition of FLT3 kinase activity abrogated the association. Since this type of controls is of general applicability, these experiments are likewise described below.

1. Standard or FLT3 inhibitor pre-treatment (*see* **Note 2**): Sediment $3–4 \times 10^6$ well-proliferating THP-1 cells ($500 \times g$, 5 min), wash cells once with serum-free RPMI1640 medium, and resuspend for starvation in serum-free RPMI1640 medium containing 0.2% fatty acid-free BSA at a density of $3–4 \times 10^5$ cells/ml. Starve for 5–7 h at 37 °C, 5% CO_2. In case of treatment with FLT3 kinase inhibitor, add compound at desired final concentration from 500-fold stock in DMSO (e.g., 1 mM cpd.102 resulting in 2 μM final concentration).
2. siRNA transfection before in situ PLA (optional, *see* **Note 3**): Sediment $1.5–2 \times 10^6$ well-proliferating THP-1 cells and resuspend in 100 μl AMAXA nucleofection solution V. Add 8 μl 20 μM siRNA solution (2.1 μg; DEP-1 siRNA or control siRNA), transfer in the (4 mm) electroporation cuvette, and pulse with the program V-01. Add immediately 0.5 ml complete cell culture medium. Disperse all cell clumps by repeated pipetting up and down, without foaming, to get a homogenous cell suspension and transfer the suspension into a well of a 6-well plate containing 2 ml complete medium, supplemented with Penicillin/Streptomycin. Add 1.5–2 ml fresh medium the next day. After 2 days, prepare cells for analysis.
3. Cell plating: Place coverslips in wells of a 12-well plate and add poly-L-lysine to each coverslip. 150 μl is sufficient for covering the surface of 13 mm (ID) coverslips; the volume may need adjustment for larger areas (*see* **Note 4**). Incubate at room temperature for at least 1 h (or longer, e.g., over the cell starvation period). Wash wells twice with PBS. Sediment the starved cells and resuspend at a concentration of $1–2 \times 10^5$ cells in 120 μl serum-free medium. Add 120 μl of this solution per well to the coated coverslips and allow adhesion of the cells at room temperature for 10 min. Aspirate nonadhered cells and medium, and add 1.0 ml fresh serum-free medium per well (add FLT3 inhibitor again at this stage, if required).
4. Ligand stimulation (*see* **Note 5**): Dilute FLT3 ligand (FL) in serum-free RPMI1640 medium to 10 μg/ml (e.g., 13 μl 100 μg/ml stock plus 117 μl medium for stimulation of 12 wells). Label plate from bottom according to the different conditions, such as different ligand stimulation time points and unstimulated controls. Add 10 μl diluted ligand per well (final concentration 100 ng/ml) for FL stimulation, starting with the sample with the longest incubation time (30 min), subsequently the shorter incubation times (after 10, 20, 25, and 27.5 min for incubation of 20, 10, 5, and 2.5 min, respectively) and place plate in the 37 °C, 5% CO_2 incubator between additions. After 30 min, aspirate medium and wash once with 1 ml ice-cold PBS, then place plate on ice.

5. For cell fixation (*see* **Notes 1** and **6**), add 1 ml ice-cold 70% ethanol to each well and incubate on ice for 1 h. Aspirate the ethanol and allow the plate to air-dry at room temperature for 30 min. Store plate at 4 °C (*see* **Note 7**) or proceed directly to in situ PLA.
6. In situ PLA staining procedure: All treatments are performed with the fixed cells on coverslips in the 12-well plate. Make a ring around the cell layer with a wax pen and let dry for approximately 15 min until the ring is completely dry. Wash the fixed cells once with 1 ml PBS. From now on the slides must not dry as this will lead to unspecific signals! To prevent drying of cells, liquids are removed from the cells with a pipet tip connected via a flexible tube to a vacuum driven pump (in one hand) and fresh liquid is immediately added with a pipet (in the other hand).
7. Blocking: Add one drop of DUOLINK blocking solution (*see* **Note 8**), incubate in a wet chamber at 37 °C for 90 min.
8. Primary antibody incubation (*see* **Note 9**): Dilute the primary antibodies 1:50 in the DUOLINK-antibody-solvent. Anti-FLT3 (S18, rabbit), and anti-DEP1 (AF1934, goat), 1 µl of each antibody per sample combined (*see* **Note 1**) in 48 µl solvent. Put the 50 µl diluted antibodies on each coverslip, incubate at 4 °C in a wet chamber overnight. Wash coverslips two times with DUOLINK wash buffer A (5 min incubation in each washing step).
9. Secondary antibody-probe (*see* **Note 10**) incubation: For one sample, mix 8 µl anti-rabbit PLA "PLUS" probe and 8 µl anti-goat PLA "MINUS" probe with 24 µl DUOLINK antibody diluent. Put 40 µl on each coverslip, incubate at 37 °C in the wet chamber for 1 h. Wash coverslips two times with DUOLINK wash buffer A (5 min incubation in each washing step).
10. Ligation: Per sample, mix 31 µl H_2O, 8 µl DUOLINK-5× ligation buffer, plus 1 µl ligase. Add 40 µl of ligation mix to each coverslip and incubate at 37 °C for 30 min. Wash coverslips two times with DUOLINK wash buffer A (2 min incubation in each washing step).
11. Amplification and detection: For one sample, mix 31.5 µl H_2O, 8 µl 5× DUOLINK amplification buffer, and 0.5 µl polymerase. Add 40 µl of amplification mix to each coverslip and incubate at 37 °C for 100 min. Wash coverslips two times with DUOLINK wash buffer B (10 min incubation in each washing step). Wash coverslips once with DUOLINK wash buffer B, diluted 1:10 with H_2O (10 min incubation in the washing step).
12. Mounting: Pipet 6 µl mounting solution containing 1 µg/ml HOECHST 33347 (*see* **Note 11**) on a microscope slide. Remove

the coverslip from the 12-well plate (use injection needle and forceps for lifting) and put it on the drop of mounting solution with the cell layer downwards facing the slide. Fix the coverslip with three to four drops nail polish around the edges.

13. Microscopic imaging: For each experiment, acquire five to ten images per condition of cell treatment using identical microscope and camera settings (*see* **Note 12**). As a possible microscope configuration, an APOPTOME II Zeiss Imager Z1 microscope (Carl Zeiss Microimaging, Jena, Germany), and a Plan Apochromat 40×/1.3 oil (DIC/UV VIS-IR M27) objective, or an AXIOVERT 200 M microscope (Carl Zeiss Microimaging, Jena, Germany) with an EC Plan Neofluar 40×/1.3 oil (DIC, M27) may be used, equipped with an AXIOCAM AutoCam MR Rev3 camera and Axiovision software (release 4.8.2). For each image, acquire signals sequentially in the red (e.g., excitation 540–550 nm, emission 570–580 nm) and blue (e.g., excitation 359, emission 461) fluorescence channel (for the RCP and Hoechst staining, respectively). Optionally, signals in additional channels may be recorded (e.g., to monitor cellular expression and distribution of the analyzed PTP and/or its interaction partner, or to obtain a reference for cell structures).
14. Quantification: Use TIF files generated in the red and blue fluorescent channel for quantification of the number of rolling circle amplification products (RCP) per cell using BlobFinder (Version 3.2) (*see* **Note 13**) with the following settings: 3×3 pixel mask for RCPs, detection of nuclei with minimum diameter of 100 pixels. Count all RCP signals in each individual image and divide this number by the number of nuclei to obtain an average of signals per cell. Generate means and standard deviations of the independently acquired images for each condition.
15. Control experiments with transiently transfected cells: These experiments provided qualitative data for FLT3-DEP-1 interaction, and allowed controls by performing in situ PLA with cells lacking overexpression of one potential interaction partner or of both (Fig. 3). A substrate trapping variant of hDEP-1 (C1239S) was used to enhance interactions. Counterstaining of FLT3 was also employed in some cases to score transfected cells (Fig. 4, *see* **Note 14**). Place coverslips in a 12-well plate and incubate with a solution of collagen (100 µg/ml in PBS, sterile) at room temperature for 2 h. Wash two times with PBS. Seed $1.2–1.5 \times 10^5$ HEK293 cells or 2.5×10^4 COS7 cells per well in 1 ml medium. Perform transient transfection, e.g., with the polyethylenimine (PEI) method [36], with expression plasmids for hDEP-1 C1239S, and hFLT3 (in pcDNA3.1) using a total amount of 2 µg DNA per well. Allow expression for 24 h, then,

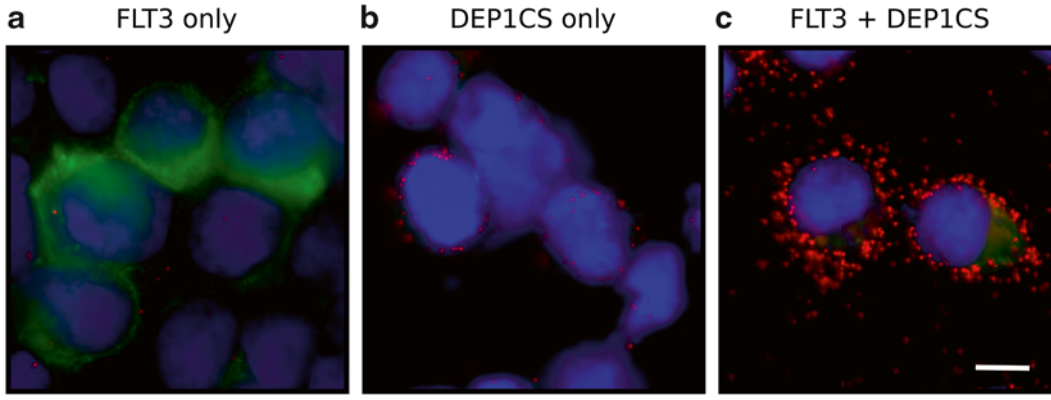

Fig. 3 Control experiments for in situ PLA using transfection of only one or both interaction partners (DEP-1, FLT3) in HEK293 cells. HEK293 cells were transiently transfected with expression constructs for human FLT3 or the C1239S "trapping" variant of human DEP-1, or both as indicated. Incubation with antibodies against both proteins and subsequent in situ PLA were carried out. Additionally, FLT3 (decorated with a rabbit antibody) was visualized by staining with FITC-labeled anti-rabbit-IgG (*green*). Note that a pronounced in situ PLA (*red*) occurs only in cells expressing both FLT3 and DEP-1C1239S. (Scale bar 5 μm)

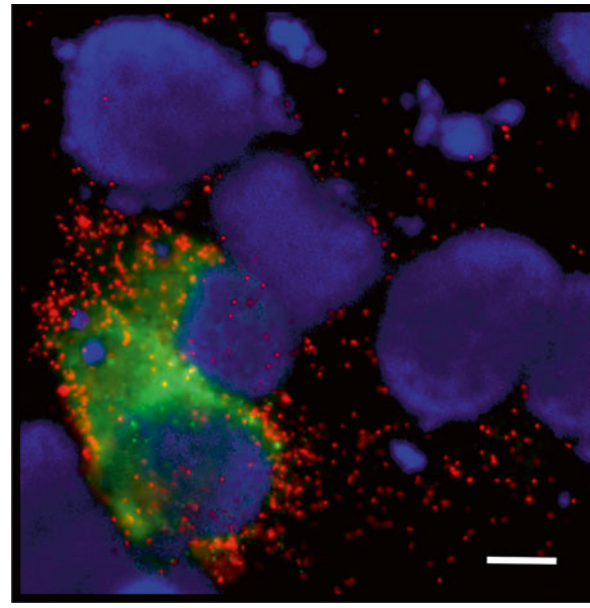

Fig. 4 Specificity of in situ PLA signals in transfected COS7 cells. COS7 cells were transiently co-transfected with expression constructs for human FLT3 and human DEP-1. Incubation with antibodies against both proteins and subsequent in situ PLA were carried out. Additionally, FLT3 (decorated with a rabbit antibody) was visualized by staining with FITC-labeled anti-rabbit-IgG (*green*). Note that a pronounced in situ PLA (*red*) occurs only in transfected cells, which are labeled *green* for FLT3 expression. (Scale bar 5 μm)

after washing with 1 ml ice-cold PBS, subject samples to fixation with 70% ethanol and perform in situ PLA as described in **steps 6–11**. Counterstain coverslips with FITC-labeled anti-rabbit-IgG to visualize FLT3: Dilute antibody 1:600 in 1.5% BSA in PBS. Add 50 µl per coverslip and incubate in the dark for 1 h in a wet chamber. Wash three times with PBS, then once with Milli-Q H_2O, then proceed to mounting (*see* **step 12**).

3.2 In Situ PLA Detection of VE-PTP/PTPRB Interaction with VEGFR2 or Tie2 in Endothelial Cells

The following protocol describes the detection of the interaction of endothelium-specific vascular endothelial-phosphotyrosine phosphatase (VE-PTP) with the RTKs VEGFR2 or Tie2 in Human Umbilical Vein Endothelial cells (HUVEC), a human endothelial cell line endogenously expressing these three molecules at easily detectable levels. VE-PTP, VEGFR2, and Tie2 form a trimeric complex. VEGF, the ligand for VEGFR2, induces activation of VEGFR2 and dissociation from VE-PTP, enabling VEGFR2 signaling in tip cells of the vessel sprout. In contrast, in stalk cells, where Ang1, the ligand for Tie2, is additionally present, the trimeric complex is translocated to cell junctions, where VE-PTP dephosphorylates both activated RTKs (Fig. 5). The repression of RTK signaling at junctions is crucial for the maintenance of vascular quiescence. VE-PTP knockdown abolishes RTK silencing in junctions resulting in excess RTK signaling and loss of polarization of endothelial cells (EC) and of lumen formation [25].

For the establishment of the in situ PLA protocol, different variables were tested (*see* **Note 1**). Control experiments using none or only one of the two primary antibodies as well as VE-PTP knockdown were also performed. Since this type of controls is of general applicability, these experiments are included below. The protocol is suitable to visualize association of VE-PTP and VEGFR2 (see examples in [24, 25]) as well as VE-PTP and Tie2 (Fig. 5).

1. Ligand stimulation of cells: HUVECs are seeded (50,000 cells per cm^2) in glass bottom 8-well chamber slides and cultivated until confluent. They are then starved in MV2 medium with 1% FCS and without growth factor supplements for 2 h. Starved HUVECs are treated with 200 ng/ml COMP-Ang1 for 30 min, or with 20 ng/ml murine VEGF164 for 5 min. Alternatively, HUVECs are incubated with 200 ng/ml COMP-Ang1 for 30 min followed by addition of 20 ng/ml murine VEGF164 for 5 min.
2. Fixation of cells: HUVECs are fixed with 4% PFA for 10 min at room temperature, and subsequently permeabilized with 0.2% Triton X-100 in PBS for 5 min at room temperature (*see* **Note 6**). After several washes with PBS containing 0.1% Tween 20, the polystyrene vessels of the 8-well chamber slides are removed with the included removal tool. Be careful to never let the cells dry out during this procedure and at all later steps.

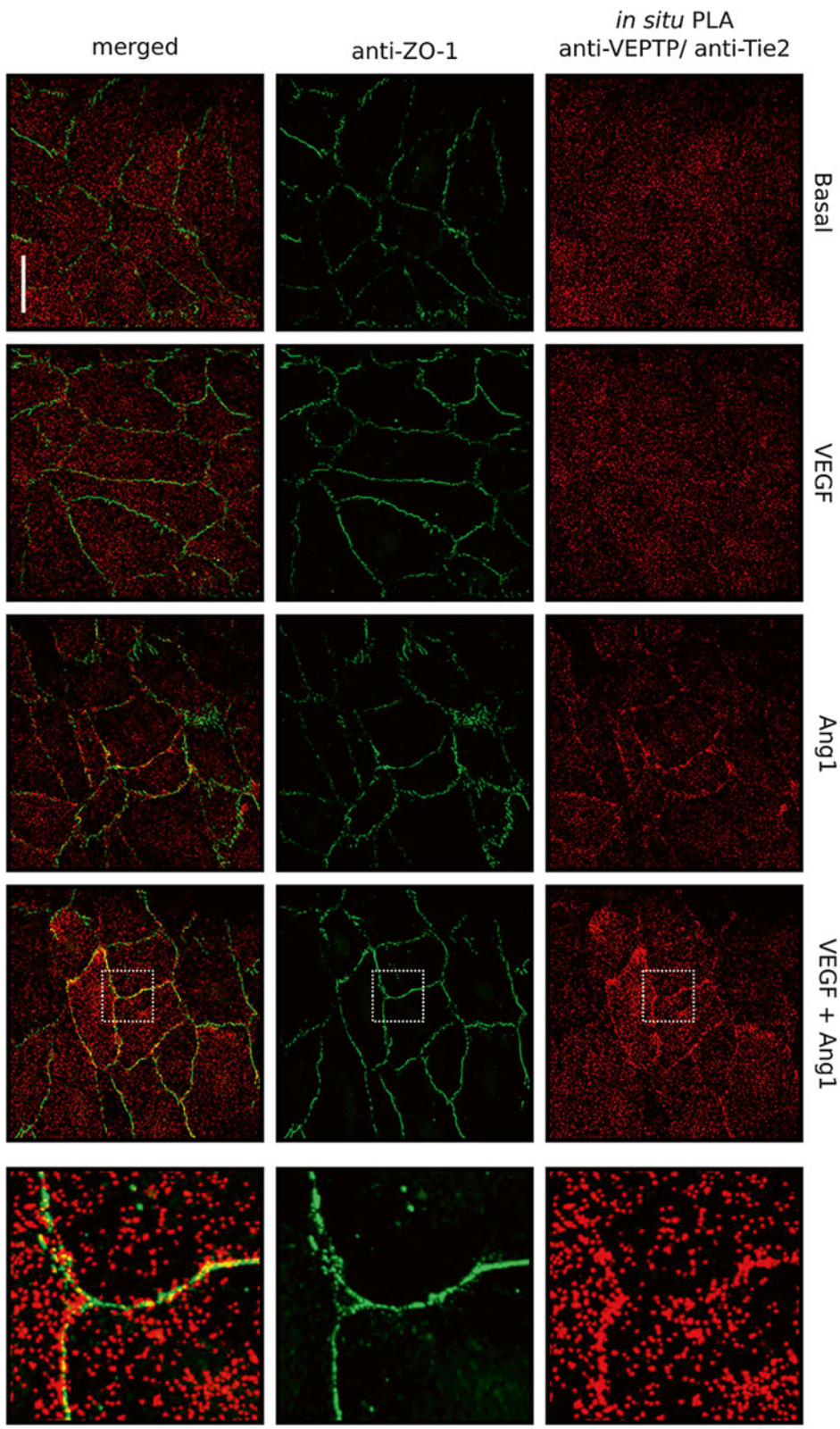

Fig. 5 Angiopoietin 1-mediated translocation of constitutive VE-PTP/Tie2 complexes to junctions of HUVEC cells visualized by in situ PLA. HUVECs were stimulated with VEGF and Angiopoietin 1 (Ang1) individually or in combination or left untreated (basal), followed by in situ PLA to detect VE-PTP/Tie2 complexes (*red dots*)

3. In situ PLA staining procedure: All following treatments are performed with the fixed cells on 8-well chamber slides (without the removable polystyrene vessel and in the wet chamber, *see* **Note 15**). Liquids are removed from the cells with a pipet tip connected via a flexible tube to a vacuum driven pump (in one hand) and fresh liquid is immediately added with a pipet (in the other hand) to prevent drying of cells.
4. Blocking: Add one drop of DUOLINK blocking solution per well of the 8-well slide, incubate in a wet chamber at 37 °C for 90 min.
5. Primary antibody incubation: Dilute the primary antibodies in the DUOLINK-antibody-solvent (amounts for one well): Anti-Tie2 (goat), 1 μl, anti-VE-PTP (rabbit), 1 μl and anti-ZO1 (mouse), 0.25 μl combined (*see* **Note 1**) in 47.75 μl solvent. Alternatively, dilute anti-VEGFR2 (goat), 1 μl, anti-VE-PTP (rabbit), 1 μl and anti-ZO1 (mouse), 0.25 μl combined (*see* **Note 1**) in 47.75 μl solvent. Put 50 μl diluted antibodies per well (*see* **Note 16**), incubate at 4 °C in the wet chamber overnight. Wash 8-well slides twice with DUOLINK wash buffer A (5 min incubation in each washing step) (*see* **Note 17**).
6. Secondary antibody-probe (*see* **Note 10**) incubation: For one sample, mix 8 μl anti-rabbit PLA "PLUS" probe and 8 μl anti-goat PLA "MINUS" probe with 24 μl DUOLINK antibody diluent. Put 40 μl on each well of the 8-well slide, incubate at 37 °C in a wet chamber for 1 h. Wash 8-well slides twice with DUOLINK wash buffer A (5 min incubation in each washing step).
7. Ligation: Per sample, mix 31 μl H_2O, 8 μl DUOLINK 5× ligation buffer, plus 1 μl ligase. Add 40 μl of ligation mix per well and incubate at 37 °C for 30 min. Wash 8-well slides twice with DUOLINK wash buffer A (2 min incubation in each washing step).
8. Amplification and detection: Per well, mix 31.4 μl H_2O, 0.3 μl anti-mouse IgG-conjugated Alexa-488 (1:100, to detect anti-ZO1), 8 μl 5× DUOLINK amplification buffer, and 0.6 μl polymerase. Add 40 μl of amplification mix to each 8-well slide and incubate at 37 °C for 100 min. Wash 8-well slides twice

Fig. 5 (continued) and stained for Zona occludens 1 (ZO1; *green*) to visualize cell-cell junctions. Scale bar 10 μm. High magnification *insets* show PLA products at junctions. It is known that Tie2 accumulates at cell-cell contacts in response to Ang1 [41]. Moreover, as shown here, VE-PTP/Tie2 complexes are constitutive and evenly distributed within cells under basal conditions, but translocate to cell-cell junctions upon Ang1 stimulation. VEGF stimulation also slightly contributed to this translocation. Together with results shown in Hayashi et al. [25], this shows that the three components (VE-PTP, Tie2 and VEGFR2) communicate to balance vascular quiescence preferentially at cell-cell junctions

with DUOLINK wash buffer B (10 min incubation in each washing step). Include 0.1 μg/ml HOECHST 33347 (*see* **Note 11**) in the second washing step. Wash 8-well slides once with DUOLINK wash buffer B, diluted 1:10 with H_2O (10 min incubation in the washing step). This washing step can also be done with TBS.

9. Mounting: Pipet approximately 50–100 μl Vectashield mounting solution as a line over the rectangular coverslip. Starting from one side, lay the coverslip slowly down on the 8-well chamber slide, so that the mounting medium is covering the cells without air bubbles.
10. Microscopic imaging: Analysis can be done with a Nikon Eclipse E1000 microscope (Nikon) with a Hamamatsu Digital Camera C10600 (Hamamatsu), or a LSM 510 Meta or a LSM 700 confocal microscope (Carl Zeiss, Oberkochen, Germany). A used configuration of the Zeiss LSM700 comprised a Plan Apo 63× NA 1.4 oil objective, 488 nm excitation at 30%, emission range 505–530, pinhole size 190 μm, and 555 nm excitation at 30%, emission range 566–615, with pinhole size 216 μm. A z-stack of six images was scanned with line scanning (scanning speed 4), *z*-steps of 698 nm, and pixel size 95×95 nm.
11. Control experiments: These experiments enable qualitative evaluation of the technique by performing in situ PLA on cells with knocked down expression of one potential interaction partner (VE-PTP, biological control) or by omitting one or both of the primary antibodies (technical controls). *Biological controls:* Seed cells in 8-well chamber slides as described under **step 1**. Perform transient transfection with Lipofectamine RNAiMax according to the manufacturer's recommendations, using VE-PTP siRNA, Tie2 siRNA, Tie1 siRNA, or control siRNA with a total amount of 3 pMol siRNA per well. Change culture medium 6 h after transfection and culture cells for 24 h, then subject samples to fixation with 4% PFA and perform in situ PLA as described in **steps 3–9**. *Technical controls*: Perform in situ PLA as described in **steps 3–9**, but omit either the anti-VE-PTP antibody or the anti-Tie2 antibody or both primary antibodies (Example results can be found in [25]).
12. Counterstain 8-well slides with anti-ZO1 and anti-mouse IgG conjugated to Alexa488 to visualize cell-cell junctions as described in **step 5**.

4 Notes

1. A generic strategy for establishing an in situ PLA assay using suitable controls is depicted in Fig. 6. Some important aspects shall be outlined:

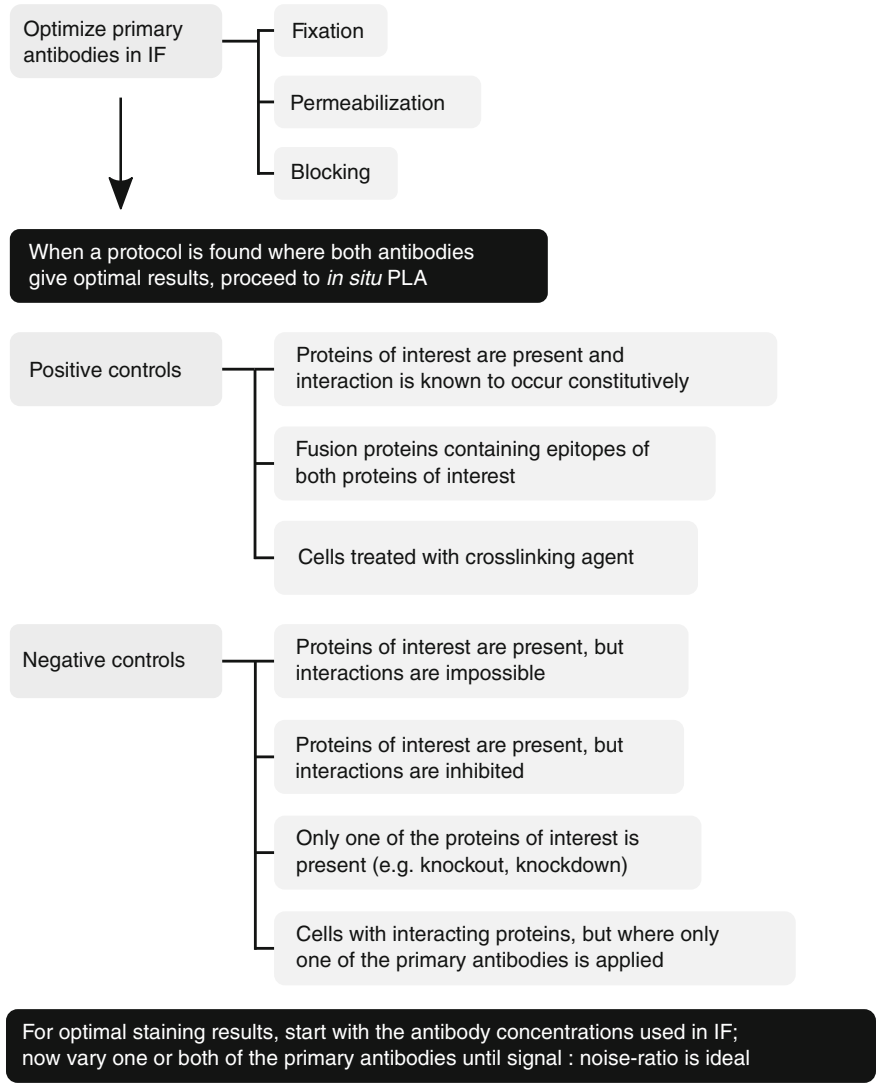

Fig. 6 Schematic presentation of a generic strategy for establishing an in situ PLA assay. The strategy comprises initial experiments to establish selective immunofluorescence protocols working with antibodies against both interaction partners. In subsequent in situ PLA experiments, several types of controls can be employed to ensure that in situ PLA signals are selective. Finally, optimization of signal-to-noise will be achieved by titrating antibodies once more. The individual steps are discussed in detail in the text

Antibodies used as primary binders should be pre-tested using conventional immunostaining protocols. Optimization should be guided by staining patterns reflecting the correct localization with high intensity and low background and should include the check of different fixation methods (e.g., ethanol, acetone, paraformaldehyde), permeabilization conditions (e.g., Triton X-100, ethanol, methanol), and of different blocking (e.g., respective normal sera, BSA, milk). Also time and temperature for incubation may be varied.

For the immunostainings, always include controls without primary antibodies. Further useful controls may involve cells which do not express the antigen (e.g., cells from mice with knockout of the gene encoding the antigen), or cells treated appropriately to provoke known alterations in antigen levels. Note that for in situ PLA both primary antibodies have to work under the same conditions!

If you can chose freely whether the epitopes for detecting the interaction are on the inside or outside of the cell, choosing the outside will make it possible to omit the cell permeabilization. However, then only proteins outside the cells are detected, e.g., internalized proteins will not be stained. If the antibodies recognize epitopes that are located on either side of the cell membrane (i.e., intra- and extracellular), then in the in situ PLA all oligonucleotides have to cross the membrane and ligate over it. Although this is not impossible [37] setting up an in situ PLA assay of this format will decrease the efficiency. Also, the assay will be very sensitive to minor changes in the fixation/permeabilization protocol.

For in situ PLA assays, again technical controls omitting both or only one primary antibody should be done. An example for a negative control is, e.g., a cell, where the interaction that should be detected is not induced by stimulation (Fig. 6). To optimize the signal-to-noise ratio, run experiments, where one antibody concentration is held constant, while the other antibody is decreased in concentration and vice versa. If no interaction can be detected at all, it should always be considered that the interaction may potentially block the antibody binding sites. To control, that the assay procedure as such is working correctly, two antibodies from two different species against two epitopes on the same protein may be used as this detection is not dependent on proximity.

Antibodies may suffer batch-to-batch and vendor-to-vendor variations. Especially polyclonal antibodies are prone to variations between batches and it might be required to validate each batch again. Care should also be taken, when storing antibodies: If they are stored at −20 °C, the storage buffer should contain glycerol to prevent them from freezing. Otherwise, aliquot the antibodies, freeze them only once, and store them at 4 °C after thawing. Aliquoting is also recommended when storing antibodies at 4 °C. Here addition of anti-bacterial agents, like sodium azide, is required to prevent bacterial growth in the antibody solution.

2. Kinase inhibition was used to demonstrate that DEP-1-FLT3 association depends on FLT3 kinase activity (Fig. 7). Inhibition of upstream kinases may also be used as a general tool to demonstrate specificity for PTP-substrate interactions.

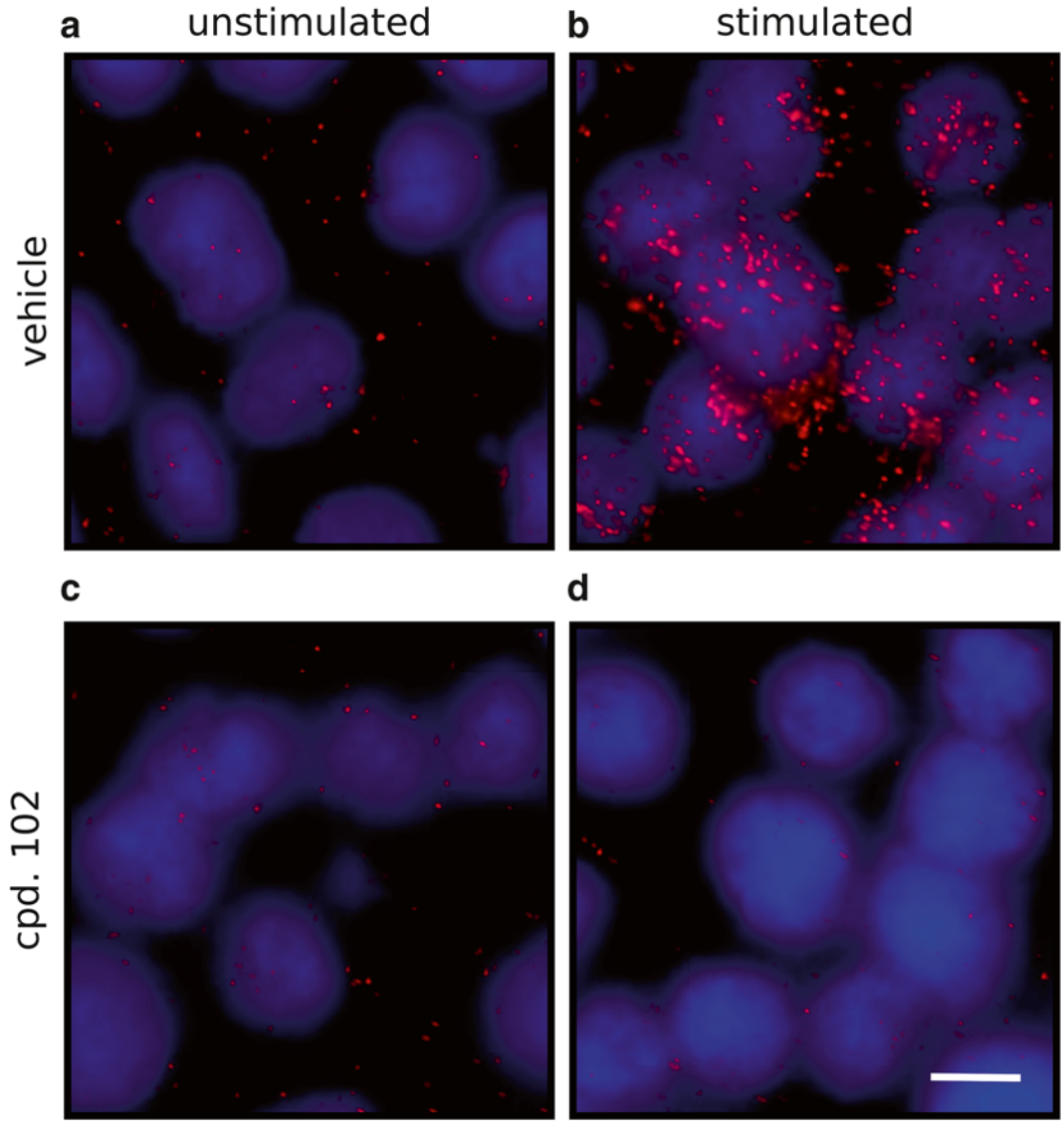

Fig. 7 Inhibition of FLT3 tyrosine kinase activity abrogates complex formation with DEP-1 PTP. FLT3 ligand-stimulated complex formation of DEP-1 and FLT3 in THP-1 cells was detected as described in Fig. 1 except that cells in (**c**) and (**d**) were pre-incubated with the FLT3 kinase inhibitor cpd.102 (2 μM). Cells in (**a**) and (**b**) were only pre-treated with vehicle (0.2 % DMSO). (Scale bar 10 μm)

3. In addition to controls described under **Note 1**, siRNA-mediated knockdown of one of the interaction partners can serve as control (Fig. 8). This may already be considered for establishing the immunostaining conditions. Since knockdowns are never complete, attenuation but not complete abolishment of the immunostaining/in situ PLA signal is expected.
4. Poly-L-lysine pre-coating of the coverslips was necessary to immobilize the THP-1 cells used in this study, which grow in

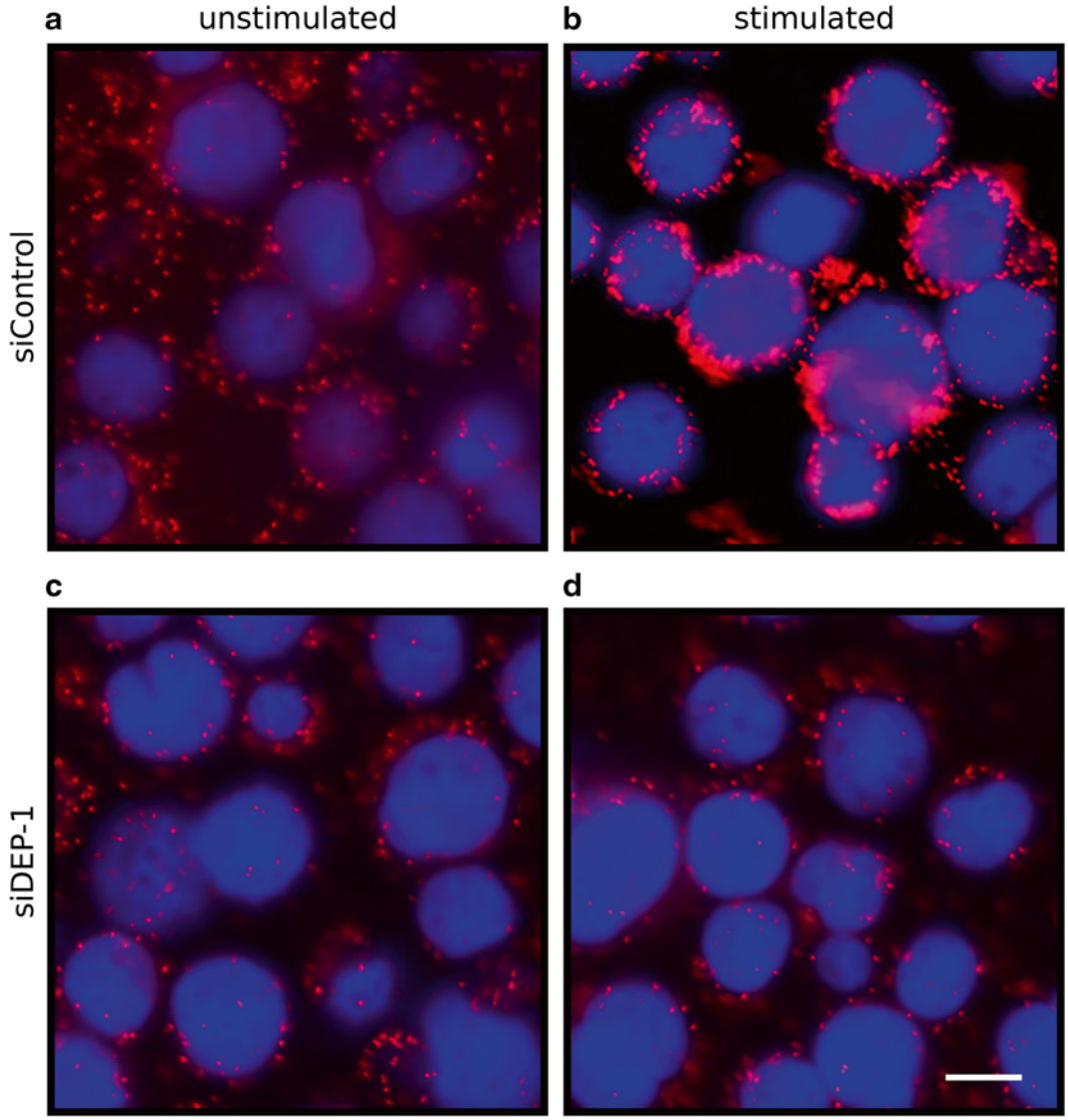

Fig. 8 Knockdown of DEP-1 PTP by siRNA attenuates complex formation with FLT3. THP-1 cells were subjected to transfection with control siRNA (**a** and **b**) or DEP-1 targeting siRNA (**c** and **d**). 48 h later, cells were starved and stimulated with FLT3 ligand (or left unstimulated, as indicated). In situ PLA was performed as in Fig. 1. Note that siRNA-mediated DEP-1 knockdown (validated with immunoblotting) causes signal reduction, which further indicates specificity of the detected complex formation. (Scale bar 5 μm)

suspension. Coating with collagen was instead used to improve adherence of COS7 and HEK293 cells throughout transfection and in situ PLA procedures. We generally recommend considering and testing pre-coating of the coverslips before starting with the in situ PLA experiments.

5. Ligand stimulation was specifically used here to test the effect on association of FLT3 with DEP-1. It may be generally considered to use activation of substrate phosphorylation by

appropriate modulation of upstream signaling for assessing its effect on PTP association.

6. Different fixation methods were tested. Fixation with PFA was not compatible with in situ PLA in case of the FLT3-DEP-1 association study; no signals were obtained. In contrast, for the VE-PTP/Tie2 and VE-PTP/VEGFR2 experiments, fixation with PFA and permeabilization with 0.2% Triton X-100 were successful. Be aware of the influence fixation, permeabilization, and blocking have on the detected signals. In unfortunate antibody combinations, changing the fixation method may completely change, where signals are detected. It is therefore of outermost importance to include appropriate positive and negative controls at all steps.
7. Storage of fixed cells at 4 °C was possible for up to 14 days to still obtain robust in situ PLA signals. Longer storage may also be possible but was not tested.
8. We have also used successfully 10% normal donkey serum (compatible with primary antibodies from goat and rabbit) filtered through a 0.22 μm filter before use, and diluted in PBS with 1.5% bovine serum albumin as blocking solution and antibody solvent.
9. For detection of DEP-1-FLT3 interaction, alternative antibody combinations were tested. Specific but fewer in situ PLA signals were also obtained using another anti-DEP-1 antibody (mouse monoclonal 143-41, Santa Cruz sc-21761) in combination with rabbit anti-FLT3 S18 antibody. Another DEP-1 antibody (goat polyclonal C17, Santa Cruz sc-13798) as well as anti-FLT3 rabbit polyclonal antibody C20 (Santa Cruz sc-479) were less satisfying in the immunostainings and were therefore not pursued for in situ PLA.
10. In case secondary antibody probes are purchased separately, it is essential that among the appropriate species-selective probes, a "PLUS" and a "MINUS" probe are combined. 40 μl was just sufficient to cover the wax pen-encircled area we have used. Drying has to be absolutely avoided! If required use somewhat larger volumes.
11. Alternatively, DAPI can be used as stain for nuclei. Mounting solutions can be purchased with DAPI already included (Duolink® In situ Mounting Medium with DAPI, DUO82040). It should be avoided to stain the nuclei too intensely to prevent "bleeding" of the signal into the red channel. HOECHST 33347 may also be used at lower concentration (e.g., 0.1 μg/μl) for preventing too intense staining.
12. Retrieving good images of a sufficient number of cells will be critical for obtaining statistically significant results. Before starting, it is important to consider, which microscope to use for acquiring the images, and in what mode to run the micro-

scope. For single cell layers it is often sufficient to use conventional epifluorescence microscopes. For taking the image, either a focussed layer with the highest amount of signals is chosen or z-stacks are taken to acquire all images spread over the whole depth of the cell. If signals need to be analyzed in thicker slices (e.g., tissue sections) or a high spatial resolution is required, it is also possible to apply confocal microscopy. Note that the image analysis method (*see* **Note 13**) needs to be compatible with the microscopy method. Also Selective Plane Illumination Microscopy (SPIM) may be used (especially for thick tissue sections or pieces).

When acquiring the images it is of outermost importance to keep the exposure time and all other settings of the channel with in situ PLA signals constant between different positions on the same slide, but also between different controls belonging to the same experiments. If the same experiment is run several times, it should even be possible to keep the exposure time constant between experiments as the brightness of in situ PLA signals is very reproducible under the same experimental conditions. For images detecting the cell nucleus, it is desirable to also keep the exposure time constant. However, some stainings, e.g., HOECHST staining for cell nuclei, bleach fast and may make it impossible to keep the exposure time constant. In these cases it is also acceptable to use the "automatic" exposure time to acquire images from the cell nuclei, which was routinely done throughout the DEP-1-FLT3 study.

A final issue concerns choice of the regions to image, and the number of images which should be analyzed per condition. To avoid subjective bias in choosing the imaged regions, they should be selected in the nuclei channel. Five to ten images per condition were found sufficient for statistical analysis in our experiments.

13. A common public-domain software tool to analyze in situ PLA signals is designated "Blobfinder" (http://www.cb.uu.se/~amin/BlobFinder/). A more advanced commercial software version is the "Duolink image tool" (http://www.olink.com/products-services/duolink/how-use-duolink/software). These analysis tools use either individual TIF or zvi images and can also generate maximum intensity projections (MIPs) from z-stacks. For each position that should be analyzed, an image (or z-stack) from the channel, which is used to detect the cell nuclei, and an image (or z-stack) from the in situ PLA signal channel are required. The software defines the nuclei and the in situ PLA signals [38] and offers the possibility to define the cell cytoplasm as amount of pixels with a certain distance from the nucleic border. In the output file, it can be chosen, whether the signals are counted per cell and in the background or per image. An example for analysis by Blobfinder is shown in Fig. 9.

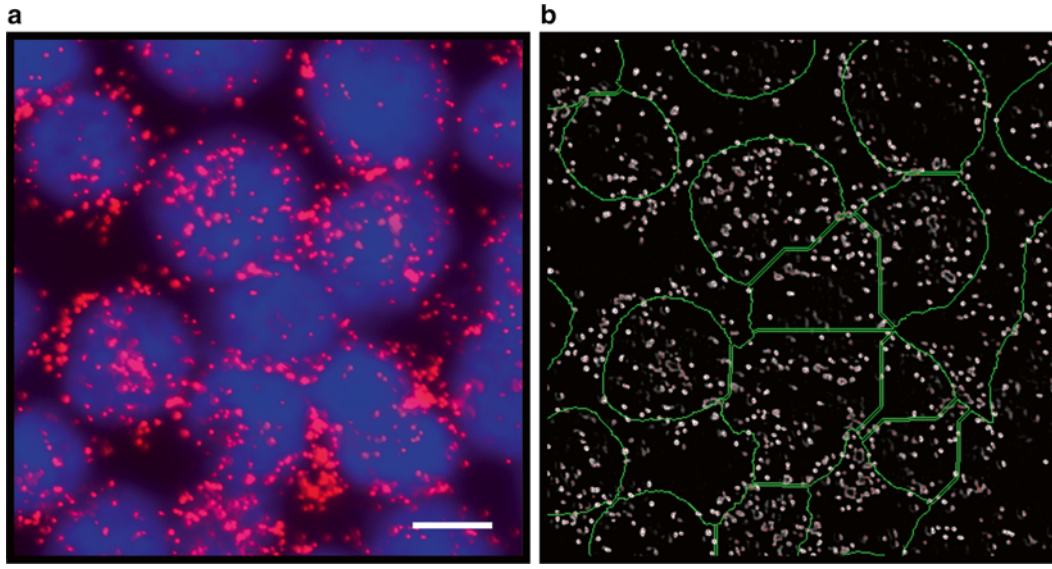

Fig. 9 Automatic assignment of cell areas by BlobFinder for quantification of in situ PLA RCA signals. (**a**) An example image from the detection of FLT3 DEP-1 complexes in FLT3 ligand-stimulated cells (*red channel*—RCA signals; *blue channel*—HOECHST 33347 staining of nuclei) is shown. (**b**) BlobFinder analysis of the image revealing cell assignment (*green circles*) and RCA signals recognized by the program (*red*). Quantification of RCA signals per cell is based on these assignments. (Scale bar 10 μm)

Another tool to analyze images for in situ PLA signals is CellProfiler [39, 40]. This software tool from the Broad Institute (http://www.cellprofiler.org/) allows the user to build user-specific image analysis pipelines using different building blocks. With this tool, it is also possible to include steps to detect the cytoplasm from a counterstaining. The homepage offers even some pre-made pipelines to use as a starting point.

Also other image analysis software may be applied to analyze in situ PLA images: For example, ImageJ can be applied to count speckles and nuclei and in that way create own Plugins or Macros to analyze images.

Please be aware of the fact that, due to binding efficiencies of less than 100% of the different components of the assay, only a small fraction of all interactions that occur in a cell are detected by in situ PLA. However, it can be assumed that the amount of detected RCPs is proportional to the amount of protein-protein interactions in that cell.

14. Counterstaining to monitor additional informative cell features can be done and the corresponding immunofluorescence can be layered on top of the in situ PLA signal. For example, after the detection step, it is possible to either detect primary antibodies employed for in situ PLA with a fluorescently labeled secondary antibody to reveal the localization of the

total pool of one or the other interaction partner. Also, a third primary antibody, either directly labeled or from a third species, which is subsequently detected with a fluorescently labeled species-specific antibody can be applied. Obviously, it is important to choose a fluorescent label different from the PLA label. Also, the staining should be performed in the dark as the in situ PLA signals are light sensitive. However, apply these additional stainings late in the experiment series, i.e., after in situ PLA has been established for your proteins of interest. Always prepare samples with and without stainings in order to be able to compare and test if the PLA signal is altered by the stainings. In addition, add one extra staining at a time and compare between no extra staining, one and several extra stainings etc., always making sure that your PLA signal is similar between those different conditions.

15. The procedure can also be performed in 2-, 4-, or 6-well chamber slides according to your needs.
16. The antibody solution should cover the wax pen-circled area completely and drying has to be avoided. We have used routinely 50 μl but lower volumes are possible with some experience when required.
17. Washing can also be done by hanging the whole slide into the washing buffer. This is faster, but should only be done if cells attach very tightly to the slide. Alternatively, the washing buffer can be pipetted on each well separately.

Acknowledgments

The authors acknowledge grant support from Deutsche Forschungsgemeinschaft and Deutsche Krebshilfe (to F.D.B.), the Community's 7th Framework Program (FP7/2007–2013) under grant agreement no 278568 "PRIMES" and the Swedish Research Council (to O.S.), the Knut and Alice Wallenberg foundation (Wallenberg Scholar Award), the Swedish Science Council, and the Swedish Cancer Foundation (to L.C-.W.).

References

1. Tonks NK (2006) Protein tyrosine phosphatases: from genes, to function, to disease. Nat Rev Mol Cell Biol 7:833–846
2. Östman A, Böhmer FD (2001) Regulation of receptor tyrosine kinase signaling by protein tyrosine phosphatases. Trends Cell Biol 11:258–266
3. Böhmer FD, Friedrich K (2014) Protein tyrosine phosphatases as wardens of STAT signaling. JAKSTAT 3:e28087
4. Östman A, Hellberg C, Böhmer FD (2006) Protein-tyrosine phosphatases and cancer. Nat Rev Cancer 6:307–320
5. Julien SG, Dube N, Hardy S, Tremblay ML (2011) Inside the human cancer tyrosine phosphatome. Nat Rev Cancer 11:35–49
6. Flint AJ, Tiganis T, Barford D, Tonks NK (1997) Development of "substrate-trapping" mutants to identify physiological substrates of

protein tyrosine phosphatases. Proc Natl Acad Sci U S A 94:1680–1685

7. Tiganis T, Bennett AM (2007) Protein tyrosine phosphatase function: the substrate perspective. Biochem J 402:1–15
8. Chagnon MJ, Wu CL, Nakazawa T, Yamamoto T, Noda M, Blanchetot C, Tremblay ML (2010) Receptor tyrosine phosphatase sigma (RPTPsigma) regulates, p250GAP, a novel substrate that attenuates Rac signaling. Cell Signal 22:1626–1633
9. Bugga L, Ratnaparkhi A, Zinn K (2009) The cell surface receptor Tartan is a potential in vivo substrate for the receptor tyrosine phosphatase Ptp52F. Mol Cell Biol 29:3390–3400
10. Sakuraba J, Shintani T, Tani S, Noda M (2013) Substrate specificity of R3 receptor-like protein-tyrosine phosphatase subfamily toward receptor protein-tyrosine kinases. J Biol Chem 288:23421–23431
11. Haj FG, Verveer PJ, Squire A, Neel BG, Bastiaens PI (2002) Imaging sites of receptor dephosphorylation by PTP1B on the surface of the endoplasmic reticulum. Science 295:1708–1711
12. Boubekeur S, Boute N, Pagesy P, Zilberfarb V, Christeff N, Issad T (2011) A new highly efficient substrate-trapping mutant of protein tyrosine phosphatase 1B (PTP1B) reveals full autoactivation of the insulin receptor precursor. J Biol Chem 286:19373–19380
13. Biskup C, Böhmer A, Pusch R, Kelbauskas L, Gorshokov A, Majoul I, Lindenau J, Benndorf K, Böhmer FD (2004) Visualization of SHP-1-target interaction. J Cell Sci 117:5165–5178
14. Boute N, Boubekeur S, Lacasa D, Issad T (2003) Dynamics of the interaction between the insulin receptor and protein tyrosine-phosphatase 1B in living cells. EMBO Rep 4:313–319
15. Monteleone MC, Gonzalez Wusener AE, Burdisso JE, Conde C, Caceres A, Arregui CO (2012) ER-bound protein tyrosine phosphatase PTP1B interacts with Src at the plasma membrane/substrate interface. PLoS One 7:e38948
16. Haj FG, Sabet O, Kinkhabwala A, Wimmer-Kleikamp S, Roukos V, Han HM, Grabenbauer M, Bierbaum M, Antony C, Neel BG, Bastiaens PI (2012) Regulation of signaling at regions of cell-cell contact by endoplasmic reticulum-bound protein-tyrosine phosphatase 1B. PLoS One 7:e36633
17. Roda-Navarro P, Bastiaens PI (2014) Dynamic recruitment of protein tyrosine phosphatase PTPD1 to EGF stimulation sites potentiates EGFR activation. PLoS One 9:e103203
18. Söderberg O, Gullberg M, Jarvius M, Ridderstrale K, Leuchowius KJ, Jarvius J, Wester K, Hydbring P, Bahram F, Larsson LG, Landegren U (2006) Direct observation of individual endogenous protein complexes in situ by proximity ligation. Nat Methods 3: 995–1000
19. Jarvius M, Paulsson J, Weibrecht I, Leuchowius KJ, Andersson AC, Wahlby C, Gullberg M, Botling J, Sjöblom T, Markova B, Östman A, Landegren U, Söderberg O (2007) In situ detection of phosphorylated platelet-derived growth factor receptor beta using a generalized proximity ligation method. Mol Cell Proteomics 6:1500–1509
20. Petri MK, Koch P, Stenzinger A, Kuchelmeister K, Nestler U, Paradowska A, Steger K, Brobeil A, Viard M, Wimmer M (2011) PTPIP51, a positive modulator of the MAPK/Erk pathway, is upregulated in glioblastoma and interacts with 14-3-3beta and PTP1B in situ. Histol Histopathol 26:1531–1543
21. Mistafa O, Ghalali A, Kadekar S, Hogberg J, Stenius U (2010) Purinergic receptor-mediated rapid depletion of nuclear phosphorylated Akt depends on pleckstrin homology domain leucine-rich repeat phosphatase, calcineurin, protein phosphatase 2A, and PTEN phosphatases. J Biol Chem 285:27900–27910
22. Jeon M, Zinn K (2015) R3 receptor tyrosine phosphatases: conserved regulators of receptor tyrosine kinase signaling and tubular organ development. Semin Cell Dev Biol 37: 119–126
23. Böhmer SA, Weibrecht I, Söderberg O, Böhmer FD (2013) Association of the protein-tyrosine phosphatase DEP-1 with its substrate FLT3 visualized by in situ proximity ligation assay. PLoS One 8:e62871
24. Mellberg S, Dimberg A, Bahram F, Hayashi M, Rennel E, Ameur A, Westholm JO, Larsson E, Lindahl P, Cross MJ, Claesson-Welsh L (2009) Transcriptional profiling reveals a critical role for tyrosine phosphatase VE-PTP in regulation of VEGFR2 activity and endothelial cell morphogenesis. FASEB J 23:1490–1502
25. Hayashi M, Majumdar A, Li X, Adler J, Sun Z, Vertuani S, Hellberg C, Mellberg S, Koch S, Dimberg A, Koh GY, Dejana E, Belting HG, Affolter M, Thurston G, Holmgren L, Vestweber D, Claesson-Welsh L (2013) VE-PTP regulates VEGFR2 activity in stalk cells to establish endothelial cell polarity and lumen formation. Nat Commun 4:1672
26. Koos B, Andersson L, Clausson CM, Grannas K, Klaesson A, Cane G, Söderberg O (2014) Analysis of protein interactions in situ by prox-

imity ligation assays. Curr Top Microbiol Immunol 377:111–126

27. Gu GJ, Friedman M, Jost C, Johnsson K, Kamali-Moghaddam M, Pluckthun A, Landegren U, Söderberg O (2013) Protein tag-mediated conjugation of oligonucleotides to recombinant affinity binders for proximity ligation. N Biotechnol 30:144–152
28. Clausson CM, Allalou A, Weibrecht I, Mahmoudi S, Farnebo M, Landegren U, Wählby C, Söderberg O (2011) Increasing the dynamic range of in situ PLA. Nat Methods 8:892–893
29. Clausson CM, Arngården L, Ishaq O, Axel Klaesson A, Kühnemund M, Grannas K, Koos B, Qian X, Ranefall P, Krzywkowski T, Brismar H, Nilsson M, Wählby C, Söderberg O (2015) Compaction of rolling circle amplification products increases signal integrity and signal-to-noise ratio. Sci Rep 5:12317
30. Leuchowius KJ, Clausson CM, Grannas K, Erbilgin Y, Botling J, Zieba A, Landegren U, Söderberg O (2013) Parallel visualization of multiple protein complexes in individual cells in tumor tissue. Mol Cell Proteomics 12:1563–1571
31. Gross S, Knebel A, Tenev T, Neininger A, Gaestel M, Herrlich P, Böhmer FD (1999) Inactivation of protein-tyrosine phosphatases as mechanism of UV-induced signal transduction. J Biol Chem 274:26378–26386
32. Schmidt-Arras DE, Böhmer A, Markova B, Choudhary C, Serve H, Böhmer FD (2005) Tyrosine phosphorylation regulates maturation of receptor tyrosine kinases. Mol Cell Biol 25: 3690–3703
33. Cho CH, Kammerer RA, Lee HJ, Steinmetz MO, Ryu YS, Lee SH, Yasunaga K, Kim KT, Kim I, Choi HH, Kim W, Kim SH, Park SK, Lee GM, Koh GY (2004) COMP-Ang1: a designed angiopoietin-1 variant with nonleaky angiogenic activity. Proc Natl Acad Sci U S A 101:5547–5552
34. Winderlich M, Keller L, Cagna G, Broermann A, Kamenyeva O, Kiefer F, Deutsch U, Nottebaum AF, Vestweber D (2009) VE-PTP controls blood vessel development by balancing Tie-2 activity. J Cell Biol 185:657–671
35. Arora D, Stopp S, Böhmer SA, Schons J, Godfrey R, Masson K, Razumovskaya E, Rönnstrand L, Tänzer S, Bauer R, Böhmer FD, Müller JP (2011) Protein-tyrosine phosphatase DEP-1 controls receptor tyrosine kinase FLT3 signaling. J Biol Chem 286: 10918–10929
36. Boussif O, Lezoualc'h F, Zanta MA, Mergny MD, Scherman D, Demeneix B, Behr JP (1995) A versatile vector for gene and oligonucleotide transfer into cells in culture and in vivo: polyethylenimine. Proc Natl Acad Sci U S A 92:7297–7301
37. Leuchowius KJ, Jarvius M, Wickstrom M, Rickardson L, Landegren U, Larsson R, Söderberg O, Fryknas M, Jarvius J (2010) High content screening for inhibitors of protein interactions and post-translational modifications in primary cells by proximity ligation. Mol Cell Proteomics 9:178–183
38. Allalou A, Wählby C (2009) BlobFinder, a tool for fluorescence microscopy image cytometry. Comput Methods Programs Biomed 94: 58–65
39. Carpenter AE, Jones TR, Lamprecht MR, Clarke C, Kang IH, Friman O, Guertin DA, Chang JH, Lindquist RA, Moffat J, Golland P, Sabatini DM (2006) Cell Profiler: image analysis software for identifying and quantifying cell phenotypes. Genome Biol 7:R100
40. Ke R, Mignardi M, Pacureanu A, Svedlund J, Botling J, Wahlby C, Nilsson M (2013) In situ sequencing for RNA analysis in preserved tissue and cells. Nat Methods 10:857–860
41. Saharinen P, Eklund L, Miettinen J, Wirkkala R, Anisimov A, Winderlich M, Nottebaum A, Vestweber D, Deutsch U, Koh GY, Olsen BR, Alitalo K (2008) Angiopoietins assemble distinct Tie2 signalling complexes in endothelial cell-cell and cell-matrix contacts. Nat Cell Biol 10:527–537

Chapter 14

Use of Dominant-Negative/Substrate Trapping PTP Mutations to Search for PTP Interactors/Substrates

Vegesna Radha

Abstract

Phosphorylation of proteins on tyrosine residues is the consequence of coordinated action of tyrosine kinases (TKs), and protein tyrosine phosphatases (PTPs). Together, they regulate intermolecular interactions, subcellular localization, and activity of a variety of proteins. The level of total protein-associated tyrosine phosphorylation in eukaryotic cells is only a small fraction of the total phosphorylation. PTPs, which have high specific activity compared to tyrosine kinases, play an important role in maintaining the tyrosine phosphorylation state of proteins and regulate signal transduction pathways and cellular responses. PTPs depend on specific invariant residues that enable binding to substrates phosphorylated at tyrosine and aid catalytic activity. Identification of PTP substrates has helped understand their role in distinct intracellular signaling pathways. Because of their high specific activity, the interaction between tyrosine phosphatases and their substrates is often very transient in the cellular context, and therefore identification of physiological substrates has been difficult. Single-site mutations in the enzymes stabilize interaction between the enzyme and its targets and have been used extensively to identify substrates. The mutations are either of the catalytic cysteine (Cys) residue or other invariant residues and have been classified as substrate-trapping mutants (STMs). These mutants often serve as dominant negatives that can inactivate effector functions of a specific PTP within cells. Considering their association with human disorders, inhibiting specific PTPs is important therapeutically. Since the catalytic domains are largely conserved, developing small-molecule inhibitors to a particular enzyme has proven difficult and therefore alternate strategies to block functions of individual enzymes are seriously being investigated. We provide a description of methods that will be useful to design strategies of using dominant-negative and substrate-trapping mutants for identifying novel interacting partners and substrates of PTPs.

Key words Protein tyrosine phosphatases, Dominant negative, Substrate-trapping mutants, Substrate identification, Interacting proteins, Phospho-tyrosine

1 Introduction

Studies carried out over the last quarter of a century have highlighted the role of protein tyrosine phosphatases (PTPs) as key players in signaling events that regulate a variety of cellular functions [1, 2]. Genome sequencing, genetic, and biochemical studies have shown their presence across all classes of life forms including the prokaryotes. In humans, 38 classical tyrosine-specific forms are

Rafael Pulido (ed.), *Protein Tyrosine Phosphatases: Methods and Protocols*, Methods in Molecular Biology, vol. 1447,
DOI 10.1007/978-1-4939-3746-2_14, © Springer Science+Business Media New York 2016

known and about 60 more with dual specificity, which can dephosphorylate phospho-serine (p-Ser) and phospho-threonine (p-Thr) in addition to phospho-tyrosine (p-Tyr) [3]. In addition, enzymes that dephosphorylate lipids and carbohydrates share catalytic domains with PTPs [4]. In mammalian cells, phosphorylation at tyrosine residues forms a very small fraction of total acid-stable phosphorylation on proteins, and it has been shown that PTPs have an order of magnitude higher activity compared to the tyrosine kinases [5]. It may also be noted that contraindicatory to its catalytic function, the activation of PTPs can enhance tyrosine phosphorylation status of cellular proteins because of their ability to activate tyrosine kinases [6, 7]. Identifying the substrates and interacting partners of PTPs has been crucial to understand their distinct role in signaling to cellular responses [2]. In vitro, PTPs dephosphorylate a variety of substrates, but show high selectivity in the cellular context [8]. Residues adjoining the p-Tyr in the target, subcellular localization, presence of non-catalytic regulatory domains, dimerization, protein-protein interactions, and posttranslational modifications are determinants of substrate selectivity for the PTPs [8, 9]. Though the catalytic domain of PTPs is specific for recognition of p-Tyr, it does so with 10,000-fold greater affinity for p-Tyr in proteins and peptides compared to free p-Tyr. This higher affinity is due to interaction of amino acids in the catalytic cleft with residues flanking the p-Tyr in protein targets [10]. Unlike in the case of tyrosine kinases it is difficult to identify or predict a tyrosine phosphatase that targets a specific protein based on the primary sequence adjoining the p-Tyr in the substrate. Using peptide libraries, it has been shown that electrostatic interaction between basic residues near the catalytic site and acidic residues, generally N-terminal to the p-Tyr in the substrate, determines target selectivity of PTPs [8].

A stretch of about 280 amino acids constitute the catalytic domain of p-Tyr-specific PTPs, and invariant residues essential for catalytic activity are Cys and arginine (Arg) in the signature motif at the base of the catalytic cleft; aspartate (Asp) in the WPD loop; and glutamate (Glu) in the Q loop, which form the sides of the cleft [4]. In addition, the catalytic domain has a p-Tyr recognition motif which is responsible for substrate selectivity, as well as other conserved residues which provide structural stability to the cleft. The depth of the cleft determines the specificity of the enzyme towards p-Tyr, or p-Ser/p-Thr [11]. Structural and biochemical analysis using mutants has revealed the exact steps involved in catalysis, which is conserved across all PTPs [10].

The transient nature of the enzyme substrate complex has made the task of researchers attempting to identify interacting partners and substrates of PTPs difficult. Few attempts at identifying substrates using wild-type (WT)-PTP in interaction assays have been successful [12]. Generation of mutant enzymes that

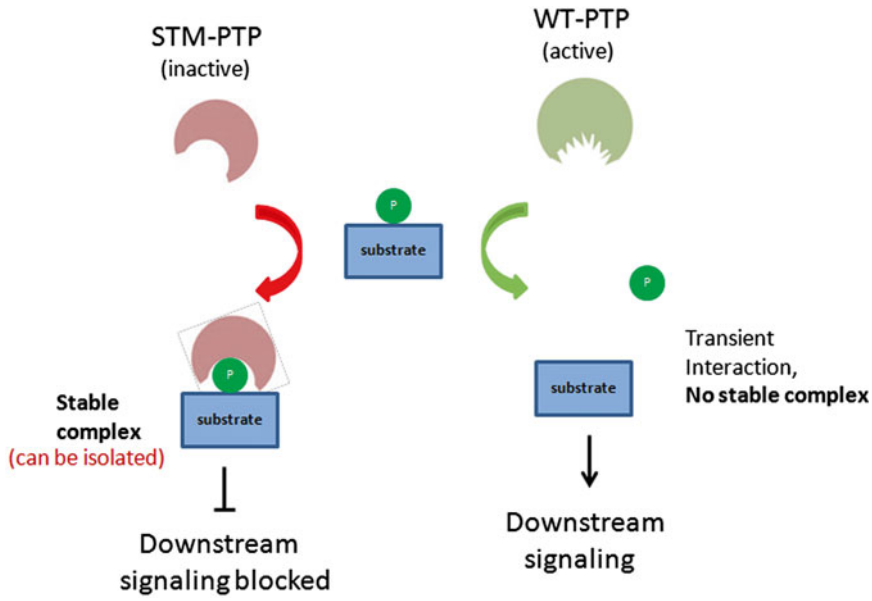

Fig. 1 Schematic figure showing principle of using STMs for identifying interacting partners of PTPs. While the WT enzyme acts on the substrate transiently to release the phosphate, the STM binds to the phospho-substrate and forms a stable complex which can be isolated. Formation of a stable complex and absence of dephosphorylation of the target in the cellular context inhibit downstream signaling and therefore STM mutants function as dominant negatives

lack or have poor catalytic activity and therefore form stable complexes with their substrates has been the principle of substrate-trapping mutants (STMs) (Fig. 1). These have been extremely helpful in identifying substrates and therefore enabled understanding of the physiological functions of specific PTPs [13–16]. Mutation of residues essential for catalytic activity like Cys or Arg in the P-loop; Asp in WPD; and Glu in the Q-loop results in STMs [17, 18]. In some instances, mutations in other residues like Thr466 in SHP2 and Tyr676 in PTPH1 also serve as STMs [19, 20]. It is important that the mutation does not alter the site or substrate-binding specificity of the enzyme [17]. Very often, mutation of two residues has improved their ability to function as an STM. The effectiveness of single and double mutants as substrate traps is different for individual PTPs. The ideal residue/s to be mutated to generate STM in the case of each enzyme has to be examined, as it has been found that simple inhibition of activity is not sufficient to cause substrate trapping. Cloning of STM PTPs into adenovirus and lentiviral expression systems has enabled very efficient expression of the variants and more effectiveness in finding interacting proteins. These mutants have also been helpful in obtaining complexes of enzyme-substrate for structural studies and also to isolate specific inhibitors [21, 22]. Because of their

ability to form stable complexes, STMs are useful in determining subcellular location at which dephosphorylation occurs.

In addition to catalytic site mutants, residues outside the catalytic cleft that are involved in substrate binding also serve as good STMs [23]. Mutations generated in non-catalytic domain that disable interaction with cellular proteins are useful in identifying interacting partners of PTPs that are not necessarily substrates [24, 25]. Very often, STMs function as dominant negatives to inhibit cellular functions of the enzymes. But not all STMs have known cellular consequences that are inhibitory to downstream signaling [26]. In these instances, other strategies of generating dominant negatives are employed, and are also validated using knockdown approaches. Some dominant-negative variants have also helped understand fine-tuned regulation of signaling involving inhibitory feedback loops [27].

It is interesting to note that naturally occurring catalytic inactive forms of PTPs have been identified to function as dominant negatives to block function of the active isoform suggesting that nature also uses dominant-negative strategies to regulate signaling by PTPs [28]. Some of the pseudophosphatases also function through protein interactions and show signaling activity independent of catalytic activity [29].

Therefore, it is important that for any specific PTP being studied, various mutants are checked and optimized for efficacy. A high-efficiency STM of the PTP should have high substrate binding affinity (i.e., low Km); low rate of dissociation (i.e., low Kd); and low enzyme activity (i.e., low Kcat). Efficacy of binding can be determined in vitro using phosphopeptides or artificial substrates through methods like isothermal calorimetry [30]. In the case of some PTPs, dephosphorylation of a substrate is dependent on interaction of its non-catalytic sequences which enables association of the enzyme with its substrate or subcellular organelles where the substrate is present. A good example of this is seen in the case of TC48 isoform of PTPN2/TC-PTP which dephosphorylates Bcr-Abl, but not c-Abl or its activated forms [31]. This difference is due to the ability of TC48 to interact with Bcr domain of Bcr-Abl, which enables the enzyme and the substrate to be brought together. SHP2 also dephosphorylates substrates dependent on interactions with its substrate through its SH2 domain [32]. In identifying such interactions, truncated PTPs lacking the catalytic domain can be used as dominant-negative variants.

Once the appropriate mutant is generated by cloning in bacterial or eukaryotic expression vectors, with a tag, it can be used to identify previously unknown interacting partners. It can be tested for interaction with a known protein substrate prior to using it for finding novel substrates. The bacterial GST-fusion protein (GST-FP) expression system is often used to enable purification of the protein for in vitro interaction (Fig. 2). The substrate pool to

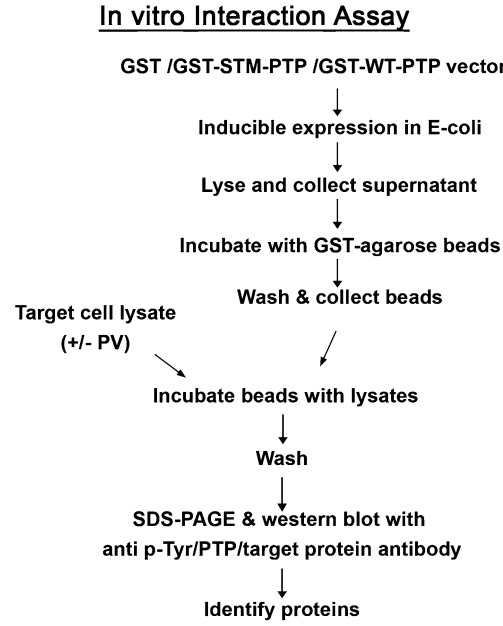

Fig. 2 Schematic showing steps involved in identifying molecules that interact in vitro with substrate-trapping mutant PTP. GST fusion proteins of the WT and STM constructs of the PTP in study are expressed in *E. coli* and purified by coupling to glutathione agarose beads. Cell lysates are prepared, and incubated with the beads. The beads are obtained after washes and bound proteins from the lysates recovered by boiling in SDS-PAGE buffer. Western blotting is used to detect the proteins which are then compared between pull downs carried out using WT and mutant PTPs

be used in the interaction assays is usually lysates of cells known to express the PTP, and treated with agonists or phosphatase inhibitors to increase tyrosine phosphorylation of all likely targets. This is essential, as the catalytic site of PTPs is designed to interact only with proteins phosphorylated on tyrosine residues. Having enabled the enzyme substrate interaction, the complex is isolated using glutathione-agarose beads to which the GST-PTP is coupled and resolving the bound protein and detecting them by Western blotting with anti-p-Tyr antibodies. The substrate trapped with the PTP can be identified by informed guess based on their molecular weight, or by carrying out mass spectroscopy analysis [33]. Interaction in the cellular context is generally identified by overexpressing the tagged STM PTP, carrying out immunoprecipitation, and then identifying the associated proteins (Fig. 3). The STM can also be used in an yeast-2-hybrid system to isolate novel interacting partners [34].

A large number of PTPs have been implicated in human disorders and therefore identifying the regulators and signaling effectors is of interest [35]. In situ interactions in distinct subcellular regions

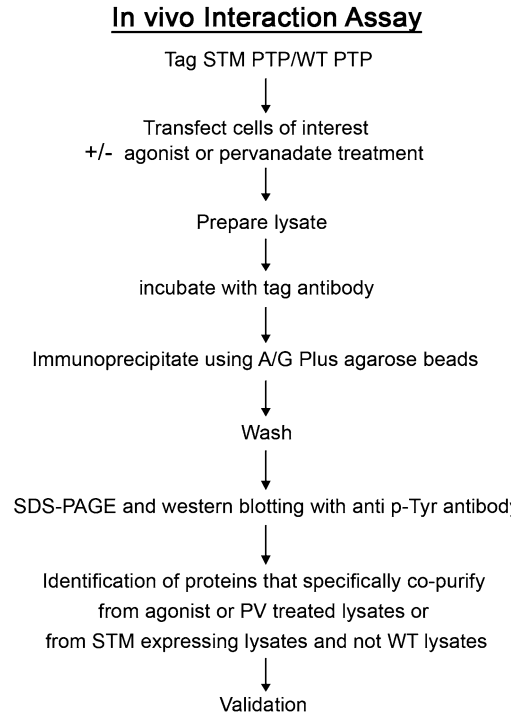

Fig. 3 Schematic showing steps involved in identifying molecules that interact in vivo with substrate-trapping mutant PTP. Mammalian cells are transfected with the WT or STM-PTP of interest and immunoprecipitation carried out using anti-tag or anti-PTP antibodies. Associated proteins are examined by western blotting using anti-p-Tyr or phospho-site-specific antibodies. Lysates are prepared in the presence or absence of vanadate/agonists

can be identified by overexpression and colocalization using immunofluorescence methods like colocalization analysis, FRET, and BRET [14] (Fig. 4). In this chapter, we provide a description of methods that will be useful to design strategies for using STM and dominant mutants of PTP to identify novel cellular interacting proteins and substrates. Methods to validate these molecules using various assays are also described. Though the strategies described in this chapter refer to PTPs, they can also be applied to dual-specificity phosphatases and low-molecular-weight phosphatases.

2 Materials

All solutions are made in autoclaved deionized water and stocks are stored after autoclaving.

1. GST-FP expression vector with WT and mutant PTP, and parental vector.
2. Glutathione sepharose beads.

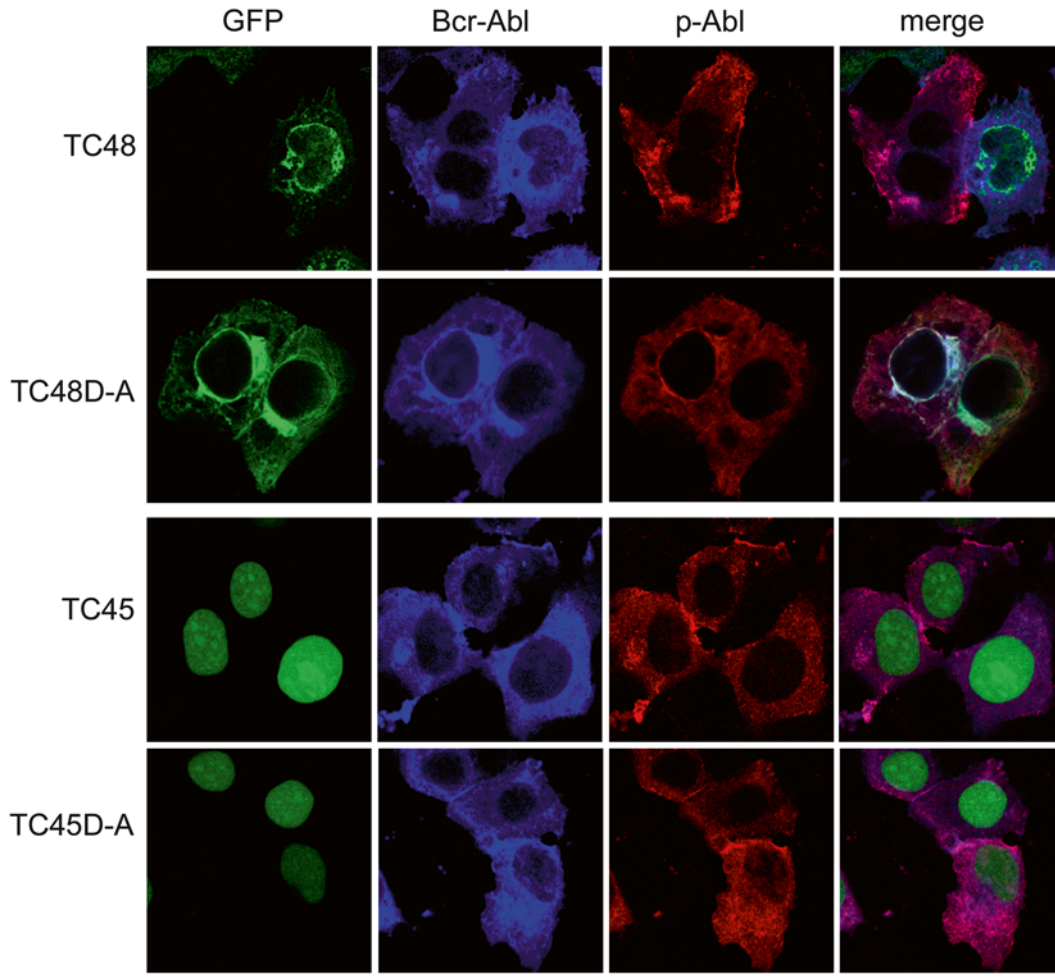

Fig. 4 Distinct substrate specificity shown by isoforms of TC-PTP and identification of Bcr-Abl as a substrate of TC48 and not its nuclear isoform, TC45: GFP-tagged WT and STM mutants of TC48 and TC45 are co-expressed with Bcr-Abl and stained to detect Abl (*blue*) and p-Abl (*red*). TC48 expression results in dephosphorylation of Bcr-Abl, and therefore no p-Abl is seen; also no colocalization is seen with Bcr-Abl. TC48D-A-expressing cells show no dephosphorylation of Bcr-Abl, but showed colocalization with Bcr-Abl. Expression of either TC45 or TC45D-A showed no dephosphorylation of Bcr-Abl indicating that Bcr-Abl is not a substrate of the nuclear phosphatase. Subcellular localization of the PTP enables substrate dephosphorylation and STM mutants show colocalization with their substrates

3. Isopropyl β-D-1-thiogalactopyranoside (IPTG).
4. Media and reagents for growth of mammalian cells in culture.
5. Exponentially growing mammalian cells which possess likely interacting partners and substrates of the specific PTP, or tissue from which a substrate is to be identified. This can be decided based on cell type and tissue-specific expression of the PTP being studied.
6. Pervanadate solution: Stock freshly made by combining equal volumes of 100 mM sodium orthovanadate and 100 mM

H_2O_2, and added to cells at a concentration of 50 μM within 5 min of preparation.

7. Anti-p-Tyr-, PTP-, or Tag-specific antibodies, and antibodies to likely targets. Wherever available, phospho-site-specific antibodies can be used.
8. Protease inhibitor cocktail.
9. Reagents for SDS-polyacrylamide gel electrophoresis (SDS-PAGE) and Western blotting.
10. Enhanced chemiluminescence kit.
11. Nitrocellulose or PVDF membranes for protein transfer.
12. Phosphatase inhibitors, NaF, Na_3VO_4, iodoacetamide/iodoacetic acid (IAA).
13. Lysis buffer: 10 mM Tris pH 7.4, 150 mM NaCl, 5 mM EDTA, 1 mM PMSF, 1% Triton X-100, 0.1% BSA, 5 mM IAA, 2 mM sodium orthovanadate, 10 mM NaF, and protease inhibitors (this buffer is freshly prepared from stocks; phosphatase inhibitors and protease inhibitors are added just before use).
14. Wash buffer: 20 mM Tris pH 7.4, 150 mM NaCl, 10% glycerol, 0.1% Triton X-100, and protease inhibitors.
15. Phosphate-buffered saline (PBS): 1.85 mM NaH_2PO_4, 8.4 mM $NaHPO_4$, 137 mM NaCl, and 2.7 mM KCl, pH 7.4.
16. WT-PTP and STM-PTP cloned in eukaryotic expression vector (preferable to use a tag that will enable immunoprecipitation with tag-specific antibody).
17. Immunoprecipitation (IP) buffer: 20 mM Tris pH 7.4, 1% Triton X-100; 5 mM EDTA, 0.1% BSA; 150 mM NaCl; 1 mM PMSF, 1 mM Na orthovanadate or 1 mM IAA, EDTA-free protease inhibitor.
18. GFP agarose conjugated beads; or protein A/G Plus agarose beads.
19. Transfection reagents.
20. Antibodies to GFP and control IgG; anti-p-Tyr antibodies; or other required primary and secondary antibodies.
21. 1× SDS sample buffer: 60 mM Tris pH 6.8; 2% SDS, 10% glycerol, 5% β-mercaptoethanol, and 0.005% bromophenol blue.
22. Staining solution: 0.1% Coomassie Brilliant Blue R-250 (CBB), 50% methanol, and 10% glacial acetic acid.
23. Destaining solution: 40% methanol and 10% glacial acetic acid.
24. Transfer buffer: 39 mM glycine, 48 mM Tris–HCl, 0.0375% SDS, and 20% methanol.
25. Ponceau S solution: 10× stock containing 2% Ponceau S, 30% TCA, and 30% sulfo-salycylic acid in H_2O.

26. TBST: 10 mM Tris pH 8.0, 150 mM NaCl, 0.1% Tween.
27. Blocking solution: 5% Blotto or 2% BSA in TBST (*see* **Note 1**).
28. Deprobing buffer: 62.5 mM Tris pH 6.8, 2% SDS, and 100 mM β-mercaptoethanol in H_2O.

3 Methods

Based on studies of a large number of PTPs, we have some hints on the residues which are to be mutated or regions to be deleted to generate STMs or dominant-negative forms. It has been found that mutation of Asp to Ala functions better than Cys to Ala/Ser in those enzymes where substrate recognition is primarily restricted to residues immediately surrounding the phosphorylation site. Examples of such enzymes are PTP1B, TC-PTP, and PTP-PEST. For enzymes in which the recognition is dependent on contacts distal to the Tyr, the Cys-to-Ser mutant generally forms a complex stable enough to be isolated. The residues Cys, Asp, and Trp are usually mutated to Ala or Ser, and Tyr to Phe (*see* **Note 2**). For identifying interactions involving non-catalytic domains of PTPs, deletion constructs lacking catalytic sequences can be used in interaction assays.

3.1 In Vitro Substrate Trapping

This method is dependent on isolation of recombinant STM with a tag (usually GST) that enables purification and incubation with a lysate of cells or tissues that have likely substrates of the phosphatase. The main steps involved are shown in Fig. 2. To ensure that the likely substrates are phosphorylated, the lysates may be made after treatment with agonists or with pervanadate (PV), an irreversible inhibitor of PTPs [36, 37]. PV treatment results in a large number of cellular proteins being stably phosphorylated on Tyr. The steps include expression and purification of recombinant proteins (**steps 1–3**), followed by western blotting (**steps 4–8**).

1. Grow GST and GST-FP expressing cultures of BL-21(DE3) strain of *E. coli* overnight, dilute 1:20, and incubate until an OD of ~0.4, at 600 nm is reached. Add 1 mM IPTG to the exponentially growing cultures and induce for 3–4 h at 37 °C (*see* **Note 3**). Harvest the cells by centrifugation, suspend in 1 ml of cold PBS containing protease inhibitors, and sonicate with 5-s bursts on ice at 30-s intervals. Add Triton X-100 to a final concentration of 1% and leave on ice for 20 min. Centrifuge at 10,000 rpm for 20 min, and transfer the supernatant into fresh Eppendorf tubes. Add 20 μl (50% slurry) of glutathione agarose beads and incubate by slow tumbling for 30 min–1 h at 4 °C. Collect the beads coupled to either GST or the GST FPs (WT and STM) by washing thrice in cold PBS, and centrifuging at 2000 rpm for 1 min each time. The beads

can be stored in PBS containing protease inhibitors, 1 mM DTT, and 10% glycerol at 4 °C (*see* **Note 4**). Examine a small aliquot (5 µl) of the coupled beads by running on SDS-PAGE and staining with CBB to approximately quantitate the protein, and ensure that it is not degraded.

2. Plate mammalian cells that are proposed to be used for detecting PTP-interacting proteins in a 100 mm dish at 30–40% confluence. The following day, exponentially growing cells are either left untreated or treated with PV (50 µM, 10–20 min), and washed in cold PBS. Lyse the cells immediately on ice for 10 min by adding 1 ml lysis buffer. Transfer to an Eppendorf tube and vortex the lysate to ensure complete solubilization. Add DTT to the lysate at a final concentration of 1 mM (to inactivate unreacted iodoacetic acid) and collect supernatant by centrifugation at 15,000 rpm for 10 min at 4 °C. Distribute the supernatant equally to three fresh 1.5 ml tubes and add required quantity (equivalent to about 2 µg of the bound protein) of GST- or GST-FP-coupled beads. Rotate the tubes on a rotorotorque at 4 °C for 4–6 h and collect the complexes associated with the beads by washing thrice in 1 ml of wash buffer. Elute the bound proteins by boiling in 1× SDS sample buffer.
3. Subject the samples to SDS-PAGE (8–10% is most suitable to obtain a profile of the polypeptides) and carry out western blotting using anti-p-Tyr antibodies or antibodies specific to likely interacting proteins/substrates. Polypeptides positive for p-Tyr in lysates incubated with STM mutant and not seen in WT or GST incubated samples can be considered as specific substrates. The identity of the interacting proteins/substrates is to be determined using specific antibodies or by subjecting the co-purified proteins to mass spectrometric analysis.
4. Resolve proteins on an 8–10% SDS-PAGE gel and transfer to nitrocellulose membrane using a semidry apparatus. Place the gel on nitrocellulose or PVDF membrane cut to the size of the gel and place in between seven layers of Whatman 1 filter paper on either side, soaked in transfer buffer, and apply a current of 1 mA/cm^2 for 1–2 h (*see* **Note 5**). Stain the membrane using Ponceau S solution to visualize efficient transfer of proteins and mark the position of the molecular weight markers. Wash the stain off with water and place the blot in blocking solution for 1 h at RT, or overnight at 4 °C. When phospho-antibodies are used, 2% BSA and phosphatase inhibitors (50 mM NaF, and 5 mM Na_3VO_4) in TBST are used as blocking solution.
5. Carry out primary and secondary antibody incubation in blocking solution, diluted 1:10 in TBST, for 1–2 h at room temperature, or overnight at 4 °C. Give three washes of 5 min after each step. All incubations and washes are carried out on a platform shaker with sufficient volume of the solutions. Include

phosphatase inhibitors in TBST during the washes when probing with phospho-antibodies. Detect antibody-bound proteins using western lighting chemiluminescence as instructed by the manufacturer (*see* **Note 6**). Quantitate the bands for comparison of intensity, using Image J Software. Deprobe the blots prior to blotting using an alternate antibody. For deprobing, wash the blots in deprobing buffer for 30 min at 50 °C on a shaker water bath. Remove the deprobing solution and wash the blots in TBST several times at room temperature. The removal of antibodies is examined by checking for the presence of any residual signals.

6. For analyzing bound proteins using mass spectrometry (MS), fractionate the eluted proteins on an SDS-PAGE, and detect polypeptides by CBB staining that enables subsequent peptide identification (*see* **Note 10**). Excise stained protein bands from gels and digest with trypsin. Elute the tryptic peptides and concentrate before reconstitution in 10 μl of 1% formic acid. Subject the samples to MS and identify the peptides by database search. Generally, proteins that are matched by the presence of two or more unique peptides are considered positive. Detailed method is given below.
7. In vitro interactions using recombinant PTPs can also be attempted using Far-Western blotting [38]. For this, incubate purified GST/GST-PTP protein with blots onto which untreated and PV-treated cell lysates have been transferred. After three washes in TBST, incubate with anti-GST or anti-PTP antibodies, and appropriate secondary antibodies. The polypeptides detected specifically in PV-treated samples in blots incubated with purified GST-PTP will likely be the molecules with which the PTP binds.
8. GST-FPs are eluted from beads (obtained as described in previous section) by shaking with 50–100 μl of 5 mM glutathione made in 50 mM Tris–HCl, pH 9.0 for 1–2 min. The beads are spun down and the eluted protein present in the supernatant quantitated and also checked on SDS-PAGE for degradation. The pure protein can be stored frozen in buffer containing 50% glycerol and 1 mM final concentration of DTT (to prevent oxidation of enzymes). The polypeptides to which the STM binds can subsequently be identified by MS.

3.2 Identification of Proteins and Substrates That Interact with PTP in the Cellular Context

The in vitro assay systems are likely to result in some nonspecific interactions as the enzyme and substrate are brought together artificially and may not see each other within cells. Therefore, identification of true substrates has depended on detecting molecules that can be co-precipitated with the PTP from cell lysates. Expression of STM-PTP in cells will prevent dephosphorylation of its specific substrates and therefore the cellular proteins need not

necessarily be artificially phosphorylated by PV treatment or expression of a kinase. The steps involved are shown in Fig. 3.

1. Transfect mammalian cells (HEK293 or Cos generally), plated in 60 mm dishes as per the manufacturer's instructions with WT or STM-PTP. After 30–48 h (with or without agonist/PV treatment for the required time) lyse the cells in IP buffer (600 μl) (*see* **Note 7**). Vortex the lysates and leave on ice for 10 min before centrifugation at 15,000 rpm for 15 min at 4 °C. Collect the supernatant, estimate protein concentration, and keep aside a small amount (generally 1–2 %) boiled in sample buffer to be used as whole-cell lysate (WCL). Transfer the lysate (2–5 mg) equally to two tubes and incubate the lysates with equal amount (2 μg) of the tag antibody or control IgG at 4 °C for 4–16 h. Add 20 μl slurry of protein A/G plus agarose beads and incubate further for 30 min–1 h. Wash the beads three to four times with 1 ml wash buffer by centrifuging at 2000 rpm for 1 min at 4 °C to remove the supernatant (*see* **Note 8**).
2. Recover the precipitated proteins by lysing in SDS sample buffer and subject to SDS-PAGE and western blotting with anti-p-Tyr antibodies. The blots are deprobed before incubation with other antibodies. The efficiency of immunoprecipitation is examined by probing with anti-tag or anti-PTP antibodies and comparing levels between WCL and immune complexes. In the case of too much background, the lysates can be precleared by incubating with 20 μl of protein A-sepharose for 30 min at 4 °C. When examining target protein dephosphorylation, it is good to verify that the WT enzyme does not significantly alter total p-Tyr on a large number of cellular proteins by examining WCL by western blotting, or cells plated on cover slips by indirect immunofluorescence (Fig. 5) [39]. Under these conditions, overexpression can be regulated to prevent nonspecific dephosphorylation of targets.
3. When GFP fusion proteins are used to identify interacting partners, a one-step method called GFP-Trap can be used for quick and efficient pull down. This method does not require the use of regular anti-GFP antibodies and therefore has the advantage that the heavy and light chains of IgG do not appear in the pull down. Camel-derived antibodies that are stable and bind with high efficiency to GFP are coupled to agarose beads and used as a trap. On a similar principle, GST-Trap is also available for pull down of GST-FPs. The cell lysate is incubated with 10–20 μl of equilibrated beads at 4 °C for 1 h and recovered by centrifugation and washes in wash buffer. The complexes are dissociated from beads by incubating at 95 °C for 10 min in 60 μl of buffer without protease inhibitors. The beads are

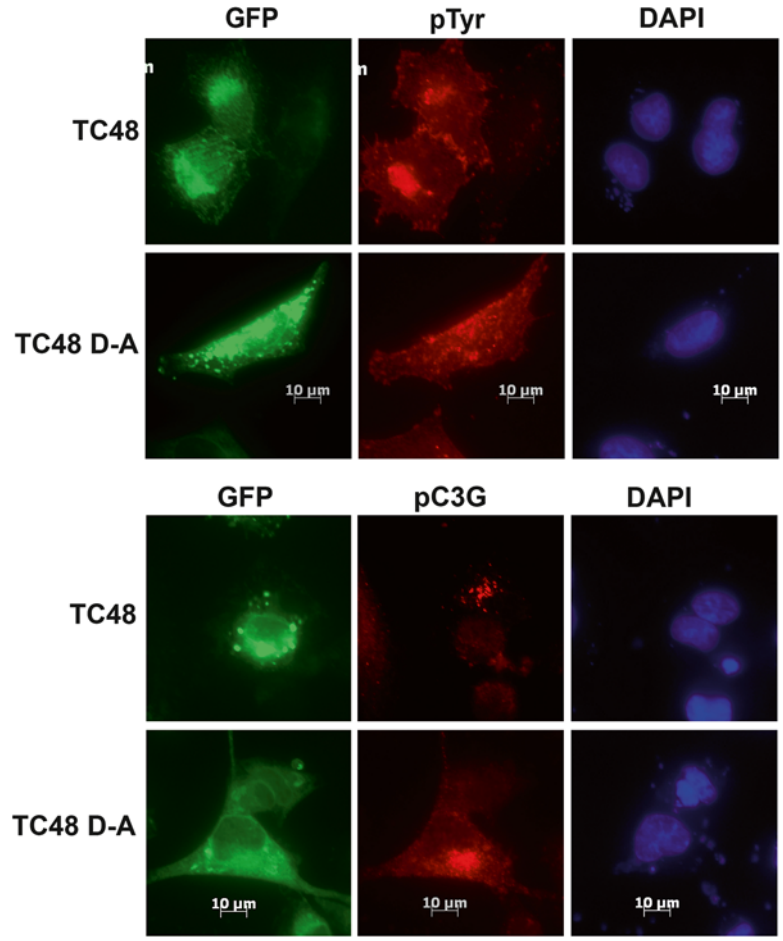

Fig. 5 TC48 dephosphorylates C3G but does not alter total cellular p-Tyr level. Cells were cotransfected with c-Src and either WT or D-A TC48 and stained for p-Tyr (*upper*) or p-C3G (*lower panels*). As seen, TC48 expression results in loss of p-C3G signals, but does not affect total cellular p-Tyr, indicating that endogenous C3G is a specific substrate of TC48. D-A mutant does not affect phosphorylation on C3G or total cellular p-Tyr

removed by centrifugation and the supernatants used for SDS-PAGE and MS analysis.

The methods mentioned above depend on the identification of the co-purified proteins. This can sometimes be done by making an informed guess based on the molecular weight of the phosphoprotein, an understanding of subcellular location of the enzyme and tyrosine-phosphorylated substrates, or the signaling events in which the enzyme is involved, and validating it by using specific antibodies. Unbiased approaches depend on identification of the interacting molecules using MS analysis [40, 41].

3.3 In-Gel Digestion and Preparation of Peptides for Mass Spectrometry (MS)

1. Analyze the samples obtained in the pull down, by 1D SDS-PAGE, and after CBB staining, cut gel slices from the entire lane for extraction, trypsinization, and analysis by MS. It is important to wear gloves and use good-quality tubes and tips for all the steps (*see* **Notes 9** and **10**). Gels are left in water overnight for processing for in-gel tryptic digestion.
2. Cut the gel pieces with bands of visible protein into small pieces using a sterile blade, and destain in 600 µl of destaining solution (30 mM ammonium bicarbonate in 50% acetonitrile [ACN]). Tumble the tubes on a rotatorque for 1 h, centrifuge, and repeat destaining until stain is completely washed off. Replace the destaining solution with 500 µl of autoclaved water and shake for 30–60 min. Centrifuge the tubes, remove water, and add 200 µl 100% acetonitrile. Repeat this step until the gel pieces appear crystalline. Air-dry for 10–15 min; add 100–500 ng of trypsin in 1% acetonitrile and 60 mM ammonium bicarbonate; and incubate at 37 °C for 20–24 h. Ensure that the gel pieces are submerged by adding 1% ACN and 60 mM ammonium bicarbonate solution. Elute the digested peptides by adding 500 µl of elution solution (0.1% trifluoroacetic acid [TFA] in 50% ACN) and tumbling for about 45 min. Collect supernatant by centrifugation, and lyophilize using a speed vacuum concentrator. Desalt the samples by vortexing in a solution of 0.1% TFA and 5% ACN, and running through rehydrated zip-tip columns (size, p10) (*see* **Note 11**). Rehydrate the zip-tip columns starting with a solution of 0.1% TFA and 100% ACN, followed by solution of 0.1% TFA and 50% ACN; and then a solution of 0.1% TFA in autoclaved MilliQ water, by pipetting in and out 10–15 times. Elute the peptides using 0.1% TFA and 50% ACN, and vacuum dry. Reconstitute the samples in 0.1% formic acid and 5% ACN, for MS analysis.

3.4 Other Methods

An alternate unbiased method to identify interacting partners as substrates of PTPs is the use of 2-hybrid screen using dominant-negative PTPs [34, 42]. The approach is based on expressing a library of cellular proteins along with constitutively active tyrosine kinase (usually Src) under an inducible promoter and using the mutant PTP as bait. Transcriptional activation of the reporter occurs when a Src-phosphorylated protein binds to the PTP-lexA fusion. The drawback of this method is the assumption that the likely PTP substrates are physiological targets of the tyrosine kinase used. This method offers the advantage of identifying low-abundance substrates and also weak enzyme substrate complexes that do not withstand washes used in conventional in vitro and in vivo interaction methods.

Other unbiased approaches to identify targets have been the use of synthetic phospho-peptide libraries [43–45] for in vitro interaction with the mutant PTP. This has been modified by direct

microsynthesis of the phospho-peptides on membranes to enable testing for interaction with purified P^{32}-labeled PTP. Specific interaction with peptides could be detected by autoradiography after incubation of the membrane with the labeled protein. In parallel, the membranes can also be incubated with the WT enzyme in dephosphorylation buffer (TBST) that contains 1 mM DTT. After the bound PTP is removed by extensive washes in PBS containing 0.1% Tween, western blotting can be performed using anti-p-Tyr antibodies.

3.5 Validation

Having identified a likely substrate of any specific PTP based on enhanced interaction with STM using the methods mentioned above, it is important that experiments are carried out to prove that the interacting protein is a substrate of the PTP. Some of the methods are detailed below.

3.5.1 In Vitro Dephosphorylation

This is carried out by immunoprecipitating cellular or exogenously expressed protein from HEK293 cells after treatment with PV, or expression of a tyrosine kinase known to phosphorylate the specific protein. Purified recombinant PTP or mutant PTP is incubated with the immunoprecipitated protein and the agarose-bound complexes are examined by western blotting with anti-p-Tyr antibodies followed by antibodies that detect the target protein. If the level of tyrosine phosphorylation on the target protein is significantly lower in the presence of WT enzyme compared to the mutant, it provides evidence that the protein is a substrate of the PTP.

3.5.2 In Vivo Dephosphorylation

This can be examined both by western blotting methods and by immunofluorescence. If phospho-specific antibodies that recognize the target site of the substrate are available, the effect of the ability of the active phosphatase to dephosphorylate the target can be examined directly. Cells can be transfected with WT or mutant PTP and subjected to PV treatment or an agonist that is known to result in tyrosine phosphorylation of the substrate. Cell lysates prepared 24–48 h after transfection are subjected to western blotting with the phospho-site-specific antibody followed by deprobing and blotting using antibody to detect the target protein. Reduced phosphorylation of the target seen in cells expressing WT enzyme compared to control vector-transfected cells would confirm that the protein is a specific cellular target of the PTP. In the event that phospho-site-specific antibodies are not available, the lysates may be subjected to immunoprecipitation using antibodies against the proposed substrate and examined using anti-p-Tyr antibodies. If cells expressing the mutant enzyme show enhanced levels of p-Tyr on the target protein compared to vector-transfected cells, it would also indicate that the mutant functions as a dominant negative and inhibits the activity of the cellular enzyme. True intracellular substrates are best identified using dominant-negative mutants, as

overexpressed enzymes have the possibility of dephosphorylating nonphysiological substrates.

Very often, PTP substrates are phosphorylated on more than one tyrosine residue and it is important to identify which of the residues are dephosphorylated by a specific enzyme. This is carried out by site-directed mutagenesis of the target tyrosines to phenylalanine. Co-transfection with the WT and mutant PTP is carried out and phosphorylation status examined using either phospho-site-specific or p-Tyr antibodies as described earlier. Tyrosine phosphorylation often results in altered mobility of the polypeptides on SDS-PAGE. Detection of a slower moving band upon western blotting has in some instances been used to study dephosphorylation by a PTP [46].

Validation of the interacting partner as an in vivo substrate can also be carried out in situ using phospho-specific antibodies. The WT or mutant PTP is transfected in cells plated on cover slips, and indirect immunofluorescence (IIF) is carried out using phospho-site-specific antibodies and fluorescent secondary antibodies. This method has the advantage of showing the subcellular site of action of the phosphatase (Fig. 5). For IIF, Cos-1 cells are plated on cover slips and grown for 24 h to achieve 70% confluency. Transfection is carried out using 400 ng of GFP-tagged WT or STM PTP and after 30 h fixed (in 4% formaldehyde in PBS) for 10 min at room temperature. After three washes in PBS, permeabilization is done by exposing cells to PBS containing 0.5% Triton X-100 and 0.05% Tween-20 for 6 min. The cover slips are rinsed thrice in PBS and incubated with 2% BSA in PBS for 1 h at room temperature. The phospho-site-specific antibody that recognizes the phosphorylated substrate is diluted in 2% BSA and added to cover slips for 2 h at room temperature or overnight at 4 °C. After washing with PBS, cells are incubated with Cy3 (or any other appropriate fluorophore) conjugated secondary antibody diluted in 2% BSA for 1 h, at room temperature. Cells are washed and mounted on clean glass slides using mountant containing 90% glycerol, 1 mg/ml of paraphenylenediamine, and 0.5 μg/ml DAPI in PBS (*see* **Note 12**).

In vivo substrates can also be validated using FRET and BRET methods. Constructs are generated where the STM-PTP is fused to YFP and the substrate/interacting partner to be validated fused to Renilla-luciferase. When cotransfected into cells, luminescence from the substrate will excite the YFP in the PTP if they are localized within 100°A of each other. These assays confirm intracellular interactions and also facilitate the understanding of subcellular site of action and dynamics of the interactions [47].

An additional approach to validate the ability of a PTP to dephosphorylate a particular substrate is by examining dephosphorylation in the presence or absence of Na_3VO_4 [16, 48]. Vanadate is a p-Tyr mimetic and can be used in in vitro dephosphorylation assays to block the substrate from binding to the PTP.

The GST-PTP-STM is incubated with 1 mM Na_3VO_4 for 10 min prior to adding to the cell lysates in interaction experiments. EDTA is not added to the buffers when vanadate competition is being tested. The decrease/loss of interaction in the presence of vanadate indicates direct interaction between the enzyme and the target.

In addition to using dominant-negative or STM mutants, it is important to confirm substrate specificity of the PTP in the physiological context by using knockdown strategies like antisense RNA, RNAi, or genetic knockouts. STM mutants can also be used to generate transgenic mice to study the role of the PTP in distinct tissue systems.

3.6 Limitations and Cautions

The approach of using STM to identify targets of PTPs is not without limitations. Some of the issues to be kept in mind are mentioned here. One drawback of using STM overexpression is that formation of a stable enzyme-substrate complex in cells may affect downstream signaling and prevent identification of alternate substrates within the cell.

The constitutive expression levels of a PTP substrate may be low in specific cell types and pull down using a STM may not yield results. Under these circumstances, putative substrates need to be overexpressed along with the STM-PTP and interaction experiments carried out after ensuring their proper subcellular localization. The in vitro interaction experiments using overexpressed recombinant proteins are likely to show nonspecific binding. It is important to use appropriate controls for comparison like untreated and PV-treated cell lysates. The blots can also be probed with an antibody to an abundant cellular protein like actin to make sure that it is not present in the pull-down samples.

Very often, expression of STM has been used to dominantly inhibit the function of a specific intracellular PTP. In some instances, STMs do not alter downstream signaling and functional consequence of their expression is similar to that of the WT enzyme. A good example has been the D181A mutant of PTP1B, which inhibits dephosphorylation of its substrate Bcr-Abl but blocks downstream signaling of Bcr-Abl by disabling its interaction with Grb2 [26]. Some STMs can trap substrates from cell lysates, but are unable to pull down complexes in the cellular context [19]. In some cases a mutant may function as a good substrate trap when generated in the truncated catalytic domain, but functions poorly when generated in the full-length enzyme—e.g., PTP-PEST [9].

It is also to be kept in mind that proteins from PV-treated cell lysates that complex with the PTP need not be substrates. Interaction could be between p-Tyr on a protein that interacts with noncatalytic domains of the PTP—e.g., SH-PTP. These can be identified as they would show similar interaction with WT or STM.

Some proteins are phosphorylated on more than one tyrosine, and require the action of more than one phosphatase, sometimes

resulting in opposing consequences [7]. Under these circumstances, identifying enzymes that selectively increase phosphorylation of one or the other residues using STM requires cautious interpretation of results. Examining dephosphorylation in response to physiological stimuli is important as a single substrate (e.g., p130Cas) may be dephosphorylated by many PTPs (e.g., PTP1B, LAR, PTP-PEST) based on the cell type and context.

3.7 Future Perspectives

Presently, we are far from having a complete map of the interactome and also knowledge of all the substrates for many of the PTPs. A combination of approaches including use of novel strategies is therefore warranted [50–52]. High-density phosphopeptide chips have been designed to be used with STM to identify targets. Quantitative proteomics can be used to identify a large number of cellular substrates by comparing tyrosine phosphorylated peptides from knockout or STM-expressing cells and WT cells [53]. This approach can be used for many of the PTPs whose function in distinct signaling pathways has not been elucidated. Other developments have been the use of a battery of STM mutants (corresponding to a large number of known PTPs) to identify which of them interacts with a specific protein phosphorylated on tyrosine. This approach has successfully been used to identify novel PTPs that target insulin receptor [54].

In addition to the 38 PTPs identified in the human genome, there are 12 pseudogenes, which have all the catalytic features of the PTPs, but lack catalytic activity due to mutations. Lately, these molecules have also been shown to have physiological functions [55]. Identifying their interacting partners and studying their function have raised challenges for design of novel strategies. PTPs and their defined targets coupled with fluorescent tags can help in understanding the dynamics of their interaction in the subcellular context [47]. It is hoped that the coming years will give us dynamic cellular maps of context-based activation of PTPs and dephosphorylation of their substrates.

Because of their ability to modulate signaling pathways, deregulated PTPs involved in disease are good therapeutic targets [56]. This is evident from examples of targeting PTP1B in type 2 diabetes and obesity. Due to high conservation of the PTP catalytic domain, it has been difficult to develop small molecules inhibiting the individual enzymes. Use of STM in viral expression systems and inducible expression to efficiently target all the cells in the tissue of interest should be possible in the near future [57]. Under certain conditions, use of dominant-negative mutants has been more effective in disabling the function of a certain molecule than knockdown strategies (like antisense siRNA) which may not remove the protein totally [58]. Due to the high specificity with which STM and dominant-negative strategies work, at least as proof of principle, they could be used therapeutically with success.

In some cases, mutations that render a PTP catalytically inactive or constitutively active have been found to be associated with specific disorders [59, 60]. Devising means to therapeutically intervene to either enhance or inhibit PTP activity is a challenge for the future.

4 Notes

1. All the western blotting steps for detection of phospho-antibodies are carried out with blocking solution containing 2% BSA and phosphatase inhibitors (1 mM Na_3VO_4 and 10 mM NaF).
2. The efficacy of the STM also depends on whether the mutation has been made in the full-length enzyme or in the catalytic domain alone [9]. Expression level of a specific substrate and its phosphorylation status determine the ability of a PTP to dephosphorylate it in various contexts. Low-abundance proteins require the use of overexpression systems and also genetic and proteomic approaches. When experiments are carried out with overexpressed proteins, care should be taken about mislocalization and nonspecific interactions due to overexpression. Substrates identified by these methods should be validated by knockdown strategies like RNAi or using physiological stimuli that activate the phosphatase.
3. If induction is poor, or the protein forms inclusion bodies, cells could be induced overnight at 28 °C with 0.1 mM IPTG.
4. The presence of DTT will prevent the catalytic site cysteine from getting oxidized and disable the PTP from interacting with its substrates.
5. Air bubbles between layers of filter paper and the gel are to be avoided. Longer transfer is required for high-molecular-weight proteins.
6. Bands are detected by exposing to X-ray film or using the chemiluminescence imaging equipment.
7. If interest is in proteins bound to cellular structures, lysis can be done in 2× IP buffer and diluted to 1× prior to antibody addition, or lysed in RIPA buffer, which has additional detergents. RIPA buffer: 50 mM Tris pH 7.4, 150 mM NaCl, 0.1% SDS, 0.5% sodium deoxycholate, 1% Triton X 100 or NP-40, and protease inhibitors.
8. GFP-coupled agarose beads can be used if the PTP is tagged with GFP.
9. When IP samples are being prepared for MS analysis, it is recommended that Triton in the IP lysis buffer is replaced by lauryl maltoside, which solubilizes protein complexes well and is easier to remove prior to MS analysis.

10. For CBB staining, a modified method is recommended when samples are to be processed for MS analysis [49]. Proteins are fixed with 10% phosphoric acid, 10% methanol, and 40% ethanol for 1 h, and treated with 1% phosphoric acid and 10% ammonium sulfate solution for 2 h. The gels are stained with a solution consisting of 5% aluminum sulfate 14–18 hydrate, 10% ethanol, 0.02% of CBB G-250, and 8% phosphoric acid for 3 h, and destained for 30 min in a solution containing 2% phosphoric acid and 10% ethanol.
11. Use a fresh zip-tip for each sample.
12. Antibody incubations are carried out by placing the cover slips on parafilm in a humid chamber, and washes are made in 35 mm dishes.

Acknowledgements

Work in VR's lab is supported by grants from DST (SR/SO/BB-0087/2012), DBT (BT/PR11921/BRB/10/698/2009), and CSIR (BSC 0108, BSC 0115, and BSC 0111). I thank Dr. Ghanshyam Swarup and Dr. E. Prem Kumar Reddy for gift of plasmids used in experiments mentioned in this chapter, and Dr. Kunal Dayma for assistance in preparing the manuscript and figures.

References

1. Fauman EB, Saper MA (1996) Structure and function of the protein tyrosine phosphatases. Trends Biochem Sci 21(11):413–417
2. Tiganis T, Bennett AM (2007) Protein tyrosine phosphatase function: the substrate perspective. Biochem J 402(1):1–15
3. Alonso A, Sasin J, Bottini N, Friedberg I, Friedberg I, Osterman A, Godzik A, Hunter T, Dixon J, Mustelin T (2004) Protein tyrosine phosphatases in the human genome. Cell 117(6):699–711
4. Tonks NK (2013) Protein tyrosine phosphatases--from housekeeping enzymes to master regulators of signal transduction. FEBS J 280(2):346–378
5. Mustelin T, Tasken K (2003) Positive and negative regulation of T-cell activation through kinases and phosphatases. Biochem J 371(Pt 1):15–27
6. Swarup G, Radha V (1992) Protein tyrosine phosphatases as regulators of proten kinase activity. Curr Sci 62:462–469
7. Roskoski R Jr (2005) Src kinase regulation by phosphorylation and dephosphorylation. Biochem Biophys Res Commun 331(1):1–14
8. Selner NG, Luechapanichkul R, Chen X, Neel BG, Zhang ZY, Knapp S, Bell CE, Pei D (2014) Diverse levels of sequence selectivity and catalytic efficiency of protein-tyrosine phosphatases. Biochemistry 53(2):397–412
9. Garton AJ, Burnham MR, Bouton AH, Tonks NK (1997) Association of PTP-PEST with the SH3 domain of p130cas; a novel mechanism of protein tyrosine phosphatase substrate recognition. Oncogene 15(8):877–885
10. Zhang ZY, Wang Y, Dixon JE (1994) Dissecting the catalytic mechanism of protein-tyrosine phosphatases. Proc Natl Acad Sci U S A 91(5):1624–1627
11. Jia Z, Barford D, Flint AJ, Tonks NK (1995) Structural basis for phosphotyrosine peptide recognition by protein tyrosine phosphatase 1B. Science 268(5218):1754–1758
12. Tian W, Qu L, Meng L, Liu C, Wu J, Shou C (2012) Phosphatase of regenerating liver-3 directly interacts with integrin beta1 and regulates its phosphorylation at tyrosine 783. BMC Biochem 13:22
13. Mercan F, Bennett AM (2010) Analysis of protein tyrosine phosphatases and substrates. Curr Protoc Mol Biol. Chapter 18:Unit 18. 16

14. Boubekeur S, Boute N, Pagesy P, Zilberfarb V, Christeff N, Issad T (2011) A new highly efficient substrate-trapping mutant of protein tyrosine phosphatase 1B (PTP1B) reveals full autoactivation of the insulin receptor precursor. J Biol Chem 286(22):19373–19380
15. Agazie YM, Hayman MJ (2003) Development of an efficient "substrate-trapping" mutant of Src homology phosphotyrosine phosphatase 2 and identification of the epidermal growth factor receptor, Gab1, and three other proteins as target substrates. J Biol Chem 278(16): 13952–13958
16. Flint AJ, Tiganis T, Barford D, Tonks NK (1997) Development of "substrate-trapping" mutants to identify physiological substrates of protein tyrosine phosphatases. Proc Natl Acad Sci U S A 94(5):1680–1685
17. Blanchetot C, Chagnon M, Dube N, Halle M, Tremblay ML (2005) Substrate-trapping techniques in the identification of cellular PTP targets. Methods 35(1):44–53
18. Xie L, Zhang YL, Zhang ZY (2002) Design and characterization of an improved protein tyrosine phosphatase substrate-trapping mutant. Biochemistry 41(12):4032–4039
19. Zhang SH, Liu J, Kobayashi R, Tonks NK (1999) Identification of the cell cycle regulator VCP (p97/CDC48) as a substrate of the band 4.1-related protein-tyrosine phosphatase PTPH1. J Biol Chem 274(25):17806–17812
20. Merritt R, Hayman MJ, Agazie YM (2006) Mutation of Thr466 in SHP2 abolishes its phosphatase activity, but provides a new substrate-trapping mutant. Biochim Biophys Acta 1763(1):45–56
21. Qiu W, Wang X, Romanov V, Hutchinson A, Lin A, Ruzanov M, Battaile KP, Pai EF, Neel BG, Chirgadze NY (2014) Structural insights into Noonan/LEOPARD syndrome-related mutants of protein-tyrosine phosphatase SHP2 (PTPN11). BMC Struct Biol 14:10
22. Scapin G, Patel S, Patel V, Kennedy B, Asante-Appiah E (2001) The structure of apo protein-tyrosine phosphatase 1B C215S mutant: more than just an S→O change. Protein Sci 10(8): 1596–1605
23. Berchtold S, Volarevic S, Moriggl R, Mercep M, Groner B (1998) Dominant negative variants of the SHP-2 tyrosine phosphatase inhibit prolactin activation of Jak2 (janus kinase 2) and induction of Stat5 (signal transducer and activator of transcription 5)-dependent transcription. Mol Endocrinol 12(4):556–567
24. Timms JF, Carlberg K, Gu H, Chen H, Kamatkar S, Nadler MJ, Rohrschneider LR, Neel BG (1998) Identification of major binding proteins and substrates for the SH2-containing protein tyrosine phosphatase SHP-1 in macrophages. Mol Cell Biol 18(7):3838–3850
25. Cong F, Spencer S, Cote JF, Wu Y, Tremblay ML, Lasky LA, Goff SP (2000) Cytoskeletal protein PSTPIP1 directs the PEST-type protein tyrosine phosphatase to the c-Abl kinase to mediate Abl dephosphorylation. Mol Cell 6(6):1413–1423
26. LaMontagne KR Jr, Hannon G, Tonks NK (1998) Protein tyrosine phosphatase PTP1B suppresses p210 bcr-abl-induced transformation of rat-1 fibroblasts and promotes differentiation of K562 cells. Proc Natl Acad Sci U S A 95(24):14094–14099
27. Chang Y, Ceacareanu B, Zhuang D, Zhang C, Pu Q, Ceacareanu AC, Hassid A (2006) Counter-regulatory function of protein tyrosine phosphatase 1B in platelet-derived growth factor- or fibroblast growth factor-induced motility and proliferation of cultured smooth muscle cells and in neointima formation. Arterioscler Thromb Vasc Biol 26(3):501–507
28. Chang HH, Tai TS, Lu B, Iannaccone C, Cernadas M, Weinblatt M, Shadick N, Miaw SC, Ho IC (2012) PTPN22.6, a dominant negative isoform of PTPN22 and potential biomarker of rheumatoid arthritis. PLoS One 7(3), e33067
29. Kharitidi D, Manteghi S, Pause A (2014) Pseudophosphatases: methods of analysis and physiological functions. Methods 65(2): 207–218
30. Zhang YL, Yao ZJ, Sarmiento M, Wu L, Burke TR Jr, Zhang ZY (2000) Thermodynamic study of ligand binding to protein-tyrosine phosphatase 1B and its substrate-trapping mutants. J Biol Chem 275(44):34205–34212
31. Mitra A, Sasikumar K, Parthasaradhi BV, Radha V (2013) The tyrosine phosphatase TC48 interacts with and inactivates the oncogenic fusion protein BCR-Abl but not cellular Abl. Biochim Biophys Acta 1832(1):275–284
32. Ren Y, Meng S, Mei L, Zhao ZJ, Jove R, Wu J (2004) Roles of Gab1 and SHP2 in paxillin tyrosine dephosphorylation and Src activation in response to epidermal growth factor. J Biol Chem 279(9):8497–8505
33. Wu J, Katrekar A, Honigberg LA, Smith AM, Conn MT, Tang J, Jeffery D, Mortara K, Sampang J, Williams SR et al (2006) Identification of substrates of human protein-tyrosine phosphatase PTPN22. J Biol Chem 281(16):11002–11010
34. Fukada M, Kawachi H, Fujikawa A, Noda M (2005) Yeast substrate-trapping system for isolating substrates of protein tyrosine phosphatases: Isolation of substrates for protein tyrosine phosphatase receptor type z. Methods 35(1): 54–63

35. Tautz L, Critton DA, Grotegut S (2013) Protein tyrosine phosphatases: structure, function, and implication in human disease. Methods Mol Biol 1053:179–221
36. Swarup G, Speeg KV Jr, Cohen S, Garbers DL (1982) Phosphotyrosyl-protein phosphatase of TCRC-2 cells. J Biol Chem 257(13): 7298–7301
37. Huyer G, Liu S, Kelly J, Moffat J, Payette P, Kennedy B, Tsaprailis G, Gresser MJ, Ramachandran C (1997) Mechanism of inhibition of protein-tyrosine phosphatases by vanadate and pervanadate. J Biol Chem 272(2):843–851
38. Pasquali C, Vilbois F, Curchod ML (2000) Hooft van Huijsduijnen R, and Arigoni F. Mapping and identification of protein-protein interactions by two-dimensional far-Western immunoblotting. Electrophoresis 21(16): 3357–3368
39. Mitra A, Kalayarasan S, Gupta V, Radha V (2011) TC-PTP dephosphorylates the guanine nucleotide exchange factor C3G (RapGEF1) and negatively regulates differentiation of human neuroblastoma cells. PLoS One 6(8), e23681
40. Chang YC, Lin SY, Liang SY, Pan KT, Chou CC, Chen CH, Liao CL, Khoo KH, Meng TC (2008) Tyrosine phosphoproteomics and identification of substrates of protein tyrosine phosphatase dPTP61F in Drosophila S2 cells by mass spectrometry-based substrate trapping strategy. J Proteome Res 7(3):1055–1066
41. Liang F, Kumar S, Zhang ZY (2007) Proteomic approaches to studying protein tyrosine phosphatases. Mol Biosyst 3(5):308–316
42. Kawachi H, Fujikawa A, Maeda N, Noda M (2001) Identification of GIT1/Cat-1 as a substrate molecule of protein tyrosine phosphatase zeta /beta by the yeast substrate-trapping system. Proc Natl Acad Sci U S A 98(12):6593–6598
43. Zhang ZY, Thieme-Sefler AM, Maclean D, McNamara DJ, Dobrusin EM, Sawyer TK, Dixon JE (1993) Substrate specificity of the protein tyrosine phosphatases. Proc Natl Acad Sci U S A 90(10):4446–4450
44. Pellegrini MC, Liang H, Mandiyan S, Wang K, Yuryev A, Vlattas I, Sytwu T, Li YC, Wennogle LP (1998) Mapping the subsite preferences of protein tyrosine phosphatase PTP-1B using combinatorial chemistry approaches. Biochemistry 37(45):15598–15606
45. Vetter SW, Keng YF, Lawrence DS, Zhang ZY (2000) Assessment of protein-tyrosine phosphatase 1B substrate specificity using "inverse alanine scanning". J Biol Chem 275(4): 2265–2268
46. Muppirala M, Gupta V, Swarup G (2012) Tyrosine phosphorylation of a SNARE protein, syntaxin 17: implications for membrane trafficking in the early secretory pathway. Biochim Biophys Acta 1823(12):2109–2119
47. Boute N, Boubekeur S, Lacasa D, Issad T (2003) Dynamics of the interaction between the insulin receptor and protein tyrosine-phosphatase 1B in living cells. EMBO Rep 4(3):313–319
48. Palka HL, Park M, Tonks NK (2003) Hepatocyte growth factor receptor tyrosine kinase met is a substrate of the receptor protein-tyrosine phosphatase DEP-1. J Biol Chem 278(8):5728–5735
49. Pink M, Verma N, Rettenmeier AW, Schmitz-Spanke S (2010) CBB staining protocol with higher sensitivity and mass spectrometric compatibility. Electrophoresis 31(4):593–598
50. He R, Zeng LF, He Y, Zhang S, Zhang ZY (2013) Small molecule tools for functional interrogation of protein tyrosine phosphatases. FEBS J 280(2):731–750
51. Zhang ZY (2005) Functional studies of protein tyrosine phosphatases with chemical approaches. Biochim Biophys Acta 1754(1-2):100–107
52. Cote JF, Charest A, Wagner J, Tremblay ML (1998) Combination of gene targeting and substrate trapping to identify substrates of protein tyrosine phosphatases using PTP-PEST as a model. Biochemistry 37(38):13128–13137
53. Mertins P, Eberl HC, Renkawitz J, Olsen JV, Tremblay ML, Mann M, Ullrich A, Daub H (2008) Investigation of protein-tyrosine phosphatase 1B function by quantitative proteomics. Mol Cell Proteomics 7(9):1763–1777
54. Walchli S, Curchod ML, Gobert RP, Arkinstall S (2000) and Hooft van Huijsduijnen R. Identification of tyrosine phosphatases that dephosphorylate the insulin receptor. A brute force approach based on "substrate-trapping" mutants. J Biol Chem 275(13):9792–9796
55. Tonks NK (2009) Pseudophosphatases: grab and hold on. Cell 139(3):464–465
56. He RJ, Yu ZH, Zhang RY, Zhang ZY (2014) Protein tyrosine phosphatases as potential therapeutic targets. Acta Pharmacol Sin 35(10):1227–1246
57. Bergeron S, Dubois MJ, Bellmann K, Schwab M, Larochelle N, Nalbantoglu J, Marette A (2011) Inhibition of the protein tyrosine phosphatase SHP-1 increases glucose uptake in skeletal muscle cells by augmenting insulin receptor signaling and GLUT4 expression. Endocrinology 152(12):4581–4588
58. Song DD, Chen Y, Li ZY, Guan YF, Zou DJ, Miao CY (2013) Protein tyrosine phosphatase 1B inhibits adipocyte differentiation and mediates TNFalpha action in obesity. Biochim Biophys Acta 1831(8):1368–1376

59. Xu D, Zheng H, Yu WM, Qu CK (2013) Activating mutations in protein tyrosine phosphatase Ptpn11 (Shp2) enhance reactive oxygen species production that contributes to myeloproliferative disorder. PLoS One 8(5), e63152

60. Goebel-Goody SM, Baum M, Paspalas CD, Fernandez SM, Carty NC, Kurup P, Lombroso PJ (2012) Therapeutic implications for striatal-enriched protein tyrosine phosphatase (STEP) in neuropsychiatric disorders. Pharmacol Rev 64(1):65–87

Chapter 15

Detection and Identification of Ligands for Mammalian RPTP Extracellular Domains

Andrew William Stoker

Abstract

Receptor protein tyrosine phosphatases (RPTPs) form a group of over 20 enzymes in vertebrates, each with unique ectodomains subject to potential extracellular interactions with ligands. It has recently become clear that a remarkably diverse range of ligands exist, including homophilic binders, adhesion molecules, neurotrophin receptors, and proteoglycans. Individual RPTPs can bind several ligands, and vice versa, suggesting that complex cell signaling networks exist. The identification of RPTP ligands and where they are located in tissues remains a challenge for a large number of these enzymes. Here we describe some powerful methods that have proved successful for several research groups, leading to our improved understanding of RPTP-ligand interactions and functional regulation.

Key words RPTP, Receptor tyrosine phosphatase, Affinity probe, RAP assay, Placental alkaline phosphatase, Ligand, Affinity chromatography, Hippocampal neuron, Synapse, Neurite

1 Introduction

The sequencing of the first cytoplasmic protein tyrosine phosphatase (PTP) PTP1b in 1989 confirmed that the catalytic domain of PTP1b was highly related to similar domains in two receptor-like protein tyrosine phosphatases (RPTPs), LAR and CD45 [1–3]. The mindset prior to the discovery of RPTPs had been that PTP enzymes were likely to be cytoplasmic scavengers of tyrosine phosphate, and few researchers had envisaged receptor versions of the enzymes. It was therefore an exciting prospect to realize that RPTPs could be subject to extracellular regulation and be directly involved in cell signaling. There has been a fascination ever since with the potential functions of RPTPs and in particular how, or if, these enzymes are controlled by ligands that bind to their ectodomains. There are 20 RPTP proteins encoded in human genome, with many orthologues in other vertebrates and invertebrates, raising the possibility of a wide range of such ligands.

Rafael Pulido (ed.), *Protein Tyrosine Phosphatases: Methods and Protocols*, Methods in Molecular Biology, vol. 1447,
DOI 10.1007/978-1-4939-3746-2_15,

In recent years a number of ligands have been identified and it is becoming clear that RPTPs bind to these *in trans* and sometimes *in cis*. RPTP ectodomains can also send signals to other cells [4], reminiscent of EphR and Ephrin signaling [5]. RPTPs could therefore be both ligand and receptor. In the methods below, therefore, we will use the term "ligand" for simplicity, although "binding partner" may be more appropriate in some cases.

There was initially some difficulty with identifying RPTP ligands, in part due to the almost complete lack of functional assays. Also, in contrast to RPTKs, we now know that most RPTP ligands are not usually small growth factor-like molecules, but rather they are usually large, often highly glycosylated matrix molecules or cell-associated receptors; these can be hard to identify by traditional affinity purification and expression cloning methods. Some RPTPs, in particular those of the type IIB subfamily, not only bind to themselves [6], but also form complexes with cadherins to regulate cell-cell adhesion [7, 8]. Heterophilic ligands of other RPTP subfamilies include proteoglycans, contactins, receptor tyrosine kinases, and a number of leucine-rich repeat (LRR) family receptors in neurons [4]. Some ligands also bind several RPTP members and individual RPTPs can have several related or distinct ligands, adding to the many signaling combinations available.

Some RPTP ligands were identified from affinity panning methods or affinity binding or chromatography, using affinity probes made from RPTP ectodomains linked to placental alkaline phosphatase (PLAP) [9], Fc dimers [10] (*see* **Note 1**), or cross-linked directly to affinity resins [11, 12]. More recently, functional assays of synaptogenesis have revealed a new range of ligands for RPTPs, such as TrkC and other LRR family proteins in synapses [13–17]. In some cases we now know how ligands bind structurally to RPTP ectodomains [12, 18] and how ligands alter the function of the associated RPTPs [14, 19, 20].

It has taken 25 years to get to this point, but many more ligands remain to be identified. This chapter presents some examples of ligand identification and tissue localization methods that have been previously employed and could still bear fruit in future. We will describe (1) use of affinity probes based on RPTP ectodomains linked to PLAP or Fc, (2) use of affinity-purified RPTP ectodomains as bait in affinity column purification of ligands, and (3) use of a hippocampal neuron coculture system for validating synaptic partners of RPTPs. Several research groups have successfully used these separately, sequentially, and sometimes concurrently. Note that we have reviewed some of these methods in 2005 and further details can be found in that document [21]. As a word of caution, these methods have worked well for some RPTPs, but they have not worked for all those tested. One stumbling block can be in the generation of sufficient RPTP ectodomain protein for these assays. We therefore suggest caution when planning

ligand-hunting studies and we recommend initial feasibility tests for fusion protein production. After this, we recommend use of more than one ligand identification approach. Lastly, the value of functional assays in these kinds of studies cannot be overstated.

2 Materials

2.1 Generating PLAP Fusion Proteins

1. HEK293T or Cos7 cell lines for transfection and high-level protein production.
2. Complete DMEM medium: DMEM, 10% fetal bovine serum, penicillin and streptomycin mixture for tissue culture (optional).
3. 200 mM 4-Nitrophenyl disodium orthophosphate (pNPP) in water.
4. A solution of 2 M diethanolamine, 1 mM $MgCl_2$.
5. Transfection reagent polyethlyenimine (PEI); 25 kDa branched form (CAS number 9002-98-6; this is a *highly* viscous solution and cannot be directly pipetted). Stocks are made in water at 100 mg/ml and stirred for potentially several days. Before use on cells, dilute the stock to 1 mg/ml in water and adjust pH to 7 with HCl; sterile filter and freeze aliquots.
6. Optimem serum-free medium.
7. Expression plasmids encoding PLAP fusion proteins, for use in mammalian cells (commercial source: http://www.genhunter.com/products/aptag/; you may also be able to obtain vectors from research groups directly).
8. Large-scale plasmid purification kits.

2.2 Performing RAP Assays and Affinity Chromatography

1. Fisherbrand™ Superfrost™ Plus microscope slides.
2. A stock of culture supernatant containing RPTP ectodomain-PLAP fusion protein (or Fc fusion protein).
3. Nitroblue tetrazolium (NBT)/5-bromo-4-chloro-3-indolyl phosphate (BCIP) stock solution: 18.75 mg/ml NBT, 9.4 mg/ml BCIP dissolved in 67% (v/v) DMSO; or commercial equivalent.
4. Anti-placental alkaline phosphatase-agarose.
5. Cyanogen bromide-activated-Sepharose® 4B.
6. PD10 desalting columns.
7. Cells or tissues from which to purify ligands.
8. Lysis buffer for cells and tissues: Here we have used: 1% Triton X100, 150 mM NaCl, Tris HCl pH 7.0, protease inhibitor cocktail (Roche).
9. 2× SEAP buffer: 2 M Diethanolamine; 1 mM $MgCl_2$.

10. AP buffer: 100 mM Tris–HCl, pH 9.5, 50 mM $MgCl_2$, 100 mM NaCl.
11. Slide wash buffer: HBSS, 20 mM Hepes pH 7.0, 0.5 mg/ml BSA.
12. A suitable FPLC setup such as AKTA FPLC system (Amersham Biosciences).

2.3 Performing Hippocampal-Cos7 Coculture

1. A source of rat hippocampal neurons from P1 rat pups.
2. Cos7 cells for transfection.
3. Transfection reagents as above.
4. Tissue culture media DMEM as above.
5. Microscope capable of phase contrast and multichannel fluorescence detection of common fluorophores such as FITC, Cy3, Cy5, and fluorescent proteins such as GFP, CFP, YFP, and RFP.
6. Round, glass cover slips.
7. Concentrated nitric acid.
8. Poly-L-lysine hydrobromide.
9. Phosphate-buffered saline (PBS): 1.85 mM NaH_2PO_4, 8.4 mM $NaHPO_4$, and 150 mM NaCl.
10. Trypsin/EDTA mixture (1× in PBS).
11. Plastic tissue culture dishes or multiwell plates.

3 Methods

3.1 Receptor Affinity Probing (RAP): In Situ Detection of Ligands in Cells and Tissues

In this approach, known often as RAP, one uses an RPTP affinity probe to identify the tissue location of ligands (or binding partners). The affinity probes are based on fusion proteins between RPTP ectodomains and either PLAP or Fc. As our experience is with PLAP fusion proteins, these will be the main focus of this review. PLAP and Fc probes have been used successfully for receptor tyrosine kinases [22] and these were also used early on in identifying contactin as a PTPζ ligand [10], and more recently for identifying HSPGs as PTPσ ligands [23, 24], Slitrk3 as a ligand for several PTPσ [16], and TrkC as a ligand for PTPσ [14]. As ligand binding is affected by affinity and avidity effects, this approach has not worked for every RPTP tried to date (*see* **Note 2**), but in successful cases it has proved very useful. If you have problems making successful RPTP probes, ligand-based probes may instead be useful (*see* **Note 3**).

1. *Making an affinity probe*. You must first identify which region of the RPTP ectodomain cDNA sequence is to be sub-cloned. It must lack the predicted transmembrane domain and PCR primers should be designed so that the product can be cloned

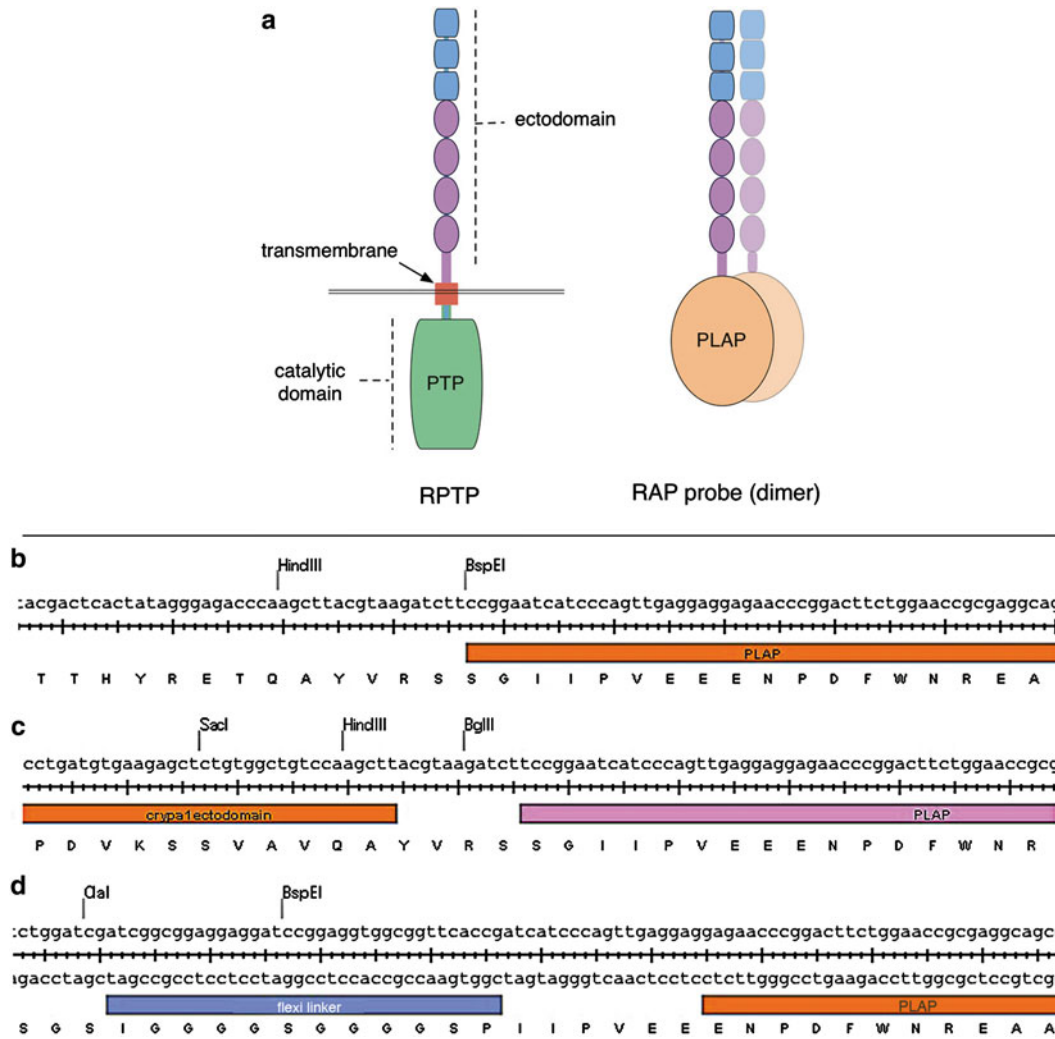

Fig. 1 (**a**) Schematic diagram of a PLAP fusion protein with the PTPσ ectodomain. This short isoform of PTPσ has four FNIII-like domains (*purple*) and three Ig-like (*blue*) domains, linked via a transmembrane domain to the catalytic domain. On the right of the figure, PLAP is shown fused to the juxtamembrane region of PTPσ; this probe will form as a dimer due to the obligate dimeric state of PLAP. (**b**–**d**) Example DNA sequences and amino acid coding frames of PLAP vectors, showing (**b**) the fusion point amino-terminal to PLAP in APTag2 [25], (**c**) the CRYPα1 (chick PTPσ) ectodomain fusion point to PLAP [23, 28], (**d**) the PLAP fusion region, but with a flexible glycine-rich linker upstream [31]. (**b**–**d**) were generated using Seqbuilder software (DNASTAR®)

in-frame with PLAP (Fig. 1). Matching the cDNA species to your cells and tissues is advised (*see* **Note 4**). Fusion to Fc can also be used, but there may be subtle differences in binding properties with Fc and PLAP probes (*see* **Note 5**). PLAP should generally be carboxy-terminal to the PTP ectodomain. Suitable expression vectors such as APTag-2 and APTag-4 were originally designed by John Flanagan [25] and have been modified by other laboratories. Examples of fusion cloning sites

are shown in Fig. 1; cloning sites are quite limited, however, making cDNA insertion difficult in some cases. Basic vectors can be obtained commercially from GeneHunter (http://www.genhunter.com/products/aptag/). Note that the original technology and vectors are patented and permission to acquire or pass on vectors requires appropriate permission. You will also need a vector that expresses a secretable form of PLAP alone (e.g., APtag-4), for use in *negative control* assays. Since PLAP (and Fc) are dimeric, it is worth considering making more than one probe, with different fusion points in the RPTP sequence (*see* **Note 6**). Once the RPTP-PLAP fusion plasmid is constructed, it should be sequenced to verify the encoded ectodomain and fusion points to PLAP. Purify the plasmid at high quality for transfection, using Qiagen plasmid kits.

2. *Generation of fusion proteins.* To generate fusion protein, first plate HEK293T cells in flasks or standard tissue culture plates in complete DMEM medium. Plate cells so that they will be at 80% confluency when transfected the next day. We recommend using at least one 25 cm^2 flask for this, to generate sufficient fusion protein for direct affinity detection work. Use several 175 cm^2 flasks for fusion protein purification. Transfect the plasmid DNA using the polethylenimine (PEI) method (for specific method, *see* ref. [26]). For a 175 cm^2 flask, transfect 50 μg of plasmid DNA (scale up or down accordingly). Add DNA to 5 ml of serum-free medium (e.g., Optimem), mix, then add 75 μl PEI stock (1 mg/ml), and vortex briefly. Incubate the mixture for 10 min at room temperature. The optimal DNA:PEI ratio is between 1:1.5 and 1:2 [26]. While the complexes form, change the cell media to 2% serum (e.g., 20 ml for a 175 cm^2 flask). Then add the DNA mixture dropwise to the flask and mix continuously; culture at 37 °C for 4–5 days. The production of PLAP fusion protein in the supernatant can be assayed daily using a pNPP assay (see below and [27]). Collect the final media, sterile filter it, and add HEPES pH 7.4 to a final concentration of 20 mM; store this then at 4 °C. When storing for several days and using aliquots, we recommend adding 0.1% sodium azide to prevent bacterial growth (this does not affect PLAP activity). Some probes are adversely affected by glycosylation and there are methods to address this (*see* **Note 7**).

3. *pNPP assay.* To assess how much active probe is in your supernatant, you can quantify the PLAP activity. Heat a 250 μl aliquot of fusion protein-conditioned medium at 65 °C for 5 min to inactivate endogenous phosphatases and cool to room temperature. Add 250 μl of water and 500 μl of 2× SEAP buffer. Vortex and stand for 5 min. Add 20 μl of 200 mM pNPP, then transfer to a cuvette or 96-well plate, and measure absorbance at 405 nm. Readings can be taken at intervals up to

30 min, and OD per minute can be calculated [27]. Use medium without fusion protein as a negative control. As a positive control for the pNPP reaction, use a very small amount of an AP-conjugated secondary antibody. We recommend using similar specific activities of probe solutions in assays, if multiple probes are used (*see* **Note 8**), and probe solutions can be further concentrated (*see* **Note 9**). Although RAP probes in supernatants can be quite stable for several weeks in the fridge, we do recommend that you initially use very fresh supernatant for RAP assays, to set the benchmark for what you will expect to see in subsequent tests.

4. Identification of ligand sites in tissue sections.
   (a) First generate 10–15 μm thick cryosections of your tissue of interest on Superfrost™ (or equivalent) glass slides and air-dry the sections. For initial studies the tissue should be unfixed and snap frozen before sectioning. Pre-fixing tissue before sectioning can be tried subsequently if necessary.
   (b) Rinse sections in Hanks' balanced salt solution (HBSS) for 2 min. Either leave tissue unfixed, or fix the sections in (1) either methanol (at –20 °C for 90 s) or (2) 4% paraformaldehyde in PBS at room temperature for 5 min. A priori, it will not be known whether or not the chemical fixation of tissue post-sectioning will be detrimental to ligand-probe interactions. We recommend trying the assay with and without post-fixation of sections.
   (c) Wash sections gently in slide wash buffer, for 5 min on a shaking platform.
   (d) Draw a hydrophobic line around the sections with a wax pen, and then add supernatants containing either (1) the fusion protein, (2) the control PLAP protein, or (3) no fusion protein; 100 μl of supernatant is easily sufficient to cover 1 cm^2. Place slides in a flat, humidified chamber for 90 min at room temperature.
   (e) Wash sections three to six times for 1 min in slide wash buffer. *Optional*: Refix the section in 4% paraformaldehyde/PBS for 1 min after the washes.
   (f) Heat the slides at 65 °C for 30 min in slide wash buffer, to inactivate endogenous AP (*see* **Note 10**).
   (g) Rinse slides in AP buffer, and then add AP buffer plus NBT/BCIP mixture (20 μl NBT/BCIP into 10 ml buffer). Leave to develop in a dark, humidified chamber; check periodically for purple/brown reaction product. Reactions can be stopped and restarted (*see* **Note 11**).
   (h) If you want to do immunohistochemistry alongside RAP, this is possible (*see* **Note 12**).

5. *RAP assay in cultured cells or tissues.* RAP assays can be done in live cells on pretreated cover slips (*see* **Note 13**), fixed cells on culture plates, and small pieces of tissue. The method is essentially similar to that described above. For tissues, you will need to first methanol fix in order to permeabilize and allow probe access; you will also need to extend probe incubation and wash times accordingly.
6. *Panning for ligand identification.* One of the first uses of RPTP ectodomain fusion probes was to pan for cell surface ligands expressed from a cDNA library in Cos7 cells [10]. Here, a plasmid-based cDNA expression library was first transfected into Cos7 and live cells probed with fusion protein. After fixation, cells were immunostained to detect the bound fusion protein. The cDNA library was then de-convoluted to identify the ligand clone (expressing contactin). This approach can be adapted for PLAP fusion proteins.
7. *Probe specificity.* When you have identified a potential ligand and have access to soluble forms of it, you should use this as a competitive agent to test the specificity of the affinity interaction. An alternative method to check for specificity is to use a specific antibody to the ligand (if available) to test for blockade of RPTP fusion protein binding. This will only work if the antibody binds to a site that is required for RPTP-ligand interactions.
8. *If you need to quantify RPTP*-ligand affinities, you can use standard binding kinetics or advanced methods such as Biacore™ if you have access to purified, soluble forms of both RPTP ectodomain and ligand. Biacore™ has also been effective for testing the structural basis of interactions, since it is straightforward to synthesize and assay the binding properties of mutated forms of either the RPTP or the ligand [12, 18].

3.2 Identification of Ligands by Affinity Chromatography

If a ligand or binding partner has reasonable affinity for the RPTP ectodomain, it can potentially be identified by direct affinity isolation. Ligands can be identified using standard affinity chromatography, or binding in batch mode. You will first need to generate sufficient recombinant proteins fused to either PLAP (described here; [9]), Fc, or other affinity tags [12]. Alternatively, RPTP ectodomains can be directly isolated from tissues if you have a good source of strongly expressing tissue and a very specific antibody [11]. For negative control assays, we recommend generating PLAP from a suitable expression vector with PLAP linked to a secretion domain (APTag-4; [29]).

1. *Purification of PLAP fusion probes.* To purify PLAP fusion proteins, we recommend first transfecting the plasmid into several 175 cm^2 flasks and collecting supernatants as above. To affinity purify the fusion protein, use anti-placental alkaline phosphatase-agarose (anti-PLAP):

(a) Pack 1 ml of anti-AP agarose into an appropriate FPLC column. Equilibrate the agarose with five column volumes of 0.05 M Tris and 0.5 M NaCl, pH 8.0 at a flow rate of 0.5 ml/min.

(b) Centrifuge the conditioned media at 400 g for 5 min and load the supernatant onto the column. Wash the column with five column volumes of the equilibration buffer.

(c) Elute the fusion protein with 50 mM glycine and 0.5 M NaCl, pH 2.8. Collect 500 µl fractions into tubes containing 50 µl of 1.0 M Tris/HCl, pH 9.0. Assay fractions for protein content by absorbance at 280 nm.

(d) Pool appropriate fractions, desalt with PD10 columns, and check purity on polyacrylamide gels. Store fractions at 4 °C, or frozen.

2. *Affinity chromatography.* To purify ligands from cell or tissue lysates, first identify the best tissue source of the ligand source, using RAP (above). Tissue should be either fresh or snap frozen. If fresh, homogenize the tissue with a glass homogenizer (or similar) in a suitable ice-cold lysis buffer (place buffer in *wet* ice). We have successfully used 4% CHAPS, 100 mM KH_2PO_4, pH 7.5, 5% glycerol, and protease inhibitor cocktail (Roche, Lewes, UK). Vortex the lysate for 1 h at 4 °C and then centrifuge at 2000 g for 15 min. If the tissue is frozen, we recommend grinding to a fine powder in a mortar sitting in dry ice, and then add the powder in small amounts to the cooled lysis buffer.
3. Dilute the lysate 1:2 in PBS.
4. Prepare some column matrix by mixing 2 mg of your pre-purified fusion protein with 1 ml of CnBr sepharose (follow the manufacturer's protocol). This cross-links the protein to the matrix.
5. Mix your lysate with the affinity matrix in batch mode, rolling overnight at 4 °C; the volume should be minimized and not be more than a few milliliters, since too high a volume will reduce the binding efficiency.
6. Load the mixture onto an appropriate HPLC column and then wash the column with five column volumes of PBS containing 0.1% Tween and 30 mM EDTA.
7. Elute the bound components with PBS containing 0.5 M NaCl. Elute in 2 ml total, in 200 µl fractions. Take small aliquots of these fractions and test them with polyacrylamide electrophoresis under reducing conditions, visualizing with silver staining.
8. A negative control column should also be run, using matrix that has been cross-linked to purified alkaline phosphatase only. The silver-stained samples must be compared to those in the experimental samples.

9. If bands of interest are located specifically in the experimental (RPTP column) samples, these can be subjected to tandem mass spectrometry for protein identification [9].

3.3 Validation of RPTP Interactions with Synaptic Partners in Hippocampal Neurons

In the 1990s it was well known that many RPTPs were strongly expressed in neural tissues during development and into adulthood. However, it has taken much longer to reveal their functions. Here, to provide an example, we describe a very specific, cell-based, functional assay that looks at the role of RPTPs in synaptogenesis. This assay uses an established technique of hippocampal neuron/Cos7 coculture and here it is used to identify and validate novel, functional partnerships between presynaptic RPTPs and postsynaptic ligands (Fig. 2c). This is a rather specialized assay and does require access to a source of hippocampal neurons.

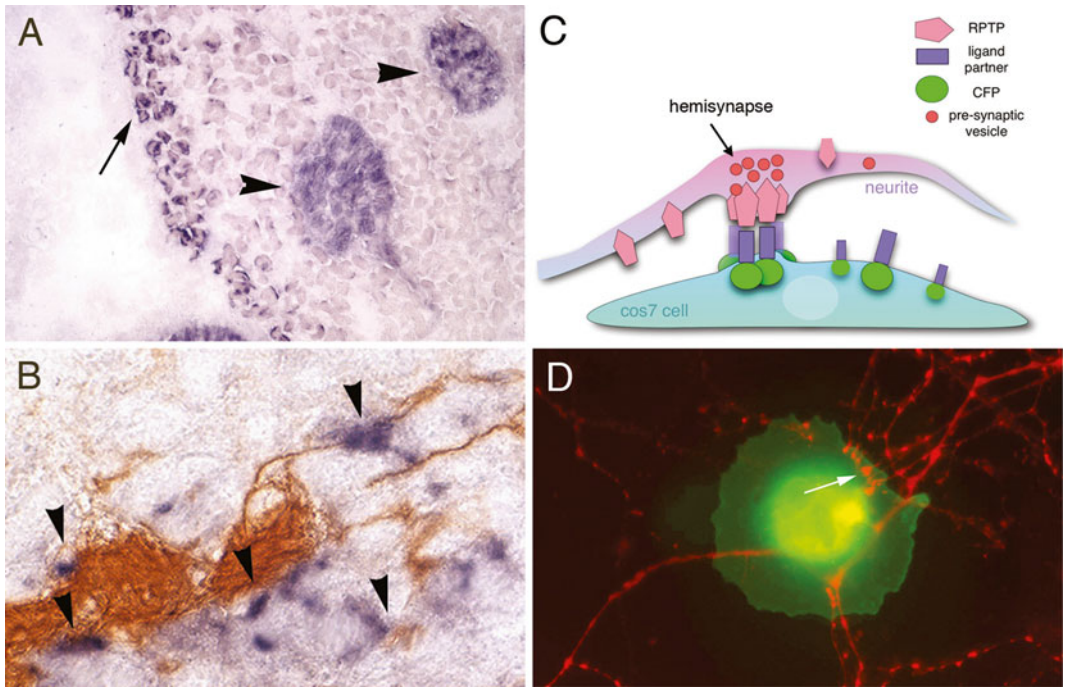

Fig. 2 (**a** and **b**) Examples of PLAP-based RAP assays on tissue sections from chick embryos (taken from [23, 28] with permission from Elsevier Ltd.). The RAP probe was chick PTPσ-PLAP. **A**, trunk muscle showing binding (*purple stain*) to ligand sites in muscle cells themselves (*arrow*) and in nerve bundles running through the tissue (*arrowheads*). (**b**) is similar to (**a**), except that this section is co-stained with an antibody to neurofilament protein 3A10 (*brown* HRP stain). *Arrowheads* here indicate points of close juxtaposition between nerves and ligand sites on muscle cells. (**c**) Schematic of a neurite (*pink* process) overlaying a Cos7 cell that is expressing ligand protein (*blue rectangle*). A contact has formed where the RPTPs form complexes with the ligands, generating a hemisynapse rich in presynaptic vesicles. (**d**) Dark-field micrograph showing CFP fluorescence in a transfected Cos7 cell, along with hippocampal neurites stained with synapsin (*red*). *White arrow* indicates a hemisynapse contact between neurite and Cos7 cells. The CFP is fused here to TrkC (for further information on this particular protein interaction, *see* [14, 18]

1. For this assay it is assumed that the RPTP is expressed on presynaptic membranes in neurites (they are also expressed postsynaptically in some cases). The ligand is presented to neurites as if it were on a dendritic surface, but in this case it is actually presented to neurites via transfected Cos7 cell membrane surfaces (Fig. 2c). Thus if there is a functional RPTP-ligand interaction, it triggers hemisynaptic structures in the neurites, rich in proteins such as synapsin (Fig. 2c, d) [14].
2. Hippocampal neuron cultures should be prepared from P1 rat pups (full methods can be found in [30]). Plate them into 35 mm culture dishes containing prepared, glass cover slips. The neurons should be cultured for 20 days before further use, to allow extensive neuritic processes to form.
3. *Coverslip preparation*: Submerge cover slips in concentrated nitric acid overnight at room temperature, in a glass beaker or rack; this cleans the glass.
4. Rinse the cover slips four times (at least 2 h each) in distilled water; finally rinse in 100% methanol.
5. Bake the cover slips at 150–225 °C overnight.
6. Place cover slips into tissue culture plates and add 100–150 µl of poly-L-lysine solution (200 µg/ml in water) to each cover slip and incubate at room temperature for several hours (*see* **Note 13**).
7. Remove the PLL solution and rinse twice with 3 ml of sterile water, 2 h each. Add tissue culture medium.
8. Plate out the cells.
9. To present the putative RPTP ligand to the neurons, it must be expressed on the cell surface of Cos7 cells. An expression vector must therefore be generated, containing the extracellular and TM portion of the ligand fused at its c-terminus to a fluorescent protein such as GFP or CFP. Transfect this into Cos7 cells. After 24 h the cells should be re-seeded at low density (around 2×10^4 per 35 mm plate) onto the cover slips of neurons.
10. After 20 h of coculture, RPTP ligands in the Cos7 cells can induce RPTP-dependent clustering of presynaptic proteins in neurites. Fix the cultures in 4% paraformaldehyde and 4% sucrose in PBS for 15 min. Immunofluorescence microscopy is then used for detection of the synaptic protein of interest, such as synapsin or VGLUT1 [14]. The ligand fusion protein in Cos7 cells is detected using the appropriate UV filter set.
11. Figure 2d shows an example of presynaptic structures forming after neuronal contact with TrkC-expressing Cos7 cells (*see* ref. [18] for more details of this study). Other experimental approaches are then needed to confirm that RPTPs are the presynaptic receptors [14–16]. These published works are

excellent examples of what can be achieved by using a mix of RAP-type assays, affinity purification systems, and functional assays to identify ligands and to assay RPTP-ligand signaling.

4 Notes

1. If you use an Fc fusion, the Fc portion can be identified using immunofluorescence microscopy or immunocytochemistry (for example *see* ref. [14]). As these probes are not phosphatase based, you will not need to carry out the heat inactivation step after probe binding.
2. It is of relevance that RPTP-ligand interactions may occur in "rafts" of molecules, relying on avidity and multiple cis interactions in vivo [8, 19]. It is therefore possible that some RPTP-ligand interactions will be of too low affinity to detect using RAP or even affinity chromatography.
3. RAP assays can be done in both directions, with probes being made from either RPTP ectodomains or the binding partner (*see* Fig. 2 in ref. [14]. This can be advantageous if you have problems making sufficient quantities of the RPTP-PLAP proteins and you know the ligand identity.
4. Depending on the conserved nature of the RPTP, some probes may be potentially used across species. However, we found that this did not work very well for PTPσ between chick and mouse for example.
5. RAP probes can be made using either PLAP or Fc fusions. Both are *dimeric*, but their conformations are not necessarily the same in this state. There have been no direct comparisons of these two fusion methods with a given RPTP, as far as we are aware. PLAP is a very sensitive enzymatic probe for use with its histochemical assay, but it is harder to detect directly with antibodies in immunohistochemistry or -cytochemistry. Fc fusions have been detected after RAP assays using immunofluorescence detection, but the sensitivity of this will depend on the nature of your particular RPTP-ligand interaction.
6. The PLAP and Fc fusion probes generate dimeric molecules. This can be advantageous as it may increase avidity, but we also have evidence that steric restriction can occur in the dimeric state with PLAP [31]. If you are concerned about this, you can introduce a flexible linker between the RPTP ectodomain and PLAP, which increases rotational freedom (Fig. 1b; [31]). We have evidence that some ligand interactions require the dimer state of the RPTP; monomer forms of PLAP probes can be made to test this [31].
7. Note that some ligands and RPTPs are glycosaminoglycans and this can interfere with assays of their interactions. The

group of Aricescu has used 293S-GnTI (a variant of HEK293 cells) and inhibitors such as kifunensine or swainsonine to reduce glycosylation for their structural studies of RPTP-ligand interactions [32].

8. If you are trying to make qualitative or semiquantitative comparisons between the binding affinity of different PLAP fusion probes in RAP assays, we recommend that you normalize the supernatants for their PLAP activities before carrying out RAP assays. Dilute the supernatants with medium until they have the same activity units per milliliter as each other.
9. For most RAP assays on cells and tissue sections, the neat cell supernatant is sufficient. If necessary it can be concentrated a little further by centrifuging through sterile filter units that trap large proteins.
10. If you use an Fc fusion, the Fc portion can be identified using immunofluorescence microscopy or immunocytochemistry (for example *see* ref. [14]). As these probes are not phosphatase based, you will not need to inactivate endogenous phosphatases and you need not carry out the heat inactivation step after probe binding.
11. You can stop the PLAP reaction and restart it again several hours later if the sections have been kept in physiological buffer. The reaction itself can keep running a long time and may reach a very high level of intensity. To slow the speed of the NBT/BCIP reaction, you can do the reaction at 4 °C, or reduce the NBT/BCIP concentration.
12. It is also possible to do both RAP assays and immunohistochemistry on the same tissue sections [23, 28]. You will need to test empirically how effective the HRP antibody staining is after NBT/BCIP development of PLAP, or vice versa. If using Fc probes, you can perform dual immunodetection and indirect fluorescence microscopy. Direct immunodetection of PLAP probes with anti-AP antibodies has, in our hands at least, proved problematic; the enzymatic detection of PLAP is more sensitive.
13. If doing assays with cells on cover slips, then the PLL coating is critical. PLL solution should flow over the cleaned glass readily. If the glass remains hydrophobic though, then more nitric acid cleaning is required.

Acknowledgements

Our work addressing RPTP ligands over the past 15 years has been generously funded by the European Commission (HPRN-CT-2000-00085), the Wellcome Trust (Studentship for John Chilton and grant 071418), the Karim Rida Said Foundation

(Studentship for F. Haj), University College London Graduate Research Scholarship (Alexandru Aricescu), and the Child Health Research Appeal Trust. We thank Radu Aricescu for helpful advice and we acknowledge Charlotte Coles for the generation of the TrkC-CFP vector used in Fig. 2d.

References

1. Charbonneau H, Tonks NK, Walsh KA, Fischer EH (1988) The leukocyte common antigen (CD45): a putative receptor-linked protein tyrosine phosphatase. Proc Natl Acad Sci U S A 85(19):7182–7186
2. Charbonneau H, Tonks NK, Kumar S, Diltz CD, Harrylock M, Cool DE, Krebs EG, Fischer EH, Walsh KA (1989) Human placenta protein-tyrosine-phosphatase: amino acid sequence and relationship to a family of receptor-like proteins. Proc Natl Acad Sci U S A 86:5252–5256
3. Tonks NK, Charbonneau H, Diltz CD, Fischer EH, Walsh KA (1988) Demonstration that the leukocyte common antigen is a protein tyrosine phosphatase. Biochemistry 27(24):8695–8701
4. Mohebiany AN, Nikolaienko RM, Bouyain S, Harroch S (2013) Receptor-type tyrosine phosphatase ligands: looking for the needle in the haystack. FEBS J 280(2):388–400
5. Lisabeth EM, Falivelli G, Pasquale EB (2013) Eph receptor signaling and ephrins. Cold Spring Harb Perspect Biol 5(9)
6. Brady-Kalnay SM, Flint AJ, Tonks NK (1993) Homophilic binding of PTPm, a receptor-type protein tyrosine phosphatase, can mediate cell-cell aggregation. J Cell Biol 122:961–972
7. Brady Kalnay SM, Rimm DL, Tonks NK (1995) Receptor protein tyrosine phosphatase PTPmu associates with cadherins and catenins in vivo. J Cell Biol 130(4):977–986
8. Aricescu AR, Hon W-C, Siebold C, Lu W, van der Merwe PA, Jones EY (2006) Molecular analysis of receptor protein tyrosine phosphatase mu-mediated cell adhesion. EMBO J 25(4):701–712
9. Alete DE, Weeks ME, Hovanession AG, Hawadle M, Stoker AW (2006) Cell surface nucleolin on developing muscle is a potential ligand for the axonal receptor protein tyrosine phosphatase-sigma. FEBS J 273:4668–4681
10. Peles E, Nativ M, Campbell PL, Sakurai T, Martinez R, Lev S, Clary DO, Schilling J, Barnea G, Plowman GD et al (1995) The carbonic anhydrase domain of receptor tyrosine phosphatase beta is a functional ligand for the axonal cell recognition molecule contactin. Cell 82(2):251–260
11. Maeda N, Nishiwaki T, Shintani T, Hamanaka H, Noda M (1996) 6B4 proteoglycan/phosphacan, an extracellular variant of receptor-like protein-tyrosine phosphatase zeta/RPTPbeta, binds pleiotrophin/heparin- binding growth-associated molecule (HB-GAM). J Biol Chem 271(35):21446–21452
12. Bouyain S, Watkins DJ (2010) The protein tyrosine phosphatases PTPRZ and PTPRG bind to distinct members of the contactin family of neural recognition molecules. Proc Natl Acad Sci U S A 107(6):2443–2448
13. Kwon SK, Woo J, Kim SY, Kim H, Kim E (2010) Trans-synaptic adhesions between netrin-G ligand-3 (NGL-3) and receptor tyrosine phosphatases LAR, protein-tyrosine phosphatase delta (PTPdelta), and PTPsigma via specific domains regulate excitatory synapse formation. J Biol Chem 285(18): 13966–13978
14. Takahashi H, Arstikaitis P, Prasad T, Bartlett TE, Wang YT, Murphy TH, Craig AM (2011) Postsynaptic TrkC and Presynaptic PTPσ Function as a Bidirectional Excitatory Synaptic Organizing Complex. Neuron 69(2):287–303
15. Yim YS, Kwon Y, Nam J, Yoon HI, Lee K, Kim DG, Kim E, Kim CH, Ko J (2013) Slitrks control excitatory and inhibitory synapse formation with LAR receptor protein tyrosine phosphatases. Proc Natl Acad Sci U S A 110(10):4057–4062
16. Takahashi H, Katayama K, Sohya K, Miyamoto H, Prasad T, Matsumoto Y, Ota M, Yasuda H, Tsumoto T, Aruga J, Craig AM (2012) Selective control of inhibitory synapse development by Slitrk3-PTPdelta trans-synaptic interaction. Nat Neurosci 15(3):389–398, S381-382
17. Takahashi H, Craig AM (2013) Protein tyrosine phosphatases PTPdelta, PTPsigma, and LAR: presynaptic hubs for synapse organization. Trends Neurosci 36(9):522–534
18. Coles CH, Mitakidis N, Zhang P, Elegheert J, Lu W, Stoker AW, Nakagawa T, Craig AM, Jones EY, Aricescu AR (2014) Structural basis for extracellular cis and trans RPTPsigma signal competition in synaptogenesis. Nat Commun 5:5209

19. Coles CH, Shen Y, Tenney AP, Siebold C, Sutton GC, Lu W, Gallagher JT, Jones EY, Flanagan JG, Aricescu AR (2011) Proteoglycan-specific molecular switch for RPTPsigma clustering and neuronal extension. Science 332(6028):484–488
20. Meng K, Rodriguez-Pena A, Dimitrov T, Chen W, Yamin M, Noda M, Deuel TF (2000) Pleiotrophin signals increased tyrosine phosphorylation of beta-catenin through inactivation of the intrinsic catalytic activity of the receptor-type protein tyrosine phosphatase beta/zeta. Proc Natl Acad Sci U S A 97(6): 2603–2608
21. Stoker A (2005) Methods for identifying extracellular ligands of RPTPs. Methods 35(1): 80–89
22. Cheng HJ, Flanagan JG (2001) Cloning and characterization of RTK ligands using receptor-alkaline phosphatase fusion proteins. Methods Mol Biol 124:313–334
23. Haj F, McKinnell I, Stoker A (1999) Retinotectal ligands for the receptor tyrosine phosphatase CRYPalpha. Mol Cell Neurosci 14(3):225–240
24. Aricescu AR, McKinnell IW, Halfter W, Stoker AW (2002) Heparan sulfate proteoglycans are ligands for receptor protein tyrosine phosphatase sigma. Mol Cell Biol 22(6):1881–1892
25. Flanagan JG, Cheng HJ (2000) Alkaline phosphatase fusion proteins for molecular characterization and cloning of receptors and their ligands. Methods Enzymol 327:198–210
26. Aricescu AR, Lu W, Jones EY (2006) A time- and cost-efficient system for high-level protein production in mammalian cells. Acta Crystallogr D Biol Crystallogr 62(Pt 10):1243–1250
27. Cullen BR, Malim MH (1992) Secreted placental alkaline phosphatase as a eukaryotic reporter gene. Methods Enzymol 216: 362–368
28. Sajnani-Perez G, Chilton JK, Aricescu AR, Haj F, Stoker AW (2003) Isoform-specific binding of the tyrosine phosphatase PTPsigma to a ligand in developing muscle. Mol Cell Neurosci 22(1):37–48
29. Cheng HJ, Flanagan JG (1994) Identification and cloning of ELF-1, a developmentally expressed ligand for the Mek4 and Sek receptor tyrosine kinases. Cell 79(1):157–168
30. Kaech S, Banker G (2006) Culturing hippocampal neurons. Nat Protoc 1(5):2406–2415
31. Lee S, Faux C, Nixon J, Alete D, Chilton J, Hawadle M, Stoker AW (2007) Dimerization of protein tyrosine phosphatase sigma governs both ligand binding and isoform specificity. Mol Cell Biol 27(5):1795–1808
32. Aricescu AR, Owens RJ (2013) Expression of recombinant glycoproteins in mammalian cells: towards an integrative approach to structural biology. Curr Opin Struct Biol 23(3): 345–356

Chapter 16

Production of Osteoclasts for Studying Protein Tyrosine Phosphatase Signaling

Eynat Finkelshtein*, Einat Levy-Apter*, and Ari Elson

Abstract

Osteoclasts, specialized cells that degrade bone, are key components of the cellular system that regulates and maintains bone homeostasis. Aberrant function of osteoclasts can lead to pathological loss or gain of bone mass, such as in osteopetrosis, osteoporosis, and several types of cancer that metastasize to bone. Phosphorylation of osteoclast proteins on tyrosine residues is critical for formation of osteoclasts and for their proper function and responses to physiological signals. Here we describe preparation and growth of osteoclasts from bone marrow of mice, use of viral vectors to downregulate expression of endogenous proteins and to express exogenous proteins in osteoclasts, and analysis of signaling processes triggered by M-CSF, estrogen, and physical contact with matrix in these cells.

Key words Tyrosine phosphatase, Osteoclast, Bone, Adenovirus, Lentivirus

1 Introduction

The physical properties and mass of bone are preserved by the opposing but generally balanced activities of specialized cells. Osteoblasts, which are derived from the mesenchymal lineage, synthesize bone matrix, while hematopoietically derived osteoclasts degrade it. Osteoclasts (OCLs) are multinucleated cells that are formed by fusion of monocyte-macrophage precursor cells, in a process driven by Macrophage Colony Stimulating Factor (M-CSF, CSF-1) and Receptor Activator of NFkB Ligand (RANKL) [1, 2]. Both factors are either secreted by osteoblasts or expressed on their surface, making close contact between both cell types essential for proper bone homeostasis. OCLs adhere to bone tightly using adhesion structures called podosomes [3, 4]. Once attached, OCLs physically isolate the area of bone to which they adhere from the

*The authors are contributed equally.

Rafael Pulido (ed.), *Protein Tyrosine Phosphatases: Methods and Protocols*, Methods in Molecular Biology, vol. 1447,
DOI 10.1007/978-1-4939-3746-2_16,

environment and secrete onto it a mixture of proteolytic enzymes and acid, which together degrade the protein and mineral components of bone matrix [1, 5].

Protein tyrosine phosphorylation plays critical roles in regulating the production and function of OCLs. Prime examples include the central role of the M-CSF receptor, c-Fms, which is a receptor tyrosine kinase, in production of OCLs [6, 7], and the significant dependence of OCL function on proper activity and regulation of the Src tyrosine kinase [8–10]. Protein tyrosine phosphatases (PTPs), which counter the activities of tyrosine kinases, also play important roles in regulating production and activity of OCLs. The non-receptor type, SH2 domain-containing PTP SHP1 inhibits OCL formation and function in vivo [11, 12] while SHP2, a distinct but structurally related PTP, performs opposite roles [13, 14]. The receptor-type PTP CD45, which is often present on hematopoietic cells, inhibits Src in OCLs and leads to increased OCL activity, increased numbers of dysfunctional OCLs, and increased bone mass in CD45-deficient mice [15]. The dual-specificity phosphatase MKP1, which belongs to a subfamily of phosphatases capable of dephosphorylating MAP kinases at both the threonine and tyrosine residues of their Thr-x-Tyr activation site, appears to assist production of OCLs but to inhibit their function [16, 17]. The non-receptor isoform of PTP Epsilon (cyt-PTPe) contributes to OCL adhesion and function by linking integrins to downstream activation of Src. OCLs of young female mice lacking cyt-PTPe exhibit reduced Src activity and reduced ability to resorb bone in vitro and in vivo [18–20]. Interestingly, the closely related PTP Alpha does not play a unique role in this cell type [21]. Studies in cell-culture systems have established the non receptor-type PTP-PEST as a positive regulator of OCL differentiation and adhesion, most likely through its role in dephosphorylating and activating Src [22–24] that may be related to its ability to promote macrophage fusion [25]. Similar findings have been obtained in culture regarding the receptor-type PTPRO (PTP-oc) [26, 27].

The biological functions of OCLs are key to maintaining proper bone health. Moreover, OCLs can interact with tumor cells present in their environment and thus support formation and expansion of bone metastases of various types of cancer in a process that degrades bone and often leads to fractures and increased morbidity. Studies of OCLs are required in order to better understand how their production and activities are regulated at the molecular level, leading to better understanding of their function and suggesting new approaches to treating disease. Production and growth of OCLs in culture poses several challenges since mature OCLs are terminally differentiated, do not divide, and cannot be passaged or frozen. OCLs are often produced in culture from precursor cells found in bone marrow, a process that works well and allows deriving cells from human samples and from genetically manipulated

mice. We describe this process, as well as protocols for expressing exogenous genes and inhibiting endogenous ones in OCLs. Alternatives to production of OCLs from bone marrow cells include production of OCLs from spleen cells, use of specific established hematopoietic cell lines, such as RAW264.7, that can be differentiated in culture to assume an OCL-like phenotype, or isolation of relatively small amounts of primary OCLs directly from bone. We do not discuss these techniques here.

2 Materials

2.1 Production of OCLs in Culture from Unselected Bone Marrow Cells Using Cytokines

1. Mice (*see* **Note 1**).
2. RANKL (Catalog # 462-TEC-110-5, R&D Systems, Minneapolis, MN, USA) and M-CSF (Catalog # 315-02, PeproTech, Rocky Hill, NJ, USA) (*see* **Note 1**).
3. Phosphate-buffered saline (1× PBS): 8.1 mM Na_2HPO_4, 1.47 mM KH_2PO_4, 2.67 mM KCl, 137 mM NaCl, sterile.
4. Sterile surgical operating tools (two to three sets of small surgical scissors, two to three forceps (5–7 cm in length) with blunt ends).
5. #11 Scalpels (do not have to be sterile).
6. OCL medium: alpha-MEM, supplemented with 10% fetal calf serum, 2 mM glutamine, 50 U/ml penicillin, 50 μg/ml streptomycin.
7. Tissue-culture plasticware: 6- and 10-cm plates, 6- and 24-well plates.
8. Glass coverslips, microscope slides (optional, if growing cells for immunofluorescence studies). The make of the glass can sometimes affect OCL differentiation. We have had good results with slides manufactured by Menzel-Glaser, Braunschweig, Germany.
9. 10 ml syringe equipped with a 27″ needle.
10. 70% ethanol.
11. 1 ml pipettor, tips, 15 ml plastic test tubes (all sterile).
12. Tissue culture facilities: hood, incubator, centrifuge.
13. Hypotonic Red Blood Cell lysis Buffer.
14. Hemocytometer (or alternative method for counting cells).

2.2 Production of OCLs in Culture from Bone Marrow Macrophages Using Cytokines

In addition to items noted in Subheading 2.1:

1. Ficoll Paque Plus (sterile).
2. MACS buffer: 1× PBS, 1 mM EDTA, 2% serum; sterilize by filtration.
3. Biotin-conjugated anti-CD115 (M-CSF receptor) antibodies.

4. Streptavidin-coated magnetic beads.
5. Cell separation magnet.
6. Ice and ice bucket.

2.3 Expressing Foreign Proteins and Knocking Down Endogenous Proteins in OCLs Using Viral Vectors

In addition to items noted in Subheadings 2.1 and 2.2:

1. Adenovirus and lentivirus preparations.
2. HEK293 adherent cells that adhere well to the plate.
3. HEK293 cell medium: DMEM, supplemented with 10% fetal calf serum, 2 mM glutamine, 50 U/ml penicillin, 50 μg/ml streptomycin.
4. 0.45 μm sterile tissue culture filter.
5. Polybrene.

2.4 Studying Cell Signaling in Cultured OCLs

In addition to items noted in Subheadings 2.1–2.3:

1. Estrogen-free OCL medium: Phenol red-free alpha MEM, supplemented with 10% charcoal-stripped fetal calf serum, 2 mM glutamine, 50 U/ml penicillin, 50 μg/ml streptomycin.
2. NP40 lysis buffer: 50 mM Tris-Cl, pH 7.5, 150 mM NaCl, 1% Nonidet NP40. Supplement with protease inhibitors (e.g., a commercial protease inhibitor cocktail) and/or phosphatase inhibitors (e.g., 0.5 mM sodium pervanadate, a tyrosine phosphatase inhibitor) as necessary.
3. Rubber policeman of a size compatible with the wells/plates used to grow OCLs.
4. Eppendorf centrifuge.
5. β-estradiol.
6. Analytical grade ethanol.
7. Fibronectin: Dilute to 20 μg/ml with sterile PBS.
8. 10 mM EDTA/PBS solution: 0.5 M EDTA solution, pH 8.0, diluted to 10 mM in PBS.
9. DMEM-HEPES medium containing 1 mg/ml bovine serum albumin (BSA).
10. Equipment and reagents for running SDS-PAGE gels and for protein blotting studies.
11. Primary antibodies for determining phosphorylation of key signaling molecules (e.g., anti-pY416 Src, anti-pY402 Pyk2, anti-pThr308 AKT, anti-AKT, anti-v-Src, anti-Pyk2, anti-pThr/pTyr ERK1/ERK2, and anti-ERK1/ERK2).
12. Secondary antibodies for protein blots (e.g., horseradish peroxidase-labeled goat anti-mouse and goat anti-rabbit).

3 Methods

3.1 Production of OCLs in Culture from Unselected Bone Marrow Cells Using Cytokines

This protocol focuses on differentiation of OCLs in culture from unpurified bone marrow precursors using exogenous purified RANKL and M-CSF, a process that yields relatively pure OCLs but with some, albeit little, presence of stromal cells. Stromal cells can be avoided if one purifies monocytes from the crude bone marrow using anti-CD115 (M-CSF receptor) antibodies, as described in Subheading 3.2. It is also possible to produce OCLs by coculturing unpurified bone marrow cells with calvarial osteoblasts. Treatment of the osteoblasts with 1,25-dihydroxy vitamin D3 and prostaglandin E2 induces them to produce M-CSF and RANKL, which drive proliferation of osteoclast precursors and their differentiation into OCLs. The osteoblasts are subsequently removed from the much more adherent OCLs [28]. The advantages of the method discussed here include the ability to easily visualize production of OCLs over time, and to examine production, morphology, and function of OCLs without possible confounding effects of supporting osteoblasts.

1. Sacrifice a mouse by cervical dislocation (*see* **Note 2**). Spray fur with 70% ethanol to mat down hair. Working on a non-sterile but clean lab bench, remove both hind legs entirely at the proximal joint of the femur, making sure that both femora and tibiae are intact (*see* **Notes 3** and **4**).
2. Remove fur and flesh from bones as much as possible. This can be done using scissors and/or scraping with a clean #11 scalpel. Separate each femur from its associated tibia; do not attempt to retain the fibula. Work carefully to ensure that the femora and tibiae retain their integrity at this stage.
3. Place individual bones together in a 6- or 10-cm tissue-culture plate. The bones are not sterile at this stage, but it is important to keep them clean: place them in a clean plate and close the plate's cover.
4. If preparing cells from more than one mouse, repeat **steps 1–3** in sequence for each mouse one after the other. In particular, sacrifice the mouse only when you are ready to harvest its tissues. Collect bones in plastic dishes together or separately depending on the experimental design (*see* **Note 5**).
5. Move the plate(s) with bones to a tissue culture room. Inside the tissue culture hood prepare three sterile 6- or 10-ml plates for each plate containing bones from **step 3**:
   - Plate #1: 3–4 ml of sterile PBS.
   - Plate #2: empty.
   - Plate #3: empty.

- In addition, prepare a larger vessel with OCL medium (complete with serum, antibiotics and glutamine, but without M-CSF or RANKL), as well as a sterile 10 ml syringe fitted with a 27″ gauge needle.

6. While still outside the tissue culture hood, pour 70% ethanol solution onto the bones while they are still in their original plastic plate. After 15–30 s transfer the plate into the tissue culture hood and rapidly transfer the bones one-by-one using fresh sterile forceps from the 70% ethanol solution into Plate #1 that contains PBS, to wash away and dilute the ethanol. When done, discard the ethanol-containing plate. From this point the bones are considered sterile; the bones and cells derived from them should remain in the tissue culture hood or removed from it only when enclosed in sterile containers (tissue culture plasticware, test tubes, etc.).
7. Transfer the bones from the PBS solution to Plate #2 to await flushing.
8. Aspirate OCL medium into the 10 ml syringe (*see* **Note 6**).
9. Pick up one bone with sterile forceps. Cut epiphyses with sterile scissors. Hold bone over empty Plate #3. Insert the syringe needle into the bone marrow cavity and flush the cavity with OCL medium to remove bone marrow cells, while gently moving the syringe and needle in and out of the bone along its long axis; in our experience, 0.5–1.0 ml of medium is required per bone. Continue flushing until the bone is empty and white (when the red bone marrow cells, which are visible through the thin bone matrix, have been removed). Marrow from multiple bones may be flushed into the same plate if the experimental design allows this. Flush only with fresh medium—do not flush with medium that contains cells (*see* **Note 7**).
10. Pipette up and down the medium and bone marrow cells collected in Plate #3 with a 1 ml pipettor to break cell clusters and to suspend the cells.
11. Transfer the cell-containing medium to a 15 ml test tube. Wash the plate with 1–2 ml OCL medium or PBS to collect remaining cells and add to the same 15 ml test tube.
12. Centrifuge at 200 × *g* for 3 min at room temperature.
13. Remove supernatant by gentle aspiration inside the tissue culture hood. Pellet should appear reddish due to presence of erythrocytes (*see* **Note 8**).
14. Remove erythrocytes by adding 1 ml of hypotonic Red Blood Lysis Buffer. Mix gently and incubate at room temperature for 1 min. Stop lysis by adding 5 ml of OCL medium or of 1× PBS.
15. Centrifuge at 200 × *g* for 3 min at room temperature.

16. Remove supernatant by gentle aspiration inside the tissue culture hood. Pellet should now appear much lighter in color compared to **step 13**.
17. Resuspend cells in 2 ml OCL medium (per mouse). Count cells; expect about 30×10^6 cells per two femur–tibia pairs from one young adult male mouse of the 129SvEv strain.
18. Seed cells in appropriate vessels: $5–7 \times 10^6$ cells per well of a 6-well plate (2 ml medium) or 35 cm dish (1 ml medium), 1×10^6 cells per well of a 24 well plate (0.5 ml medium) (*see* **Note 9**). Seed cells in OCL medium supplemented with 20 ng/ml M-CSF and 20 ng/ml RANKL. Incubate at 37 °C, 5 % CO_2 for 5 days (*see* **Note 9**). Change medium and cytokines after 24 h and then every 1–2 days during this period (*see* **Note 10**).
19. What to expect: Most of the cells plated are non-adherent (e.g., lymphocytes) and will be removed at the first medium change after 24 h. Relatively few adherent cells will remain; these will be a mixture of monocytes/macrophages and their precursors, but also some osteoblasts, fibroblasts, etc. The former cells then begin to proliferate massively under the influence of M-CSF. At day 3 or 4 cells will begin to fuse, generating somewhat larger cells that stain strongly for tartrate-resistant acid phosphatase (TRAP, an OCL marker). On days 5–6 one usually observes large flat osteoclasts forming. These very characteristic cells are markedly (up to 100×) larger than other cells, are multinuclear, and stain for TRAP (although not as strongly as their immediate precursors). These cells tend to form initially in the more crowded regions of the plate, but eventually can cover the entire plate. Small undifferentiated cells can be found in between these larger OCLs (Fig. 1). Use cells promptly, since they deteriorate rapidly and die within 1–2 days following peak of formation of large cells.
20. Troubleshooting: The quality of the RANKL, M-CSF and serum used is critical; If OCLs do not form, the fault is usually with one or more of these three reagents (*see* **Note 1**).

3.2 Production of OCLs in Culture from Bone Marrow Macrophages Using Cytokines

This protocol allows purification of monocytes/macrophages from crude bone marrow cells, thus reducing somewhat possible contamination of the OCL preparation by adherent stromal cells. This protocol is identical to the one in Subheading 3.1 up to and including **step 13**, which described obtaining a preparation of bone marrow cells from mice, ending with centrifugation of the cells.

1. Prepare mouse bone marrow cells according to Subheading 3.1, up to and including **step 13**. From this step onwards, strict sterility should be maintained.

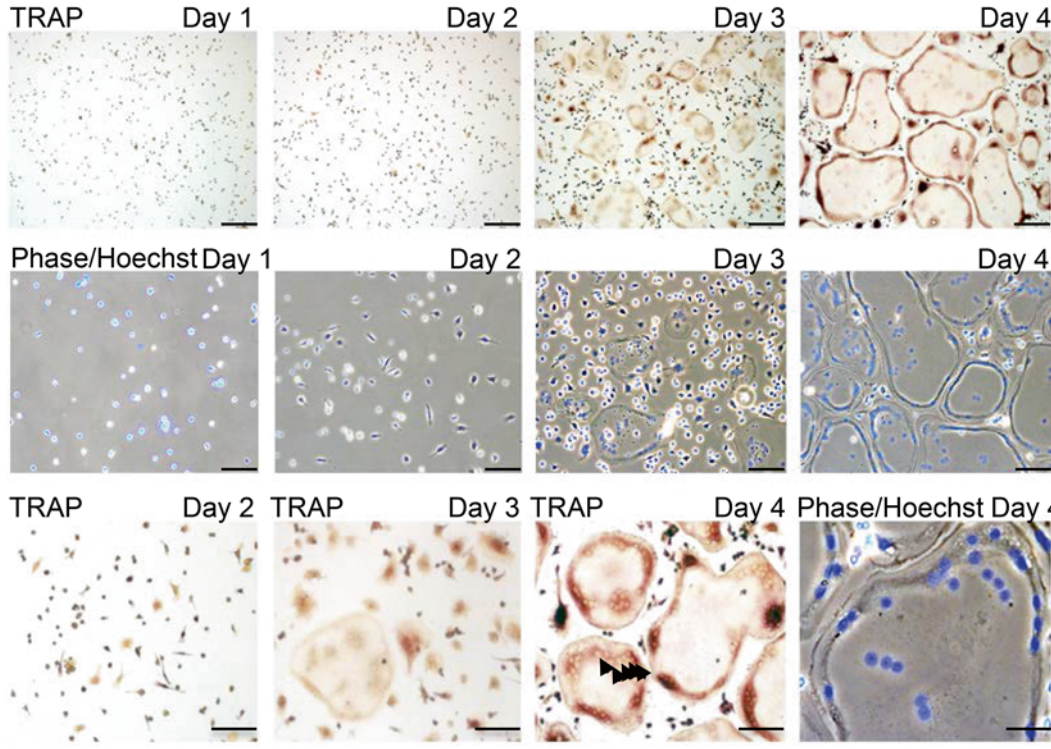

Fig. 1 Time course of differentiation of bone marrow cells in culture into OCLs. *Top panel*: Cells stained for tartrate-resistant acid phosphatase pointing upwards (TRAP, stains *red*). *Middle panel*: DNA (Nuclei) was stained with Hoechst. Pictures include phase light microscopy images of the cells overlain with fluorescence images showing nuclei (*Blue*). Note that mature OCLs include multiple nuclei per cells. *Bottom panel*: Larger magnifications of selected frames from the *top two panels. Arrowheads pointing upwards* (TRAP, day 4, *bottom panel*) indicate nuclei (not all were marked in the picture). Day of seeding is defined as Day 0. Scale bars: *Top* and *middle panels*: 200 μm. *Bottom panel*: 100 μm

2. Suspend cell pellet in 4 ml PBS per mouse and overlay carefully over 4 ml Ficoll per mouse in a sterile test tube. Use one test tube per mouse and do not overload.
3. Centrifuge at 650 × *g* at room temperature, 15 min. Set acceleration and brake of the centrifuge to zero.
4. Collect buffy coat layer in 1–2 ml. Add 12 ml 1× PBS, shake to suspend cells, centrifuge at 200 × *g* for 3 min at room temperature.
5. Suspend the cells in 50 μl of MACS buffer per mouse. At this stage one can mix cells from several mice if the experimental plan allows. Note that volumes in subsequent steps are given per mouse; take care to adjust volumes accordingly if combining cells from several mice.
6. Add anti-CD115-biotin antibody at a final dilution of 1:50. Incubate for 15 min on ice.

7. Wash cells by adding 2 ml MACS buffer per mouse. Centrifuge at $200 \times g$ for 3 min at room temperature, and aspirate supernatant.
8. Suspend the cells in 270 μl of MACS buffer per mouse. Add 30 μl of streptavidin-coated magnetic beads per mouse. Incubate on ice for 20 min with gentle mixing every 4–5 min.
9. Add 2.5 ml of MACS buffer per mouse and transfer cell suspension to a vial or test tube suitable for use with the cell-separating magnet. Use one vial per mouse; if preparation contains cells from several mice, split them among several vials.
10. Place vial in the cell-separating magnet for 10 min, at room temperature.
11. While the vial is still within the magnetic field, remove the MACS buffer (and with it unbound cells). Remove vial from magnet and wash the remaining cells with 2 ml MACS buffer. Centrifuge cells for at $200 \times g$ for 3 min at room temperature.
12. Suspend the cells in 300 μl of OCL medium per mouse. Count cells (if counting by hemocytometer, it is best to dilute a sample of the cells 1/10 before counting).
13. Seed 1.25×10^5 cells per well of a 24 well plate (or 2.5×10^5 cells per well of a 12-well plate).
14. Grow cells in OCL medium supplemented with 20 ng/ml M-CSF and 20 ng/ml RANKL. Incubate at 37 °C, 5% CO_2 for 5 days. Change medium and cytokines after 24 h and then every 1–2 days during this period (*see* **Notes 9** and **10**).

3.3 Expressing Foreign Proteins and Knocking Down Endogenous Proteins in OCLs Using Viral Vectors

OCLs are terminally differentiated, non-dividing cells; as such, they are refractory to many of the standard techniques used for gene expression or knockdown in most other cell types. Adenoviruses, as well as lentiviruses and other types of retroviruses, are often used to enable genetic manipulation of OCLs in culture. Adenoviruses and Lentiviruses, which we discuss here, differ in their use and properties. Adenoviruses are quite easy to work with and to propagate as virus-from-virus, a process that should be limited to two to three rounds to prevent accumulation of mutations; Adenovirus preparations may be stored frozen for future use. However, the cloning and packaging processes required for initial preparation of Adenoviruses are relatively complex. In contrast, Lentiviral vectors are easy to construct and the viruses themselves are easy to prepare, although in our hands they can be stored for only up to 10 days at 4 °C and need to be prepared anew often. Moreover, these viruses tend to be somewhat less effective in introducing their genetic cargo into OCLs compared with Adenoviruses. Finally, Adenoviruses are very amenable to coinfection studies; OCLs can be treated with a mixture of two (and possibly more) Adenoviruses, leading to coexpression of the protein products of

these viruses in the same cell. We describe here use of Adenoviruses to express exogenous proteins, and use of Lentiviruses to knock down expression of endogenous proteins in OCLs, singly or in combination.

1. *Adenoviruses*: Cloning and initial preparation of adenoviruses is beyond the scope of this chapter and will not be described here. We produce Adenoviruses using the commercial AdEasy XL Adenoviral Vector System (Stratagene, Agilent Technologies, Inc., Santa Clara, CA, USA). After obtaining an initial viral clone we amplify the viruses by infecting HEK293 cells (*see* **Note 11**) by adding a small amount of virus to the growth medium and waiting until most of the cells are infected. This point can be determined the significant change in the cells' morphology and widespread cell death after 24–72 h, depending on the concentration of the virus stock. Cells (adherent and floating) are then collected in the growth medium in the plate and sonicated; the sonicate is centrifuged, and the supernatant is filtered and stored in aliquots at –80 °C until used (*see* **Note 12**).
2. *Infection with Adenoviruses*: 48 h after seeding bone marrow cells and initiating their differentiation with RANKL and M-CSF, replace medium with a mixture of OCL medium containing M-CSF and RANKL (1/2 of the volume normally used, e.g., 1 ml for a well of a 6-well plate) and Adenovirus suspension (50–300 μl) (*see* **Notes 13–15**).
3. After an overnight incubation, remove the virus-containing medium and replace with fresh OCL medium supplemented with RANKL and M-CSF.
4. Replace medium once every 24 h until the cells are collected. Adenoviruses do not lyse OCLs, so no significant cell death is expected (unless the viral preparation is contaminated or the specific protein expressed by the viruses kills the cells). Collect cells and analyze (e.g., Fig. 2a).
5. *Lentiviruses*: In brief, viruses are prepared by transfecting the various plasmids of the Lentivirus system into HEK293 cells plated on poly-lysine. Following transfection, replace medium of the HEK293 cells with a minimal volume of medium containing 2% serum (e.g., 5 ml/10 cm plate). Collect medium after 36 h and filter through a 0.45 μm filter. Viruses can be stored in at this stage for up to 10 days at 4 °C.
6. *Infection with Lentiviruses*: 72 h after seeding bone marrow cells and initiating their differentiation with RANKL and M-CSF, remove medium. Replace medium with Lentivirus suspension supplemented with 8 μg/ml polybrene (*see* **Note 16**).
7. Centrifuge cells while in their plates at 500 × *g*, 30 °C, for 90 min. Wrap plates with Parafilm or equivalent prior to

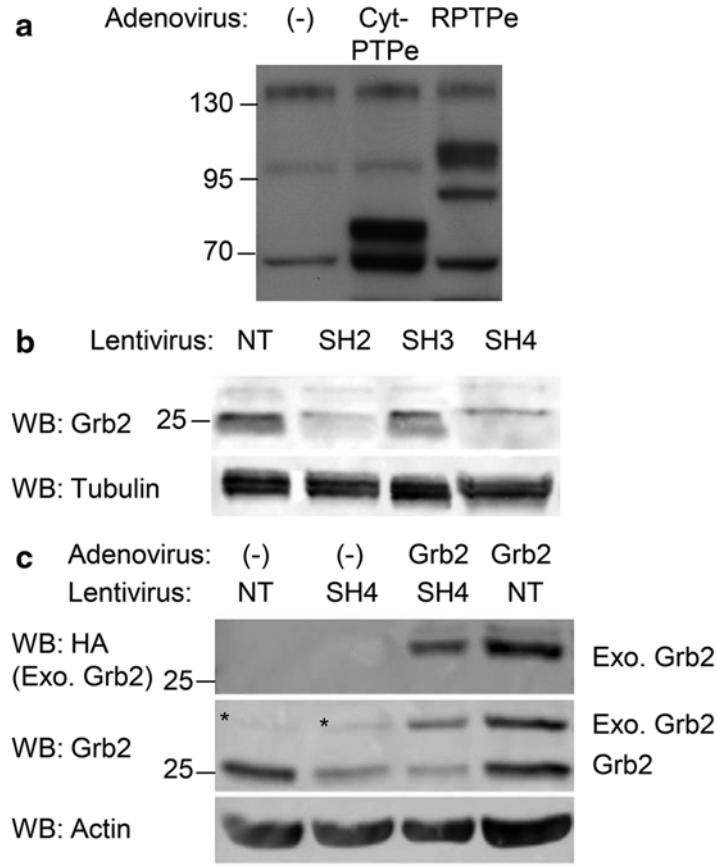

Fig. 2 Use of Adenoviruses and Lentiviruses to express exogenous genes and to inhibit endogenous genes, respectively, in OCLs. (**a**) OCLs from protein tyrosine phosphatase epsilon (PTPe) knockout mice were infected with Adenoviruses expressing cyt-PTPe and RPTPe (the cytosolic and receptor-type isoforms of PTPe, respectively). Note expression of both proteins in the infected cells. (–): uninfected knockout cells. (**b**) Inhibition of endogenous Grb2 protein expression by three shRNAs. Wild-type OCLs were prepared from mouse bone marrow and infected with Lentiviruses expressing non-targeting shRNA (NT) or one of three distinct shRNAs targeting Grb2 (SH2, SH3, and SH4). Shown are protein blots depicting Grb2 protein (*top strip*) and Tubulin (loading control, *bottom strip*). (**c**) Downregulation of endogenous Grb2 and its replacement with exogenous Grb2. Wild type OCLs were infected with lentiviruses containing the Grb shRNA SH4, and then infected with Adenoviruses expressing HA-tagged exogenous Grb2. Non-targeting shRNA (NT) served as control for downregulation of endogenous Grb2. Shown are protein blots depicting HA-Grb2 (anti-HA; *top strip*), HA-Grb2 and endogenous Grb2 (anti-Grb2; *middle strip*), and actin (loading control, *bottom strip*). Note that while SH4 downregulates the exogenous HA-Grb2 to some extent, the process results in replacing about 2/3 of endogenous Grb2 protein with the exogenous protein. The HA tag shifts migration of the 25 kDa Grb2 protein; *asterisk marks* nonspecific protein band. OCLs were prepared from mouse bone marrow as described in Subheading 3.1; Lentiviral and Adenoviral infections were performed as described in Subheading 3.3. Molecular mass markers are in kDa

centrifugation to prevent rapid loss of carbon dioxide and pH changes, and to preserve sterility.

8. Following centrifugation, remove virus suspension and replace with fresh OCL medium, supplemented with RANK and M-CSF. Return to tissue culture incubator.
9. Replace medium once per 24 h until the cells are collected. Collect cells and analyze (e.g., Fig. 2b).
10. *Infection with Lentiviruses and Adenovirus* (*see* **Note 17**): Infect cells initially with Lentiviruses 48 h after seeding, according to the above protocol.
11. 24 h later, infect with Adenoviruses as described above.
12. The day following addition of the Adenoviruses, replace medium with OCL medium/M-CSF/RANKL and repeat once every 24 h until the cells are collected (e.g., Fig. 2c).

3.4 Studying Cell Signaling in Cultured OCLs

Studying cell signaling in OCLs requires adaptations to account for the sensitivity of these cells to removal of serum or other key factors from the medium, and their very tight adherence to the surface on which they grow. Here we describe examining signaling triggered by M-CSF, estrogen, and physical adhesion to matrix.

1. Prepare OCLs from mouse bone marrow as described in Subheading 3.1 or 3.2. Grow cells in OCL medium supplemented with M-CSF and RANKL, replacing the medium every day. It is often convenient to seed cells in wells of 6-well plates; each well will contain sufficient cells for analysis of a single time point in a signaling experiment. Seed $6–7 \times 10^6$ cells per well; a single 129SvEv strain young adult male mouse (aged 2–3 months) will typically provide sufficient cells for four to five such wells.
2. *For M-CSF stimulation*: On Day 4 (seeding is counted as Day 0), starve the cells: Remove the medium, wash the cells once with PBS, and add OCL medium containing 1 % serum (without cytokines) for up to 4 h (*see* **Note 18**).
3. After the starvation period, stimulate the cells by adding M-CSF to the medium (100 ng/ml final concentration), and collect samples at times 0, 2, 5, 15, and 30 min.
4. Rinse plates with cold PBS. Remove PBS as best possible using a Pasteur pipette and vacuum. Lyse cells in NP40 lysis buffer (or any other suitable lysis buffer, supplemented with protease and phosphatase inhibitors), collect cells with the aid of a rubber policeman (*see* **Note 19**) into an Eppendorf tube, incubate on ice for 10 min, and spin down nuclei and debris at $14{,}000 \times g$ for 5 min.
5. Remove supernatant to a new tube and determine protein concentrations using an appropriate method, such as the Bradford technique.

6. Analyze by protein (Western) blotting M-CSF receptor amounts and phosphorylation (e.g., at Y809), phosphorylation of ERK and AKT.
7. *For acute Estrogen signaling*: Prepare, seed and grow cells as described in **step 1** above, in OCL medium supplemented with M-CSF and RANKL. Feed cells with fresh OCL medium with cytokines daily.
8. On the morning of Day 3, remove the medium and wash the cells once with PBS. Add estrogen-free OCL medium supplemented with M-CSF and RANKL (*see* **Note 20**). Feed cells once again with estrogen-free OCL medium supplemented with cytokines in the evening of Day 3.
9. On the morning of Day 4 examine the cells. If the culture looks well-differentiated proceed to **step 10** below. If not, wait a few hours to allow the cells to complete their differentiation.
10. Add estrogen directly to the medium for a final concentration of 10 nM. Collect cells at times 0, 2, 5, 15, 30 min (*see* **Note 21**). Collect cells as described in **steps 4** and **5** above.
11. Analyze cell lysates by protein blotting for phosphorylated (activated) ERK, AKT.
12. *Adhesion*: In this protocol adherent cells are detached from the plate, held in suspension, and then replated on surfaces coated with various proteins, thus triggering integrin signaling. OCLs adhere to matrix very strongly; in our hands, mature OCLs cannot be detached without damaging them. To circumvent this difficulty we often work with pre-OCLs, which are easier to detach and which can withstand this process better (*see* **Note 22**).
13. Prepare, seed (*see* **Note 23**) and grow cells as described in **step 1** above, in OCL medium supplemented with M-CSF and RANKL.
14. Grow cells until Day 4 with daily changes of medium.
15. On Day 4, starve cells for 4 h in OCL medium containing 1% serum, (no M-CSF or RANKL) as described in **step 2** above.
16. In parallel, on Day 4 coat plates with fibronectin or other proteins you may wish to study. Dilute stock solution with PBS, to a working concentration of 20 μg/ml. Add 1.5 ml per well of a 6-well plate and incubate for 1 h at 37 °C (or overnight at 4 °C, if prepared the day before). Remove fibronectin solution and replace with OCL medium until used in **step 18** below (*see* **Notes 24** and **25**).
17. After starvation, wash the plates containing the cells with PBS. Add 10 mM EDTA/PBS solution (1.5 ml per well of a 6 well plate) and incubate at room temperature for 10 min.

After incubation for 10 min, detach cells by gently pipetting and washing the plate with the volume of EDTA/PBS solution it contains.

18. Collect the cells into a 15 ml test tube.
19. Wash plate once again with a similar volume of 10 mM EDTA/PBS. Add the washings to the cells collected previously.
20. Spin down the cells by centrifugation at 200 × *g* for 3 min at room temperature.
21. Suspend cells in 5 ml of DMEM-HEPES medium (containing 1 mg/ml BSA).
22. Keep cells in suspension for 1 h with gentle mixing to keep the cells suspended throughout this period. This step is performed in the tissue-culture incubator to maintain proper temperature.
23. Seed cells on fibronectin-coated plates. Collect adherent cells at various time points (15, 30, 60 and 120 min) and analyze integrin signaling as indicated in **steps 4** and **5** above (followed by protein blotting for, for example, activated Src or Pyk2). Alternatively it is possible to monitor spreading of the cells by following their appearance using a suitable microscope.

4 Notes

1. M-CSF and RANKL can be purchased from commercial providers or produced and purified in-house using any of a variety of bacterial or cellular systems that overexpress M-CSF or RANKL cDNAs. In some cases M-CSF can be used in the form of conditioned media from cells that overexpress it. The choice of source should balance the relatively high cost of these cytokines when obtained commercially with the need for reagents of consistent high quality. The specific brands and types of M-CSF and RANKL noted work well in our hands, but are by no means the only sources for these reagents.
2. The strain of mice used can result in significant differences in the yield of OCLs. Mice from strain 129 SvEv provide excellent cultures and we routinely use this strain in our work. C57Black/6 mice can be used, but in our hands yield cultures that contain fewer cells than 129 SvEv mice. One can also prepare OCLs from bone marrow of mice that carry a floxed allele that has not been recombined by Cre. Cre recombinase can later be expressed in these cells using adenoviruses, leading to recombination in culture.
3. The femur contributes the highest amount of bone marrow cells, followed by the tibia. An additional relatively small number of cells can be obtained from the humerus, if forelimbs are collected as well.

4. Sterility: As the cells collected will be kept in culture for several days, it is critical to ensure that the cells entering culture are sterile. On the other hand, good tissue culture practice prevents presence of mice (live or after sacrifice) in tissue culture rooms for fear of contamination. Our practice is then to isolate intact bones from mice in a standard clean, but not sterile, laboratory using sterilized surgical equipment and sterile plasticware (even though they rapidly lose their sterility), and then to sterilize the bones with 70% ethanol prior to moving them into the tissue culture hood as described in Stage 6. From that point on, the bones and later on cells are handled in absolute sterility and are manipulated with a fresh set of sterile surgical instruments. We do not experience contaminations using this protocol.
5. We have not verified the maximal length of time a given bone can wait for subsequent bones to be collected without loss of viability of bone marrow cells. However, as a rule of thumb, if the maximal wait is expected to exceed 1 h we either reduce the number of mice processed or increase the number of people performing the dissections.
6. A 27″ needle is used since it is thin enough to enter the bone marrow cavity of both the tibia and femur and facilitates easy flushing. Due to the narrow diameter of the 27″ needle, it is easiest to aspirate the medium into the syringe with the needle removed, and only then to attach the needle. Also, it is possible to use PBS for flushing instead of OCL medium.
7. The femur is relatively easy to flush from either end as its internal diameter is constant and relatively large, and the needle fits in it well. The internal diameter of the tibia, on the other hand, narrows as one moves distally. Consequently, we cut off the distal third of the tibia to ensure proper flow. If the distal end of the tibia is too narrow for the flushing process, shorten this end further and repeat flushing.
8. At this point one may shift to the protocol from Subheading 3.2 to isolate monocytes from the bone marrow cells.
9. If cells are to be examined using immunofluorescence methods, plate them on glass coverslips (one round 13 mm diameter coverslip per well of a 24-well plate, or several round or square coverslips per larger plate). When removing the medium by vacuum suction, take care not to lift or break glass coverslips that may be present in the plates/wells.
10. It is possible to omit RANKL from the medium on the day of seeding without harming the eventual differentiation process.
11. Adenoviruses can be packaged any subclone of HEK293 cells, so long as they adhere well to the plate.
12. Adenoviruses can infect human cells and tissues. Take care to handle adenoviral preparates with care and to dispose of them

and of objects that come in contact with them according to your Institution's regulations.

13. We use the viruses without titering. It has been our experience that adenoviruses prepared from HEK293 cells that appear completely infected 24 h after adding the virus stock to the uninfected cells are concentrated enough for use with OCLs.
14. In order to conserve adenoviral stock, use the minimal volume required to cover the plate at this stage (e.g., 4.5 ml/10 cm plate).
15. Cells may be coinfected with a mixture of more than one type of adenovirus.
16. Polybrene is conveniently prepared and stored as a 1000× stock of 8 mg/ml in water.
17. This protocol is convenient if one wishes to downregulate expression of an endogenous protein (using siRNA expressed by lentiviruses) and express an exogenous protein in its place (using adenoviruses).
18. OCLs are quite sensitive to withdrawal of M-CSF or RANKL. Removal of these factors should be for a relatively short time, such as 4 h, which allows signaling to reduce to baseline values without significantly harming the cells.
19. OCLs are markedly adherent. Use rubber policeman to ensure complete removal of cells from the plate.
20. Although many stimuli activate the same cellular molecules and pathways, the sensitivity of OCLs to removal of M-CSF and RANKL makes it imperative to avoid their removal unless required. We find that removal of estrogen from the medium (by using medium devoid of phenol red and containing charcoal-stripped serum) while leaving M-CSF and RANKL maintains health of the cells and succeeds to reduce phosphorylation of relevant signaling molecules to a minimum.
21. Preparation of estrogen: Dissolve powder in pure ethanol, 1 mg/ml. Note that estrogen dissolves with some difficulty and may require gentle heating. Use glass tubes for preparation and storage of the stock solution. It is possible to dilute the stock to 20 μg/ml in OCL alpha-MEM medium without phenol red and store frozen. Do not refreeze thawed aliquots.
22. Alternative protocols that are not discussed here include growing OCLs on a collagen gel. The gel can be degraded with collagenase, thus releasing the mature OCLs to be used as described here. OCLs held in suspension can also be treated with activating anti-integrin antibodies as an alternative to allowing them to readhere to matrix.
23. Be prepared to experience significant cell loss once cells are detached from the plate. To counter this, seed more plates/wells

for those cultures that are meant to be detached. For example, we seed 9 wells of a 6-well plate as follows: 1 well to analyze adherent cells, 4 wells to analyze cells held in suspension, and 4 wells to analyze suspended cells that have been allowed to reattach to the plate. Cell loss can be reduced if the cells are plated and grown on plates made of bacteriological-grade plastic, to which they adhere relatively weakly.

24. It is possible to leave the fibronectin solution in the wells and remove it only prior to use.
25. It is possible to coat the plates with other proteins, vitronectin (an αvβ3 integrin ligand) or BSA, which is not an integrin ligand, for control purposes.

Acknowledgements

This study was supported by grants from The Israel Science Foundation, from the Chief Scientist, Israel Ministry of Heath, and from the Kekst Family Institute for Medical Genetics and the David and Fella Shapell Family Center for Genetic Disorders Research, both of the Weizmann Institute of Science (to A.E.).

References

1. Bruzzaniti A, Baron R (2006) Molecular regulation of osteoclast activity. Rev Endocr Metab Disord 7(1–2):123–139
2. Teitelbaum SL (2011) The osteoclast and its unique cytoskeleton. Ann N Y Acad Sci 1240: 14–17
3. Jurdic P, Saltel F, Chabadel A, Destaing O (2006) Podosome and sealing zone: specificity of the osteoclast model. Eur J Cell Biol 85(3–4):195–202
4. Georgess D, Machuca-Gayet I, Blangy A, Jurdic P (2014) Podosome organization drives osteoclast-mediated bone resorption. Cell Adh Migr 8(3):191–204
5. Teitelbaum SL (2007) Osteoclasts: what do they do and how do they do it? Am J Pathol 170(2):427–435
6. Wada T, Nakashima T, Hiroshi N, Penninger JM (2006) RANKL-RANK signaling in osteoclastogenesis and bone disease. Trends Mol Med 12(1):17–25
7. Ross FP (2006) M-CSF, c-Fms, and signaling in osteoclasts and their precursors. Ann N Y Acad Sci 1068:110–116
8. Miyazaki T, Sanjay A, Neff L, Tanaka S, Horne WC, Baron R (2004) SRC kinase activity is essential for osteoclast function. J Biol Chem 279(17):17660–17666
9. Lowe C, Yoneda T, Boyce BF, Chen H, Mundy GR, Soriano P (1993) Osteopetrosis in Src-deficient mice is due to an autonomous defect of osteoclasts. Proc Natl Acad Sci U S A 90(10):4485–4489
10. Soriano P, Montgomery C, Geske R, Bradley A (1991) Targeted disruption of the c-src proto-oncogene leads to osteopetrosis in mice. Cell 64(4):693–702
11. Umeda S, Beamer WG, Takagi K, Naito M, Hayashi S, Yonemitsu H, Yi T, Shultz LD (1999) Deficiency of SHP-1 protein-tyrosine phosphatase activity results in heightened osteoclast function and decreased bone density. Am J Pathol 155(1):223–233
12. Aoki K, Didomenico E, Sims NA, Mukhopadhyay K, Neff L, Houghton A, Amling M, Levy JB, Horne WC, Baron R (1999) The tyrosine phosphatase SHP-1 is a negative regulator of osteoclastogenesis and osteoclast resorbing activity: increased resorption and osteopenia in me(v)/me(v) mutant mice. Bone 25(3):261–267
13. Bauler TJ, Kamiya N, Lapinski PE, Langewisch E, Mishina Y, Wilkinson JE, Feng GS, King PD (2011) Development of severe skeletal defects in induced SHP-2-deficient adult mice: a model of skeletal malformation in humans with

SHP-2 mutations. Dis Model Mech 4(2): 228–239

14. Zhou Y, Mohan A, Moore DC, Lin L, Zhou FL, Cao J, Wu Q, Qin YX, Reginato AM, Ehrlich MG, Yang W (2015) SHP2 regulates osteoclastogenesis by promoting preosteoclast fusion. FASEB J. doi:10.1096/fj.14-260844
15. Shivtiel S, Kollet O, Lapid K, Schajnovitz A, Goichberg P, Kalinkovich A, Shezen E, Tesio M, Netzer N, Petit I, Sharir A, Lapidot T (2008) CD45 regulates retention, motility, and numbers of hematopoietic progenitors, and affects osteoclast remodeling of metaphyseal trabecules. J Exp Med 205(10):2381–2395
16. Carlson J, Cui W, Zhang Q, Xu X, Mercan F, Bennett AM, Vignery A (2009) Role of MKP-1 in osteoclasts and bone homeostasis. Am J Pathol 175(4):1564–1573
17. Sartori R, Li F, Kirkwood KL (2009) MAP kinase phosphatase-1 protects against inflammatory bone loss. J Dent Res 88(12): 1125–1130
18. Levy-Apter E, Finkelshtein E, Vemulapalli V, Li SS, Bedford MT, Elson A (2014) Adaptor protein GRB2 promotes Src tyrosine kinase activation and podosomal organization by protein-tyrosine phosphatase in osteoclasts. J Biol Chem 289(52):36048–36058
19. Granot-Attas S, Luxenburg C, Finkelshtein E, Elson A (2009) PTP epsilon regulates integrin-mediated podosome stability in osteoclasts by activating Src. Mol Biol Cell 20(20):4324–4334
20. Chiusaroli R, Knobler H, Luxenburg C, Sanjay A, Granot-Attas S, Tiran Z, Miyazaki T, Harmelin A, Baron R, Elson A (2004) Tyrosine phosphatase epsilon is a positive regulator of osteoclast function in vitro and in vivo. Mol Biol Cell 15(1):234–244
21. Finkelshtein E, Lotinun S, Levy-Apter E, Arman E, den Hertog J, Baron R, Elson A (2014) Protein tyrosine phosphatases epsilon and alpha perform nonredundant roles in osteoclasts. Mol Biol Cell 25(11):1808–1818
22. Chellaiah MA, Kuppuswamy D, Lasky L, Linder S (2007) Phosphorylation of a Wiscott-Aldrich syndrome protein-associated signal complex is critical in osteoclast bone resorption. J Biol Chem 282(13):10104–10116
23. Chellaiah MA, Schaller MD (2009) Activation of Src kinase by protein-tyrosine phosphatase-PEST in osteoclasts: comparative analysis of the effects of bisphosphonate and protein-tyrosine phosphatase inhibitor on Src activation in vitro. J Cell Physiol 220:382–393
24. Eleniste PP, Du L, Shivanna M, Bruzzaniti A (2012) Dynamin and PTP-PEST cooperatively regulate Pyk2 dephosphorylation in osteoclasts. Int J Biochem Cell Biol 44(5):790–800
25. Rhee I, Davidson D, Souza CM, Vacher J, Veillette A (2013) Macrophage fusion is controlled by the cytoplasmic protein tyrosine phosphatase PTP-PEST/PTPN12. Mol Cell Biol 33(12):2458–2469
26. Amoui M, Sheng MH, Chen ST, Baylink DJ, Lau KH (2007) A transmembrane osteoclastic protein-tyrosine phosphatase regulates osteoclast activity in part by promoting osteoclast survival through c-Src-dependent activation of NFkappaB and JNK2. Arch Biochem Biophys 463(1):47–59
27. Lau KH, Stiffel V, Amoui M (2012) An osteoclastic protein-tyrosine phosphatase regulates the beta3-integrin, syk, and shp1 signaling through respective src-dependent phosphorylation in osteoclasts. Am J Physiol Cell Physiol 302(11):C1676–C1686
28. Itzstein C, van't Hof RJ (2012) Osteoclast formation in mouse co-cultures. Methods Mol Biol816:177–186.doi:10.1007/978-1-61779-415-5_12

Chapter 17

Functional Analysis of Protein Tyrosine Phosphatases in Thrombosis and Hemostasis

Souad Rahmouni*, Alexandre Hego*, Céline Delierneux, Odile Wéra, Lucia Musumeci, Lutz Tautz*, and Cécile Oury*

Abstract

Platelets are small blood cells derived from cytoplasmic fragments of megakaryocytes and play an essential role in thrombosis and hemostasis. Platelet activation depends on the rapid phosphorylation and dephosphorylation of key signaling molecules, and a number of kinases and phosphatases have been identified as major regulators of platelet function. However, the investigation of novel signaling proteins has suffered from technical limitations due to the anucleate nature of platelets and their very limited levels of mRNA and de novo protein synthesis. In the past, experimental methods were restricted to the generation of genetically modified mice and the development of specific antibodies. More recently, novel (phospho) proteomic technologies and pharmacological approaches using specific small-molecule inhibitors have added additional capabilities to investigate specific platelet proteins.

In this chapter, we report methods for using genetic and pharmacological approaches to investigate the function of platelet signaling proteins. While the described experiments focus on the role of the dual-specificity phosphatase 3 (DUSP3) in platelet signaling, the presented methods are applicable to any signaling enzyme. Specifically, we describe a testing strategy that includes (1) aggregation and secretion experiments with mouse and human platelets, (2) immunoprecipitation and immunoblot assays to study platelet signaling events, (3) detailed protocols to use selected animal models in order to investigate thrombosis and hemostasis in vivo, and (4) strategies for utilizing pharmacological inhibitors on human platelets.

Key words Platelets, Aggregation, Secretion, Signaling, Flow cytometry, Aggregation under flow, Selectin, JON/A, Calcium, Bleeding time, Collagen, CLEC-2, GPVI, ADP, Thrombin, Intravital microscopy, Ferric chloride, Thromboembolism, DSPs, Dual-specificity phosphatases, PTPs, Protein tyrosine phosphatases, DUSP3, VHR, Small molecule inhibitors, Western blots, Immunoprecipitation

1 Introduction

Platelets are small anucleate cytoplasmic fragments of megakaryocytes produced in the bone marrow [1, 2]. Human platelets circulate for approximately 7–10 days in the blood stream before being cleared by macrophages in the spleen and liver. Only when the endothelial

*These authors are contributed equaly to this work.

Rafael Pulido (ed.), *Protein Tyrosine Phosphatases: Methods and Protocols*, Methods in Molecular Biology, vol. 1447,
DOI 10.1007/978-1-4939-3746-2_17,

cell layer of blood vessels is damaged by injuries or pathological alterations, the adhesive potential of platelets becomes evident. Under these conditions, components of the subendothelial extracellular matrix (ECM) are exposed and trigger sudden platelet activation and adhesion [3]. The first step in the hemostatic cascade is the interaction of platelets with the exposed ECM, which contains a large number of adhesive macromolecules, such as laminin, fibronectin, collagen, and von Willebrand factor (vWF). The initial tethering of platelets to the ECM is mediated by the interaction between the platelet receptor glycoprotein (GP) Ib and vWF bound to collagen. The binding of GPIb to vWF has a fast off-rate and is therefore insufficient to mediate stable adhesion. 'Rolling' platelets establish contacts with the thrombogenic ECM protein collagen through their immunoglobulin superfamily receptor GPVI. This receptor triggers intracellular signals that shift platelet integrins to a high-affinity state and induce the release of the secondary mediators adenosine diphosphate (ADP) and thromboxane A_2 (TXA_2). These agonists, together with locally produced thrombin, contribute to cellular activation by stimulating G-protein coupled receptors, which induce various signaling events and act synergistically to induce full platelet activation [4, 5].

Platelet activation depends on the rapid phosphorylation and dephosphorylation of key signaling proteins, particularly on tyrosine residues. The repertoire of protein tyrosine kinases (PTKs) has been well described in platelet activation (reviewed in ref. 6). However, the expression, regulation, specificity, and function of the platelet-expressed protein tyrosine phosphatases (PTPs) are largely unknown. Quantitative proteomic analyses revealed that 14 out of 37 known classical, phosphotyrosine-specific PTPs are expressed in human platelets [7, 8]. However, only a few of these enzymes, including PTP1B, SHP1, SHP2, and CD148, have been investigated in platelet signaling [8, 9]. Expression and function of the dual-specificity phosphatases (DSPs), the largest subgroup of PTPs with (additional) activity towards phosphoserine and phosphothreonine or non-protein substrates, are largely unknown.

Because platelets have no nucleus and only very limited levels of mRNA and de novo protein synthesis, standard RNA interference or recombinant DNA techniques cannot be used to investigate novel regulatory platelet proteins. Instead, such studies depend on the generation of knockout animals and the development of specific antibodies, tool compounds, and new technologies such as (phospho)proteomics. Using both genetic knockout and pharmacological inhibition, we recently identified the dual-specificity phosphatase 3 (DUSP3) as a major player in platelet biology [10]. This was the first time a DSP had been implicated in platelet function. We showed that DUSP3 is essential for platelet activation and thrombus formation in vivo. We also demonstrated that signaling via the canonical GPVI and C-type lectin-like receptor (CLEC) 2-induced pathways is impaired in DUSP3-deficient platelets. To investigate DUSP3

function in human platelets, we developed a novel small-molecule inhibitor of DUSP3. We showed that inhibition of DUSP3 activity in human platelets phenocopies the effect of DUSP3 deficiency in murine cells, providing proof-of-principle for a DUSP3-based therapeutic approach in arterial thrombosis.

In this chapter we describe methods to investigate the role of DUSP3 in platelet signaling and activation. These methods are generally applicable also to other PTPs or signaling proteins. We provide detailed instructions on how to study platelet function both ex vivo (mouse and human platelets) and in vivo in mice.

2 Materials

All chemicals used should be of analytical grade. Distilled water (dH_2O) should be used for preparation of all buffers.

2.1 Anesthetic Reagents

1. Ketamine–xylazine mix: Ketamine 1000 and xylazine (Xyl-m; 2%). Stock concentrations: ketamine 100 mg/μL, xylazine 20 mg/μL. Prepare an anesthetic cocktail just before the anesthesia with a final concentration 100 mg/kg of ketamine and 10 mg/kg of xylazine. Add (body weight × 1 × 1.5 μL) of ketamine stock and (body weight × 0.5 × 1.5 μL) of xylazine stock. Complete with NaCl 0.9% to 300 μL. Inject to mice intraperitoneally (i.p.) 200 μL of the ketamine–xylazine mix using a 1 mL syringe with 26 G needle. Check for depth of anesthesia after 10–15 min by pinching the footpad of the mouse using forceps or fingertips. If the animal withdraws the foot or even "cries," anesthesia is not deep enough to proceed. If required, mice should be maintained under anesthesia by injecting Nembutal (*see* **Notes 1** and **2**).

2.2 Anticoagulants

Anticoagulant usage depends on the type of experiment as they can influence the results. For human and mouse platelet preparations, we recommend acid citrate dextrose (ACD) as anticoagulant when working with washed platelets, and citrate when working with whole blood or platelet-rich-plasma (PRP). Heparin should be avoided because of its platelet activating properties [11].

1. Acid-citrate dextrose (ACD) buffer: Dissolve 27.35 g sodium citrate (93 mM), 1.471 g citric acid (7 mM), and 0.252 g dextrose (14 mM) in a final volume of 1 L of dH_2O. This buffer can be kept at 4 °C for up to 6 months. Use 1 volume of anticoagulant for 6 volumes of blood. Just before the blood collection, add 1 U/mL of apyrase grade I. Once thawed, apyrase should not be frozen a second time.
2. Citrate buffers:
   - Sodium citrate tribasic dehydrate 3.2%: dissolve 40 g in 1 L dH_2O.

- Sodium citrate tribasic dehydrate 3.8%: dissolve 47.5 g in 1 L dH_2O.

Buffers can be kept at 4 °C for up to 6 months.

Use 1 volume of citrate 3.2% for 9 volumes of human blood, and 1 volume of citrate 3.8% for 9 volumes of mouse blood.

2.3 Blood Collection

1. 1 mL syringes with 26 G needles and 10 mL syringes with 18 G needles.
2. 1.5 mL polypropylene Eppendorf tubes.
3. Disposable Capillaries (10 μL).
4. 50 mL polypropylene conical tube.
5. Apyrase.

2.4 Platelet Preparation and Aggregation

1. Stock $CaCl_2$: 21.9 g (100 mM) $CaCl_2$ in 1 L dH_2O.
2. Stock solutions for Tyrode's buffer:
   - Stock solution 1: 8.01 g (137 mM) NaCl; 1.01 g (12 mM) $NaHCO_3$; 0.149 g (2 mM) KCl; 0.060 g (0.34 mM) Na_2HPO_4. Dissolve in 1 L of dH_2O.
   - Stock solution 2: Dissolve 119.2 g (5 mM) HEPES powder in 1 L of dH_2O.
   - Stock solution 3: Dissolve 203.3 g (1 mM) $MgCl_2$ in 1 L of dH_2O.

   Stock solutions can be kept at 4 °C for up to 6 months.
3. Tyrode's buffer: dissolve 10 mg of glucose and 35 mg of BSA in 10 mL of stock solution 1. Add 100 μL of stock solution 2 and 10 μL of stock solution 3. Bring to room temperature and use within the day of preparation.
4. Microcentrifuge.
5. Benchtop centrifuge with swinging bucket rotor.
6. 15 and 50 mL polypropylene conical tubes.
7. Hematology analyzer. We used Cell-Dyn 3700 from Abbott.
8. Cuvettes 450 μL (ChronoLog Corporation).
9. ChronoLog siliconized stir bars (ChronoLog Corporation).
10. Lumi-Aggregometer. We used ChronoLog Lumi-Aggregometer from ChronoLog Corporation.
11. 200 μL gel loading tips.

2.5 Platelet Secretion Using Flow Cytometry

1. FITC-conjugated anti-mouse CD62P antibody (clone RB40.34, BD Biosciences).
2. PE-conjugated anti-mouse active form of $\alpha_{IIb}\beta_3$ (clone JON/A, Emfret Analytics).

3. PE-conjugated anti-human CD62P antibody (clone AC 1.2, BD Biosciences).
4. FITC-conjugated anti-PAC1 antibody (clone PAC-1, BD Biosciences).
5. 5 mL polystyrene round bottom tube.
6. 1 % of Paraformaldehyde (PFA) (*see* **Note 3**).
7. BD FACS™ lysing solution (BD Biosciences); 10× concentrate. To be diluted in dH_2O.

2.6 Platelet Activation, Lysis, Immunoprecipitation (IP), and Immunoblot

1. Cuvettes 450 µL (ChronoLog Corporation).
2. Siliconized stir bars (ChronoLog Corporation).
3. 200 µL gel loading tips.
4. 96-well flat bottom plates.
5. Pierce Coomassie (Bradford) Protein Assay Kit (Thermo Scientific).
6. Spectrophotometer.
7. Complete EDTA-free protease inhibitor cocktail.
8. PhosphoSTOP phosphatase inhibitor cocktail.
9. Stock solutions for platelet 4× lysis buffer:
   - 5 M NaCl: dissolve 292.2 g NaCl in 1 L dH_2O.
   - 1 M Tris–HCl, pH 7.5: dissolve 60.55 g of Tris (hydroxymethyl aminomethane) in 460 mL dH_2O. Adjust the pH to 7.5 with conc. HCl. Bring to 500 mL with dH_2O.
   - 0.5 M EDTA pH 8: Dissolve 93.05 g EDTA in 460 mL dH_2O. Adjust the pH to 8.0 using 1 M NaOH. Bring to 500 mL with dH_2O.
   - 0.5 M EGTA pH 8: dissolve 95.1 g of EGTA in 460 mL dH_2O. Adjust the pH 8.0 with 1 M NaOH. Bring to 500 mL with dH_2O.
10. Platelet 4× lysis buffer: 60 mL of 5 M NaCl; 20 mL of 0.5 M Tris–HCl; 4 mL of 0.5 M EGTA; 4 mL of 0.5 M EDTA, and 20 mL of 100% NP-40. Bring to 500 mL with dH_2O. Mix well. Store the buffer at 4 °C for up to 6 months.

    When needed, prepare 2× platelet lysis buffer and add fresh complete EDTA-free protease inhibitor cocktail and PhosphoSTOP phosphatase inhibitor cocktail. Stocks of protease and phosphatase inhibitor cocktails can be prepared in advance (concentration 20×) and stored at –20 °C in small aliquots.
11. Stock solutions for Laemmli 2× sample buffer.
    - 20% SDS: dissolve 20 g SDS in 100 mL dH_2O.
    - 1 M Tris–HCl pH 6.8: dissolve 121.14 g Tris in 1 L dH_2O and adjust pH to 6.8 with HCl.

12. Laemmli 2× sample buffer: (4% SDS) 2 mL of 20% SDS; (20% glycerol) 2 mL of 100% glycerol; (50 mL Tris–HCl) 1 mL of 500 mM Tris–HCl; 1 mg of bromophenol blue (0.01%). Adjust to 9 mL with dH_2O. Stock in 800 µL aliquots at −20 °C. When needed, defreeze an aliquot and add 200 µL of 2-mercaptoethanol. This solution can be kept at room temperature (RT) under a fume hood and is stable for up to 3 months.
13. Immunoblot Assays:
    - Vertical acrylamide electrophoresis unit with power supply.
    - Electroblotting unit, fully submerged.
    - Nitrocellulose membrane (0.45 µm pore size).
    - Whatman #1 filter paper.
    - Methanol.
    - Precast 4–20% Tris–Glycine gradient gels.
    - SDS running buffer; 10× stock solution (2 L): 60.4 g Tris base, 288 g glycine, 20 g SDS. Make up the solution close to the desired volume using dH_2O. Stir for 10 min. Adjust the pH to be between 8.1 and 8.5. Adjust with dH_2O to the final desired volume.
    - TBST buffer; 10× stock solution (1 L): 24.2 g Tris base, 80 g NaCl, add 800 mL of cold dH_2O, adjust pH to 7.6 by adding ~15 mL conc. HCl, and add 10 mL Tween 20. Stir until Tween is completely dissolved and adjust the final volume to 1 L using cold dH_2O.
    - Blocking buffer: 3% BSA in 1× TBST; 5% fat-free milk in 1× TBST.
    - Molecular weight marker: Mix equal volumes of MagicMark (Life Technologies) and SeeBlue Plus2 Prestained Protein Standards (Life Technologies). This will allow visual control of migration of proteins on the gel (SeeBlue) and visualize the marker (MagicMark) together with proteins of interest after ECL.
    - Optional: phospho-specific antibodies and pan-antibodies directed against the signaling molecules involved in the platelet receptor pathway of interest.
    - Anti-phosphotyrosine antibody (4G10 clone); anti-actin or anti-GAPDH antibodies; HRP-conjugated anti-mouse and anti-rabbit secondary antibodies.
    - Chemiluminescent detection kit (ECL).

2.7 In Vivo Thrombosis Models

1. Carboxyfluorescein succinimidyl ester (CFSE). Add 50 µL of DMSO to one vial of 50 µg CFSE dye until fully dissolved. The stock solution is 1 µg/µL. Keep stocks at −20 °C protected from light.

2. Ferric chloride ($FeCl_3$). Prepare 10% solution of $FeCl_3$ in dH_2O. In 1.5 mL Eppendorf tube, dissolve 100 mg of $FeCl_3$ powder in 100 μL of dH_2O and vortex the mix. The solution should be freshly prepared.
3. NaCl 0.9% sterile: Mini Plasco NaCl 0.9.
4. Horm Collagen (Takeda Austria GmbH).
5. Epinephrine (1 mg/mL, Sterop laboratories).
6. Forceps: Dumont 7 and Dumont 7b.
7. Surgical scissor: Hardened Fine Iris Scissors.
8. Spring Scissor: Spring Scissors—8 mm Blades.
9. BD Intramedic™ Polyethylene Tubing (Non-Sterile). ID 0.28 mm, OD 0.6 mm.
10. Sponge: Sugi® points sterile (Kettenbach).
11. 0.5 × 0.5 × 0.5 cm triangle black plastic: from thin black plastic bag.
12. 4-0 silk suture.
13. 1 mm × 1 mm square Whatman filter paper.
14. 1.5 mL Eppendorf tubes.
15. 1 mL syringes with 26 G needles.
16. Balance.
17. Heating plate.
18. Binocular stereomicroscope equipped with a double-arm led illuminator.
19. Epifluorescence Microscope equipped with 10× dry objective.

3 Methods

Appropriate licensing and ethical permissions must be obtained from the researcher's local ethical committee for all animal procedures and experiments. Experiments using human samples should be approved by the researcher's institutional review board, and should be in accordance with the Helsinki Declaration.

Platelets easily become activated during preparation, and shape change, aggregation, and release of granule content may occur. The ideal preparation method should provide resting platelets that respond to ex vivo stimulation similarly as they would do in vivo. Platelets should also maintain their responsiveness to stimuli for few hours after blood collection to allow in vitro experiments. To prevent platelet activation during preparation, strong mechanical forces such as vigorous shaking, fast pipetting, use of needles with small gauge numbers (<21 G), or of vacuum blood collection system should be avoided.

3.1 Retro-orbital Mouse Blood Collection

This method allows the collection of large blood volumes (up to 1 mL) and therefore can only be used as a terminal procedure that should be performed by well-trained personnel. Cardiac puncture can also be used as a terminal procedure to allow the collection of 0.8–1 mL of blood. However, this method requires the use of a syringe/needle that may lead to the activation/desensitization of platelets. In contrast, the retro-orbital method allows for free-flow blood collection with lower risk of platelet disturbances.

1. Anesthetize mice by intraperitoneal (i.p.) injection of ketamine–xylazine mix as described in Subheading 2.1.
2. Prepare one Eppendorf tube (1.5 mL) for each mouse. Add 1 volume of ACD and 1 U/mL of apyrase as described in Subheading 2.2. Swirl the tubes to allow the anticoagulant mix to come into contact with tube walls.
3. Verify that the mouse is deeply anesthetized by pinching its footpad with forceps or fingertips. With your first finger and thumb, scruff the animal firmly enough to pull the skin around the eye (Fig. 1a).
4. Detach gently the eyeball from adjacent tissues with the help of the capillary (Fig. 1b).
5. Insert the glass capillary into the medial canthus of the eye under the nictitating membrane (Fig. 1c). Apply a rotation motion to the capillary to enter the slightly resistant sinus membrane (Fig. 1c). When the vein is broken, the blood enters the capillary and flows into the collection tube.
6. Stop collecting when the blood volume reaches 1 mL (*see* **Note 4**).
7. Mix immediately the blood with the anticoagulant with a gentle up and down movement (do no vortex).
8. Euthanize the mouse immediately after blood collection by cervical dislocation and make sure the animal is dead.

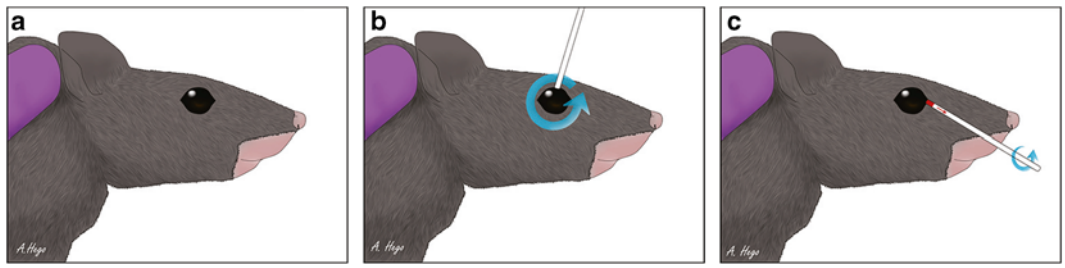

Fig. 1 Retro-orbital mouse blood collection. (**a**) With your index finger and thumb, scruff the animal firmly enough to pull the skin around the eye. (**b**) Detach gently the eyeball from adjacent tissues with the help of the capillary. (**c**) Insert the glass capillary into the medial canthus of the eye under the nictitating membrane and apply a rotation motion to the capillary to enter the sinus membrane

3.2 Isolation of Mouse Washed Platelets

1. Centrifuge the Eppendorf tube containing the collected mouse blood for 5 s at 800 × *g* followed by 5 min at 100 × *g* at room temperature.
2. Collect carefully the upper layer supernatant containing the platelet rich plasma (PRP) and transfer to a clean 15 mL conical tube. PRP from different mice of the same genotype can be pooled in one sample (*see* **Note 5**). Mix by gentle pipetting using a 1 mL tip.
3. To wash platelets, dilute the PRP three times in ACD containing 1 U/mL apyrase at room temperature.
4. Centrifuge at 800 × *g* 10 min at room temperature.
5. Discard supernatant and dry the 15 mL tube walls using Tork wiping paper.
6. Resuspend washed platelets pellet in 1 mL of 1× Tyrode's buffer containing 1 U/mL apyrase (room temperature). Mix gently by pipetting using 1 mL tips.
7. To count cells, take an aliquot of 20 μL of washed platelet suspension and add 180 μL of Tyrode's buffer. Mix gently by pipetting using a 1 mL tip and proceed with counting using a hematology analyzer. Set up the machine for mouse protocol.
8. Platelets should be resuspended in 1× Tyrode's buffer containing 1 U/mL apyrase to a concentration of 350×10^3 platelets/μL for aggregation and secretion experiments, and to 500×10^3 platelets/μL for immunoblot and immunoprecipitation (IP) experiments.

3.3 Mouse Platelet Aggregation Assay

Light transmission aggregometry is a widely used method to assess platelet responses to agonists, inhibitors, or after depletion of a specific protein [12]. Platelet aggregation can be monitored by measuring the transmission of light (expressed as percentage of light transmission) through a platelet suspension (PRP or washed platelets). Single platelets in suspension form a turbid solution that reduces the transmission of light. After addition of a platelet receptor agonist, platelets form aggregates that reduce the sample turbidity resulting in an increase of light transmission [13, 14]. Light transmission aggregometry is considered the 'gold standard' for testing platelet function and allows rapid collection of data for platelet responsiveness to a variety of platelet receptor agonists in small sample volumes [15]. Thus, we recommend this method as the first step to screen for platelet function defects in knockout animals. However, because this method is only semi-quantitative and performed under non-physiological conditions that do not fully mimic aggregate formation in vivo, it should be combined with additional experiments (as described below) to assess platelet function.

1. Aliquot 270 μL (350×10^3/μL mouse platelets) of washed platelets in 450 μL cuvettes containing one siliconized stir bar.
2. Let the platelets rest for 15 min at room temperature.
3. Meanwhile, set the aggregometer to optical mode at 37 °C and 1200 rpm.
4. Start the AGGRO/LINK8 program and select the test procedure within the Aggregometer window. Select the number of channels to be used (usually two or four, depending on the available equipment. We used the ChronoLog Lumi-Aggregometer).
5. Select "run patient" within the aggregometer window and indicate the test conditions when prompted.
6. Make sure to place the cuvette with 500 μL Tyrode's buffer in appropriate reference well.
7. Start the assay by clicking on "OK".
8. Press "set baselines" pushbutton for each test channel.
9. After baselines have stabilized, click on "Stop test" button and restart current test within the aggregometer window.
10. Using the 200 μL gel loading tips, add 2.7 μL of the 100 mM $CaCl_2$ stock solution to each cuvette.
11. About 30 s later, add the receptor agonist to be tested to each cuvette/sample. Start with the highest concentration agonist to be tested. For example, 0.5–1 μg/mL of collagen-related peptide (CRP) induces a full, irreversible aggregation of wild type (WT) mouse platelets 2 min after stimulation. Platelets from WT mice should always be used as a reference. Complete aggregation should be reached in the control conditions.
12. When a complete (80–100%) irreversible aggregation is achieved under control conditions, stop the assay and proceed with the next sample. If very low concentrations of platelet receptor agonist are used, aggregation may not be complete (usually lower than 50%). In these cases, the assay should be stopped when the aggregation is plateauing.
13. To calculate slope and amplitude, click on edit and set the start and stop time. Place the "start line" to where the agonist was added and the "stop line" to where the aggregation tracing was at full amplitude. Click on "done" and select "calculate result" within the Edit window. This command will allow calculation of the percentage of aggregation and the slope. Click the "OK" button to reveal the final data in the data box. This setting is specific to the ChronoLog Lumi-Aggregometer (ChronoLog Corporation).

3.4 Platelet Secretion Assay by Flow Cytometry

Flow cytometry is a quantitative, reliable, and sensitive method for the evaluation of platelet function. When activated, platelets undergo a shape change and release their granule content. As a result, several antigens are exposed on the platelet surface and can be utilized to discriminate between activated and resting platelets. P-selectin (also known as CD62P) resides within the alpha-granules and becomes exposed on the membrane surface after platelet degranulation [16]. It is probably the most widely used laboratory marker of platelet activation, either alone or in combination with other markers [17]. Monoclonal antibodies directed against P-selectin allow labeling and quantification of degranulated platelets. Additionally, during platelet activation, integrin $\alpha_{IIb}\beta_3$ (also known as GPIIb/IIIa) undergoes a conformational change by an inside-out activation phenomenon. The active form can be recognized using specific antibodies such as JON/A for mice and PAC-1 for humans [18]. Moreover, the conformational change allows fibrinogen to bind to its integrin receptor, and FITC-conjugated fibrinogen can be used to detect platelet activation.

Platelet secretion can be analyzed on washed platelets, PRP, or whole blood. We describe two methods using either washed platelets or whole blood. Specifically, we provide experimental details for the analysis of $\alpha_{IIb}\beta_3$ integrin activation and P-selectin exposure on CRP-activated mouse platelets. Similar methods can be used with other platelet agonists.

3.4.1 Mouse Platelet Secretion Assay in Whole Blood

Platelet secretion in whole blood is fast, requires a very small volume of blood, and does not require platelet isolation, thereby limiting the steps that may lead to accidental platelet activation. However, this method requires the use of higher concentrations of platelet receptor agonists as compared to washed platelet suspensions. It is most useful when the amount of available blood is a limiting factor.

1. Prepare three aliquots (25 μL each) of citrate-anticoagulated mouse blood in three tubes (1 volume of 3.8% citrate buffer for 9 volumes of mouse blood). Label the tubes as follows: no stimulation (NS), 1 and 3 μg/mL CRP.
2. To tube NS, add of 0.9% NaCl or Tyrode's buffer; to the other tubes add 1 or 3 μg/mL of CRP (final concentration), respectively.
3. Incubate for 15 min at room temperature.
4. Add 2.5 μL of FITC-CD62P and PE-JON/A antibodies. Mix gently and incubate for 15 min in the dark at room temperature.
5. Add 1 mL of 1× BD FACS lysing solution and incubate for 30 min.
6. Analyze cells by flow cytometry within 48 h.

3.4.2 Mouse Platelet Secretion Assay in Washed Platelets

1. Prepare five aliquots of 50 μL each (350×10^3/μL platelets) in five tubes. Label the tubes as follow: NS; 0.1, 0.3, 0.5, and 1 μg/mL CRP.
2. To tube NS, add of 0.9% NaCl or Tyrode's buffer, and to the other tubes add 0.1, 0.3, 0.5, and 1 μg/mL CRP (final concentrations).
3. Incubate for 15 min at RT.
4. Add 2.5 μL of FITC-CD62P and PE-JON/A antibodies. Mix gently and incubate for 15 min in the dark at room temperature.
5. Analyze cells by flow cytometry immediately. Otherwise, fix stained cells by adding 1% PFA and perform flow cytometry analysis within 48 h. In our experience, results do not significantly differ between non-fixed and PFA-fixed platelets.
6. Flow cytometry analysis: Use the logarithmic scale to visualize platelets in forward-scatter (FSC) and side-scatter (SSC) axis and gate on platelets (P1) as shown in Fig. 2a. On P1, analyze the expression of JON/A and CD62P under resting and CRP-activated conditions. Resting platelets should not result in any staining. An example is given in Fig. 2b. If the platelets are even slightly positive for Anti-JON/A and/or anti-CD62P, the sample should be discarded as this indicates that platelets were activated during the preparation procedure. An example is shown in Fig. 2c. Figure 2d shows an example of CRP-activated platelets.

3.5 Platelet Activation, Lysis, IP, and Immunoblot

Light transmission aggregometry and the platelet secretion assay by flow cytometry are powerful methods to rapidly and directly assess platelet responses to different receptor agonists. They allow the identification of receptor signaling pathways affected by a specific protein deletion or inhibition. After the identification of such a pathway, immunoblot assays and IP of target proteins are the methods of choice to dissect signaling defects and perhaps identify the direct targets of the PTP of interest. For instance, the tyrosine phosphorylation pattern of CRP-activated platelets is well known in the platelet signaling field. An example of an anti-phosphotyrosine immunoblot on CRP-activated WT and DUSP3$^{-/-}$ mouse platelets is shown in Fig. 3a. The major tyrosine phosphorylated bands are located between 40 and 80 kDa molecular weights. Because CRP activation of platelets leads to tyrosine phosphorylation of the Src family kinases (SFKs, 50–55 kDa) and the spleen tyrosine kinase (Syk, 70 kDa), anti-phosphotyrosine immunoblots can be very informative. Next, if phosphospecific antibodies are available (as is the case for most SFKs and Syk), immunoblot assays on total lysates can be performed. Otherwise, IP of the target protein followed by anti-phosphotyrosine immunoblot is required. As before, details

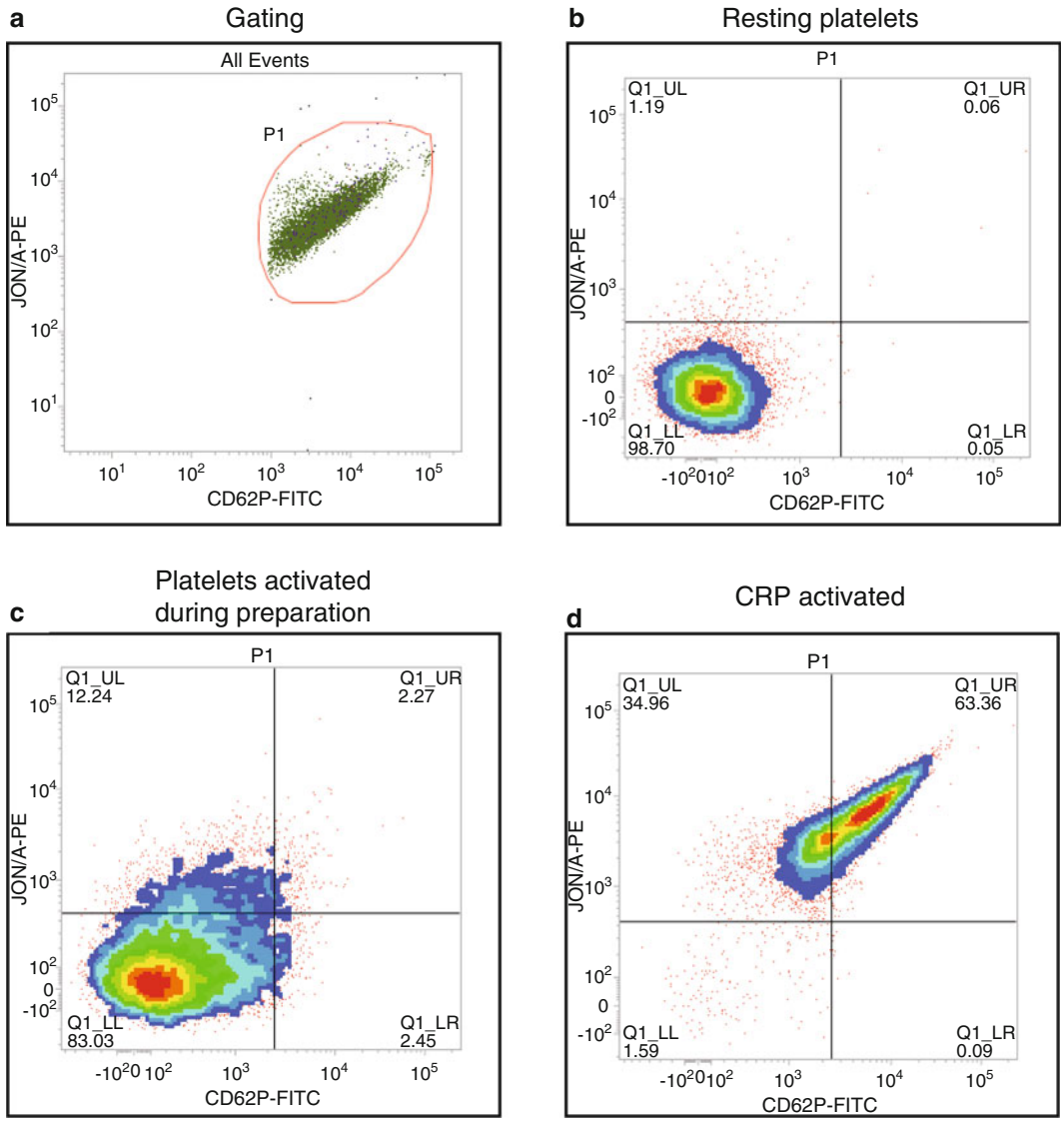

Fig. 2 Gating strategy to analyze platelet secretion by flow cytometry. (**a**) FSC and SSC axis (log scale) and gate on platelets (P1). (**b**) An example of resting platelets based on the analysis of JON/A and CD62P on P1 gated platelet population. (**c**) An example of platelets activated during preparation based on the analysis of JON/A and CD62P on P1 gate. (**d**) An example of CRP-activated platelets based on the expression of JON/A and CD62P

are provided for experiments using CRP to activate platelets through the GPVI receptor. However, the protocol can be easily adapted for experiments using other platelet receptor agonists.

3.5.1 Platelet Activation and Lysis

1. Adjust the concentration of washed platelets (WPs) (Subheading 3.2) to 500×10^3 platelets/μL in Tyrode's buffer without BSA. From the blood of two mice, up to 1 mL WPs can be obtained, which is enough to perform four IPs.

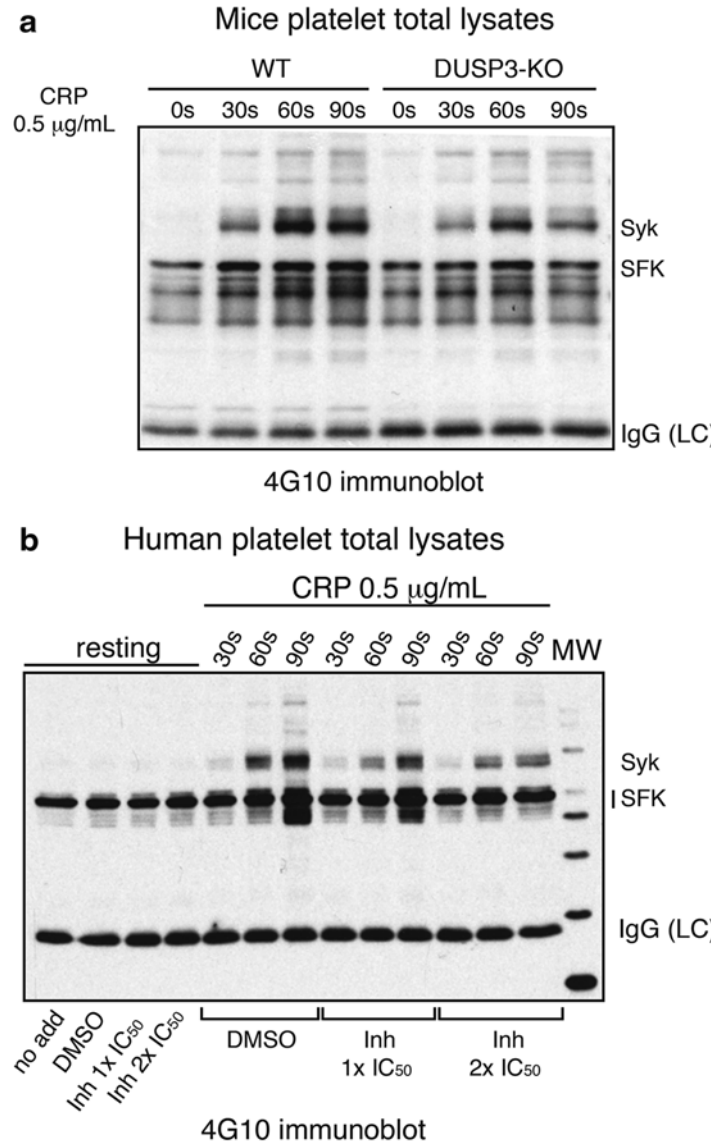

Fig. 3 Examples of an anti-phosphotyrosine immunoblot assay on total lysates from mouse and human platelets. (**a**) Lysates were prepared from non-activated or CRP (0.3 μg/mL)-activated WT and DUSP3-KO washed platelets for the indicated periods of time. Western blot was performed using anti-phosphotyrosine (4G10) antibodies. (**b**) Lysates were prepared from vehicle (DMSO) or DUSP3 inhibitor (MLS-0437605) pretreated washed human platelets. Cells were non-activated or CRP-activated (0.3 μg/mL) for the indicated periods of time, lysed, and immunoreacted using anti-phosphotyrosine antibody

2. Aliquot 270 μL WPs in a 450 μL cuvettes containing one siliconized stir bar. One cuvette of pooled WPs from each mice genotype should be kept with no stirring (as a control for resting conditions).

3. Perform pipetting carefully as rapid flows may activate platelets.
4. Let the platelets rest at room temperature for 25 min.
5. Meanwhile, set the aggregometer on optical mode at 37 °C and 400 rpm.
6. Prepare highly concentrated CRP working solutions in Tyrode's buffer for each CRP concentration to be tested. This will ensure the addition of equal volume of CRP in all cuvettes (2 μL of CRP working solution to 270 μL WPs). Keep working solutions on ice until needed. Equilibrate at room temperature for 5 min before use.
7. To analyze the tyrosine phosphorylation profile of platelets on western blots, titration and time course activation with CRP (or other platelet receptor agonists) should be performed.
8. Place the cuvettes in aggregometer set at 37 °C with stirring at 400 rpm and equilibrate WPs for 30 s.
9. Add 2 μL room temperature concentrated CRP solution using the long gel loading tips and stimulate for different time points (e.g., 30, 60, 90 s)
10. Stop platelet activation by adding an equal volume of 2× lysis buffer containing 2× concentrated protease and phosphatase inhibitors.
11. Transfer the cuvettes immediately on ice and transfer lysates into 1.5 mL Eppendorf tubes using long tips (Keep samples on ice or at 4 °C to preserve phosphorylated sites)
12. Lyse for 30 min on rotator at 4 °C (in cold room).
13. Centrifuge lysates at 7500 × *g* at 4 °C and transfer supernatants into fresh 1.5 mL Eppendorf tubes.
14. Determine the protein concentration of each sample using the Bradford assay in a 96-well plate.
15. Prepare samples by adding equal volumes of 2× SDS Sample Buffer (e.g., 50 μL lysate + 50 μL 2× SDS sample buffer).
16. Boil at 95 °C for 5 min to denature proteins. Use Eppendorf tubes that close tightly to avoid loss of samples by evaporation. Freeze the rest of lysates at −80 °C or proceed immediately with IP.
17. Load denatured samples directly on 4–20% Tris–Glycine gradient acrylamide gels for western blot assay or freeze at −20 or −80 °C for longer storage.
18. Perform western blot as previously described [19].

When performing immunoblot assays using anti-phosphotyrosine antibodies (4G10) on activated vs. non-activated platelets, a gradual increase (over time of stimulation) of

tyrosine-phosphorylated bands should be observed in activated platelets, especially at molecular weights between 45 and 80 kDa (Fig. 3a). The band corresponding to Syk (70 kDa) is of particular interest. Under non-activated conditions, no tyrosine-phosphorylated band should be observed at 70 kDa. When activated, Syk gets rapidly (30 s) phosphorylated on tyrosine and becomes visible on the total lysate blot. If Syk appears phosphorylated under resting conditions, WPs were likely activated during preparation, and results should be discarded (*see* also **Note 6**). The identity of tyrosine-phosphorylated proteins should be confirmed using phosphotyrosine-specific antibodies if available, or by IP of the candidate protein, followed by immunoblot assays using anti-phosphotyrosine antibodies.

3.5.2 Immunoprecipitation

1. Thaw lysates from non-activated and activated WPs on ice for 20 min.
2. Meanwhile, prepare Protein A-Sepharose (or Protein G) beads for preclearing lysates from platelet-bound murine IgGs. Use 20 µL slurry per sample and wash beads with 1 mL ice cold PBS three times by centrifuging beads at 800 × *g* for 1 min at 4 °C.
3. After centrifugation, let the beads rest for 2 min on ice before discarding supernatant.
4. Resuspend washed beads in 1 mL PBS and aliquot them in clean prelabeled 1.5 mL Eppendorf tubes for as many samples as needed. Centrifuge again at 800 × *g* for 1 min at 4 °C to eliminate extra PBS.
5. Add thawed lysates into the beads-containing tubes and incubate for 30 min at 4 °C with rotation.
6. Meanwhile, add 2 µg of selected antibody to a clean Eppendorf prelabeled tube and keep on ice.
7. As a negative control, perform an additional IP with rabbit-IgG or mouse-IgG, depending on the origin of the used antibody.

   For such a control, pooled lysates from WT and PTP-KO mouse WPs can be used to limit the number of mice needed for the experiment. When using human platelets, one negative IP for each donor should be performed.
8. Centrifuge the tubes containing WPs lysates and beads at 800 × *g* for 1 min at 4 °C and transfer precleared supernatants to the new tubes containing the antibody. Discard beads used for preclearing.
9. Incubate for 1 h at 4 °C with rotation to allow binding of the antibody to the target protein.
10. During this time, prepare protein A-Sepharose (or protein G) beads for all samples.
11. 40 µL beads slurry are needed per sample (40 µL × n (number of samples) = total volume of beads slurry to be prepared).

12. Add 1 mL of ice-cold-PBS to the required volume of beads slurry and mix by pipetting up and down.
13. Centrifuge for 1 min at 800 × *g* and carefully discard supernatant. Repeat the washing procedure two more times.
14. For the last wash, split the mixture of PBS/beads in as many clean 1.5 mL Eppendorf tubes as samples to be tested, plus one tube for the negative IP control.
15. Centrifuge at 4 °C for 1 min at 800 × *g* and carefully discard supernatants. Keep the beads on ice at all times.
16. Centrifuge the lysate/antibody mixtures at 5000 × *g* for 30 s and transfer them to the corresponding beads-containing tubes.
17. Incubate overnight at 4 °C with rotation (cold room).
18. Centrifuge samples at 4 °C for 1 min at 800 × *g*.
19. Save the flow through (FT) at 4 °C and proceed with beads.
20. Wash beads three times with 1 mL of ice-cold PBS or with 1× WPs lysis buffer.
21. After the last wash, aspirate the supernatant carefully without disturbing the beads. Add 30 μL of 2× SDS loading buffer to the beads, vortex, and boil at 95 °C for 5 min.
22. Vortex again and centrifuge at 15,000 × *g* for 1 min.
23. Load 10 μL of supernatants on acrylamide gel and proceed for western blotting as described in [19].

3.6 In Vivo Mouse Thrombosis Models

3.6.1 Ferric Chloride ($FeCl_3$) Carotid Injury Model

Intravital video-microscopy is a widely used technology to directly visualize, in real time, the initiation and progression of thrombus formation in live small animals. Importantly, this technique allows the investigation of thrombotic and hemostatic processes under physiological conditions. Thrombus formation in mice can be induced by different methods such as mechanical destruction of the endothelium, systemic infusion of Rose Bengal (a photoreactive chemical) followed by low-power laser excitation, activation of the endothelial cells by a high power nitrogen laser, or by chemical injury using topical application of $FeCl_3$ solution [5, 20]. Here, we provide a detailed protocol for the $FeCl_3$ injury model, which is a simple and well-established model known to be sensitive to both anticoagulants as well as antiplatelet drugs [5, 20].

$FeCl_3$ is an oxidative agent that can penetrate through the vessel, leading to the denudation of the endothelium and subendothelial matrix exposition. The severity of the damage induced depends on the $FeCl_3$ concentration used and the duration of the application [21]. $FeCl_3$ can be applied on small vessels like cremaster and mesenteric arterioles or on larger vessels like carotid artery [21]. In order to visualize and quantitate thrombus formation, platelets are labeled using CFSE and injected through the jugular vein before thrombus initiation. Quantification can be performed

by monitoring the time until full occlusion of the blood vessel or by comparing the fluorescence intensity between different conditions.

Staining of Washed Platelet with CFSE

1. Prepare PRP from one mouse as described in Subheading 3.2.
2. Transfer PRP (200 µL of 200×10^3/platelets per µL) to a 15 mL conical tube and add 3 mL of Tyrode's buffer and 200 µL of ACD containing Apyrase.
3. Add 15 µL of CFSE at 1 µg/µL and incubate 2 min at room temperature protected from light.
4. Centrifuge at $950 \times g$ for 10 min at room temperature.
5. Resuspend the pellets gently in 200 µL PBS and keep at room temperature protected from light (*see* **Note** 7).

Preparation of Material and Mouse Surgery

1. Cut 10 cm of an Intramedic™ Polyethylene catheter tube. Cut one end of the tube diagonally (preferably using a binocular loupe) in order to ease insertion of the tube into the blood vessel.
2. Few millimeters away from the diagonal cut, make three to four very slight diagonal incisions to create a kind of "self-retaining harpoon catheter". This will help maintaining the catheter inside the blood vessel.
3. Fill an insulin syringe with sterile 0.9% NaCl avoiding bubbles and insert it to the non-diagonally cut end of the catheter.
4. Using a binocular loupe, make sure that the liquid (NaCl) does not leak through the diagonal incisions/winglets.
5. Weigh the mice and inject i.p. the appropriate volume of the ketamine–xylazine mix. Overdosing may occur if animals are not properly weighed.
6. Following deep anesthesia, place the mouse in dorsal recumbency on a heating plate set to 37 °C.
7. Secure the front legs on the plate using rubber bands. Ensure that the mouse is positioned in a comfortable position to optimize breathing.
8. Gently scrub the surgical area with 70% ethanol solution.
9. Perform a midline skin incision in the mouse neck using a surgical scissor as indicated in Fig. 4, steps A and B.

Fig. 4 (continued) catheter tubing to the jugular vein with an additional suture on the cephalic end of the jugular vein. (**J**) Separate gently the sternomastoid and the sternohyoid to visualize the vagus nerve and the carotid artery. Place a black plastic triangle under the carotid artery vessel. (**K**) Place a $FeCl_3$-soaked filter on the carotid artery for 5 min. (*a*) submaxillary gland. (*b*) platysma. (*c*) jugular vein. (*d*) sternohyoid muscle. (*e*) sternomastoid muscle. (*f*) fat on the jugular vein. (*g*) jugular catheter with harpoon-like structure. (*h*) vagus nerve. (*i*) carotid artery. (*j*) black plastic triangle. (*k*) $FeCl_3$-soaked filter (site of injury)

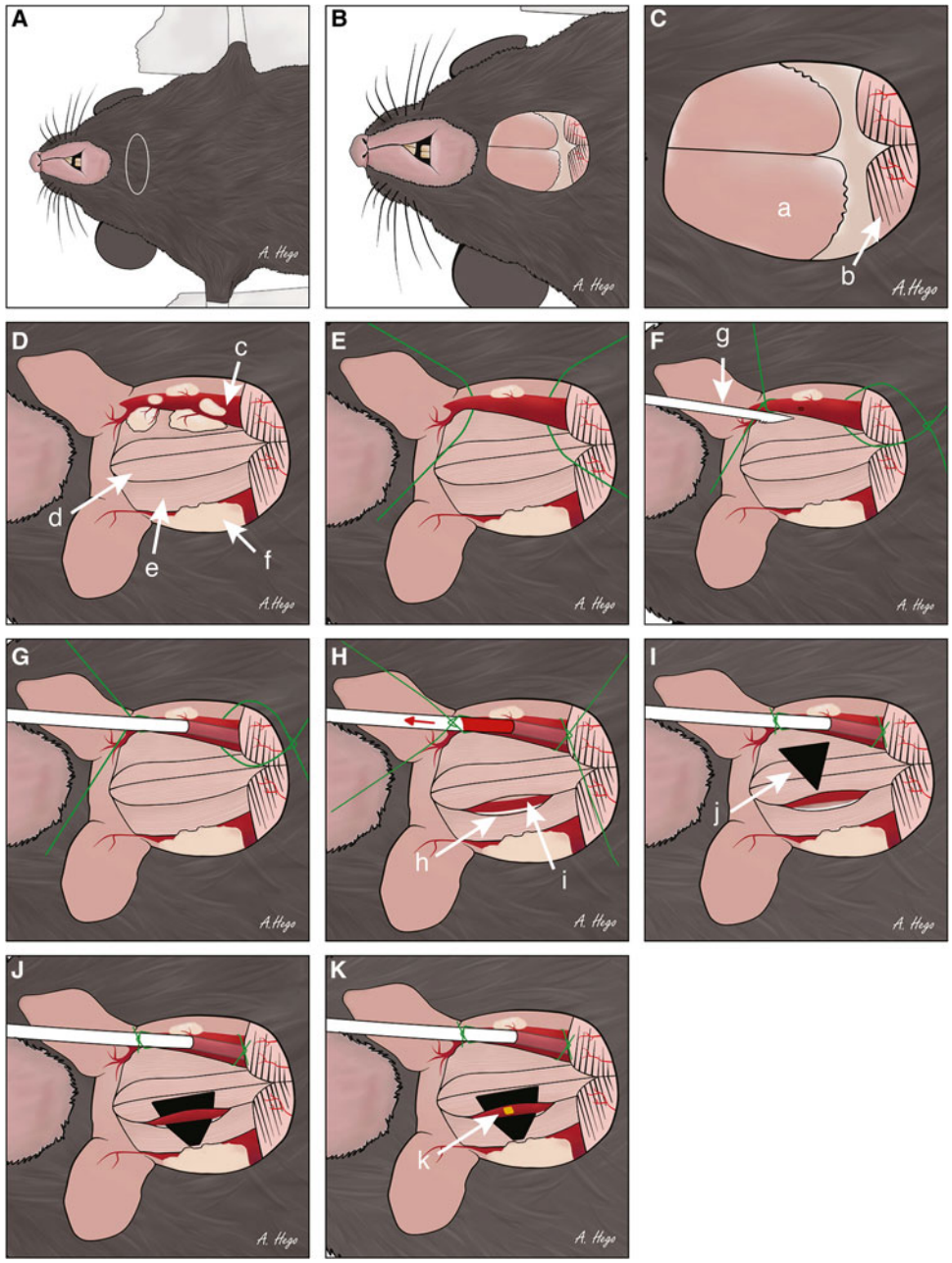

Fig. 4 Ferric chloride ($FeCl_3$) carotid injury model, surgical procedure. (**A**) Secure the front legs on the plate using rubber bands. (**B** and **C**) Perform a midline skin incision in the mouse neck and expose the submaxillary glands. (**D**) Separate the submaxillary glands and the muscle and place them near the mouse's face. (**E**) Isolate carefully the jugular vein on both sides and underneath for a distance of 1–1.5 cm and place a loose tie on both cranial and caudal ends of the vessel using suture silk. (**F**) Tie the cranial ligature around the vessel and make a very small incision in line with the vessel between the two ligatures. (**G**) Insert the free diagonally cut end of the catheter into the vessel incision toward the heart and push carefully the catheter until the entire cut end is inside the vessel. (**H**) Tie up the ligature at the caudal end to secure the catheter into the vessel and verify leaking by injecting 0.9 % NaCl in the jugular vein and aspirate blood. (**I**) Secure the position of the

10. Expose the submaxillary glands (Fig. 4, step C).
11. Gently separate the submaxillary glands and the muscle using surgical forceps and place them near the mouse's face (Fig. 4, step D).
12. The jugular veins and the sternohyoid muscle are now exposed.
13. Isolate carefully the jugular vein on both sides and underneath (with the help of the forceps) for a distance of 1–1.5 cm. Do not touch directly the jugular vein with the end of the forceps since this could damage the vein. Both left and right veins can be used.
14. Place a loose tie on both cranial and caudal ends of the vessel using suture silk (Fig. 4, step E). This will maximize the exposure of the vessel.
15. Tie the cranial ligature around the vessel (Fig. 4, step F).
16. Make a very small incision using microsurgical scissors in line with the vessel between the two ligatures (Fig. 4, step F). No blood should flow out of the vessel. If hemorrhage occurs, it may be controlled by gently pulling the cranial ligature end.
17. Insert the free, diagonally cut end of the catheter tubing into the vessel incision toward the heart with the help of the forceps (Fig. 4, step G). Push carefully the catheter until the entire end is inside the vessel.
18. Use the ligature at the caudal end to secure the catheter into the vessel. Verify licking by injecting 0.9% NaCl in the jugular vein and aspirate blood (Fig. 4, step H) (*see* **Note 8**).
19. Secure further the position of the catheter tubing to the jugular vein with additional suture on the cephalic end of the jugular vein (Fig. 4, step I).
20. Gently separate the sternomastoid and the sternohyoid muscles using the forceps; the carotid artery is located underneath (Fig. 4, step H). The vagus nerve, white and easily visible, resides also near the carotid artery.
21. Carefully separate the vagus nerve from the carotid artery by opening and closing the forceps placed between the nerve and artery.
22. Place the black plastic triangle under the vessel as shown in Fig. 4, steps I and J. The black plastic triangle will elevate the vessel and prevent autofluorescence from the adjacent tissue.
23. Prepare an insulin syringe with 120 μL of the CFSE loaded platelets.
24. Inject i.v. 100 μL of stained platelets through the jugular vein catheter.
25. Incubate a 2 × 2 mm square of Whatman paper in 10% $FeCl_3$ buffer.

26. Dry completely the carotid artery using a Sugi® sponge. Dilution of the $FeCl_3$ in residual liquid can induce significant variations between experiments.
27. Basal level fluorescence (488 nm band pass filter) in the vessels should be acquired before adding $FeCl_3$.
28. Take at least 50 snapshots using the Slidebook software (or equivalent) following the instructions of the manufacturer. Heart beating of the artery may influence the quality of images (mainly blurring).
29. Put the $FeCl_3$-soaked filter on the carotid artery and leave it for 5 min (Fig. 4, step K).
30. Remove the $FeCl_3$-soaked filter and clean the carotid artery using a pipette filled with 1× PBS.
31. Dry completely the vessel using the Sugi® sponge in order to prevent diffraction during image acquisition.
32. Start recording the thrombus formation with a 488 nm band pass filter. Take 50 snapshots every 2 min for 30 min or up to total occlusion of the blood vessel.
33. Stop the recording and euthanize the mouse either by injecting 50 µL of Nembutal or by cervical dislocation.
34. Analyze of the acquired images. Slidebook software, for example, can determine and compare the mean fluorescence intensities (MFI) between basal conditions and after $FeCl_3$-induced injury.

3.6.2 Collagen and Epinephrine-Induced Pulmonary Embolism Model

Collagen and epinephrine-induced pulmonary embolism is a very simple and reliable in vivo model to study the effectiveness of antithrombotic drugs or to investigate the role of a signaling molecule in thrombosis. The method was described for the first time by DiMinno and Silver in 1983 [22]. In this model, thromboembolism in mice is induced by injecting a combination of a platelet-aggregating agent such as collagen together with epinephrine. The time to death and the rate of survival is recorded, and the number and size of thrombi in lung sections can be analyzed. The protocol provided here is specific to C57BL/6 male mice. The dose of collagen and epinephrine should be adjusted if other mouse genetic backgrounds or female mice are used.

1. Weigh and label 8–12 weeks old male mice (WT and target PTP-KO, ten mice in each group). Labeling can be performed on tails using permanent marker.
2. Anesthetize the mice with an i.p. injection of ketamine–xylazine mix as described in Subheading 2.1.
3. Place the mice in lateral recumbency on the heating plate set at 37 °C.

4. While waiting for the mice to sleep, label Eppendorf tubes and prepare the mixture of epinephrine (170 μg/kg) and collagen (60 μg/kg) for every mouse (one Eppendorf tube per mouse).
5. Load 1 mL syringes/30 G needles with the appropriate volume of collagen/epinephrine mix for each mouse.
6. When mice are deeply anesthetized, inject each mouse into the plexus retro-orbital vein with the appropriate volume of collagen/epinephrine mix. Plexus retro-orbital vein injection can be achieved by inserting the needle into the medial canthus of the eye under the nictitating membrane (Fig. 2c).
7. Mice need to be kept on the heating plate during the entire procedure.
8. Monitor mice for vital signs such as breathing and heart beating. Under the conditions described here, time to death in WT mice was recorded between 10 and 20 min. The animals are considered as dead when they stop breathing/heart beating.
9. Animals that do not die after 40 min should be sacrificed by cervical dislocation.
10. Perfuse the lungs with 4% formaldehyde and collect them for histological analysis.
11. Results obtained can be presented as the percentage of survival and time to death. It is also possible to analyze the number and size of thrombi in lung sections from different groups (WT and target PTP-KO) using a simple hematoxylin eosin staining method.

3.7 Pharmacological Inhibition of Platelet PTPs

Platelets are anucleate cells that are not amenable to RNA interference or recombinant DNA technologies. Thus, chemical probes to pharmacologically inhibit (or activate) the function of a specific PTP (or other signaling molecule) in human platelets are invaluable tools to corroborate findings that originate from animal models in human cells.

3.7.1 General Considerations

All PTPs share a common catalytic mechanism based on a nucleophilic cysteine that is part of the active-site signature motif C(X)5R [23]. Sodium orthovanadate, which binds to the active site and functions as transition state analog, is a standard reagent to inhibit PTP activity in cells including platelets [24]. More potent general PTP inhibitors with proven activity in cells include peroxovanadium compounds such as potassium bisperoxo(1,10-phenanthroline) oxovanadate [bpV(phen)] [25]. The number of reported specific PTP inhibitors with selectivity for a particular target and efficacy in cells is very limited. This is due to the fact that the vast majority of small-molecule PTP inhibitors target the highly conserved active site, and thus lack sufficient selectivity for the PTP of interest. Nonetheless, several promising compounds have been

reported for PTPs known to be important for platelet signaling including PTP1B and SHP2 [8]. However, there is a paucity of data demonstrating efficacy of these compounds in platelets. Moreover, we found that our previously identified DUSP3 inhibitors, which showed excellent specificity and efficacy in HeLa cells [26], caused spontaneous aggregation of human platelets [10]. Thus, there appears to be an even more rigorous requirement for compound specificity when working with platelets. Several new strategies to generate PTP inhibitors with increased specificity are currently being investigated. For further reading on this topic we refer to our recently published review articles [8, 23].

3.7.2 *Inhibition of DUSP3 in Human Platelets*

Using a chemical genomics approach, we developed a novel inhibitor of DUSP3 (MLS-0437605; Fig. 5) [10]. MLS-0437605 specifically inhibited human platelet aggregation in response to stimulation of the GPVI and CLEC-2 receptors, analogous to the effect of DUSP3 deficiency in murine cells. Tests on platelets from WT mice yielded similar results, while MLS-0437605 only minimally affected aggregation of DUSP3-deficient platelets [10]. Inhibition of DUSP3 by MLS-0437605 in human platelets reduced tyrosine phosphorylation of immunoprecipitated Syk and PLCγ2 in response to GPVI and CLEC-2 stimulation, while global tyrosine phosphorylation was not affected. These results demonstrated that pharmacological inhibition of DUSP3 in human platelets phenocopies the effect of DUSP3 deficiency in murine platelets. Here, we provide detailed protocols for testing the effects of small-molecule inhibitors on human platelet activation and aggregation. Methods related to the development of specific PTP inhibitors

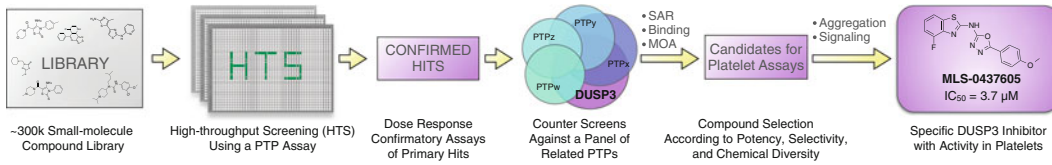

Fig. 5 Development of a DUSP3-specific inhibitor. High-throughput screening (HTS) of a drug-like compound collection was used in the search for novel DUSP3 inhibitors. Primary hits, i.e., compounds that inhibited DUSP3 activity by at least 50 %, were taken into dose response hit confirmation assays using two orthogonal assay formats. Cross-active hits with IC_{50} values <20 μM in both assays were subjected to counter screens against four additional PTPs. Based on potency and selectivity, several hits were selected for structure–activity relationship (SAR), binding, and mechanism-of-action (MOA) studies, resulting in several candidate compounds for tests on human platelets. These tests included platelet aggregation assays as well as biochemical assays assessing the tyrosine-phosphorylation levels of various signaling proteins involved in DUSP3-regulated pathways. Compound MLS-0437605 effectively inhibited mouse and human platelet aggregation, specifically in response to GPVI and CLEC-2 platelet stimulation, thereby phenocopying the effect of DUSP3 deficiency on mouse platelets. In contrast, aggregation of DUSP3-deficient platelets was only marginally affected by MLS-0437605. MLS-0437605 also decreased tyrosine phosphorylation of Syk and PLCγ2 in human platelets in response to GPVI and CLEC-2 stimulation, similar to the effect of DUSP3 deficiency on mouse platelets. (*see* ref. 10 to review the actual data.)

have been previously described [27, 28]. The major steps for the identification of the DUSP3 inhibitor MLS-0437605 are summarized in Fig. 5.

3.7.3 Human Blood Collection

For blood collection, make sure to not include donors that have taken aspirin or any other antiplatelet medication during the 15 days prior to blood donation.

1. Collect blood from a forearm vein using an 18 G needle (*see* **Note 9**). Blood collected should be free-flowing.
2. Discard the first 5 mL of blood. (The first 5 mL of blood should be discarded because it contains activated platelets that have been in contact with collagen released from the wound.)
3. Use a conical tube containing ACD and 1 U/mL of apyrase grade I (1 volume ACD + 1 U/mL of apyrase for 6 volumes of blood) to collect ~30 mL of blood.
4. Immediately after collection, close the tube and mix the blood gently with the anticoagulant.
5. Platelet assays should be performed within 3 h after blood collection.

3.7.4 Isolation of Human Platelets

1. Centrifuge blood for 15 min at 100 × *g* at room temperature to obtain PRP.
2. Carefully transfer PRP into a new 15 mL conical tube.
3. Wash platelets by adding 2 volumes of ACD containing 1 U/mL of apyrase grade I at RT and centrifuge at 800 × *g* 10 min and room temperature.
4. Proceed as described in Subheading 3.2, **steps 5–8**. Select human protocol for counting platelets when using the hematology analyzer.
5. Resuspend washed platelet pellets in Tyrode's buffer containing 1 U/mL apyrase to a concentration of 250×10^3 platelets/μL for aggregation and secretion experiments, and to 500×10^3 platelets/μL for immunoblot and IP experiments.

3.7.5 Effects of Small-Molecule Inhibitors on Human Platelet Aggregation

1. Prepare 20 mM inhibitor stock solutions in DMSO, which will allow testing of inhibitors in platelets at up to 40 μM final concentration at the nontoxic concentration of 0.2% DMSO (*see* **Note 10**). Store stock solutions as small aliquots as needed at −20 or −80 °C and avoid repeated thawing and freezing. For inhibitor treatment, platelets are resuspended in Tyrode's buffer with glucose and BSA.
2. Prepare 500× concentrated inhibitor working solutions in DMSO for each inhibitor concentration to be tested. This will ensure equal amounts of DMSO in inhibitor dose–response assays. (A 500× working solution results in 0.2% DMSO final

concentration.) For dose–response studies prepare 1/3-log steps serial dilutions (highest final concentration 5- or 10-times inhibitor IC_{50} value, but not exceeding 40 μM). We recommend four to five inhibitor dilutions (e.g., 30–10–3–1–0.3–0 μM final inhibitor concentration), so that the lowest final concentration is well below the inhibitor IC_{50} value.

3. Prepare human WPs as described in Subheading 3.7.4.
4. Aliquot 270 μL (250×10^3 human platelets/μL) of WPs in 450 μL cuvettes containing one siliconized stir bar.
5. Let the platelets rest for 25 min at room temperature.
6. Make sure the inhibitor does not spontaneously cause platelet aggregation (*see* **Note 11**).
7. Add DMSO or inhibitor working solution to WPs and incubate at room temperature for 30 min (to allow inhibitor uptake). Since the ChronoLog aggregometer can analyze only two cuvettes in parallel, prepare only two cuvettes at a time and allow an interval of at least 10 min between additional inhibitor/DMSO incubations. Some aggregometers allow the analysis of four cuvettes at a time. Adjust the number of cuvettes depending on the available equipment.
8. Proceed with the aggregation assay as described in Subheading 3.3. Determine the percentage of aggregation inhibition by comparing to the vehicle (DMSO) control. Human platelet responses to receptor agonists are highly variable between individuals. We recommend determining the optimal concentration of a platelet receptor agonist (e.g., CRP) for every donor before proceeding with the inhibitor dose–response aggregation assay.
9. Repeat the aggregation assays with more fine-tuned, narrower range of inhibitor concentrations. The goal is to find the lowest concentration of inhibitor that yields maximal inhibition of platelet aggregation. MLS-0437605 inhibited CRP- and rhodocytin-induced platelet aggregation at a concentration of $1\times$ IC_{50}.

3.7.6 Effects of Small-Molecule Inhibitors on Human Platelet Secretion

Platelet secretion analysis using flow cytometry is a quantitative and highly sensitive method for the evaluation of platelet function. This method allows for further characterization of the effects of selected inhibitors. Since secretion can be performed on small aliquots of WPs, several conditions can be tested simultaneously for the same donor. Thus, dose response data for both the inhibitor and the agonist can be obtained. Typically, for WPs from a particular donor, the highest concentration of platelet receptor agonist used in the secretion experiment corresponds to the lowest concentration of the same agonist used in the platelet aggregation assay (Subheading 3.7.5). We here describe a method analyzing

JON/A and p-Selectin exposure on CRP-activated human washed platelets using three CRP and two inhibitor concentrations plus vehicle control. The same method can be used with other platelet receptor agonists.

1. Prepare 12 aliquots of 100 µL (250×10^3/µL) each of washed human platelet. Label the tubes as shown in the table:

NS—DMSO	0.1 µg/mL CRP DMSO	0.3 µg/mL CRP DMSO	0.5 µg/mL CRP DMSO
NS—inhibitor conc. 1	0.1 µg/mL CRP inhibitor conc. 1	0.3 µg/mL CRP inhibitor conc. 1	0.5 µg/mL CRP inhibitor conc. 1
NS—inhibitor conc. 2	0.1 µg/mL CRP inhibitor conc. 2	0.3 µg/mL CRP inhibitor conc. 2	0.5 µg/mL CRP inhibitor conc. 2

2. Add the appropriate amounts of DMSO or inhibitor working solution to the tubes. Mix gently by pipetting twice up and down using 1 mL pipette tips and incubate at room temperature for 30 min.
3. Add CRP at the indicated concentrations and mix gently. Add the equivalent volume of 0.9% NaCl or Tyrode's buffer to the NS samples. Incubate for 15 min at room temperature.
4. Add 10 µL of FITC-conjugated anti-human CD62P and 10 µL of PE-PAC1 antibodies. Mix gently and incubate for 15 min in the dark at room temperature.
5. Fix cells using 1 mL of 1% PFA. Proceed with flow cytometry analysis within 48 h (*see* **Note 12**).

3.7.7 Effects of Small-Molecule Inhibitors on Human Platelets Using Immunoblot Assays

The aggregation assay is a relatively simple method that can be used as screening assay to prioritize compounds. However, aggregation assays only measure the final effect of a compound on platelet activation. More direct effects of PTP inhibitors can be evaluated by determining the overall and specific change in tyrosine phosphorylation using immunoblot analyses with anti-phosphotyrosine (4G10) or phospho-specific antibodies on total lysates or IPs from activated vs. non-activated platelets. A specific PTP inhibitor is not expected to increase global tyrosine phosphorylation, but should phenocopy the effect of the PTP deficiency in mouse platelets. If the inhibitor induces a dramatic change in global tyrosine phosphorylation, the compound is likely acting unspecifically. An example of a phosphotyrosine immunoblot using the specific DUSP3 inhibitor MLS-0437605 on human platelets is shown in Fig. 3b. Further, if the direct substrate(s) of the target PTP is known, and phospho-specific antibodies for this/these substrate(s) are available, immunoblot assays probing directly the phosphorylation site of the substrate(s) can be performed on total lysates. If phospho-specific antibodies are not available, IP of the substrate protein using a

pan-antibody, followed by an anti-phosphotyrosine (4G10) western blot can be performed. For dose–response experiments with inhibitors, platelets are prepared and treated similarly as described above for aggregation assays. However, platelet activation should be performed at a lower stirring speed of 400 rpm. This is because stirring speeds higher than 400 rpm lead to the formation of tight platelet aggregates and highly variable lysis efficiency. We recommend repeating the dose–response aggregation assay (as described in the previous section) for the selected inhibitor and vehicle control (DMSO) at 400 rpm and determine optimal concentrations of CRP (or other agonist) and inhibitor. Once optimal conditions are found, a time course stimulation of inhibitor- and DMSO-treated platelets should be performed at 400 rpm stirring condition. For lysis and immunoblotting, follow the steps described in Subheading 3.6. Because platelet activation is highly variable between donors, experiments should be performed on platelets from at least three donors.

4 Notes

1. Nembutal stock solution: 6 mg/mL in 9% NaCl. Prepare 1 mL. If the experiment lasts more than 30 min, inject mice with Nembutal (10 μg/g) to maintain anesthesia. Repeat the injection every 30 min if required.
2. Many factors such as genotype, age, and stress levels can result in variation in anesthetic depth and time to recover. Therefore, the anesthesia protocol should be adjusted accordingly. We provide the conditions that worked well for DUSP3$^{-/-}$ and WT littermates in C57BL/6 mice background.
3. Preparation of paraformaldehyde (PFA): Weigh 4 g of PFA in beaker. Add 80 mL of 1× PBS. Cover with Parafilm. Place the beaker on magnetic stirrer/heater (52 °C). Mix with moderate stirring until the solution becomes clear. Heating and a slight alkaline pH are necessary to dissolve PFA. Since the pH of PBS is around 7.4, PAF dissolves easily in the PBS. Adjust the final volume to 100 mL with PBS. Store the solution in small aliquots, depending on the usage, at −20 °C. PFA solution can also be stored at room temperature up to 1 week; longer storage at room temperature will lead to formation of formic acid.
4. Take a small aliquot of collected blood and make sure (using the hematology analyzer (Cell-Dyn 3700 in our case)) that platelet counts are higher than 8×10^5 platelets/μL. Lower platelet concentrations indicate that the blood contains small platelet aggregates, and those samples should be discarded.
5. Collect 0.8–1 mL of blood from one mouse. Less blood volume usually means that the quality of the collected blood is not good enough to proceed, and the sample should be discarded.

About ten aggregation cuvettes can be prepared out of a pool of PRP from three mice. Secretion assays using flow cytometry can be performed on non-pooled PRP because smaller platelet numbers are required.

6. Care should be taken when the primary antibody against the target protein to be detected in western blot is raised in mouse and the target protein is at the same size of immunoglobulins (IgGs) heavy or light chains. Indeed, murine IgGs bind to platelet surface and contaminate PRP lysates. They are visible on immunoblots when secondary HRP-conjugated anti-mouse antibodies are used. One way to get partially rid of these contaminants is to preclean WP lysates with protein G or protein A sepharose beads. This is particularly useful in IPs.
7. CFSE loaded platelets should be used within 2 h after staining, as the staining intensity decreases rapidly.
8. Vessels surrounding tissues should not swell when injecting NaCl. If this happens, the catheter is likely not well inserted.
9. To minimize platelet activation, use <21 G needles to avoid shear stress. Further, discard the first few milliliters of blood, which can be in contact with collagen. Finally, gently mix the collected blood with the anticoagulant immediately, minimize the time from sample collection to analysis, and avoid sudden manipulation.
10. DMSO concentrations higher than 0.2% significantly inhibit both human and mouse platelet aggregation.
11. The inhibitor should be highly pure, and we strongly recommend repurification of commercial screening compounds using preparative HPLC. Platelets are a highly reactive cell type and may get activated by nonspecific binding of contaminants. Therefore, a platelet aggregation assay in response to the compound alone (with no platelet receptor agonist added) should be performed to test for unspecific, spontaneous platelet aggregation.
12. When dealing with a large number of blood donors, an alternative method can be used. Platelets can be fixed in 1% PFA after activation and stored for up to 5 days at 4 °C. However, anti-PAC1 antibodies do not work on fixed platelets. Anti-fibrinogen antibodies can be used in this case. For analysis, centrifuge the fixed cells at 800 × *g* for 5 min at 4 °C. Discard the supernatant and add 1 mL of PBS to the washed platelets. Centrifuge again at 800 × *g* for 5 min at 4 °C. Discard supernatant and add 150 μL of PBS. Add 10 μL of anti-CD62P antibody 2 μL of anti-Fibrinogen antibody (Dako #F0111; diluted 5× in PBS). Incubate for 15 min at RT in the dark. Add 1 mL of 1% PFA and proceed with flow cytometry analysis.

Acknowledgement

This work was supported by the Belgian National Fund for Scientific Research (F.R.S.-FNRS: PDR N° T.0105.13), the University of Liège (Fonds Spéciaux pour la Recherche) to (CO and SR), the National Institutes of Health (Grants 1R21CA132121 and 1R03MH084230 to LT), and the American Heart Association (Innovative Research Grant 14IRG18980075 to LT).

References

1. Italiano JE, Patel-Hett S, Hartwig JH (2007) Mechanics of proplatelet elaboration. J Thromb Haemost 5:18–23
2. Junt T, Schulze H, Chen Z, Massberg S, Goerge T, Krueger A, Wagner DD, Graf T, Italiano JE, Shivdasani RA, von Andrian UH (2007) Dynamic visualization of thrombopoiesis within bone marrow. Science 317:1767–1770
3. Varga-Szabo D, Pleines I, Nieswandt B (2008) Cell adhesion mechanisms in platelets. Arterioscler Thromb Vasc Biol 28:403–413
4. Offermanns S (2006) Activation of platelet function through G protein-coupled receptors. Circ Res 99:1293–1304
5. Furie B, Furie BC (2007) In vivo thrombus formation. J Thromb Haemost 5:12–17
6. Watson SP, Auger JM, McCarty OJT, Pearce AC (2005) GPVI and integrin alphaIIb beta3 signaling in platelets. J Thromb Haemost 3:1752–1762
7. Karisch R, Fernandez M, Taylor P, Virtanen C, St-Germain JR, Jin LL, Harris IS, Mori J, Mak TW, Senis YA, Östman A, Moran MF, Neel BG (2011) Global proteomic assessment of the classical protein-tyrosine phosphatome and "redoxome". Cell 146:826–840
8. Tautz L, Senis YA, Oury C, Rahmouni S (2015) Perspective: Tyrosine phosphatases as novel targets for antiplatelet therapy. Bioorg Med Chem 15:2786–2797
9. Ming Z, Hu Y, Xiang J, Polewski P, Newman PJ, Newman DK (2011) Lyn and PECAM-1 function as interdependent inhibitors of platelet aggregation. Blood 117:3903–3906
10. Musumeci L, Kuijpers MJ, Gilio K, Hego A, Théâtre E, Maurissen L, Vandereyken M, Diogo CV, Lecut C, Guilmain W, Bobkova EV, Eble JA, Dahl R, Drion P, Rascon J, Mostofi Y, Yuan H, Sergienko E, Chung TD, Thiry M, Senis Y, Moutschen M, Mustelin T, Lancellott RS (2015) Dual-specificity phosphatase 3 deficiency or inhibition limits platelet activation and arterial thrombosis. Circulation 131: 656–668
11. Gao C, Boylan B, Fang J, Wilcox DA, Newman DK, Newman PJ (2011) Heparin promotes platelet responsiveness by potentiating αIIbβ3-mediated outside-in signaling. Blood 117:4946–4952
12. Cattaneo M, Cerletti C, Harrison P, Hayward CPM, Kenny D, Nugent D, Nurden P, Rao AK, Schmaier AH, Watson SP, Lussana F, Pugliano MT, Michelson AD (2013) Recommendations for the standardization of light transmission aggregometry: a consensus of the working party from the platelet physiology subcommittee of SSC/ISTH. J Thromb Haemost 11:1183–1189
13. Born GV, Cross MJ (1963) The aggregation of blood platelets. J Physiol 168:178–195
14. Born G (1962) Aggregation of blood platelets by adenosine diphosphate and its reversal. Nature 194:927–929
15. Zhou L, Schmaier AH (2005) Platelet aggregation testing in platelet-rich plasma: description of procedures with the aim to develop standards in the field. Am J Clin Pathol 123:172–183
16. McEver RP, Bennett EM, Martin MN (1983) Identification of two structurally and functionally distinct sites on human platelet membrane glycoprotein IIb-IIIa using monoclonal antibodies. J Biol Chem 258:5269–5275
17. Nieuwenhuis HK, van Oosterhout JJ, Rozemuller E, van Iwaarden F, Sixma JJ (1987) Studies with a monoclonal antibody against activated platelets: evidence that a secreted 53,000-molecular weight lysosome-like granule protein is exposed on the surface of activated platelets in the circulation. Blood 70:838–845
18. Shattil SJ, Hoxie JA, Cunningham M, Brass LF (1985) Changes in the platelet membrane glycoprotein IIb.IIIa complex during platelet activation. J Biol Chem 260:11107–11114

19. Rahmouni S, Delacroix L, Liu WH, Tautz L (2013) Evaluating effects of tyrosine phosphatase inhibitors on T cell receptor signaling. Methods Mol Biol 1053:241–270
20. Furie B, Furie BC (2005) Thrombus formation in vivo. J Clin Invest 115:3355–3362
21. Kurz KD, Main BW, Sandusky GE (1990) Rat model of arterial thrombosis induced by ferric chloride. Thromb Res 60:269–280
22. DiMinno G, Silver MJ (1983) Mouse antithrombotic assay: a simple method for the evaluation of antithrombotic agents in vivo. Potentiation of antithrombotic activity by ethyl alcohol. J Pharmacol Exp Ther 225:57–60
23. Tautz L, Critton DA, Grotegut S (2013) Protein tyrosine phosphatases: structure, function, and implication in human disease. Methods Mol Biol 1053:179–221
24. Chiang TM (1992) Okadaic acid and vanadate inhibit collagen-induced platelet aggregation; the functional relation of phosphatases on platelet aggregation. Thromb Res 67:345–354
25. Posner BI, Faure R, Burgess JW, Bevan AP, Lachance D, Zhang-Sun G, Fantus IG, Ng JB, Hall DA, Lum BS, Shaver A (1994) Peroxovanadium compounds. A new class of potent phosphotyrosine phosphatase inhibitors which are insulin mimetics. J Biol Chem 269:4596–4604
26. Wu S, Vossius S, Rahmouni S, Miletic AV, Vang T, Vazquez-Rodriguez J, Cerignoli F, Arimura Y, Williams S, Hayes T, Moutschen M, Vasile S, Pellecchia M, Mustelin T, Tautz L (2009) Multidentate small-molecule inhibitors of Vaccinia H1-related (VHR) phosphatase decrease proliferation of cervix cancer cells. J Med Chem 52:6716–6723
27. Tautz L, Sergienko EA (2013) High-throughput screening for protein tyrosine phosphatase activity modulators. Methods Mol Biol 1053:223–240
28. Tautz L, Mustelin T (2007) Strategies for developing protein tyrosine phosphatase inhibitors. Methods 42:250–260

Chapter 18

Functional Analysis of Dual-Specificity Protein Phosphatases in Angiogenesis

Mathieu Amand, Charlotte Erpicum, Christine Gilles, Agnès Noël, and Souad Rahmouni

Abstract

Therapeutic perspectives targeting angiogenesis in cancer stimulated an intense investigation of the mechanisms triggering and governing angiogenic processes. Several publications have highlighted the importance of typical dual-specificity phosphatases (DSPs) or MKPs in endothelial cells and their role in controlling different biological functions implicated in angiogenesis such as migration, proliferation, apoptosis, tubulogenesis, and cell adhesion. However, among atypical DSPs, the only one investigated in angiogenesis was DUSP3. We recently identified this DSP as a new key player in endothelial cells and angiogenesis. In this chapter we provide with detailed protocols and models used to investigate the role of DUSP3 in endothelial cells and angiogenesis. We start the chapter with an overview of the role of several DSPs in angiogenesis. We continue with providing a full description of a highly efficient transfection protocol to deplete DUSP3 using small interfering RNA (siRNA) in the primary human umbilical vein endothelial cells (HUVEC). We next describe the major assays used to investigate different processes involved in angiogenesis such as tube formation assay, proliferation assay and spheroids sprouting assay. We finish the chapter by validating our results in DUSP3-knockout mice using in vivo angiogenesis assays such as Matrigel plug and Lewis lung carcinoma cell subcutaneous xenograft model followed by anti-CD31 immunofluorescence and ex vivo aortic ring assay. All methods described can be adapted to other phosphatases and signaling molecules.

Key words DSPs, DUSP3, Angiogenesis, Endothelial cells, HUVEC, LLC, Sprouting, Spheroid assay, Aortic ring assay, Proliferation, Immunofluorescence, Matrigel plug assay

1 Introduction

Angiogenesis is critical for both normal development and homeostasis and for tumor growth. Understanding the mechanisms of angiogenesis will open new avenues for better targeting and treatment of several pathologies. Genomic approaches demonstrated that several dual-specificity phosphatases (DSPs) genes are differentially expressed in a variety of diseases including cancers and could contribute to cancer initiation and/or progression [1, 2]. However, the role of this subset of phosphatases is not well

Rafael Pulido (ed.), *Protein Tyrosine Phosphatases: Methods and Protocols*, Methods in Molecular Biology, vol. 1447,
DOI 10.1007/978-1-4939-3746-2_18,

known in angiogenesis. So far, only three typical DSPs, also called MAPK phosphatases or MKPs, and one atypical DSP (A-DSP) were investigated in angiogenesis, namely DUSP1 (MKP-1), DUSP6 (MKP-3), DUSP2 (PAC1), and DUSP3 (VHR). Based on results obtained from knockout mice, DUSP1 seems to play a proangiogenic role in vivo. Indeed, vascular endothelial growth factor (VEGF)- and thrombin-induced sprout formation in an ex vivo aortic ring assay (ARA) is reduced in the *Mkp1–/–* mice compared to the wild-type controls [3]. The *Mkp1–/–* mice also displayed blunted angiogenesis in a model of distal hindlimb ischemia, which further confirmed this in vivo proangiogenic role [4]. In both models, the reduced angiogenesis was associated with decreased migratory properties of endothelial cells (EC) in response to VEGF upon DUSP1 deletion. In line with this, in vitro DUSP1 depletion impaired the angiogenic potential of H460 NSCLC cells [5]. In addition, DUSP1 inhibition, combined to gemcitabine treatment of pancreatic ductal adenocarcinoma in mice attenuates angiogenesis and enhances apoptotic cell death, as compared to gemcitabine alone [6]. DUSP6 was also reported to contribute to angiogenesis control/regulation. Indeed, in melanoma cells, DUSP6 protein degradation was associated with increased ERK activity and upregulation of VEGF-A which drives angiogenesis [7]. These results suggest that DUSP6 acts as an antiangiogenic factor through the dephosphorylation of ERK. Another potential reported antiangiogenic DSP is DUSP2. The overexpression of this MKP causes tumor regression and downregulates angiogenic genes. In line with this, its expression is reduced in many human cancers [8].

Among all A-DSPs, DUSP3 is the only one for which a role in angiogenesis has been investigated. Based on results obtained from *Dusp3–/–* mice and from in vitro DUSP3 depletion using small interfering RNA (siRNA) in HUVEC cells, DUSP3 seems to play a proangiogenic role [9]. Indeed, in vivo DUSP3 deficiency prevented the neovascularization of transplanted basic-fibroblast growth factor (b-FGF)-containing Matrigel and LLC xenograft tumors. Furthermore, we found that DUSP3 is required for b-FGF-induced microvessel outgrowth in the aortic ring assay. The in vitro downregulation of DUSP3 using siRNA in HUVECs reduced significantly the tube formation on Matrigel and the angiogenic sprouting in a spheroid assay. Surprisingly, this defect was not associated with an altered phosphorylation of the documented in vitro DUSP3 substrates, ERK1/2, JNK1/2, and EGFR, but instead with an increased PKC phosphorylation [9].

The following sections describe in detail the in vivo, ex vivo, and in vitro methods we used to investigate the role of DUSP3 in endothelial cells and angiogenesis [9].

2 Materials

All material for cells and tissue culture should be sterile.

2.1 Basic Required Material

1. Heat-inactivated fetal bovine serum (FBS).
2. Penicillin–streptomycin, L-glutamine, and sterile phosphate-buffered saline (PBS).
3. Trypsin (170,000 U/mL)–Versene (EDTA, 200 mg/mL) mixture 1×.
4. Dimethyl sulfoxide (DMSO).
5. Trypan blue 0.4%.
6. Matrigel basement membrane matrix.
7. Basic-Fibroblast growth factor (b-FGF).
8. Drabkin's reagent.
9. Marienfeld counting chamber.

2.2 Cell Culture and Transfection

1. EBM basal medium (Lonza), EGM singlequot kit supplements and growth factors (product CC4133, Lonza) (*see* **Note 1**).
2. Early cell passages (two to six) pooled human umbilical vein endothelial cells (HUVECs).
3. Dulbecco's modified Eagle's medium (DMEM).
4. Lewis Lung Carcinoma (LLC or 3LL) cells.
5. 6-well flat-bottom sterile tissue culture plates.
6. Gene*Trans*II transfection reagent.
7. Two different double stranded siRNAs for the specific gene target and a control non-targeting siRNA.

2.3 Proliferation

1. 96-wells flat-bottom plates.
2. Tritiated thymidine (^{3}H-TdR); specific activity: 20 Ci (740 GBq)/mmol; concentration: 1 mCi/mL. Prepare ^{3}H-TdR working solution by adding 100 µL ^{3}H-TdR stock solution to 5.9 mL of sterile EGM (EBM + singlequots), EBM + 2% FBS, or EBM + bFGF 100 ng/mL.
3. Omnifilter-96 Cell Harvester.
4. Scintillation analyzer.
5. MultiScreen harvest 3H, FC plates (96-well plates).
6. Scintillation liquid buffer.
7. White adhesive bottom seal for 96-well backing tape.
8. Adhesive seal for 96-well plate.

2.4 Tube Formation Assay and Time Lapse

1. 24-wells flat-bottom plates.
2. Lab-Tek II chamber slides (2-well glass slide).
3. Matrigel basement membrane matrix.
4. Inverted bright-field phase-contrast microscope with long-working distance, dry objectives, and camera for images acquisition. We used Leica DM IRE2 inverted microscope equipped with digital QImaging Retiga 2000R high sensitivity grayscale CCD camera. Image capture was driven by ImagePro 6.3 software.
5. Image J software (National Institutes of Health: http://rsb.info.nih.gov/ij/index.html).
6. Confocal microscope equipped with *x*, *y*, and *z* axes, a chamber maintained at 37 °C and 5 % CO_2 and 4D analysis software. We used Nikon A1R microscope and Nis Elements software.

2.5 Spheroid Sprouting Assay

1. Methyl-cellulose.
2. 96-well round bottom non-adherent plates.
3. Rat Tail Collagen I, High Concentration.
4. EBM basal medium and EGM singlequot kit supplements.
5. Phase-contrast microscope (we used Leica DM IRE2).

2.6 In Vivo Matrigel Plug Assay and LLC Subcutaneous Tumors Model

1. Heparin 1 mg/mL.
2. 1 mL sterile syringes with 25G sterile needles.
3. Scalpel or scissors.
4. Dispase 5000 U/mL.
5. NaCl 0.9 % in dH_2O.
6. 30 % (w/v) Brij 35 solution.
7. Hemoglobin from bovine blood.
8. FITC-Dextran (20 mg/mL).
9. Tissue-tek O.C.T compound.
10. Multiscan MS microplate reader capable of measuring absorbance at 540 nm.
11. Tissue homogenizer.
12. Dry ice.

2.7 Immunofluorescence

1. Superfrost plus microscope slides and coverslips #1.
2. Frozen Matrigel plugs sections of 7 μm.
3. Ice-cold acetone.
4. 80 % methanol (4 °C) diluted in water.
5. 10 and 2 % normal goat serum diluted in PBS.
6. Anti-CD31 antibody.

7. Anti-rat Alexa 594 secondary antibody.
8. Vectashield mounting medium with DAPI.
9. Epifluorescent microscope. We used Olympus Vanox AHBT3 epifluorescent microscope.
10. Analysis software. We used Imaris software.

2.8 Aortic Ring Assay (ARA)

1. Inverted bright-field phase-contrast microscope with long-working distance, dry objectives, and camera for images acquisition. We used Leica DM IRE2 inverted microscope equipped with digital QImaging Retiga 2000R high sensitivity grayscale CCD camera. Image capture was driven by ImagePro 6.3 software.
2. Insulin syringes.
3. 100 mm culture petri dish.
4. 86 × 12 mm petri dish.
5. 10 and 17 mm punchers.
6. Microdissection forceps, microdissection scissor, and sterile dissection board.
7. Beaker 100 mL.
8. Magnetic stirrer and stir bars.
9. DMEM 10×, DMEM 1×, and MCDB131 mediums.
10. $NaHCO_3$.
11. NaOH 1 N.
12. Agarose.
13. Rat Tail Collagen I.

3 Methods

All mice experiments and procedures should be carried out following the guidelines and in agreement with the author's local animal ethics committee. Experiments using human samples should be approved by the authors' institutional review board and in accordance with the Helsinki Declaration.

Isolating and culturing large population of primary mice endothelial cells (EC) is challenging. The overgrowth of contaminating cells, in addition to the fact that EC are prone to phenotypic drift during culture, render long term culture of these cells a difficult task to achieve. Therefore, to investigate the role of DUSP3 in EC functions, we used the human primary endothelial HUVEC cells as an in vitro model. These adherent cells are isolated from the vein of the umbilical cord and are commonly used as cellular model of angiogenesis. We optimized siRNA transfection protocol using different commercially available reagents and identified GeneTrans II

reagent as the best transfection reagent yielding a high efficiency of gene knockdown without compromising cellular viability. The role of DUSP3 in EC functions was evaluated using the tube formation, sprouting and proliferation assays. We provide with all these detailed protocols in the sections bellow.

3.1 Cell Culture and Transfection

Cells are maintained in complete EGM medium (EBM supplemented with the EGM singlequot, 10% FBS, and 1× penicillin–streptomycin). In vitro doubling time for HUVECs is about 30 h.

3.1.1 HUVECs Culture

1. Prewarm at 37 °C (in a water bath) the needed amount of all reagents.
2. To thaw HUVECs, incubate them at 37 °C for 2 min.
3. Transfer thawed cells to 50 mL conical tube containing 15 mL of complete prewarmed EGM medium and homogenize HUVECs suspension.
4. Transfer the cell suspension to a T75 cell culture flask and incubate in a cell incubator at 37 °C with 5% CO_2.
5. Aspirate the initial culture medium and replace with fresh 37 °C prewarmed complete EGM medium 16–24 h after the initiation of the culture and every 48 h thereafter. Cells should be split at 70–85% confluence.
6. To split cells, remove the complete EGM medium from the flask.
7. Wash cells twice with 5 mL prewarmed sterile PBS.
8. Add 5 mL of prewarmed trypsin–Versene solution to the T75 and incubate at 37 °C for 3–5 min. Regularly ensure microscopically for cell detachment (*see* **Note 2**).
9. When all cells are detached from the flask bottom, add 12 mL of complete EGM to inhibit trypsin (*see* **Note 3**) and transfer the HUVECs suspension to a sterile 50 mL conical tube.
10. Centrifuge at 200×*g* for 5 min and discard the supernatant without dislodging the cell pellet.
11. Resuspend homogenously the HUVECs in 2 mL prewarmed complete EGM.
12. Perform trypan blue exclusion viability test and count cells using Marienfeld counting chamber (live cells, due to their intact membrane, exclude trypan blue).
13. Seed the cells in new culture vessels at an initial concentration of 2500 live cells/cm^2 in the appropriate amount of complete EGM (1 mL/5 cm^2).
14. Incubate at 37 °C and 5% CO_2.
15. For freezing, prepare complete EGM supplemented with 10% DMSO and 10% FBS (cryopreservation medium) and cool down to 4 °C.
16. Resuspend and centrifuge cells as mentioned above (**steps 7–10**).

17. Resuspend the pellets in cold cryopreservation medium at 5×10^5 cells/mL.
18. Keep the freezing vials at −80 °C overnight and transfer the next day in liquid nitrogen tank.

3.1.2 RNA Interference (RNAi) Transfection in HUVECs

The following instructions are for a 6-well flat-bottom tissue culture plate. Adjust all volumes accordingly for other culture plates. Reconstitution of the GeneTransII is performed according to the instructions of the manufacturer.

1. Rehydrate with the appropriate volume of Hydration Buffer (component of the kit) (1.5 mL for GeneTrans II 0202B) and vortex at maximal speed for 10 s. Store at 4 °C and briefly vortex before each use.
2. The day before transfection, harvest HUVECs as described in Subheading 3.1.1, **steps 1–12** and seed 1.2×10^5 HUVECs per well in 1.5 mL complete EGM medium (*see* **Note 4**).
3. Incubate overnight at 37 °C, 5 % CO_2, and 90 % humidity.
4. For each well, mix 22.75 μL of DNA diluent B (component of the kit) with 2.25 μL of siRNA (100 μM).
5. In another 1.5 mL tube, and for each well, dilute 5.25 μL of GeneTrans II Reagent with 19.75 μL of serum-free DMEM.
6. Mix well by pipetting up and down and incubate at room temperature for 5 min. Do not vortex the DNA diluent B.
7. Mix the siRNA-DNA diluent B with the diluted GeneTrans II Reagent and incubate at room temperature for 10 min to maximum 20 min to allow the formation of lipoplexes.
8. Wash the HUVECs twice with 1 mL serum-free DMEM and add 1.5 mL of serum-free DMEM to each well.
9. Add, dropwise, 50 μL of the GeneTrans II/SiRNA lipoplexes mix to each well and mix gently by pipetting up and down. Final siRNA concentration should be 150 nM.
10. Incubate for 4 h at 37 °C, 5 % CO_2, and 90 % humidity.
11. Wash cells once with 1 mL PBS and once with 1 mL of complete DMEM.
12. Add 1.5 mL of complete EGM medium to each well and incubate overnight at 37 °C, 5 % CO_2, and 90 % humidity.
13. Change the complete EGM medium 16 h after transfection and incubate at 37 °C, 5 % CO_2, and 90 % humidity.
14. Use the cells for experimentation 72 h post-transfection (*see* **Note 5**).

3.2 Endothelial Cells Tube Formation Assay

Tube formation assay is based on the differentiation of EC (here HUVECs) into tube-like structures and is a suitable assay to compare the angiogenic properties of cells after downregulation of

genes of interest. This model can also be used to test proangiogenic or antiangiogenic properties of different agents. Quantification can be achieved by measuring the number, length, intersection of the tubes, or the area of the capillary structures formed using light microscope in 2D culture. Other advantages include the fact that this assay is easy to optimize, fast, require a short culture period, can be used for live imaging and high-throughput analysis. However, tube formation may vary between different lots of support matrix and sometimes between different lots of HUVECs. Therefore, results obtained using this assay should be further confirmed in vivo [10].

1. Thaw the Matrigel overnight at 4 °C and keep on ice as it polymerizes and solidifies at room temperature (*see* **Note 6**).
2. Dispense 200 and 300 μL of Matrigel in 24-well flat-bottom tissue culture plates and glass Lab-Tek II chamber slides (chamber slides for live imaging), respectively. Avoid the introduction of air bubbles.
3. Incubate for 2 h at 37 °C, 5% CO_2, and 90% humidity.
4. Add 250 and 750 μL of complete EGM to the 24 well plate and Lab-Tek chamber, respectively.
5. To allow Matrigel polymerization, incubate for at least 1 h at 37 °C, 5% CO_2, and 90% humidity.
6. 48 h after HUVECs transfection, harvest cells as described above (Subheading 3.1.1, **steps 1–12**).
7. For one time point analysis, add 3×10^4 (24-wells) HUVEC cells on the top of polymerized Matrigel dropwise and mix gently by rotating the plate without disturbing the Matrigel layer.
8. Incubate at 37 °C, 5% CO_2, and 90% humidity for 16 h.
9. Visualize tube formation using a phase-contrast microscope and take pictures of different fields in the middle of the wells. Avoid taking pictures of the wells edges.
10. Total tube length and number of intersections can be quantified using image J software or equivalent. Follow the software guideline.
11. To perform time-lapse video microscopy, add 1×10^5 of HUVEC cells suspension drop by drop on the top of polymerized Matrigel in the chamber slides and mix gently by rotating the slide. Avoid touching the Matrigel layer with the pipette tip.
12. Transfer directly the Lab-Tek chamber containing transfected cells to the stage of a confocal microscope equipped with *x*, *y*, and *z* axes and maintained at 37 °C, 5% CO_2, and 90% humidity. Acquire images every 10 min during 16 h (*see* **Note 7**). We used Nikon A1R confocal microscope and Nis Elements software to capture and analyze the time-lapse microscopy images.

3.3 Spheroid Sprouting Assay

Spheroid sprouting assay is a standardized three-dimensional method to study in vitro angiogenesis. The principle of this assay is based on the sprouting from gel-embedded self aggregated ECs that mimic the formation of new capillaries from preexisting vessels. The 3D nature of this model allows for better comparison with the in vivo situation. In addition, the model can be adapted for multiple applications and allows investigations of signaling pathways involved in angiogenesis [11, 12].

1. Prepare the 1.2% methylcellulose: autoclave 6 g of carboxymethylcellulose in a 500 mL glass bottle with a magnetic stir bar.
2. Preheat 500 mL of EBM medium for 1 h at 60 °C.
3. Add 250 mL of the preheated EBM to the autoclaved carboxymethylcellulose and mix by stirring under sterile conditions for 20 min.
4. Add the remaining 250 mL of EBM to the solution and mix by stirring overnight at 4 °C.
5. Aliquot the solution into 50 mL tubes and centrifuge them for 3 h at 3500 × *g* at 4 °C. The solution can be kept at 4 °C for 3 months. Use only the upper 45 mL from the 50 mL aliquots.
6. Harvest HUVEC cells as described in Subheading 3.1.1.
7. Seed 1500 HUVECs in each well of a non-adherent 96-round bottom well plate in a total volume of 200 μL of a reduced medium EBM containing 0.24% of high-viscosity methylcellulose (20% EGM-MV + 60% EBM + 20% of the 1.2% methylcellulose solution).
8. Incubate for 24 h at 37 °C and 5% CO_2.
9. Cut the end of a 1 mL pipet tip to have a wide-bore style tip.
10. Use the wide-bore tip to collect ten spheroids and transfer into a 2 mL Eppendorf tube.
11. Centrifuge at 100 × *g* for 5 min and discard the supernatant.
12. On ice, dilute the collagen stock solution at 2 mg/mL following the manufacturer instructions and mix at 1:1 with 1.2% methylcellulose solution.
13. Embed the ten spheroids in 500 μL of the collagen solution and mix gently with 1 mL wide-bore tip.
14. Plate immediately in a 24-well plate and incubate at 37 °C and 5% CO_2 for 20 min.
15. Add 500 μL of the complete medium at the top of the gel. Recombinant protein such as b-FGF (10 ng/mL) or VEGF-A (10 ng/mL) can be used as positive controls.
16. Take pictures immediately and after 24 and 48 h using a phase-contrast microscope.

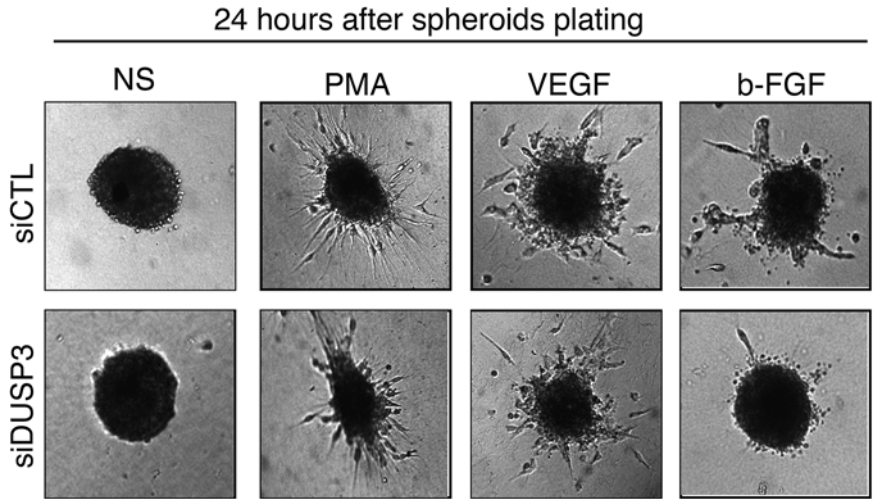

Fig. 1 Representative images of spheroid sprouting assay performed with HUVEC cells 72 h after transfection with non-targeting siRNA (siCTL) or with DUSP3 targeting siRNA (siDUSP3) with no stimulation (NS), in the presence of PMA as positive control (75 ng/mL), VEGF (10 ng/mL), or b-FGF (10 ng/mL)

A representative illustration of the sprouting assay in response to PMA, VEGF, and b-FGF is shown in Fig. 1.

3.4 HUVECs Proliferation Assay

The cellular proliferation can be evaluated by the rate of DNA synthesis that can be measured by the metabolic incorporation of tritiated thymidine (^{3}H-TdR) into cellular DNA. We used our previously described protocol for T cells proliferation [12] to perform the proliferation assay of HUVEC cells with few modification described bellow.

1. 48 h post-transfection, seed in triplicate 7.5×10^3 HUVECs in a total volume of 100 µL per well (96-well flat-bottom plate) of EBM medium (supplemented with 2% FBS), sterile EGM (EBM + singlequots) or EBM + bFGF 100 ng/mL.
2. Incubate the plate overnight at 37 °C, 5% CO_2, and 90% humidity.
3. Add 25 µL ^{3}H-TdR working solution into each well and continue incubation for another 6 h.
4. Remove the cell supernatant using a multichannel pipette.
5. Wash the wells once with 50 µL PBS.
6. Add 50 µL of trypsin to each well and incubate for 5 min at 37 °C, 5% CO_2 and 90% humidity.
7. Harvest cells onto a UniFilter plate using an Omnifilter-96 cell harvester (PerkinElmer).
8. Let the plate dry at room temperature for at least 24 h.

9. Attach the backing tape to the bottom of the dried plate and add 25 µL scintillation liquid buffer in all wells using a multichannel pipette.
10. Cover the plate with the MicroAmp optical adhesive film.
11. Place the plate into the scintillation counter and measure the radioactivity of the incorporated ^{3}H-TdR as counts per min (cpm). CAUTION: DISPOSE OF RADIOACTIVE WASTES INTO APPROPRIATE WASTE CONTAINERS.

3.5 Matrigel Plug Assay

When injected subcutaneously, together with proangiogenic factors, Matrigel solidifies and becomes the site of an intense vascular development. Therefore, this simple angiogenesis model, initially developed by Passaniti, is widely used to assess the angiogenic response in vivo [13, 14]. Mice can be injected in both flanks.

1. Thaw the Matrigel overnight at 4 °C and keep on ice (*see* **Note 6**).
2. For each plug, prepare on ice 500 µL of Matrigel supplemented with 250 ng/mL b-FGF and 0.138 mg/mL heparin (*see* **Note 8**).
3. Inject subcutaneously 500 µL of the Matrigel mixture in each flank of the anesthetized mouse using ice-cold syringe with a 25G needle (*see* **Notes 9** and **10**).
4. 10 days after Matrigel injection, proceed with mice euthanasia following the local ethical committee agreement.
5. Excise carefully the Matrigel plug using a scalpel or scissors.
6. To determine the hemoglobin content by a colorimetric reaction, weight each Matrigel plug and digest with 250 µL dispase 5000 U/mL for 1 h at 37 °C.
7. Add 200 µL NaCl 0.9% in dH_2O and mechanically ground the plugs using a tissue grinder with glass pestle.
8. Centrifuge 5 mL at 370 × *g* and recover the supernatant.
9. Reconstitute the Drabkin's solution by adding 1 mL dH_2O to one vial of Drabkin's reagent and add 0.5 mL of the 30% Brij 35 Solution. Protect from light.
10. Use bovine hemoglobin as a standard. Resuspend hemoglobin in a mix of 55% dispase and 45% NaCl 0.9% (v/v) solution.
11. Prepare an eight-point standard curve using twofold serial dilutions, starting from 500 µg/mL hemoglobin.
12. Add 20 µL of the digested Matrigel supernatant to 0.1 mL Drabkin solution and incubate for 15 min at room temperature.
13. Read absorbance at 540 nm using a Multiscan MS microplate reader and determine hemoglobin concentration using the

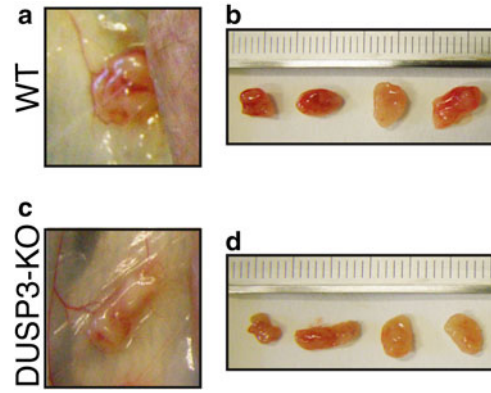

Fig. 2 Matrigel plug assay representative images. Matrigel plugs were retrieved from wild type (WT) and DUSP3-KO mice 7 days after Matrigel subcutaneous injection. (**a**) and (**c**): Matrigel plugs before dissecting them out of WT (**a**) and DUSP3-KO (**c**) right flanks of the mice. (**b**) and (**d**): Matrigel plugs retrieved from WT (**b**) and DUSP3-KO (**d**) mice (two plugs per mouse)

standard curve. Calculated values are normalized by dividing the hemoglobin percentage by the plug weight and are expressed as g/dL of hemoglobin per milligram of Matrigel [15] (*see* **Note 11**). An illustrative example of Matrigels retrieved from wild type and DUSP3-KO mice is shown in Fig. 2.

An alternative method to quantify microvessels in Matrigel plugs is the quantification of fluorescein isothiocyanate (FITC)-dextran staining in the Matrigel sections. To perform this, separated group of mice should be used.

14. Proceed as described above (from **steps 1–3**).
15. At day 10 after Matrigel injection, and 5 min prior to mice sacrifice, inject the mice intravenously in the tail vein with freshly prepared FITC-Dextran (100 mg/kg).
16. Excise carefully Matrigel plugs and freeze immediately on dry ice in Tissue-Tek O.C.T then at −80 °C until use.

3.6 LLC Subcutaneous Tumors

The Lewis lung carcinoma cells, also called LLC or 3LL, is a C57BL/6 lung tumor derived cell line and is widely used as a transplantable malignant model to study angiogenesis, tumor growth and metastasis formation in syngeneic C57BL/6 mice [16, 17]. We used this model to evaluate the role of DUSP3 in angiogenesis-dependent tumor growth. Mice can be injected in both flanks with LLC cells.

LLC cells are maintained in complete DMEM (supplemented with 10% FBS, 2 mM glutamine, and 1× penicillin–streptomycin). In vitro doubling time for LLC cells is approximately 12 h.

3.6.1 LLC Cells Culture

For thawing and growing LLC cells, proceed as described for HUVECs in Subheading 3.1.1, **steps 1–12** except that the medium used for LLC is DMEM.

1. Seed the cells in new culture vessels at an initial concentration of 3×10^4 live cells/cm^2 in the appropriate amount of complete DMEM (1 mL/5 cm^2).
2. Incubate LLC cells at 37 °C, 5% CO_2, and 90% humidity.

For freezing, proceed as described for HUVECs in Subheading 3.1.1, **steps 15–18** except that the medium used is DMEM and with 1×10^6 cells/mL concentration.

3.6.2 LLC Subcutaneous Injection

1. Harvest the LLC cells as described in Subheading 3.6.1.
2. Wash cells once in cold DMEM and centrifuge at 200 × *g* for 5 min.
3. Discard supernatant and dilute cells in cold non-supplemented DMEM at a concentration of 1×10^6 cells/50 µL. Keep the cells on ice until injection.
4. Inject subcutaneously 50 µL of the cell suspension (1×10^6 cells) in each flank of anesthetized mice using a syringe with 25G sterile needle (*see* **Note 10**).
5. After 7 days, proceed with mice euthanasia and carefully harvest the LLC tumors. At this stage, in wild type mice, the size of LLC tumor should be around 4 mm.
6. For the determination of the hemoglobin content by a colorimetric reaction, weight each tumor and mechanically ground the tumors in 450 µL NaCl 0.9% using a homogenizer.
7. Centrifuge 3 min at 825 × *g* and recover the supernatant.
8. Proceed with Drabkin reagent and hemoglobin determination as described in Subheading 3.5, **steps 9–13**.

3.7 Anti-CD31 Immunofluorescence

To quantify the number of endothelial cells, anti-CD31/PECAM can be used on both retrieved Matrigel plugs and LLC frozen sections. Combined to the use of the FITC-Dextran and in addition to the quantification of functional blood vessels, this method allows the identification of perfused vasculature structures [17].

1. Prepare frozen FITC-Dextran Matrigel sections of 7 µm (*see* **Note 12**).
2. Put the slides on a rack and fix in ice-cold acetone for 2 min.
3. Remove the acetone and add 80% cold methanol. Incubate at 4 °C for 5 min.
4. Wash 3 × 5 min with PBS.
5. Delimitate the sections on slides using Dakopen. Cover the sections with a drop of normal goat serum and incubate the slides for 30 min at room temperature in dark humid chamber.
6. Aspirate the serum and wash 3 × 5 min with PBS.

7. Add sufficient volume (to cover the sections) of anti-CD31 (1/100 dilution) antibody diluted in 5% normal goat serum/PBS and incubate for 1 h at room temperature in dark humid chamber.
8. Wash 3×5 min with PBS.
9. Add sufficient volume of anti-rat Alexa 594 secondary (1/200) antibody diluted in 2% normal goat serum/PBS and incubate for 1 h at room temperature in dark humid chamber.
10. Wash 5 min with PBS, three times.
11. Mount the slides using Vectashield mounting medium with DAPI.
12. Visualize the Matrigel stained sections under epifluorescent microscope using red filter (for Alexa 594) and green filter (for FITC-Dextran) and 20× objective. We used Olympus Vanox AHBT3 (*see* **Note 13**).
13. Quantify the number of $CD31^+$ blood vessels sections and total FITC-Dextran fluorescence intensity using Imaris software (*see* **Note 14**).

3.8 Aortic Ring Assay (ARA)

The aortic ring assay (ARA) consists in the outgrowth of blood capillaries from a small fragment of the aorta embedded in a type I collagen gel. This assay recapitulates all the steps of capillaries formation. The ARA is a suitable model used to investigate the molecular basis of angiogenesis, to evaluate the efficacy of proangiogenic or antiangiogenic agents or to phenotype transgenic mice [13, 18].

1. Add 1.5 g of agarose to 100 mL of dH_2O, autoclave and cool down at room temperature.
2. Melt the autoclaved 1.5% agarose in a microwave.
3. Add 30 mL of melted agarose in 100 mm culture petri dish and incubate at 4 °C to allow polymerization (at least 12 h).
4. Meanwhile, prepare the MCDB131 medium: Add 5 mL of penicillin–streptomycin, 5 mL of L-glutamine, 5 mL of sterile $NaHCO_3$ at 92.4 mg/100 mL, and 50 mL of FCS to 500 mL of MCDB131. Keep at room temperature.
5. Anesthetize the mice in a saturated isoflurane bell-jar and proceed with euthanasia by decapitation to allow blood elimination.
6. Surface-sterilize the mouse with 70% ethanol.
7. Lay mice back-down on a dissecting board in a laminar flow tissue culture hood to maintain sterility, fixing the legs to the board with pins.
8. Open the ventral skin with a single cut. Thereafter, use dissection scissors and blunt dissection to peel back the skin.
9. Open the thoracic cavity and cut around the rib cage.

10. Remove the liver, the lungs, the stomach, and the intestine, to expose the aorta visible as a fat-covered blood vessel tracking down along the spine.
11. Starting from the aorta separation into the iliac, detach the aorta from the spinal column, running the small scissors between the aorta and the spine toward the diaphragm.
12. When the aorta is separated from the spine, cut it near to the heart and transfer it into a petri dish containing ice-cold serum-free DMEM. CAUTION: Do no let the aorta dry.
13. Eliminate any blood residues by flushing carefully the aorta using a 1 mL syringe containing DMEM.
14. Fix the aorta to the sterile board with pin and remove carefully all the peri-aortic fibro-adipose tissue and the branching vessels with forceps.
15. Cut the aorta into 1 mm long fragments with a scalpel and transfer them into a petri dish containing ice-cold serum-free DMEM. A total of 15–20 aortic rings can be obtained per aorta.
16. Prepare the working collagen solution: on ice, mix gently 7.5 mL of rat-tail type 1 collagen, 1 mL DMEM 10×, and 1.5 mL $NaHCO_3$ at 15.6 mg/100 mL. Add NaOH 1 N till obtaining of a light pink color solution.
17. Punch agarose cylinders out of the previously prepared agarose gel (**steps 1–3**) with a 17 mm puncher and then, punch the cylinders in the center using a 10 mm puncher to obtain empty rings.
18. Put five rings in a 86 × 12 mm petri dish.
19. Add 200 µL of the collagen solution in each ring and incubate 10 min at 37 °C.

CAUTION: Avoid the formation of bubbles.

20. Prepare a solution with ¾ DMEM and ¼ of the working collagen solution.
21. Soak the aortic rings (prepared in **step 15**) in the DMEM/collagen solution and place each aortic ring on the collagen layer in the center of the agarose ring. Incubate for 10 min at 37 °C, 5 % CO_2.
22. Add 200 µL of the working collagen solution and incubate for 10 min at 37 °C, 5 % CO_2.
23. Add 6 mL of complete MCDB131 medium in the petri dish and incubate at 37 °C 5 % CO_2. We used additif-free-MCDB131 medium as a negative control. Mouse recombinant VEGF-A (10 ng) can be used as a positive control.
24. Take pictures after 6 and 9 days of culture under a phase-contrast microscope.

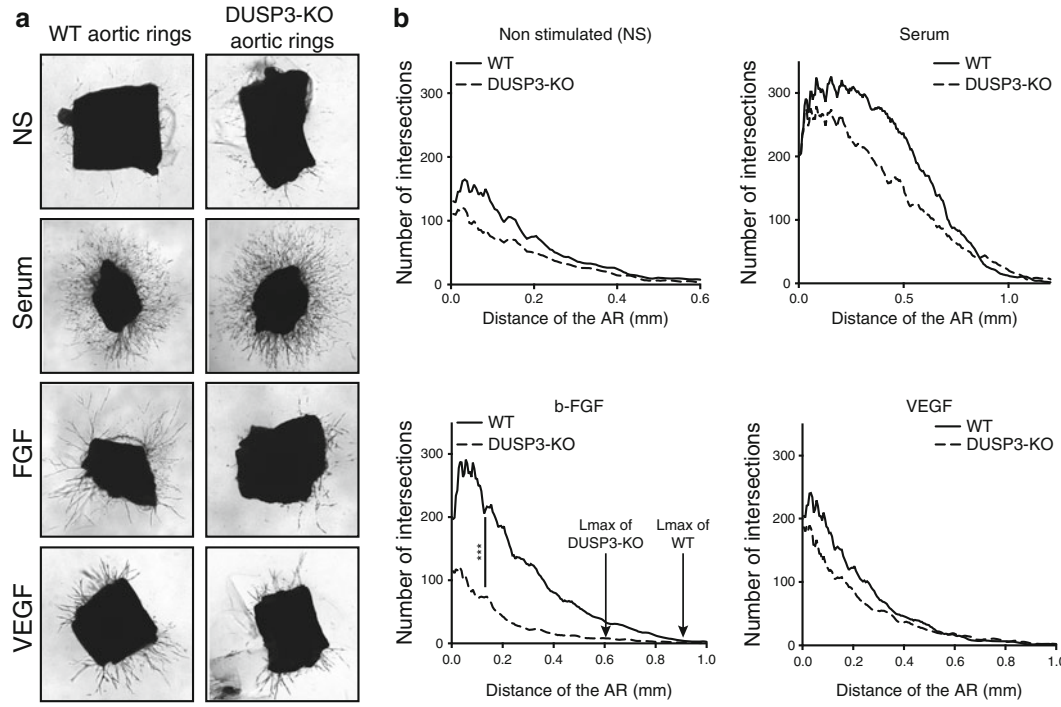

Fig. 3 Ex-vivo microvasculature outgrowth assay illustrative images. (**a**) Phase-contrast micrographs of thoracic aortas from 17-week-old WT and DUSP3-KO mice grown for 9 days in collagen additive-free (no stimulation: NS), in 2.5 % serum containing collagen gels, in 20 ng/mL of b-FGF- or 20 ng/mL of VEGF-supplemented collagen gels. Magnification ×25. (**b**) Computerized quantification of number of microvessel intersections and maximal length of vessels from culture conditions shown in (**a**). *X*-axis represents the length of the aortic microvessel outgrowth and *Y*-axis represents the number of intersections of the microvessels. The *arrows* in the b-FGF stimulated conditions indicate the maximal vessel growth, Lmax (mm) for DUSP3$^{-/-}$ and for DUSP3$^{+/+}$ aortas. ***$p < 0.001$ (*t*-student test)

25. Quantification of the microvessel distribution around the ring as well as the maximum distance of cell migration (Lmax) can be evaluated using a computer assisted method as reported in detail elsewhere [18]. An illustrative example of the expected results is shown in Fig. 3.

4 Notes

1. The EGM singlequot kit supplements and growth factors contain 0.5 mL of hEGF, 0.5 mL hydrocortisone, 0.5 mL gentamicin and amphotericin B, 2 mL bovine brain barrier extracts, 0.5 mL ascorbic acid, and 10 mL FBS. We obtained better results by culturing the HUVECs in 10 % of FBS instead of 2 %.
2. About 90 % of cells should be detached from the bottom of the flask. To facilitate cells detachment, gently tap the corner of the culture dish. The entire procedure should not take

more than 5 min to avoid cells damage. If the HUVECs do not detach, trypsin may be not enough prewarmed or not active enough.

3. Complete EGM is supplemented with 10% FBS. FBS is known to inhibit trypsin. Hence, the addition of complete EGM to the flask at the end of the trypsinization procedure inhibits the process. It is also essential to remove traces of serum before trypsinization by washing the cells carefully with PBS without Ca^{2+} and Mg^{2+}.
4. For optimal RNA interference efficiency, HUVEC confluence should be approximately 60–70% at the time of transfection.
5. For DUSP3, the best protein extinction was observed at 72 h post-transfection as evaluated by western blot. This time point should be determined for each protein of interest and depend on the protein half-life.
6. Avoid freezing–thawing cycles of the Matrigel and use precooled material (tips, pipets, tubes, culture plates) to ovoid polymerization of the Matrigel.
7. Setting up of the time lapse conditions and image acquisition is performed at time 0 on a *z*-axis. During acquisition, cells move into the Matrigel and the focal point may be lost. To limit this, z-stack images should be taken for every time point: one in the top of cells, one in the middle and a third one at the cells bottom. Images acquisition should also be taken in the center of the slide (avoid the edges). Laser capture system may also be toxic to cells and may perturb tube formation if the time lapse exceed 16 h.
8. Several growth factors and drugs can be used in this assay. VEGF, cancer cell (and other cell type) conditioned medium, and even cancer cells can be used. Concentrations of growth factors and compounds used should be adjusted by the users.
9. The mixture should be injected slowly. Wait for 10–20 s before removing the needle to allow the Matrigel to solidify and avoid leaking.
10. To facilitate the injection, the skin on each flank must be shaved prior to injection.
11. Determination of hemoglobin concentration in Matrigel plug is an indirect simple method to quantify the number of blood vessels in the Matrigel plug or in LLC tumor mass [15, 19]. Results obtained using this method should be confirmed using a histological method.
12. Matrigel sections should be prepared on superfrost microscope slides. Cryostat chamber atmosphere should be around −30 °C and a temperature object of −13 °C.

13. To ensure best quality results, examine the slides immediately after performing the immunofluorescence staining. Use nail polish to seal the coverslip on the slide. If not possible, store the slides in the dark at 4 °C for a maximum of 1 week.
14. We used Imaris software to quantify the number of $CD31^+$ blood vessels sections and total FITC-Dextran fluorescence intensity. Among many other possibilities, this software allows the semi-automated detection and quantification of fluorescence on 2D. The use of a manually predefined filter (fluorescence intensity threshold to remove background staining, area threshold to remove nonspecific signal from antibodies precipitates) saves time and limits the manual analysis bias. Such quantification of positive fluorescent blood vessels and the fluorescence intensity can also be performed manually using Image J software (National Institutes of Health).

Acknowledgement

This work was supported by grants from the Fonds de la Recherche Scientifique (FRS-FNRS) (Belgium), the Fonds Spéciaux pour la Recherche from the University of Liège (Belgium), from the Léon Fredericq Funds (FLF) and the "Centre Anti-cancéreux" (CAC). AM and EC are Télévie PhD fellows.

References

1. Patterson KI, Brummer T, O'Brien PM, Daly RJ (2009) Dual-specificity phosphatases: critical regulators with diverse cellular targets. Biochem J 418:475–489
2. Jeffrey KL, Camps M, Rommel C, Mackay CR (2007) Targeting dual-specificity phosphatases: manipulating MAP kinase signalling and immune responses. Nat Rev Drug Discov 6:391–403
3. Kinney CM, Chandrasekharan UM, Mavrakis L, DiCorleto PE (2008) VEGF and thrombin induce MKP-1 through distinct signaling pathways: role for MKP-1 in endothelial cell migration. Am J Physiol Cell Physiol 294:C241–C250
4. Boerckel JD, Chandrasekharan UM, Waitkus MS, Tillmaand EG, Bartlett R, DiCorleto PE (2014) Mitogen-activated protein kinase phosphatase-1 promotes neovascularization and angiogenic gene expression. Arterioscler Thromb Vasc Biol 34:1020–1031
5. Moncho-Amor V, Ibañez de Cáceres I, Bandres E, Martínez-Poveda B, Orgaz JL, Sánchez-Pérez I, Zazo S, Rovira A, Albanell J, Jiménez B, Rojo F, Belda-Iniesta C, García-Foncillas J, Perona R (2010) DUSP1/MKP1 promotes angiogenesis, invasion and metastasis in non-small-cell lung cancer. Oncogene 30:668–678
6. Liu F, Gore AJ, Wilson JL, Korc M (2014) DUSP1 is a novel target for enhancing pancreatic cancer cell sensitivity to gemcitabine. PLoS One 9:e84982
7. Martin MJ, Hayward R, Viros A, Marais R (2012) Metformin accelerates the growth of BRAF V600E-driven melanoma by upregulating VEGF-A. Cancer Discov 2:344–355
8. Lin SC, Chien CW, Lee JC, Yeh YC, Hsu KF, Lai YY, Lin SC, Tsai SJ (2011) Suppression of dual-specificity phosphatase-2 by hypoxia increases chemoresistance and malignancy in human cancer cells. J Clin Invest 121:1905–1916
9. Amand M, Erpicum C, Bajou K, Cerignoli F, Blacher S, Martin M, Dequiedt F, Drion P, Singh P, Zurashvili T, Vandereyken M, Musumeci L, Mustelin T, Moutschen M, Gilles C, Noel A, Rahmouni S (2014) DUSP3/VHR

is a pro-angiogenic atypical dual-specificity phosphatase. Mol Cancer 13:108

10. Donovan D, Brown NJ, Bishop ET, Lewis CE (2001) Comparison of three in vitro human "angiogenesis" assays with capillaries formed in vivo. Angiogenesis 4:113–121
11. Korff T, Augustin HG (1998) Integration of endothelial cells in multicellular spheroids prevents apoptosis and induces differentiation. J Cell Biol 143:1341–1352
12. Rahmouni S, Delacroix L, Liu WH, Tautz L (2013) Evaluating effects of tyrosine phosphatase inhibitors on T cell receptor signaling. Methods Mol Biol 1053:241–270
13. Berndt S, Perrier d'Hauterive S, Blacher S, Pequeux C, Lorquet S, Munaut C, Applanat M, Herve MA, Lamande N, Corvol P, van den Brule F, Frankenne F, Poutanen M, Huhtaniemi I, Geenen V, Noel A, Foidart JM (2006) Angiogenic activity of human chorionic gonadotropin through LH receptor activation on endothelial and epithelial cells of the endometrium. FASEB J 20:2630–2632
14. O'Reilly MS, Holmgren L, Shing Y, Chen C, Rosenthal RA, Moses M, Lane WS, Cao Y, Helene Sage E, Folkman J (1994) Angiostatin: a novel angiogenesis inhibitor that mediates the suppression of metastases by a Lewis lung carcinoma. Cell 79:315–328
15. Passaniti A, Taylor RM, Pili R, Guo Y, Long PV, Haney JA, Pauly RR, Grant DS, Martin GR (1992) A simple, quantitative method for assessing angiogenesis and antiangiogenic agents using reconstituted basement membrane, heparin, and fibroblast growth factor. Lab Invest 67:519–528
16. Eklund L, Bry M, Alitalo K (2013) Mouse models for studying angiogenesis and lymphangiogenesis in cancer. Mol Oncol 7:259–282
17. Tigges U, Hyer EG, Scharf J, Stallcup WB (2008) FGF2-dependent neovascularization of subcutaneous Matrigel plugs is initiated by bone marrow-derived pericytes and macrophages. Development 135:523–532
18. Blacher S, Devy L, Burbridge MF, Roland G, Tucker G, Noël A, Foidart JM (2001) Improved quantification of angiogenesis in the rat aortic ring assay. Angiogenesis 4:133–142
19. Masson V, Devy L, Grignet-Debrus C, Bernt S, Bajou K, Blacher S, Roland G, Chang Y, Fong T, Carmeliet P, Foidart J-M, Noël A (2002) Mouse aortic ring assay: a new approach of the molecular genetics of angiogenesis. Biol Proced Online 4:24–31

Chapter 19

Studying Protein-Tyrosine Phosphatases in Zebrafish

Alexander James Hale and Jeroen den Hertog

Abstract

Protein-tyrosine phosphatases (PTPs) are a large family of signal transduction regulators that have an essential role in normal development and physiology. Aberrant activation or inactivation of PTPs is at the basis of many human diseases. The zebrafish, *Danio rerio*, is being used extensively to model major aspects of development and disease as well as the mechanism of regeneration of limbs and vital organs, and most classical PTPs have been identified in zebrafish. Zebrafish is an excellent model system for biomedical research because the genome is sequenced, zebrafish produce a large number of offspring, the eggs develop outside the mother and are transparent, facilitating intravital imaging, and transgenesis and (site-directed) mutagenesis are feasible. Together, these traits make zebrafish amenable for the analysis of gene and protein function. In this chapter we cover three manipulations of zebrafish embryos that we have used to study the effects of PTPs in development, regeneration, and biochemistry. Microinjection at the one-cell stage is at the basis of many zebrafish experiments and is described first. This is followed by a description for measuring regeneration of the embryonic caudal fin, a powerful and robust physiological assay. Finally, the considerable but manageable troubleshooting of several complications associated with preparing zebrafish embryos for immunoblotting is explained. Overall, this chapter provides detailed protocols for manipulating zebrafish embryo samples with a compilation of tips collected through extensive experience from the zebrafish research community.

Key words Zebrafish, Protein-tyrosine phosphatases, PTP, Microinjection, Regeneration assay, Tissue lysis

1 Introduction

Protein-tyrosine phosphatases (PTPs) are a large family of signal transduction regulators, determining rate and duration of phosphotyrosine (pTyr) phosphorylation cascades [1]. Disruption of PTP activity leads to aberrant pTyr signaling and is at the basis of many human diseases [2]. Much is already known of the mechanisms PTPs employ to regulate signal transduction [3] and the regulation of their dephosphorylating activity [4–6]. Yet, a full appreciation of the importance of temporal and spatial control of PTP activity is best acquired in vivo. Model organisms used to acquire such insights include the invertebrates *Drosophila* [7] and *C. elegans* [8] and the vertebrates *Danio rerio* [9], mouse [10], and rat [11].

Rafael Pulido (ed.), *Protein Tyrosine Phosphatases: Methods and Protocols*, Methods in Molecular Biology, vol. 1447,
DOI 10.1007/978-1-4939-3746-2_19,

The zebrafish *Danio rerio* is being used extensively to model major aspects of development [12] and diseases including cancer [13, 14], metabolic disease [15–17], and cardiovascular disease [18]. Zebrafish are even used to study the mechanism of regeneration of limbs and vital organs [19, 20]. Evidently, zebrafish studies are a key aspect of translational research and are enabling advancements in human health [21]. Zebrafish are oviparous, provide up to 200 embryos per mating pair per week and develop within 5 days, with most organs forming within 48 h. Many existing genetic mutants are available from stock centers (Zebrafish International Resource Center in Eugene, USA, and European Zebrafish Resource Center in Karlsruhe, Germany) and mutagenesis is highly feasible using optimized transcription activator-like effector nucleases (TALENs) [22] or the combination of Clustered Regularly Interspaced Short Palindromic Repeats (CRISPR) with the CRISPR associated protein (CAS) [23–25]. Transient overexpression or stable transgenesis can readily be achieved through microinjection of synthetic messenger RNA (RNA) or plasmid DNA respectively at the one-cell stage [26]. In addition, mutagenesis-based gene inactivation is carried out using reagents such as *N*-ethyl-*N*-nitrosourea (ENU) to generate random single nucleotide mutations [27].

Zebrafish embryos are transparent, allowing for easy analysis of developmental progression and defects as well as disease phenotypes. Intravital imaging of fluorescent markers expressed in a tissue- or cell type-specific manner provides a powerful tool for studying developmental processes. This has been taken advantage of extensively to study angiogenesis [28], lymphangiogenesis [29], convergence and extension cell movements during development [30] and even to capture embryonic development in 3D [31, 32]. Intravital imaging of fusion proteins facilitates the analysis of protein localization, protein–protein interactions, and protein function in a whole organism in vivo. In addition, several techniques are now being refined and will augment the advantages of zebrafish as an experimental system. These include proteomics analysis of zebrafish embryos using mass-spectrometry following selection by immunoprecipitation [33–35], analysis of the plasma proteome following blood collection [36] and derivation of cell lines from single embryos [37].

Finally, the relative simplicity of adding compounds to either the water of the adults or the medium of the embryos, combined with the possibility for large sample number and rapid reproducibility has led to several bioactive compound screens [18, 38]. Notably, combining knockouts or embryos with transient overexpression with timed drug treatments provides an unparalleled opportunity to pinpoint the exact temporal role of proteins in vivo.

An important experimental consideration is that the zebrafish genome was duplicated early in evolution [39, 40]. Whilst some of

the duplicated chromosomes were lost, the duplicated genes that remain may have complementary or diverging expression patterns and exhibit redundant or complementary functions. Therefore, gene duplications may complicate the creation of knockout mutants by requiring two redundant genes to be targeted. The translational value is another essential consideration when choosing an experimental system and the reason the zebrafish is regularly used to model disease is in part due to 84% of human genes associated with a disease having a zebrafish counterpart [41].

All classical PTPs, except *ptpn7*, *ptpn12*, and *ptpn14*, have been identified in the zebrafish genome and 14 are duplicated [42]. Van Eekelen et al. 2010 also characterize expression duration and localization using in situ hybridization, identifying that some of the duplicated PTP pairs have divergent expression patterns, indicative of diverging functions. A good example of the complexity arisen from PTP duplication is that of *ptpn11*, encoding the Shp2 protein. Bonetti et al. 2014 demonstrate that zebrafish *ptpn11a* and *ptpn11b* encode highly homologous proteins, Shp2a and Shp2b respectively. Yet, whilst *ptpn11a–/–* mutants have severe developmental defects and are embryonic lethal, *ptpn11b–/–* mutants show no obvious developmental defects. This difference may suggest that Shp2a and Shp2b proteins are functionally distinct. Shp2b does have a function in development, because *ptpn11a–/– ptpn11b–/–* mutants exhibit a slightly more severe phenotype than *ptpn11a–/–* mutants. Furthermore, severe developmental defects displayed by *ptpn11a–/– ptpn11b–/–* double mutant embryos are rescued by transient overexpression of either Shp2a or Shp2b, demonstrating functional similarity of Shp2a and Shp2b proteins. The expression patterns of *ptpn11a* and *ptpn11b* are distinct; *ptpn11a* is constitutively expressed at a high level throughout development, whereas *ptpn11b* expression is at a relatively low level during early development and increases steadily through later stages. Hence, we conclude that the difference in expression patterns of *ptpn11a* and *ptpn11b*, rather than an intrinsic difference in protein function of Shp2a and Shp2b is at the basis of the difference in function of *ptpn11a* and *ptpn11b* during development [43]. The accompanied complexity of gene duplication can be used to extensively delineate gene function and the advantages of zebrafish as an experimental system make it ideal for elucidating the intricate function and regulation of PTPs in vivo. Hence, zebrafish are often used to understand the role of PTPs in signaling in development [44–47] and, lately more, in disease [34].

2 Materials

All solutions are prepared in double-distilled, deionized Milli-Q filtered water (resistivity of 18 MΩ cm at 25 °C).

2.1 Microinjection

1. Bright-field/Nomarski optics stereomicroscope.
2. Micromanipulator.
3. Pneumatic microinjector.
4. Nitrogen (N_2) gas.
5. Glass capillaries: Outer diameter 1 mm, inner diameter 0.78 mm, length 100 mm.
6. 0.01 mm micrometer slide.
7. 10 μl microloader pipette tips.
8. 0.5% phenol red.
9. Thermomixer.
10. E3 medium: 5 mM NaCl, 0.17 mM KCl, 0.33 mM $CaCl_2$, 0.33 mM $MgSO_4$.
11. 0.05% methylene blue; dilute in E3 medium to 0.01% prior to use.
12. Micropipette puller P97.
13. Putty or tape.
14. Slanted lane mold.
15. Plastic 15 and 10 cm plates.
16. Ultrapure agarose.
17. 70% ethanol.
18. Mineral oil.

2.2 Regeneration Assay

1. Stereomicroscope.
2. Bright-field/Nomarski optics stereomicroscope with camera function.
3. 0.4% MS222: 0.4% ethyl 3-aminobenzoate methanesulfonate salt (MS222), 50 mM Tris–HCl pH 7.5; dilute in E3 medium to desired concentration prior to use.
4. Stainless steel surgical blade.
5. Plastic and glass Pasteur pipettes.
6. Plastic 10 cm dish and multi-well plates.
7. 10 μl microloader pipette tips.
8. E3 medium: 5 mM NaCl, 0.17 mM KCl, 0.33 mM $CaCl_2$, 0.33 mM $MgSO_4$.

2.3 Tissue Lysis for Protein Extraction

1. 1.5 ml tubes.
2. Mini-pestle (to fit in the 1.5 ml tubes).
3. 1 ml syringe and 0.2–0.8 mm needles.
4. Sonicator.
5. Degassed lysis buffer: 25 mM 4-(2-hydroxyethyl)-1-piperazineethanesulfonic acid (HEPES) pH 7.4, 150 mM

NaCl, 0.25% deoxycholate, 1% Triton X-100, 10 mM $MgCl_2$, 1 mM ethylenediaminetetraacetic acid (EDTA), 10% glycerol.

6. RIPA buffer: 25 mM Tris–HCl pH 7.6, 150 mM NaCl, 1% NP-40, 1% sodium deoxycholate, 0.1% sodium dodecyl sulfate.
7. Ginzburg fish Ringers buffer: 111.2 mM NaCl, 3.35 mM KCl, 2.38 mM $NaHCO_3$.
8. Liquid nitrogen (N_2).
9. Thermomixer.
10. Cold centrifuge.
11. Protease inhibitors, aprotinin and leupeptin (both 1 mg/ml).
12. Phosphatase inhibitors sodium fluoride (0.5 M), beta-glycerophosphate (1 M), and sodium orthovanadate (200 mM).
13. 70% ethanol.
14. 2× Laemmli sample buffer: 2% β-mercaptoethanol, 20% glycerol, 0.125 M Tris–HCl pH 6.8, 4% sodium dodecyl sulfate, (a pinch) bromophenol blue.

3 Methods

The underlying principle of the protocols and notes that follow is that zebrafish embryos are a living organism, useful for analyzing phenotypes, but can also be considered a compact factory of cells malleable to existing molecular techniques. All procedures involving zebrafish described were approved by the local animal experiments committee and performed according to local guidelines and policies in compliance with national and European law. Zebrafish maintenance and breeding were performed following published protocols [48].

An absolute must for the genetic manipulation of zebrafish is the skill to microinject at the one-cell stage. This is covered first (Subheading 3.1) and following this a plethora of manipulations are available. Here, a description for measuring regeneration of the embryonic caudal fin, a powerful and robust physiological assay, is given (Subheading 3.2). Also the method of lysing zebrafish tissue for protein extraction to perform SDS-PAGE and immunoblotting will be detailed (Subheading 3.3), which requires considerable but manageable troubleshooting due to the complications that arise from obtaining a homogenous zebrafish cell lysate and lack of antibodies that recognize the zebrafish ortholog.

In Subheading 3.1 we cover the use of microinjection for introduction of alien genetic material into an organism, which began in 1971 when it was used to introduce DNA into Xenopus oocytes [49]. Since then the technique has been adapted for microinjection of zebrafish embryos at the one-cell stage and early mouse blastocysts for transgenesis [50, 51] and cells in culture [52]. A detailed

video protocol for microinjection of zebrafish embryos can be found on Jove entitled "Microinjection of zebrafish embryos to analyse gene function" [53]. Needles for holding and injecting RNA or DNA are made using a glass capillary micropipette puller, which contains a heating filament that slowly melts the glass and as the two halves separate the tip is stretched to the correct diameter. Each machine model will need to be calibrated according to the manufacturer's instructions before use.

RNA microinjection leads to efficient, and usually high, expression within several hours and will be described below, though the reader can consider all uses of "RNA" interchangeable with "DNA." The only significant factor when microinjecting DNA is that accuracy needs to be high to ensure that the DNA ends up in the cell. For this reason, significant effort is made to align embryos properly in the microinjection plate to improve accuracy of injecting directly into the cell. Microinjection is a technique that develops and improves with experience. It is easy to learn but difficult to teach as a lot is based on a singular coordinated movement of fingers moving the needle into the embryo and feet ejecting the RNA or DNA, and this is a "comfortable" feeling once mastered. For example, it takes practice to be able to estimate just how much of the needle needs to be shortened once mounted; there is no way to measure this. Practice is essential, and once the technique is acquired the individual tends to improve without any further guidance.

In Subheading 3.2 an embryonic caudal fin regeneration assay is described. Some urodeles and teleosts are capable of epimorphic regeneration, perfect or near-perfect replacement of lost tissue, throughout their lifetime [54]. Zebrafish are capable of regenerating multiple tissues, including fins, the brain, retina, spinal cord, and heart [19]. Zebrafish are therefore an excellent model to study and understand the mechanism of epimorphic regeneration. The results that emerge from such research may pave the way to enabling adult mammal organs to regenerate, most of which are currently limited to inflammation and formation of a collagen-rich connective tissue scar following injury [55]. Adult zebrafish caudal fin regeneration takes 10–12 days to complete. In comparison, embryo caudal fins only take 3 days, making the embryonic regeneration assay an efficient and reproducible technique. A previously established caudal fin regeneration model [56] was adapted to amputate at 2 days post fertilization and regeneration is then completed by 3 days post amputation (5 days post fertilization).

Importantly, as regeneration rate is higher in embryos, wound healing is also more rapid. For this reason it is paramount that a picture of the amputated caudal fin be taken as soon as possible to capture the wound margin as accurately as possible. Another consideration with an embryonic caudal fin regeneration assay is that changes in regeneration rate could also be due to changes in rate of embryonic development. It is ideal to compare amputated

embryos with same stage uncut embryos and, therefore a picture of an uncut embryo is taken at the same time as the embryo with the wound margin. This technique can easily be combined with microinjection of RNA or DNA or drug treatments.

Subheading 3.3 describes tissue lysis of whole zebrafish embryos for extraction of protein. Zebrafish embryos, up to 6 days, can be considered tissue extracts for applying molecular techniques. Thus, the method remains the same regardless of age but becomes more laborious with older, more defined tissue. Preparation of zebrafish embryos for SDS-PAGE requires deyolking, and then lysis buffer is applied before the sample is homogenized. A general method can be found on the ZFIN database [57] but we have developed our own lysis buffers and homogenization techniques for specific uses of the protein extract and this will be explained in detail below.

Zebrafish embryos have a yolk sac, providing nutrients for growth until day 6 when the embryos can eat particle food [48]. This yolk sac contains a high concentration of vitellogenin, a phospholipo-glycoprotein composed of multiple subunits, the most predominant two at around 150 and 80 kDa. Unfortunately, the yolk proteins interfere with detection of specific proteins by immunoblotting, presumably due to the high expression levels of the yolk proteins. Particularly detection of specific proteins of similar sizes as the yolk proteins is problematic. This interference can be largely reduced by deyolking embryos using Ginzburg fish Ringers solution [58]. After deyolking, lysis buffer is applied. We use one of two lysis buffers, each has advantages and disadvantages. Whereas RIPA lysis buffer is fast and provides high yield, the presence of SDS may disrupt delicate protein-protein interactions. In comparison, degassed lysis buffer will yield less protein but the absence of SDS protects delicate protein-protein interactions, which is useful if intending to perform co-immunoprecipitation. Following the choice of lysis buffer there are three options for homogenization. The least challenging, but also the least effective in terms of yield, is using a mini-pestle to crush the embryo in the 1.5 ml tube containing lysis buffer. A higher yield can be obtained by using a syringe and needle to aspirate and push the tissue through a small (<0.4 mm) needle opening (shearing). Complications arise with larger tissue (e.g., fin clips and embryos approaching 5 days post fertilization) which may clog the needle. Though laborious, this complication can be resolved by first choosing an appropriately sized (>0.6 mm) needle for the dense tissue extract and repeating homogenization with a smaller needle afterwards. The final alternative is to use a sonicator, which works well on embryos up to 4 days old but may take considerably longer on defined tissue such as fin-clips.

Following successful lysis of zebrafish tissue, the lysate can be loaded onto an SDS-PAGE gel following a standard protocol.

The only exception is that a protein concentration assay (e.g., Biorad Bradford assay) is not performed on zebrafish embryos because the sample is less pure than from cells and there is an abundance of yolk protein which will skew the estimation. Instead protein level is correlated with the number of embryos per unit volume of lysis buffer used. A standard protocol for immunoblotting can also be applied. A far greater problem is the sheer lack of antibodies that recognize the zebrafish protein homologs. It is not uncommon that when the zebrafish and mammalian homologs share a high percentage amino acid sequence similarity, the antibody raised against the mammalian homolog does not bind the zebrafish homolog. Even when the epitope sequence is conserved the antibody does not necessarily work for the zebrafish homolog; sometimes the antibody will simply not bind anything but more often the problem is increased nonspecific binding (including sequestration of the antibody by the yolk protein). This antibody issue may be partially circumvented by raising an antibody against the purified target zebrafish protein. However, functionality of these antibodies is not necessarily guaranteed and should be tested thoroughly for validation. Also of note is that these antibodies do not always have the same efficiency on endogenous proteins in zebrafish embryos. Hopefully, with time, a range of antibodies produced and validated by different labs will become available on the commercial market. Some are already available at the Zebrafish International Resource Centre (ZIRC).

3.1 Microinjection

1. Dissolve ultrapure agarose in E3 medium with 0.01% methylene blue to prepare a 2% agarose solution.
2. Pour 2% agarose into a plastic 10 cm dish and gradually apply the plastic lane mold onto the surface of the agarose. Leave new microinjection plate (Fig. 1) to set (*see* **Note 1**).

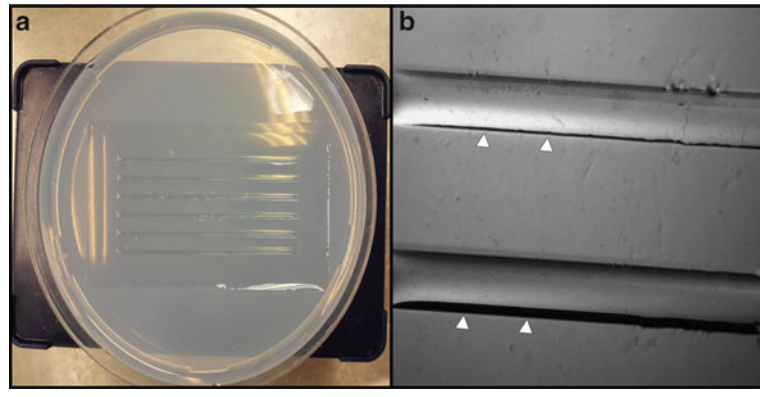

Fig. 1 Example of a microinjection plate made of 2% agarose (**a**) and higher magnification showing the grooves with the beveled edge (*arrow heads*) on the bottom side (**b**)

3. Remove the mold and pour E3 medium with 0.01% methylene blue to cover the surface. Store at 4 °C (*see* **Note 2**).
4. Prepare RNA by diluting as required in a mixture of Milli-Q water and 0.5% phenol red (*see* **Note 3**).
5. Heat RNA for 5–10 min at 65 °C and 1150 rpm in a thermomixer (*see* **Note 4**). Keep RNA on ice.
6. Switch on pneumatic microinjector and open the N_2 gas valve. The "regulator" pressure should not exceed 30 psi.
7. Wipe base of stereomicroscope with 70% ethanol and adjust lamp brightness as desired.
8. Place needle under stereomicroscope and use the micrometer slide to determine the point at which the needle tip width is equal to 20 μm. Use tweezers to remove the excess of the needle that extends beyond this point.
9. Use microloader pipette tips to transfer 1–2 μl of RNA into the cut needle.
10. Position micromanipulator and mount needle half way up the shaft of the pressure dispenser.
11. Position needle tip in a small dish of mineral oil and check pneumatic microinjector is set to "gated".
12. In "gated" mode apply pressure to the foot pump for 1–2 s to eject some RNA solution (*see* **Note 5**).
13. Switch pneumatic microinjector to "timed," switch the "range" to "100 ms" and the "period" to maximum "2.0" so that duration of ejection is 200 ms. Now, a single push of the foot pump will eject a single drop of RNA.
14. Press down on foot pump to eject a single drop of RNA into the mineral oil. Use the micrometer slide to measure size of droplet (*see* **Note 6**).
15. Adjust droplet size to 1 nl by first reducing the duration of ejection. Lower the "period" slightly and repeat **step 15**. If droplet size is still too small when duration of ejection is 70 ms ("period" is "0.70"), use the tweezers to remove more of the needle tip and repeat adjustment with "period" (*see* **Note 7**). Once a droplet of 1 nl is obtained rest the needle in mineral oil.
16. Collect fresh fertilized embryos in a plastic 10 cm dish with E3 medium. From this point on you have ~30 min before the single cell of the embryo divides. Work fast (*see* **Note 8**).
17. Transfer embryos to the lanes in the microinjection plate using a plastic Pasteur pipette (*see* **Note 9**).
18. Under the stereomicroscope the single cell of the embryo will be clearly visible. Position embryo such that the cell is at the top (*see* **Note 10**).

19. Use micromanipulator to adjust needle position and penetrate through the chorion and into the cell of the embryo. Almost simultaneously, press the foot pump to eject some RNA into the cell and withdraw the needle (*see* **Note 11**).
20. Move to the next embryo and repeat the microinjection until the desired number of embryos has been microinjected.
21. When finished use a plastic Pasteur pipette and E3 medium with 0.01% methylene blue to rinse the embryos into a plastic 10 cm dish with fresh E3 medium with 0.01% methylene blue. Incubate at 28.5 °C (*see* **Note 12**).
22. Discard needle in sharps bin and remaining embryos in designated waste bin. Close the N_2 gas valve, switch pneumatic microinjector to "gated" again and use foot pump to eject remaining N_2 gas. Switch off pneumatic microinjector and stereomicroscope light.

If injecting RNA encoding a fluorescent protein, a standard fluorescence microscope with appropriate filter can be used to visually assess success rate. It is common for protein expression to vary between embryos (Fig. 2) as each embryo is microinjected in a slightly different position and embryos have varying rates of protein synthesis, depending on health and developmental stage. Practice microinjections using mRNA encoding Green Fluorescent Protein (GFP) is convenient for evaluation of success rate. The technique is considered "mastered" once a success rate of 95% or higher is reached.

RNA or DNA injection into the cell at the one-cell stage of zebrafish should lead to expression in all subsequent daughter cells, but mosaicism is frequently observed. If RNA is microinjected at a late one-cell stage or whilst the first cell division is in progress

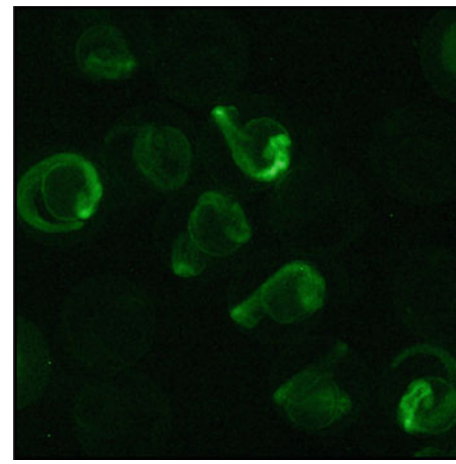

Fig. 2 Twenty-four hour post fertilization zebrafish embryos, still in their chorion, displaying variation in GFP protein expression between embryos following microinjection of GFP RNA

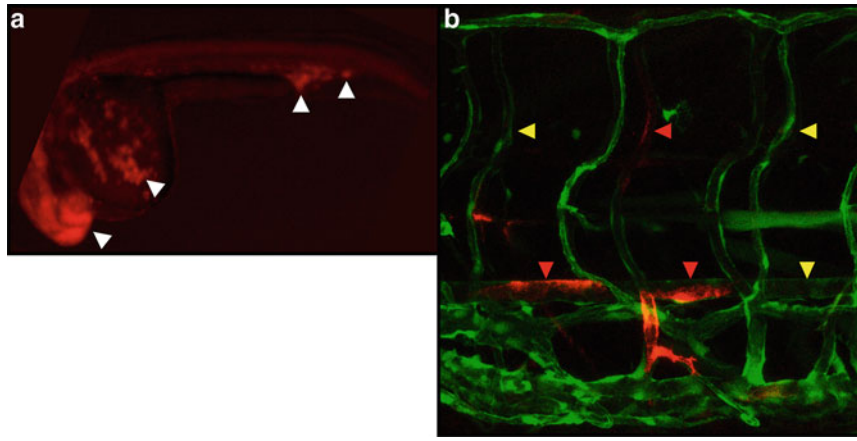

Fig. 3 Examples of non-ubiquitous expression following microinjection of RNA. (**a**) Example of patchy expression from RNA microinjection. An embryo microinjected with RNA encoding wild-type human Pten tagged with mCherry is imaged at 2dpf. Mosaic mCherry expression is found in a few clusters of cells scattered around the body of the embryo (*arrow heads*), suggesting RNA was not microinjected at the one-cell stage. (**b**) Example of mosaic expression in the trunk of an embryo at 5 days post fertilization. A transgenic embryo expressing *flt4:mCit* to mark the vasculature, shown in *green*, is microinjected with plasmid DNA encoding *prox1a:KalTA4,UAS:tagRFP,* shown in *red*, at the one-cell stage. Despite accurate microinjection only some vessels express RFP (*red arrow heads*), demonstrating mosaicism. *Yellow arrow heads* show similar vessels without RFP expression for comparison

mosaicism in the form of patchy expression, with only small clusters of cells translating the RNA, may arise (Fig. 3a). When RNA is microinjected accurately there may be considerably less mosaicism but it will still be present (Fig. 3b). Depending on the purpose of the experiment, the presence of mosaicism can offer some advantages in that a comparison can be made, for example, between the same population of cells expressing the microinjected protein and those without in the same embryo.

3.2 Regeneration Assay

1. Dechorionate embryos using tweezers.
2. Anesthetize embryos by transferring to 0.1% MS222 in E3 medium with 0.01% methylene blue for 2–4 min (*see* **Note 13**).
3. Place the lid of a 10 cm plastic dish over the light source of a stereomicroscope (*see* **Note 14**).
4. Transfer one embryo at a time to surface of plastic lid in a droplet of 0.1% MS222 in E3 medium with 0.01% methylene blue using a plastic Pasteur pipette (*see* **Note 15**).
5. Use a stainless steel surgical blade to amputate the caudal fin of the embryo immediately distal to the notochord under the stereomicroscope (*see* **Note 16**).
6. Use a glass Pasteur pipette to transfer embryo to fresh 0.1% MS222 in E3 medium with 0.01% methylene blue (*see* **Note 17**).

7. Capture wound margin of amputated caudal fin using a stereomicroscope with an attached camera (*see* **Note 18**).
8. Wash embryo in fresh E3 medium.
9. Use a glass Pasteur pipette to transfer embryo to a well in a multi-well plate containing fresh E3 medium with 0.01% methylene blue (*see* **Note 19**).
10. Repeat **steps 4–9** until multi-well plates of both amputated and uncut controls are filled. Incubate embryos at 28.5 °C for 3 days (*see* **Note 20**).
11. Prepare 0.2% MS222 in E3 medium by mixing half volume 0.4% MS222 and half volume E3 medium. Use a plastic Pasteur pipette to add three to four droplets of 0.2% MS222 in E3 medium to each well.
12. Use a glass Pasteur pipette to transfer one embryo per time to a 10 cm plate containing fresh 0.1% MS222 in E3 medium with 0.01% methylene blue.
13. Capture size of caudal fin using a stereomicroscope with an attached camera (*see* **Note 21**).
14. Repeat **steps 12–13** until all embryos of multi-well plates for both amputated and uncut controls have been imaged.

The images captured at 2 and 5 days post fertilization are of uncut controls and amputated embryos (Fig. 4). The change in

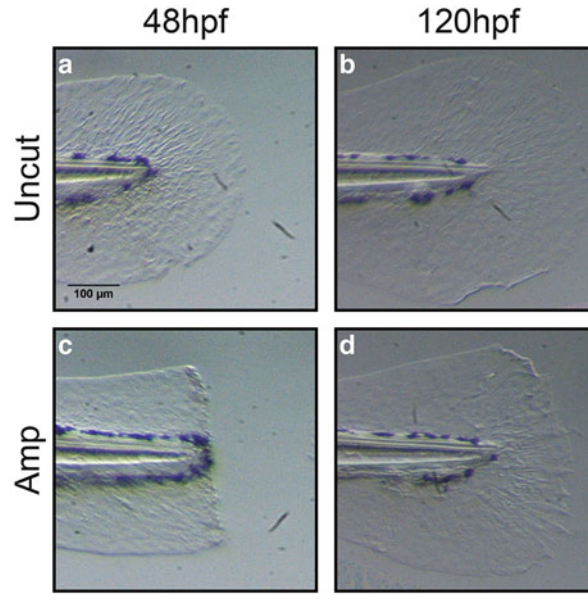

Fig. 4 Bright-field images of the caudal fin of zebrafish embryos. Fin margins are captured at 48 h post fertilization (**a** and **c**), and again at 5 days post fertilization (**b** and **d**), of uncut controls (**a** and **b**) and embryos amputated adjacent to the notochord (**c** and **d**). Scale bar is equivalent for all panels

caudal fin length after 3 days is calculated by subtracting the length of the fin from the tip of the notochord at day 5 from that at day 2 for each embryo. This is easily quantified using the measure tool in ImageJ and the difference calculated is a measure of regenerative outgrowth.

3.3 Tissue Lysis for Protein Extraction

1. Dechorionate embryos using tweezers (*see* **Note 22**).
2. Transfer embryos to a 1.5 ml tube, 96-well plate or similar. Remove as much system water or E3 medium as possible.
3. Prepare Ginzburg fish Ringers solution by adding protease and phosphatase inhibitors (10 μl/ml sodium fluoride, 5 μl/ml beta-glycerophosphate, 5 μl/ml sodium orthovanadate, 1 μl/ml aprotinin, 1 μl/ml leupeptin) and add sufficient volume to the embryos to allow repeated pipetting with a P200 tip (~600 μm wide).
4. Repeatedly pipette up and down in a gentle steady motion or invert regularly. Do not create air bubbles. Alternatively, place multiple embryos in a well of a 6-well plate filled with Ginzburg fish Ringers solution and place plate on a thermomixer set to 28.5 °C and 400–800 rpm for 30–45 min (*see* **Note 23**).
5. Wash deyolked embryos with fresh Ginzburg fish Ringers solution and transfer to chosen vessel (1.5 ml tube or 96-well plate).
6. Centrifuge briefly at 4 °C to collect embryos at bottom of tube or well.
7. Aspirate Ginzburg fish Ringers solution and snap-freeze embryos in liquid nitrogen (*see* **Note 24**).
8. Defrost frozen tissue on ice.
9. Prepare chosen lysis buffer by adding protease and phosphatase inhibitors (10 μl/ml Sodium Fluoride, 5 μl/ml beta-Glycerophosphate, 5 μl/ml Sodium Orthovanadate, 1 μl/ml Aprotinin, 1 μl/ml Leupeptin) and add volume according to age (Table 1).

Next, there are three homogenization options available for proceeding with tissue lysis; the steps required for homogenization using a mini-pestle (A), a syringe and needle (B), or sonication (C), are described below.

A. Mini-pestle homogenization (1.5 ml tubes only):

   10A. Quickly, with the tissue still frozen, start applying pressure using a mini-pestle that fits in a 1.5 ml tube (*see* **Note 25**).

   11A. Withdraw pestle and use a pipette to wash head of pestle to maximize amount of lysate collected.

12A. Clean pestle by rinsing with 70% ethanol followed by water and repeat **steps 10** and **11** for each sample.

13A. Rest on ice.

B. Syringe and needle homogenization:

10B. Wait for tissue to defrost in lysis buffer.

11B. Attach a sterile needle, width 0.2–0.8 mm, to a 1 ml syringe. No larger than 0.2 mm is highly recommended for 24 h post fertilization (hpf).

12B. Aspirate and dispense suspension repeatedly until tissue has been completely sheared (see Note 26).

13B. Rest on ice.

C. Sonication homogenization:

10C. Wait for tissue to defrost in lysis buffer.

11C. Incubate on ice for 30 min.

12C. Sonicate at "high" intensity for 10–15 min with a repeated cycle of 30 s ON, followed by 30 s OFF.

13C. Rest on ice.

14. Once homogenized with the chosen method centrifuge samples at 17,970 rcf and 4 °C for 20 min.

15. Transfer supernatant to a fresh tube or plate and discard the pellet. Can store supernatant at −80 °C at this point if required.

16. Mix equal volume lysate and 2× Laemmli buffer.

17. Boil samples for 5–10 min (*see* **Note 27**).

18. Store at −20 °C or continue loading samples onto an SDS gel.

Please note that there are many variations on the deyolking and homogenization procedures. For example, deyolking can be carried out *after* mini-pestle homogenization by centrifuging lysate and resuspending the pellet in Ginzburg fish Ringers solution. The sample is then centrifuged again to remove the Ginzburg fish Ringers

Table 1
Volume of lysis buffer to be used per embryo of the indicated age

Tissue age	Volume lysis buffer
<24 hpf	1 µl/embryo
24–48 hpf	1–2 µl/embryo
48–96 hpf	2–5 µl/embryo
>96 hpf	>5 µl/embryo
Adult fin clips	>10 µl

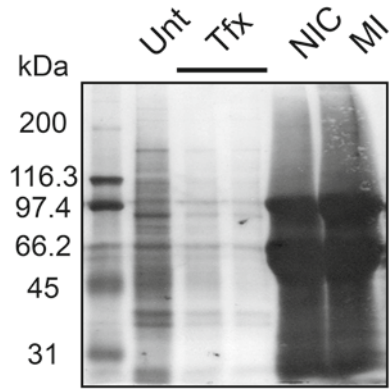

Fig. 5 Coomassie stain of PVDF membrane showing differences between HEK 293T cells lysed with RIPA buffer (*lanes 2–4*) and zebrafish embryos lysed with RIPA buffer and subjected to mini-pestle homogenization (*lanes 5* and *6*). A typical experiment comparing non-transfected (Unt) and transfected (Tfx) HEK 293T cells with non-injected control (NIC) and microinjected (MI) zebrafish embryo samples (7.5 embryo equivalents per lane). *Lane 1* contains a molecular weight marker

solution and resuspended in 1× sample buffer (created by mixing equal volumes of chosen lysis buffer and 2× Laemmli buffer). This way the deyolking procedure is more convenient but a possible consequence is greater variation in protein concentration between samples as some lysed protein may have been lost in the multiple centrifugations where supernatants are discarded. Another alternative is to only disrupt the integrity of the embryos a little using mini-pestle homogenization and follow that with sonication to achieve more efficient lysis. One's choice will be determined by a combination of purpose for the lysate, embryo age, and, ultimately, experience.

Preparation of zebrafish embryo lysates requires more diligence than for cell lysates. This is partly due to the high protein content compared to cultured cells, resulting in the bands being "fatter" and more "smiley" (Fig. 5). This can also cause protein bands to run slightly slower, but offsets size estimation by no more than 5 kDa. The right combination of deyolking, lysis buffer and homogenization optimizes the result. For example, embryos can be lysed in RIPA buffer prepared for SDS-PAGE using mini-pestle homogenization without dechorionating and deyolking (Fig. 6a). But when embryos are dechorionated, deyolked, lysed using degassed lysis buffer and prepared for SDS-PAGE using mini-pestle homogenization the result is less yield but almost as clean as that obtained from pure cell lysate (Fig. 6b). Then again, Fig. 6b clearly shows that deyolking can lead to unequal protein concentration between samples, as a result of both the lysate that remains on the head of the pestle and the centrifugation step required.

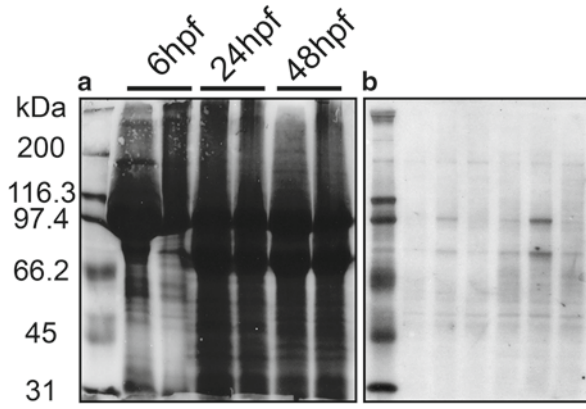

Fig. 6 Coomassie stains of PVDF membranes containing zebrafish embryo samples. (**a**) Samples, not dechorionated or deyolked, lysed in RIPA buffer and subjected to mini-pestle homogenization (5 embryo equivalents per lane). Zebrafish embryos were lysed at 6, 24, and 48 h post fertilization (hpf). Notice how "fat" and "smiley" the bands are. (**b**) Samples after dechorionating, deyolking, lysed in degassed lysis buffer and subjected to mini-pestle homogenization (1 embryo per lane). Zebrafish embryos were lysed at 48 hpf. Notice that the protein content is considerably less, but that the lysate profile is more "clean" and similar to that of the cell lysates seen in Fig. 5. A typical experiment with six different conditions is depicted. *Lane 1* in (**a**) and (**b**) contains a molecular weight marker

4 Notes

1. The plastic mold is embossed with ramps with a 45° beveled side (Fig. 1b). This aids microinjection as the embryo will be pushed into the corner of the lane, allowing the needle to more easily penetrate the chorion and yolk or cell.
2. The agarose microinjection plates will keep for 1–2 weeks, after which molds will begin to grow and the borders of the lanes begin to soften and break. The molds do not interfere with the embryos as long as the embryos are washed afterwards but the breaks in the lanes can inconvenience injections.
3. In general not more than 500 pg of RNA is injected in zebrafish embryos (this is achieved using 1 nl of RNA at 500 ng/μl). The phenol red is only used as a dye to observe successful injection (once competent this aid is no longer required), and 1 μl for every 15 μl is more than sufficient.
4. Heating the RNA removes secondary structures such as hairpin loops. This ensures that most of the RNA injected is available for translation and ultimately increases the efficiency of microinjection. This step is not necessary if injecting DNA.
5. This action removes air bubbles from the RNA. The RNA is now under pressure. If "hold" pressure is too great the RNA will now begin to leak from the needle tip, adjust if necessary.

6. Calibration of the RNA droplet to 1 nl is measured using a 0.01 mm micrometer slide. Briefly, according to $V=4/3\pi r^3$, a droplet of 1 nl has a radius of 62 μm and the diameter is hence 124 μm. The micrometer slide has divisions of 10 μm; meaning 1 nl is equivalent to 12 divisions. The needle width is measured to approximately 20 μm wide prior to mounting and the width of each new needle then needs to be adjusted to create a 1 nl droplet using the micrometer slide to calibrate.
7. Duration of ejection MUST NOT be <70 ms ("period" not <0.70) as this results in ejection of unreliable droplet size with repeated injections. If needle tip is shortened too much, a new needle will have to be prepared. Resting the needle tip in mineral oil avoids RNA drying up and forming a plaque that blocks the ejection of RNA. If, despite best efforts, the needle does become blocked there are two options; switch the pneumatic pump back to "gated" and try to flush the plaque off, or if the duration of ejection is still set relatively high (>100 ms for example) remove the tip of the needle with the tweezers and recalibrate droplet size using the micrometer slide and reducing the duration of ejection by lowering the "period."
8. If too much time is lost and RNA is microinjected at the two-cell stage, the mosaicism that arises will be considerable (Fig. 3a).
9. Under the stereomicroscope the lanes will be clearly visible. Use a truncated microloader pipette tip to position embryos in the lanes. At this point it is prudent to eject a single RNA droplet and check it is still 1 nl on the micrometer slide. It is good to do this before every round of microinjecting as well in case the yolk from the embryos microinjected in the previous round has blocked the needle and causes <1 nl to be ejected in subsequent rounds of microinjecting.
10. Bright field is usually sufficient for identifying the cell and microinjecting but Nomarski optics can be used to improve contrast between the yolk and the transparent cell of the zebrafish embryo.
11. This movement is extremely fluid such that it is one move, once competent a rate of >50 embryos per minute is achievable. If the cell is missed and instead the RNA is deposited into the yolk of the embryo, then continue. During development most of the RNA from the yolk will be taken up into the cell. Especially when learning the technique the first few times it is easier to aim right under the cell, providing a wider target area, as the RNA will be taken up within minutes following injection through cytoplasmic streaming. If injecting DNA be aware that DNA is a considerably larger molecule and is therefore barely taken up through cytoplasmic streaming!
12. If development needs to be accelerated or decelerated for any reason then incubate at maximum 31 °C (faster development) or minimum 21.5 °C (slower development), respectively.

13. MS222 is sensitive to light and loses potency with time. For this reason, I often wrap the plastic dish with 0.1 % MS222 in E3 medium 0.01 % methylene blue in aluminum foil when intending to amputate many embryos.
14. Preferably cut on the lid so that the rim does not obstruct the motion of incision. The plastic will not break. A microscope with a small base is preferable as it provides free vertical movement of the arm when performing amputations.
15. In parallel I usually transfer an uncut control embryo to the plastic 10 cm dish with fresh 0.1 % MS222 in E3 medium with 0.01 % methylene blue mentioned in **step 6**.
16. The main focus area for improvement in this technique is accuracy to perform the amputation as close to the notochord as possible without damaging the notochord. The notochord does not regenerate, hence if nicked or amputated the embryo will die. Also, avoiding tearing of the fin tissue by pulling the surgical blade away from wound margin is desirable to simplify the analysis of regenerative outgrowth. The optimal incision motion is made using downward pressure to sever the caudal fin tissue and not slicing towards you, as this can create a pulling force on the fin tissue and lead to a sheared fin instead of a clean cut.
17. Preferably use a glass Pasteur pipette from this point forward as the amputated caudal fin readily sticks to plastic, causing damage to the caudal fin.
18. Use microloader pipette tips to position embryo with the posterior end flat on the bottom of the plastic dish. Nomarski optics can be used to improve contrast of the transparent caudal fin of the zebrafish embryo. For comparing different embryos it is paramount to use the same zoom settings on the stereomicroscope. Using the abovementioned Leica setup there is enough space to take a picture of both the amputated embryo and the uncut control in the same image.
19. Smaller than a 24-well plate is not recommended as the embryos have insufficient space to grow.
20. By performing the assay this way each uncut control is near enough at the same developmental stage as the amputated embryos and changes in embryonic growth rate can be accounted for.
21. The caudal fin of 5 dpf embryos is substantially bigger than at 2 dpf. Hence, each embryo for both amputated and uncut controls requires a separate image.
22. The chorion contains maternal DNA and proteins; this needs to be removed for accurate estimation of embryonic protein content.

23. The temperature is simply set to a comfortable temperature in which the embryo will survive. If using a 1.5 ml tube or multi-well plate it is easy to look under a standard stereomicroscope to check how much of the yolk has dissociated from the embryo.
24. If not deyolking, any excess system water or E3 medium can be removed from fin-clips or embryos respectively and directly subjected to snap-freezing in liquid nitrogen. By snap-freezing the tissue becomes more brittle, increasing homogenization efficiency. Can store tissue at this point at –80 °C.
25. Accompany a firm up-down motion with a gentle rotation for maximum efficiency. The tissue will shear. When removing the pestle some buffer or tissue may adhere to the head.
26. Creating air bubbles is practically unavoidable with this method but if the appropriate needle is used the tissue will be better sheared than it would have been with a mini-pestle. A small amount of suspension is always lost in the tip of the syringe which cannot be dispensed.
27. This removes quaternary and tertiary structures of proteins. Take into consideration that, after preparation with sample buffer and boiling, the sample may be very viscous, especially if little lysis buffer is used for many embryos. Upon such an occurrence the sample usually needs to be diluted with more sample buffer for accurate loading to be feasible. It is therefore very important to follow the guidelines set out in **step 9** to avoid this complication.

Acknowledgements

We would like to make a special mention of Miriam Stumpf who optimized sonication of zebrafish embryos in our lab and was kind enough to share her expertise. Also we thank Jelte Sikkens and Andreas van Impel for providing Fig. 3a and b respectively. We are grateful to all our colleagues, both within the den Hertog group and in the wider field of zebrafish research, for sharing their experiences with us and helping to make this chapter as comprehensive as possible with contributions from experts in zebrafish research.

References

1. Tonks NK (2006) Protein tyrosine phosphatases: from genes, to function, to disease. Nat Rev Mol Cell Biol 7(11):833–846. doi:10.1038/nrm2039
2. Hendriks WJ, Elson A, Harroch S, Pulido R, Stoker A, den Hertog J (2013) Protein tyrosine phosphatases in health and disease. FEBS J 280(2):708–730. doi:10.1111/febs.12000
3. Tonks NK (2013) Protein tyrosine phosphatases—from housekeeping enzymes to master regulators of signal transduction. FEBS J 280(2):346–378. doi:10.1111/febs.12077
4. Andersen JN, Mortensen OH, Peters GH, Drake PG, Iversen LF, Olsen OH, Jansen PG, Andersen HS, Tonks NK, Moller NP (2001) Structural and evolutionary relationships

among protein tyrosine phosphatase domains. Mol Cell Biol 21(21):7117–7136. doi:10.1128/MCB.21.21.7117-7136.2001

5. Chiarugi P, Cirri P (2003) Redox regulation of protein tyrosine phosphatases during receptor tyrosine kinase signal transduction. Trends Biochem Sci 28(9):509–514. doi:10.1016/s0968-0004(03)00174-9
6. den Hertog J, Groen A, van der Wijk T (2005) Redox regulation of protein-tyro sine phosphatases. Arch Biochem Biophys 434(1):11–15. doi:10.1016/j.aab.2004.05.024
7. Zinn K (1993) Drosophila protein tyrosine phosphatases. Semin Cell Biol 4(6):397–401
8. Gutch MJ, Flint AJ, Keller J, Tonks NK, Hengartner MO (1998) The Caenorhabditis elegans SH2 domain-containing protein tyrosine phosphatase PTP-2 participates in signal transduction during oogenesis and vulval development. Genes Dev 12(4):571–585
9. van der Sar AM, de Fockert J, Betist M, Zivkovic D, den Hertog J (1999) Pleiotropic effects of zebrafish protein-tyrosine phosphatase-1B on early embryonic development. Int J Dev Biol 43(8):785–794
10. Revuelta-Cervantes J, Mayoral R, Miranda S, Gonzalez-Rodriguez A, Fernandez M, Martin-Sanz P, Valverde AM (2011) Protein tyrosine phosphatase 1B (PTP1B) deficiency accelerates hepatic regeneration in mice. Am J Pathol 178(4):1591–1604. doi:10.1016/j.ajpath.2010.12.020
11. Zabolotny JM, Bence-Hanulec KK, Stricker-Krongrad A, Haj F, Wang YP, Minokoshi Y, Kim YB, Elmquist JK, Tartaglia LA, Kahn BB, Neel BG (2002) PTP1B regulates leptin signal transduction in vivo. Dev Cell 2(4):489–495. doi:10.1016/s1534-5807(02)00148-x
12. Haffter P, Granato M, Brand M, Mullins MC, Hammerschmidt M, Kane DA, Odenthal J, van Eeden FJM, Jiang YJ, Heisenberg CP, Kelsh RN, Furutani-Seiki M, Vogelsang E, Beuchle D, Schach U, Fabian C, Nusslein-Volhard C (1996) The identification of genes with unique and essential functions in the development of the zebrafish, Danio rerio. Development 123:1–36
13. Feitsma H, Cuppen E (2008) Zebrafish as a cancer model. Mol Cancer Res 6(5):685–694. doi:10.1158/1541-7786.MCR-07-2167
14. Blackburn JS, Langenau DM (2014) Zebrafish as a model to assess cancer heterogeneity, progression and relapse. Dis Model Mech 7(7):755–762. doi:10.1242/dmm.015842
15. Seth A, Stemple DL, Barroso I (2013) The emerging use of zebrafish to model metabolic disease. Dis Model Mech 6(5):1080–1088. doi:10.1242/dmm.011346
16. Intine RV, Olsen AS, Sarras MP Jr (2013) A zebrafish model of diabetes mellitus and metabolic memory. J Vis Exp 72:e50232. doi:10.3791/50232
17. Vliegenthart AD, Tucker CS, Del Pozo J, Dear JW (2014) Zebrafish as model organisms for studying drug-induced liver injury. Br J Clin Pharmacol 78(6):1217–1227. doi:10.1111/bcp.12408
18. Peterson RT, Link BA, Dowling JE, Schreiber SL (2000) Small molecule developmental screens reveal the logic and timing of vertebrate development. Proc Natl Acad Sci U S A 97(24):12965–12969. doi:10.1073/pnas.97.24.12965
19. Gemberling M, Bailey TJ, Hyde DR, Poss KD (2013) The zebrafish as a model for complex tissue regeneration. Trends Genet 29(11):611–620
20. Goessling W, North TE (2014) Repairing quite swimmingly: advances in regenerative medicine using zebrafish. Dis Model Mech 7(7):769–776. doi:10.1242/dmm.016352
21. Phillips JB, Westerfield M (2014) Zebrafish models in translational research: tipping the scales toward advancements in human health. Dis Model Mech 7(7):739–743. doi:10.1242/dmm.015545
22. Sun N, Zhao H (2013) Transcription activator-like effector nucleases (TALENs): a highly efficient and versatile tool for genome editing. Biotechnol Bioeng 110(7):1811–1821. doi:10.1002/bit.24890
23. Irion U, Krauss J, Nusslein-Volhard C (2014) Precise and efficient genome editing in zebrafish using the CRISPR/Cas9 system. Development 141(24):4827–4830. doi:10.1242/dev.115584
24. Jao LE, Wente SR, Chen W (2013) Efficient multiplex biallelic zebrafish genome editing using a CRISPR nuclease system. Proc Natl Acad Sci U S A 110(34):13904–13909. doi:10.1073/pnas.1308335110
25. Hwang WY, Fu Y, Reyon D, Maeder ML, Tsai SQ, Sander JD, Peterson RT, Yeh JR, Joung JK (2013) Efficient genome editing in zebrafish using a CRISPR-Cas system. Nat Biotechnol 31(3):227–229. doi:10.1038/nbt.2501
26. Holder N, Xu Q (1999) Microinjection of DNA, RNA, and protein into the fertilized zebrafish egg for analysis of gene function. Methods Mol Biol 97:487–490. doi:10.1385/1-59259-270-8:487
27. de Bruijn E, Cuppen E, Feitsma H (2009) Highly efficient ENU mutagenesis in zebrafish. Methods Mol Biol 546:3–12. doi:10.1007/978-1-60327-977-2_1
28. Lawson ND, Weinstein BM (2002) In vivo imaging of embryonic vascular development

using transgenic zebrafish. Dev Biol 248(2): 307–318

29. van Impel A, Schulte-Merker S (2014) A fish-eye view on lymphangiogenesis. Adv Anat Embryol Cell Biol 214:153–165. doi:10.1007/978-3-7091-1646-3_12
30. van Eekelen M, Runtuwene V, Overvoorde J, den Hertog J (2010) RPTPalpha and PTPepsilon signaling via Fyn/Yes and RhoA is essential for zebrafish convergence and extension cell movements during gastrulation. Dev Biol 340(2):626–639. doi:10.1016/j.ydbio.2010.02.026
31. Keller PJ, Schmidt AD, Wittbrodt J, Stelzer EH (2008) Reconstruction of zebrafish early embryonic development by scanned light sheet microscopy. Science 322(5904):1065–1069. doi:10.1126/science.1162493
32. Schmid B, Shah G, Scherf N, Weber M, Thierbach K, Campos CP, Roeder I, Aanstad P, Huisken J (2013) High-speed panoramic light-sheet microscopy reveals global endodermal cell dynamics. Nat Commun 4:2207. doi:10.1038/ncomms3207
33. Paardekooper Overman J, Preisinger C, Prummel K, Bonetti M, Giansanti P, Heck A, den Hertog J (2014) Phosphoproteomics-mediated identification of Fer kinase as a target of mutant Shp2 in Noonan and LEOPARD syndrome. PLoS One 9(9):e106682. doi:10.1371/journal.pone.0106682
34. Paardekooper Overman J, Yi JS, Bonetti M, Soulsby M, Preisinger C, Stokes MP, Hui L, Silva JC, Overvoorde J, Giansanti P, Heck AJ, Kontaridis MI, den Hertog J, Bennett AM (2014) PZR coordinates Shp2 Noonan and LEOPARD syndrome signaling in zebrafish and mice. Mol Cell Biol 34(15):2874–2889. doi:10.1128/MCB.00135-14
35. Lemeer S, Jopling C, Gouw J, Mohammed S, Heck AJ, Slijper M, den Hertog J (2008) Comparative phosphoproteomics of zebrafish Fyn/Yes morpholino knockdown embryos. Mol Cell Proteomics 7(11):2176–2187. doi:10.1074/mcp.M800081-MCP200
36. Babaei F, Ramalingam R, Tavendale A, Liang Y, Yan LS, Ajuh P, Cheng SH, Lam YW (2013) Novel blood collection method allows plasma proteome analysis from single zebrafish. J Proteome Res 12(4):1580–1590. doi:10.1021/pr3009226
37. Choorapoikayil S, Overvoorde J, den Hertog J (2013) Deriving cell lines from zebrafish embryos and tumors. Zebrafish 10(3):316–325. doi:10.1089/zeb.2013.0866
38. den Hertog J (2005) Chemical genetics: drug screens in zebrafish. Biosci Rep 25(5–6):289–297. doi:10.1007/s10540-005-2891-8
39. Meyer A, Schartl M (1999) Gene and genome duplications in vertebrates: the one-to-four (-to-eight in fish) rule and the evolution of novel gene functions. Curr Opin Cell Biol 11(6):699–704
40. Woods IG, Kelly PD, Chu F, Ngo-Hazelett P, Yan YL, Huang H, Postlethwait JH, Talbot WS (2000) A comparative map of the zebrafish genome. Genome Res 10(12): 1903–1914
41. Howe K, Clark MD, Torroja CF, Torrance J, Berthelot C, Muffato M, Collins JE, Humphray S, McLaren K, Matthews L, McLaren S, Sealy I, Caccamo M, Churcher C, Scott C, Barrett JC, Koch R, Rauch GJ, White S, Chow W, Kilian B, Quintais LT, Guerra-Assuncao JA, Zhou Y, Gu Y, Yen J, Vogel JH, Eyre T, Redmond S, Banerjee R, Chi J, Fu B, Langley E, Maguire SF, Laird GK, Lloyd D, Kenyon E, Donaldson S, Sehra H, Almeida-King J, Loveland J, Trevanion S, Jones M, Quail M, Willey D, Hunt A, Burton J, Sims S, McLay K, Plumb B, Davis J, Clee C, Oliver K, Clark R, Riddle C, Elliot D, Threadgold G, Harden G, Ware D, Begum S, Mortimore B, Kerry G, Heath P, Phillimore B, Tracey A, Corby N, Dunn M, Johnson C, Wood J, Clark S, Pelan S, Griffiths G, Smith M, Glithero R, Howden P, Barker N, Lloyd C, Stevens C, Harley J, Holt K, Panagiotidis G, Lovell J, Beasley H, Henderson C, Gordon D, Auger K, Wright D, Collins J, Raisen C, Dyer L, Leung K, Robertson L, Ambridge K, Leongamornlert D, McGuire S, Gilderthorp R, Griffiths C, Manthravadi D, Nichol S, Barker G, Whitehead S, Kay M, Brown J, Murnane C, Gray E, Humphries M, Sycamore N, Barker D, Saunders D, Wallis J, Babbage A, Hammond S, Mashreghi-Mohammadi M, Barr L, Martin S, Wray P, Ellington A, Matthews N, Ellwood M, Woodmansey R, Clark G, Cooper J, Tromans A, Grafham D, Skuce C, Pandian R, Andrews R, Harrison E, Kimberley A, Garnett J, Fosker N, Hall R, Garner P, Kelly D, Bird C, Palmer S, Gehring I, Berger A, Dooley CM, Ersan-Urun Z, Eser C, Geiger H, Geisler M, Karotki L, Kirn A, Konantz J, Konantz M, Oberlander M, Rudolph-Geiger S, Teucke M, Lanz C, Raddatz G, Osoegawa K, Zhu B, Rapp A, Widaa S, Langford C, Yang F, Schuster SC, Carter NP, Harrow J, Ning Z, Herrero J, Searle SM, Enright A, Geisler R, Plasterk RH, Lee C, Westerfield M, de Jong PJ, Zon LI, Postlethwait JH, Nusslein-Volhard C, Hubbard TJ, Roest Crollius H, Rogers J, Stemple DL (2013) The zebrafish reference genome sequence and its relationship to the human genome. Nature 496(7446):498–503. doi:10.1038/nature12111

42. van Eekelen M, Overvoorde J, van Rooijen C, den Hertog J (2010) Identification and expression of the family of classical protein-tyrosine phosphatases in zebrafish. PLoS One 5(9):e12573. doi:10.1371/journal.pone.0012573
43. Bonetti M, Rodriguez-Martinez V, Paardekooper Overman J, Overvoorde J, van Eekelen M, Jopling C, Hertog J (2014) Distinct and overlapping functions of ptpn11 genes in Zebrafish development. PLoS One 9(4):e94884. doi:10.1371/journal.pone.0094884
44. Liao WH, Cheng CH, Hung KS, Chiu WT, Chen GD, Hwang PP, Hwang SP, Kuan YS, Huang CJ (2013) Protein tyrosine phosphatase receptor type O (Ptpro) regulates cerebellar formation during zebrafish development through modulating Fgf signaling. Cell Mol Life Sci 70(13):2367–2381. doi:10.1007/s00018-013-1259-7
45. van Eekelen M, Runtuwene V, Masselink W, den Hertog J (2012) Pair-wise regulation of convergence and extension cell movements by four phosphatases via RhoA. PLoS One 7(4):e35913. doi:10.1371/journal.pone.0035913
46. Hayashi M, Majumdar A, Li X, Adler J, Sun Z, Vertuani S, Hellberg C, Mellberg S, Koch S, Dimberg A, Koh GY, Dejana E, Belting HG, Affolter M, Thurston G, Holmgren L, Vestweber D, Claesson-Welsh L (2013) VE-PTP regulates VEGFR2 activity in stalk cells to establish endothelial cell polarity and lumen formation. Nat Commun 4:1672. doi:10.1038/ncomms2683
47. Wyatt L, Wadham C, Crocker LA, Lardelli M, Khew-Goodall Y (2007) The protein tyrosine phosphatase Pez regulates TGFbeta, epithelial-mesenchymal transition, and organ development. J Cell Biol 178(7):1223–1235. doi:10.1083/jcb.200705035
48. Kimmel CB, Ballard WW, Kimmel SR, Ullmann B, Schilling TF (1995) Stages of embryonic-development of the zebrafish. Dev Dyn 203(3):253–310. doi:10.1002/aja.1002030302
49. Gurdon JB, Lane CD, Woodland HR, Marbaix G (1971) Use of frog eggs and oocytes for the study of messenger RNA and its translation in living cells. Nature 233(5316):177–182
50. Kola I, Sumarsono SH (1995) Microinjection of in vitro transcribed RNA and antisense oligonucleotides in mouse oocytes and early embryos to study the gain- and loss-of-function of genes. Methods Mol Biol 37:135–149. doi:10.1385/0-89603-288-4:135
51. Gordon JW, Scangos GA, Plotkin DJ, Barbosa JA, Ruddle FH (1980) Genetic transformation of mouse embryos by microinjection of purified DNA. Proc Natl Acad Sci U S A 77(12):7380–7384
52. Graessmann M, Graessmann A (1983) Microinjection of tissue culture cells. Methods Enzymol 101:482–492
53. Rosen JN, Sweeney MF, Mably JD (2009) Microinjection of zebrafish embryos to analyze gene function. J Vis Exp 25:1115. doi:10.3791/1115
54. Agrawal V, Johnson SA, Reing J, Zhang L, Tottey S, Wang G, Hirschi KK, Braunhut S, Gudas LJ, Badylak SF (2010) Epimorphic regeneration approach to tissue replacement in adult mammals. Proc Natl Acad Sci U S A 107(8):3351–3355. doi:10.1073/pnas.0905851106, Epub 0905852009 Dec 0905851104
55. Poss KD, Keating MT, Nechiporuk A (2003) Tales of regeneration in zebrafish. Dev Dyn 226(2):202–210
56. Kawakami A, Fukazawa T, Takeda H (2004) Early fin primordia of zebrafish larvae regenerate by a similar growth control mechanism with adult regeneration. Dev Dyn 231(4):693–699
57. Bradford Y, Conlin T, Dunn N, Fashena D, Frazer K, Howe DG, Knight J, Mani P, Martin R, Moxon SA, Paddock H, Pich C, Ramachandran S, Ruef BJ, Ruzicka L, Bauer Schaper H, Schaper K, Shao X, Singer A, Sprague J, Sprunger B, Van Slyke C, Westerfield M (2011) ZFIN: enhancements and updates to the Zebrafish Model Organism Database. Nucleic Acids Res 39(Database issue):D822–D829. doi:10.1093/nar/gkq1077
58. Westerfield M (2000) The zebrafish book. A guide for the laboratory use of zebrafish (Danio rerio), 4th edn. University of Oregon Press, Eugene

Chapter 20

Live Staining of *Drosophila* Embryos with RPTP Fusion Proteins to Detect and Characterize Expression of Cell-Surface RPTP Ligands

Namrata Bali, Hyung-Kook (Peter) Lee, and Kai Zinn

Abstract

The activity and/or localization of receptor tyrosine kinases and phosphatases are controlled by binding to cell-surface or secreted ligands. Identification of ligands for receptor tyrosine phosphatases (RPTPs) is essential for understanding their in vivo functions during development and disease. Here we describe a novel in vivo method to identify ligands and binding partners for RPTPs by staining live-dissected *Drosophila* embryos. Live dissected embryos are incubated with RPTP fusion proteins to detect ligand binding in embryos. This method can be streamlined to perform large-scale screens for ligands as well as to search for embryonic phenotypes.

Key words Receptor tyrosine phosphatases, Live dissection, Fusion proteins, Ligand screening, Schneider cells

1 Introduction

Receptor tyrosine phosphatases (RPTPs) are transmembrane receptor proteins that reverse reactions catalyzed by tyrosine kinases. Phosphotyrosine signaling is essential for cell-cell communication in all metazoans [1]. We know a great deal about interactions of ligands with receptor tyrosine kinases, but relatively little about ligands for RPTPs. For example, of the six *Drosophila* RPTPs (*Ptp10D*, *Ptp69D*, *Ptp99A*, *Ptp4E*, *PTP52F*, and *Lar*) ligands and/or co-receptors have only been described for Ptp10D and Lar [2–4].

The first reported screen for *Drosophila* RPTP ligands was conducted by our group in 2002–2005 using live embryo staining with RPTP fusion proteins. This was a screen of a genome-wide collection of deletion mutations, called deficiencies (*Dfs*). It identified a deletion that eliminated a portion of the staining pattern observed with Lar fusion proteins, and we found that the responsible gene within the deletion was *Syndecan* (*Sdc*), which encodes

Rafael Pulido (ed.), *Protein Tyrosine Phosphatases: Methods and Protocols*, Methods in Molecular Biology, vol. 1447,
DOI 10.1007/978-1-4939-3746-2_20,

a heparan sulfate proteoglycan [2]. This screen did not identify ligands for other RPTPs. Data from the ectopic expression screen described below suggested that this is because each RPTP binds to multiple ligands that are expressed in overlapping patterns.

More recently, we conducted an ectopic expression screen for RPTP ligands using live embryo staining and identified an in vivo ligand for Ptp10D, Stranded at second (Sas). This screen also identified several other candidate Ptp10D ligands [4], in addition to candidate ligands for Lar, Ptp69D, and Ptp99A (unpublished results). In the ectopic expression screen, 311 fly lines with "UAS"-containing insertion elements ("EP-like elements") upstream of genes encoding cell surface and secreted (CSS) proteins were screened by driving ectopic expression of each individual CSS protein using a pancellular (Tubulin-GAL4) driver. The available EP insertions covered 30–40 % of all CSS proteins, and the screen identified more than 20 candidate RPTP ligands, implying that there might be 50–60 proteins encoded in the genome that can bind to these four RPTPs in this assay. Our data also suggest that new ligands for vertebrate RPTPs can be identified by characterizing ligands that bind to their *Drosophila* orthologs (unpublished results).

For all of these screens, the extracellular domain (XCD) of an RPTP (or other cell surface protein) was fused to multimeric human placental alkaline phosphatase (AP) constructs to create RPTP-AP fusion proteins. These were expressed using baculovirus or *Drosophila* Schneider 2 cell (S2) systems, and the supernatant from infected or transfected cells was used directly for binding to live-dissected embryos. Dissected, unfixed embryos must be used because the fusion proteins cannot penetrate the vitelline membrane, and fixation destroys binding. Results from such screens can be confirmed by performing "reverse-binding" experiments. In these experiments, the RPTP is ectopically expressed in embryos using the GAL4 system and the embryos are incubated with candidate CSS ligand-AP fusion proteins to detect ectopic binding [4]. If specific binding patterns are observed in both the forward and reverse directions, this proves that the CSS protein can bind to the RPTP. However, it does not show that it can bind without additional cofactors that might be expressed in the embryo. For Sdc and Sas, we were able to show that they could bind to Lar and Ptp10D, respectively, in the absence of additional cofactors by performing in vitro binding studies [2, 4].

Here, we describe in detail live embryo dissections in *Drosophila* as a technique to detect ligands for RPTPs and other orphan receptors. Briefly, stage 16 *Drosophila* embryos are collected and dechorionated, followed by dissection with a glass needle on a slide (*see* Fig. 1 for staging criteria). Dissected embryos are then incubated with dimeric or pentameric RPTP-AP fusion proteins (or other CSS-AP fusion proteins), followed by fixation and anti-AP antibody staining to visualize bound AP fusion proteins. If a strong staining pattern such as those shown in Fig. 2 and in refs. 2, 4, 5 is

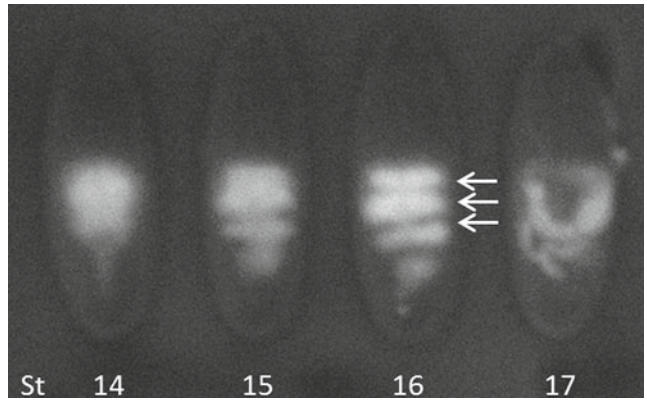

Fig. 1 Gut morphology in different stages of *Drosophila* embryos. The gut appears like a blob at early stage 13–14. A fissure appears in the gut and it starts to separate into bands at early stage 15. By stage 16, the gut has clearly divided into three distinct bands (*arrows*). This is the ideal stage for dissection. As the embryos age to stage 17–18, the gut forms spirals and the embryos can no longer be properly dissected

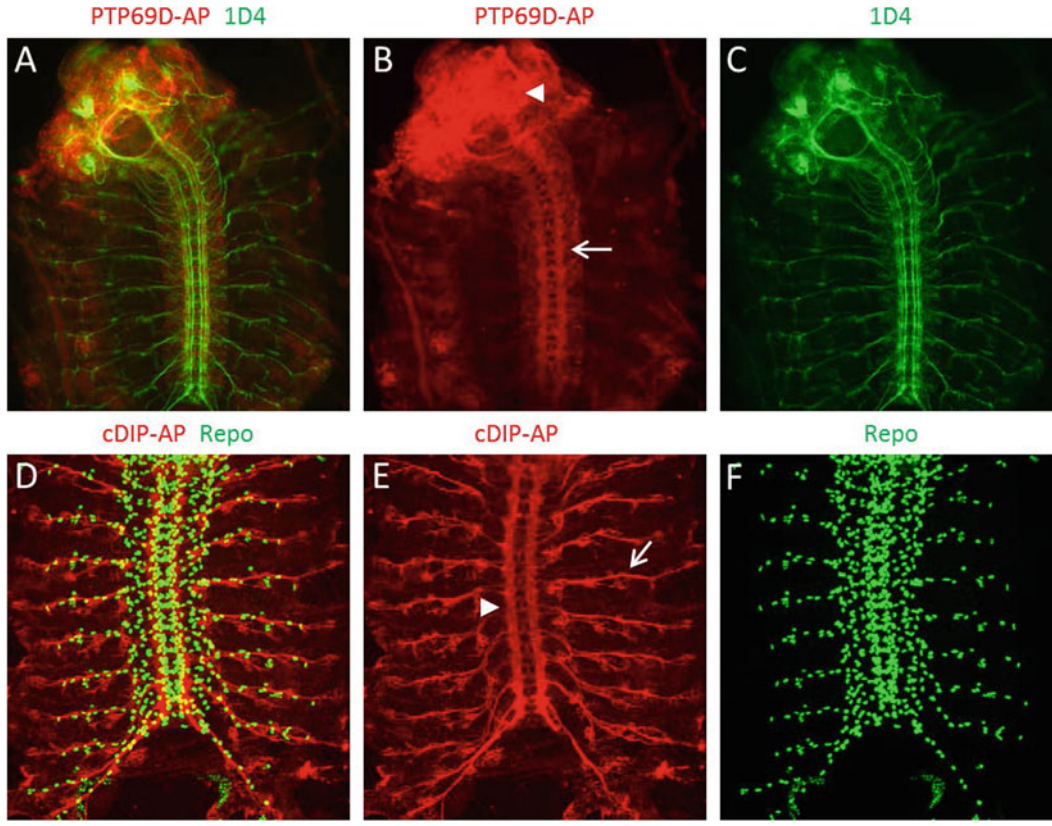

Fig. 2 Dissected and stained *Drosophila* stage 16 embryos. (**a**) A live dissected stage 16 embryo incubated with PTP69D-AP fusion protein and stained with anti-AP (*red*, **b**) and mAb 1D4 (*green*, **c**) antibodies. PTP69D-AP fusion protein binds specifically to longitudinal and commissural axon tracts in the ventral nerve cord (*arrow* in **b**) and also shows strong binding in the brain (*arrowhead* in **b**). (**d**) A live dissected stage 16 embryo incubated with cDIP-AP fusion protein and stained with anti-AP (*red*, **e**) and anti-Repo (*green*, **f**). cDIP is a cell surface protein and shows binding to CNS axons (*arrowhead* in **e**) and motor axons (*arrow* in **e**)

observed, this can be used as the basis for a *Df*, ectopic expression, or candidate gene screen to molecularly identify the responsible ligand(s). In the protocol below, we describe methods for expressing pentamerized AP fusion proteins in S2 cells, which is the easiest method. If adequate expression levels cannot be obtained in this system, it may be necessary to express the fusion proteins using baculovirus systems. The protocol for live embryo dissection and staining can be streamlined for many other applications including screening for embryonic phenotypes [5]. This live dissection technique is much faster than fixed embryo dissections for the purpose of screening for phenotypes as fixed embryo dissections take much longer than live dissections. Moreover, AP fusion protein staining can also be performed on third instar larvae to study ligand binding patterns of CSS proteins at later developmental stages (*see* **Note 1**).

2 Materials

1. Egg collection chambers: Arrange five 50 ml conical tubes upside down on a 100 × 15 mm plastic petri dish and glue them together using silicon rubber adhesive sealant. Then, glue the lid of the petri dish to the conical ends of the tubes to create a 'Five-barrel' chamber. Make holes in each tube using a hot needle for air circulation (*see* **Note 2**).
2. Egg collection plates: Make 1% grape agar gel by first mixing 50 g Bacto-Agar in 1.5 L distilled water. Secondly, add 177 ml frozen grape juice concentrate (*see* **Note 3**) and 25 g sucrose to 500 ml water. Autoclave both solutions separately for 45 min. Remove both solutions from autoclave and cool to approximately 60 °C. Mix the Bacto-Agar solution with the grape juice solution. Add 30 ml 10% Nipagin (*p*-hydroxybenzoic acid methyl ester) and 0.4 g Streptomycin sulfate to the mixed solution. Pour 10–11 ml of grape agar gel in each 100 × 15 ml plastic petri dish and let solidify (*see* **Note 4**). Store upside down sealed at 4 °C.
3. AP fusion proteins: Clone the extracellular domains (XCD) of desired proteins into an expression vector containing a pentamerization sequence and a human placental alkaline phosphatase (AP) tag [6]. Plasmid containing the XCD domain fused to AP tag can be transfected into Schneider cells (S2 cells). We use the Effectene transfection reagent to routinely transfect DNA into S2 cells with good yields of fusion protein in the supernatant. Collect the supernatant from transfected cells 2–3 days after transfection and concentrate the 1× fusion proteins up to 5× using Amicon Ultra-15 Centrifugal Filter Units. Store the fusion proteins at −80 °C for long term storage and at 4 °C for immediate use.

4. Dry yeast.
5. Superfrost Plus Micro slides.
6. Double-sided scotch tape.
7. Hydrophobic barrier pen.
8. Pulled glass needle for dissection: Pre-pulled glass microcapillary needles are available commercially. Alternately, glass capillary tubes can be bought and pulled individually. The glass capillary tubes have a 1 mm outer diameter and 0.6 mm internal diameter.
9. Phosphate buffered saline (PBS, 10×): Add 80 g NaCl, 25.6 g $Na_2HPO_4{\cdot}7H_2O$, 2 g KCl, and 2 g KH_2PO_4 to 800 ml water. Bring final volume up to 1 L with water and adjust pH to 7.4. Autoclave for 45 min. Store at room temperature.
10. PBT: PBS containing 0.05% Triton X-100 and 1% bovine serum albumin (BSA) (*see* **Note 5**).
11. 20% paraformaldehyde.
12. Fix solution: 4% paraformaldehyde in 1× PBS (*see* **Note 6**).
13. Normal goat serum.
14. Blocking buffer: PBT containing 5% normal goat serum (*see* **Note 7**). Store at 4 °C.
15. Rabbit anti-human placental alkaline phosphatase antibody.
16. Goat anti-Rabbit IgG (H + L) Secondary Antibody, Alexa Fluor 568.
17. Antifade mounting medium.
18. Rectangular glass coverslips: #1 thickness, 22 mm × 40 mm.
19. Clear nail polish.

3 Methods

All procedures are carried out at room temperature unless specified otherwise. Ref. [7] contains a video demonstration of the live embryo dissection process and staining of embryos.

3.1 Preparation of Flies and Embryo Collection

1. Set up a cross using >50 virgins and >20 males and transfer the flies to one chamber of the five-barrel chamber. Label each barrel carefully with the correct genotype of the cross. Egg collection plates are used as the lid of the five-barrel chamber. Put a small amount of yeast paste at five spots on an egg collection plate in the center of each chamber. Cover the five-barrel chamber with the egg collection plate and gently press down. Tape the chamber and grape plate together using lab labeling tape. Flies in the five-barrel chamber should be incubated at 18 °C to prolong lifespan (*see* **Note 8**).

2. Use a fresh egg collection plate for each embryo collection. Put a very small amount of yeast paste on an egg collection plate in the center of each chamber. While holding the old plate on top of chamber carefully, gently tap the whole chamber down to tap down the flies. Tap flies down a few times and replace the old plate with the new egg collection plate.
3. Incubate the flies at room temperature for 2–4 h to allow sufficient embryos to accumulate on the plate. Replace the egg collection plate with a new one and return flies to 18 °C. Place a Whatman filter paper inside the lid of the grape plate and add enough water to completely soak it. Cover the egg collection plate with the lid and incubate at 18 °C overnight.
4. Change the grape plate of the chamber every day even if not collecting embryos (*see* **Note 9**).

3.2 Aging Embryos, Sorting, and Staging

1. Embryos are best suited for live dissections at stage 16 (Fig. 1) as the CNS can be fully visualized at that stage. It becomes harder to dissect stage 17 embryos as their outer chorion becomes tougher and we have found that stage 17 embryos do not stick well to the glass slide. Incubate embryos at 18 °C for ~22 h after collection to get stage 15 embryos. For studies using the UAS/GAL4 system, incubate embryos at 18 °C for ~20 h. Transfer embryos to a 29 °C incubator for 1–2 h to activate the UAS/GAL4 system.
2. GFP balancers are used to differentiate between different genotypes in a line or a cross. We use CyO arm-GFP as the second chromosome balancer, TM3 arm-GFP as third chromosome balancer and FM7 Kr-GAL4, UAS-GFP as the X chromosome balancer. GFP negative embryos are used to select homozygotes. GFP sorting is done under a GFP dissecting microscope where embryos are sorted and dechorionated at the same time.
3. Embryos are sorted using gut morphology around stages 14–16. The gut has autofluorescence under the GFP microscope and is visible as white and opaque under normal white light if using a regular dissecting microscope. At stage 16 the gut appears as three distinct bands. At earlier stages the gut looks like a single blob. This is closer to stage 14. As aging progresses from stage 14 to 16, the gut can be seen separating into bands. At stage 15 the gut has started to divide into bands, but the bands are not completely separate from each other. It is best to sort embryos and dechorionate them between stages 14 and 15, so that as soon as they reach the three band gut stage (stage 16) they are ready for dissections (Fig. 1) (*see* **Note 10**).

3.3 Embryo Dechorionation and Preparation for Dissection

1. Stick a long piece of double-sided sticky tape on a regular glass slide and place small pieces of grape plate agar slabs beside the sticky tape. Dechorionated embryos are placed on the agar slab for aging.

2. Transfer the collected embryos from the egg collection plate to the sticky tape on the slide using a fine paint brush. Wet the brush a little and spread the embryos evenly across the sticky tape. Break up any large embryo clusters gently using the brush.
3. Dechorionate the embryos on the double sided tape by gently rolling them on the tape using a blunted dissecting needle (*see* **Note 11**). Pick up the dechorionated embryos with the needle and place them gently on the agar slab beside the tape.
4. Dechorionate ~100 embryos so that there will be enough embryos of the right age at the time of dissection. Sort the dechorionated embryos according to age and place stage 16 embryos on a new agar slab. Place the embryos dorsal side down against the agar slab with their posterior ends facing toward you. Arrange the embryos in a row of five to ten embryos per genotype (*see* **Note 12**).
5. Prepare a super-frost plus slide for live dissection as follows. Cut a small piece of double-sided sticky tape (the size of the tape should be sufficient to accommodate the rows of embryos). Place the piece of sticky tape near one end of the super-frost plus slide.
6. Draw a rectangle around the sticky tape using a wax pen. We have found the ImmEdge hydrophobic barrier pen to be best suited for detergent-based washes during the immunohistochemistry steps. The rectangle should be big enough to allow dissection of all embryos on the agar slab. Sometimes a slightly larger rectangle can be drawn to allow more space option for embryos that do not stick very well.
7. Transfer the aligned embryos from the agar slab to the piece of sticky tape on the super-frost plus slide by gently lowering the tape on the slide over the embryos on the agar slab. The embryos now will be dorsal side up on the slide.
8. Add cold 1× PBS on top of the embryos. The wax rectangle will help to retain the PBS within the boundaries of the wax seal.

3.4 Embryo Live Dissection: See Ref. [7] for a Video Demonstration of the Live Embryo Dissection Process

1. A pulled glass dissection needle is used for the actual dissections. Make a superficial cut in the embryo along the dorsal midline starting from the posterior end of the embryo going all the way to the anterior end. This will rip open the interior vitelline membrane.
2. Poke the anterior end of the embryo with the needle and gently lift it up, keeping the embryo submerged in the PBS at all times. Transfer the embryo to one corner of the slide surface. A stage 16 embryo should stick to the slide surface easily. Using this same technique transfer all embryos from the tape to the slide surface in the same order as on the tape. Take extra caution to keep embryos arranged properly in neat rows to avoid confusion about the genotype of the embryos later on.

3. Once all embryos have been transferred to the slide surface, start dissecting the embryos one by one using the same glass needle. The cut made in the embryo in **step 1** should also cut open the embryo to separate the two sides of the body wall. However, this is not always the case. In this scenario, make another shallow cut along the dorsal midline starting at the posterior end. The two ends of the body wall should now be separate.
4. Gently paste the body wall flaps onto the slide on both sides. Make sure to not stretch the body wall or remove material from the surface. The best way to ensure least damage to the embryo is by only touching the anterior and posterior ends of the body walls and only at the dorsal-most edges since motor axons do not extend this far dorsally.
5. Fillet all embryos in this manner while leaving the gut intact on top of the ventral nerve cord. Once all embryos have been "filleted", begin to remove the gut from all embryos one by one (*see* **Note 13**). Make a cut where the hindgut is attached to the body wall. The gut can now be removed from the embryo in one of two ways. The gut can either be completely removed from the embryo by cutting the foregut which lies under the brain lobes, which would result in a free-floating gut which can be transferred back to the sticky tape to get it out of the way of other embryos. Alternately the gut can be simply displaced beside the embryo by pulling it away from the embryo toward the anterior end and sticking it on the slide. The foregut will stay attached to the embryo but this will not interfere with the staining of the embryos.

3.5 Fixation and Immunohistochemistry

1. After dissection, embryos are incubated with AP fusion proteins for 2 h. This is done before fixation. We typically use AP fusion proteins at 5× concentration if made using transfected Schneider (S2) cells. However the ideal concentration for optimal signal to noise ratio of the fusion protein binding signal should be titrated and optimized for individual AP fusion proteins. Weakly expressed fusion proteins will need to be used at a higher concentration (~5×) compared to strongly expressed ones.
2. Remove the sticky tape from the slide using a blunt-ended forceps and discard. Remove as much PBS as possible using a P200 pipette tip (*see* **Note 14**). Add 150–200 μl AP fusion protein, depending upon the size of the rectangle containing the dissected embryos.
3. Incubate at room temperature in a covered and humidified chamber for 2 h.
4. Prepare fresh fix solution (4% PFA in PBS) and replace the AP fusion protein with the fix. Wash using the fix five times, using

1 ml fix per wash to a total of 5 ml fix per slide. Use a pipette tip fitted at the end of a vacuum to remove solutions from the slide. A waste receptacle is attached to the end of the vacuum to collect solutions as they are removed from the slide. Fix embryos for 30 min. Again, take care to not expose the embryos to the meniscus of solutions. Keep embryos submerged in solution at all times.

5. Remove fix solution and replace with PBS. Wash three times with PBS, using 1 ml PBS per wash. Let the embryos sit in PBS for 5 min.
6. Replace PBS with PBT. Wash three times, using 1 ml per wash. Let embryos sit in PBT 5 min.
7. Once the embryos have come into contact with detergent in the PBT, embryos become less sensitive to the meniscus and solutions containing detergent (PBT, Block and antibody solutions) can be removed from the slide by blotting off with a Kimwipes. Place a folded Kimwipes at the edge of the wax seal and gently tip the slide over the Kimwipes. This will remove most of the solution from the slide and minimize carryover of solutions from a previous step.
8. Replace PBT with Block, by removing the PBT as described in **step 7**. Use ~200 μl Block per slide. Incubate in Block at least 30 min, up to 1 h. Additional blocking over an h does not seem to enhance signal to noise ratio.
9. Replace Block with desired primary antibody in Block solution. Remove Block using Kimwipes method (*see* **step 7**) and add ~200 μl primary antibody solution. Incubate in primary antibody overnight at 4 °C.
10. Next day, wash three times with PBT. Each wash should include four changes of PBT, 1 ml per change for a total of 4 ml per wash.
11. Replace last wash solution with secondary antibody in Block. Add ~200 μl secondary antibody solution and incubate at room temperature for 2 h.
12. Wash three times with PBT, similar to **step 10**.
13. Replace the last PBT wash with PBS. Wash with PBS two times, each wash with four changes of PBS, 1 ml per change. Incubate in the last PBS wash for 10 min.
14. Remove as much PBS as possible using a P200 pipette tip. Add ~40 μl Vectashield mounting medium for fluorescence around all embryos. Gently place a #1 glass coverslip over the embryos making sure there are no bubbles over the embryos. The Vectashield should diffuse evenly and cover the entire area of the coverslip. Place one drop of clear nail polish at each end of the coverslip and let dry in the dark for ~10 min (*see* **Note 15**).

15. Once the nail polish drops have dried, swipe with the clear nail polish around all edges of the coverslip, sealing the coverslip in place.
16. Store sealed slides horizontally at 4 °C.

4 Notes

1. In order to study ligand binding patterns in third instar larvae, dissect and fillet the larvae as described in [8]. Following the dissections, incubate the dissected larvae in AP fusion proteins. The concentration of the AP fusion proteins used will need to be optimized for each individual protein. Incubate larvae in AP fusion proteins for 2 h, followed by fixation and routine immunohistochemistry procedures.
2. Each chamber of the five-barrel chamber can hold up to 300 flies without overcrowding. However, if more flies are needed for an experiment, a larger plastic container can be used in place of the five-barrel chamber. Individual embryo collection cages are available commercially in three different sizes from flystuff.com (Catalog No: 59-100—59-106, Flystuff.com, San Diego, CA, USA). Small petri dishes of comparable size are also available from the same supplier, which can be filled with the grape juice solution to make appropriate sized egg collection plates.
3. Frozen grape juice can be bought at any grocery store and stored at −20 °C until used. We prefer to buy the juice in cardboard cans vs. tin cans as the juice is thawed in the can itself. Place the frozen cardboard container in a microwave and heat at 30 s to 1 min intervals until fully thawed. Measure out the thawed juice using a measuring cylinder.
4. Since the grape juice solution is a 1% agar solution, it will start to solidify as it cools in the flask. To minimize this, keep the solution submerged in a 55–60 °C water bath while you pipette out the solution into petri dishes. It may be useful to use an automatic solution dispenser to help make this process faster.
5. First add Triton X-100 to 1× PBS and mix thoroughly until fully dissolved. Then add BSA and mix thoroughly. This solution should be filtered using a bottle-top vacuum filter of pore size 0.45 μm. Once filtered, store PBT at 4 °C. Do not leave PBT at room temperature for extended periods of time. Filtered PBT can be used for up to 6 months if stored properly at 4 °C.
6. Fix solution should be made fresh just prior to use.
7. Thaw and aliquot the 10 ml normal goat serum received from the company into 0.5 ml aliquots in 15 ml conical tubes.

Freeze the conical tube aliquots at −20 °C until used. To make Blocking solution, thaw an aliquot of serum and add 9.5 ml PBT. Gently mix and store at 4 °C.

8. Keep the chamber containing flies with the egg collection plate end elevated at ~30–45° angle. We use a piece of Styrofoam to make a "pillow" to keep the grape plate end of the chamber elevated. This helps in the embryos being deposited mostly on the plate and not on the interior walls of the chamber.
9. Changing the grape plate every day is essential as the grape solution provides moisture to the flies and the agar tends to dry out after 1 day. If the plate is not changed daily, large numbers of embryos begin developing on the agar resulting in crawling larvae in the chamber. Moreover, the grape agar tends to fall down into the chamber if it dries out.
10. Place the slide containing dechorionated embryos on the agar slab in a humidified chamber such as a petri dish with a soaked Whatman filter paper to prevent the embryos from getting dried out.
11. After dechorionation, the embryos will stick more strongly to the needle than to other embryos or to the removed chorion. But they will still stick strongly to the sticky tape. To pick up the embryos effectively with the needle, roll the embryos either on top of each other or on top of their removed chorions. Embryos lying on the sticky tape may be difficult to pick up.
12. Do not put more than ~50 embryos on one slide for dissection, as the yolk released from the gut during dissections makes it difficult for later embryos to stick to the slide.
13. The gut can be removed right after dissecting each embryo as well. However, in this case it might be difficult for later-dissected embryos to stick well to the glass slide as the yolk released from the gut during gut-removal makes the PBS fatty. This can become a problem if the embryos have already been transferred to the slide surface, as the body walls of the embryos will not stick to the slide.
14. Take extra care to not remove too much PBS from the slide, as removing too much will expose the dissected embryos to the PBS meniscus. If this happens, the dissections are ruined as the embryos "explode" towards the meniscus. Some become detached from the slide surface and some lose the ventral nerve cord.
15. Once the coverslip has been placed over the embryos, make sure to not move the coverslip even a little bit. Any movement of the coverslip over the embryos will move the ventral nerve cord from its normal position and will ruin the dissections.

References

1. Lim WA, Pawson T (2010) Phosphotyrosine signaling: evolving a new cellular communication system. Cell 142(5):661–667. doi:10.1016/j.cell.2010.08.023
2. Fox AN, Zinn K (2005) The heparan sulfate proteoglycan syndecan is an in vivo ligand for the Drosophila LAR receptor tyrosine phosphatase. Curr Biol 15(19):1701–1711. doi:10.1016/j.cub.2005.08.035
3. Johnson KG, Tenney AP, Ghose A, Duckworth AM, Higashi ME, Parfitt K, Marcu O, Heslip TR, Marsh JL, Schwarz TL, Flanagan JG, Van Vactor D (2006) The HSPGs Syndecan and Dallylike bind the receptor phosphatase LAR and exert distinct effects on synaptic development. Neuron 49(4):517–531. doi:10.1016/j.neuron.2006.01.026
4. Lee HK, Cording A, Vielmetter J, Zinn K (2013) Interactions between a receptor tyrosine phosphatase and a cell surface ligand regulate axon guidance and glial-neuronal communication. Neuron 78(5):813–826. doi:10.1016/j.neuron.2013.04.001
5. Wright AP, Fox AN, Johnson KG, Zinn K (2010) Systematic screening of Drosophila deficiency mutations for embryonic phenotypes and orphan receptor ligands. PLoS One 5(8):e12288. doi:10.1371/journal.pone.0012288
6. Ozkan E, Carrillo RA, Eastman CL, Weiszmann R, Waghray D, Johnson KG, Zinn K, Celniker SE, Garcia KC (2013) An extracellular interactome of immunoglobulin and LRR proteins reveals receptor-ligand networks. Cell 154(1):228–239. doi:10.1016/j.cell.2013.06.006
7. Lee HK, Wright AP, Zinn K (2009) Live dissection of Drosophila embryos: streamlined methods for screening mutant collections by antibody staining. J Vis Exp (34). doi:10.3791/1647
8. Brent JR, Werner KM, McCabe BD (2009) Drosophila larval NMJ dissection. J Vis Exp (24). doi:10.3791/1107

Chapter 21

Methods to Study Protein Tyrosine Phosphatases Acting on Yeast MAPKs

Almudena Sacristán-Reviriego, María Molina, and Humberto Martín

Abstract

Mitogen activated protein kinases (MAPK) pathways play a key role in orchestrating the eukaryotic cellular response to different stimuli. In this process, phosphorylation of both conserved threonine and tyrosine residues of MAPKs is essential for their activation. Identification of tyrosine and dual specificity protein phosphatases capable of dephosphorylating these phosphosites is thus critical to gain insight into their regulation. Due to the conservation of pivotal elements in eukaryotic signaling, yeast has turned into a valuable tool to increase the knowledge of MAPK signaling in other cell types. Here we describe an in vivo method to evaluate the capacity of a protein, from yeast or other origin, to act as a MAPK phosphatase. It relies on the ability of the phosphatase to reduce, when overexpressed, both the amount of activated MAPK and the transcription from a specific promoter regulated by the corresponding pathway. To this end, the pathway has to be previously activated, preferentially through overexpression of a hyperactive allele of an upstream component within the MAPK module. Additionally, the ability of an overexpressed "trapping" inactive phosphatase version to modify these readouts is also analyzed. Western blotting analysis with specific anti-phospho MAPK antibodies and flow cytometry-based determination of fluorescence produced by GFP whose expression is driven by MAPK-regulated promoters are the selected techniques for monitoring these readouts.

Key words Protein tyrosine phosphatase, Dual specificity phosphatase, PTP, DSP, MAPK, MAPK phosphatase, Anti-phospho MAPK antibody, Yeast, GFP, Flow cytometry

1 Introduction

1.1 Yeast MAPK Signaling and Their Regulation by Tyrosine Phosphatases

Reversible protein phosphorylation is a central mechanism in the regulation of signal transduction pathways in eukaryotic cells and depends on the opposing actions of protein kinases and protein phosphatases. Among the latter, protein tyrosine phosphatases (PTPs) specifically eliminate phosphate groups from tyrosine residues within proteins previously phosphorylated by protein tyrosine kinases. Compared to mammalian cells, the extent of tyrosine phosphorylation in yeast is extremely low [1]. In fact, there are not true protein tyrosine kinases but dual-specificity kinases that include members of the MAPKK (MAP kinase kinase) family and cell cycle

Rafael Pulido (ed.), *Protein Tyrosine Phosphatases: Methods and Protocols*, Methods in Molecular Biology, vol. 1447,
DOI 10.1007/978-1-4939-3746-2_21,

regulators [2]. However, both classical tyrosine phosphatases (PTPs) and dual specificity phosphatases (DSPs) are present in yeast cells. PTPs and DSPs have a common mechanism for hydrolysis and share the $HC(X)_5R$ motif at their catalytic site, although the latter are able to accommodate not only phosphotyrosine but also phosphoserine or phosphothreonine within the active pocket [3].

The MAPK is the last component of a three tiered-protein kinase cascade that constitutes the highly conserved common module of MAPK signal transduction pathways. Upon stimulation, the MAPK is activated by phosphorylation on both threonine and tyrosine residues within the signature motif T-X-Y by a dual specificity MAPKK. Therefore, both PTPs and DSPs can act on MAPKs, playing a crucial role in their negative regulation [4]. Among DSPs, those that specifically act on MAPKs are known as MKPs (for MAPK phosphatases) [5]. In the yeast *Saccharomyces cerevisiae*, there are five MAPKs pathways that trigger cellular adaptation to different stimuli [6]. The most extensively studied are those involved in the regulation of the response to pheromones (Mating pathway), in the compensatory mechanism against cell wall damage (CWI pathway) and in the osmoregulation under osmotic stress conditions (HOG pathway). A scheme of these three pathways mediated, respectively, by the MAPKs Fus3, Slt2, and Hog1 is depicted in Fig. 1. Stimulation of these pathways gives rise to a

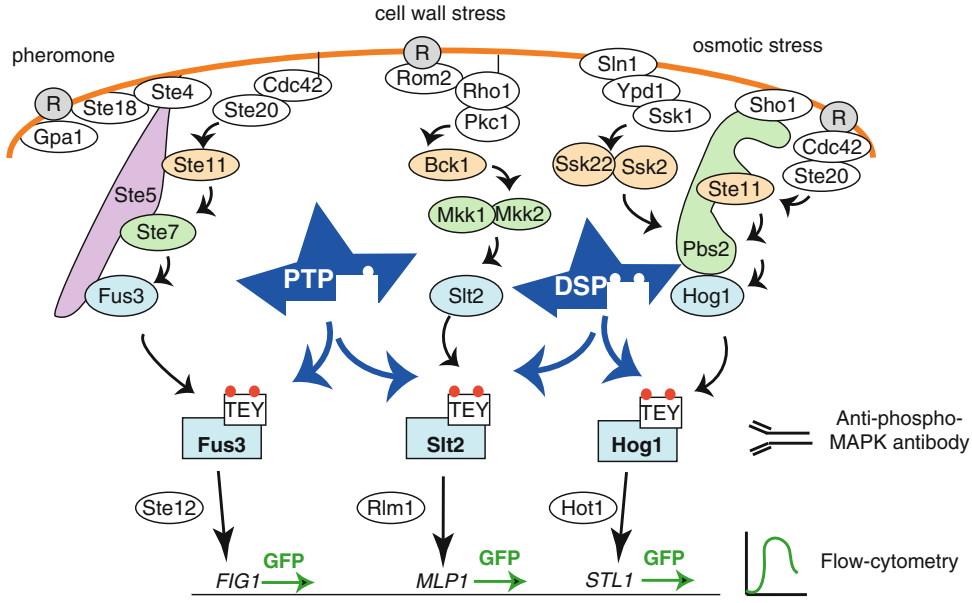

Fig. 1 Scheme depicting components and signaling flow of the mating, CWI and HOG MAPK pathways of *S. cerevisiae*. A transcriptional readout of each pathway is also indicated. Phosphorylation of MAPKs in threonine and tyrosine at the activation loop is illustrated with *small red circles*. The two proposed methods for analyzing signaling through the pathways, namely immunodetection of phosphorylated MAPK and flow cytometry measurement of fluorescence from the transcriptional reporter, are schematized

wide transcriptional response through the activation of specific transcription factors by the MAPKs [7–9]. The PTPs Ptp2 and Ptp3 have been shown to regulate these three MAPKs with different impact and physiological consequences in each pathway [3]. Very recently, our group has shown that another member of this family, Ptp1, also downregulates the mating and CWI pathways and physically interacts with both Fus3 and Slt2, suggesting that this PTP is acting at the MAPK level [10]. On the other hand, the MKP Msg5 is known to dephosphorylate Fus3 and Slt2, whereas the MKP Sdp1 seems to be selective for Slt2 [3]. No DSPs have been described to act on Hog1 to date.

The easiness of manipulation combined with the increasing number of genomic tools available for genetic, biochemical, and phenotypic analysis either at small or large scale makes yeast a valuable system to study cell signaling. Furthermore, MAPKs pathways are very well conserved in fungi and structural and/or functional homologs of the *S. cerevisiae* protein phosphatases have been identified in numerous fungal species [11]. Such conservation is also evident in *Drosophila*, *Caenorhabditis*, plant, and mammalian cells [12]. For all these reasons, research on MAPK regulation in yeast has greatly helped to increase the knowledge of MAPK signaling in other eukaryotic cell types.

1.2 A Strategy to Detect Yeast MAPK Regulation by a Specific PTP

The usual redundancy of phosphatases that regulate yeast MAPKs makes overexpression of these negative regulators a better strategy than their deletion for obtaining information of their activity on MAPKs. When the aim is to study the effect of phosphatases from other organisms in yeast, the overexpression approach is obviously nearly the only possibility. For simplicity, from this point and throughout the article we will refer to both classical PTPs and DSPs as PTPs. For analyzing the dephosphorylating activity of an overexpressed PTP, the putative target MAPK needs to be previously phosphorylated and therefore activated. To this end, yeast cells can be treated with a pathway-specific activating stimulus. An alternative way to trigger the activation of the pathway relies on the expression of a hyperactive version of a component upstream of the MAPK. In particular, the use of a hyperactive MAPKKK or MAPKK version should be the strategy of choice as it allows activation specifically at the level of the MAPK module.

On the other hand, overexpression of a PTP mutant version without catalytic activity but intact substrate affinity leads to what is known as "substrate trapping" [13, 14]. The formation of a stable complex between the inactive phosphatase and the MAPK results in accumulation of the phosphorylated form of the kinase, even in the absence of the pathway activating stimulus. However, in spite of the high amount of activated MAPK, the formation of such complexes antagonizes binding between the MAPK and its substrates, impeding downstream signaling [15]. Therefore, the use of

phosphatase-dead versions of PTPs not only serves as a tool to investigate PTP-MAPK interactions but to uncover the activity of a PTP on a specific MAPK.

Here we describe a yeast-based approach to investigate whether a PTP is acting as a negative regulator of a MAPK pathway by specifically targeting the MAPK. We make use of specific readouts of yeast MAPK pathways, namely MAPK phosphorylation and induction of reporter gene expression, to analyze the impact on MAPK signaling of the overexpression of both wild type and "substrate-trapping" phosphatase-dead versions of the protein phosphatase under study. The mating and CWI MAPKs Fus3 and Slt2, like mammalian Erk1/2 and Erk5, bear a T-E-Y sequence at the phosphorylation loop, whereas the osmoregulatory MAPK Hog1 is homolog to mammalian p38 and possesses a T-G-Y activation motif. Therefore, the commercial antibodies that specifically recognize the dual phosphorylated forms of either Erk-type or p-38 mammalian MAPKs are also routinely used to detect Fus3 and Slt2 or Hog1 activation, respectively. We propose the use of the *FIG1*, *MLP1*, and *STL1* promoters fused to GFP for monitoring the transcriptional induction mediated by the mating, CWI and HOG1 pathways, respectively (Fig. 1). Whereas a reduction in both MAPK phosphorylation and reporter gene expression is expected upon overexpression of a wild type phosphatase acting on the corresponding MAPK, an increase in MAPK phosphorylation but a decrease in reporter gene expression should be observed when the inactive phosphatase version is overexpressed.

The method detailed here proved useful to identify novel yeast regulators of the mating and CWI pathways [10]. Due to the conservation of PTPs along the evolutionary scale, we believe that this strategy could also be successfully used with members of this phosphatase family from any eukaryotic cell origin.

2 Materials

2.1 Yeast Plasmids and Strains

1. PTP overexpression plasmids: To overexpress the PTP under study fused to GST in *Saccharomyces cerevisiae*, we suggest the use of pEG(KG) plasmid (2μ *URA3 leu2-d GAL1-GST*) [16]. This plasmid carries the *GAL1* promoter that can be induced by galactose and repressed by glucose (*see* **Note 1**).
2. MAPK-activating plasmids: To get MAPK activation, cells can be transformed with plasmids carrying hyperactive alleles of the MAPKKK or the MAPKK of the CWI, mating or HOG pathways (Table 1). For example, the pYES3-BCK1^{CT} plasmid (*2μ TRP1 GAL1-BCK1CT*) carries a *BCK1* version lacking the N-terminal regulatory domain that, when overexpressed from the *GAL1* promoter, leads to a hyperactivation of the CWI pathway [10] (*see* Fig. 2a).

Table 1
Stimulation conditions and tools for monitoring yeast MAPK activation

Pathway/ MAPK	MAPK activation			
	External stimuli	Hyperactive allele	Phospho-MAPK detecting antibody	Transcriptionally regulated genes
CWI/Slt2	Congo red 15 mg/ml (2–4 h)	*MKK1S386P* [19] *BCK1CT* [10]	Anti-phospho-p44/p42 MAPK (Thr202/Tyr204)	*MLP1*
Mating/Fus3	Alpha factor 10 μM (30 min to 2 h)	*STE7P368* [20] *STE11-4* [21]	Anti-phospho-p44/p42 MAPK (Thr202/Tyr204)	*FIG1*
HOG/Hog1	KCl 0.4 M (5–30 min)	*PBS2S514E T518E* [22]	Anti-phospho-p38 MAPK (Thr180/Tyr182)	*STL1*

3. Reporter plasmids: Inducible promoters *FIG1*, *MLP1*, and *SLT1* (from the mating, CWI, and HOG pathways, respectively) (Table 1) are fused to GFP in plasmids pRS315-FIG1p-GFP, pRS315-MLP1p-GFP, pRS315-STL1p-GFP [10, 17] (*see* **Note 2**).
4. Yeast strains: Any strain with the appropriate genetic markers for selecting transformants with the abovementioned plasmids can be used. For example, strain YPH499 (*MATa ade2-101 trp-63 leu2-1 ura3-52 his3-Δ200 lys2-801*) [18].

2.2 Culture Media and Solutions

Media are autoclaved at 121 °C for 20 min. Agar 2% is added for obtaining solid media.

1. Yeast extract peptone dextrose (YPD): Complete medium for yeast growth composed of 1% yeast extract, 2% peptone, 2% dextrose. Add deionized water to a final volume of 1 l.
2. Synthetic dextrose (SD): Often called drop-out media because, depending on the markers used for selection, one or several nutrients are missing: 2% dextrose, 0.17% yeast nitrogen base, 0.5% ammonium sulfate, 0.19% dropout mixture (–His, –Leu, –Trp, –Ura). Add histidine, leucine, tryptophan, or uracil when necessary for selection of transformants (0.2 g/l of each amino acid). Add deionized water to a final volume of 1 l.
3. Synthetic Raffinose (SR): Same composition as SD but with 2% of raffinose as carbon source instead of dextrose.
4. Galactose stock solution: 20% galactose in deionized water.

2.3 Transformation of Yeast Cells

1. Transformation mix solution: 40% PEG 3350, 200 mM LiOAc, 0.1% (v/v) β-mercaptoethanol. Prepare fresh just prior to transformation using the following stock solutions (amount

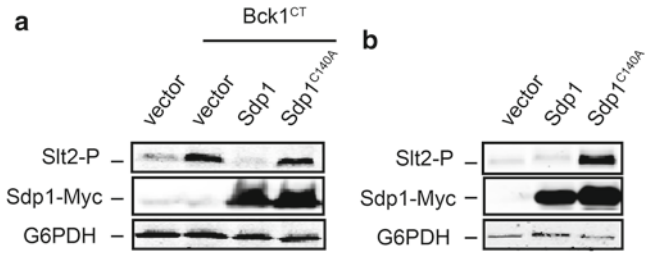

Fig. 2 Western blotting analysis of the effect of overexpressing the yeast DSP Sdp1 on the phosphorylation of the CWI MAPK Slt2. (**a**) Overexpression of wild type Sdp1 but not of inactive Sdp1^{C104A} causes a strong reduction in the high phospho-Slt2 level of CWI-activated cells. Yeast cells from the *msg5*Δ strain DD1-2D [15] transformed with pEG-KG (vector), pEG-KG-Sdp1 or pEG-KG-Sdp1^{C104A}, and pYES3 (vector) or pYES3-BCK1^{CT} plasmid, which contains a hyperactive N-terminally truncated version of the MAPKK Bck1 [10] to constitutively activate the pathway, were grown to mid-log phase in SR at 24 °C, then galactose was added to a final 2% concentration for 4 h at 24 °C, and protein extracts were prepared. Phosphorylated Slt2, Sdp1-Myc, and G6PDH (as loading control) were detected with anti-phospho-p42/44 (*upper panel*), anti-Myc (*middle panel*), and anti-G6PDH antibodies (*lower panel*), respectively. (**b**) Overexpression of the inactive "substrate trapping" version Sdp1^{C104A} leads to an increase in Slt2 phosphorylation in non CWI-activated cells. Yeast cells from strain YPH499 [18] transformed with pEG-KG (vector), pEG-KG-Sdp1 or pEG-KG-Sdp1^{C104A} were grown to mid-log phase in SR at 24 °C, then galactose was added to a final 2% concentration for 4 h at 24 °C, and protein extracts were prepared. Immunodetection was performed as in (**a**)

to prepare 1 ml): 50% PEG 3350 (800 µl); 1 M LiOAc (200 µl); β-mercaptoethanol (1 µl).

2. Salmon sperm DNA: 5% solution in water (v/v).

2.4 Preparation of Cell Extracts

1. Lysis buffer: 50 mM Tris–HCl pH 7.5, 10% glycerol, 1% Triton X-100, 0.1% SDS, 0.1% NP40, 150 mM NaCl, 5 mM EDTA, 50 mM NaF, 50 mM β-glycerophosphate, 5 mM sodium pyrophosphate, 1 mM sodium orthovanadate. Prior to use, add PMSF (1 mM) and one protease inhibitor cocktail tablet from Roche (complete, Mini, EDTA-free) per 10 ml of lysis buffer.
2. Glass beads (0.4–0.6 mm).
3. Fast prep centrifuge (MP Biomedicals, California, USA).

2.5 SDS-Polyacrylamide Gel Electrophoresis (SDS-PAGE)

1. Preparative 10% acrylamide gel for SDS-PAGE: 1.9 ml water, 1.7 ml 30% acryl-bisacrylamide mix, 1.3 ml 1.5 M Tris–HCL pH 8.8, 50 µl 10% SDS, 50 µl 10% ammonium persulphate, 2 µl TEMED.
2. Stacking 5% acrylamide gel for SDS-PAGE: 1.4 ml water, 333 µl 30% acryl-bisacrylamide mix, 250 µl 1.5 M Tris–HCl pH 6.8, 20 µl 10% SDS, 20 µl 10% ammonium persulfate, 1 µl TEMED.

3. 2× SDS-PAGE gel loading buffer: 100 mM Tris–HCl pH 6.8, 4% SDS, 20% glycerol, 0.1% bromophenol blue, 200 mM DTT. Store the SDS-PAGE gel loading buffer without DTT at room temperature. Prior to use, add DTT from a 1 M stock.
4. SDS-PAGE gel running buffer: 190 mM glycine, 25 mM Tris–HCl base, 0.1% SDS.

2.6 Western Blotting

1. Nitrocellulose membranes.
2. Molecular weight protein marker.
3. Transfer buffer: 190 mM glycine, 25 mM Tris–HCl base, 20% methanol.
4. Blocking buffer: 5% dry skimmed milk in PBS.
5. Washing buffer: 0.1% Tween 20 in PBS.
6. Primary antibodies: anti-GST antibodies (Santa Cruz Biotechnology, 1:2000) to immunodetect the tagged PTP (*see* **Note 3**). Anti-phospho-P44/42 and anti-phospho-p38 antibodies (Cell Signaling, 1:2000) to immunodetect dually phosphorylated MAPKs. Anti-G6PDH antibody (Sigma, 1:50,000) for loading control.
7. Secondary antibodies: IRDye 800CW Goat anti-rabbit (LI-COR Biosciences, USA) and IRDye 680LT Goat anti-mouse (LI-COR Biosciences, USA). Use both at 1:5000 dilution.

2.7 Data Analysis

1. Odyssey Infrared Imaging System (LI-COR Biosciences): To detect and quantify fluorescence signal from conjugated IRDye secondary antibodies. This system allows the simultaneously detection of two different antigens (e.g., phosphorylated MAPK and tagged-PTP) on the same blot using antibodies labeled with IRdyes that are visualized in different fluorescence channels (700 and 800 nm).

2.8 Flow Cytometry GFP Fluorescence Quantification

1. Cycloheximide: 10 mg/ml solution in PBS.
2. CyAn MLE Flow cytometer (Dako, Glostrup, Denmark): to acquire green fluorescence through a 488 excitation laser and a 525/30 BP emission filter (BFP) for GFP-positive cells.

3 Methods

3.1 Overexpression of PTPs in Saccharomyces cerevisiae

When considering an overexpression approach, the *GAL1* promoter is probably the most used among the strong inducible promoters in yeast. Transcription of *GAL1* gene is repressed by the presence of glucose and strongly activated by the galactose-dependent Gal4 activator. Addition of galactose to 2% in a medium containing raffinose, a carbon source that neither repress nor

induce the *GAL1* promoter, leads to a fast induction of this promoter and it is therefore a simple and very efficient way to express high levels of a specific protein, for example a PTP, in yeast cells. It is also very convenient to mark the phosphatase with a tag in order to easily check the efficient expression of the phosphatase by western blotting. The pEG-KG vector [16] provides a very versatile and widely used system for *GAL1*-based expression of GST-tagged proteins in yeast. Here we describe a detailed protocol for transformation of yeast cells with a pEG-KG-based plasmid carrying either the wild-type or the catalytically inactive allele of the *PTP* gene under study. Phosphatase-dead versions for substrate trapping can be obtained by mutating the conserved cysteine residue within the $HC(X)_5R$ catalytic motif of PTPs to alanine. Other plasmids with *GAL1*-driven expression of the *PTP* alleles could be similarly used.

A plasmid with a compatible marker carrying the transcriptional reporter should be co-transformed in order to check the transcriptional activity mediated by the MAPK. In order to get the MAPK activated, cells could be treated with a specific stress agent; alternatively, a plasmid with a compatible marker carrying either a MAPKKK or MAPKK hyperactive allele could be co-transformed. Depending on the target MAPK to analyze as a substrate for a specific phosphatase, different possibilities regarding the external stimuli or the hyperactive allele, the anti-phospho-MAPK antibody and the distinct reporters to be used are shown in Table 1.

3.1.1 Transformation of Yeast Cells

1. Inoculate yeast cells previously grown in YPD plates into 5 ml YPD liquid medium and incubate overnight (O/N) at 30 °C, 200 rpm.
2. Dilute the overnight culture into fresh medium to make 100 ml of culture (per ten transformations) with $OD_{600} = 0.2$ and incubate the flask for 3 h (30 °C, 200 rpm).
3. Collect yeast cells from the culture by centrifugation (1006–2795 × *g*) for 3 min at room temperature and remove carefully the supernatant with a micropipette.
4. Resuspend cells in 1 ml of freshly prepared transformation mix solution and vortex gently.
5. Make aliquots of 100 μl.
6. Add 1 μl of each plasmid solution (around 0.2 μg of DNA) and then vortex again (*see* **Note 4**).
7. Optional: 5 μl of denatured salmon sperm DNA (10 mg/ml) can be added per 100 μl of transformation mix in order to increase transformation efficiency.
8. Incubate for 10 min at room temperature (RT).
9. Heat shock at 45 °C, 30–45 min.

10. Plate the cell suspension onto appropriate selective medium depending on the carried plasmids (SD plate lacking uracil, leucine or tryptophan). If cells have settled, mix by pipetting up and down before plating.
11. Place the plates at 30 °C. Colonies should be visible in 3 days.

3.1.2 Yeast Cells Growth, Expression of PTPs, Pathway Activation, and Cell Collection

1. Inoculate a single colony of the yeast transformant from a plate of selective medium used for plasmid maintenance in 5 ml of SR selective liquid medium. Incubate at 30 °C overnight with shaking.
2. Dilute the overnight culture into SR fresh medium lacking uracil, leucine and tryptophan to $OD_{600} = 0.2$ (30 ml of culture for western-blotting analysis and 2 ml of culture for transcriptional assays). In order to induce the overexpression of PTPs, add galactose stock solution for a 2 % final concentration to the liquid SR medium and incubate for 4–6 h. Addition of galactose also leads to the activation of the MAPK pathway in cells carrying hyperactive alleles of the MAPKKKs or MAPKKs (Table 1).
3. Alternatively to the use of hyperactive alleles, to get CWI, mating or HOG pathway activation, add Congo red, α-factor or KCl respectively to the cultures following the concentrations and times indicated in Table 1.
4. Collect cells at $1006 \times g$ at 4 °C.
5. Resuspend cells with 0.8 ml of ice-cold water and transfer to an eppendorf tube.
6. Wash once with 0.8 ml of ice-cold water and collect the cells at $1006 \times g$ at 4 °C.
7. Remove water. For western blotting analysis, freeze straightaway the pellet in liquid nitrogen and store at –80 °C until you are ready to carry on with the experiment. For transcriptional assays performed by flow cytometry, resuspend the pellet in 1 ml of cycloheximide in PBS (10 mg/ml) to block protein synthesis and keep the samples at 4 °C. By doing this, cells can be analyzed afterwards, even 24 h later.

3.2 Analysis of the Effect of PTPs Overexpression on Yeast MAPK Phosphorylation

The effect of overexpressing either the wild type or the trapping mutant version of the PTP under study on MAPK phosphorylation is analyzed by western blotting. The previously collected cells are glass-beads disrupted, protein extracts separated by SDS-PAGE, and the comparative amount of activated MAPK analyzed using specific antibodies that detect the dually phosphorylated form of the MAPK. Whereas phosphorylated Slt2 and Fus3 are similarly recognized by anti-phospho p42/p44 antibodies, activated Hog1 is specifically detected by anti-phospho-p38 antibody (Table 1).

3.2.1 Preparation of Yeast Cell Extracts

1. Thaw on ice the pellets obtained as described in Subheading 3.1.2, resuspend each one in 150 μl of cold lysis buffer containing phosphatase and protease inhibitors and add an equal volume of glass beads.
2. Disrupt cells by placing tubes in a FastPrep centrifuge and set speed at highest setting (5.5). Bead-beat the cells twice for 30 s placing tubes on ice for 5 min in between.
3. Collet the debris by centrifugation (18894 × *g*) for 10 min at 4 °C.
4. Transfer the supernatants to cold 1.5 ml eppendorf tubes and place on ice.
5. Measure the protein concentration of each lysate using a spectrophotometer at 280 nm.
6. Adjust lysate concentration to 1.5 μg/μl with lysis buffer. To this end, use the general equation: Protein Concentration (μg/μl) = OD_{280} divided by cuvette width (cm).
7. Add 25 μl of 2× SDS-PAGE loading buffer per 25 μl of lysate, boil for 5 min at 99 °C, and load 10 μl of the samples on a SDS polyacrylamide gel (*see* **Note 5**).

3.2.2 SDS-PAGE and Western Blotting

1. Prepare the polyacrylamide gel.
2. Load the samples and run the gel (150 V) in running buffer for 1 h.
3. Set up transfer from the gel to a nitrocellulose membrane in transfer buffer. Run at 100 V for 1 h.
4. Block the blot by soaking in blocking buffer for 30–60 min with gentle shaking in a rocker.
5. Add primary anti-phospho-MAPK antibody at proper dilution. Incubate the membrane for 1 h with shaking. Alternatively, incubation can be done overnight at 4 °C.
6. Wash the membrane five times with washing buffer for 5 min.
7. Incubate with secondary antibodies for 45–60 min with shaking.
8. Wash the membrane five times with washing buffer for 5 min.
9. Scan protein bands using an Odyssey Infrared Imaging System (*see* **Note 6**).

Figure 2 shows the western blotting analysis of the effect of overexpressing the yeast DSP Sdp1 and its trapping inactive version on the dual phosphorylation of Slt2, the MAPK of the CWI pathway.

3.2.3 Data Analysis (Quantification/Ratios/ Statistics)

1. Quantify the fluorescent signals corresponding to the amount of phosphorylated MAPK and G6PDH protein (loading control) with the Odyssey Software.

2. Normalize the amount of phospho-MAPK in each sample to the corresponding loading control.
3. Calculate the ratio between the normalized phospho-MAPK amount of the sample from cells overexpressing the PTP and that of the control cells bearing the empty plasmid.

Perform the experiment in triplicate to calculate the average ratio, standard deviation, and *p*-value.

3.3 Analysis of the Effect of PTPs Overexpression on Yeast MAPK-Mediated Transcriptional Induction

In order to analyze the impact of the overexpression of either the wild type or the trapping mutant version of the PTP under study on the activity of the distinct MAPKs, the transcriptional induction of a reporter gene under the control of promoters specifically regulated by each MAPK pathway should be studied. Measurement of *LacZ* expression through β-galactosidase activity determination has been very used. However, here we propose the use of GFP as reporter gene since fluorescence determination with a flow cytometer is a fast and simple non-enzymatic method.

3.3.1 Flow Cytometry GFP Quantification

1. Use cell suspension in 1 ml of cycloheximide (10 mg/ml), obtained as described in Subheading 3.1.2.
2. Optimize the appropriate excitation laser (488 nm) and emission filter (525 nm) in the flow cytometer to acquire green fluorescence.
3. Fix the low threshold setting (blank) using yeast cells that do not carry any GFP-bearing plasmid and therefore do not express this fluorescent protein.
4. Obtain the GFP fluorescence of cells and calculate the mean.

An example of the effect of overexpressing the yeast PTP Ptp1 and the DSP Msg5 on the mating pathway *FIG1-GFP* reporter under pheromone stimulation (α-factor) is shown in Fig. 3.

3.3.2 Data Analysis (Ratios/Statistics)

1. Calculate the ratio of GFP fluorescence emission derived from the transcriptional reporter between cells under pathway stimulating conditions in the presence or absence of PTP and control cells under basal conditions.

Perform the experiment in triplicate using three single and independent transformants to calculate the average ratio, standard deviation and *p*-value.

4 Notes

1. Other similar plasmids with compatible markers, bearing either *GAL1* or other strong promoter, could also be used for PTP expression induction. For example, the *ADH1* promoter leads

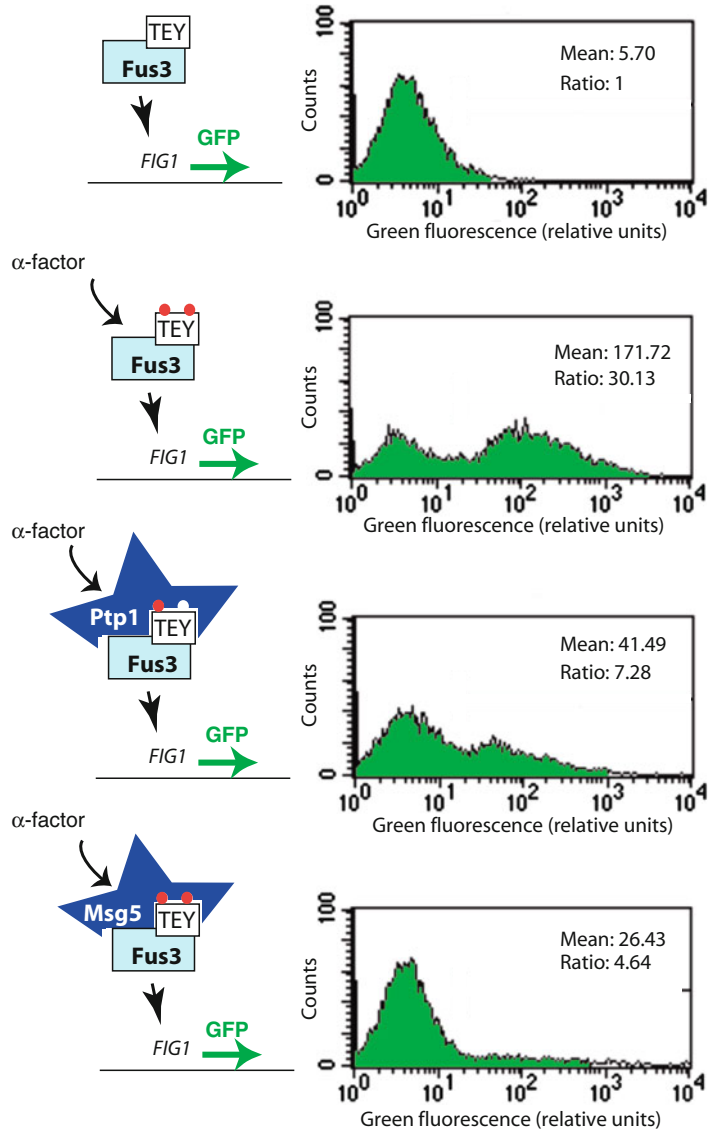

Fig. 3 Flow cytometry analysis of the effect of overexpressing yeast PTP Ptp1 and DSP Msg5 on expression of the mating *FIG1-GFP* reporter. Quantification of GFP signal in cells of strain BY4741 carrying pRS315-FIG1p-GFP and pEG-KG, pEG-KG-PTP1, or pEG-KG-MSG5 plasmids, as indicated, in the absence (*upper panel*) or presence of α-factor (10 μM for 2 h) was performed. Histograms show relative units of green fluorescence in logarithmic scale in the abscissae. For each sample, the mean relative fluorescence and the ratio relative to control cells in non-stimulating conditions are shown

to high-level constitutive expression during logarithmic growth of the yeast cells. This promoter can only be used when overexpression of the PTP is not toxic for yeast cells.

2. Plasmids in which the inducible promoters are fused to the reporter gene *lacZ* can also be used for transcriptional assays.

In this case, determination of β-galactosidase activity instead of fluorescence detection should be performed.

3. Alternative specific antibodies (anti-Myc, anti-HA, anti-His) can be used depending on the tag used for PTP tagging.
4. Include a negative control of transformation by adding 3 μl of water in one of the cell suspension aliquot in order to check that no colonies appear unless cells are transformed with DNA.
5. Samples can be stored at −80 °C prior to load them on a gel.
6. Alternatively to the fluorescent method described here, a traditional chemiluminescent method can be used to develop the blot.

Acknowledgements

We acknowledge the Centro de Citometría y Microscopía de Fluorescencia (UCM, Madrid, Spain) for flow cytometry analysis. This work was made possible thanks to grant BIO2013-44112-P from Ministerio de Economía y Competitividad, (Spain) and S2011/BMD-2414 from Comunidad Autónoma de Madrid (Spain). A.S-R is a recipient of a FPU fellowship from Ministerio de Educación y Ciencia (Spain).

References

1. Chi A, Huttenhower C, Geer LY et al (2007) Analysis of phosphorylation sites on proteins from *Saccharomyces cerevisiae* by electron transfer dissociation (ETD) mass spectrometry. Proc Natl Acad Sci U S A 104:2193–2198
2. Hunter T, Plowman GD (1997) The protein kinases of budding yeast: six score and more. Trends Biochem Sci 22:18–22
3. Martin H, Flandez M, Nombela C et al (2005) Protein phosphatases in MAPK signalling: we keep learning from yeast. Mol Microbiol 58:6–16
4. Tonks NK, Neel BG (2001) Combinatorial control of the specificity of protein tyrosine phosphatases. Curr Opin Cell Biol 13:182–195
5. Caunt CJ, Keyse SM (2013) Dual-specificity MAP kinase phosphatases (MKPs): shaping the outcome of MAP kinase signalling. FEBS J 280:489–504
6. Engelberg D, Perlman R, Levitzki A (2014) Transmembrane signaling in *Saccharomyces cerevisiae* as a model for signaling in metazoans: state of the art after 25 years. Cell Signal 26:2865–2878
7. Roberts CJ, Nelson B, Marton MJ et al (2000) Signaling and circuitry of multiple MAPK pathways revealed by a matrix of global gene expression profiles. Science 287:873–880
8. Garcia R, Bermejo C, Grau C et al (2004) The global transcriptional response to transient cell wall damage in *Saccharomyces cerevisiae* and its regulation by the cell integrity signaling pathway. J Biol Chem 279:15183–15195
9. Posas F, Chambers JR, Heyman JA et al (2000) The transcriptional response of yeast to saline stress. J Biol Chem 275:17249–17255
10. Sacristan-Reviriego A, Martin H, Molina M (2015) Identification of putative negative regulators of yeast signaling through a screening for protein phosphatases acting on cell wall integrity and mating MAPK pathways. Fungal Genet Biol 77:1–11
11. Rispail N, Soanes DM, Ant C et al (2009) Comparative genomics of MAP kinase and calcium-calcineurin signalling components in plant and human pathogenic fungi. Fungal Genet Biol 46:287–298
12. Qi M, Elion EA (2005) MAP kinase pathways. J Cell Sci 118:3569–3572
13. Tonks NK, Neel BG (1996) From form to function: signaling by protein tyrosine phosphatases. Cell 87:365–368

14. Blanchetot C, Chagnon M, Dubé N et al (2005) Substrate-trapping techniques in the identification of cellular PTP targets. Methods 35:44–53
15. Sacristan-Reviriego A, Madrid M, Cansado J et al (2014) A conserved non-canonical docking mechanism regulates the binding of dual specificity phosphatases to cell integrity mitogen-activated protein kinases (MAPKs) in budding and fission yeasts. PLoS One 9:e85390
16. Mitchell DA, Marshall TK, Deschenes RJ (1993) Vectors for the inducible overexpression of glutathione S-transferase fusion proteins in yeast. Yeast 9:715–722
17. Martin H, Shales M, Fernandez-Pinar P et al (2015) Differential genetic interactions of yeast stress response MAPK pathways. Mol Syst Biol 11:800
18. Sikorski RS, Hieter P (1989) A system of shuttle vectors and yeast host strains designed for efficient manipulation of DNA in *Saccharomyces cerevisiae*. Genetics 122:19–27
19. Watanabe Y, Irie K, Matsumoto K (1995) Yeast RLM1 encodes a serum response factor-like protein that may function downstream of the Mpk1 (Slt2) mitogen-activated protein kinase pathway. Mol Cell Biol 15:5740–5749
20. Irie K, Gotoh Y, Yashar BM et al (1994) Stimulatory effects of yeast and mammalian 14-3-3 proteins on the Raf protein kinase. Science 265:1716–1719
21. Stevenson BJ, Rhodes N, Errede B et al (1992) Constitutive mutants of the protein kinase STE11 activate the yeast pheromone response pathway in the absence of the G protein. Genes Dev 6:1293–1304
22. Wurgler-Murphy SM, Maeda T, Witten EA et al (1997) Regulation of the *Saccharomyces cerevisiae* HOG1 mitogen-activated protein kinase by the PTP2 and PTP3 protein tyrosine phosphatases. Mol Cell Biol 17:1289–1297

Index

Rafael Pulido (ed.), *Protein Tyrosine Phosphatases: Methods and Protocols*, Methods in Molecular Biology, vol. 1447,
DOI 10.1007/978-1-4939-3746-2, © Springer Science+Business Media New York 2016

H

I

K

L

M

N

O

P

R

S

T

V

W

Y

Z